Vol. 190, May 15, 1987 ISSN 0003-2670
Complete in one issue Special Issue

10TH INTERNATIONAL SYMPOSIUM ON MICROCHEMICAL TECHNIQUES, ANTWERP, BELGIUM, AUGUST 25–29, 1986
PART II

ANALYTICA CHIMICA ACTA

International journal devoted to all branches of analytical chemistry

ELSEVIER

ANALYTICA CHIMICA ACTA

International journal devoted to all branches of analytical chemistry
Revue internationale consacrée à tous les domaines de la chimie analytique
Internationale Zeitschrift für alle Gebiete der analytischen Chemie

PUBLICATION SCHEDULE FOR 1987

	J	F	M	A	M	J	J	A	S	O	N	D
Analytica Chimica Acta	192	193	194	195	196	197	198	199	200	201	202	203

Scope. *Analytica Chimica Acta* publishes original papers, short communications, and reviews dealing with ev aspect of modern chemical analysis both fundamental and applied.

Submission of Papers. Manuscripts (three copies) should be submitted as designated below for rapid a efficient handling:

Papers from the Americas to: Professor Harry L. Pardue, Department of Chemistry, Purdue University, W Lafayette, IN 47907, U.S.A.

Papers from all other countries to: Dr. A. M. G. Macdonald, Department of Chemistry, The University, P.O. Box 3 Birmingham B15 2TT, England. Papers dealing particularly with computer techniques to: Professor J. T. Cl Universität Bern, Pharmazeutisches Institut, Baltzerstrasse 5, CH-3012 Bern, Switzerland.

Submission of an article is understood to imply that the article is original and unpublished and is not be considered for publication elsewhere. Upon acceptance of an article by the journal, authors will be asked to trans the copyright of the article to the publisher. This transfer will ensure the widest possible dissemination information.

Papers in English, French and German are published. There are no page charges. Manuscripts should conform layout and style to the papers published in this Volume. See inside back cover for "Information for Authors".

Reprints. Fifty reprints will be supplied free of charge. Additional reprints (minimum 100) can be ordered. order form containing price quotations will be sent to the authors together with the proofs of their article.

Publication. *Analytica Chimica Acta* appears in 12 volumes in 1987. The subscription for 1987 (Vols. 192–203 Dfl. 2700.00 plus Dfl. 300.00 (p.p.h.) (total approx. US $1333.30). All earlier volumes (Vols. 1–191) except V 23 and 28 are available at Dfl. 243.00 (US $118.54), plus Dfl. 18.00 (US $8.78) p.p.h., per volume.

Our p.p.h. (postage, packing and handling) charge includes surface delivery of all issues, except to subscribers the U.S.A., Canada, Australia, New Zealand, P.R. China, India, Israel, South Africa, Malaysia, Thailand, Singapo South Korea, Taiwan, Pakistan, Hong Kong, Brazil, Argentina and Mexico, who receive all issues by air deliv (S.A.L. — Surface Air Lifted) at no extra cost. For Japan, air delivery requires 50% additional charge; for all ot countries airmail and S.A.L. charges are available upon request.

Subscription. Subscription should be sent to: Elsevier Science Publishers B.V., Journals Department, P.O. B 211, 1000 AE Amsterdam, The Netherlands. Tel: 5803 911, Telex: 18582, to which requests for sample copies c also be sent.

Claims for issues not received should be made within three months of publication of the issues. If not they can be honoured free of charge.

Readers in the U.S.A. and Canada can contact the following address: Elsevier Science Publishing Co. Inc., Jour Information Center, 52 Vanderbilt Avenue, New York, NY 10017, U.S.A., Tel: (212) 916-1250, for furt information, or a free sample copy of this or any other Elsevier Science Publishers journal.

Advertisements. Advertisement rates are available from the publisher.

0003-2670/87/$0

Printed in The Netherlands

ANALYTICA CHIMICA ACTA

tracted, indexed in: Anal. Abstr.; Biol. Abstr.; Chem. Abstr.; Curr. Contents Phys. Chem. Earth Sci.; Sci.; Index Med.; Mass Spectrom. Bull.; Sci. Citation Index; Excerpta Med.)

196 **CONTENTS** May 15, 1987

ial issue on Microchemical Techniques, Proceedings of the 10th International Symposium held at verp, Belgium, August 25–29, 1986. Part II. For Part I see Vol. 195.

(Continued overleaf)

(Contents continued)

ANALYTICA CHIMICA ACTA
VOL. 196 (1987)

ANALYTICA CHIMICA ACTA

International journal devoted to all branches of analytical chemistry

ELSEVIER Amsterdam–Oxford–New York–Tokyo

Anal. Chim. Acta, Vol. 196 (1987)

SPECIAL ISSUE

Proceedings of the 10th International Symposium on Microchemical Techniques, Antwerp, Belgium, August 25–29, 1986. Part II

Foreword

Microanalysis is one of the oldest specialities in analytical chemistry. Its primary goal is to analyze small samples that may range from a few milligrams or milliliters to submicrograms or submicroliters. The first symposium on microchemical techniques was held in Graz (Austria) in 1950; the emphasis of that meeting was naturally on wet-chemical and light-microscopic techniques.

In a modern laboratory, the analytical scientist is confronted with requests not only to determine residues, impurities and dopants at ever lower levels in smaller and smaller samples, but also very often to establish where the analyte of interest is located, how it is distributed in the sample, and in which chemical form. Consequently, microanalysis has shifted to a larger variety of subjects in recent years. As in all areas of analysis, rapid advances have taken place with the advent of a profusion of instrumental techniques.

Research in quantitative chemical analysis using microprobes in particular has become a very active research area in analytical sciences. It is thus understandable that at the 10th International Symposium on Microchemical Techniques, held in Antwerp (Belgium) in August 1986, emphasis was given to the application of microbeam techniques for the in-situ analysis of microscopic features in solid samples and on techniques for surface chemical analysis of both inorganic and organic samples. Among the techniques featured were laser-microprobe mass spectrometry, particle-induced x-ray emission, and ion and Raman microprobe methods. This does not mean, however, that the more classical techniques of microchemical and trace analysis were neglected. We have witnessed a considerable interest in electrochemical and optical methods of analysis and in separation and preconcentration. And applications to the life sciences, environmental sciences, materials science and industry were well represented.

A selection of all the above techniques is collected in two special issues of Analytica Chimica Acta. For convenience, the microbeam techniques have been separated from the more classical techniques of microchemical and trace analysis. We hope that the journal's readers will find these issues useful reference samples.

Renaat Gijbels

Analytica Chimica Acta, 196 (1987) 1—21
Elsevier Science Publishers B.V., Amsterdam — Printed in The Netherlands

TRENDS IN OPTICAL SPECTROCHEMICAL TRACE ANALYSIS WITH PLASMA SOURCES

J. A. C. BROEKAERT

Institut für Spektrochemie und angewandte Spektroskopie (ISAS), Bunsen-Kirchhoff-Str. 11, D-4600 Dortmund 1 (Federal Republic of Germany)

(Received 14th July 1986)

SUMMARY

The state-of-the-art and trends in the development of optical spectrochemical trace analysis with inductively-coupled plasmas (i.c.p.), direct current plasmas (d.c.p.) and microwave-induced plasmas (m.i.p.) are discussed. Innovation in plasma optical emission spectrometry (o.e.s.) is shown to lie in new sources such as the low-gas-consumption i.c.p., the air and helium i.c.p. as well as the toroidal m.i.p., which is operated at medium power and possibly with molecular gases. Sample introduction has been improved by using new pneumatic nebulizers, flow injection, electrothermal vaporization, hydride generation, direct sample insertion and direct solid sampling. Progress in the acquisition of spectral information is attained by high-resolution spectrometry, Fourier-transform spectrometry and by the use of multichannel detectors. D.c.p./o.e.s. is a mature technique for routine work and m.i.p./o.e.s. is a powerful tool for element-specific detection in chromatography. Plasma sources are also suitable atom reservoirs for atomic fluorescence spectrometry and for laser-enhanced ionization spectrometry. Trends in the figures of merit of optical plasma spectrochemical analysis are discussed.

Plasma sources were developed for emission spectrometric analysis in the late 1960s. At that time, several new radiation sources brought considerable innovation in optical emission spectrometry which previously had been confined to flame, arc and spark spectrometry (Fig. 1). For the analysis of solids, glow discharges with flat cathodes [1] and hollow cathodes [2], graphite furnaces operated at atmospheric [3] and at reduced pressure, denoted by Falk as f.a.n.e.s. (Furnace Atomic Non-resonant Emission Spectrometry) [4], and laser evaporation were described. Mainly for work with liquids, the inductively-coupled plasma (i.c.p.), the direct current plasma (d.c.p.), the microwave-induced plasma (m.i.p.) and the capacitively-coupled microwave plasma (c.m.p.) have been developed.

These sources are denoted as plasma sources and will be treated in this paper. They result from a development of sources with a geometry which enables the efficient introduction of aerosols as into flames, but with a higher temperature. Both conditions must be fulfilled to enable efficient evaporation of aerosol particles, dissociation of molecules and analyte excitation, and also to avoid matrix interferences from the formation of thermally stable compounds. As residence times of milliseconds in regions with temperatures

0003-2670/87/$03.50

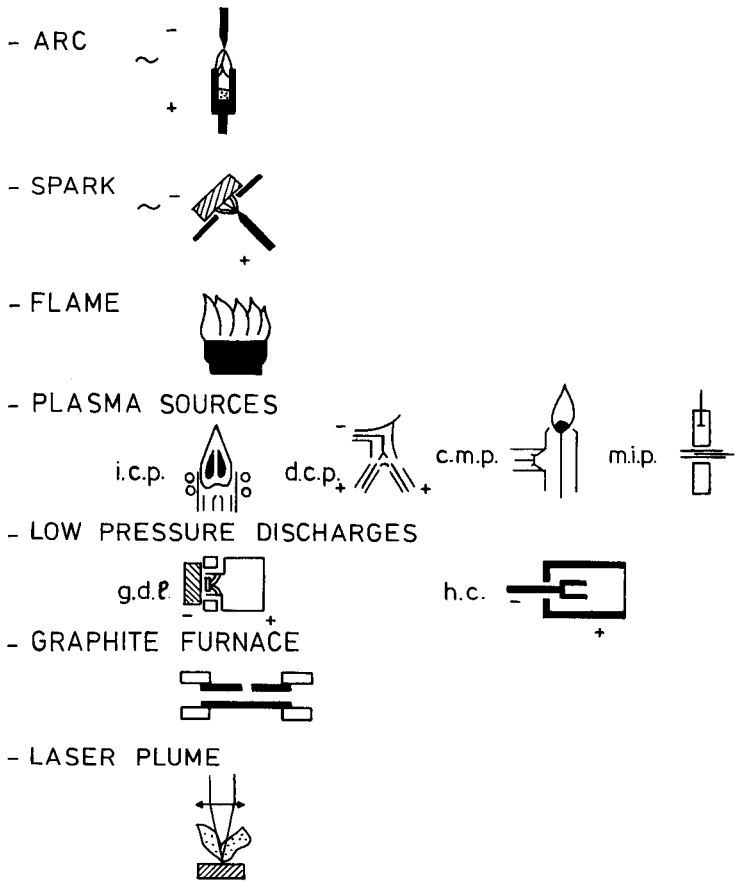

Fig. 1. Radiation sources for optical emission spectrometry.

above 5000 K are realized in the i.c.p., the d.c.p. and the m.i.p., these developments brought considerable progress compared to flames, where temperatures are below 3000 K.

Plasma optical emission spectrometry allows the sequential or simultaneous determination of a large number of elements down to absolute amounts of $\leqslant 10^{-10}$ g depending mainly on the method of sample introduction. Calibration for liquids is easy, the matrix effects can be well controlled in several ways and analyses can be obtained within a large concentration range. Accordingly, it became an established method for elemental determinations alongside other spectrometric methods such as atomic absorption spectrometry (a.a.s.).

The trends of development in optical spectrochemical trace analysis with plasma sources follow several directions. Though the sources themselves are mature, they still need further development, especially to improve their reliability and reduce their instrument and operation costs. Considerable innova-

tion is needed in sample presentation to the different sources. Also, new techniques for signal acquisition and the use of other types of signal than emission will enlarge their possibilities.

INDUCTIVELY-COUPLED PLASMA OPTICAL EMISSION SPECTROMETRY (i.c.p./o.e.s.)

With i.c.p./o.e.s. more than 70 elements can be determined; their detection limits in solutions are at the 0.5—50 ng ml^{-1} level [5]. There are restrictions in the case of the argon i.c.p. as generally used for applications to the halogens, to a certain degree to the alkali metals as well as for the working and environmental gases.

The figures of merit, however, strongly depend on the sample introduction techniques which Browner and Boorn [6, 7] called the "Achilles heel" of plasma spectrometry. With the pneumatic nebulizers presently used (Fig. 2), the sample consumption is 0.3—2 ml min^{-1}, whereas the aerosol generation efficiency is up to a few percent. As is known from flame a.a.s., much of the systematic error relates to pneumatic nebulization. Accordingly, concentrations of acids or of fluxes used for dissolution of solids should be matched in the calibration solutions, and special attention must be given to surfactants which might be present in real samples.

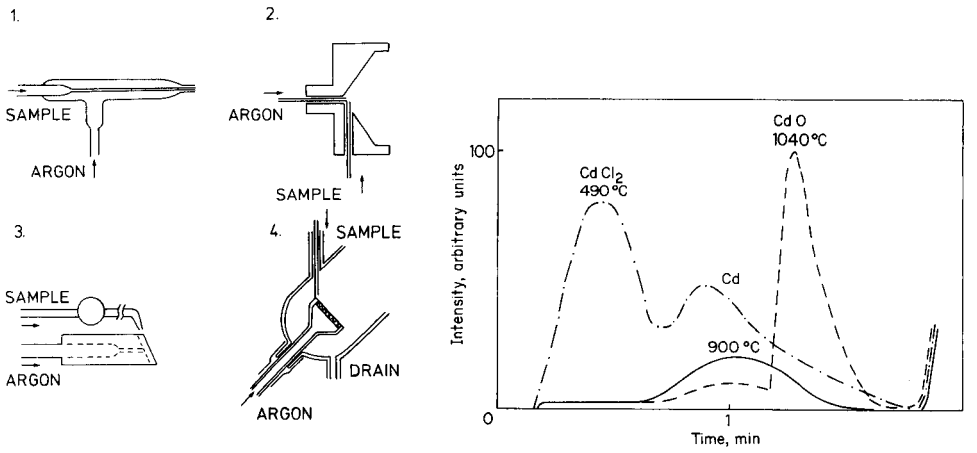

Fig. 2. Pneumatic nebulizers for optical plasma spectrometry: (1) concentric nebulizer; (2) cross-flow nebulizer; (3) Babington nebulizer; (4) fritted disc nebulizer.

Fig. 3. Thermoanalytical study of cadmium for 50-μl samples in a graphite furnace: (—) 10 μg ml^{-1} cadmium nitrate aqueous solution; (— — —) 10 μg ml^{-1} Cd added to a 0.1 g ml^{-1} solution of NBS 1571 (c_{Cl} = 690 μg g^{-1}); (— · —) 10 μg ml^{-1} Cd added to NBS 1577 (c_{Cl} = 2700 μg g^{-1}). Drying (95°C for 60 s and 350°C for 60 s) with gradual temperature increase from 350°C to 2400°C (600°C min^{-1}); 3-kW Ar/N_2 plasma; Cd II 226.5-nm line. (Reproduced, with permission, from [29].)

A main cause of systematic errors lies in spectral interferences hampering the isolation of the true analytical signal. Data on spectral interferences are now partly available in Tables [8, 9], which are helpful for adequate line selection. However, accurate acquisition of line and background intensities is also required and is only possible with advanced types of sequential and simultaneous computerized spectrometers and the appropriate software.

I.c.p. sources

Considerable work has been done on miniaturization of the plasma torch. This should allow gas consumption and power, and instrument as well as operation costs all to be decreased. Re-designed torches for which the power required is only 600 W and the gas consumption only 6 l argon min^{-1} without loss of analytical performance have been described (see for instance ref. 10). They are available in commercial instrumentation. However, Kornblum et al. [11] in 1979, already showed that an i.c.p. can be operated at a power as low as 200 W and a total argon consumption down to 0.2 l min^{-1}. This was achieved by replacing the outer gas flow by water cooling. Later, an i.c.p. with a power of 600 W and a total argon consumption of 1 l argon min^{-1} could be run by using a torch with an air-cooled ceramic outer tube [12]. Such systems will find practical application provided that their detection limits and interferences for real samples are also similar to those of conventional i.c.p. spectrometry.

Further progress in the development of i.c.p. sources lies in the use of gases other than argon. With nitrogen or air as the outer gas, and at high power, a robust plasma is obtained, as already known from the early paper of Greenfield et al. [13]. Later, all-nitrogen [14], air and oxygen plasmas [15] operating at 2 kW were found to have lower gas consumption costs but higher limits of detection than an argon i.c.p. Recently, Chan and Montaser [16] described a 600 W helium i.c.p., which might have an improved power of detection for halogens and other elements with high excitation energies (As, Bi, Cd, Se, Zn, etc.). Work with gases other than argon was promoted by the availability of generators working at high frequencies, but the effect of frequency on the excitation processes has not yet been clearly elucidated.

In order to improve operational stability and noise characteristics, work has been done on laminar-flow torches for i.c.p./o.e.s. [17].

Sample introduction

There are several possibilities for generating from a liquid or solid sample an aerosol which has suitable properties for being evaporated, atomized and excited in the i.c.p. They include pneumatic nebulization, ultrasonic nebulization, electrothermal vaporization, hydride generation (for As, Se, etc.), direct solid sampling by electroerosion or laser ablation, and direct sample insertion.

Pneumatic nebulizers (Fig. 2), because of their general applicability, are standard devices for routine work. The concentric pneumatic nebulizer for

i.c.p. work does not differ from the one described by Gouy [18] in 1879. Like the cross-flow nebulizer, it has undergone only slight modification. Currently, i.c.p. nebulizers made of materials such as Ryton have become available; in combination with spray chambers made of other plastics (e.g., PTFE) and torches with a ceramic inner tube, they are suitable for work with solutions containing hydrofluoric acid. The Babington nebulizer has been adapted to i.c.p. work, e.g., as described by McKinnon et al. [19], and is free of clogging even when slurries or suspensions are used. For titanium dioxide powder with a particle size down to a few μm, direct nebulization of a suspension containing 10 g l^{-1} powder and calibration with titanium solutions, for instance, is possible [20]. Injection and flow-injection techniques enable most efficient use to be made of pneumatic nebulization. Whereas the former especially facilitates work with microsamples [21] and decreases nebulization effects [22], the latter [23] facilitates automation and coupling with liquid chromatography. For such applications, nebulizers through which the liquid flow can be widely varied, such as the Babington type, and which can work efficiently at very low liquid throughput, such as the fritted-disk type [24], are promising. The direct insertion nebulizer developed by Kimberly et al. [25], because of its negligible dead volume (ca. 10 μl) and high aerosol transport efficiency, is also suitable for interfacing liquid chromatography and i.c.p./o.e.s. The question as to whether systems producing monodispersive aerosols or thermal spray systems, as used in conjunction with liquid chromatography [26], will improve the analytical performance of i.c.p./o.e.s., has not been answered satisfactorily.

Techniques for sample introduction other than pneumatic nebulization do not offer a general approach, but allow the specific requirements of various analytical problems to be met very well. Instrumentation for ultrasonic nebulization, apart from some improvements, still performs as described by Taylor et al. [27]. In combination with desolvation, detection limits are a factor of ten lower than with pneumatic nebulizers. Accordingly, for elements such as arsenic and lead, direct analyses of fresh waters can be achieved. As memory effects, salt depositions and desolvation interferences are considerable even for solutions of only moderate salt content, however, ultrasonic nebulization has not yet become of general use.

Electrothermal vaporization from a graphite rod [28] or furnace [29] in combination with i.c.p./o.e.s. allows the absolute and concentration detection limits to be improved by up to a factor of ten compared to pneumatic nebulization (Table 1). By suitable vapour transport, routine operation at compromise conditions for multi-element determinations can be achieved. As shown by the thermoanalytical study for cadmium in Fig. 3, the anions present govern the analyte evaporation and therefore calibration must be done by standard addition. So, for instance, in 50-μl serum aliquots, multi-element determinations at the sub-μg ml^{-1} level become possible. As the analytical signals are transient (1–2 s) and considerable changes of the spectral background may occur during analyte evaporation, time-resolved and simultaneous measurements of line and background intensities are desirable.

TABLE 1

Detection limits obtained with i.c.p./o.e.s. and m.i.p./o.e.s.

Element and line (nm)		Detection limit (ng ml^{-1})		
		I.c.p./o.e.s., pneumatic nebulization[a]	Electrothermal vaporization[b]	
			I.c.p./o.e.s.[c]	M.i.p./o.e.s.[d]
Ca I	345.3	—	—	80
Cd I	228.8	—	8	35
Cd II	226.5	20	6	250
Co II	238.9	20	—	—
Cr I	425.4	—	—	30
Cr II	283.6	20	4	84
Cu I	324.8	40	10	18
Fe I	371.9	—	—	220
Fe II	260.0	5	2	90
Mg I	285.2	—	—	2
Mo II	279.6	1	0.1	2
Mn I	279.4	—	—	60
Mn II	257.6	2	0.4	7
Ni I	341.4	—	90	80
Ni II	227.0	100	—	—
Pb I	405.7	400	130	50
Tl I	276.7	500	90	—
Tl I	377.6	—	—	90
Zn I	213.8	40	6	10

[a] 3-kW Ar/N_2 i.c.p., Meinhard nebulizer. [b] With 50-μl aliquots. [c] 3-kW Ar/N_2 i.c.p., graphite furnace; according to [29]. [d] 40-W Ar m.i.p. graphite furnace; see later section for detail.

By applying flow-cell hydride generation [30, 31], the i.c.p. detection limits for arsenic, selenium, etc. can be decreased to the ng ml^{-1} level, whereas the sample throughput and the analytical precision remain as with pneumatic nebulization (RSD $\leqslant$1%, 1—2 samples per min). However, as known from a.a.s. work (see, e.g. [32]), systematic errors may occur with real samples. They may arise because the hydride-forming elements are present as organic compounds; this can be eliminated by applying a suitable sample digestion (for instance by treatment with H_2SO_4/H_2O_2). Interferences caused by transition metals (the effect of traces of copper is well known) may be avoided by removal of the interferent by coprecipitation (e.g., with lanthanum hydroxide) or masking (e.g., with tartaric acid) [33]. Hydride-generation i.c.p./o.e.s. is used for water analysis [31] and has the advantage over hydride-generation a.a.s. that in principle several elements with volatile hydrides can be determined simultaneously.

Even in the first publications on i.c.p./o.e.s., the desire to achieve direct sampling of solids with the same analytical performance as for work with solutions was mentioned. Indeed, practical spectroscopists would like to

analyze solids without dissolution, which is not only time-consuming, but introduces risks of contamination and, for many materials (e.g., Al_2O_3 and TiO_2), is difficult. However, the processes of evaporation, dissociation and excitation in the i.c.p. dictate conditions that are difficult to achieve, namely a large number of particles sized below 2–3 μm and with the same composition as the sample must be generated and the particles must be carried without loss in the transport line into the i.c.p. by a maximum gas flow of 2—3 l min^{-1}. For compact, conducting samples, these conditions, to a certain extent, can be fulfilled by spark erosion, as was shown by Human et al. [34]. Spark sources providing high repetition rates for different matrices were found to be most suitable in this respect [35]. Accordingly, spark ablation coupled to i.c.p./o.e.s. for metals now enables detection limits similar to spark emission spectrometry to be achieved [36]. Moreover, the matrix effects are slight as has been shown by the results for various types of aluminium alloys [37]. Laser evaporation coupled to i.c.p./o.e.s. has also been shown to be useful for non-conducting solids [38]. The low precision and the power of detection compared to analysis of dissolved samples mainly originate from the laser sources available.

Direct sample insertion [39, 40] excludes any analyte vapour or aerosol transport and the resulting losses. It has been found to achieve detection limits down to 10^{-12} g for dry solution residues [41] as well as for direct determination of volatile elements in solids [42], and it might be the most sensitive plasma emission spectrometric technique.

Spectrometric signal acquisition

Because of the high temperatures in the i.c.p., the spectra are line-rich and spectral interferences occur. As the physical widths of the analytical lines are between 0.002 and 0.02 nm, spectrometers with a practical resolution of at least this magnitude would be desirable. However, they would not eliminate the problem as the analytical lines often coincide with other lines or lie on the wings of matrix lines or on bands emitted by the working or environment gases (N^{2+}, CN, NH, etc), by species from the solvents (OH, C_2 from organics, etc.) or by analyte metal oxide species (AlO, YO, etc.). Even at the highest resolution, the power of detection for real samples, because of residual interferences, may be decreased considerably [43, 44]. For high-resolution work, classical grating spectrometers, but also echelle systems which might have fewer stray radiation limitations, can be used.

Sequential i.c.p. spectrometers are flexible with respect to elements and lines. Computer control provides reliable line presetting, rapid sequential multi-element determinations and thus, low sample consumption. The information required for correcting background interferences can be obtained from automated scans of the spectral ambience of the analytical lines. Criteria for selecting the wavelength for background measurement may be included in the software, thus providing for "objective" background estimation [45]. However, the complex spectra of real samples often necessitate the

critical intervention of the operator and automatic signal acquisition in i.c.p. spectrometric trace determinations is still a long way off. In i.c.p./o.e.s. with continuous pneumatic nebulization, steady-state conditions are reached and signals can be acquired with a one-channel spectrometer. Techniques producing transient signals (flow injection, electrothermal vaporization, etc.) could be considerably improved by using "dual-channel" spectrometers allowing simultaneous and time-resolved measurements of line and background signals [46].

Simultaneous i.c.p. spectrometry provides the determination of a large number of elements at high sample throughput and is a routine technique in fields such as water pollution control, geological prospecting, and clinical analysis. Current innovation lies in improved background measurement such as is possible with multiple optics, improved software for calibration, automated sample preparation using robots, etc. Internal standardization, which is a well-known principle from early d.c. arc spectrometry, has also been found useful for i.c.p./o.e.s., when high analytical precision is required [47].

The acquisition of spectral data may make progress by the use of multichannel detectors with parallel input such as diode arrays. Photodiode arrays coupled with a microchannel plate (Fig. 4) are as sensitive as high-quality photomultipliers, even at vacuum ultraviolet wavelengths. Their dimensions (ca. 15 mm), and the diode densities (50 per mm) and pixel dimensions (15 μm), limit the wavelength coverage and resolution. Accordingly, they can at present only be used for simultaneous recordings of small spectral windows which have to be preset sequentially. Nevertheless, they provide data acquisition for real-time background and interference corrections as well as for line identification.

Considerable innovation can be expected from Fourier-transform spectrometry, which can now be used at u.v. wavelengths and has been introduced to i.c.p. spectrometry [48]. The features lie in software-controlled adaptation of the spectral resolution to the analytical problem and parallel input

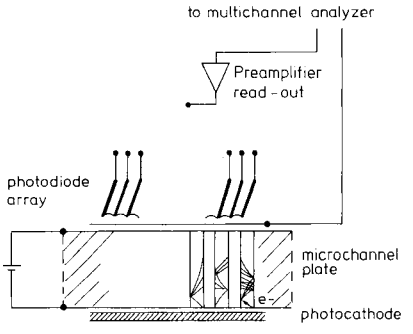

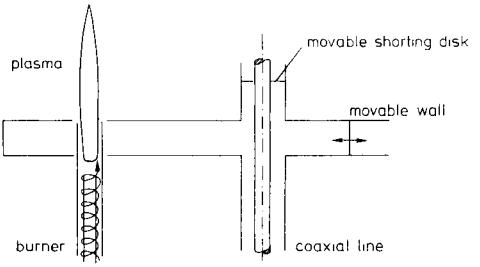

Fig. 4. Principle of microchannel plate/photodiode array detector.

Fig. 5. Resonant rectangular TE-102 resonator and plasma torch for the 800-W m.i.p. (Reproduced, with permission, from [82].)

of data. However, in order to be able to apply the technique successfully in i.c.p./o.e.s. at trace concentrations, sources with improved noise characteristics must become available.

DIRECT-CURRENT ARC PLASMA EMISSION SPECTROMETRY (d.c.p./o.e.s.)

The three-electrode d.c. arc plasma source [49] now available is the result of a long period of development aimed at the efficient use of a d.c. arc for the analysis of solutions. It unifies the advantages of "transferred" plasmas which are rather insensitive to easily ionized elements and "current-carrying" plasmas which automatically compensate for cooling caused by the introduction of wet aerosols, as known from work in the 1960s. As the analytical zone

TABLE 2

Papers on d.c.p./o.e.s. cited in a 1986 review on emission spectrometry [50]

Source development:	
two-jet plasmatron	[51]
new three-electrode plasma	[52]
rotating arc d.c.p.	[53]
Vacuum-u.v. work with d.c.p.; S, Cl, P	[54]
Interference studies:	
models for analyte emission enhancement	[55]
Pt-group metals in alumina base	
alkali metal interferences	[56]
non-alkali metal interferences	[57]
transition metals, sodium interference	[58]
lead, interferences caused by alkali and alkaline earth elements	[59]
uranium, enhancements in ground water and wine analysis	[60]
Applications:	
alkali and alkaline earth elements in orange juice	[61]
NBS coal	[62]
engine coolants	[63]
Fe—Nd and Fe—Nd—B alloys	[64]
urine and blood	[65]
natural waters	[66]
steel	[67]
mineral suspensions	[68]
estuarine sediments	[69]
blood and fish samples	[70]
Hydride generation and detection in chromatography:	
selenium and tellurium with hydride generation	[71]
arsenic with continuous hydride-generation d.c.p./o.e.s. in spiked waters and tuna samples,	[72]
h.p.l.c./hydride-generation d.c.p./o.e.s. for analysis of spiked waters, clam juice, sea water, tuna	[73]
h.p.l.c./d.c.p./o.e.s. interfacing	[74]
determination of polyphosphate oligomers by h.p.l.c./d.c.p./o.e.s.	[75]

is small (0.2×0.2 mm^2) and radiances are high, the d.c.p. can be efficiently combined with an echelle spectrometer with crossed dispersion resulting in high spectral resolution.

During the last decade, d.c.p./o.e.s. has not undergone much change. It is a routine technique which is used in many fields of application, as shown by a list of recently published work (Table 2). The power of detection and the precision obtainable are very similar to i.c.p. values. Varying concentrations of alkali elements cause higher matrix effects than in i.c.p./o.e.s. However, high concentrations of dissolved salts can be used without risks of salt deposition on the aerosol tube and electrodes. Accordingly, d.c.p./o.e.s. has frequently been applied for analyses of sea water, leaching solutions and biological fluids. The high spectral resolution of d.c.p. echelle spectrometers has promoted their use for the analysis of materials with line-rich spectra such as metal alloys. They can also successfully be used for element-specific detection in gas and liquid chromatography.

Innovation may arise from recent research on new d.c. plasma sources. In particular, attempts have been made to find a plasma geometry where a wet aerosol can pierce a hot, but current-free, d.c.-arc plasma. Masters and Piepmeier [52], for instance, used three concentric quartz tubes with electrodes running parallel to the tubes in the space between the sample and the middle quartz tubes. It is, however, still uncertain if a better power of detection and lower concomitant effects can be obtained with such sources than with a conventional three-electrode d.c.p.

MICROWAVE-INDUCED PLASMA OPTICAL EMISSION SPECTROMETRY (m.i.p./o.e.s.)

Electrodeless microwave-induced plasmas became of importance as spectrometric radiation sources after Beenakker [76] succeeded in operating them at atmospheric pressure in 1977. His low-power m.i.p. was operated in a TM-010 resonator and powered by a 2.45-GHz microwave generator. At a power of 40—100 W an argon or helium m.i.p. can be sustained with a gas flow below 1 l min^{-1}. These discharges, similar to that in the i.c.p., have high excitation temperatures ($\geqslant$5000 K) and thus also allow sensitive detection of many elements. Their gas temperatures, however, may be considerably lower, as is known from measurements of the intensity distributions in rotation–vibration spectra (e.g., of OH or N_2^+, which indicate ca. 2000 K). Moreover, they have a filament structure by which the uptake of wet aerosols without desolvation is difficult. Accordingly, these plasmas cannot be used for the direct analysis of solutions after pneumatic nebulization as in i.c.p./o.e.s. Nevertheless, they have excellent performance for dry analyte vapours. Progress in m.i.p./o.e.s. now lies in work with new types of m.i.p. discharges which can take up wet aerosols and be operated with different gases. However, progress in the use of the original m.i.p. in combination with chromatography and electrothermal vaporization also continues.

Microwave discharges

A toroidal m.i.p. can be obtained in a TM-010 cavity by using a quartz tube with an internal diameter of up to 4 mm instead of 1 mm as originally used by Beenakker, and by increasing the power to 150 W. Kollotzek et al. [77] therefore accurately centered the discharge tube in the resonator and optimized the gas flows. They obtained both toroidal and multifilament plasmas during their optimization work. The toroidal m.i.p. accepted wet aerosols as generated by a Meinhard pneumatic nebulizer. The detection limits were between 2 and 100 ng ml^{-1}, being higher only by a factor of 3—10 than in i.c.p.-o.e.s. However, the sample uptake had to be kept low ($\leqslant$0.4 ml min^{-1}) and matrix effects caused by alkali metals were high [78]. Bollo-Kamara and Codding [79] obtained similar results by using a multitube micro torch and a tangentially introduced gas flow. In both cases, it was found that by adding oxygen organic solvents could also be used.

A m.i.p. produced by surface wave propagation (surfatron) was described some years ago by Hubert et al. [80]. It is also operated at atmospheric pressure and at 100—200 W. Diagnostic studies have been performed and the surfatron is expected to accommodate all the techniques of sample introduction discussed above.

Plasmas with excellent operation stability and sample uptake capacities have been obtained in argon, helium and nitrogen at 200—300 W. They are, to some degree, interesting alternatives to the i.c.p. Deutsch and Hieftje [81] described a nitrogen m.i.p. which they called MINDAP (Microwave-Induced Nitrogen Discharge at Atmospheric Pressure). It is operated at 2 l min^{-1} argon and 200 W, and wet aerosols as generated by pneumatic nebulization can be introduced. The detection limits lie in the range 0.3—120 ng ml^{-1} and are especially low for alkali metals and rather volatile elements with sensitive atom lines (e.g., copper). The authors also used combinations with desolvation and vaporization in a microarc. Leis and Broekaert [82] developed a high-power m.i.p. for the direct analysis of solutions. A rectangular TE-102 cavity was used to generate an 800-W argon/nitrogen m.i.p. inside and outside a torch consisting of two concentric quartz tubes (Fig. 5). The aerosol was produced by pneumatic nebulization with argon and introduced into the plasma without desolvation. The detection limits here lie between the i.c.p. and MINDAP values. Similar systems for work with helium, argon only and air also have been described (see, e.g. [83]). Despite the fact that these plasmas have a geometry similar to that of the i.c.p., they are more sensitive to effects of alkali metals. To what extent further modification of the plasma geometry and the gas flows can bring more improvements and how far these interferences are inherent in the excitation mechanism have still to be discovered.

The single electrode microwave plasma (c.m.p.) known from the work of Kessler and Gebhardt [84] and others in the 1960s have recently been studied again. Hanamura et al. [85] reported diagnostic studies of an argon and a helium c.m.p. and described the determination of oxygen and hydrogen in metals [86].

Microwave plasmas in combination with electrothermal vaporization

A low-power Beenakker m.i.p. has been successfully applied in combination with electrothermal vaporization from a graphite cup [87] or furnace [88] or from a wire loop [89]. It is a most powerful technique for trace multi-element determinations in microaliquots of liquids. The instrument and operational costs are low compared to electrothermal vaporization/i.c.p./o.e.s. With a 40-W argon m.i.p. and a graphite furnace [88], the power of detection (Table 1) and the accuracy were similar to those attainable with the analogous i.c.p. method [29]. Direct sampling of powders is possible [90] by using the powder sampling syringe described by Grobenski (Fig. 6). Absolute detection limits down to the pg ml^{-1} range can be obtained by electrodeposition of the elements to be determined on graphite cups and subsequent electrothermal vaporization into the m.i.p. [91]. A similar technique for mercury based on reduction to elemental mercury, fixation on a gold wire and subsequent release by heating has also been described [92]. As the new types of plasmas, because of their discharge geometry, have greater sample uptake capacities, the re-investigation of some sample introduction techniques (electrothermal vaporization, laser evaporation, etc.) might bring further improvements in detection power.

Microwave plasmas for element-specific detection in chromatography

Numerous papers have described work on interfacing i.c.p./o.e.s. or d.c.p./o.e.s. with gas or liquid chromatography. The m.i.p., owing to its high absolute power of detection, can perform as well as these in many cases and has, moreover, lower instrument and operational costs. As helium can also be used as the working gas, the halogens can be detected with high sensitivity, so that the m.i.p. has become a valuable tool in pesticide residue analysis.

Element-specific detection in gas chromatography by means of m.i.p./o.e.s.

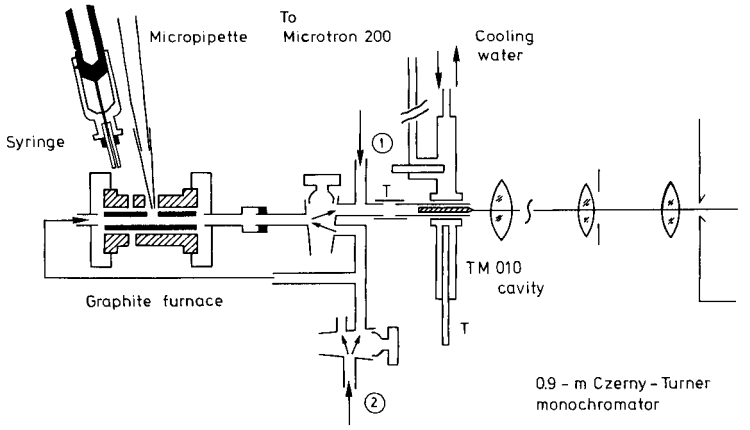

Fig. 6. Instrumentation for electrothermal vaporization m.i.p./o.e.s. The syringe is for direct solid sampling. (Reproduced, with permission, from [90].)

has been reviewed, for instance, by Uden [93]. Recent applications range from detection of organo-silicon content [94] to the determination of dioxins. For the latter, Bruce and Caruso [95] designed a laminar-flow m.i.p., with which detection limits of 8—60 pg s^{-1} for carbon, hydrogen, bromine, chlorine and fluorine emission signals were obtained. Derivatization (see, e.g. [96]) allows the detection of organic substances via the halides. Thermally stable organometallic compounds (for Hg, Se and As, see [97]) or metal complexes (such as acetylacetonates) can be detected directly by g.c./m.i.p./o.e.s. Metal complexes are of special interest for the matrix-free detection of these elements in complex mixtures. The performance of the m.i.p. with respect to organic compounds can be substantially improved by using a tangential flow torch [98], which provides a self-centering plasma, increased emission intensity and improved stability.

Since a low-power m.i.p. which can take up wet aerosols has become available, m.i.p./o.e.s. is also of potential interest for element-specific detection in liquid chromatography. As shown by Kollotzek et al. [99], different mercury species can be detected in soil samples after separation of their 2-mercaptoethanol complexes. When an argon/oxygen m.i.p. is used, carbon deposits from organic compounds can be avoided.

Because of these properties, m.i.p./o.e.s. is a powerful technique for water quality control, and there are many papers on the determination of halogenated compounds in water, for instance. Also, the coupling of m.i.p./o.e.s. to hydride generation [100] or to other techniques for the formation of volatile compounds is of topical interest.

PLASMA SOURCES FOR ATOMIC FLUORESCENCE AND LASER-ENHANCED IONIZATION SPECTROMETRY

Atomic fluorescence spectrometry (a.f.s.), as known from work with flames, unifies the advantages of the "zero background" of absorption methods with the large dynamic range of emission techniques, but without the implications of line-rich spectra which arise in o.e.s. The a.f.s. technique with flames as atom reservoirs was intensively investigated in the 1970s [101]. In the case of continuum primary sources (such as xenon lamps) simultaneous multi-element determinations are possible, but saturation of the excited level and the full power of detection can only be reached with powerful line sources such as lasers. The detection limits obtained are then in the ng ml^{-1} range. However, in flames, elements with thermally stable oxides give a poor response and chemical interferences occur. Therefore, the i.c.p. was proposed as an atom reservoir for a.f.s. by Montaser and Fassel [102] as early as 1976. In the system described later by Demers and Allemand [103], multi-element atomic fluorescence was achieved by arranging a hollow-cathode lamp, an interference filter to isolate the resonant fluorescence line and a photomultiplier around the i.c.p. The detection limits for As, Cd, Se, Tl and Zn were at least as low as in i.c.p./o.e.s. By adding propane to the

carrier gas and optimizing the torch parameters, further improvements were achieved [104].

When laser excitation is used instead of hollow-cathode lamps, non-resonant fluorescence signals can be measured and stray radiation limitations vanish. As shown by Omenetto and Human [105], detection limits in laser-excited non-resonant i.c.p./a.f.s. are similar to those in i.c.p./o.e.s. For Ga,

TABLE 3

Detection limits obtained by i.c.p./a.f.s. and flame/laser-enhanced ionization

Element	Detection limit (ng ml^{-1})			
	Hollow-cathode lamp/ i.c.p./a.f.s. [104]	Laser/ i.c.p./a.f.s. [105]	I.c.p./ i.c.p./a.f.s. [106]	Flame/ laser-enhanced [109]
Ag	1	—	—	—
Al	40	0.4	10	—
B	2000	4	10	—
Ba	—	0.7	0.9	—
Ca	—	—	0.4	0.1[a]
Cd	0.6	—	—	—
Cr	8	—	10	—
Cu	4	—	0.4	—
Ga	—	1	—	0.07[a]
Hf	—	—	30	—
Ho	—	—	10	—
In	—	—	—	0.006[a]
K	—	—	100	1[a]
Li	—	—	—	0.001[a]
Mg	—	—	0.2	—
Mo	200	5	—	—
Na	—	—	1	0.05[a]
P	—	—	80	—
Pb	250	1	—	—
Pt	—	—	30	—
Rb	—	—	—	2[a]
Si	—	1	7	—
Sm	—	—	20	—
Sn	300	3	—	—
Sr	—	—	0.2	0.4[b]
Th	—	—	100	—
Ti	—	1	—	—
Tl	—	7	—	—
V	—	3	40	—
Y	—	0.6	20	—
Yb	—	—	10	—
Zn	—	—	2	—
Zr	0.5	3	10	—

[a]Pulsed laser. [b]Continuous wave laser.

Pb, Sn and Zn they are considerably lower, but at the expense of multi-element capability and with the need for a complicated tunable laser system (Table 3).

Most interesting is the approach of using two i.c.p. sources as proposed by Greenfield and Thompson [106] and Krupa et al. [107]. The elements to be determined are introduced into the first i.c.p. which acts as the radiation source, whereas the second i.c.p. serves as the atom reservoir. This approach is most promising for real applications as multielement determinations can be performed, detection limits lie at the level of i.c.p./o.e.s. values and spectral interferences are almost completely absent. However, two i.c.p. sources are required.

Plasma sources are not only excellent atom reservoirs for a.f.s. but, as with flames, they can also be used for laser-enhanced ionization spectrometry. This technique, as described by Turk and Travis (see, e.g. [108]) for flames, is based on the measurement of the increase in ionization caused by selectively populating excited states with the aid of radiation from a tuned laser. The experimental set-up (Fig. 7) comprises a flame, a laser which can be tuned to a wavelength corresponding to the energy of a suitable level in the term scheme of the analyte element and which has sufficient output to saturate the level, as well as a collector electrode and sensitive electronics to measure the ion current, which is the analytical signal. In the flame laser-enhanced ionization method, the detection limits for some elements are at the sub-ng ml^{-1} level. This might result from the fact that the signal is measured over a solid angle of 4π instead of over a few degrees as, for instance, in o.e.s. It has already been shown that the i.c.p. can also be used with laser-enhanced ionization [110], which opens further prospects for elements with thermally stable oxides, and decreases chemical interferences. By using two lasers and applying two-photon spectroscopy, the selectivity and the power of detection can be further improved. Moreover, as Doppler-free signals are then obtained, single isotopes can be detected and isotopic dilution could become practicable in optical atomic spectroscopy. A further increase of the

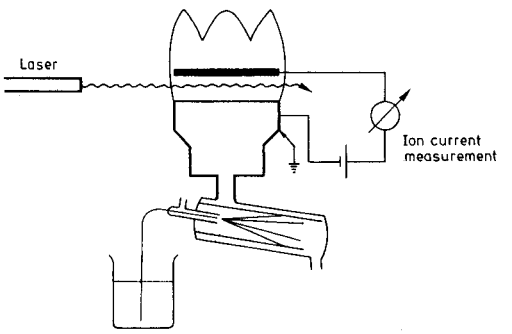

Fig. 7. Principle of flame/laser-enhanced ionization. Pneumatic nebulization is used.

power of detection becomes possible by thermionic diode detection, as described in a recent paper of Niemax et al. [111].

EVALUATION OF PLASMA OPTICAL SPECTROCHEMICAL ANALYSIS WITH RESPECT TO OTHER METHODS FOR INORGANIC ANALYSIS

Reliable instrumentation for plasma spectrometry has been available for a decade, and the technique has taken its place among other techniques for inorganic analysis, such as x-ray fluorescence spectrometry, electrochemical techniques, u.v.-visible spectrophotometry, spectrofluorimetry and in some cases, mass spectrometry and radiochemistry. The developments in plasma spectrometry discussed above, however, might change its value relative to these other techniques. Therefore, it is interesting to consider the influence of these developments with respect to the figures of merit of an analytical method (Fig. 8).

Power of detection

Detection limits in solution for i.c.p./o.e.s. and d.c.p./o.e.s. with pneumatic nebulization are between those for flame a.a.s. and furnace a.a.s. For solid samples, they are at the same level as those of x-ray fluorescence spectrometry, but they are considerably poorer than in mass spectrometry. As shown above, considerable improvements in detection limits have been realized by optimizing sample introduction. Work in this direction will certainly continue, as it also allows the implications of the physical state of the

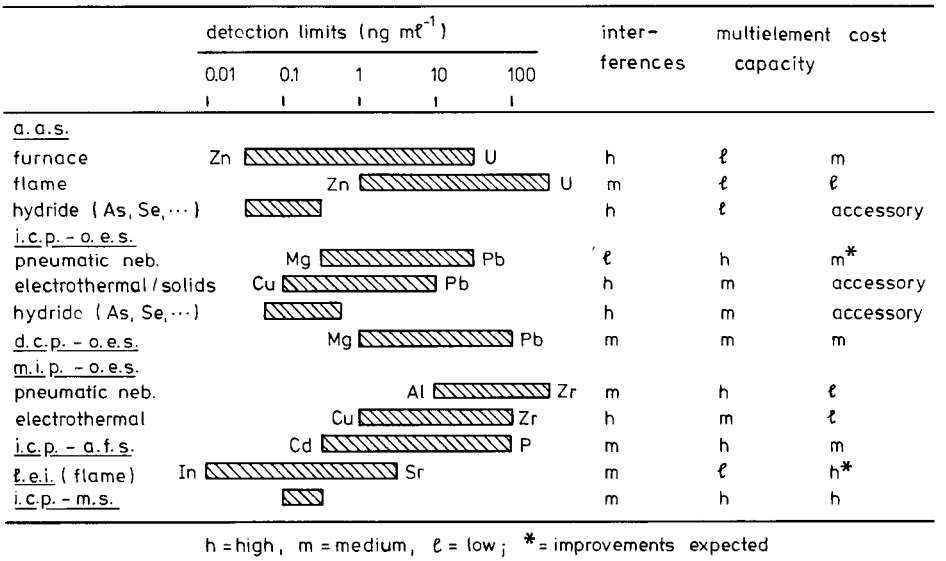

Fig. 8. Comparison of figures of merit for plasma atomic spectrometry. L.e.i. is laser-enhanced ionization.

sample (microsamples, solids which are difficult to dissolve etc.) to be considered. Especially, it has been shown that by modifying the mode of sample introduction, the i.c.p. often can be replaced by cheaper sources (m.i.p. in the case of electrothermal volatilization or hydride generation) without much loss of analytical performance.

Most progress in improving the power of detection, however, has arisen from the use of information other than emission. In this respect, laser-enhanced ionization techniques are most promising. The detection limits of plasma laser-enhanced ionization may be expected to be lower than those for flames, and such detection, moreover, might find interest for element-specific detection in chromatography and in the direct analysis of solids with glow-discharge techniques. Laser-enhanced ionization will become important for routine work, because versatile alternatives to the present complex tunable-dye laser systems are under investigation. These make use of semiconductor lasers which have become available and are simple and cheap. They are a step along the route towards a low-cost wavelength-tunable high-intensity source covering the whole u.v.-visible range.

The detection of ions by mass spectrometry (m.s.), which is beyond the scope of this paper, has also brought considerable improvements in the power of detection in plasma spectrometry. Indeed, the detection limits for i.c.p./m.s. are at the 0.1 ng ml^{-1} level [112]. Therefore, at present it is an adequate but expensive tool for ultratrace analyses of, for example, water samples. However, in the case of sample solutions with high salt content, aperture restrictions may hamper reliable operation. Also easily ionizable elements seem to cause greater interferences [113] than in i.c.p./o.e.s. Considerable progress in plasma m.s. can still be expected from the use of other working gases, work with plasma sources other than the i.c.p., and from refinements in the plasma/mass spectrometer interface. For the analysis of solids, suitable developments may be expected from glow-discharge m.s., some current progress in which has been described by Harrison et al. [114].

Both the developments discussed above narrow the gap in detection power between atomic spectrometry and the complicated, but very sensitive, radiochemical methods of analysis.

Multi-element capacity and other features

Plasma o.e.s. has a high multielement capacity under compromise conditions. This especially applies to i.c.p./o.e.s., which is in this respect superior to spectrophotometry and spectrofluorimetry, which it has displaced in many cases. In d.c.p./o.e.s., the optimum conditions differ more from one element to another and considerable losses in detection power, for instance, may result from using compromise conditions.

Accuracy and precision. If suitable reference signals are used, solids can be analyzed by plasma o.e.s. with the same precision as by x-ray fluorescence spectrometry [115]. Plasma laser-enhanced ionization and m.s. can also make use of isotopic dilution resulting in improved accuracy and precision.

Speciation. Combinations of chromatography and plasma spectrometry are very powerful tools for speciation. M.i.p./o.e.s. is very suitable for element-specific detection in gas chromatography. As well as the i.c.p.s. with low gas consumption, the new types of microwave plasma are becoming of use for liquid chromatographic detection.

Automation. Spectrometer control and automated data acquisition are possible with the use of computers. Background correction and parameter optimization, however, are so complex that it is still questionable if they can be controlled completely by artificial intelligence.

Instrument and operational costs. Advanced i.c.p. emission spectrometers are expensive. Prices start in the range of good-quality furnace a.a.s. instrumentation. However, modest sequential systems including those with a low gas consumption i.c.p. could decrease the price to that of flame a.a.s. systems. They would have a similar power of detection, but less chemical interference and a larger multi-element capacity. Their costs would also approach those of electrochemical techniques, which are useful, only for a limited number of elements (Cd, Tl, Pb, etc.) and moreover, have a higher degree of interferences as well as much lower sample throughput.

Conclusions

Progress in optical spectrochemical analysis with plasma sources has been shown to lie in improvements of sample introduction, of i.c.p., d.c.p. and m.i.p. sources as well as in better acquisition of the analytical signals. Up to now, it has been the optical emission which has been selected as the analytical signal, but other types of detection such as plasma a.f.s., laser-enhanced ionization and m.s. are showing great promise. Their use will enlarge the possibilities of plasma spectrometry for inorganic analysis.

This work has been supported by the "Ministerium für Wissenschaft und Forschung des Landes Nordrhein-Westfalen" and by the "Bundesministerium für Forschung und Technologie".

REFERENCES

1 W. Grimm, Spectrochim. Acta, Part B, 23 (1968) 443.
2 S. Caroli, Progr. Anal. At. Spectrosc., 6 (1983) 253.
3 D. Littlejohn and J. M. Ottaway, Analyst, 104 (1979) 208.
4 H. Falk, E. Hoffmann and Ch. Lüdke, Spectrochim. Acta, Part B, 39 (1984) 283.
5 R. K. Winge, V. J. Peterson and V. A. Fassel, Appl. Spectrosc., 33 (1979) 206.
6 R. F. Browner and A. W. Boorn, Anal. Chem., 56 (1984) 786A.
7 R. F. Browner and A. W. Boorn, Anal. Chem., 56 (1984) 875A.
8 P. W. J. M. Boumans, Line Coincidence Tables for Inductively Coupled Plasma Atomic Emission Spectrometry, 2nd edn., Pergamon Press, Oxford, 1984.
9 R. K. Winge, V. A. Fassel, V. J. Peterson and M. A. Floyd, Inductively Coupled Plasma Atomic Emission Spectroscopy, an Atlas of Spectral Information, Elsevier, Amsterdam, 1985
10 R. Rezaaiyaan, G. M. Hieftje, H. Anderson, H. Kaiser and B. Meddings, Appl. Spectrosc., 36 (1982) 627.

11 G. R. Kornblum, W. Van de Waa and L. de Galan, Anal. Chem., 51 (1979) 2378.
12 P. S. C. van der Plas, A. C. de Waaij and L. de Galan, Spectrochim. Acta, Part B, 40 (1985) 1457.
13 S. Greenfield, I. L. Jones and C. T. Berry, Analyst, 89 (1964) 713.
14 R. M. Barnes and G. A. Meyer, Anal. Chem., 52 (1980) 1523.
15 G. A. Meyer and R. M. Barnes, Spectrochim. Acta, Part B, 40 (1985) 893.
16 S. K. Chan and A. Montaser, Spectrochim. Acta, Part B, 40 (1985) 1467.
17 J. Davies and R. D. Snook, Analyst, 110 (1985) 887.
18 G. L. Gouy, Ann. Chim. Phys., 18 (1879) 5.
19 P. W. McKinnon, K. C. Giess and T. V. Knight, in R. M. Barnes (Ed.), Developments in Atomic Plasma Spectrochemical Analysis, Heyden, London, 1981, p. 287.
20 J. A. C. Broekaert, F. Leis and B. Radziuk, unpublished work.
21 A. Aziz, J. A. C. Broekaert and F. Leis, Spectrochim. Acta, Part B, 36 (1981) 251.
22 J. A. C. Broekaert and F. Leis, Anal. Chim. Acta, 109 (1979) 73.
23 S. Greenfield, Spectrochim. Acta, Part B, 38 (1983) 93.
24 L. R. Layman and F. E. Lichte, Anal. Chem., 54 (1982) 638.
25 E. L. Kimberly, G. W. Rice and V. A. Fassel, Anal. Chem., 56 (1984) 289.
26 G. A. Meyer, J. S. Roeck and M. L. Vestal, ICP Inf. Newsl., 10 (1985) 955.
27 C. E. Taylor and T. L. Floyd, Appl. Spectrosc., 35 (1981) 408.
28 A. M. Gunn, D. L. Millard and G. F. Kirkbright, Analyst, 103 (1978) 1066.
29 A. Aziz, J. A. C. Broekaert and F. Leis, Spectrochim. Acta, Part B, 37 (1982) 369.
30 M. Thompson, B. Pahlavanpour and S. J. Walton, Analyst, 103 (1978) 568.
31 J. A. C. Broekaert and F. Leis, Fresenius' Z. Anal. Chem., 300 (1980) 22.
32 B. Welz and M. Melcher, Spectrochim. Acta, Part B, 36 (1981) 439.
33 M. Thompson, B. Pahlavanpour, S. J. Walton and G. F. Kirkbright, Analyst, 103 (1978) 705.
34 H. G. C. Human, R. H. Scott, A. R. Oakes and C. D. West, Analyst, 101 (1976) 265.
35 B. Raeymaekers, P. Van Espen, F. Adams and J. A. C. Broekaert, Applied Spectrosc., in press.
36 J. A. C. Broekaert, F. Leis and K. Laqua, in B. Sansoni (Ed.), Instrumentelle Multielementanalyse, Verlag Chemie, Weinheim, 1985, p. 359.
37 A. Aziz, J. A. C. Broekaert, F. Leis and K. Laqua, Spectrochim. Acta, Part B, 39 (1984) 1091.
38 T. Ishizuka and Y. Uwamino, Spectrochim. Acta, Part B, 38 (1983) 519.
39 E. D. Salin and G. Horlick, Anal. Chem., 51 (1979) 2284.
40 D. Sommer and K. Ohls, Fresenius' Z. Anal. Chem., 304 (1980) 97.
41 G. F. Kirkbright and S. J. Walton, Analyst, 107 (1982) 276.
42 Y. Shao and G. Horlick, Appl. Spectrosc., 40 (1986) 386.
43 P. W. J. M. Boumans and J. J. A. M. Vrakking, Spectrochim. Acta, Part B, 39 (1984) 1261.
44 P. W. J. M. Boumans and J. J. A. M. Vrakking, Spectrochim. Acta, Part B, 40 (1985) 1085.
45 P. Taylor and P. Schutyser, Spectrochim. Acta, Part B, 41 (1986) 81.
46 J. A. C. Broekaert, W.-D. Hagenah, K. Laqua, F. Leis and D. Stüwer, Spectrochim. Acta, Part B, 41 (1986) 1357.
47 S. A. Myers and D. H. Tracy, Spectrochim. Acta, Part B, 38 (1983) 1227.
48 L. M. Faires, B. A. Palmer, R. Engelmann Jr. and T. M. Niemczyk, Spectrochim. Acta, Part B, 39 (1984) 819.
49 J. Reednick, Am. Lab., (May) (1979) 127.
50 P. N. Keliher, W. J. Boyko, R. H. Clifford, J. L. Snyder and S. F. Zhu, Anal. Chem., 58 (1986) 335R.
51 I. G. Yudelevich, A. N. Cherovko, V. S. Engelsht, V. V. Pikalov, A. P. Tagiltsex and Zh. Zh. Zheenbajev, Spectrochim. Acta, Part B, 39 (1984) 777.
52 R. A. Masters and E. H. Piepmeier, Spectrochim. Acta, Part B, 40 (1985) 85.

53 L. Y. Hara and M. L. Parsons, Anal. Chem., 57 (1985) 841.
54 J. W. Carr and M. W. Blades, Spectrochim. Acta, Part B, 39 (1984) 667.
55 M. H. Miller, D. Eastwood and M. S. Hendrick, Spectrochim. Acta, Part B, 39 (1984) 13.
56 R. L. Fox, Appl. Spectrosc., 38 (1984) 645.
57 R. L. Fox, Spectrochim. Acta, Part B, 40 (1985) 287.
58 M. Miller, E. Keating, D. Eastwood and M. S. Hendrick, Spectrochim. Acta, Part B, 40 (1985) 593.
59 J. Sneddon and V. A. Fuavao, At. Spectrosc., 5 (1984) 108.
60 B. Greene, A. Uranga and J. Sneddon, Spectrosc. Lett., 18 (1985) 425.
61 J. A. McMard, K. M. Twigg, D. T. Bach and J. D. Winefordner, Spectrosc. Lett., 17 (1984) 285.
62 D. L. McCurdy, M. D. Wichman and R. C. Fry, Appl. Spectrosc., 39 (1985) 984.
63 N. M. Potter and R. R. Lovelace, Anal. Chim. Acta, 162 (1984) 419.
64 N. M. Potter and H. E. Vergasen, Talanta, 32 (1985) 545.
65 L. Pyy, E. Hakala and L. H. J. Lajunen, Anal. Chim. Acta, 158 (1984) 297.
66 I. T. Urasa, Anal. Chem., 56 (1984) 904.
67 L. A. Fernando, Anal. Chem., 57 (1985) 1970.
68 R. Derie, Anal. Chim. Acta, 166 (1984) 61.
69 A. Y. Cantillo, S. A. Sinex and G. R. Heiz, Anal. Chem., 56 (1984) 33.
70 L. H. J. Lajunen, A. Kinnunen and E. Yrjanheikki, At. Spectrosc., 6 (1985) 49.
71 H. Hayrynen, L. H. J. Lajunen and P. Peramaki, At. Spectrosc., 6 (1985) 88.
72 D. L. McCurdy, M. D. Wichman and R. C. Fry, Appl. Spectrosc., 39 (1985) 984.
73 I. S. Krull and K. W. Panaro, Appl. Spectrosc., 39 (1985) 960.
74 D. J. Mazzo, W. G. Elliot, P. C. Uden and R. M. Barnes, Appl. Spectrosc., 38 (1984) 585.
75 W. R. Briggs, J. T. Gano and R. J. Brown, Anal. Chem., 56 (1984) 2653.
76 C. I. M. Beenakker, Spectrochim. Acta, Part B, 32 (1977) 173.
77 D. Kollotzek, P. Tschöpel and G. Tölg, Spectrochim. Acta, Part B, 37 (1982) 91.
78 D. Kollotzek, P. Tschöpel and G. Tölg, Spectrochim. Acta, Part B, 39 (1984) 625.
79 A. Bollo-Kamara and E. G. Codding, Spectrochim. Acta, Part B, 36 (1981) 973.
80 J. Hubert, M. Moissan and A. Ricard, Spectrochim. Acta, Part B, 33 (1979) 1.
81 R. D. Deutsch and G. M. Hieftje, Appl. Spectrosc., 39 (1985) 214.
82 F. Leis and J. A. C. Broekaert, Spectrochim. Acta, Part B, 39 (1984) 1459.
83 K. G. Michlewicz, J. J. Uhr and J. W. Carnahan, Spectrochim. Acta, Part B, 40 (1985) 493.
84 W. Kessler and F. Gebhardt, Glastechn. Ber., 40 (1967) 194.
85 S. Hanamura, B. W. Smith and J. D. Winefordner, Can. J. Spectrosc., 29 (1984) 13.
86 S. Hanamura, W. J. Wang and J. D. Winefordner, Can. J. Spectrosc., 30 (1985) 46.
87 C. I. M. Beenakker, P. W. J. M. Boumans and P. J. Rommers, Philips Techn. Rev., 39 (1980) 65.
88 A. Aziz, J. A. C. Broekaert and F. Leis, Spectrochim. Acta, Part B, 37 (1982) 381.
89 E. I. Brooks and K. J. Timmins, Analyst, 110 (1985) 557.
90 J. A. C. Broekaert and F. Leis, Mikrochim. Acta, (II) (1985) 261.
91 G. Volland, P. Tschöpel and G. Tölg, Spectrochim. Acta, Part B, 36 (1981) 1901.
92 G. Kaiser, D. Götz, P. Schoch and G. Tölg, Talanta, 22 (1975) 889.
93 P. C. Uden, in R. M. Barnes (Ed.), Developments in atomic plasma spectrochemical analysis, Heyden, London, 1981, p. 302.
94 K. J. Slatkavitz, L. D. Hoey, P. C. Uden and R. M. Barnes, Anal. Chem., 57 (1985) 1846.
95 M. L. Bruce and J. A. Caruso, Appl. Spectrosc., 39 (1985) 942.
96 D. F. Hagen, J. S. Marhevka and L. G. Haddad, Spectrochim. Acta, Part B, 40 (1985) 335.
97 K. B. Olson, D. S. Sklarev and J. C. Evans, Spectrochim. Acta, Part B, 40 (1985) 357.

98 S. R. Goode, B. Chambers and N. P. Buddin, Spectrochim. Acta, Part B, 40 (1985) 329.
99 D. Kollotzek, D. Oechsle, G. Kaiser, P. Tschöpel and G. Tölg, Fresenius' Z. Anal. Chem., 318 (1984) 485.
100 N. W. Barnett, L. S. Chen and G. F. Kirkbright, Spectrochim. Acta, Part B, 39 (1984) 1141.
101 N. Omenetto and J. D. Winefordner, Progr. Anal. At. Spectrosc., 2 (1979) 1.
102 A. Montaser and V. A. Fassel, Anal. Chem., 48 (1976) 1490.
103 D. R. Demers and Ch. Allemand, Anal. Chem., 53 (1981) 1915.
104 E. B. M. Jansen and D. R. Demers, Analyst, 110 (1985) 541.
105 N. Omnetto and H. G. C. Human, Spectrochim. Acta, Part B, 39 (1984) 115.
106 S. Greenfield and S. Thomsen, Spectrochim. Acta, Part B, 40 (1985) 1369.
107 R. J. Krupa, G. L. Long and J. D. Winefordner, Spectrochim. Acta, Part B, 40 (1985) 1485.
108 J. C. Travis, G. C. Turk, J. R. Devoe and P. K. Schenk, Progr. Anal. At. Spectrosc., 7 (1984) 199.
109 G. J. Havrilla, S. J. Weeks and J. C. Travis, Anal. Chem., 54 (1982) 2566.
110 G. C. Turk and R. L. Watters, Anal. Chem., 57 (1985) 1979.
111 K. Niemax, J. Lawrenz, A. Obrebski and K. H. Weber, Anal. Chem., 58 (1986) 1566.
112 A. L. Gray, Spectrochim. Acta, Part B, 40 (1985) 1525.
113 J. A. Olivares and R. S. Houk, Anal. Chem., 58 (1986) 20.
114 W. W. Harrison, K. R. Hess, R. K. Markus and F. L. King, Anal. Chem., 58 (1986) 341A.
115 J. A. C. Broekaert, R. Klockenkämper and J. B. Ko, Fresenius' Z. Anal. Chem., 316 (1983) 256.

Analytica Chimica Acta, 196 (1987) 23—31
Elsevier Science Publishers B.V., Amsterdam — Printed in The Netherlands

DETERMINATION OF TRACE METALS IN NATURAL WATERS AT NANOGRAM PER LITER LEVELS BY ELECTROTHERMAL ATOMIC ABSORPTION SPECTROMETRY AFTER EXTRACTION WITH SODIUM DIETHYLDITHIOCARBAMATE

DIPANKAR CHAKRABORTI

Department of Chemistry, Jadavpur University, Calcutta 700032 (India)

F. ADAMS* and WILLY VAN MOL

Department of Chemistry, University of Antwerp (U.I.A.), B-2610 Wilrijk (Belgium)

KURT J. IRGOLIC

Department of Chemistry, Texas A&M University, College Station, TX 77843 (U.S.A.)

(Received 11th August 1986)

SUMMARY

The determination of trace metals (Cd, Co, Cu, Fe, Ni and Pb) at concentrations found in fresh and sea waters is described. The metals are extracted as diethyldithiocarbamates from 500-ml samples into carbon tetrachloride, the extracts are evaporated to dryness and the residues are mineralized with 0.1 ml of concentrated nitric acid. This solution is used for graphite-furnace atomic absorption spectrometry after appropriate dilution. The detection limits are 10 pg Cd, 150 pg Co, 125 pg Cu, 100 pg Fe, 250 pg Ni and 100 pg Pb. The extraction/mineralization method is almost free from interferences, e.g., from trace elements at 500-fold and Na, K, Ca and Mg at million-fold amounts. The procedure is successfully applied to the determination of the above metals in deionized water, and river and sea waters.

Knowledge about the concentrations of heavy metals present at trace levels in natural waters is required to judge the "environmental health" of water bodies, to evaluate risks to users of such waters, and to estimate the degree to which organisms accumulate metals [1]. The most frequently used technique for this purpose is graphite-furnace atomic absorption spectrometry (AAS), which has high sensitivity for most metals with absolute detection limits in the low nanogram range when the sample matrix approaches distilled water in composition. However, in more complex matrices such as sea water, the determination of trace metals becomes difficult if not impossible. For instance, cadmium present in unpolluted sea water at 10 ng l^{-1} is generally determined after preconcentration or extraction, althougn the electrothermal AAS detection limit of 3 ng l^{-1} obtained for distilled water solutions of cadmium should allow direct determination in the absence of interferences. To avoid the interferences caused by the sample matrix and to increase the sensitivity, metals and metalloids

0003-2670/87/$03.50

are often extracted from the samples and preconcentrated. This step isolates the analytes from other cations and anions that may otherwise interfere with the analysis even if present only at low concentrations [2]. The determination of arsenic, for instance, is seriously impeded by low concentrations of anions such as chloride, sulfate or phosphate [3—7].

Extraction as dithiocarbamates is one of the most widely used techniques for the preconcentration of trace metals before their determination by electrothermal AAS [8—14]. When the organic extracts are injected into the furnace, the metal complexes might be volatilized and lost during drying and ashing. To prevent such losses, the metals are usually transferred back into an aqueous phase by shaking with aqueous nitric acid for AAS. The back-extraction is often slow and inefficient for metals such as cobalt, copper and iron [13]. To obtain acceptable results, concentrated nitric acid and long shaking times are necessary.

This paper documents the interferences caused by common cations in the direct determination of cadmium, cobalt, copper, lead, nickel and iron by graphite-furnace AAS, and reports a procedure involving extraction of the metal diethyldithiocarbamates into carbon tetrachloride, evaporation of the extracts to dryness, mineralization of the residues with nitric acid, and use of the nitric acid solutions for AAS. This procedure preconcentrates, prevents interferences, and avoids the difficulties associated with the extraction of the organic phase by nitric acid.

EXPERIMENTAL

Instrumentation

Cadmium (228.8 nm), Co (240.7 nm), Cu (324.8 nm), Fe (248.3 nm), Ni (232.0 nm) and Pb (283.3 nm) were determined with a Perkin-Elmer 3030 atomic absorption spectrometer equipped with a HGA-500 graphite-furnace atomizer and a deuterium background corrector. The instrumental conditions were as follows for all the elements investigated: drying temperature, 110°C at 5-s ramp time and 20-s hold time; hold time for ashing, 20 s; atomization, no ramp time, 5-s hold time; clean-up temperature, 2700°C at 1-s ramp time and 2-s hold time. The element-specific parameters were (element, ashing temperature (°C), ashing ramp time, atomization temperature (°C)): Cd, 250°, 5 s, 1100°; Co, 1000°, 5 s, 2500°; Cu, 900°, 8 s, 2300°; Fe, 1200°, 10 s, 2500°; Ni, 1200°, 10 s, 2700°; Pb, 500°, 5 s, 1300°. During atomization a nitrogen flow of 50 ml min^{-1} through the furnace was maintained. The autosampler (AS-40) was set to inject 20 μl of sample into the furnace.

Reagents

Standard solutions of the six elements were prepared from Merck Titrisol 1000 mg l^{-1} solutions. All other materials were of analytical-reagent grade. Suprapur acids (Merck) were used for the mineralization of the metal dithiocarbamates. All solutions were prepared with deionized water (Milli-Q;

Millipore). Aqueous solutions (0.5% w/v) of sodium diethyldithiocarbamate (Na-DDTC) were obtained by dissolving Na-DDTC (Merck) in deionized water and purifying the solution (100 ml) by extraction with carbon tetrachloride (10 ml) and rejecting the extract. An acetate buffer was prepared by mixing equal volumes of acetic acid (0.2 M) and sodium acetate (0.2 M) and adding one of the components until a pH of 4.5 was reached. The buffer (1 l) was purified by mixing with the Na-DDTC solution (5 ml) and extracting with carbon tetrachloride (20 ml) and rejecting the extract.

General procedure

The water samples were filtered first through 1.2-μm and then through 0.45-μm Millipore membranes. The filtered sample (500.0 ml) was placed in a separatory funnel and mixed with the buffer (10.0 ml) and the Na-DDTC solution (4.0 ml). The solution was shaken twice for 2 min with 5-ml portions of carbon tetrachloride. The two extracts were combined and placed in a 50-ml Erlenmeyer flask with a ground-glass aperture. The carbon tetrachloride was removed in a rotary evaporator at 30°C in a water bath. Concentrated nitric acid (0.1 ml) was cautiously added to the dry residue and the mixture was heated gently on a hot plate, in a well ventilated hood. Brown fumes were evolved and the solution rapidly became colorless. The colorless solution was quantitatively transferred to a volumetric flask (2 or 5 ml). The solution was diluted to the mark with deionized water and the resulting solution was used for graphite-furnace AAS. The volumes of water sample to be extracted and the final volumes of the solutions obtained by mineralization of the residues from the extracts depend on the concentration of the metal ions present in the water samples. The appropriate volumes must be estimated from preliminary experiments.

Interference studies

Solutions of Cd, Co, Cu, Fe, Ni and Pb (concentrations as in Table 1) were prepared in deionized water. Appropriate quantities of salts were added to these solutions to obtain a series of samples with increasing concentrations of salts. Aliquots (500 ml) of these samples were extracted with diethyldithiocarbamate and the extracts mineralized as described above. The mineralized extracts were diluted to 5.0 ml for AAS. For the direct injection of the aqueous samples, solutions (5 ml) were made with concentrations of analytes and salts equal to the concentrations in the 5-ml mineralized extract solutions, at the desired analyte/salt ratios.

RESULTS AND DISCUSSION

Graphite-furnace atomic absorption spectrometry is a widely used method for the determination of trace elements in a variety of matrices. The determination of trace elements by direct injection of water samples into the graphite cup or tube is, unfortunately, often unreliable, because other

dissolved cations and anions cause chemical and physical interferences [15—20]. Even low concentrations of salts may interfere [2].

Interferences in the direct injection mode

To define better the extent of interference caused by various salts, solutions of Cd^{2+}, Co^{2+}, Cu^{2+}, Fe^{3+} and Ni^{2+} chlorides and of lead nitrate, containing various amounts of other salts were analyzed by direct injection into the furnace. The weight concentration ratios of interfering element to analyte at which the analyte signal in the presence of an interfering element differs by 5% from the signal obtained in the absence of interfering elements are listed in Table 1. These data show clearly that many elements interfere with the direct determination of the six analytes and especially with the determination of Fe, Ni and Pb. The interferences caused by Cd, Co, Cr, Cu, Fe, Hg, Mn, Ni, Pb and Zn generally present at trace levels in environmental samples are not as serious as the interferences observed with Ca, K, Mg and

TABLE 1

Interference of cations in the determination of cadmium, cobalt, copper, iron, nickel, and lead before and after extraction with diethyldithiocarbamate

Interfering element as	Ratio[a] causing reduction/enhancement of signal by 5%[b,c]											
	Cd^{2+} (0.025 $\mu g\ l^{-1}$)		Co^{2+} (0.5 $\mu g\ l^{-1}$)		Cu^{2+} (0.5 $\mu g\ l^{-1}$)		Fe^{3+} (0.5 $\mu g\ l^{-1}$)		Ni^{2+} (1.0 $\mu g\ l^{-1}$)		Pb^{2+} (0.25 $\mu g\ l^{-1}$)	
	DI	DG	DI	DG	DI	DG	DI	DG	DI	DG	DI	DG
$AlCl_3$	*	**	*	**	*	**	2	**	25	**	*	**
$NaAsO_2$	*	*	*	*	*	*	*	*	50	*	*	*
$CaCl_2$	*	**	10	**	*	**	2	**	2.5	**	10	**
$CdCl_2$	—	—	*	*	*	*	*	*	25	*	100	**
$CoCl_2$	*	*	—	—	*	*	*	*	250	250	10	50
K_2CrO_4	50	*	200	250	20	400	1	250	25	25	10	*
$CuCl_2$	5	*	100	*	—	—	2	*	25	*	100	*
$FeCl_3$	5	*	100	*	20	*	—	—	2.5	75	0.1	*
$Hg(NO_3)_2$	*	*	*	400	*	**	150	400	25	*	*	*
KCl	5	**	*	**	*	**	20	**	2.5	**	5	**
$MgCl_2$	5	**	10	**	200	**	20	**	25	**	10	**
$MnCl_2$	*	*	*	*	*	*	200	*	250	*	250	*
NaCl	0.5	**	*	**	*	**	20	**	25	**	10	**
$NiCl_2$	5	*	10	*	20	*	20	*	—	—	10	50
$Pb(NO_3)_2$	*	*	*	*	200	*	20	*	25	*	—	—
$ZnCl_2$	*	*	100	*	200	*	2	*	25	*	*	*

[a]Ratio of concentration ($\mu g\ l^{-1}$) of interferent to analyte. [b]The relative standard deviations of the signals from analytes at the indicated concentrations in the absence of interfering cations and of the signals changed by 5% in the presence of interfering ions are ca. 4%. With 12 determinations each, the 5% difference between the signals is significant at the 0.01% level. [c]DI, direct injection mode; DG, DDTC/graphite-furnace AAS.

* No interference at an element/analyte ratio of 500, the highest ratio tested.

** No interference at an element/analyte ratio of 10 000, the highest ratio tested.

Na elements that are found in most aqueous samples and often at high concentrations. For instance, sodium (as NaCl) interferes even at as little as 1 mg l^{-1} in the determination of Fe, Ni and Pb. Interferences can be avoided by removing the analytes from the matrix by extraction.

The DDTC/graphite-furnace procedure

An improved procedure for the extraction of Cd, Co, Cu, Fe, Ni and Pb with diethyldithiocarbamate into carbon tetrachloride and subsequent determination of these metals was developed. The extraction of the six metals from acetate-buffered solutions is quantitative at pH >4.3 (Fig. 1). Therefore, pH 4.5, at which the acetate buffer is most effective, was chosen for all experiments. The residues obtained by evaporation of the extract were readily mineralized with concentrated nitric acid. Volumes of concentrated nitric acid from 25 to 250 µl gave identical results. The appropriately diluted solutions were used for graphite-furnace AAS.

Calibration graphs were constructed in the following manner. Analyte solutions (500 ml) were extracted. The extracts were evaporated, the residues mineralized, and the resulting solutions diluted to 2.0 ml. Aliquots of 20 µl were taken from the diluted solutions and injected into the graphite furnace. The detection limits and the concentration ranges that were used in these experiments are listed in Table 2. The absolute detection limits of this

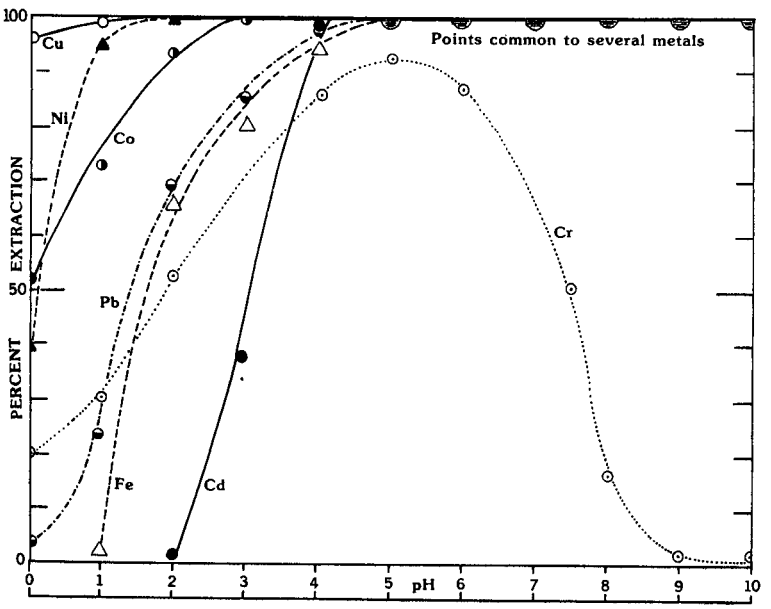

Fig. 1. The % extraction of Cd^{2+}, Co^{2+}, Cu^{2+}, Fe^{3+}, Ni^{2+}, Pb^{2+} and chromate as a function of pH (0.5% w/v Na-DDTC in water, carbon tetrachloride as organic phase).

TABLE 2

Detection limits and calibration ranges for determination by the recommended method

Ion	2σ detection limits expressed as				Calibration range[c] ($\mu g\ l^{-1}$)
	Conc. in water sample[a] ($ng\ l^{-1}$)	Amount in 500-ml sample (ng)	Conc. in 2 ml of digest ($\mu g\ l^{-1}$)	Amount injected[b] (pg)	
Cd^{2+}	2 (200, 80)	1	0.5	10	0.6—2.5
Co^{2+}	30 (200, 80)	15	7.5	150	10.0—62.5
Cu^{2+}	25 (5000, 3000)	12.5	6.25	125	7.5—50.0
Fe^{3+}	20 (670 000, 3000)	10	5.0	100	7.5—50.0
Ni^{2+}	50 (300, 2000)	25	12.5	250	25.0—150.0
Pb^{2+}	20 (3000, 30)	10	5.0	100	6.2—37.5

[a]The numbers in parentheses are the average concentrations in river water and sea water, respectively, in $ng\ l^{-1}$ [21]. [b]In 20 μl. [c]In the 2-ml of solution obtained by mineralization. Division of these by 250 will give the concentrations in the samples that were extracted.

procedure for the six analytes are ca. two to fifty times below the limits claimed for the direct injection of distilled water solutions. Better detection limits, as might be expected from the preconcentration, were not achieved because of the operating conditions selected for the furnace. To achieve maximal sensitivity, the nitrogen flow of 2 l min^{-1} through the furnace is generally stopped during atomization. However, repeatability and precision are sacrificed under these conditions, especially when the analytes are in complex matrices. A good compromise between sensitivity and precision was achieved by setting the nitrogen flow at 50 ml min^{-1}. This nitrogen flow is responsible for the poorer detection limits. Such detection limits, however, are much below the average concentration of the six analytes in unpolluted river water and sea water (Table 2) [21].

Interferences in the recommended procedure

The procedure was checked for potential interferences by other cations. The results obtained, when the six analytes were extracted from solutions containing a variety of salts and then determined in the mineralized extracts, are summarized in Table 1. The procedure was found to be almost free from interferences. Of special significance is the observation that the six metals can be determined without interference in the presence of a 10 000-fold excess of alkali and alkaline earth metal cations. The data in Tables 3 and 4 indicate that these ions will not interfere even at a million-fold excess. The extraction does not remove all interferences. Interfering ions (Table 1) such as Ni^{2+}, Co^{2+} and Fe^{3+} that are extractable will be carried into the extract. However, in most samples these interfering ions will not be present at concentrations that would impede the measurements.

TABLE 3

Cadmium, cobalt, copper, iron, nickel and lead in water samples determined by the recommended procedure.

Water sample	Concentration ($\mu g\ l^{-1}$)[a]					
	Cd	Co	Cu	Fe	Ni	Pb
Deionized	0.0028 ±0.0003	<0.03	0.090 ±0.003	0.18 ±0.02	0.040 ±0.004	0.052 ±0.005
Tap	0.20 ±0.01	0.06 ±0.04	3.9 ±0.1	5.0 ±0.1	0.98 ±0.05	1.13 ±0.07
Synthetic river[b]	0.0060 ±0.0004	0.060 ±0.003	0.24 ±0.01	1.00 ±0.09	0.120 ±0.007	0.096 ±0.009
River Scheldt	0.17 ±0.01	0.23 ±0.02	6.3 ±0.2	29.3 ±3	1.92 ±0.09	1.44 ±0.08
Lake (U.I.A.)	0.090 ±0.003	0.04 ±0.02	0.92 ±0.04	3.2 ±0.1	0.79 ±0.06	0.97 ±0.05
Synthetic sea water[c]	0.098	0.10	0.50	1.4	0.24	0.13
Coastal North Sea	0.060 ±0.002	0.060 ±0.003	1.60 ±0.09	1.5 ±0.1	0.57 ±0.03	0.48 ±0.04
SRM 1643b	20.6 ±0.7	24.0 ±0.8	22.3 ±0.7	104 ±9	48.5 ±4	24.0 ±0.5
Certified	20.3 ±1	26 ±1	21.9 ±0.4	99 ±8	49.8 ±3	24.1 ±0.7

[a]Mean ± standard deviation of 3 determinations. [b]Composition in mg l^{-1}: $CaCl_2 \cdot 2H_2O$, 294; NaCl, 216; $MgSO_4 \cdot 7H_2O$, 8.6; KCl, 9.5; $(NH_4)_2HPO_4$, 7.3. [c]Composition in gl^{-1}: NaCl, 23.9; $MgCl_2$, 5.07; Na_2SO_4, 3.99; $CaCl_2$, 1.12; KCl, 0.667; $NaHCO_3$, 0.196; KBr, 0.098; H_3BO_3, 0.027; $SrCl_2$, 0.024; NaF, 0.003.

TABLE 4

Recovery of metals from spiked water samples by the recommended method

Amount (ng) added to 250 ml/% recovered[a]					
Cd	Co	Cu	Fe	Ni	Pb
Deionized water					
6.25/110 ± 2	250/97 ± 4	125/109 ± 2	125/105 ± 3	250/114 ± 3	62.5/106 ± 3
12.5/107 ± 4	500/93 ± 4	250/104 ± 4	250/104 ± 4	500/106 ± 3	125.0/105 ± 4
25.0/95 ± 5	750/89 ± 3	500/102 ± 3	500/102 ± 4	1000/102 ± 5	250.0/98 ± 6
Synthetic river water[b]					
6.25/109 ± 3	250/106 ± 2	125/112 ± 4	125/109 ± 2	250/114 ± 5	62.5/106 ± 2
12.5/108 ± 4	500/105 ± 4	250/108 ± 2	250/106 ± 3	500/106 ± 4	125.0/105 ± 1
25.0/106 ± 3	750/103 ± 6	500/109 ± 1	500/109 ± 2	1000/100 ± 3	250.0/106 ± 2
Synthetic sea water[b]					
6.25/110 ± 2	250/94 ± 3	125/103 ± 3	125/109 ± 4	250/108 ± 5	62.5/111 ± 4
12.5/108 ± 5	500/101 ± 4	250/107 ± 4	250/108 ± 2	500/106 ± 2	125.0/107 ± 3
25.0/104 ± 3	750/97 ± 1	500/109 ± 2	500/109 ± 4	1000/100 ± 3	250.0/106 ± 2

[a]Mean of 3 determinations; recoveries calculated from the concentrations corrected with the appropriate values given in Table 3 for deionized water. [b]Compositions as in Table 3.

Analysis of water samples

The recommended procedure was used to determine the six metals in natural and synthetic water samples and in the NBS SRM 1643b (Trace Elements in Water). The results are summarized in Table 3. The concentrations found in river water and sea water are in good agreement with published data [22, 23]. The trace elements detected in the synthetic water samples came from impurities in the salts used for their preparation. The concentrations of the analytes in NBS SRM 1643b are not significantly different from the certified values.

The efficiency of diethyldithiocarbamate as an extractant was checked with spiked samples of deionized water, synthetic river water, and synthetic sea water. The extractions removed Cd, Co, Cu, Fe, Ni, and Pb quantitatively from the aqueous samples. The bias toward extraction efficiencies higher than 100% (range 95—111%, average 105%, standard deviation ±4%) might be caused by a slight underestimation of the blanks.

Conclusions

Cations commonly present in natural waters interfere seriously in the direct determination of Cd, Co, Cu, Fe, Ni and Pb by graphite-furnace AAS. The extraction and mineralization procedures described avoid interferences, and provide detection limits suitable for the determination of these metals in unpolluted, natural water samples. The mineralization of the residues from the extracts makes the troublesome back-extraction of the analytes from the carbon tetrachloride phase into an aqueous medium unnecessary. If several extractions and evaporations are done simultaneously, at least ten samples can be analyzed per hour.

Financial support of these investigations by the Robert A. Welch Foundation of Houston, Texas; Texas A&M University Center for Energy and Mineral Resources; the Department of Chemistry, Jadavpur University, Calcutta; and a Fulbright Institutional Grant from the Commission for Educational Exchange is gratefully acknowledged.

REFERENCES

1 K. J. Irgolic and A. E. Martell (Eds.), Environmental Inorganic Chemistry, VCH, Deerfield Beach, FL, 1985.
2 M. Bengtsson, L.-G. Danielsson and B. Magnusson, Anal. Lett., Part A, 12 (1979) 1367.
3 D. Chakraborti, W. De Jonghe and F. Adams, Anal. Chim. Acta, 119 (1980) 331.
4 D. Chakraborti, K. J. Irgolic and F. Adams, Int. J. Environ. Anal. Chem., 17 (1984) 241.
5 D. Chakraborti, K. J. Irgolic and F. Adams, J. Assoc. Off. Anal. Chem., 67 (1984) 277.
6 F. D. Pierce and H. R. Brown, Anal. Chem., 49 (1977) 1417.
7 D. Chakraborti, W. De Jonghe and F. Adams, Anal. Chim. Acta, 20 (1980) 121.

8 R. R. Brooks, B. J. Presley and I. R. Kaplan, Talanta, 14 (1967) 809.
9 K. Kremling and H. Peterson, Anal. Chim. Acta, 70 (1974) 35.
10 J. D. Kinrade and J. C. Van Loon, Anal. Chem., 46 (1974) 1894.
11 L. Danielsson, B. Magnusson and S. Westerlund, Anal. Chim. Acta, 98 (1978) 47.
12 T. K. Jan and D. R. Young, Anal. Chem., 50 (1978) 1250.
13 B. Magnusson and S. Westerlund, Anal. Chim. Acta, 131 (1981) 63.
14 K. W. Bruland, R. P. Franks, G. A. Knauer and J. H. Martin, Anal. Chim. Acta, 105 (1979) 233.
15 F. J. Fernandez and D. C. Manning, At. Absorpt. Newsl., 10 (1971) 3.
16 D. A. Segar and J. G. Gonzalez, Anal. Chim. Acta, 58 (1972) 7.
17 B. R. Culver and T. Suries, Anal. Chem., 47 (1975) 920.
18 W. Frech and A. Cedergren, Anal. Chim. Acta, 88 (1977) 57.
19 S. Yasuda and H. Kakiyama, Anal. Chim. Acta, 89 (1977) 369.
20 E. J. Czobik and J. P. Matousek, Anal. Chem., 50 (1978) 2.
21 J. R. Riley and R. Chester, Introduction to Marine Chemistry, Academic, New York, 1971, p. 64.
22 H. Watabanabe, K. Goto, S. Taguchi, J. W. McLaren, S. S. Berman and D. S. Russell, Anal. Chem., 53 (1981) 730.
23 H. Tao, A. Miyazaki, K. Bansho and Y. Umizaki, Anal. Chim. Acta, 156 (1984) 159.

Analytica Chimica Acta, 196 (1987) 33—40
Elsevier Science Publishers B.V., Amsterdam — Printed in The Netherlands

DETERMINATION OF BARIUM IN SEA WATER BY CATION-EXCHANGE SEPARATION AND ELECTROTHERMAL ATOMIC ABSORPTION SPECTROMETRY

FRANK DEHAIRS, MARIA DE BONDT, WILLY BAEYENS* and PIERRE VAN DEN WINKEL

Free University of Brussels, Pleinlaan 2, 1050 Brussels (Belgium)

MICHEL HOENIG

Institute for Chemical Research, Ministry of Agriculture, Museumlaan 5, 1980 Tervuren (Belgium)

(Received 24th July 1986)

SUMMARY

A method is described for the routine determination of barium in sea water by graphite-furnace atomic absorption spectrometry. Barium is separated from the main sea-water cations by collection on a cation-exchange resin. The barium is extracted into nitric acid from a portion of the resin for injection into the pyrolytically-coated graphite furnace. The method is satisfactory for the low $\mu g\ l^{-1}$ levels of barium present in ocean water, with recoveries $\geq 99\%$ and a relative standard deviation of $< 5\%$.

Precise measurements of dissolved barium in sea water were reported on a world ocean scale by Chan et al. [1]. They used isotope-dilution mass spectrometry after the separation of barium by ion-exchange chromatography [1, 2]. Several investigators have tried to optimize conditions for direct determination of barium in sea water by graphite-furnace atomic absorption spectrometry (AAS) [3, 4] and atomic emission spectrometry [5, 6]. Direct-current plasma atomic emission spectrometry is also possible [7]. While these techniques are sufficiently sensitive and the background signal from the sea water matrix can be eliminated, none, with the possible exception of the last, appears to be useful for routine determination of barium in sea water. In graphite-furnace AAS the rapid degradation of pyrolytically-coated graphite tubes on repeated injection of sea water [4, 5] is a major impediment to its routine use. In this study, a method is described for ion-exchange separation of barium from the major sea salt components, followed by elution of barium in an acidic medium and subsequent determination by graphite-furnace AAS.

EXPERIMENTAL

Apparatus

A Varian AA-1275BD atomic absorption spectrometer equipped with a GTA-95 graphite furnace and programmable autosampler was used. The

0003-2670/87/$03.50

barium hollow-cathode lamp (Instrumentation Laboratory) was operated at 8 mA. All measurements were made at the 553.6-nm barium line at a spectral band width of 0.5 nm (with decreased slit height). Pyrolytically-coated tubes (Le Carbone Lorraine) were used throughout. The furnace program is shown in Table 1. All absorbance readings were in peak-height mode. A Hamilton Microlab 1000 diluter was used for diluting. The ^{133}Ba activity was measured with a 2-in. pit crystal NaI scintillation detector (Canberra).

Sample preparation and reagents

Conditioning of the cation-exchange resin. Dowex 50W-X8 resin (200—400 mesh, H^+-form; BioRad) was used throughout. After a few preliminary rinses, and discard of the floating fines, the resin was packed in a column, washed with 7.5 M hydrochloric acid (analytical grade) and rinsed with Milli-Q (Millipore) water until the pH was 5—6. The resin was converted to the ammonium form with 30% ammonia (analytical grade) and again rinsed with Milli-Q water to pH 5—6. The resin was dried at 60°C.

Batch experiments. The resin (1 g) was equilibrated overnight with 0.33 meq of the cation studied in 41 ml of solution. Cations were all used as their chlorides. Elements were determined in batch experiments by flame atomic absorption spectrometry (Varian AA-275 spectrometer). Ammonium chloride solutions used for column experiments were purified from barium on Dowex resin (NH_4^+ form) prepared as above.

Column experiments. For processing sea-water samples ($\leqslant$120 ml), columns (13.4 mm i.d.) were filled with 2.5 g of the ammonium-form resin. Before the samples were applied, the resin was conditioned with 0.6 M ammonium chloride. Flow through the column was maintained at 1.5 ml min^{-1} with a peristaltic pump. After the major cations had been eluted (see below), the resin was washed chloride-free with Milli-Q water, dried at 60°C and homogenized for one hour in a Buchler vortex mixer. From this dry resin, small portions were weighed for subsequent exchange of barium into nitric acid in the autosampler cup.

Sample volumes of 100 ml were processed here, but this volume can be conveniently reduced, which allows a reduction of resin amount and eluant.

TABLE 1

Electrothermal program used for the determination of barium

Temp. (°C)	80	150	1200	1200	2500	2500	80
Time (s)	1.0	20	10	2.0	0.7[a]	2.5[b]	11
Argon (l min^{-1})	3	3	3	0	0	0	3

[a]Maximum heating rate. [b]Peak-height absorbance measured during this period.

RESULTS AND DISCUSSION

Separation of barium from sea water

The effect of three counter-ions (H^+, K^+ and NH_4^+) on the distribution coefficients, K_d, of barium and sodium, the main cation in sea water, was measured; K_d (in ml g^{-1}) is given by the ratio of the equivalents on the resin to the equivalents in solution, as deduced from the concentrations of Ba^{2+} or Na^+ added and those measured in solution after batch equilibration of the resin with 0.4 M hydrochloric acid. The results are shown in Table 2. It is clear that the ammonium form of the resin produces the best conditions for the separation of barium and sodium ions. Successful separation of the alkaline earth elements has been described by others, with ammonium malonate as the eluant [8]. In this investigation, satisfactory results for the separation of barium ions from a matrix containing Na^+, K^+, Ca^{2+} and Mg^{2+} as major cations were obtained with ammonium chloride as eluant.

Distribution coefficients for Ba^{2+}, Ca^{2+}, Mg^{2+}, Na^+ and K^+ were obtained from separate batch experiments with 0—2 M ammonium chloride. The results are shown in Fig. 1. For each ammonium chloride concentration, selectivity coefficients, K_{B,NH_4}, were calculated:

$$K_{B,NH_4} = (B_R)\,(NH_4^+)^n/(NH_{4R})^n\,(B^{n+})$$

where ( ) represents equivalent concentrations, B is the competing cation and R is the resin phase. Table 3 lists the arithmetic means of the selectivity coefficients for ammonium chloride concentration ranges that produced <5% relative standard deviation (*RSD*). These average selectivity coefficients can be used, within the corresponding ammonium chloride concentration range, to calculate K_d for any ammonium chloride concentration (see Appendix). These calculated K_d values are identified in Fig. 1.

The K_d value for barium ions in sea water is required to predict the breakthrough of barium when a sea-water sample is applied to the column. A batch experiment was done with an artificial sea-water solution with concentrations of the major cations close to their natural values (0.6 M Na^+, 0.01 M K^+, 0.01 M Ca^{2+}, 0.08 M Mg^{2+}). The Ba^{2+} content was 0.33 meq. This gave a K_d value for barium of 109 ml g^{-1}, a value that indicates that barium will have passed over 0.9 g of resin after the application of a 100-ml sea-water sample.

TABLE 2

Distribution constants of sodium and barium ions as a function of the counter-ion for a batch experiment with 0.4 M HCl (duplicate measurements)

Counter-ion	H^+	NH_4^+	K^+
$K_d(Na^+)$	18.5	10.7	8.2
	17.6	9.8	9.0
$K_d(Ba^{2+})$	484	795	664
	476	808	672

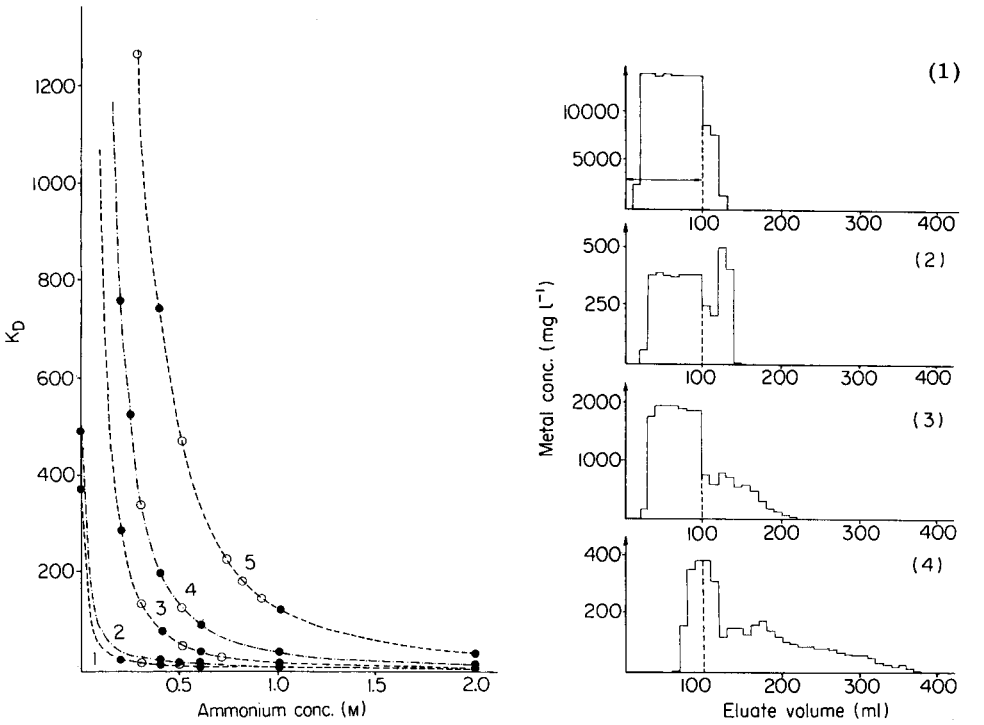

Fig. 1. K_d values vs. ammonium concentration: (1) Na^+; (2) K^+; (3) Mg^{2+}; (4) Ca^{2+}; (5) Ba^{2+}. (•) Experimental values; (○) calculated values, based on formulae in Appendix.

Fig. 2. Elution profiles: (1) Na^+; (2) K^+; (3) Mg^{2+}; (4) Ca^{2+}. A 100-ml sea water sample was passed through a column containing 2.5 g of NH_4^+-form resin; Na^+, K^+, Mg^{2+}, Ca^{2+} were eluted with 0.6 M ammonium chloride solution. The dashed lines indicate the end of the 100-ml sample introduction.

TABLE 3

Selectivity coefficients of Na^+, K^+, Mg^{2+}, Ca^{2+} and Ba^{2+} over various ammonium chloride concentration ranges

Ion	K_{B,NH_4}	*RSD* (%)	NH_4Cl (M)
Na^+	0.89	4.8	0.2—0.6
K^+	1.73	1.5	0.4—1.0
Mg^{2+}	24.4	3.6	0.2—1.0
Ca^{2+}	66.3	1.3	0.2—0.6
Ba^{2+}	241	1.3	0.2—2.0

From the distributions of K_d values as a function of ammonium chloride concentrations, a 0.6 M solution was selected as eluant, ensuring both maximum retention of barium and optimum elimination of Na^+, K^+, Ca^{2+} and Mg^{2+}. The calculated column parameters and K_d values are given in Table 4. These parameters can be used to calculate that the peak maximum of Na^+ elutes at 21 ml, K^+ at 33 ml, Mg^{2+} at 89 ml and Ca^{2+} at 227 ml with 0.6 M ammonium chloride. Experimental elution profiles for the different cations are shown in Fig. 2, confirming the calculated data. In practice, the sea-water samples were eluted with 250 ml of 0.6 M ammonium chloride. The Ca^{2+} tail was eliminated with 20 ml of 1.0 M ammonium chloride.

Barium recovery. Aliquots (100 ml) of a natural sea-water sample were spiked with 0.5 μCi ^{133}Ba and applied to columns containing 2.5 g of the ammonium form resin. The major cations were eluted as described above; barium was eluted with 8 M nitric acid and precipitated as its sulphate.

The activity of the precipitate was measured with the scintillation counter and compared with a standard processed in the same way, except for the column separation. Recoveries were $\geqslant 99\%$.

For the determination of barium in sea-water, the resin was retained instead of the barium being eluted from the column. Barium ion exchange between the ammonium-form resin and a barium standard in 7.5 M nitric acid was examined. Amounts of resin ranging from 10 to 20 mg suspended in 1 ml of barium standard solutions (5—15 μg l^{-1}) resulted in recoveries of >99% (10 mg of resin) and >90% (20 mg of resin), relative to the standards with no resin added.

Determination of barium

Barium was desorbed from 15—20 mg portions of dry resin suspended in 1.5 ml of 7.5 M nitric acid within the microvials used for the furnace autosampler. The graphite tube was changed after ca. 200 firings, at which stage the absorbance had decreased by ca. 20%. Throughout the work, periodic recalibrations were made (every 6 firings). After 200 firings, no macroscopical degradation of the pyrolytic coating was observed; this only occurred after some 500 firings, the actual tube lifetime. The achieved temperature, as

TABLE 4

Column parameters and K_d values at two ammonium chloride concentrations

NH_4Cl (M)	i[a]	ρ[b] (ml g^{-1})	h[c] cm	K_d (ml g^{-1})				
				Na^+	K^+	Mg^{2+}	Ca^{2+}	Ba^{2+}
0.6	0.62	1.92	3.42	7.06	11.9	34.3	89.4	316
1.0	0.62	1.85	3.29	4.24	7.2	12.8	33.8	179

[a]Interstitial volume fraction. [b]Specific volume of resin. [c]Height of resin column (13.4 mm i.d.).

measured with an optical pyrometer, did not differ by more than 5% from the selected temperature throughout the tube lifetime [4].

Standard solutions were prepared in 7.5 M nitric acid, as used for the sample desorption. A direct calibration graph and a standard addition graph for a natural sea-water sample had similar slopes, indicating that there was no matrix effect and that direct calibration with acidified aqueous standards is valid. This is in agreement with the fact that only small amounts of residual sea-water matrix elements remained on the column after elution with 0.6 M ammonium chloride (Na $\approx$ 0.5, K $\approx$ 0.2, Ca $\approx$ 0.2, Mg $\approx$ 0.07 $\mu g\ ml^{-1}$).

The resin particles were allowed to stand in the nitric acid in the sample cup for a few minutes. This was sufficient for the cation exchange to reach equilibrium. Under these conditions, the barium concentration in the final solution is no greater than in the sea water, but the sensitivity of graphite-furnace AAS is sufficient (4 pg Ba for 0.0044 absorbance) for determination at the levels obtained.

Reproducibility. Ten determinations of a single supernatant solution from a sample solution containing 8 $\mu g\ l^{-1}$ barium produced an *RSD* < 2%. To check the entire procedure (column separation and graphite-furnace AAS), four 100-ml aliquots of filtered, aged Mediterranean sea water spiked with 10.0 $\mu g\ l^{-1}$ barium were processed. The mean barium concentration found was 21.2 $\mu g\ kg^{-1}$, and the *RSD* was 3.0%. For six samples collected within a 70-m depth interval, close to the sea floor in the NE Atlantic (FLUXATLANTE, Station 7, 46° 22.01′ N, 12° 23.7′ W; 3850 m), the mean concentration was 8.03 $\mu g\ kg^{-1}$, and the *RSD* was 4.1%. Within such a small depth interval no gradients of barium are expected to occur.

Blanks. Untreated commercial Dowex 50W-X8 (200—400 mesh, H^+-form) resin contains relatively large concentrations of barium, up to 1 $\mu g\ g^{-1}$ of dry resin. Rinsing and conversion to the ammonium form decreases this barium blank to 0.04 $\mu g\ g^{-1}$ of dry resin. Procedural blanks, run under the identical conditions used for the samples gave blank values of 0.05 $\mu g\ g^{-1}$ barium. Depending on the initial barium content, this is equivalent to 10% (initial concentration, 15 $\mu g\ l^{-1}$) to 25% (initial concentration, 5 $\mu g\ l^{-1}$) of the sample concentration.

Application to sea-water samples from a N.E. Atlantic profile. Table 5 gives the data for dissolved barium along a vertical profile (4500 m) in the N.E.

TABLE 5

Concentration of dissolved barium along a vertical profile in the N.E. Atlantic, collected during the FLUXATLANTE campaign at Station 3, position 36° 15.2′ N, 13° 45.6′ W; 4460 m

Depth (m)	Barium ($\mu g\ kg^{-1}$)	Depth (m)	Barium ($\mu g\ kg^{-1}$)	Depth (m)	Barium ($\mu g\ kg^{-1}$)	Depth (m)	Barium ($\mu g\ kg^{-1}$)
19	5.1	310	6.5	1193	8.8	2961	10.2
41	5.0	506	7.3	1241	9.1	3443	12.0
61	5.3	761	7.5	1984	8.5	3924	12.9
113	6.3	1143	8.8	2473	10.0	4376	12.1

Atlantic sampled in April 1985, during FLUXATLANTE. The concentration was found to increase from a minimum value in surface water (5.1 $\mu g\ kg^{-1}$) to 12.9 $\mu g\ kg^{-1}$ in the deep sea. At the nearest GEOSECS station (station 115; position 28° 1.5′ N, 26° 0.0′ W) the surface and deep water concentrations are 5.3 and 10.8 $\mu g\ kg^{-1}$, respectively [1].

Conclusions

The method presented here is suitable for the routine determination of barium in sea water. The ion-exchange operation allows quantitative recovery of barium, with elimination of the major fraction of the major salt components. Barium remains on the resin, allowing for a more convenient storage of samples, as compared to its elution from the column. The subsequent batch-type desorption of barium from only milligram amounts of resin into nitric acid, just prior to the determination of barium by graphite-furnace AAS is straightforward. Further testing is required in order to decrease the barium blank values. Despite this, and the relatively complex nature of the whole procedure, barium determinations are possible with a RSD <5% at very low levels.

We are indebted to Dr. C. E. Lambert (CFR-CNRS, Gif/Yvette), who provided the samples. F. D. is a Research Associate of the Belgian National Fund for Scientific Research.

APPENDIX

Calculation of the distribution coefficient K_d for the ammonium chloride concentration range producing constant selectivity coefficients.

For monovalent/monovalent ion exchange,

$$NH^+_{4R} + B^+ \rightleftharpoons NH^+_4 + B^+_R$$

The selectivity coefficient can be defined as

$$K_{B,NH_4} = [X_{BR}/(1 - X_{BR})]\ [(1 - X_B)/X_B] \qquad (1)$$

Here, X_{BR} is the equivalent fraction of B^+ on the resin, i.e., $(B^+_R)/(R)$ where (B^+_R) is the number of equivalents of B^+ on the resin and (R) is the total number of equivalents on the resin; X_B is the equivalent fraction of B^+ in solution, i.e., $(B^+)/(S)$, where (B^+) is the number of equivalents of B^+ in solution and (S) the total equivalents in solution. $(B^+_R) + (B^+) = (B_t)$, the total equivalents of B^+.

Equation 1 can be written as

$$(1 + K_{B,NH_4})(B^+_R)^2 + [(B_t) - (S) - K_{B,NH_4}(B_t) - K_{B,NH_4}(R)]\ [B^+_R] +$$

$$+ K_{B,NH_4}(B_t)(R) = 0$$

Because K_{B,NH_4}, (B_t), (S) and (R) are known, solution of this quadratic equation for (B^+_R) gives $K_d = (B^+_R)/(B^+)$ in ml g^{-1}.

For monovalent/divalent ion exchange,

$$2NH^+_{4R} + B^{2+} \rightleftharpoons 2NH^+_4 + B^{2+}_R$$

The selectivity coefficient is then

$K_{B,NH_4} = [X_{BR}/(1 - X_{BR})^2]\ [(1 - X_B)^2/X_B]\ [(S)/(R)]$

with all terms defined as above. This equation can be written as

$$[-1 - K_{B,NH_4}]\ (B_R^{2+})^3 + [2\,K_{B,NH_4} - 2(S) + K_{B,NH_4}\,(B_t) + 2\,(B_t)]\ (B_R^{2+})^2 +$$
$$+ [2\,(B_t)\,(S) - 2\,(B_t)\,K_{B,NH_4}\,(R) - K_{B,NH_4}\,(R)^2 - (S)^2 - (B_t)^2]\ (B_R^{2+}) +$$
$$+ (B_t)\,(R^2)\,K_{B,NH_4} = 0$$

Because K_{B,NH_4}, (B_t), (S) and (R) are known, solution of this cubic equation for (B_R^{2+}) gives $K_d = (B_R^{2+})/(B^{2+})$ in ml g^{-1}.

REFERENCES

1 L. H. Chan, D. Drummond, J. M. Edmond and B. Grant, Deep-Sea Res., 24 (1977) 613.
2 M. P. Bacon and J. M. Edmond, Earth Planet. Sci. Lett., 16 (1972) 66.
3 M. K. Conley, J. J. Sotera and H. L. Kahn, Instrum. Lab., 11 (1979) 1.
4 M. Hoenig, F. Dehairs and A. M. De Kersabiec, J. Anal. At. Spectrom., 1 (1986) 449.
5 M. S. Epstein and A. T. Zander, Anal. Chem., 51 (1979) 915.
6 H. Hui-Ming and L. Yao-Han, Spectrochim. Acta, Part B, 39 (1984) 493.
7 D. C. Bankston, Proc. Int. Winter Conf. on Developments in Atomic Plasma Spectrochemical Analysis, 1981, p. 627.
8 F. W. E. Strelow, C. R. Van Zijl and C. R. Nolte, Anal. Chim. Acta, 40 (1968) 145.

Analytica Chimica Acta, 196 (1987) 41—47
Elsevier Science Publishers B.V., Amsterdam — Printed in The Netherlands

SENSITIVE DETERMINATION OF TRACES OF BORON IN WATERS, FERTILIZERS AND GEOLOGICAL AND BIOLOGICAL MATERIALS BY ISOTOPE-DILUTION MASS SPECTROMETRY

N. L. DUCHATEAU, A. VERBRUGGEN, F. HENDRICKX and P. DE BIÈVRE*

CEC, Joint Research Centre, Geel Establishment, Central Bureau for Nuclear Measurements, Steenweg op Retie, B-2440 Geel (Belgium)

(Received 28th July 1986)

SUMMARY

A method is described for determining traces of boron in water, fertilizers, geological and biological (reference) materials by isotope-dilution mass spectrometry after separation on an Amberlite IRA-743 borate-selective ion-exchange column. Boron (5—250 ng g^{-1}) in water can be determined with an accuracy of 5—20% (computed on a 2*s* basis). After correction for weighing errors and for moisture content, which varied from 0 to 8% for the samples tested, 1—35 $\mu g\ g^{-1}$ boron in "dry" fertilizer, biological or geological sample can be assayed with an accuracy of 5—30% (2*s*). In an IAEA interlaboratory program on a simulated fresh water, the method yielded a value of 24.3 ± 2 $\mu g\ l^{-1}$, compared to the make-up value of 25 $\mu g\ l^{-1}$.

A study by the National Bureau of Standards, Washington, of boron assays for the reference material SRM 1571 Orchard Leaves over the period 1974–1982 resulted in values from 23 to 40 $\mu g\ g^{-1}$ produced by 32 laboratories using nine different methods [1]. Thus it was shown once more that reference measurement methods and reference materials are necessary for calibration of different techniques. Because of its characteristics, isotope-dilution mass spectrometry (IDMS) is suitable for "absolute" determinations (i.e., when it is done properly) with an uncertainty that takes into account all components that contribute to the total uncertainty of an assay [2–4], and so has the potential to produce an uncertainty which, for all practical purposes, can claim to contain the "true" value.

Assay of boron by IDMS

In IDMS, the unknown amount N_X of an element in a sample is calculated from the change induced in the isotope ratio R_X of two isotopes in that element, when a known amount N_Y (spike) of the same element with another isotope ratio R_Y is added to the unknown sample, the isotope ratio of the spiked sample being R_B:

$$N_X = N_Y\ [(R_Y - R_B)/(R_B - R_X)]\ [(1 + R_X)/(1 + R_Y)]$$

In the case of boron $R = {}^{10}B/{}^{11}B$. A boric acid material isotopically enriched to 95% ^{10}B (NBS-SRM 952) was used as the spike.

0003-2670/87/$03.50

The accuracy of the determination is defined by the accuracy of the measured isotope ratios. A fundamental advantage of IDMS is that the absolute isotope ratios can be measured with high precision and accuracy by calibration with isotopic reference materials or synthetic mixtures of isotopes. Additional advantages are that it is not necessary to separate the spiked element quantitatively from the sample, and that the method is rather insensitive to chemical interference [2].

The $^{10}B/^{11}B$ isotope ratios R_B of the spiked samples ranged between that for natural boron ($R_X \approx 20/80$) and that of the spike ($R_Y \approx 95/5$). By use of "natural" boric acid (CBNM-IRM 011) and "^{10}B-enriched" boric acid (NBS-SRM 952) isotopic reference materials, an isotope fractionation correction factor $K = 0.9947 \pm 0.0028$ was evaluated. The "true" isotope ratio can then be calculated from $R = K\,R'$, where R is the true isotope ratio, K the isotope fractionation correction factor and R' the measured isotope ratio (see Table 1).

EXPERIMENTAL

Chemical preparation

Accurate weighing. For accurate mass determinations, accurate weighing is essential. Weights were used which had been traced directly to the Primary Standard Kilogram at the Bureau International des Poids et Mesures, Sèvres. Care was taken to prevent electrostatic forces during the weighing of small samples and to correct for "buoyancy", in order to achieve accurate weighings free from systematic errors.

The correction factor for buoyancy is

$$\rho_v\,(\rho_g - \rho_1)/\rho_g\,(\rho_v - \rho_1)$$

where ρ_1, ρ_v, ρ_g are the specific gravities of, respectively, air, sample and reference weights. For temperatures between 10°C and 35°C, relative humidity between 10% and 90%, atmospheric pressure ranging from 730 to 780 mm Hg, ρ_1 varies between 0.00108 and 0.00128 g cm^{-3}. Figure 1 shows the correction factor on the weighings as a function of ρ_v. It appears that for certain samples a correction must be applied. The correction factor is independent of the amount weighed.

TABLE 1

Isotope fractionation correction factor K (2s uncertainties)

Isotope reference material	Certified $^{10}B/^{11}B$ isotope ratio	Observed $^{10}B/^{11}B$ isotope ratio	Isotope fractionat correction factor
CBNM-IRM 011 natural boric acid	0.24726 ± 0.00032	0.24858 ± 0.00064	0.9947 ± 0.0028
NBS-SRM 952 ^{10}B-enriched boric acid	18.80 ± 0.02	18.902 ± 0.050	0.9946 ± 0.0028
Mean			0.9947 ± 0.0028

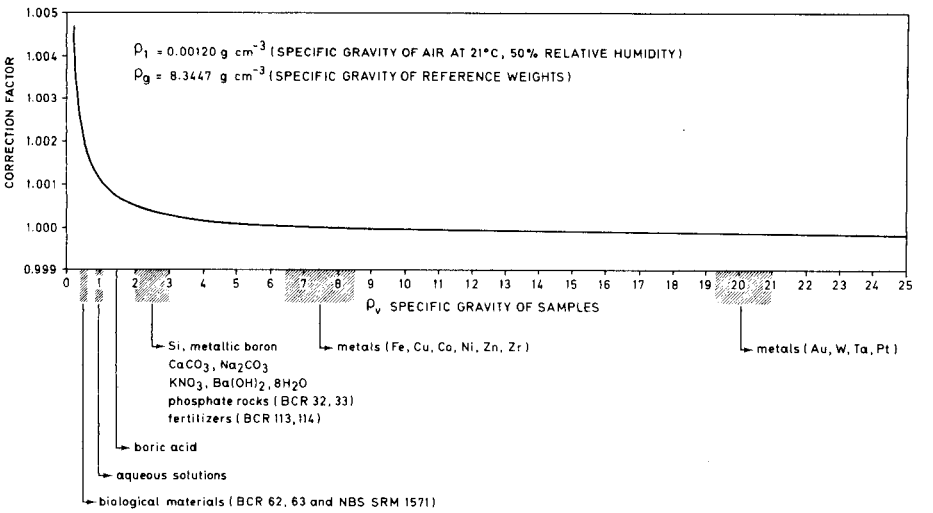

Fig. 1. Correction factor on the weighings as a function of specific gravity of samples ρ_v.

Moisture content in fertilizers, biological and geological materials. Most materials contain a certain amount of moisture. In reporting results, it is essential to indicate whether or not a correction for this moisture content has been applied.

In a conditioned room (21°C, 50% relative humidity), 2.0000 ± 0.0005-g samples were weighed into porcelain crucibles. Then these crucibles were placed in a thermostated oven (108.5 ± 1.0°C) for 120 ± 5 min. After 2 h, the crucibles were placed in a box with a continuously passing dry air current (21°C, <5% relative humidity). After cooling for 18—20 h, crucibles were weighed in this box. The procedure was repeated until changes in mass were less than 0.0005 g. Three repeats were sufficient for all samples, except for the BCR 33 Superphosphate. Changes in mass induced by the porcelain crucibles themselves were negligible (<0.0002 g). Moisture content in the biological materials tested varied between 5 and 8%. In geological materials and fertilizers, less than 2% loss of mass was detected (except 4.8% for BCR 33 Superphosphate) (see Table 2).

Separation of boron on an Amberlite IRA-743 ion-exchange column. Samples comprising 50—400 g of water, 0.25—1.00 g of fertilizer, 0.10—0.60 g of geological material, and 0.06—1.60 g of biological material, as well as spike solutions, were weighed accurately. To achieve isotope-dilution analysis under optimal spiking conditions [5] and to arrive at a large enough amount of boron on the filament in order to avoid the influence of boron contamination [6], about 30 μg of boron spike (about 0.1 g of a 0.3 mg g^{-1} boron NBS-SRM 952 solution) were added.

Water samples were homogenized by shaking and were not further treated before separation. Fertilizers were dissolved in hydrochloric acid (if necessary,

TABLE 2

Moisture content in fertilizers, biological and geological materials (2*s* uncertainties)

Sample[a]	% Dry mass	Sample[a]	% Dry mass
BCR 33 Superphosphate (lot 0041)[b]	95.2 ± 0.1	NBS SRM 1571 Orchard Leaves	94.6 ± 0.1
BCR 113 KCl (lot 0054)[b]	99.5 ± 0.1	USGS-AGV 1 (split 60 pos. 24)	98.9 ± 1.9
BCR 114 K_2SO_4 (lot 0059)[b]	99.9 ± 0.1	USGS-G2 (split 41 pos. 2)	99.9 ± 0.1
BCR 62 Olive Leaves (lot 0324)	94.5 ± 0.1	GSJ-JG 1 (split 7)	99.9 ± 0.1
BCR 63 Skimmed Milk Powder (lot 0560)	92.5 ± 0.1	BCR 32 Phosphate Rock (2499)	98.5 ± 0.2

[a]BCR, Community Bureau of Reference, Brussels. USGS, United States Geological Survey, Denver. GSJ, Geological Survey of Japan. NBS, National Bureau of Standards, Washington, D.C. [b]Fertilizer.

small amounts of hydrofluoric or sulphuric acid were added) [7]. Geological materials were mixed with an excess of 40/1 sodium carbonate/potassium nitrate, dried at 100°C, fused in a platinum crucible for 4 h at 1000°C and redissolved in concentrated hydrochloric acid [8]. Biological materials were mixed with an excess of barium hydroxide, dried for 4 h at 60°C and ashed for 10 h at 600°C; the ash was dissolved in a 1/3/15 concentrated hydrochloric/concentrated nitric acid/water mixture [9]. All sample solutions were adjusted to a pH $\geqslant$ 7 with concentrated ammonia. If small amounts of precipitate were formed, the solutions were decanted. Only the clear solutions were used for separation on the ion-exchange column.

For the separation, 4 ml of Amberlite IRA-743 ion-exchanger (20—50 mesh) in suspension was placed in an 11-ml polypropylene column. Before use, the loaded ion-exchange column was washed successively with 50 ml of 2 M HCl, 20 ml of 3 M ammonia, 50 ml of water, 30 ml of 2 M HCl, 10 ml of 3 M ammonia (until neutral) and 20 ml of water. Then the sample solution was placed on the column. Boron is adsorbed on the ion exchanger. The column was washed with 30 ml of water and the boron was eluted by means of 35 ml of 2 M HCl. More than 95% of the boron was recovered. Although IDMS itself does not require quantitative separation, high yields overcome the possible suspicion of isotope fractionation on an ion-exchange column when yields are <40% [10]. To the solution collected, about 0.3 mg of calcium carbonate was added. The solution was then lyophilized, and the residue was dissolved in 60 μl of water and used for mass spectrometric measurements.

Thermal ionization mass spectrometry

A mass spectrometer with a 68° magnetic-field sector and 30.5-cm radius of curvature was used for this work. The sample was thermally ionized from a single filament. Ion currents, typically 10^{-11}—10^{-9} A, were collected in a deep Faraday bucket connected to a 10^9—10^{11} ohm input resistor and measured by a vibrating reed electrometer (Cary 401). After analog/digital conversion, the ion-current intensities were read on a digital voltmeter.

Rhenium filaments (0.7 mm wide, 0.025 mm thick) were outgassed under vacuum by passing a current of 3.5 A through them for 100 min. A portion

(2 μl) of the sample solution was deposited on the filament and dried by means of a filament current of 0.7—1.0 A. The filament current was then increased until incipient red heat was observed (1.7—1.9 A).

The sample was mounted in the ion source and heated to 800°C until the pressure reached 1×10^{-4} Pa. This temperature is just below the 850°C required for BO_2^- ion emission [11]. With an accelerating potential of —3833 V, the sample was heated to 1000°C, and after an ion-beam focusing period of 30 min, four runs, each consisting of ten isotope-ratio measurements, were recorded. Peak-height measurements were made at masses 42 ($^{10}B^{16}O^{16}O^-$) and 43 ($^{11}B^{16}O^{16}O^-$). The baseline was monitored at masses 41.75, 42.5, 43.25 and measured before and after the peak-height determinations. A correction was made for $^{10}B^{16}O^{17}O^-$ interference at mass 43 [12]. No other (isobaric) interferences were observed.

Correction for blank. To avoid the influence of boron contamination from the filament during the mass spectrometric measurements [6], all samples were spiked with about 30 μg of boron. To determine the boron blank of the method, a "sample addition" method was used (see Fig. 2). For different masses of sample $x_n \pm \Delta x_n$, the boron mass $y_n \pm \Delta y_n$ was determined. After a first-order least-squares fitting, the boron concentration in the sample is given by the slope of the line (tan α), while the boron blank value $y \pm \Delta y$ is fixed by the intersection point with the ordinate.

Compared to the usual way of blank determination where the sample matrix element(s) are not present in the blank solutions, this method compensates for possible effects of separation techniques (e.g., yields) caused by the presence or absence of a matrix element.

Measured boron blanks varied from 0.3 to 3.0 μg and became relatively

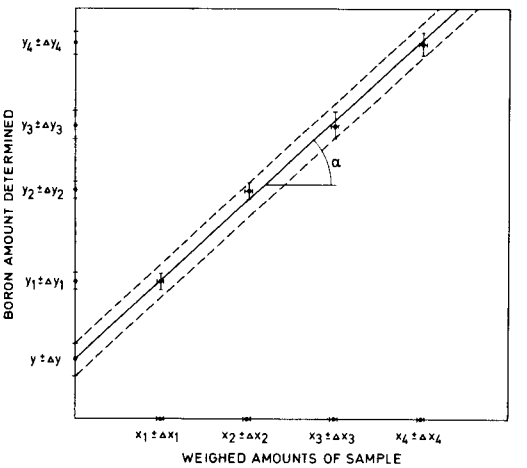

Fig. 2. Evaluation of the boron blank by the "sample addition" method: $y = \alpha x + b$ with blank $b = y \pm \Delta y$ and concentration α (tan α).

more important with increasing number of treatment steps in the total procedure and with decreasing boron concentrations in the samples or with decreasing sample weights. Only the use of ultra-purified reagents (acids, salts, ion-exchange material) and clean-air facilities might further reduce the blank level.

RESULTS AND DISCUSSION

In the interpretation of results from water analysis and their comparison with literature information, two features must be kept in mind: no pretreatment of water samples with acid and no prefiltration were done in the present assay. The method developed is very sensitive for boron in water with a limit of detection of 0.001 $\mu g\ g^{-1}$ and from recent literature information [13], only inductively-coupled plasma/atomic emission spectrometry achieves the same sensitivity. As Geel tapwater was used as the supply for the Milli-RO4/Milli-Q water purification system, it was confirmed that this installation also removed boron from water very effectively (Table 3). It must be mentioned that water from this system was used throughout the entire experimental work.

In fertilizers, the water-acid-soluble boron was determined, because agriculturalists are interested in this [7]. However, it is also possible to determine the total boron content by using the dissolution procedure developed for geological materials. All boron content for fertilizers, geological and biological materials are expressed as μg of boron per g of "dry mass" sample (see Table 2).

The accuracy of the method developed may be illustrated by an interlaboratory comparison organised by the International Atomic Energy Agency (IAEA) [13]. The boron content of 24.3 ± 2.0 $\mu g\ l^{-1}$ found in the Simulated

TABLE 3

Boron content in different samples (2*s* uncertainties)

Sample	Boron content ($\mu g\ g^{-1}$)	Sample	Boron cont ($\mu g\ g^{-1}$)
Water from Milli-RO4/Milli-Q system	0.0002 ± 0.0010	BCR 33 Superphosphate	18.2 ± 0.5
Commercial water (Spa; low sodium content)	0.0048 ± 0.0011	BCR 113 KCl	5.9 ± 0.2
		BCR 114 K_2SO_4	0.77 ± 0.2
Commercial water (Chevron)	0.0237 ± 0.0015	GSJ-JG1	5.9 ± 1.2
Tapwater[b] (CBNM, Geel)	0.0602 ± 0.0020	USGS-AGV 1	8.0 ± 1.3
Tapwater[b] (University of Antwerp, Wilrijk)	0.0799 ± 0.0035	USGS-G 2	2.7 ± 1.0
		BCR 32 Phosphate Rock	22.5 ± 0.5
River-water[b] (Schelde, Steen Antwerp)	0.2445 ± 0.0069	BCR 62 Olive Leaves	13.1 ± 0.2
		BCR 63 Skimmed Milk Powder	2.1 ± 0.2
River-water[b] (Jeker, Sluizen)	0.1465 ± 0.0070	NBS SRM 1571 Orchard Leaves	33.8 ± 2.3
IAEA Interlaboratory Comparison: Simulated Freshwater W4 solution	0.0243 ± 0.0020		

[a] Designations and lot or split data as in Table 2. [b] All samples were taken in mid-June 1984.

Freshwater W4 sample, differs by only 2.9% from the 25.0 $\mu g\ l^{-1}$ make-up value.

N. Duchateau acknowledges a European Community fellowship during part of his stay at the Central Bureau for Nuclear Measurements. Thanks also go to Mrs. H. Nagel-Kerslake for editing and typing assistance.

REFERENCES

1 E. S. Gladney, C. E. Burns, D. R. Perrin, I. Roelandts and T. E. Gills, 1982 Compilation of Elemental Concentration Data for NBS Biological, Geological and Environmental Standard Reference Materials, National Bureau of Standards, March 1984.
2 P. De Bièvre, Nukleare Analysenenverfahren bei der Erzeugung und Industriellen Nutzung von Edelmetallen, Symposium, Brussels, Nov. 1971, Report No. 71, Commission of the European Communities, Brussels, Euristop (1973) 519.
3 P. De Bièvre, Adv. Mass Spectrom., Part A, 8 (1976) 395.
4 J. P. Cali and W. P. Reed, National Bureau of Standards, Special Publication, 422 (1976) 41.
5 P. De Bièvre and G. Debus, Nucl. Instrum. Methods, 32 (1965) 224.
6 N. L. Duchateau, Ph.D. Thesis, UIA, Antwerpen, 1985.
7 J. R. Melton, W. L. Hoover and P. A. Howard, J. Ass. Offic. Anal. Chem., 52 (1969) 950.
8 P. G. Jeffrey, Chemical Methods of Rock Analysis, Pergamon, Oxford, 1975.
9 F. J. Szydlowski, Anal. Chim. Acta, 106 (1979) 121.
10 H. Kakihana, M. Kotaka, S. Satoh, M. Nomura and M. Okamoto, Bull. Chem. Soc. Jpn., 50 (1977) 158.
11 N. L. Duchateau and P. De Bièvre, Int. J. Mass Spectrom. Ion Phys., 54 (1983) 289.
12 P. De Bièvre and G. Debus, Int. J. Mass Spectrom. Ion Phys., 2 (1969) 15.
13 L. Pszonicki, A. Hanna and O. Suschny, Report on Intercomparison IAEA/W4 of the Determination of Trace Elements in Simulated Freshwater, International Atomic Energy Agency, Wien, IAEA/RL/118, May 1985.

Analytica Chimica Acta, 196 (1987) 49—58
Elsevier Science Publishers B.V., Amsterdam — Printed in The Netherlands

DETERMINATION OF PRECIOUS METALS IN ORES AND ROCKS BY THERMAL NEUTRON ACTIVATION/γ-SPECTROMETRY AFTER PRECONCENTRATION BY NICKEL SULPHIDE FIRE ASSAY AND COPRECIPITATION WITH TELLURIUM

I. SHAZALI, L. VAN'T DACK and R. GIJBELS*

Department of Chemistry, University of Antwerp (U.I.A.), B-2610 Wilrijk (Belgium)

(Received 4th August 1986)

SUMMARY

The six platinum group elements (Ru, Rh, Pd, Os, Ir and Pt) can be determined in geological samples down to the $\mu g\ kg^{-1}$ level, by using nickel sulphide fire assay and neutron activation of the residue remaining after dissolution of the nickel sulphide button in concentrated hydrochloric acid. Losses for the platinum group elements during this dissolution step are usually insignificant, except when the elements are present at ultra-trace levels. They can be recovered from the filtrate by coprecipitation with tellurium. The latter approach also permits determination of silver, which is significantly lost in the hydrochloric acid treatment (recovery >98% instead of typically ≈10%). The coprecipitation with tellurium considerably improves the results for gold (recovery ≈95% instead of typically 75%).

The precious metals include gold, silver, and the platinum group elements palladium, platinum, iridium, ruthenium, rhodium and osmium. The precious metals in geological materials are known [1, 2] to behave differently from the purified metals in their reaction with acids and other reagents. These reactions are not quantitatively predictable as they depend on the composition of the alloy or compound in which the elements occur. There is little information about the mode of occurrence of precious metals in natural materials [3]. As the species are unknown, acid attack and chlorination are not reliable in analytical work.

The precious metals are often present in rocks and ores at very low levels and their distribution can be very inhomogeneous. These two factors favour the fire-assay approach where a large sample can be used and where the precious metals are concentrated into small buttons or beads. Many fire-assay procedures have been proposed for the collection of precious metals, the most common using lead, tin, copper/nickel/iron, or nickel sulphide as the collector. Detailed accounts of practical procedures and the advantages and disadvantages of the various collectors are readily available [1, 3—7]. Quite often, the resulting buttons are parted with acid(s); hydrochloric acid is

0003-2670/87/$03.50

commonly used. Some investigators [1, 6—10] have studied the effect of single acids on the corrosion of precious metals after dissolution of samples or buttons from fire assays. Yet few attempts have been made to assess the errors in the analytical results caused by losses that may occur during the dissolution process. The economic importance of precious metals makes it essential that the results be as accurate as possible. Therefore, it was decided to study the recovery, by coprecipitation with tellurium, of precious metals which might have passed into the filtrate after attack of the nickel sulphide button in the fire-assay technique described by Robért et al. [3]. The separation of precious metals from complex matrices and solutions by coprecipitation with tellurium has been described [1, 6, 11—13]. The effectiveness of this method has been assessed by using radiotracers in rock digestion solution [12].

The present work describes a combination of coprecipitation with tellurium and thermal neutron activation to detect precious metals that have passed into solution during dissolution of the nickel sulphide button by hydrochloric acid. Both precipitates (i.e., tellurium and the precious metal sulphide originally contained in the nickel sulphide button) are examined by using thermal neutron activation.

EXPERIMENTAL

Materials and standards

Fire assay crucibles (No. 4) were cut to a height of 9 cm (yielding a capacity of 230 cm^3). An electric furnace capable of holding three crucibles was used at 1000°C. Whatman No. 542 (5.5 cm) filter paper in Gelman funnels was used to filter the solution obtained after dissolution of the nickel sulphide button (see below). Several blank fire charges were analysed to make sure that all chemicals were free of precious metals. All reagents were crushed and sieved (400 mesh). The following analytical-grade reagents were used: sodium borate, sodium carbonate, sulphur powder, carbonyl nickel powder and silica. Solutions containing 1 mg ml^{-1} tellurium and tin(II) chloride solutions were prepared as described by Sandell and Neumayer [13].

Standards were prepared by pipetting 100—250 μl of a standard solution of each precious metal onto filter papers, onto 0.1—0.2 g of black nickel sulphide residue prepared from a blank fire assay, and onto 0.1—0.2 g of the residue from a granite powder fire assay, to ensure that the effect of neutron and gamma self-absorption in the standard was similar to that of the samples.

Irradiation

All the neutron irradiations were done in the Thetis research reactor of the State University at Ghent. The pneumatic system of channel 9 allowed for quick transfer of samples into the reactor and back within 2.4 s. This channel, with a thermal neutron flux of 2.56×10^{12} cm^{-2} s^{-1} was chosen for determining rhodium in the samples and standards; a nickel flux monitor was used to correct for differences in neutron dose from one irradiation to

the next. The remaining elements were measured after a 7-h irradiation in channels 5 or 14 at a neutron flux of 1.0×10^{12} cm^{-2} s^{-1}. To correct for vertical flux gradients within the rabbit, a copper flux monitor was co-irradiated. The countings for rhodium and palladium were done at Ghent, and those for the other elements at Antwerp. The counts were based on γ-ray spectrometry using a low-energy photon detector (Ge; LEPD) and a conventional Ge(Li) detector similar to those described earlier [14]. To obtain the same geometrical shape and same density, the precipitates on the filters of the samples and standards were pressed into pellets of identical dimensions (diameter 12.7 mm) using a hydraulic press.

Procedures

Fire assay. Nickel sulphide fire assay buttons were prepared from 20—50 g samples following the fusion procedure of Robért et al. [3] with some modifications. The crucible contents were allowed to solidify in situ and the resulting buttons were dissolved in 12 M hydrochloric acid without crushing. No hydrogen sulphide was bubbled through the solution as recommended by Robért et al. [3]. For chromite samples or rocks rich in chromium, lithium tetraborate was used instead of sodium tetraborate. The most important modification was that the filtrate was not discarded. The precious metal residue retained on the filter paper was folded and pressed into pellets prior to irradiation.

Coprecipitation with tellurium. The filtrate was collected in a 600-ml beaker and the solution in the covered beaker was evaporated slowly to dryness overnight. The residue was dissolved in 100 ml of 1 M HCl by heating to boiling. Then 1 ml of the tellurium solution (1 mg Te) and, with stirring, 10—12 ml of freshly prepared tin(II) chloride solution were added. The mixture was kept near boiling for 30 min or until the precipitate was well coagulated. Sometimes a second portion of reducing agent was added to ensure complete reduction. The precipitate was filtered and washed with hot water. The filter paper was folded and pressed to a pellet.

Instrumental neutron activation. Nuclear data for the radioisotopes used are listed in Table 1. The procedure was similar to that of Hoffman et al. [15]. The procedure involved two irradiations. To determine rhodium in the samples, the pellets were irradiated for 5 min; after transfer to the detector (about 40 s), counts were collected for 1200 s at 10 cm from the top of the LEPD. For the determination of Pd, Os, Ir, Au, Ru, Pt and Ag, seven samples in one rabbit were irradiated for 7 h. Samples were allowed to decay for 16 h and the palladium content was measured for 3000-s counting intervals. Figure 1 shows a γ-ray spectrum of the precious metal sulphide from SARM-7 after 16-h decay, obtained with the LEPD; SARM-7 is a South African platinum ore standard [16]. The Os, Pt, Ir and Au were also measured for 3000 s after a 7-day cooling time. Figure 2 shows the γ-ray (LEPD) spectrum of the irradiated sulphide residue of the same sample recorded after 7 days. The ruthenium and silver were measured by counting for 10 000 s after 4—5 weeks. A typical

TABLE 1

Nuclear data for the radioisotopes used

Element	Reaction	Half-life of nuclide produced	γ-ray energy (keV)	Detector used	Decay time
Rhodium	^{103}Rh (n, γ) ^{104m}Rh	4.35 min	51	LEPD	40—5
Platinum	^{198}Pt (n, γ) ^{199}Pt (β^-) ^{199}Au	3.15 d	158; 208	LEPD	7 d
Palladium	^{108}Pd (n, γ) ^{109}Pd	13.47 h	88	LEPD	16 h
Iridium	^{191}Ir (n, γ) ^{192}Ir	74.02 d	316	LEPD	7 d
Osmium	^{190}Os (n, γ) ^{191}Os	14.6 d	129	LEPD	7 d
Ruthenium	^{102}Ru (n, γ) ^{103}Ru	38.9 d	497	Ge(Li)	4—5
Gold	^{197}Au (n, γ) ^{198}Au	2.69 d	412	LEPD	7 d
Silver	^{109}Ag (n, γ) ^{110m}Ag	249.9 d	658	Ge(Li)	4—5

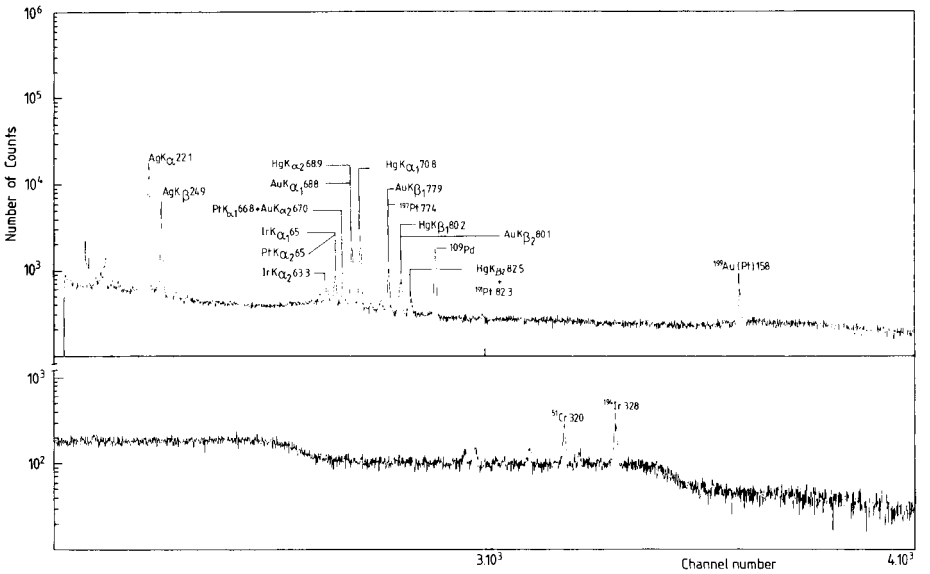

Fig. 1. LEPD γ-ray spectrum of neutron-irradiated precious metal sulphide residue from SARM-7, obtained after nickel sulphide dissolution, recorded after 16-h decay.

γ-ray spectrum, with a Ge(Li) detector, is shown in Fig. 3. By means of suitable computer programs [17, 18], the concentrations of the element(s) of interest can be calculated from the γ-ray spectra of the irradiated samples. Corrections for flux, irradiation, decay and counting times were made manually.

RESULTS AND DISCUSSION

A detailed discussion of nuclear considerations and interfering reactions has been given by Gijbels [19]. Gold-199 has been used to determine platinum

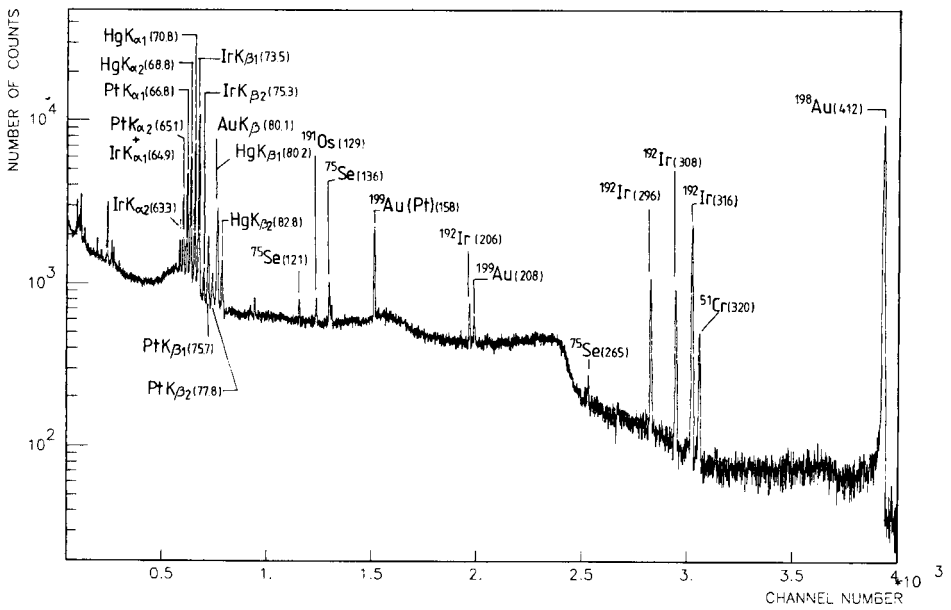

Fig. 2. LEPD γ-ray spectrum of neutron-irradiated precious metal sulphide residue from SARM-7, obtained after nickel sulphide dissolution, recorded after 7-d decay.

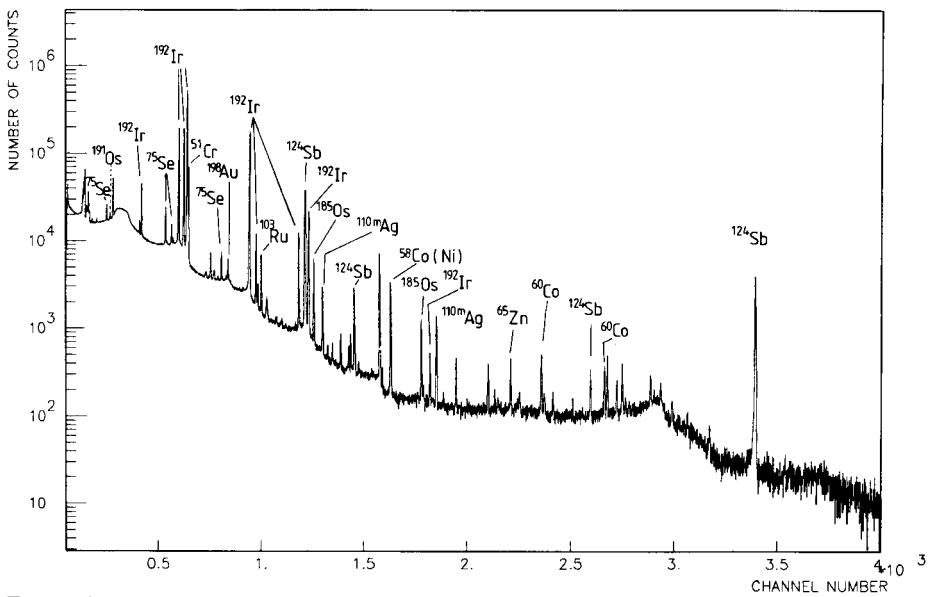

Fig. 3. Conventional Ge(Li) γ-ray spectrum of neutron-irradiated precious metal sulphide residue from SARM-7, obtained after nickel sulphide dissolution, recorded after several weeks decay.

via its 158-keV peak; in the tellurium precipitate, however, this peak suffers from strong interference from a ^{123m}Te peak. The ^{199}Au 208-keV peak, although less sensitive, was therefore used. In principle, a correction for the tellurium interference at 158 keV can also be made by recounting the samples after ^{199}Au (half-life 3.15 d) has decayed, because the half-life of ^{123m}Te is 117 days. Heating the samples at 525°C for 0.5 h to reduce tellurium [12] by evaporation is not recommended here even after measurement of osmium, because ruthenium can be lost as its tetroxide and has to be measured later. Generally speaking, the gross activity induced in 1 mg of tellurium poses no problem for γ-ray spectrometry.

The black residue of the dissolved button consists only of nickel sulphide with small amounts of chromium, bromine, cobalt and antimony and arsenic sulphides as well as (sub)microgram amounts of precious metal sulphides. Some of these elements come from the reagents used (e.g. bromide from hydrochloric acid). Chromium, arsenic, antimony and cobalt may also come from the sample. The presence of chromium could indicate that chromite in the samples has not been completely dissolved. Thermal neutron activation combined with nickel sulphide fire assay proved to be a very sensitive and accurate technique for precious metal determinations. The data in Table 2 show the precious metal content found for SARM-7 (PTO-I) based on the residue of the dissolved button. The results are in good agreement with the overall data obtained from 36 laboratories [16] which analysed this material in a round-robin study, except for silver and gold. Although silver is almost completely collected by nickel sulphide, some of it can pass into solution as dichloroargentate becasue of the solubility of silver chloride in a concentrated nickel chloride solution. Kallmann and Maul [7] stated that the conversion of silver chloride to a soluble complex depends to a large extent on the amount of other precious metal sulphides. This may partly explain the lesser extent of silver dissolution in chromite from the Sudan compared to that of SARM-7 (Table 3), 36—40% versus >90%. The dissolved silver is recovered by coprecipitation with tellurium. The total amount of silver then matches the recommended value for SARM-7. This treatment also improves the results for chromites from the Sudan. However, no data are available about the silver content of these samples by other techniques, thus it is difficult to prove that tellurium completely recovered the dissolved silver. The incomplete recovery of silver from acid-digested samples of SARM-7 (no fire assay) by tellurium reported by Elson and Chatt [12] may be due to the sample size which was not sufficiently representative (0.3—1.3 g) or to errors arising from incomplete dissolution of the sample: a residue often remained, indeed, after simple acid treatment of ore samples, which is definitely a disadvantage as compared to fire assay.

The losses of other precious metals during the nickel sulphide parting were found to be insignificant for all these metals except gold. Nickel sulphide is not a very suitable collector for gold, but the results are still semiquantitative. Gold is largely reduced by sulphur to the free metal during the fusion process,

TABLE 2

Average concentrations of precious metals found in the standard platinum ore SARM-7[a]

	Element							
	Rh	Pd	Os	Pt	Ir	Au	Ru	Ag
NiS residue	0.234	1.495	0.071	3.702	0.075	0.232	0.415	0.028
Tellurium precipitation	0.008	0.042	0.0002	0.026	0.002	0.051	0.003	0.386
Total	0.242	1.537	0.0712	3.728	0.077	0.283	0.418	0.414
Recommended values	0.24	1.53	0.063	3.74	0.074	0.31	0.43	0.42
Recovery by Te (%)	3.3	2.7	0.3	0.7	2.7	18	0.7	93

[a]The data (mg kg^{-1}) are the averages of five separate determinations.

TABLE 3

Average concentrations (mg kg^{-1}) of precious metals in two samples of chromite from the Sudan[a]

	Element							
	Rh	Pd	Os	Pt	Ir	Au	Ru	Ag
Sample A								
NiS residue	0.004	0.0	0.006	0.003	0.012	0.003	0.021	0.209
Tellurium precipitation	0.002	0.0	0.0	0.0	0.003	0.002	0.003	0.120
Total	0.006	0.0	0.006	0.003	0.015	0.005	0.024	0.329
Recovery by Te (%)	33	—	—	—	20	40	12.5	36
Sample B								
NiS residue	0.008	0.0	0.043	0.002	0.074	0.003	0.0462	0.323
Tellurium precipitation	0.002	0.0	0.0	0.0	0.003	0.0007	0.0	0.214
Total	0.010	0.0	0.043	0.002	0.077	0.0037	0.0462	0.537
Recovery by Te (%)	20	—	—	—	4	18.9	—	39.9

[a]The data are the averages of three separate determinations.

passing into the slag and partially being retained by the wall of the assay crucible. Hoffman and Ernst [20] reported poor reproducibility even when 50-g samples were used; this was attributed to the heterogeneous nature of gold-containing minerals. From the present work, another source of irreproducibility was identified when the nickel sulphide fire assay was used; it was found that about 20% (in the case of SARM-7) of gold could pass into solution, and even more in the case of the chromites.

The recovery of Rh, Ir and Ru by tellurium precipitation is also high considering their low contents (Table 3). The effect of dissolution by hydrochloric acid is not constant but significant amounts of precious metals can pass unnoticed. It is difficult to predict the percentage losses relative to the levels of precious metals in the samples. Therefore it is always advantageous to include a tellurium precipitation step after the precious metal sulphide residue has been filtered.

The loss of precious metals passing into solution was also studied as follows: 250 μl of each solution of Rh (19.57 μg), Ag (76.5 μg), Au (53.6 μg), Ir (0.639 μg), Os (651 μg), Ru (9.695 μg), Pt (136.14 μg) and Pd (45.3 μg) was pipetted into a fire-assay crucible containing 25 g of acidic rock powder (granite). The crucibles were left to air-dry for 3—4 weeks and then treated with nickel sulphide, etc., in the same way as before. The amount of precious metals which passed into the filtrate was less than 1.5% (relative) for all metals concerned except for silver and gold. For silver, 90—96% passed into solution; for gold 5—15% passed the filter. These results are in agreement with the data of Kuznetsov et al. [9] and Dixon et al. [10] except for gold; 98—101% of the dissolved precious metals were recovered by tellurium.

Several investigators have tried to explain the losses of precious metals during the parting of the nickel sulphide buttons in hydrochloric acid. Robért and Van Wyk [21] reported that tin causes losses of precious metals. They conjectured that the small amount of tin sulphide that enters the button promotes dissolution of precious metals by the concentrated hydrochloric acid used for dissolving the button. The effect of base metals in increasing the solubility of precious metals was investigated by Agrawal and Beamish [22]. They found that the solubility of platinum and especially iridium in an acid increased with increasing copper content in a lead button.

Palmer and Watterson [8], using radiotracer techniques, found that the losses of Au, Ir, Ru and Os were 1.4, 1.2, 2.3, 4.5%, respectively, in dissolving the nickel sulphide button by hydrochloric acid. In the same study, they found that the losses of these metals during the parting of a tin button were much greater than during the parting of the nickel sulphide button. It was considered that this could be due to the formation of alloys of tin and the noble metals, which are much more soluble in hydrochloric acid than the noble metals alone. The noble metals present as sulphide are more insoluble in hydrochloric acid.

There is some controversy about the loss of precious metals during prolonged heating in the dissolution process. Kallmann and Maul [7] reported no precious metal losses except for silver, even when the solution was evaporated to incipient crystallization of nickel chloride. Kuznetsov et al. [9] pointed out that losses of Pt and Pd could reach 5—15% when the insoluble residue was allowed to remain for a long time in contact with the hydrochloric acid solution after all the hydrogen sulphide had ceased to come off. Beamish and Van Loon [23] pointed out that precious metals react with silica to form corrosion-resisting compounds and/or solid solutions when the

TABLE 4

Detection limits (in $\mu g\ kg^{-1}$) for precious metals in SARM-7 with nickel sulphide fire assay and thermal neutron activation

Pt	Pd	Rh	Au	Os	Ir	Ru	Ag
15	7	2	0.2	5	0.5	3	2.5

sample is subjected to high temperature. No data were given. Fritz et al. [24] stated that some oxidation may occur, resulting in loss of precious metals as soluble sulphites or sulphates left on the filter without removal of all the acid, which is not the case in this study.

CONCLUSION

From this study, it is clear that thermal neutron activation after nickel sulphide fire assay is a very sensitive and accurate technique for the determination of precious metals at ultra-trace level in geological samples (Table 4). The behaviour of the precious metals during hydrochloric acid attack of the nickel sulphide is unpredictable and there is a risk of losing part of the precious metals by dissolution. The proposed method of treating the filtrate with tellurium and using tin(II) chloride as reducing agent to coprecipitate the precious metals is simple and essential to improve the results, particularly for the silver determination and to a lesser extent for the gold assay.

REFERENCES

1 F. E. Beamish, The Analytical Chemistry of the Noble Metals, Pergamon, Oxford, 1966.
2 J. B. Mertie, U.S. Geological Survey, Professional paper 630, 1969.
3 R. V. D. Robért, R. Van Wyk and R. Palmer, Nat. Institute for Metallurgy, Report 1371, 1971.
4 R. V. D. Robért, E. Van Wyk and R. Palmer, Journal of South African Chemical Institute, 25 (1972) 179.
5 S. G. Wall and A. Chow, Anal. Chim. Acta, 69 (1974) 439.
6 Z. Sulcek, P. Povondra and J. Dolezal, Crit. Rev. Anal. Chem., 6 (1976) 265 (and references therein.)
7 S. Kallmann and C. Maul, Talanta, 30 (1983) 21.
8 R. Palmer and J. I. W. Watterson, Nat. Institute for Metallurgy, Report 1185, 1971.
9 A. P. Kuznetsov, Yu N. Kukushkin and D. Makarov, Zh. Anal. Khim, 29 (1974) 2155.
10 K. Dixon, E. A. Jones, S. Rasmussen and R. V. D. Robért, Nat. Institute for Metallurgy, Report 1714, 1975.
11 H. W. Stockman, J. Radioanal. Chem., 78 (1983) 307.
12 C. Elson and A. Chatt, Anal. Chim. Acta, 155 (1983) 305.
13 E. B. Sandell and J. J. Neumayer, Anal. Chem., 23 (1951) 1863.
14 J. Hertogen and R. Gijbels, Anal. Chim. Acta., 56 (1971) 61.
15 E. L. Hoffman, A. J. Naldrett and J. C. Van Loon, Anal. Chim. Acta, 102 (1978) 157.
16 T. W. Steele, J. Levin and T. Copelowitz, Nat. Institute for Metallurgy, Report 1696, 1975.
17 J. Op de Beeck, At. Energy Rev., 113 (1975) 743.

18 J. Op de Beeck and J. De Donder, The OLIVE program package, Internal report, State University at Ghent, 1977.
19 R. Gijbels, Talanta, 18 (1971) 587.
20 E. L. Hoffman and P. C. Ernst, J. Radioanal. Chem., 71 (1982) 447.
21 R. V. D. Robért and E. Van Wyk, Nat. Institute for Metallurgy, Report 1705, 1975.
22 K. C. Agrawal and F. E. Beamish, Talanta, 11 (1964) 1449.
23 F. E. Beamish and E. Van Loon, Miner. Sci. Eng., 4 (1972) 3.
24 J. S. Fritz, S. H. R. Grady and W. H. Hartford, in I. M. Kolthoff and P. J. Elving (Eds.), Treatise on Analytical Chemistry, Part II, Vol. 8, Wiley, New York, 1963.

Analytica Chimica Acta, 196 (1987) 59—68
Elsevier Science Publishers B.V., Amsterdam — Printed in The Netherlands

RAPID, AUTOMATIC, HIGH-PRECISION METHOD FOR MICRO, ULTRAMICRO, AND TRACE DETERMINATIONS OF SULFUR

WOLFGANG J. KIRSTEN*[a] and BERNT S. NORDENMARK
Mikro Kemi AB, Prästgårdsgatan 8C, Box 19025, S-750 19 Uppsala (Sweden)
(Received 28th July 1986)

SUMMARY

Samples are burned in a Carlo Erba 1106 elemental analyzer over copper oxide with oxygen injected into the carrier gas. Combustion gases are reduced with copper. Water is absorbed, and sulfur dioxide is separated from carbon dioxide and nitrogen in a very short column of Porapak QS. Sample size is up to 0.7 mg, one determination takes 5 min, and the sampler takes up to 196 samples. It can be continuously loaded, and the instrument can be left to work automatically overnight. For the micro determination, helium is the carrier gas, and sulfur dioxide is measured with a thermal conductivity detector. The standard deviation of 18 analyses of pure organic compounds was 0.046% S. The detection limit is 0.5 μg S, or about 0.1% S in a normal 0.5-mg sample. For ultramicro and trace determinations, nitrogen is the carrier gas, and the measurement is made with an electron capture detector. The detection limit is 0.002 μg S, or about 0.0004% (4 mg kg^{-1} S) in a normal 0.5-mg sample.

A flash combustion/gas chromatographic separation method [1] for the automatic simultaneous determination of carbon, hydrogen, nitrogen, and sulfur, which was based upon a work of Pella and Colombo [2], has been used in this laboratory for the elemental analysis of all sulfur-containing materials for several years. In general, however, the demand for CHNS results was found to be rather small compared with the demand for CHN results without sulfur and for sulfur results without CHN. This meant that many unnecessary determinations were being conducted. It appeared, therefore, more economic to produce the CHN results by a separate method [3], which is simpler and faster than the CHNS method, and to develop a simple and rapid method for the micro, ultramicro, and trace determination of sulfur alone.

EXPERIMENTAL

Apparatus

An automatic elemental analyzer (model 1106; Carlo Erba, Milan, Italy) was arranged as shown in Fig. 1. The electron capture detector was from

[a]Present address: Department of Chemistry and Molecular Biology, Swedish University of Agricultural Sciences, S-750 07 Uppsala, Sweden.

0003-2670/87/$03.50

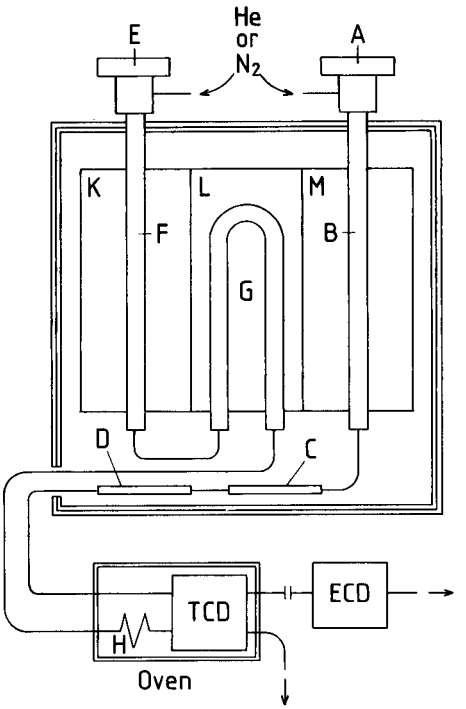

Fig. 1. Automatic elemental analyzer. A-B-C-D-TCD-ECD is the train for sulfur determination; E-F-G-H-TCD is the train for carbon, hydrogen and nitrogen determinations. (A, E) Samplers; (B) reactor tube for S; (C) water absorption tube, glass, 130 mm long, 8 mm i.d., filled with magnesium perchlorate; (D) separation column, teflon, 200 mm long, 3 mm i.d., filled with acetone-washed Porapak QS; (C) and (D) are mounted vertically between the furnace housing and the front plate of the instrument, so that the gas flow passes downward through (D). (F) Combustion tube for CHN; (G) reduction tube for CHN; (H) separation column for CHN; (TCD) thermal conductivity detector; (ECD) electron capture detector; (K) combustion furnace for CHN, 1020°C; (L) reduction furnace for CHN, 600°C; (M) reactor furnace for S, 1000°C. The bottom hole of the reactor furnace housing with the protruding beak of the reactor tube is tightened well with an insulating fiber material in order to keep the whole copper filling hot.

Brechbühler (Steinwiesenstr. 3, Schlieren, Switzerland) controlled with the ECD-control model 180 (Carlo Erba).

Materials and reagents

Tungsten(VI) oxide (Merck, No. 829) was purified by boiling with 2% (v/v) acetic acid solution for 1 h, filtering and washing several times with hot redistilled water; the material was then dried and heated at 1000°C in a flow of oxygen for 3 h [1]. Vanadium(V) oxide (Merck, No. 824) was used as received, as was copper oxide from wire (Merck). Copper was prepared by reduction of the copper oxide with a slow flow of pure, sulfur-free hydrogen at 300°C. Tin capsules (No. 76 1308 83 from Lüdi Metallwarenfabriken,

Flawil, Switzerland, or No. 240 053 00 from Carlo Erba), teflon tubing (3 mm i.d.), and Porapak QS (50—80 mesh, acetone-washed, from Carlo Erba, or prepared as described by De Souza and Bhatia [4]) were also required.

Carbonized sucrose was prepared by heating reagent-grade sucrose to 1100°C under nitrogen, cooling and grinding to a fine powder.

Modification of apparatus

The holes in the end plates of the furnace are too small to accept the reactor tube shown in Fig. 2. Thus the furnace must be taken out and the ceramic end plates removed. During handling of the furnace, care is needed not to bend the Kanthal wire at the points where it comes out from the ceramic tube, because it is very brittle there. Alternatively, a narrower reactor tube can be used, but the number of determinations which can be done with one tube filling is then smaller.

The apparatus is assembled as shown in Fig. 1. A 10-ml loop is used for

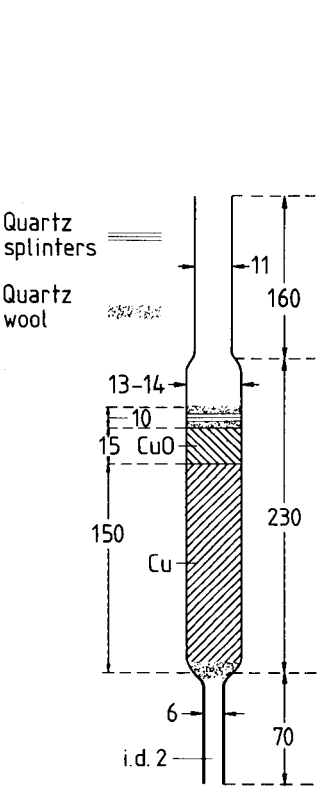

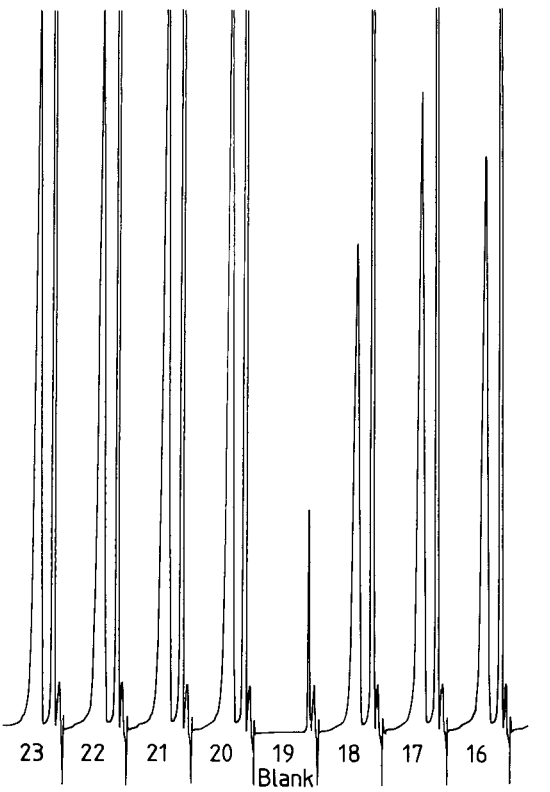

Fig. 2. Reactor tube of thick-walled opaque quartz. All dimensions in mm.

Fig. 3. Recorder traces for samples 16—23 from Table 1.

the oxygen injection and a 10-ml delay loop is introduced between the oxygen injection valve and the sampler. If the instrument is provided with gas flow regulators, these should be opened completely and left always open. The gas flow rate is adjusted with the pressure regulator to about 60 ml min^{-1} and the oxygen gauge pressure to 0.5 atm.

Accurate timing of the sample inlet is very important in this method: a 0.5 mg sample of carbonized sucrose is encapsulated and the sample inlet delay is adjusted to 10 s. The analysis is started and the time is measured from that moment to the moment when the sample begins to burn. The duration of the oxygen flow over the sample is calculated from the oxygen content of the loop and the flow rate of the carrier gas. The oxygen content, V, of the loop is V = volume of loop × (1 + atm. gauge pressure). The sample inlet delay time is then adjusted to the time measured above plus half of the calculated duration. This means that the sample falls right after the middle of the oxygen plug.

Micro method. Helium is used as the carrier gas with the thermal conductivity detector. The electron capture detector is detached from the instrument.

Ultramicro and trace method. Nitrogen from a separate tank is used as the carrier gas. The thermal conductivity detector is switched off and the electron capture detector is attached to the outlet opening of the instrument. The carrier gas pressure and the sample inlet delay time must be changed when the carrier gas is changed. Nitrogen requires a higher pressure than helium for the same outflow rate, and the linear flow in the system is lower at higher pressure. An equilibration time of about 2 h is needed after a change of carrier gas.

Procedure

Weigh out and encapsulate samples containing up to 0.7 mg of normal organic material. Larger samples of inorganic materials and other materials of low oxygen demand can be weighed out. It is possible to use up to 1 mg of coke and coal and similar materials which do not liberate large volumes of reducing gases on pyrolysis. Hydrocarbon samples should not exceed 0.5 mg. Add about 5 mg of tungsten(VI) oxide to every sample before closing the capsule. For extremely refractory inorganic materials, better results have sometimes been obtained by adding 5 mg of vanadium(V) oxide instead of the tungsten(VI) oxide. Weigh out hygroscopic, volatile, or otherwise difficult substances as described by Kirsten [5].

Conduct the determinations as described in the manual of the instrument. About 300 determinations can be done with one reactor tube filling. Generally, the quartz tube is so strongly attacked by the copper oxide and tin oxide that it must then be discarded. The upper part and the beak end can be reused to make new tubes.

The instrument does not contaminate the atmosphere and requires very little laboratory space. A single run takes 5 min. The sampler accepts up to

196 samples. It can be continuously loaded while the instrument is running, and the instrument can be left on, working automatically overnight.

RESULTS

Table 1 shows the results obtained for a series of pure organic compounds; these determinations were done with the thermal conductivity detector and with helium as the carrier gas. The standard deviation of 18 analyses of

TABLE 1

Sulfur determinations in pure organic compounds[a]

No.	Substance	Sample weight (μg)	Integr. counts	Sulfur (%)		Deviation (%)
				Calc.	Found	
1	Sulfanilic acid	525.3	42511	18.51	18.45	−0.06
2	Sulfanilic acid	538.3	43758	18.51	18.53	+0.02
3	*S*-Benzylthiuronium chloride	432.1	30153	15.82	15.91	+0.09
4	*S*-Benzylthiuronium chloride	490.2	34053	15.82	15.84	+0.02
5	3-Bromo-2-thiophenic acid	544.0	36865	15.48	15.45	−0.03
6	3-Bromo-2-thiophenic acid	446.9	30223	15.48	15.42	−0.06
7	5-Chloro-4-hydroxy-3-methoxy benzylthiuronium phosphate	521.0	21538	9.30	9.43	+0.13
8	5-Chloro-4-hydroxy-3-methoxy benzylthiuronium phosphate	406.3	16340	9.30	9.17	−0.13
9	7-Iodo-8-oxyquinoline-5-sulfonic acid	464.8	18655	9.13	9.15	+0.02
10	Sulfanilic acid	494.4	40157	18.51	18.52	+0.01
11	Sulfanilic acid	437.5	35559	18.51	18.53	+0.02
12	*S*-Benzylthiuronium chloride	530.0	36608	15.82	15.75	−0.07
13	*S*-Benzylthiuronium chloride	449.1	31271	15.82	15.88	+0.06
14	3-Bromo-2-thiophenic acid	501.1	33939	15.48	15.44	−0.04
15	3-Bromo-2-thiophenic acid	410.6	27629	15.48	15.34	−0.14
16	7-Iodo-8-oxyquinoline-5-sulfonic acid	537.8	21835	9.13	9.26	+0.13
17	5-Chloro-4-hydroxy-3-methoxy benzylthiuronium phosphate	583.2	23932	9.30	9.36	+0.06
18	5-Chloro-4-hydroxy-3-methoxy benzylthiuronium phosphate	454.1	18789	9.30	9.43	+0.13
19	Blank (Capsule + WO_3)	0.0	0	0.00	0.00	0.00
20	*S*-Benzylthiuronium chloride	432.6	30140	15.82	15.89	+0.07
21	*S*-Benzylthiuronium chloride	474.3	32894	15.82	15.81	−0.01
22	3-Bromo-2-thiophenic acid	422.1	28471	15.48	15.38	+0.10
23	3-Bromo-2-thiophenic acid	409.0	27749	15.48	15.47	−0.01

[a]The average of the sulfanilic acid results was used for the calibration. When these results and the blank are excluded from the calculation, the standard deviation for the remaining sulfur-containing compounds is 0.046%. Running conditions: He pressure 0.25 atm., oxygen pressure 1.0 atm., carrier gas flow rate 60 ml min^{-1}, furnace temperature 1005°C, length of separation column 150 mm, sample inlet 18 s after start, time per sample 5 min.

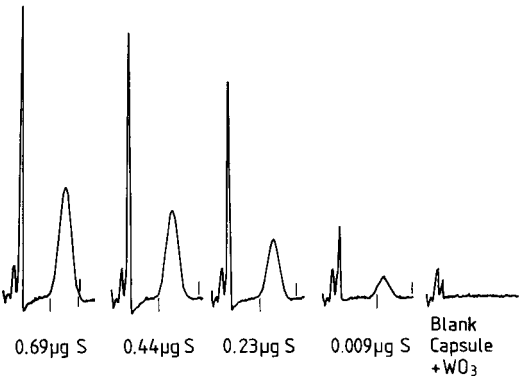

Fig. 4. Recorder traces from trace determinations. Samples were solutions of diphenyl disulfide in dinonyl phthalate; electron capture detector, Spectraphysics SP-4290 recording integrator.

sulfur-containing compounds was 0.046% S. The detection limit with this detector is 0.5 μg S or about 0.1% in a normal 0.5-mg sample. Figure 3 shows recorder traces for samples 16—23 (Table 1). The calibration curve is linear and passes through the origin.

Figure 4 shows recorder traces obtained with the electron capture detector (ECD) and with nitrogen as the carrier gas. The detection limit is 0.002 μg S or about 0.0004%, i.e., 4 μg g^{-1} in a normal 0.5-mg sample. The calibration

TABLE 2

Trace determinations of sulfur with the proposed method and with the Leco SC-32 Sulfur Analyzer
(Both instruments were calibrated with the Leco carbon standard, declared to contain 0.53 ± 0.04% sulfur. When this standard was analyzed with the 1106 instrument, with a solution of dibenzyl disulfide in dinonyl phthalate containing 0.108% sulfur as standard, the following results were obtained: 0.57%, 0.55%, 0.55%, 0.55%.)

No.	Substance	Sulfur (%) obtained with			
		Carlo Erba 1106		Leco SC-32	
1	Wheat flour	0.11	0.10	0.12	0.10
2	Cocoa	0.23	0.24	0.20	0.22
3	Maize flour	0.015	0.013	0.012	0.014
4	Glucose	0.0051	0.0053	0.0060	0.0058
5	Agarose I	0.065	0.064	0.066	0.065
6	Agarose II	0.067	0.065	0.066	0.069
7	Nitrocellulose I	0.015	0.016	0.013	0.015
8	Nitrocellulose II	0.0091	0.0093	<0.015[a]	<0.015[a]
9	Methylmethacrylate	0.0072	0.0076	—[b]	—[b]

[a]The SC-32 analyzer cannot cope with nitrocellulose samples larger than about 300 mg. The sensitivity is, therefore, too low to give more precise results. [b]The amount of this sample available was too small for analysis with the SC-32.

curve was convex, because the tritium plate of the ECD used was 12 years old. When a newer Carlo Erba ^{63}Ni detector was used, a very slightly concave calibration curve was obtained, which is what would be expected from the chemical and physical processes in the instrument.

In Table 2, the results of trace determinations of sulfur in different materials are compared with the results obtained with the Leco Sulfur Analyzer SC-32 in the same materials.

Various inorganic and metal-containing organic compounds, ordinary laboratory reagents, were also examined. The results are shown in Table 3.

DISCUSSION

Combustion and reduction

Culmo [6] used tungsten(VI) oxide as combustion catalyst and metallic copper at 820—880°C as reducing agent in his sulfur determination method. Dugan [7] used copper oxide for the combustion and investigated the reactions involved. He obtained slightly low results when copper and copper oxide were held at lower temperature than 800°C, and he ascribed this to the for-

TABLE 3

Sulfur determinations in inorganic and metal-containing organic compounds (laboratory reagents)[a]

No.	Substance	Sulfur (%)		Deviation (%)
		Found	Calc.	
1	Potassium-4-hydroxybenzene sulfonate	15.4	15.1	+0.3
2	Potassium-4-hydroxy-2-methylbenzene sulfonate	14.1	14.2	−0.1
3	Potassium-3,5-diisopropyl-2-hydroxy-benzene sulfonate	10.8	10.8	±0.0
4	Barium diphenylamine sulfonic acid	10.1	10.1	±0.0
5	Potassium sulfate	18.6	18.4	+0.2
6	Barium sulfate	13.0	13.7	−0.7
7	Cerium(IV) sulfate, 4 H_2O	15.8	15.9	−0.1
8	Bismuth sulfide	13.2	13.3	−0.1
9	Sodium lauryl sulfate	12.0	11.1	+0.8
10	Sodium lauryl sulfate[b]	11.27	11.12	+0.15
11	Sodium lauryl sulfate[b]	11.24	11.12	+0.12
12	Sodium lauryl sulfate[b]	11.22	11.12	+0.10
13	Barium sulfate[b]	13.67	13.73	−0.06
14	Barium sulfate[b]	13.79	13.73	+0.06
15	Barium sulfate[c]	13.72	13.73	−0.01
16	Barium sulfate[c]	13.83	13.73	+0.10
17	Barium sulfate[c]	13.83	13.73	+0.10

[a]For samples 10—17, barium sulfate and sodium lauryl sulfate were finely ground and barium sulfate was dried at 800°C. They were then mixed with tungsten(VI) oxide or vanadium(V) oxide. [b]Mixed with tungsten(VI) oxide. [c]Mixed with vanadium(V) oxide.

mation of copper sulfate. Kirsten [8] stated that copper sulfate is decomposed at much lower temperature, and ascribed the small losses of sulfur mainly to the formation of sulfates of other metals, which are present as impurities in the catalysts.

During this work, strong tailing was obtained at temperatures between 730 and 760°C, when very small amounts of sulfur were determined. When larger amounts were determined, the sulfur peaks became more and more symmetrical. This is the normal pattern of adsorption tailing, caused by a limited number of retaining sites. When these are occupied, the excessive sulfur dioxide passes through as a symmetrical peak. If the retention were caused by formation of copper sulfate, one would expect a different behavior, because the number of retaining sites would not be limited.

The limited number of retaining sites explains why Kirsten [8] could obtain good microanalytical results at temperatures between 730 and 760°C, when the carrier gas was doped with a small amount of sulfur dioxide, which occupied these retaining sites and allowed the sulfur dioxide from the sample to pass. Unfortunately such doping was found to be less successful in the determination of nanogram amounts of sulfur. The addition of oxygen to the carrier gas produced invariably a negative dip, caused by the formation of sulfate, followed by a tailing positive peak caused by the decomposition of the sulfate when the oxygen disappeared. When the sulfur peak from the sample was large enough to cover both dip and peak, the results were satisfactory. Smaller peaks were erroneous. Good results were obtained when ultrapure copper was used.

The use of copper at 730—760°C would be very advantageous, because copper is oxidized to CuO below 775°C, whereas at higher temperature it is oxidized to Cu_2O. The lifetime of a tube filling would, therefore, be twice that of a tube filling at higher temperature. However, ultrapure copper is not commercially available in a suitable form, its preparation is very tedious, and the raw materials are extremely expensive. It was, therefore, preferable to use ordinary copper for elemental analysis at 1000°C. This temperature is higher than the temperature (up to 900°C) recommended by earlier authors. Much better results and much less tailing were obtained at this temperature, however, and even nanogram amounts of sulfur can be determined without doping. Because the quartz tube lasts through the lifetime of the copper filling, after which it must be discarded even when it has been held only at 850°C, there seems to be no reason to use a lower temperature.

If it is assumed that the retention is caused by metallic impurities like lead, manganese, nickel, silver, the better results at 1000°C are easy to understand. In air, lead sulfate is decomposed at 1000°C, though the decomposition is not complete at this temperature. Manganese sulfate is decomposed at 850°C, nickel sulfate at 840°C and silver sulfate at 1085°C. In pure helium, the decomposition occurs probably at lower temperatures, but the helium in the combustion chamber contains oxygen for quite a while after the sample has been burned.

TABLE 4

Upper limits of metallic impurities in copper

	Riedel	Mallinckrodt
Lead	0.005%	0.005%
Manganese	0.001%	0.001%
Silver	0.001%	≈0.0005%

Merck and Fluka give no information about the content of metallic impurities in their copper and copper oxide for elemental analysis. In Table 4 the limits of metallic impurities in copper wire (31284; Riedel de Haën) and in copper grains (4649; Mallinckodt) are listed. A 5-cm layer of Mallinckrodt copper in the reactor tube weighs about 25 g. If it is assumed, probably not quite correctly, that the impurities are at the stated limits, and that they all react to form sulfate, then the oxidized 5-cm layers of either specimen would retain about 340 μg of sulfur. This is more than the total sulfur content of most of the samples examined here. Obviously, the order of magnitude of metallic impurities is such that significant errors can be caused.

When the reactor tube, filled as shown in Fig. 2, is heated to the working temperature, the copper(II) oxide is decomposed to copper(I) oxide, and a corresponding layer of copper is oxidized to copper(I) oxide. A 30-mm deep layer of copper(I) oxide is thus obtained.

When the sample falls into the combustion chamber, a reducing cloud of pyrolysis gases is immediately formed, in which sulfur is partially present as hydrogen sulfide. This cloud can reduce copper(I) oxide to metallic copper, which reacts with the hydrogen sulfide to form copper sulfide. Copper sulfide is very stable and is only partly oxidized in the short time during which oxygen is in the reactor tube. Such reactions would, therefore, cause low analytical results. When the sample is dropped into the middle of the oxygen plug, the oxygen which precedes the sample momentarily oxidizes the upper layer of the copper(I) oxide to copper(II) oxide, and the formation of copper sulfide is avoided provided that the oxygen demand of the sample is not to high.

Tungsten(VI) oxide is not used as a combustion catalyst in this laboratory, because it has been found that the oxide is slowly reduced in the course of the analyses, and that the reduced material retains sulfur. As described earlier [8], a small amount of tungsten(VI) oxide is added to the sample in order to ensure that any inorganic sulfur compounds are completely decomposed. These small amounts do not cause any noticeable errors.

Separation and measurement

The use of the very small chromatographic column was suggested by Colombo [9]. The gases which leave the reactor tube are nitrogen, carbon dioxide, water and sulfur dioxide. The column cannot separate the sulfur

dioxide from the water. The water must, therefore, be removed with magnesium perchlorate first. Also nitrogen and carbon dioxide are not separated from each other. The main advantages of the arrangement are the speed of the procedure and the higher sensitivity, which is due to the much smaller molecular diffusion in the short time available.

Because there is no water in the gases, the thermal conductivity detector can be kept at a low temperature, which enhances its sensitivity. However, because the other channel of the 1106 instrument is used for CHN determinations, the CHN temperature, 95°C, is preferred so that it is possible to change over quickly from one analytical method to the other. If the other channel is used for the determination of oxygen or of nitrogen alone, the oven can always be kept at a lower temperature, which improves the sensitivity of the detector.

The high precision and the linearity of response obtained with the thermal conductivity detector are due to the efficiency of the pressure regulators, the high temperature of the reactor tube, the accurate timing of the sample inlet, and also to the use of small samples and the low gas flow resistance of the column/detector system. A high concentration of sulfur dioxide combined with a high flow resistance would cause a decrease of the gas flow rate during the measurement, which would result in nonlinear (concave) calibration graphs.

In earlier experiments with the electron capture detector, poor stability was encountered. This was eventually traced to the fact that nitrogen from the same gas cylinder was used both as carrier gas and as the service gas for the instrument; the service gas activity caused small variations of the carrier gas pressure, which influenced the signal of the detector. Excellent stability was obtained when separate gas cylinders were used.

The Department of Chemistry and Molecular Biology of the Swedish University of Agricultural Sciences kindly placed the elemental analyzer at our disposal.

REFERENCES

1 W. J. Kirsten, Organic Elemental Analysis, Academic, New York, 1983, p. 53.
2 E. Pella and B. Colombo, Mikrochim. Acta Part I, (1978) 271.
3 W. J. Kirsten, Organic Elemental Analysis, Academic, New York, 1983, p. 43.
4 T. L. C. De Souza and S. P. Bhatia, Anal. Chem., 47 (1975) 543.
5 W. J. Kirsten, Organic Elemental Analysis, Academic, New York, 1983, pp. 21—29.
6 R. F. Culmo, Microchem. J., 17 (1972) 499.
7 G. Dugan, Anal. Lett., 10 (1977) 639.
8 W. J. Kirsten, Anal. Chem., 51 (1979) 1173.
9 B. Colombo, Carlo Erba Strumentazione, Milan, Italy, private communication, 1985.

Analytica Chimica Acta, 196 (1987) 69—74
Elsevier Science Publishers B.V., Amsterdam — Printed in The Netherlands

OUTGASSING OF POLYMERS BY THERMAL-DESORPTION GAS CHROMATOGRAPHY/FOURIER-TRANSFORM INFRARED SPECTROMETRY

J. A. J. JANSEN* and W. E. HAAS

Plastics Laboratory PMR, Nederlandse Philips Bedrijven B.V., P.O. Box 218, 5600 MD Eindhoven (The Netherlands)

(Received 18th July 1986)

SUMMARY

Applications of on-line thermal-desorption gas chromatography/Fourier-transform infrared spectroscopy are described for the evaluation of outgassing phenomena of polymers. Details of the experimental configuration and system operation are given. Examples discussed are degradation products in a dimethylsiloxane rubber, trioxane formation in polyacetal production, and monomers and additives in poly(methylmethacrylate). The detection limits are in the $\mu g\ g^{-1}$ range for 100-mg samples.

During processing and in product applications of polymeric materials, especially at elevated temperatures, evaporation of low-molecular-weight products, possibly accompanied by degradation products, may occur and cause deterioration of the properties of the material [1]. In addition, outgassing phenomena may be related to contact and environmental contamination in product applications, toxicological and aesthetic aspects [2], suitability of plastic products for finishing processes (e.g., glueing, welding, lacquering and plating), admissible temperatures for processing and use, mould contamination and reprocessability. Therefore evaluation of the type and amounts of volatile components is of considerable practical interest, and is also an analytical challenge.

To determine the contents of volatile compounds, various methods have been used such as thermogravimetry (TGA), head-space gas chromatography (GC), mass spectrometry (MS), infrared spectrometry (IR) and combinations of these methods. In TGA the weight loss is measured as a function of temperature and time, but no information is given about the nature of the evolved species [3]. In head-space GC, the sample is heated in a closed vessel so that the volatile compounds diffuse from the polymer into the gas phase. The gas phase is injected onto the chromatographic column for separation and detection. As polymeric samples contain complex mixtures of various volatile compounds, it can be difficult to identify all the peaks in the chromatogram [4]. The gas phase can also be introduced into a mass spectrometer or the gas cell of an IR spectrometer for recording a characteristic spectrum,

0003-2670/87/$03.50

but interpretation of these spectra is often very difficult for mixtures. Therefore, GC must be coupled with a technique such as mass or IR spectrometry. The application of GC/MS is well known [5]. With the introduction of Fourier-transform (FT) IR spectrometry, GC/FTIR is possible because of the high speed and sensitivity of the spectrometer [6].

Infrared spectrometry is indispensable for polymer characterization, and FTIR has brought about a revival of interest because of its increased speed, higher signal-to-noise ratio, lower detection limits, better spectral resolution and sophisticated data-processing techniques [7, 8]. In this laboratory, GC/FTIR is only one of the many daily applications of the spectrometer. The changeover from one type of operation to another should be simple and trouble-free. A combined simulation and characterization technique has been developed, capable of on-line temperature-controlled outgassing of polymeric materials, separation of the gaseous components and subsequent detection and identification. In this paper, the thermal-desorption GC/FTIR configuration is described and several examples of outgassing phenomena of polymeric materials are given.

EXPERIMENTAL

Equipment and operation

The equipment is shown schematically in Fig. 1. A thermal-desorption cold-trap injector (TCT, Chrompak) is used as an oven for temperature-controlled outgassing of polymeric materials. The finely chopped sample is transferred to the glass tube in the desorption oven and heated to a maxi-

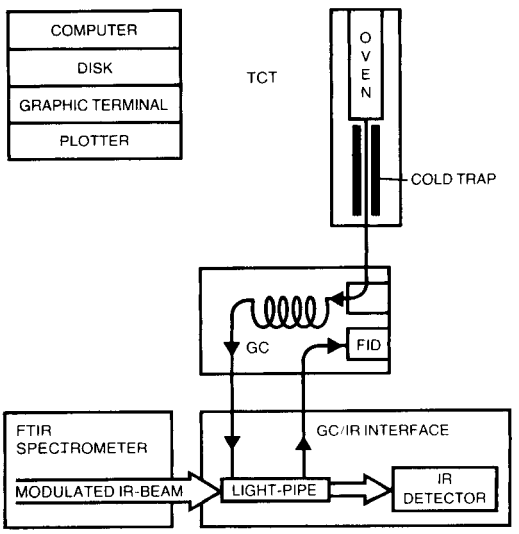

Fig. 1. Configuration for thermal-desorption gas chromatography/Fourier-transform infrared spectrometry.

mum temperature of 350°C. The volatile compounds from the sample are transferred to the cooled trap by the carrier gas stream. The components are trapped at <—100°C in a wall-coated open tubular fused-silica capillary tube (12 cm long, 0.32 mm i.d., coated with 1.2-μm Cp-Sil-5CB obtained from Chrompak). The trap is kept at a sub-ambient temperature by leading a gas flow, cooled by liquid nitrogen, through the trap compartment. After completion of the transfer of components from the sample to the cold trap, the metal capillary around the silica capillary tube is heated (direct resistance) and the cooling flow is stopped. This heating of the cold silica trap provides the injection of the trapped sample components onto the analytical capillary column, which is coupled directly with a nut of low dead volume. A narrow injection band is obtained as required for high-resolution gas chromatography. In the design, much attention was paid to avoiding cold spots, and all the flow paths are glass-lined. A control unit regulates the different temperature/time functions.
matograph (PU-4500/11, Pye Unicam) for separation. The chromatograph is equipped with a wall-coated open tubular fused-silica capillary column (25 m long, 0.32 mm i.d., coated with 1.2-μm Cp-Sil-5CB), temperature-programming control, flame ionization detector and computing integrator. The separated components are detected by means of a FTIR spectrometer (20SXB, Nicolet) with GC interface. The interface is provided with a gold-covered capillary light-pipe (15 cm long, 1.5 mm i.d.) and a liquid nitrogen-cooled mercury cadmium telluride A (MCT-A) detector. The spectrometer is software-controlled by a Nicolet 1280 minicomputer (192-K, 20 bit) with Winchester drive (36 Mbyte), color raster display and 8-pen drum plotter. GC/FTIR software is available, including library search routines and a vapor-phase spectra data base.

Procedure

Depending on the analytical problem, the amount of sample, desorption temperature program and gas flows are selected. The volatile compounds are separated on the capillary column by using a temperature gradient chosen for optimal resolution and detection. The eluting GC fractions are led through the light-pipe, and IR spectra are taken on-line. After the light-pipe, components are detected with a conventional flame ionization detector. Software is available to control the total GC/FTIR run from injection up to the identification of the peaks. During each 4-s time interval, sixteen consecutive scans with 4-cm^{-1} resolution are added together and the interferogram is stored on the Winchester drive. For real-time monitoring, high-speed, low-resolution (16 cm^{-1}) Fourier transforms are done and the resulting IR spectra are displayed on the monitor as a three-dimensional plot. Simultaneously, the integrated absorbances in five selectable wavelength windows, representing specific group frequencies, are printed on the plotter giving five spectral traces of the chromatogram. At the end of the elution, full-resolution (4 cm^{-1}) Fourier transforms and absorbance calculations are made on the

stored, added interferograms. A chromatogram is reconstructed from all the IR spectra. The locations of the peaks in this reconstructed chromatogram are calculated and qualitative analyses (i.e., library search and identification of these peaks) are conducted.

A special data base, EPA, with 3300 vapor-phase spectra, is available. The IR spectrum of the peak, a number of the best fits and the corresponding fit factors are plotted.

RESULTS AND DISCUSSION

During the year that the system has been operational, numerous polymer samples have been examined: thermoplastics such as polystyrene, polystyrene copolymer, polyacrylate, polycarbonate, polyamide and polyacetal; phenolic, polyester and epoxy thermosets; and elastomers and lacquers. Some examples are given below of product applications and problems.

Stringent demands are made on the outgassing of silicone rubber products in some applications. Outgassed products from sealing rings in light-armatures can settle on the reflector and window so that the light transmission decreases. In computer keyboards, the outgassed products of contact mats can settle on relays, forming a non-conductive layer. A dimethylsiloxane rubber mixture which is vulcanized with the aid of a peroxide has been examined. Figure 2(a) shows the reconstructed chromatogram of the volatile compounds from a 10-mg sample after 10 min at 200°C. Figure 2(b) shows the IR spectra of some of the peaks which could be characterized with the library search routine. Carbon dioxide and 2,4-dichlorobenzene are degradation products

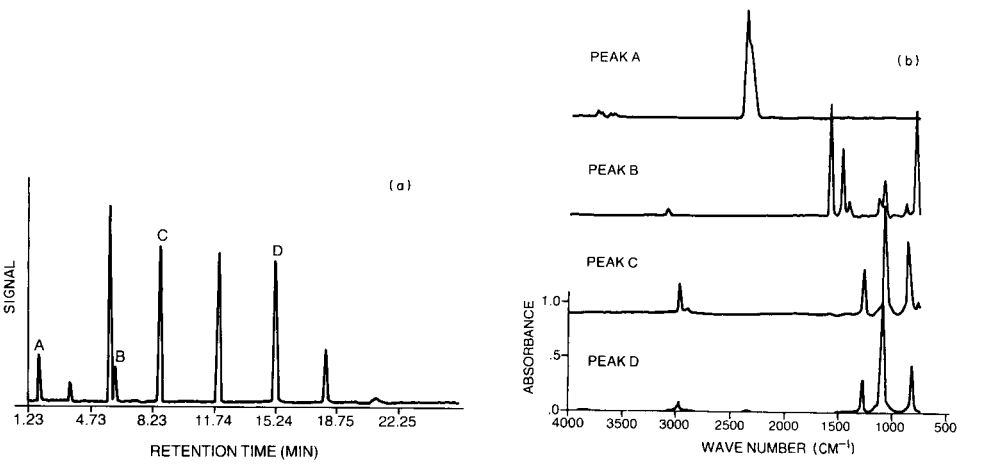

Fig. 2. (a) Reconstructed chromatogram of the volatile compounds from 10 mg of dimethylsiloxane rubber after 10 min at 200°C (signal in arbitrary units). (b) IR spectra of peaks A–D: (A) carbon dioxide; (B) 2,4-dichlorobenzene; (C, D) dimethylsiloxane oligomers.

of the peroxide used. The other peaks are low-molecular-weight dimethylsiloxanes which cause problems in the applications described above [9]. Proper post-curing of silicone rubber products can bring the outgassing down to acceptable levels.

In an assembly process a specific batch of polyacetal components caused smell and headache complaints. Therefore, 100 mg of the polyacetal sample was outgassed for 10 min at 100°C. Besides water, a peak in the chromatogram could be characterized as trioxane, the cyclic trimer of formaldehyde. Figure 3 shows the IR spectrum of the trioxane peak corresponding to ca. 1 μg of compound. At the same time another batch of polyacetal components was analysed; this batch showed a trioxane emission lower by a factor of 10. Trioxane is the starting monomer of polyacetal copolymers.

For the development of optical discs (as used in laser vision, compact discs, digital optical recording, etc.) many alternative materials have been investigated; generally these are polycarbonates and copolymers of acrylates and methacrylates. The investigation included measurement of the contents of residual monomer and additives, the monomers being determined by outgassing of poly(methylmethacrylate) at elevated temperatures at which the starting monomers are the most important degradation products [10]. Figure 4(a) shows the reconstructed chromatogram of the volatile compounds from 10 mg of sample after 10 min at 300°C. Figure 4(b) shows the IR spectra of the monomers (methylacrylate and methylmethacrylate) and the chain-length regulator and the releasing agent. The other peaks could be characterized as low-molecular-weight acrylate oligomers.

An interpretable IR spectrum is obtained from ca. 10^{-7} g of a component depending upon its IR sensitivity. This means that the detection limits of outgassing for 0.1-g samples are in the $\mu g\ g^{-1}$ range. Quantitative analyses can be made on the basis of extinction coefficients measured on standards.

Besides on-line analysis of the volatile compounds of samples at elevated temperatures, it is possible to proceed off-line by using Tenax TA adsorption cartridges, thus allowing collection for longer times, e.g., 24 hours. Off-line sampling with pre-concentration of working place atmospheres is also possible. For a 10 l gas sample the detection limit is ca. 10 $\mu g\ m^{-3}$.

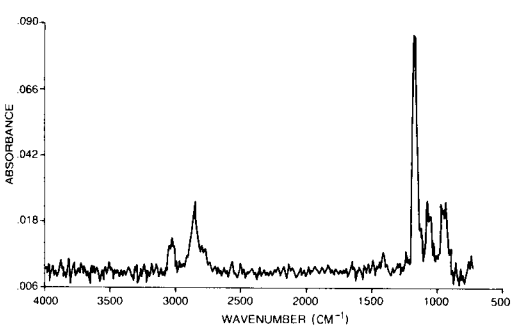

Fig. 3. IR spectrum of 1 μg of trioxane from 100 mg of polyacetal after 10 min at 100°C.

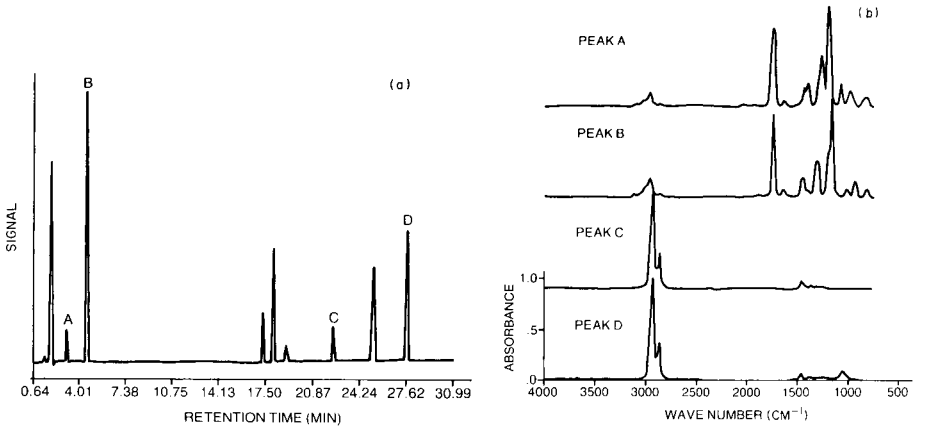

Fig. 4(a) Reconstructed chromatogram of the volatile compounds from 10 mg of poly-(methylmethacrylate) after 10 min at 300°C (signal in arbitrary units). (b) IR spectra of peaks A—D: (A) acrylic acid methyl ester; (B) methacrylic acid methyl ester; (C) n-dodecyl mercaptan; (D) 1-hexadecanol.

REFERENCES

1 S. Sharma and S. DasGupta, Proc. Electron. Components Conf., 33 (1983) 418.
2 A. Hoff, S. Jacobsson, P. Pfäffli, A. Zitting and H. Forstling, Scand. J. Work. Environ. Health, 8 (1982) suppl. 2.
3 M. Luda di Cortemiglia, G. Camio, L. Costa and M. Guaita, Thermochim. Acta, 93 (1985) 187.
4 B. Ioffe and T. Reznik, Zh. Anal. Khim., 35 (1980) 1410.
5 W. Ligon and M. George, J. Polym. Sci. Polym. Chem. Ed., 16 (1978) 2703.
6 W. Herres, in P. Schreier (Ed.), Analysis of Volatiles, Walter de Gruyter, Berlin, 1984, p. 183.
7 J. Koenig, Advances in Polymer Science, Vol. 54, Springer, Heidelberg, 1983, p. 87.
8 J. Chalmers, M. Mackenzie and H. Willis, Appl. Spectrosc., 38 (1984) 763.
9 D. Barnes, 14th North American Thermal Analysis Society Conference, Williamsburg, VA, 1983, paper 144.
10 W. Herres and U. Fölster, Farbe + Lack, 91 (1985) 6.

Analytica Chimica Acta, 196 (1987) 75—83
Elsevier Science Publishers B.V., Amsterdam — Printed in The Netherlands

SOME NEWER APPROACHES TO ANALYTE ISOLATION IN PESTICIDE RESIDUE ANALYSIS

S. FORBES

Shell Research Limited, Sittingbourne Research Centre, Sittingbourne, Kent ME9 8AG (Great Britain)

(Received 8th August 1986)

SUMMARY

Some newer approaches to analyte isolation: "digital" chromatography, semi-preparative high-performance liquid chromatography, column-switching and sweep distillation, are described and their applications in pesticide residue analysis illustrated. These techniques have enabled trace levels of a range of pesticides and their degradation products to be separated from various sample matrices. Moreover, because the newer approaches can be readily automated, there is more scope for unattended operation than with the traditional clean-up techniques, which has resulted in greater productivity.

Pesticides, by definition, are compounds with some form of high biological activity and it is important therefore to monitor the fate of these materials following their introduction into the environment. Because there is a need to determine trace levels of pesticides and their associated breakdown products in a variety of sample matrices (crops, soil, water, air, animal tissues) the analytical methods used have to be both highly sensitive and selective.

Most procedures for pesticide residue analysis involve the following major steps: sample preparation, extraction, purification of extract, determination and confirmation of identity. Although the aim of the extraction step is to isolate quantitatively the pesticide residue from the sample matrix, many co-extracted materials are usually present in the crude sample extract. These materials can interfere directly with the determination of the pesticide residue, by masking analyte peaks on a chromatogram, or indirectly, by leading to the rapid deterioration of chromatographic columns and detectors. Consequently, it is usually necessary to purify (clean-up) the crude extract before the determination step.

Traditionally, liquid/liquid partition and gravity-fed chromatographic column procedures have been most widely used for the purification of crude extracts containing pesticide residues. Such procedures can be done with basic laboratory equipment and have also been fairly well documented. McMahon and Burke [1], for example, have reported on the behaviour of over 300 pesticidal and/or industrial chemicals on chromatographic columns packed with Florisil. Automation of these techniques with custom-built

equipment is possible [2, 3]. However, as pesticides have become more chemically diverse and the residue laboratory has had to become more cost-effective, the traditional techniques have been replaced by newer approaches which can be more readily automated and/or provide a greater degree of clean-up. Some of these newer approaches, "digital" chromatography, semi-preparative high-performance liquid chromatography (HPLC), column-switching and sweep distillation, are described below.

"DIGITAL" CHROMATOGRAPHY

"Digital" chromatography involves the selective retention of analyte or co-extracted materials on a short bed of liquid chromatographic adsorbent contained in a ready-to-use disposable cartridge (e.g., Bond-Elut, Sep-Pak). The cartridges contain 40—50-μm particles of adsorbent and are available in a range of phases (Si, C18, CN, NH_2, ion-exchange). By careful selection of adsorbent and elution solvent(s) the analyte can be isolated from the bulk of co-extracted substances present in a crude extract. The operating principles of "digital" chromatography are the same as in traditional chromatographic column clean-up procedures but the speed and reproducibility of the technique have resulted in more efficient analyses.

A chromatogram obtained from an extract of wheat grain that had been cleaned-up by passage through two Sep-Pak silica cartridges is shown in Fig. 1. In the method used to determine residues of the wild oat herbicide, flamprop-isopropyl, each sample of milled wheat grain (10 g) was extracted by tumbling with acetone/hexane (1 + 4, v/v, 40 ml) for 2 h. The mixture was filtered and the residue washed with extraction solvent (3 × 10 ml). The filtrate and washings were combined and taken to dryness, and the resulting residue was redissolved in acetone/hexane (1 + 9, v/v, 5 ml). The extract was partitioned three times with water/acetonitrile (3 + 7, v/v, 3 ml) and the aqueous phases were combined and added to aqueous sodium chloride (7% w/v, 50 ml). This mixture was extracted with hexane (3 × 10 ml) and the resulting extract was dried with anhydrous sodium sulphate and taken to dryness before being redissolved in diethyl ether/hexane (1 + 1, v/v, 2.5 ml). An aliquot (0.5 ml) of the extract was injected onto two Sep-Pak silica cartridges connected in series and the pesticide residue was eluted with diethyl ether/hexane (3 + 7, v/v), discarding the first 6 ml and collecting the next 10 ml. This fraction was decreased in volume and analysed by gas chromatography with electron capture detection.

Automation

Automation of "digital" chromatography is possible with use of the Varian Advanced Automated Sample Preparation (AASP) System. This instrument uses disposable cassettes, each of which contains ten cartridges packed with adsorbent. Crude extracts are loaded onto the cartridges by use of a special manifold to apply vacuum or pressure, and the cartridges are transferred to

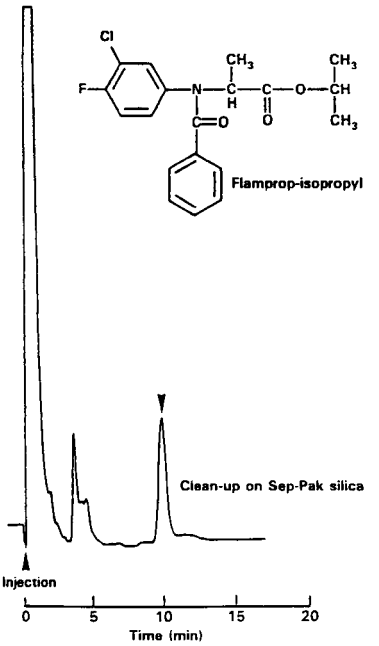

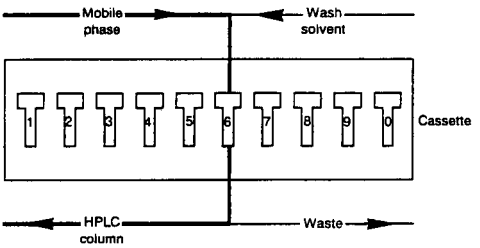

Fig. 1. Gas chromatogram illustrating the clean-up of a crude wheat grain extract containing residues of flamprop-isopropyl. Conditions: column, glass, 0.90 m × 4.0 mm i.d.; stationary phase, OV-225 2% (m m^{-1}); support, GasChrom Q (100/120 mesh); mobile phase, nitrogen; flow rate, 45 ml min^{-1}; column temperature, 200° C; detector, electron capture (^{63}Ni source); sample, 2.5 mg equivalent of grain extract fortified with 0.1 mg kg^{-1} of flamprop-isopropyl.

Fig. 2. Schematic diagram of the Varian AASP sample transfer module for HPLC.

the sample transfer module which is shown schematically in Fig. 2. Each cartridge is first washed with a solvent to remove co-extracted materials, which are diverted to waste, and the HPLC mobile phase is passed through the cartridge. The analyte is eluted directly from the cartridge onto the HPLC separation column. The sample transfer module can process up to ten cassettes (100 cartridges) fully automatically resulting in a higher throughput of samples without an increase in manpower.

The Varian AASP System has been used in the analysis of crude extracts of animal tissues for residues of the anticoagulant rodenticide, flocoumafen. Tissue samples (5 g) were first extracted by blending with anhydrous sodium sulphate (20 g) and acetone/chloroform (1 + 1, v/v, 25 ml) for 60 s. The mixture was filtered and the residue re-extracted with fresh extraction solvent (25 ml) and filtered. Both filtrates were combined and taken to dryness, and the resulting residue was redissolved in hexane (5 ml). An aliquot (10 μl) of the extract was loaded, under slight positive pressure, onto an AASP NH_2-phase cartridge. The cartridge was transferred to the HPLC sample transfer

module where co-extracted substances were first eluted to waste with ethanol (1.5 ml) and the analyte was eluted directly onto the HPLC column and quantified with fluorescence detection. A chromatogram obtained from an extract of quail liver containing flocoumafen residues is shown in Fig. 3.

Although the AASP system is designed to be interfaced to an HPLC column, it is possible to replace the column with a fraction collector. Such a configuration enables the instrument to be used for the purification of extracts containing an analyte which is not amenable to determination at the trace level by HPLC.

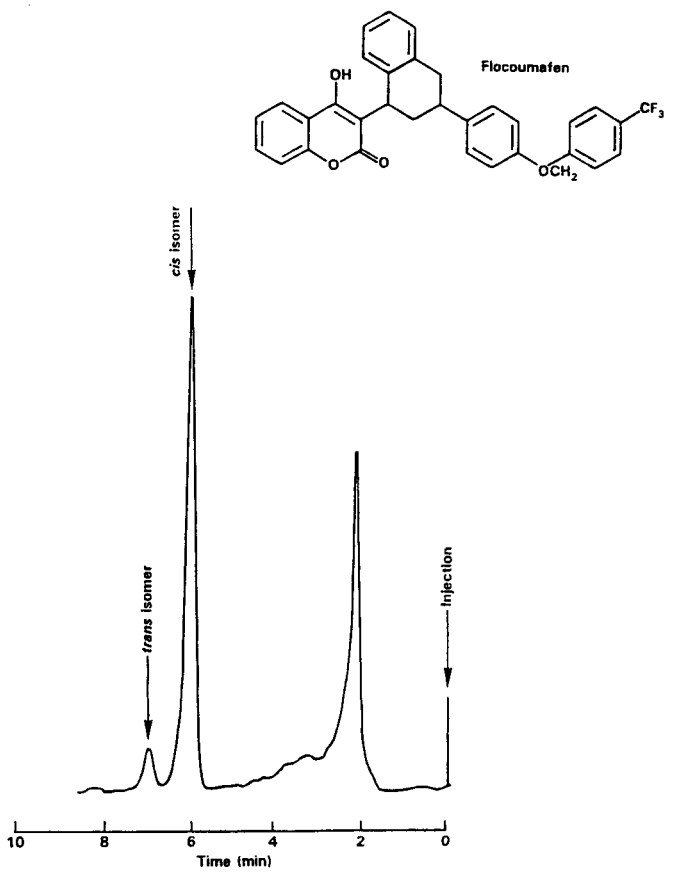

Fig. 3. Liquid chromatogram illustrating the clean-up of a crude extract of quail liver containing 0.5 mg kg^{-1} *cis* and 0.05 mg kg^{-1} *trans* flocoumafen. Conditions: column, stainless steel, 0.25 m × 4.6 mm i.d.; packing, Spherisorb-5-ODS-2 (5 μm); mobile phase, acetonitrile + water + acetic acid (80 + 20 + 0.1, v/v/v); flow rate, 2 ml min^{-1}; post column reagent, methanol + triethylamine (90 + 10, v/v); flow rate, 0.3 ml min^{-1}; detection, fluorescence, excitation 310 nm, emission 390 nm; sample, 10 mg equivalent of crude extract loaded onto AASP NH_2-phase cartridge. The cartridge was washed with ethanol (1.5 ml) and eluted with mobile phase.

SEMI-PREPARATIVE HIGH-PERFORMANCE LIQUID CHROMATOGRAPHY

Semi-preparative HPLC is used when a high degree of purification is required prior to determination. In most cases, it is used as a second-stage clean-up technique following initial purification of the crude extract by liquid-liquid partition or "digital" chromatography [4].

A schematic diagram of an automated HPLC clean-up system is shown in Fig. 4. In use, the system is first calibrated with an appropriately fortified extract, to establish the elution profile of the analyte. Extracts (0.5—1 ml) are injected onto the column and, using the information obtained from the calibration procedure, fractions are collected corresponding to elution of the analyte from the column. Because repeated injection of crude extracts onto the HPLC column results in an accumulation of co-extracted materials and loss of column efficiency, it is necessary to wash the column with appropriate solvent(s) between injections. The system illustrated enables the mobile phase and up to two wash solvents to be pumped through the HPLC column. All the operations (sample injection, fraction collection, wash cycle) are done automatically under the control of the microcomputer.

Figure 5 indicates the high degree of purification possible by HPLC. Whereas passage through two Sep-Pak silica cartridges was sufficient to clean-up wheat grain extracts containing residues of flamprop-isopropyl (Fig. 1), application of the same procedure to wheat straw extracts resulted in interfering peaks on the chromatogram as shown in Fig. 5(a). However, further purification of the wheat straw extracts by normal-phase HPLC on a LiChrosorb—NH_2 column (20 cm × 10 mm i.d.) with propan-2-ol + hexane (1 + 99, v/v) as the mobile phase at a flow rate of 4 ml min^{-1} led to the removal of the interfering peaks, as shown in Fig. 5(b).

COLUMN SWITCHING

In column-switching operations a fraction containing the analyte is transferred on-line from one chromatographic column to another. The technique can be applied to both gas and liquid chromatographic separations and is particularly useful when the analyte cannot be separated from co-extracted materials on a single column system.

In HPLC column-switching, different separation mechanisms are generally used, e.g., adsorption followed by ion-pairing or size exclusion followed by reversed-phase. Such combinations can result in a highly selective separation system and enable the analyte to be quantified following injection of a relatively crude extract onto the first column [5]. This technique has been used to analyse extracts of wheat grain and straw for residues of the chemical hybridising agent azetidine-3-carboxylic acid. In the procedure, the processed cereal sample (10 g) was blended with water (200 ml) for 60 s to extract residues of the compound. After filtration, an aliquot (5 ml) of filtrate was

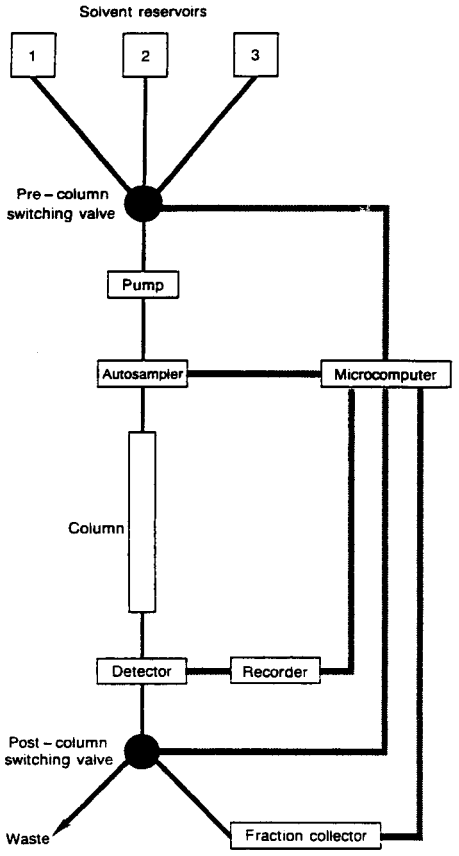

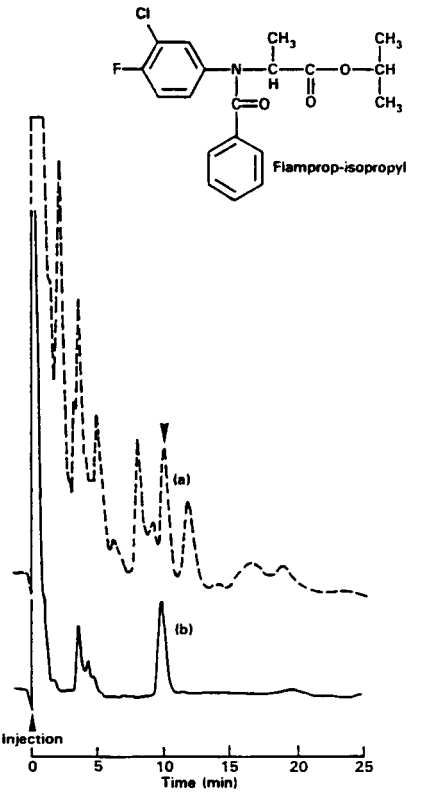

Fig. 4. Schematic diagram of the automated HPLC clean-up system.

Fig. 5. Gas chromatograms illustrating the clean-up of crude wheat straw extracts containing residues of flamprop-isopropyl: (a) clean-up on Sep-Pak silica; (b) clean-up on Sep-Pak silica and by HPLC on a LiChrosorb NH_2 column. General conditions: column, glass, 0.90 m × 4.0 mm i.d.; stationary phase, OV-225 2% (m m^{-1}); support, GasChrom Q (100/120 mesh); mobile phase, nitrogen; flow rate, 45 ml min^{-1}; column temperature, 200° C; detector, electron capture (^{63}Ni source); sample, 2.5 mg equivalent of straw extract fortified with 0.1 mg kg^{-1} flamprop-isopropyl.

passed through a Bond-Elut NH_2-phase cartridge and the cartridge was eluted with water (3 ml). The eluate was then passed through a Bond-Elut SCX-phase cartridge which was eluted with water (2 ml) and the eluate was discarded. The analyte was eluted from the cartridge with water/ammonia (200 + 1, v/v, 17 ml) and 0.8 ml of dansyl chloride solution (0.4% w/v in acetone) was added to the ammoniacal extract. The mixture was allowed to react at 50° C for 5 min, then water (10 ml) was added and the resulting solution was partitioned twice with ethyl acetate/hexane (75 + 25, v/v, 20 ml), the organic

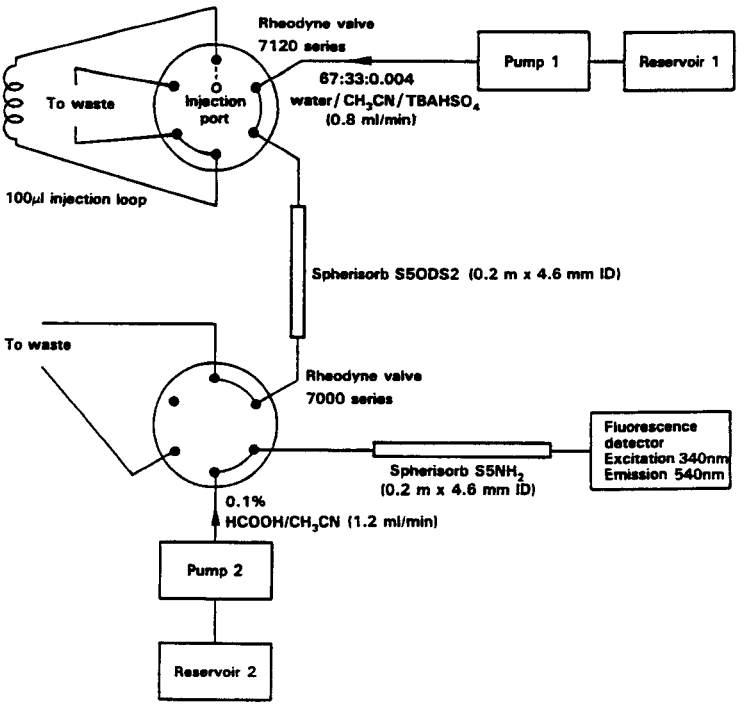

Fig. 6. Schematic diagram of the HPLC column-switching system.

phases being discarded. Formic acid (8 drops) was added to the aqueous phase, which was partitioned with the ethyl acetate/hexane mixture (2 × 20 ml). The organic phases were combined and taken to dryness, and the resulting residue was redissolved in water/acetonitrile/tetrabutylammonium hydrogensulphate (67 + 33 + 0.004, v/v/w, 2 ml). An aliquot (100 µl) of this solution was injected for the HPLC column-switching separation using the system shown schematically in Fig. 6. A chromatogram obtained from an extract of wheat grain fortified at 0.2 mg kg^{-1} with the chemical hybridising agent is shown in Fig. 7.

SWEEP DISTILLATION

Sweep distillation is particularly useful for the isolation of the more volatile pesticides from complex matrices. The technique involves separating the analyte, in the vapour phase, from a crude extract and trapping it in a solvent or on a solid adsorbent.

Although the technique of sweep distillation is not new [6], the introduction of modern equipment, such as the SGE universal trace residue extractor (Unitrex), has made the technique more attractive for routine use. The Unitrex equipment enables ten samples to be processed simultaneously. Each

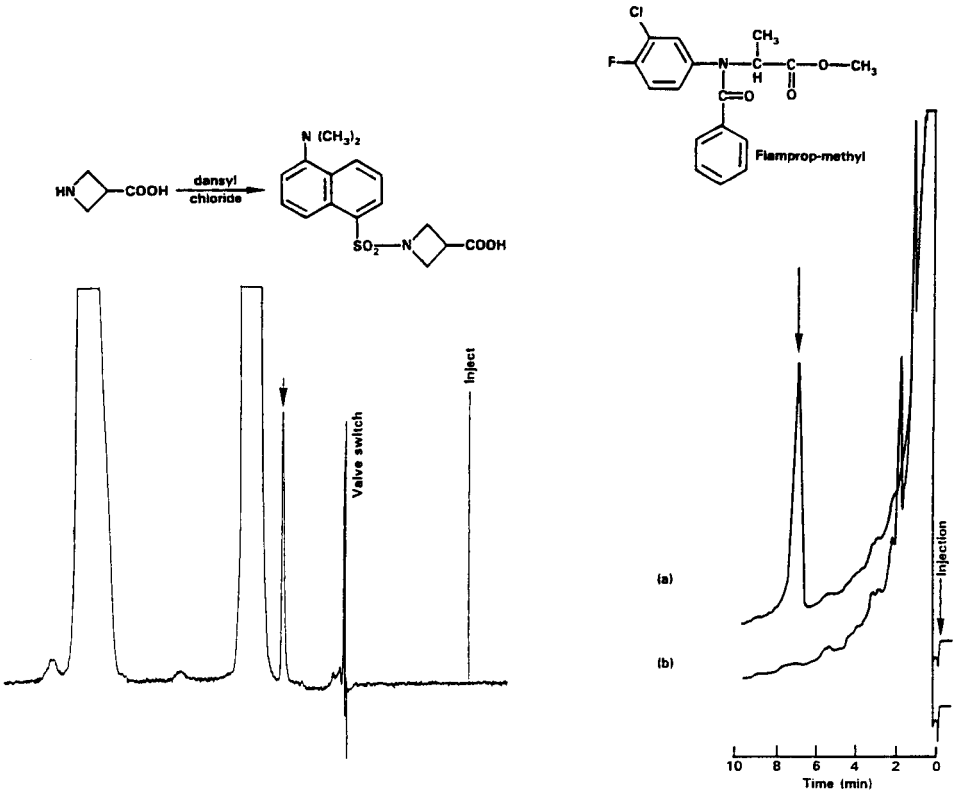

Fig. 7. Liquid chromatogram of an extract of wheat grain fortified with azetidine-3-carboxylic acid at 0.2 mg kg^{-1} (conditions as in Fig. 6).

Fig. 8. Gas chromatograms illustrating the isolation of flamprop-methyl from fortified soya bean oil: (a) oil fortified at 0.2 mg kg^{-1}; (b) control oil. Conditions: column, glass, 0.90 m × 4.0 mm i.d.; stationary phase, OV-225 2% (m m^{-1}); support, GasChrom Q (100/120 mesh); mobile phase, nitrogen; flow rate, 45 ml min^{-1}; column temperature, 200° C; detector, electron capture (^{63}Ni source); sample, 1 ml of oil distilled at 200° C for 30 min using nitrogen flow of 230 ml min^{-1}. Flamprop-methyl collected on Florisil and eluted with acetone/ethyl acetate (1 + 9, v/v).

sample is injected through a septum into a distillation tube packed with silanised glass beads and maintained at an elevated temperature. Nitrogen carrier gas flowing through the tube sweeps the pesticide into a trap packed with solid adsorbent, leaving fewer volatile components on the glass beads.

With the Unitrex system, Mes and Davies [7] obtained good recoveries of various organochlorine pesticides from fortified samples of rapeseed oil, and Luke and Richards [8] were able to isolate five organophosphorus compounds quantitatively from fortified samples of beef fat. Figure 8 shows a chromatogram obtained for the wild oat herbicide, flamprop-methyl, following isolation of the compound from soya bean oil by sweep distillation. A

sample (1 ml) of oil, fortified at 0.2 mg kg^{-1} with the herbicide, was distilled in the Unitrex and the analyte was collected on a trap packed with Florisil. After distillation, the adsorbent was eluted with acetone/ethyl acetate (1 + 9, v/v), and the eluate was analysed by gas chromatography with electron capture detection.

Although sweep distillation has often been used to isolate pesticide residues from animal and vegetable fats, it is applicable to a wide range of sample matrices. The principal requirement of the technique is that the compound to be isolated should be considerably more volatile than the majority of sample components present.

CONCLUSIONS

The techniques described have enabled trace levels of a range of pesticides and their degradation products to be isolated from various sample matrices. In some cases, these approaches have provided a higher degree of purification than is possible by the traditional clean-up techniques of liquid-liquid partition and gravity-fed column chromatography. In all cases, the techniques can be readily automated, leading to unattended analysis and greater productivity.

Present developments in the area of analyte isolation include the application of laboratory robotics and the use of other chromatographic techniques such as super-critical fluid chromatography and high-speed counter-current chromatography. However, the routine use of highly selective detection systems, such as mass spectrometers or immunochemical techniques, may eventually negate the need for extensive clean-up procedures in pesticide residue analysis.

The author acknowledges the work carried out by colleagues at Sittingbourne Research Centre which is presented in this paper.

REFERENCES

1 B. McMahon and J. A. Burke, J. Assoc. Off. Anal. Chem., 61 (1978) 640.
2 F. M. Gretch and J. D. Rosen, J. Assoc. Off. Anal. Chem., 67 (1984) 108.
3 F. M. Gretch and J. D. Rosen, J. Assoc. Off. Anal. Chem., 67 (1984) 783.
4 A. P. Woodbridge and E. H. McKerrell, in E. Reid (Ed.), Trace Organic Sample Handling, Vol. 10, Ellis Horwood, Chichester, 1981, p. 128.
5 C. J. Little, D. J. Tompkins, O. Stahel, R. W. Frei and C. E. Werkhoven-Goewie, J. Chromatogr., 264 (1983) 183.
6 R. W. Storherr and R. R. Watts, J. Assoc. Off. Anal. Chem., 48 (1965) 1154.
7 J. Mes and D. J. Davies, Int. J. Environ. Anal. Chem., 19 (1985) 203.
8 B. G. Luke and J. C. Richards, J. Assoc. Off. Anal. Chem., 67 (1984) 902.

Analytica Chimica Acta, 196 (1987) 85—93
Elsevier Science Publishers B.V., Amsterdam — Printed in The Netherlands

HOME-MADE THERMAL DESORPTION UNIT AS AN AID IN GAS CHROMATOGRAPHIC/MASS SPECTROMETRIC IDENTIFICATION OF ENVIRONMENTAL POLLUTANTS

T. RYMEN*, F. VEN and F. LIEVENS

Analytical Chemistry Service and Organic Chemistry Section, Centre for Nuclear Energy Studies, Boeretang 200, 2400 Mol (Belgium)

(Received 9th June 1986)

SUMMARY

The design, assembly and operation of a home-made thermal desorption unit is described. A special effort was made to obtain a system which does not require a substantial modification of the standard split/splitless inlet port of the gas chromatograph. As a consequence, a change-over to the split/splitless analysis of liquid samples can be done quickly and easily, thereby improving the cost-effectiveness of analysis by gas chromatography/mass spectrometry. Its analytical performance is shown to be adequate for both identification and determination of trace components.

One of the problems frequently encountered in studies of environmental pollution is the unambiguous identification of organic compounds present at trace and ultra-trace levels. In order to achieve this goal, the use of a suitable preconcentration technique is still imperative [1]. It has become common practice to use collection on solid sorbents for this purpose [2, 3]. Subsequent recovery of the trapped compounds requires either liquid/liquid extraction or thermal desorption. The latter has several advantages over liquid extraction; the elimination of sample dilution, component losses and sample contamination are the most important [4]. Thermal desorption systems available on the market, however, are expensive. Moreover, their installation often requires a substantial modification of the gas chromatograph inlet port, thereby hindering quick and easy change-over for the analysis of other types of samples. In consequence, their use leads to an important reduction in the cost-effectiveness of analysis by gas chromatography/mass spectrometry (g.c./m.s.). This paper describes the design, assembly and operation of a thermal desorption system in which these drawbacks have been decreased to acceptable levels without deterioration of the analytical performance.

EXPERIMENTAL

Equipment

Figure 1 shows a schematic representation of the system. The main components are an oven, which allows thermal desorption of the compounds

0003-2670/87/$03.50

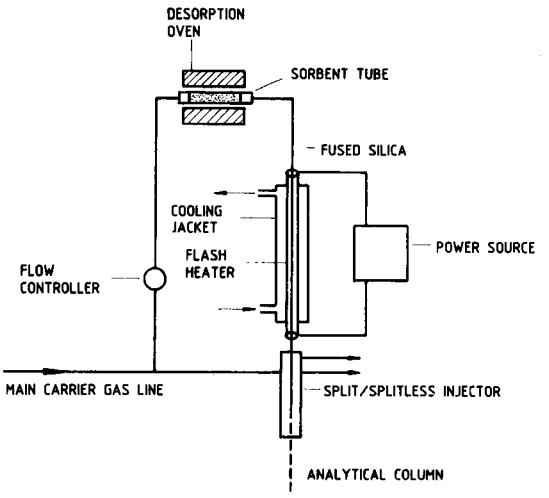

Fig. 1. Schematic representation of the thermal desorption unit.

trapped in the sorbent tube and a cold trap/flash heater combination, which allows refocussing of the gaseous compounds into a small volume followed by fast vaporization of the condensate and quantitative transfer into the separating column. Figure 2 shows a fully detailed drawing of the system. The oven, transfer line and trap/vaporizer unit are mounted in three separate cabinets of a stainless steel housing. The oven, supported by a plate of thermally isolating material, consists of an aluminium block that can be heated to 400°C by a heater cartridge linked to an on/off regulating power supply (Eurotherm, type 103-158-03-020-19-24-00). The final temperature is controlled through a NiCr/NiAl thermocouple connected to the power supply. The thermocouple and sorbent tube are positioned symmetrically relative to the heating cartridge.

The cold trap/flash vaporization combination is formed by a fused silica capillary (uncoated, deactivated, 55 cm long, 0.32 mm internal diameter), passing through a stainless steel tube (1 mm internal diameter) which itself is surrounded by an all-glass cooling jacket. The trap temperature is monitored by an extra thin NiCr/NiAl thermocouple (Pyrotenax) slid inside the stainless tube to the middle of the full tube length, and connected to a digital readout (Fluke, 2166-A). The cooling action of the jacket, resulting from a controlled flow of vaporized liquid nitrogen, is restricted to a 20-cm zone in the middle of the cold trap/flash vaporizer. At both ends, this trapping region (20 cm long, 3 mm internal diameter) is joined to a piece of narrow-bore glass tube (6 cm long, 1.5 mm internal diameter). In these end tubes, any space remaining between the stainless steel tube and the inner glass wall is filled with a cement resistant to high temperatures.

The adsorbent tube and trapping capillary are coupled through a stainless steel Swagelok reducing union (1/4 in. to 1/16 in.), which was drilled in order

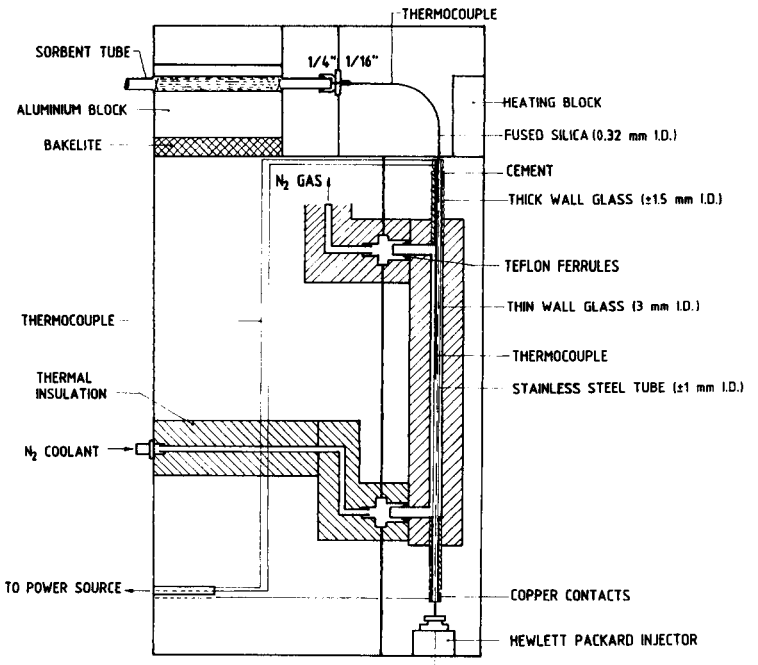

Fig. 2. Detailed drawing of the thermal desorption unit.

to allow the adsorbent tube to reach the seat of the 1/4-in. fitting. The capillary, protrudes only 1 mm into the adsorbent tube, and then passes through a thermally isolated and separately heatable compartment (transfer region). A flexible, out-of-line type of connection is absolutely essential at this point. It allows the capillary to cope with the repetitive thermal shocks originating from the repetitive cooling/heating cycles of the trap/vaporizer unit. Heating and temperature control of this transfer region is done as described above for the desorption oven.

This combination eliminates cold spots between desorption and trapping sections and permits the restriction of sample collection to a region well within the heating section of the flash vaporizer. Cooling is achieved by admitting a flow of vaporized liquid nitrogen. Flow and vaporizing speed can be controlled within very narrow limits thanks to the rather simple arrangement shown in Fig. 3.

The heart of the flash vaporizer is a home-made power supply which is connected to the outer ends of the steel tube in the cold trap. As is evident from Fig. 4, this power supply, at the start, will provide a selectable current to the heating tube through Variac V1 and transformers T1 and T2. The duration of this fast heating period can be set by using time relay BB. Once time BB is reached, time relays CC and B are activated. This results in the flash heater being powered via Variac V2 and transformers T2 and T3 until time CC has elapsed.

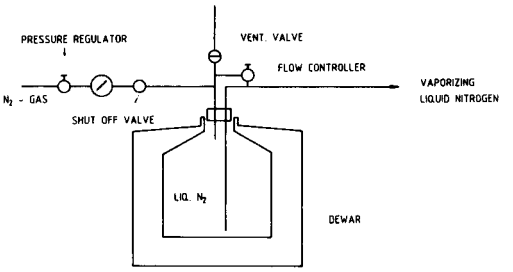

Fig. 3. Coolant supplying arrangement.

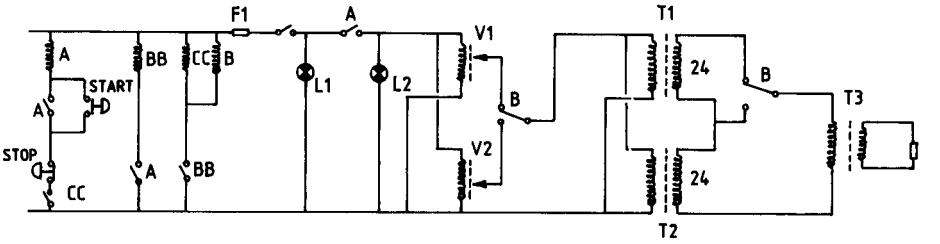

Fig. 4. Power source, circuit: BB, CC, time relay; A, B, relay; V1, V2, Variac, 220 V, 14 A; T1, T2, transformer, 220 V, 24 V; T3, transformer, 220 V, 40 V, 15 A.

On installation, the glass inlet port liner of the normal split/splitless g.c. injection port is replaced. The new liner has the same external dimensions but its internal diameter is only 0.5 mm. The analytical column enters this liner over a distance of 1 cm. The septum retaining nut is slid on to the trap capillary which is then passed through a high-temperature septum. Fixing the septum can only be done by using, for guidance, a wider bore injection needle, piercing the septum from the opposite direction. It is extremely important that the needle punctures the septum in its centre from a vertical direction. Subsequently, the system is placed directly on top of the injection port, while the trapping capillary is pushed in gently until it touches the analytical column. After alignment of capillary and injection port, the thermal desorption box is fixed by four screws, the septum is shifted down to its seat and the septum retaining nut is tightened. Subsequently, the injector block is heated to 350°C. In this way, the 1-cm long piece of transfer line, in the space between the exit of the flash vaporizer and the entrance of the heated injection block, is sufficiently heated to avoid cold spots on injection of the sample.

In a stand-by situation, the oven-to-trap transfer region will be kept at 250° C and the g.c. injector at 350° C. Starting from this situation, the column inlet pressure and split flow are adjusted via the original g.c. injector pneumatics and flow controllers. During the desorption/refocussing stage, the injector is operated in the split mode with a split flow of 100 ml min^{-1}. The sorbent tube is mounted in the desorption oven at room temperature and

under no-flow conditions. Vaporizing liquid nitrogen is fed to the trapping section of the trap/flash heater unit by adjusting the nitrogen pressure and bypass flow in the liquid nitrogen feeding device in such a way as to maintain a trap temperature of —183 ± 3°C. Following a stabilization period of 5 min, carrier gas is fed through the sorbent tube at 10 ml min^{-1} and the tube is heated immediately to the required temperature. Throughout the thermal desorption period, which takes 30 min from the start of the heating process, the trap temperature is monitored and maintained at —183 ± 3°C. Eventually, the bypass flow of nitrogen might require some minor adjustments.

After 30 min, heating of the sorbent tube is stopped and the trap flow is decreased to a value slightly smaller than the flow through the analytical column. The split flow through the g.c. injector is decreased to 40 ml min^{-1} and the split is closed. Cooling is stopped by shutting off the pressure source and opening the vent valve of the system, thus eliminating the pressure on the liquid nitrogen surface. The temperature of the cold trap is monitored and, as soon as it starts increasing, the trap heater and the chromatographic run are started simultaneously. The trap is heated from —180 to 400°C in ca. 10 s and it is held there for 2 min. Subsequently, the heating is stopped and the injection cycle is completed by activating the injector split.

Performance evaluation

The performance of the thermal desorption/flash vaporization unit was checked by comparing, for the same samples, the resulting chromatograms with those obtained by routine splitless injection. All tests were done on a test mixture containing (a) n-decane, (b) n-undecane, (c) n-dodecane, (d) n-tridecane, (e) n-tetradecane, (f) 2,6-dimethylphenol, (g) 2,6-dimethylaniline, (h) toluene and (i) an unknown impurity. These compounds were dissolved in diethyl ether at ca. 30 μg ml^{-1} and 1-μl aliquots were used for splitless injection, with activation of the split after 0.7 min.

Additionally, 1 μl of the same mixture was loaded onto a Tenax tube. The bulk of the solvent was removed by purging with helium at 50 ml min^{-1} for 15 min. Subsequently, the test compounds were desorbed thermally at 270°C, refocussed and injected as described above. Before injection, the trap flow was adjusted to 2 ml min^{-1}. The remaining analytical conditions were the same in both types of analyses: fused silica column, 25 m × 0.34 mm, loaded with Sil-5 and df = 0.22 μm; helium carrier gas at 0.8 bar inlet pressure (2.8 ml He min^{-1}); flame ionization detector set at 300°C; column oven temperature kept at 40°C for 1 min and then increased to 160°C at a rate of 7°C/min.

A series of tests was also set up in order to check system performance for very volatile compounds. The conditions were set as during normal thermal desorption (10 ml min^{-1} desorption flow; desorption oven temperature, 250°C; oven-to-trap transfer line, 250°C; g.c. injector at 350°C, purge at 100 ml min^{-1}). Under these conditions, 1-μl aliquots of pure diethylether were injected into an empty sorbent tube, with the cold trap either at room temperature or cooled to —183 ± 3°C.

RESULTS AND DISCUSSION

The results of the performance experiments are shown in Fig. 5. It is clear that the new system does not degrade the chromatographic resolution, rather there was improved peak shape for all compounds tested. Thus there is no evidence for the presence of dead volumes, active surfaces or cold spots. A comparison of the resulting peak areas (Table 1) indicates that sample transfer into the separating column is obtained more quantitatively with the thermal desorption/flash vaporization unit. As can be expected from the physical processes occurring upon injection, this is most evident for the lowest and highest boiling compounds. Tables 2 and 3 summarize the results

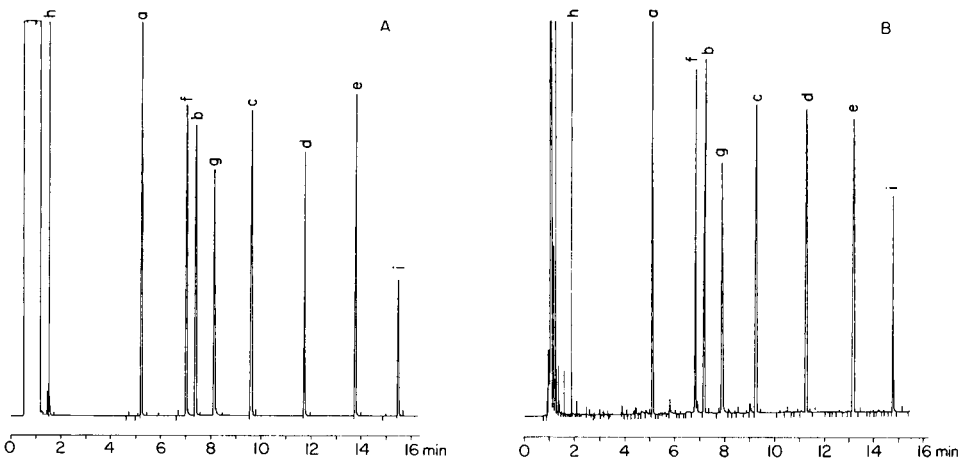

Fig. 5. Analyses of test mixture (1 μl): (A) in the splitless mode with a total run time of 16.2 min; (B) via thermal desorption with a total run time of 15.4 min. See text for peak identification.

TABLE 1

Comparison of peak areas obtained for splitless and thermal-desorption treatment of the same sample

Elution order	Compound	Area in arbitrary counts	
		Splitless	Thermal des.
1	Toluene	16940	18910
2	n-Decane	16060	17010
3	2,6-Dimethylphenol	13800	14500
4	n-Undecane	16380	17070
5	2,6-Dimethylaniline	14470	15020
6	n-Dodecane	16250	16800
7	n-Tridecane	16440	16690
8	n-Tetradecane	16430	16680
9	Unknown	7266	12240

TABLE 2

Precision of retention time data obtained by thermal-desorption g.c./m.s.

Compound code[a]	Retention time (min)				Mean	*RSD*[b] (%)
h	1.92	1.93	1.93	1.93	1.928	0.26
a	5.99	6.00	6.03	6.01	6.008	0.28
f	7.87	7.90	7.89	7.89	7.888	0.16
b	8.23	8.21	8.25	8.23	8.230	0.20
g	9.00	8.98	9.00	9.00	8.995	0.11
c	10.37	10.31	10.37	10.35	10.35	0.27
d	12.38	12.34	12.39	12.38	12.37	0.18
e	14.29	14.27	14.31	14.29	14.29	0.11
i	15.97	15.95	15.98	15.98	15.97	0.09
Run no.	1	2	3	4		

[a]See text. [b]Relative standard deviation.

TABLE 3

Precision of peak area measurements resulting from thermal desorption analysis

Compound code [a]	Peak areas in arbitrary counts				Mean	*RSD*[b] (%)
h	19220	20710	20850	20100	20220	3.7
a	18420	18690	18380	18450	18485	0.8
f	15310	15500	15220	15390	15355	0.8
b	18590	19070	18880	18570	18775	1.3
g	15760	15390	15570	15440	15540	1.1
c	17380	17480	17280	16920	17265	1.4
d	17370	17810	17560	17490	17557	1.1
e	17270	17870	17640	17310	17522	1.6
i	12480	12880	12490	12570	12605	1.5
Run no.	1	2	3	4		

[a]See text. [b]Relative standard deviation.

obtained by repetitive thermal-desorption g.c./m.s. of the same sample during a one-day period. It is evident that precisions of peak areas and retention times are well within acceptable limits, indicating the full applicability of the system in both quantitative and qualitative analysis.

For very volatile compounds (i.e., diethyl ether) when the cold trap was at ambient temperature, the resulting diethyl ether peak had an average area of 92800 ± 900 counts. At −183°C, the peak area was always less than 11 counts. The resulting collection efficiency for diethyl ether (b.p. 34.6°C) is calculated to be better than 99.9%.

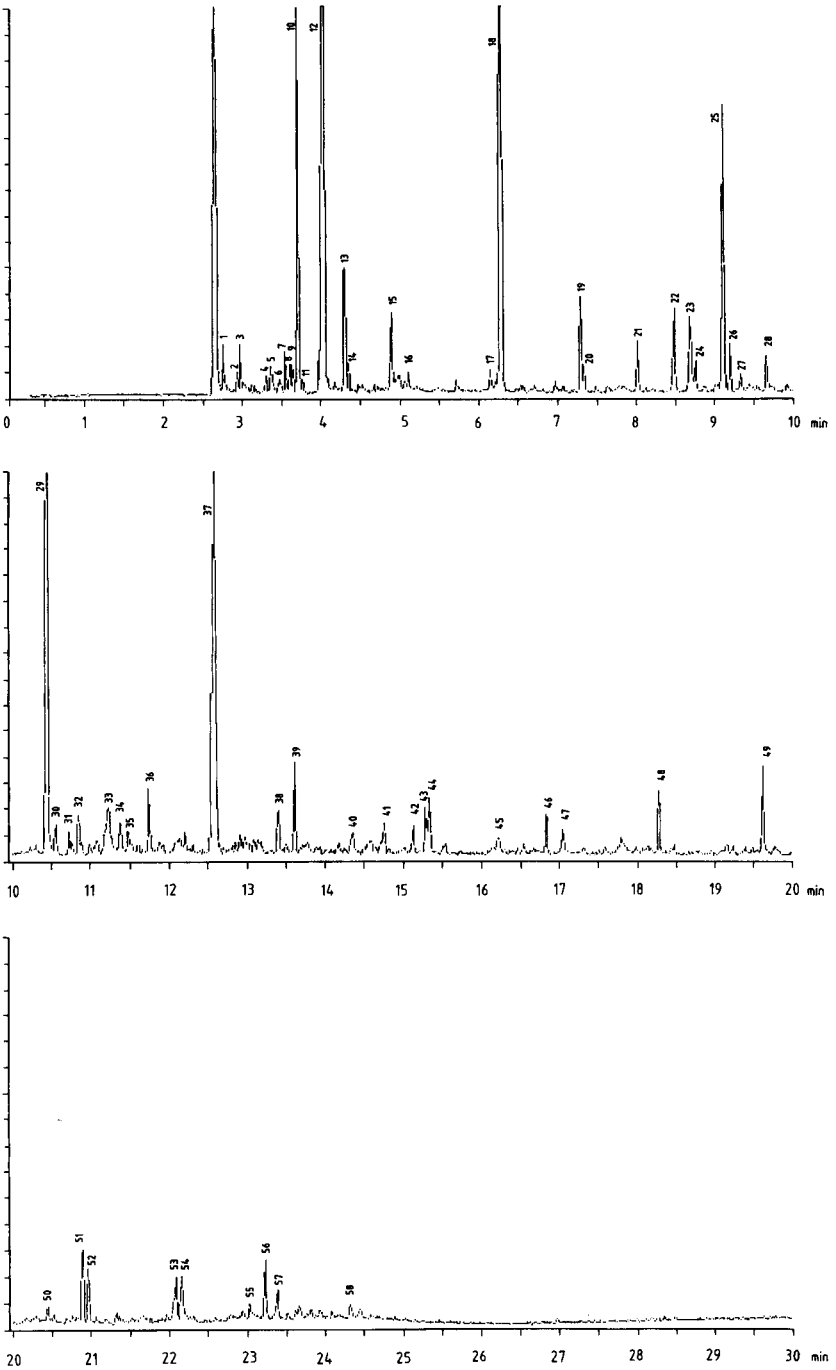

Fig. 6. Analysis of a real sample by thermal-desorption g.c./m.s. Total run time, 30 min. See Table 4 for peak identification.

TABLE 4

Compounds identified in a real sample (Fig. 6) by thermal-desorption g.c./m.s.

Peak no.	Compound	Peak no.	Compound	Peak no.	Compound
1	methylpropene	19	tetrachloroethene	38	nonanal
2	2-propenol	20	n-octane	39	n-undecane
3	2-propanone	21	hexamethyl-trisiloxane	40	1-phenyl-1,2-propane dione
4	dichloroethene isomer	22	xylene isomer	41	PAH, m.w. 128
5	dichloroethane isomer	23	xylene isomer	43	n-dodecane
6	3-buten-2-one	24	ethynylbenzene	42	decanal
7	methylpropanal isomer	25	styrene	44	benzothiazole
8	dichloroethene isomer	26	xylene isomer	45	unidentified hydrocarbon
9	n-hexane	27	tetrachloroethane isomer	46	n-tridecane
10	chloroform	28	n-nonane	47	1(3*H*)-isobenzo-furanone
11	ethyl acetate	29	benzaldehyde	48	n-tetradecane
12	dichloroethane isomer	30	propylbenzene	49	n-pentadecane
13	benzene	31	trimethylbenzene isomer	50	diethylphthalate
14	carbon tetra-chloride	32	benzonitrile	51	n-hexadecane
15	trichloroethene	33	phenol	52	diphenylmethanone
16	n-heptane	34	trimethylbenzene isomer	53	n-heptadecane
17	trichloroethane isomer	35	2-methylbicyclo-heptane	54	diphenylmethane dione
18	toluene	36	n-decane	55	$(C_6H_5CH_2CH_2)_2$
		37	methylethyl-benzene	56	n-octadecane
				57	octadecane isomer
				58	n-nonadecane

Testing the system for even more volatile compounds seemed more or less senseless because of the limits imposed by the sampling sorbents actually available. Nevertheless, g.c./m.s. of real samples, collected on Tenax in an industrialized area, systematically revealed the presence of a butene isomer (Fig. 6, Table 4). Taking into account the volatility of such a compound, it must be concluded that at least the qualitative applicability of the system extends to below the limits normally set for quantitative sorbent trapping. Obviously, the limits in the high-boiling-point region are imposed by the thermal desorption characteristics of the sorbents used.

REFERENCES

1 F. W. Karasek, R. E. Clement and J. A. Sweetman, Anal. Chem., 53 (1981) 1050A.
2 K. Grob and G. Grob, J. Chromatogr., 62 (1971) 1.
3 G. Bertoni, F. Bruner, A. Liberti and C. Perrino, J. Chromatogr., 203 (1981) 263.
4 W. D. Bowers, L. Parsons, R. E. Clement, G. A. Eiceman and F. W. Karasek, J. Chromatogr., 206 (1981) 279; 207 (1981) 203.

Analytica Chimica Acta, 196 (1987) 95—102
Elsevier Science Publishers B.V., Amsterdam — Printed in The Netherlands

UNIVERSAL EXTRACTION/CLEAN-UP PROCEDURE FOR SCREENING OF PESTICIDES BY EXTRACTION WITH ETHYL ACETATE AND SIZE EXCLUSION CHROMATOGRAPHY

A. H. ROOS, A. J. VAN MUNSTEREN, F. M. NAB[a] and L. G. M. Th. TUINSTRA*

State Institute for Quality Control of Agricultural Products, Bornsesteeg 45, 6708 PD Wageningen (The Netherlands)

(Received 24th July 1986)

SUMMARY

Size exclusion chromatography (SEC) is used as a clean-up procedure after extraction of pesticides with the compatible solvent ethyl acetate. Recoveries better than 90% are obtained for organochlorine and organophosphorus pesticides, fungicides and chlorobiphenyls from fats, fish oils, vegetables, fruits, cereals and liver. A comparison with other procedures is made. The use of a 10-mm i.d. SEC column provides the same limits of determination as those attainable with commercial systems but requires only 15% of the amount of solvents normally used.

The use of size exclusion chromatography (SEC) for pesticide determinations was first introduced by Stalling et al. [1]. The technique is based on separation by molecular size. An advantage is that, in contrast to other clean-up procedures based on Florisil, silica gel or alumina, polar as well as non-polar compounds are isolated in the same fraction. In current environmental analyses, SEC is frequently used as a clean-up procedure for organochlorine pesticides, organophosphorus pesticides, carbamates, herbicides, fungicides, polychlorobiphenyls, phthalates, aflatoxins and anabolic steroids [1—10]. It is striking that for the mobile phase so many different solvents have been used, including cyclohexane [1, 2], ethyl acetate/toluene [3, 9], cyclohexane/dichloromethane [4—6], hexane/dichloromethane [11] and cyclohexane/ethyl acetate [12]. For extraction solvents like chloroform, acetonitrile, acetone/water and dichloromethane, an extra step, evaporation of the extraction solvent and redissolution in the SEC eluent, is necessary.

This paper deals with the use of ethyl acetate as an extractant for fish oils, animal fats, cereals, vegetables, fruits and liver in the determination of organochlorine and organophosphorus pesticides, fungicides and polychlorobiphenyls (PCB's).

---

[a]Present address: Food Inspection Service, Assen, The Netherlands.

0003-2670/87/$03.50

EXPERIMENTAL

Apparatus and chemicals

The SEC system consisted of a Waters M-45 HPLC pump, a Waters automatic injection system (WISP), and a Quickfit glass column (inner diameter 10 mm, height 450 mm) filled with Bio Beads SX-3 (BioRad). The column was placed in a jacket and thermostatted at 40°C. The eluting solvent was ethyl acetate/cyclohexane (1:1, v/v) pumped at 1.0 ml min^{-1}. The pesticide/PCB fraction was collected in a fraction collector on a time basis.

The gas chromatograph used for chlorine-containing compounds was a Tracor Model 550 gas/liquid chromatograph equipped with a ^{63}Ni electron-capture detector and a capillary column (fused silica, Chrompak CP-Sil-5CB, length 25 m, inner diameter 0.25 mm, film thickness 0.1 μm). For organophosphorus pesticides, a Perkin-Elmer Model 990 gas/liquid chromatograph equipped with a nitrogen/phosphorus detector and a capillary column (fused silica, Chrompak CP-Sil-19CB, length 10 m, inner diameter 0.22 mm, film thickness 0.4 μm) was used. In both systems, 10 μl of sample was injected in the splitless mode and the splitter was opened after 3 min.

The temperature program for organochlorine and organophosphorus pesticide analysis was generally 4 min at 90°C then 10°C min^{-1} to 200°C. The inlet temperature should not exceed 200°C to avoid decomposing captafol and iprodione. To improve the limit of detection for bitertanol (0.2 mg kg^{-1} at a final temperature of 200°C), a final temperature of 250°C was used. For PCBs, the inlet and final temperatures were 240°C for optimal responses.

Ethyl acetate was redistilled in glass to eliminate interferences with pesticides.

Procedures

Fats and fish oil were diluted in the SEC eluent to 100 mg ml^{-1}, and 1.0 ml was injected onto the SEC column. For cereals, vegetables and fruits, a 50-g sample was macerated with 50 g of anhydrous sodium sulphate and 100 ml of ethyl acetate in a Waring blender. An aliquot of the ethyl acetate extract was concentrated and 1.0 ml (corresponding to 2.5 g of sample) was injected onto the SEC column. For liver, a 20-g sample was treated in the same way, and 1.0 ml (corresponding to 1.0 g of sample) was injected. The SEC eluent was collected in vials in the fraction collector. An internal standard was added to the cleaned extracts and the samples were placed without evaporation in the automatic injection system for gas chromatography.

RESULTS AND DISCUSSION

Conditions for SEC

The clean-up efficiency of the SEC column was tested with different quantities of fat. It was observed that with 150 mg of fat, especially egg fat, compression of the Bio Beads SX-3 column occurred and separations deteriorated. No compression was observed with 100 mg of fat for all kinds of fat.

The elution profile of pesticides in several fat samples diluted in the SEC solvent (ethyl acetate/cyclohexane, 1:1, v/v) was evaluated by fractionation. The dump-time at a flow rate of 1.0 ml min^{-1} for 100 mg of fat was 16.5 min and the collection time for the pesticide fraction was 13 min. In this fraction, recoveries better than 90% were obtained for the tested pesticides. The fat residue in the collected fraction was generally lower than 25 μg ml^{-1}. The same conditions were used for cereals, vegetables, fruits and liver, with the restriction of a maximum of 100 mg of fat injected onto the SEC column.

The advantage of the SEC system with a column of 10-mm inner diameter compared to the 25-mm columns normally used is that, in spite of a 6.25 times lower fat capacity, a 6.25 times smaller pesticide fraction is obtained (13 ml), resulting in less use of organic solvents. The limit of determination is the same. An advantage of the total procedure is the use of ethyl acetate for extraction, which eliminates the need for complete evaporation and redissolution before the SEC clean-up. Depending on the required limit of determination or maximum residue limit (MRL), often no concentration is necessary.

Recovery experiments

Table 1 shows the elution ranges of 19 organochlorine pesticides and fungicides tested for cereals and shows that the limit of determination related to the MRL is generally satisfactory for screening of pesticides at the sub-mg kg^{-1} level. Dutch legislation gives MRL values for pesticides in foods. In those cases where zero tolerances are stated, the limit of detection to be used is indicated. Therefore the limit of determination here was chosen to be not lower than the indicated detection limit (see Table 1). Figure 1 shows a standard chromatogram for these pesticides. The internal standards are, with increasing retention times, 4-chlorobiphenyl, hexabromobenzene and 2,2′,3,-3′,4,5,5′,6-octachlorobiphenyl. Based on a acceptable fat residue and recovery after SEC clean-up, the elution range 16.5—29.5 ml was chosen for the analysis of the pesticides.

Results of recovery experiments with cereals are given in Table 2. In general, recoveries better than 90% were obtained. The higher results for the fungicides chlorthalonil and dichlofluanid are caused by interferences present in the reagents used. The detection limit for bitertanol was 0.05 mg kg^{-1}, obtained by using the adjusted temperature program (see above). Table 3 lists the organophosphorus pesticides for which recoveries better than 90% were obtained at the 0.02—0.05 mg kg^{-1} level in the materials stated.

The repeatability of the procedure applied to a reference sample fat twice a month is shown in Fig. 2 for PCB-153 (2,2′,4,4′,5,5′-hexachlorobiphenyl) during the period January 1985—May 1986 (n = 46). Assuming an acceptable relative standard deviation (*RSD*) of 12% for pesticide determinations, lines representing twice the standard deviation (s) and the spike level of 0.20 μg kg^{-1} PCB-153 were plotted on the control chart. In practice, a mean of 0.196 mg kg^{-1} and a *RSD* of 7.8% were obtained.

TABLE 1

Maximum residue limit (*MRL*), limit of determination (*LD*) and elution range of pesticides tested for cereals

No.	Pesticide	*MRL* (mg kg product)	*LD* (mg kg product)	Elution range (ml)
1	α-HCH	0.1	0.01	17.8—26.0
2	β-HCH	0.02	0.01	17.1—24.2
3	γ-HCH	0.5	0.01	17.5—25.8
4	Chlorthalonil	0.2	0.02	18.0—24.3
5	Dichlofluanid	0[a] (0.1)	0.1	18.5—25.0
6	Triadimenol	0.1[b]	0.1[b]	15.0—24.2
7	γ-Chlordane	0.05	0.02	16.5—26.5
8	α-Endosulfan	0[a] (0.05)	0.02	17.8—28.0
9	α-Chlordane	0.05	0.02	17.8—28.0
10	p,p'-DDE	0.05[b]	0.01	17.8—28.2
11	Endrin	0.02[b]	0.02	21.5—29.0
12	β-Endosulfan	0[a] (0.05)	0.02	21.8—29.0
13	p,p'-TDE	0.05[b]	0.01	17.6—28.1
14	o,p'-DDT	0.05[b]	0.01	17.9—28.2
15	Endosulfansulphate	0[a] (0.05)	0.02	17.9—28.2
16	p,p'-DDT	0.05[b]	0.01	19.5—28.0
17	Captafol	0.2	0.1	19.9—28.2
18	Iprodione	0[a] (0.05)	0.05	17.8—28.0
19	Bitertanol	0[a] (0.05)	0.05[a]	15.5—26.2

[a] Detection limit, not regularly used on cereals. [b] Detection limit, regularly used on cereals.

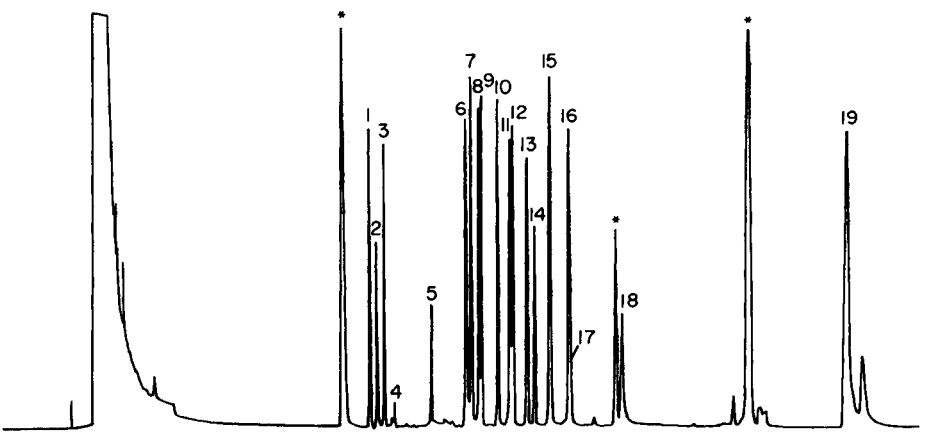

Fig. 1. Chromatogram of a standard solution of 19 pesticides tested in cereals. The numbers on the peaks correspond to the pesticides listed in Table 1. Asterisks indicate internal standards (see text).

TABLE 2

Results of recovery experiments (n = 10)

Pesticide	Mean recovery (%)			*RSD* (%)			Spike level (mg kg^{-1})
	Pure[a]	Wheat	Barley	Pure[a]	Wheat	Barley	
Bitertanol	103	108	103	12.8	8.4	18.3	8
Captafol	87	96	93	13.2	26.0	27.0	0.08
α-Chlordane	94	90	96	8.8	6.7	10.0	0.04
γ-Chlordane	97	90	97	13.3	5.4	7.1	0.04
Chlorthalonil	111	110	110	10.9	19.8	16.3	0.02
p,p'-DDE	94	89	92	14.7	4.2	9.5	0.04
o,p'-DDT	86	93	97	8.2	4.3	5.4	0.04
p,p'-TDE	90	89	102	10.2	11.2	10.8	0.04
p,p'-DDT	94	99	98	9.0	5.1	9.0	0.08
Dichlofluanid	110	86	87	12.0	12.7	10.7	0.04
α-Endosulfan	92	96	99	9.1	9.8	5.2	0.04
β-Endosulfan	93	89	96	8.8	8.0	10.1	0.04
Endosulfansulphate	96	92	96	10.7	6.9	10.2	0.04
Endrin	93	90	95	9.8	5.3	5.6	0.04
α-HCH	92	89	96	6.1	5.5	8.9	0.02
β-HCH	94	98	107	9.6	6.0	9.7	0.02
γ-HCH	97	97	101	10.3	11.3	6.4	0.02
Iprodione	99	91	98	6.1	9.0	13.0	0.2
Triadimenol	103	97	97	9.6	8.4	7.0	2

[a]Recovery of the pure compound taken through the procedure.

Comparison of extraction and clean-up procedures

To compare the extraction efficiency of the ethyl acetate and acetone [12] extractions, two cereal samples were analysed five times with each procedure. In the wheat sample, the results obtained with the ethyl acetate extraction were 0.009 mg kg^{-1} γ-HCH (*RSD* 30%), 0.024 mg kg^{-1} α-Endosulfan (*RSD* 16%) and 0.009 mg kg^{-1} β-Endosulfan (*RSD* 23%). With the acetone extraction procedure, the results were 0.012 mg kg^{-1} γ-HCH (*RSD* 19%), 0.021 mg kg^{-1} α-Endosulfan (*RSD* 8.9%) and 0.009 mg kg^{-1} β-Endosulfan (*RSD* 8.0%). In the barley sample, the results obtained with ethyl acetate extraction were 0.31 mg kg^{-1} chlorpyrifos-methyl (*RSD* 7.2%) while the acetone extraction gave a value of 0.34 mg kg^{-1} (*RSD* 14%). At these very low levels, the *RSD* values are acceptable. Figure 3 shows chromatograms obtained after each extraction procedure. Based on the results reported here and the comparison of extraction procedures reported earlier [13], it was concluded that both methods give comparable results even at very low levels. However, it was found that acetone extractions sometimes gave emulsions, unlike the ethyl acetate extraction.

TABLE 3

Organophosphorus pesticides and materials tested for which recoveries exceeded 90%

Organophosphorus pesticide	Materials[a]																	
	1	2	3	4	5	6	7	8	9	10	11	12	13	14	15	16	17	18
Azinphos-ethyl				○														
Azinphos-methyl				○														
Bromophos	○	○	○	○	○	○	○	○	○	○	○	○	○	○	○	○	○	○
Bromophos-ethyl	○	○	○	○	○	○	○	○	○	○	○	○	○	○	○	○	○	○
Carbophenothion				○														
Chloorfenvinphos																		○
Chloorpyriphos	○	○	○		○	○	○	○	○	○	○	○	○	○	○	○	○	○
Crufomate																		○
Coumaphos																		○
Dialifos				○														
Diazinon	○	○	○	○	○	○	○	○	○	○	○	○	○	○	○	○	○	○
Dichlorphos	○	○	○	○	○	○	○	○	○	○	○	○	○	○	○	○	○	○
Dimethoate	○	○	○	○	○	○	○	○	○	○	○	○	○	○	○	○	○	○
Dioxathion				○														○
Ethion	○	○	○	○	○	○	○	○	○	○	○	○	○	○	○	○	○	○
Fenchlorphos																		○
Fenitrothion				○														○
Fenthion																		○
Formothion				○														
Phosalone				○														
Phosphamidon				○														
Phosmet				○														○
Heptenophos	○	○	○	○	○	○	○	○	○	○	○	○	○	○	○	○	○	○
Jodfenphos																		○
Malathion	○	○	○	○	○	○	○	○	○	○	○	○	○	○	○	○	○	○
Methidathion				○														
Mevinphos (*cis-trans*)	○	○	○	○	○	○	○	○	○	○	○	○	○	○	○	○	○	○
Parathion	○	○	○	○	○	○	○	○	○	○	○	○	○	○	○	○	○	○
Pirimiphos-methyl	○	○	○	○	○	○	○	○	○	○	○	○	○	○	○	○	○	○
Pyrazophos	○	○	○	○	○	○	○	○	○	○	○	○	○	○	○	○	○	○
Tetrachlorvinphos	○	○	○	○	○	○	○	○	○	○	○	○	○	○	○	○	○	○
Triazophos	○	○	○	○	○	○	○	○	○	○	○	○	○	○	○	○	○	○
Thrichlorphon	○	○	○	○	○	○	○	○	○	○	○	○	○	○	○	○	○	○

[a]Materials tested: (1) potatoes, (2) strawberry, (3) endive, (4) apple, (5) beet, (6) celery, (7) cauliflower, (8) turnip, (9) purslane, (10) leeks, (11) red cabbage, (12) lettuce, (13) spinach, (14) sprouts, (15) onion, (16) white cabbage, (17) carrots, (18) swine/cattle liver.

Table 4 shows that for a few organochlorine compounds in fat samples spiked at the 0.04—0.4 mg kg^{-1} level, similar results were obtained whether the SEC or alumina clean-up was used. The comparability of the SEC clean-up procedure with the saponification procedure for the determination of individual chlorobiphenyls has already been reported [14].

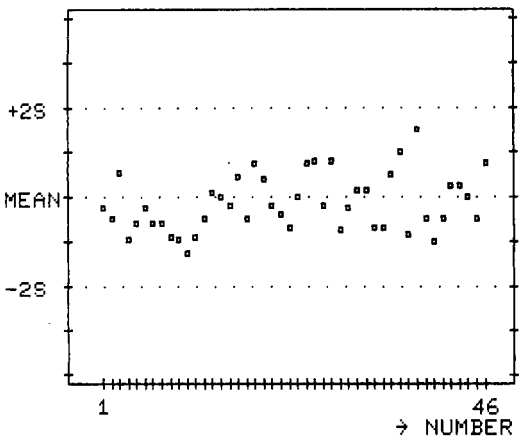

Fig. 2. Repeatability of determination of PCB-153 (spike 200 $\mu g\ kg^{-1}$) in a reference fat sample during January 1985—May 1986.

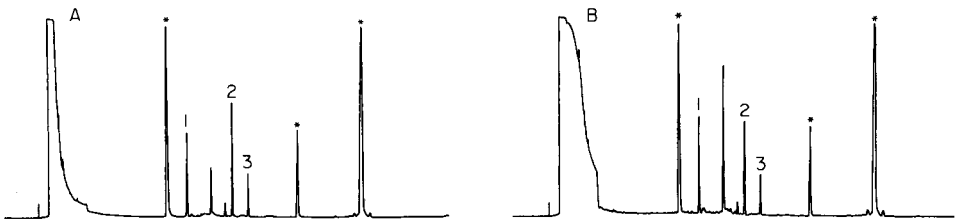

Fig. 3. Chromatogram of a wheat sample extracted with ethyl acetate (A) or acetone (B). Peaks: (1) γ-HCH at 0.013 mg kg^{-1} on wheat in A and 0.018 mg kg^{-1} in B; (2) α-Endosulfan at 0.024 mg kg^{-1} on wheat in A and 0.028 mg kg^{-1} in B; (3) β-Endosulfan at 0.01 mg kg^{-1} in A and 0.012 mg kg^{-1} in B. Electron capture detection; for chromatographic parameters, and identification of internal standards (*), see text.

TABLE 4

Comparison of recoveries after clean-up by SEC or alumina

Pesticide	Recovery[a] (%)		
	SEC (n = 57)	Alumina (n = 36)	Spike level (mg kg^{-1})
α-HCH	96 (10.9)	98 (5.5)	0.04
β-HCH	91 (10.2)	83 (11.1)	0.2
γ-HCH	107 (10.9)	100 (7.7)	0.04
p,p'-DDE	100 (9.3)	102 (8.5)	0.2
p,p'-TDE	96 (8.0)	99 (5.6)	0.2
o,p'-DDT	90 (8.6)	104 (9.4)	0.2
p,p'-DDT	95 (11.1)	105 (13.6)	0.4

[a]Mean recovery with *RSD* in parentheses.

REFERENCES

1 D. L. Stalling, R. C. Tindle and J. L. Johnson, J. Assoc. Off. Anal. Chem., 55 (1972) 32.
2 K. R. Griffitt and J. C. Craun, J. Assoc. Off. Anal. Chem., 57 (1974) 168.
3 L. D. Johnson, R. H. Waltz, J. P. Ussary and F. E. Kaiser, J. Assoc. Off. Anal. Chem., 59 (1976) 174.
4 J. A. Ault, C. M. Schofield, L. D. Johnson and R. H. Waltz, J. Agric. Food Chem., 27 (1979) 825.
5 G. Fuchsbichler, Landwirtsch. Forsch. 35 (1982) 90.
6 H. Steinwandter, Fresenius' Z. Anal. Chem., 313 (1982) 536.
7 B. G. Burns, C. J. Musial and J. F. Uthe, J. Assoc. Off. Anal. Chem., 64 (1981) 282.
8 H. Nijhuis, W. Heeschen and C. Mühlhoff, Milchwissenschaft, 38 (1983) 157.
9 L. G. M. Th. Tuinstra, W. A. Traag, H. J. Keukens and R. J. van Mazijk, J. Chromatogr., 279 (1983) 533.
10 H. Brunn, Arch. Lebensmittelhyg., 32 (1981) 116.
11 M. L. Hopper, J. Agric. Food Chem., 30 (1982) 1038.
12 W. Specht and M. Tillkes, Fresenius' Z. Anal. Chem., 301 (1980) 300; 322 (1985) 443.
13 J. Dornseiffen, G. F. Ernst, P. A. Greve, P. Olthof, G. H. Tjan and L. G. M. Th. Tuinstra, Sixth International Congress of Pesticide Chemistry, Ottawa, August, 1986.
14 L. G. M. Th. Tuinstra, J. J. M. Driessen, H. J. Keukens, A. J. van Munsteren, A. H. Roos and W. A. Traag, Int. J. Environ. Anal. Chem., 14 (1983) 147.

Analytica Chimica Acta, 196 (1987) 103—114
Elsevier Science Publishers B.V., Amsterdam — Printed in The Netherlands

CRITICAL STUDY OF THE SPECIATION OF ALUMINUM IN BIOLOGICAL FLUIDS BY SIZE-EXCLUSION CHROMATOGRAPHY AND ELECTROTHERMAL ATOMIC ABSORPTION SPECTROMETRY

H. KEIRSSE, J. SMEYERS-VERBEKE*, D. VERBEELEN and D. L. MASSART

Farmaceutisch Instituut and Academisch Ziekenhuis, Vrije Universiteit Brussel, Laarbeeklaan 103, 1090 Brussel (Belgium)

(Received 7th August 1986)

SUMMARY

Pooled serum and the serum of a healthy volunteer were spiked with aluminum and aluminum species were separated on Bio-gel columns. With the P10 column, less than 40% of the aluminum was eluted with the high-molecular-weight (m.w. >20 000) fraction; the total aluminum concentration was 600 $\mu g\ l^{-1}$. Two lower m.w. fractions were also recovered. With the P4 column, only one high m.w. (65—100%) and one low m.w. (0—35%) fraction were recovered; the total Al concentration was 10—110 $\mu g\ l^{-1}$. When a hemofiltrate obtained from uremic patients on regular hemofiltration and spiked with 60—110 μg Al l^{-1} was applied to the P4 gel, two lower m.w. fractions were detected. The adsorption/desorption of "free" aluminum on the column was studied with 0.9% NaCl solution, Earle's medium and filtrate. Normal column fractionation and frontal analysis (adsorption and desorption breakthrough curves) were used. Redistribution of aluminum seemed not to occur within the serum when in contact with the column, but contamination from extraneous aluminum could greatly alter the aluminum distribution. Different sources of errors were identified.

There is evidence that aluminum accumulation is the cause of dialysis dementia and dialysis bone disease [1]. The possible sources of the increased tissue and blood aluminum levels in patients with chronic renal failure on regular dialysis therapy are the gastrointestinal absorption from aluminum-containing phosphate-binding gels, the transfer from the dialyzate to the blood during hemodialysis, the daily exposure to aluminum present in food, drinking water and the air, and the insufficiency of renal excretion. Very little is known about the mechanism(s) by which aluminum causes its toxic effects, or how and why it is concentrated in the bones and in the gray brain matter. Speciation analysis in which individual chemical forms in the blood are determined are therefore of importance. Methods of choice for this purpose are ultrafiltration and gel filtration, but contradictory results have been reported concerning the distribution of aluminum in blood serum.

Tables 1 and 2 survey the research done on ultrafiltration and gel filtration, respectively, in this field. These contrasting results may firstly result from the use of analytical methods and procedures which are not sensitive and

0003-2670/87/$03.50

TABLE 1

Literature survey of ultrafiltration studies concerning aluminum in blood

Authors & references	Method used[a]	Serum sample[a]	Ultrafilterable fraction (%)	Sample concentration[a] ($\mu g\ Al\ l^{-1}$)	Remarks
H. Rahman et al. [2—5]	Amicon YM10 pressurized membranes	Normal	30—58 (46)[b]	6.4—11.6 (8.0)[b]	5% CO_2 in air pressure medium m.w. <10 000
		Uremic	20—47 (33)[b]	21—235 (99)[b]	
		Uremic/DFO[c]	(43)[b]	198 ± 94[c]	
Elliott et al. [6]	—	Uremic	10—30	—	Decreased at concentrations <200 $\mu g\ l^{-1}$
Leung et al. [7]	Centrifee Micropartition, Amicon YMT membranes	Normal	14.5 ± 3[e]	7.8 ± 5.8[e]	M.w. <1000
		Normal[d]	16.2 ± 4[e]	14.0 ± 5.6[e]	
		Uremic pre-DFO	19.7 ± 7[e]	140 ± 62[e]	
		Uremic post-DFO	85.8 ± 9[e]	311 ± 117[e]	
Gardiner et al. [8]	Sartorius pressure filtration at 100 kPa Ar (m.w. <10 000)	Normal + Al	45	200	pH 4.0
			50	200	pH 5.0
			57	200	pH 6.0
			27	200	pH 6.9
			20	200	pH 7.1
			10	200	pH 7.4
			2.5	200	pH 7.9
Burnatowska-Hledin et a. [9]	Amicon CF-50A and YMT membranes,	Normal rat serum + Al	2—70	20—10 800	Suprapathological concentrations. Al retention on membranes
Lundin et al. [10]	Spectropore pressurized membranes	Normal	41 ± 5.8[e]	40.2 ± 7.2[e]	Cut-off m.w. 6000—8000
			35—80	20—75	

[a] Dashes mean that no data were given. [b] Mean value. [c] Patient treated by desferrioxamine (DFO) infusion. [d] Hospital patients with normal renal function. [e] Mean ± standard deviation.

selective enough for aluminum determination at the trace levels in biological fluids. Moreover, because of the ubiquity of aluminum, contamination of the sample during preparation and handling may lead to falsely elevated values and result in the addition of new or the enlargement of existing fractions within the blood serum.

Secondly, the separation methods used are also potential sources of erroneous interpretation of results. The samples are in contact with large masses of materials and solvents which may be contaminated with aluminum, but also adsorption and consecutive desorption and binding of aluminum may alter its distribution in blood serum. It is not excluded that under certain conditions (e.g., of pH or temperature) the gel surface acts as a catalyst for the formation of certain Al species, even resulting in precipitation and thus total loss within the separation system.

It is considered that as long as the above-mentioned techniques and the handling and pretreatment of the materials are not investigated thoroughly, one will not be able to evaluate the true distribution of aluminum in blood serum. Thus, prediction of the mechanisms involved in aluminum intoxication and its prevention or detoxification will remain in an experimental state. This has prompted the present critical evaluation of speciation methods and analytical techniques and procedures.

EXPERIMENTAL

Precautions to avoid contamination

The precautions to be taken to avoid contamination with extraneous aluminum when this element is measured in biological fluids have been reported elsewhere [14]. The main points are: (a) the use of high-purity reagents, and plastic or quartz material in preference to glassware; (b) thorough rinsing of all laboratory ware in dilute (1:100) nitric acid; and (c) screening of all materials and reagents for possible sources of aluminum contamination.

Instrumentation

For routine determinations of aluminum, a Perkin-Elmer model 460 atomic absorption spectrometer equipped with a HGA 76-B graphite furnace (CT 06856) was used. Argon was used as the purging gas in the furnace. For background corrections, a deuterium background corrector was used. The wavelength was 309.3 nm. A Perkin-Elmer AS-1 autosampler delivered 20 μl of sample solution into the graphite tube. The furnace conditions were: drying at 100°C for 30 s; ramp ashing from 100 to 600°C at 6°C s^{-1}; ashing at 1450°C for 18 s; atomization, with gas interrupt, at 2650°C for 8 s.

For optimization of the aluminum determinations, checks were made with a Zeeman-3030 atomic absorption spectrometer equipped with a HGA-600 graphite furnace, a Silent Scribe Anadex printer and an AS-60 autosampler (all from Perkin-Elmer).

For gel filtration, a Pharmacia column (Pharmacia Fine Chemicals, Uppsala, Sweden), a Gilson Minipuls 2 peristaltic pump (Gilson Medical Electronics,

TABLE 2

Literature survey of gel filtration studies concerning aluminum in blood

Authors & references	Method used[a]	Serum sample[a]	Fractions recovered	Sample concentration[a] ($\mu g\ l^{-1}$)	Remarks
H. Rahman et al. [2, 3, 5]	Sephacryl S-300, Earle's medium, pH 7.4	Normal	Al-transferrin	6.4—11.6 (8.0)[b]	No total mass balance, adsorption and subsequent desorption of Al
		Uremic	Al-transferrin	21—235 (99)[b]	
		Transferrin + Al	Al-transferrin	200	
		Albumin + Al	no Al-albumin	200	
		Uremic + DFO[c]	Al-transferrin Al-DFO	198 ± 94[e]	
	CNBr-activated Sepharose coupled with antitransferrin	Uremic	35% Al in washing cycle	99 ± 54[e]	pH 7.2
			65% Al in dissociation cycle, Al-transferrin		pH 2.8 Total mass balance = 100%
King et al. [1]	Sephacryl S-200, complex buffer, pH 7.6	Normal Uremic	Al-albumin Al-high m.w. protein Al-low m.w.[d]	50 164	No total mass balance
Bertholf et al. [11]	Sephacryl S-200, complex buffer pH 7.4, 37°C	Normal + Al	Al-protein "free" Al	366	No total mass balance
		Uremic	Al-protein "free" Al Al-low m.w. protein	395	No total mass balance
Leung et al. [7]	Bio-gel P2, complex buffer, pH 7.4, Exclusion m.w. 1800	Pre-DFO uremic	Al-protein Al-low m.w. Al-low m.w. protein Al-lower m.w.	95	Transferrin + albumin No total mass balance Free Al adsorbs
		Post-DFO uremic	Al-DFO Al-lower m.w.	275	No protein coupling Free Al absorbs (Transferrin) + albumin
Gardiner et al. [8]	Sephacryl S-300, 0.1 M Tris-acetate buffer; pH 7.4; 4°C	Uremic	Al-protein Al-low m.w.	—	No total mass balance

	pH 4.15 (HCl) pH 6.0 (HCl) pH 7.4	Normal + Al	Al-protein Al-low m.w.	200	Only protein Al after incubation (37°C)
Trapp [12]	Sephadex G-200, 0.01 M Tris buffer, 0.1 M KNO_3, pH 7.2	Normal + Al	Al-high m.w. protein Al-transferrin Al-albumin	500 $\mu g\ ml^{-1}$ Al citrate	m.w. >200,000 Only after incubation with CO_2
Cochran et al. [13]	Sephacryl S-300	Post dialysis concentrated plasma	Al-transferrin	—	Only high m.w. region analysed

[a]Dashes mean that no data are available. [b]Mean value. [c]Patient treated by desferrioxamine (DFO) infusion. [d]Low molecular weight protein and/or complexed with inorganic ions. [e]Mean ± standard deviation.

Villiers, France) and an ISCO Model 563 fraction collector (Instrumentation Specialities, Lincoln, Nebraska) were used.

Materials and reagents

The water used to prepare all solutions was double-distilled from a quartz device just before use. It contained no detectable aluminum. Aluminum standards and spiked sera and buffers were prepared from a commercial 1 g l^{-1} stock solution of aluminum (Merck). All other reagents were of at least "Pro analysis" quality.

As filtration medium, Bio-gel P polyacrylamide gels P10 and P4 (Bio-Rad Laboratories) were used and columns were packed as prescribed by the manufacturer.

Filtrates were obtained from uremic patients treated with regular hemofiltration for renal replacement therapy. The hemofilter used during this procedure was the Satorius® SM-40042 type with a cut-off of ca. 20 000 Daltons.

Procedure

A first group of preliminary experiments (Table 3) was done with pooled serum spiked with aluminum, with the P10 and P4 gels. As eluent a 0.9% sodium chloride solution, pH 7, was used and aluminum concentrations in the samples were varied between 85 and 600 $\mu g\ l^{-1}$. The same experiments were repeated with aqueous (0.9% NaCl) standards and filtrate spiked with aluminum. In a second group of preliminary experiments (Table 4), the total recovery and the reproducibility were checked on serum from a healthy volunteer. Two experiments were done on the blank serum and seven with the spiked serum ($\pm 100\ \mu g\ l^{-1}$). The sample volume was 2 ml and the average

TABLE 3

Survey of preliminary experiments

Expt. no.[a]	Gel type	Column length[b] (cm)	Flow rate (ml h^{-1})	Sample origin	Sample volume (ml)	Al conc. ($\mu g\ l^{-1}$)
1	P10	42	33	Pooled serum	2	600
2	P10	42	10—12	Pooled serum	1	600
3	P10	42	10—11	Pooled serum	2	600
4	P4	24	32	0.9% NaCl	2	300
5	P4	24	32	0.9% NaCl	2	300
6	P4	24	29	Pooled serum	2	85
7	P4	24	26	Pooled serum	2	85
8	P4	24	28	Pooled serum	2	85
9	P4	27	15	Filtrate	2	110

[a]In experiments 1—8, adsorbed aluminum was not removed from the column between runs. In experiment 9, a new column was used. [b]1.5 cm diameter.

TABLE 4

Speciation of serum from a healthy volunteer spiked with aluminum (27 × 1.5 cm column, P4 gel)

Expt. no.	Sample conc. (μg Al l^{-1})	Flow rate (ml h^{-1})	Al recovered				Total % of intake
			Protein		Low m.w.		
			(ng)	(%)	(ng)	(%)	
10[a]	110	14.5	115	90	12	10	58
11	110	14.5	129	73	48	27	80
12	110	15.0	191	68	92	32	129
13	110	15.0	156	74	54	26	96
14	95	14.5	155	77	47	23	106
15	95	13.0	123	70	54	30	93
16[b]	9	15.0	72	100	0	0	400
17	95	13.5	138	78	38	22	93
18[b]	9	14.0	34	100	0	0	187

[a]Column cleaned with blank serum. [b]Blank.

flow rate was 14.5 ml h^{-1}. During the preliminary experiments, the graphite-furnace atomic absorption spectrometric procedure was studied and developed.

Investigations were made on the gel filtration of aqueous (0.9% NaCl) aluminum standards, Earle's medium spiked with aluminum and filtrates spiked with aluminum. In all experiments, the eluent used was the 0.9% sodium chloride solution. The sample volume was 2 ml in all cases. A survey of these experiments and the results obtained are given in Table 5.

The behavior of aluminum in the same buffers and on the same column was further tested by frontal analysis, by recording (adsorption/desorption) breakthrough curves (Table 6).

In a final series of experiments, the same P4 gel column was loaded with aluminum by adsorption from a 0.9% sodium chloride solution. Subsequently, serum, filtrate and Earle's medium were also contacted with the gel in order to study the uptake (desorption) of aluminum from a contaminated column. Similar experiments were performed after "loading" the column with an aluminum-spiked uremic filtrate. In all experiments, the eluent was the 0.9% sodium chloride solution (pH 7) and the sample volume was 2 ml. The results obtained are given in Table 7.

RESULTS AND DISCUSSION

From the first group of preliminary experiments, described in Table 3, it was found that three aluminum fractions were eluted from the serum when the P10 column was used. In all cases less than 40% of the aluminum was eluted together with the protein fraction (m.w. >20,000). The two lower-molecular-weight fractions were not completely separated. The overall

TABLE 5

Spiked buffer speciation

Expt. no.	Flow rate (ml h^{-1})	Sample		Al recovery (%)
		Origin	Al conc. ($\mu g\ l^{-1}$)	
19[a]	14	0.9% NaCl	140	0
20[a]	14	Earle's	100	0
21[b]	14	Earle's	200	0
22[a]	15	filtrate	110	ca. 96

[a]Cleaned column. [b]Same column as previous experiment.

TABLE 6

Adsorption breakthrough curves for spiked buffers

Expt. no.	Flow rate (ml h^{-1})	Sample			Results
		Origin	Volume (ml)	Al conc. ($\mu g\ l^{-1}$)	
23	32.5	Filtrate	60	50	Two low m.w. fractions recovered
24	15.0	Filtrate	60	110	
25	14.5	0.9% NaCl	55	140	No Al recovered
26	14.0	0.9% NaCl	50	200	No Al recovered
27	16.0	Earle's	100	200	One low m.w. fraction "desorbs" very slowly

recovery was less than 90%. With the P4 gel, two different fractions were recovered; 65—100% was found in a first fraction (m.w. >4000) hereafter called fraction I, and the overall recovery was between 60 and 125% (cf. Fig. 1). When aqueous standards were applied, all the aluminum was adsorbed, while the filtrate showed two incompletely separated low-molecular-weight fractions, hereafter called fractions II and III. The total recovery was ca. 100%.

The second group of preliminary experiments with aluminum-spiked serum (Table 4) shows an overall aluminum recovery between 58 and 129%. Fraction I contained 68—100% of the aluminum which decreased as the total serum aluminum content increased. The blank sera with no aluminum added gave a recovery of well over 100% (400 and 187%); the blank protein fraction therefore seems to be easily contaminated by extraneous aluminum and desorption of aluminum from the column. Possible explanations for fluctuations in results are systematic errors made in the volume of the different column fractions (10%). Also the spectrometric measurement was at first responsible for errors, because most sample concentrations are rather low (<20 $\mu g\ l^{-1}$) and because the absorbance signal is suppressed by the presence

TABLE 7

Survey of the "desorption" experiments from a contaminated column

Expt. no.	Flow rate (ml h^{-1})	Total Al loading (ng)	Sample		Al recovered in fraction						Total Al (ng)	(1) Remarks on procedure (2) Remarks on results
			Origin	Al conc. ($\mu g\ l^{-1}$)	I		II		III			
					(ng)	(%)	(ng)	(%)	(ng)	(%)		
28	15.0	7500	Uremic serum	45	2700	64	1500	36	0	0	4200	(1) Loaded from 0.9% NaCl
29	15.0	2200	Uremic serum	100	440	63	260	37	0	0	700	(1) Loaded from 0.9% NaCl
30	14.5	1700	Uremic serum	100	190	53	170	47	0	0	360	(1) Same column
31	15.5	10500	Filtrate	3	0	0	(±99%)		(±1%)		3900	(1) Reloaded from 0.9% NaCl (2) Two lower fractions not completely separated
32	15.5	6600	Filtrate	3	—[a]							(1) Desorption curve, 180 ml filtrate sample
33	16.5	10000	Earle's	<1	0	0	0	0	1400	100	1400	(1) Loaded from 0.9% NaCl (2) Release over very long time (70 ml)
34	16.0	8600	Earle's	<1	0	0	0	0	206	100	206	(1) Same column
35	26.5	—	Normal serum	7.5	10	100	0	0	0	0	10	(1) Column pre-contacted with 60 ml of filtrate containing 50 μg Al l^{-1} (2) No Al desorbs from column into serum after "loading" from filtrate; measurement errors because of low fraction concentrations
36	25.5	—	Normal serum	7.5	10	100	0	0	0	0	10	
37	15.0	—	Normal serum	7.5	20	100	0	0	0	0	20	(1) Precontacted with 60 ml of filtrate containing 100 μg Al l^{-1} (2) Same remark as above

[a] After 175 ml has been eluted, outlet concentration (3 μg Al l^{-1}) equals inlet concentration.

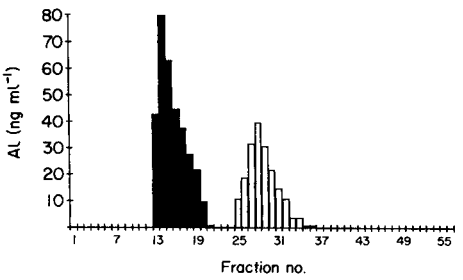

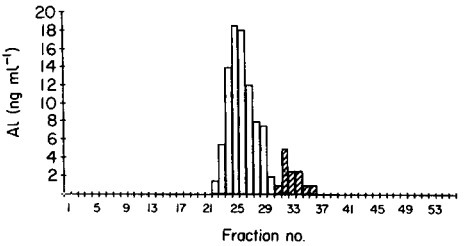

Fig. 1. Removal of aluminum from an aluminum-loaded column by serum. Fractions I (filled bars) and II (open bars) are shown. Speciation of serum spiked with aluminum showed the same elution diagram.

Fig. 2. Aluminum species in a spiked filtrate (150 μg Al l^{-1}). Fractions II (open bars) and III (hatched bars) are shown.

of sodium chloride. Because every fraction has a different matrix composition, use of a single calibration graph is impossible. Standard addition to every sample is very time-consuming and in most cases is not possible because of the small sample volumes collected from the column. As the spectrometric technique was refined during this investigation, it is advisable not to interpret these values too quantitatively. This probably explains the better results of experiments 13, 14, 15 and 17 compared with previous ones. These preliminary experiments also indicated that adsorption and subsequent desorption of aluminum may alter the aluminum distribution.

The P4 gel was selected for further research into the behavior of aluminum in different buffer solutions. As can be seen from Table 5, there is a strong interaction between aluminum and the gel matrix which, however, depends strongly on the kind of buffer. The spiked filtrate showed two low-molecular-weight fractions, the higher of which (fraction II) accounts for 83%, and the lower (fraction III) for 17% (Fig. 2). The breakthrough curves (Table 6, Fig. 3) confirmed that the filtrate contains two low-molecular-weight fractions. A low-molecular-weight fraction with the same elution time as fraction III was also detected in Earle's medium (Fig. 3). From the sodium chloride solution spiked with aluminum, no aluminum was recovered, and up to 10 μg was adsorbed by the gel. From this, it can be concluded that some of the so-called "free" aluminum found by sera speciation (e.g., fraction III) is complexed. Possible ligands are phosphate, carbonate, citrate, oxalate and fluoride. The possible formation of mixed-ligand complexes should not be excluded [8]. The lowest-molecular-weight fraction (fraction III) found in filtrate and in Earle's medium probably consists of (mixed) inorganic aluminum complexes. The other low-molecular-weight fraction (fraction II) found in filtrate and also in sera is not likely to be "free" aluminum (which adsorbs almost irreversibly onto the gel) such as Al^{3+}, $Al(OH)_4^-$, $Al(OH)_3$, $Al(OH)^{2+}$ and $Al(OH)_2^+$ but consists most probably of organic aluminum

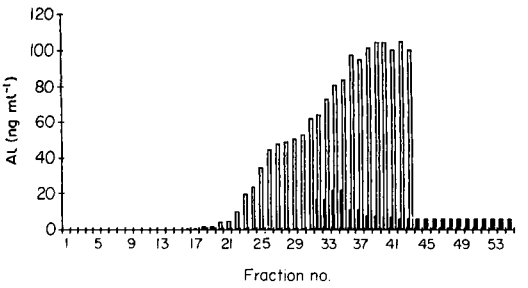

Fig. 3. Breakthrough curve for a filtrate (open bars, 110 μg Al l^{-1}) and an Earle's medium (filled bars, 200 μg Al l^{-1}).

complexes. The lowest-molecular-weight fraction (fraction III) was not recovered during speciation of sera, possibly because of the great binding affinity of the protein fraction for "free" aluminum.

The results obtained during the "desorption" experiments are given in Table 7. It is clear that large amounts of aluminum can be taken up by serum. Concentrations up to 2100 ng ml^{-1} were measured of which 64% was freed with fraction I (Fig. 1). Also filtrate "captured" up to 1900 ng ml^{-1} in fraction II, which is 2.6 times the amount found in the same fraction when serum was applied. Earle's medium freed much less aluminum, all of it in fraction III. It can therefore be stated that fractions I and II show a high affinity towards "free" aluminum and that the low-molecular-weight fraction II found in serum cannot be considered as "free" aluminum, but is possibly bound to an organic compound. However, when the two fractions are present together, as in serum, competition will occur between those two aluminum-binding components which can result in a decrease of the aluminum content of the low-molecular-weight fraction and an increase of the aluminum content in the protein fraction. This can explain the absence of aluminum in fractions II and III in the speciation of normal sera with low aluminum contents. For the same reason, fraction III will always be very low in sera samples. However, the fact that this third fraction was never detected during sera speciation, not even in samples containing large concentrations of aluminum, confirms the high affinity of the protein fraction for aluminum. No aluminum was transferred to a normal "blank" serum which was applied to a column which had first been in contact with large volumes of aluminum-spiked filtrate. The intrinsic aluminum was eluted only in fraction I. This also proved that no redistribution takes place from fractions II or III towards fraction I.

It can be concluded that gel filtration is a valid technique for studying the speciation of aluminum in biological fluids, because the overall mass balance is acceptable and no redistribution of aluminum seems to occur during the procedure. By using P4 gel, two peaks can be detected in sera, while a third peak is found in solutions which do not contain protein. No free

aluminum was detected in sera with aluminum concentrations up to 110 μg l^{-1}, either because of its absence or because it adsorbs on the column. Aluminum contamination of the eluent buffer is the major cause of erroneous results. Sodium chloride seems preferable as an eluent, because other buffers (e.g., Earle's medium) are able to bind aluminum and can be responsible for an additional peak.

This study was supported by a grant from the Belgian Medical Research Council, N.F.W.O.

REFERENCES

1 S. W. King, J. Savory and M. R. Wills, Crit. Rev. Clin. Lab. Sci., 14 (1981) 1.
2 H. Rahman, S. M. Channon, A. W. Skillen, M. K. Ward and D. N. S. Kerr, Proc. EDTA-ERA, 21 (1984) 360.
3 H. Rahman, S. M. Channon, I. S. Parkinson, A. W. Skillen, M. K. Ward and D. N. S. Kerr, Clin. Nephrol., 24 (suppl. 1) (1985) S78.
4 H. Rahman, S. M. Channon, A. W. Skillen, M. K. Ward and D. N. S. Kerr, Trace Elem. Med., 2 (1985) 143.
5 H. Rahman, A. W. Skillen, S. M. Channon, M. K. Ward and D. N. S. Kerr, Clin. Chem., 31 (1985) 1969.
6 H. L. Elliott, A. I. Macdougall, G. S. Fell and P. H. E. Gardiner, Lancet, 11 (1978) 1255.
7 F. Y. Leung, A. B. Hodsman, N. Muirhead and A. R. Henderson, Clin. Chem., 31 (1985) 20.
8 P. E. Gardiner, M. Stoeppler and H. W. Nürnberg, in P. Brätter and P. Schramel (Eds.), Trace Elements — Analytical Chemistry in Medicine and Biology, Vol. 3, Walter de Gruyter, Berlin, 1984, p. 298.
9 M. A. Burnatowski-Hledin, G. H. Mayor and K. Lau, Am. J. Physiol., 249 (1985) F192.
10 A. P. Lundin, C. Caruso, M. Sass and G. M. Berlyne, Clin. Res., 26 (1978) 63.
11 R. L. Bertholf, M. R. Wills and J. Savory, Clin. Physiol. Biochem., 3 (1985) 271.
12 G. A. Trapp, Life Sci., 33 (1983) 311.
13 M. Cochran, D. Patterson, J. H. Coates and P. T. H. Coates, in P. Brätter and P. Schramel (Eds.), Trace Elements — Analytical Chemistry in Medicine and Biology, Vol. 3, Walter de Gruyter, Berlin, 1984, p. 311.
14 J. Smeyers-Verbeke, D. Verbeelen and D. L. Massart, Clin. Chim. Acta, 108 (1980) 67.

Analytica Chimica Acta, 196 (1987) 115—122
Elsevier Science Publishers B.V., Amsterdam — Printed in The Netherlands

INFLUENCE OF TEMPERATURE IN REVERSE-PHASE HIGH-PERFORMANCE LIQUID CHROMATOGRAPHY WITH GRADIENT ELUTION

C. VISERAS, R. CELA*, C. G. BARROSO and J. A. PEREZ-BUSTAMANTE
Analytical Chemistry Department, Faculty of Sciences, University of Cadiz (Spain)
(Received 4th August 1986)

SUMMARY

The influence of temperature on the retention of several species separated by reverse-phase liquid chromatography by gradient elution is shown to be of enough importance to warrant careful control of temperature if reproducible results are to be obtained. The smaller the particle size in the column, the greater the effect of temperature, and therefore the control should be greater. Likewise, it has been verified that for a given solvent gradient, independent of its complexity, there is a linear relation between $\ln k'$ and $1/T$, which also occurs in separations by isocratic elution. Dufek's equation can be adjusted perfectly to the experimental data obtained from gradient elutions, and may be used in the simulation and optimization of gradient chromatographic processes.

In order to improve the efficiency of reverse-phase high-performance liquid chromatography (HPLC), it is necessary to consider the combined effect of the composition of the mobile phase and the column temperature on solute retention. The effect of varying the composition of the mobile phase is extremely helpful for the separation of complex mixtures. The use of more or less complicated gradients allows the resolution of peaks to be improved. Likewise, by controlling the temperature factor in such elutions, the reproducibility and selectivity of the chromatographic process can be improved.

The influence of temperature on solute retention in reverse-phase HPLC has mainly been studied in isocratic solutions [1—7]. In most of these studies, however, homologous series have been used to establish a correlation between retention and the number of carbon atoms in the solute molecule for each particular series. These studies agree that the relationship between the logarithm of the capacity factor (k') and the reciprocal of absolute temperature is linear, even over wide temperature intervals. Melander et al. [1—3] proposed an extrathermodynamic equation and a thermodynamic model [3] supporting the former, to explain the observed relationship between retention and temperature. This equation has also been verified by Vigh and Varga-Puchony [4]. Other authors [6, 7] have established another series of equations which relate temperature to the composition of the mobile phase, and the number of carbon atoms in the molecules of the homologous series.

0003-2670/87/$03.50

In theory, all these equations could not be applicable to gradient elutions, as the composition of the mobile phase varies during elution and this parameter is considered to be a constant in all the equations proposed. However, these models may be extended to gradient elutions, assuming that these behave similarly to isocratic elutions, if the same gradient is used in the study of the influence of temperature. This would allow the temperature factor readily to be included into the optimization of gradient elutions.

Unfortunately, no data are available in the literature concerning the extent of the influence of temperature on solute retention in gradient elutions, although it is almost certainly important. In practice, gradient elutions are used when the objective is to decrease separation time and increase efficiency, or when the solute mixture is too complex to be dealt with by isocratic separation. The variation in solute retention times owing to variations in temperature may provoke the cross-over or overlapping of peaks, thus invalidating laboriously developed methods. These problems are more likely to appear with more complex gradients (e.g., stepwise gradients). Common practice is to work at constant temperature to avoid such problems. Nevertheless, it is necessary to choose the temperature carefully, depending on the species to be separated. It is clear that if variation in retention times of species in gradient elutions is linear with temperature, the choice will be made considerably easier, as any of the optimization techniques proposed in the literature may be used [8]. Likewise, it is interesting to establish up to which point such an influence depends on the type of column or particle size, and therefore, up to which point the optimization of this parameter is critical for any particular working conditions. In the present paper, the influence of temperature on the gradient elution of 22 polyphenolic acids has been studied for two column types with different particle sizes.

EXPERIMENTAL

Waters HPLC equipment was used, comprising two pumps (M6000A and M45), a universal injector UK-6, a gradient programmer M680, and an M440 double-channel detector with absorbance filters of 280 and 340 nm, an Omniscribe printer and a Perkin-Elmer Sigma-15 data station. Two types of columns were used: a Waters μBondapak C18 (30 cm × 3.9 mm, particle size 10 μm) and a Waters Novapak C18 (15 cm × 3.9 mm, particle size 5 μm).

The polyphenolic acids used were from Fluka, Eastman and Merck (all >97% purity). These acids were dissolved in methanol/water mixtures (according to their solubility) in concentrations ranging from 4 to 60 μg ml^{-1}, so as to obtain adequate responses from the detector. The solvents used (HPLC grade) were filtered through 0.45-μm filters (Millipore) and degassed for 30 min in an ultrasonic bath (Selecta).

The columns and solvents were thermostatted in a bath with a Selecta cryostat. The chromatographic conditions were as follows. The mobile phase

TABLE 1

Elution programs[a]

Novapak column				μBondapak column			
Time (min)	% A	% B	Curve	Time (min)	% A	% B	Curve
0.00	100	0	—	0.00	100	0	—
9.38	100	0	1	5.00	100	0	9
22.78	87	13	1	16.33	70	30	9
37.00	75	25	1	24.33	70	30	1
49.66	62	38	1	25.88	50	50	9
59.39	50	50	1				

[a]For A and B, see text.

was solvent A [2% acetic acid, 10% methanol in water (v/v)] or solvent B [2% acetic acid, 90% methanol in water (v/v)]. The solvent flow-rate was 1 ml min^{-1}, and the detection sensitivity, 0.05 absorbance full scale. The elution programs are given in Table 1.

RESULTS AND DISCUSSION

The starting point for this study lay in the observation of variations in the retention times of a group of 22 phenolic acids, for which a plan for gradient separation had empirically been drawn up as described in Table 1 (μBondapak C18 column) [9]. This gradient had been used routinely in a non-thermostatted system. Variations in the retention times, which sometimes provoked changes in selectivity giving rise to the overlapping of species which obviously hindered their correct quantitation, had often been observed in the non-thermostatted system. It was also decided that a more efficient column of smaller particle size (Novapak) should be tried, so as to improve the separation of these 22 species.

Attempts to use this second procedure routinely gave much greater variations in retention times than those obtained with the former column, even to such an extent that 25—30% of the species in the mixture could not reliably be quantified. After making allowance for the variability which could be put down to other parameters (faults in the instrumental system, variations in the composition of the mobile phases, etc.), it was decided that the effects of temperature on separation should be studied. For this, the mixture of 22 species was eluted with the gradients developed for each of the two columns, within 14—29°C, at intervals of 2°C. In cases where peak overlapping was detected, the mixture was split into simpler mixtures in order to obtain accurate retention times. Retention-time data obtained for each species and temperature were transformed to ln k' values and least-squares plots vs. the reciprocal of absolute temperature were obtained. The results of these calculations for both columns are included in Table 2 and shown in Fig. 1. Some interesting features may be observed.

TABLE 2

Correlation coefficients (r^2), slopes and intercepts of plots in ln k' vs. $(1/T) \times 10^{-3}$ for the elution of phenolic acids from a μBondapak C18 column and a Novapak column

No.	Acid	μBondapak column			Novapak column		
		r^2 [a]	Slope	Intercept	r^2 [a]	Slope	Int
1	3,4,5-Trihydroxybenzoic	0.9974	2.70	−9.07	0.9944	3.34	−11
2	2,4,6-Trihydroxybenzoic	0.9977	3.03	−9.38	0.9864	5.33	−18
3	2,4-Dihydroxybenzoic	0.9941	2.45	−7.32	0.9982	2.99	−9
4	3,5-Dihydroxybenzoic	0.9972	2.69	−8.08	0.9940	3.53	−11
5	2,5-Dihydroxybenzoic	0.9931	2.32	−6.26	0.9983	3.12	−9
6	4-Hydroxybenzoic	0.9930	1.92	−4.84	0.9985	2.84	−8
7	2,6-Dihydroxybenzoic	0.9995	1.45	−3.18	0.9981	3.20	−10
8	3-Hydroxybenzoic	0.9958	0.99	−1.52	0.9970	2.85	−7
9	2,4-Dihydroxybenzoic	0.9988	0.95	−1.32	0.9986	3.26	−9
10	4-Hydroxy-3-methoxybenzoic	0.9925	0.67	−0.38	0.9967	2.85	−7
11	2,6-Dimethoxybenzoic	0.9798	0.40	0.58	0.9885	2.17	−4
12	3,4-Dihydroxycinnamic	0.9898	0.72	−0.49	0.9988	3.55	−9
13	3,5-Dimethoxy-4-hydroxybenzoic	0.9867	0.60	−0.63	0.9924	1.75	−3
14	4-Hydroxycinnamic	0.9905	1.03	−1.36	0.9959	1.95	−3
15	2,4-Dimethoxybenzoic	0.9915	0.50	−0.56	0.9954	1.64	−2
16	4-Hydroxy-3-methoxycinnamic	0.9902	0.90	−0.84	0.9942	1.74	−3
17	3-Hydroxycinnamic	0.9922	0.86	−0.68	0.9961	2.13	−4
18	3,4-Dimethoxybenzoic	0.9945	0.78	−0.43	0.9961	2.13	−4
19	2-Hydroxycinnamic	0.9920	0.43	0.83	0.9868	1.70	−2
20	3,5-Dimethoxy-4-hydroxycinnamic	0.9909	0.75	−0.32	0.9941	1.83	−3
21	3,5-Dimethoxybenzoic	0.9817	0.52	0.65	0.9897	1.37	−1
22	3,4,5-Trimethoxycinnamic	0.9992	0.38	1.10	0.9954	1.20	−0

[a] 5 points.

In all cases, irrespective of the type of column or gradient configuration, linear relationships are obtained between ln k' and $1/T$ (van't Hoff graphs), just as for isocratic elution. In general, the slope decreases with increasing affinity of the compound for the stationary phase, the decrease being greater for all species on the 5-μm column; important changes are produced in the order of elution of several compounds. Figure 1 shows the occurrence of several peak cross-overs between different species. For instance, peaks 3 and 4 show cross-over for the two types of column. While peak 3 hardly changes its behaviour as a function of column type, peak 4 shows a much greater variation in retention in the μBondapak column, so that it is possible, by using this column, to obtain a good resolution of this pair of peaks at temperatures higher than 23°C.

Some peaks show important behavioural differences as a function of column type (e.g., peak 15) but their behaviour as a function of the temperature remains very similar no matter which column is used. Although the temperature range considered is relatively small and corresponds approximately to a normal temperature range in laboratories that are not thermally conditioned,

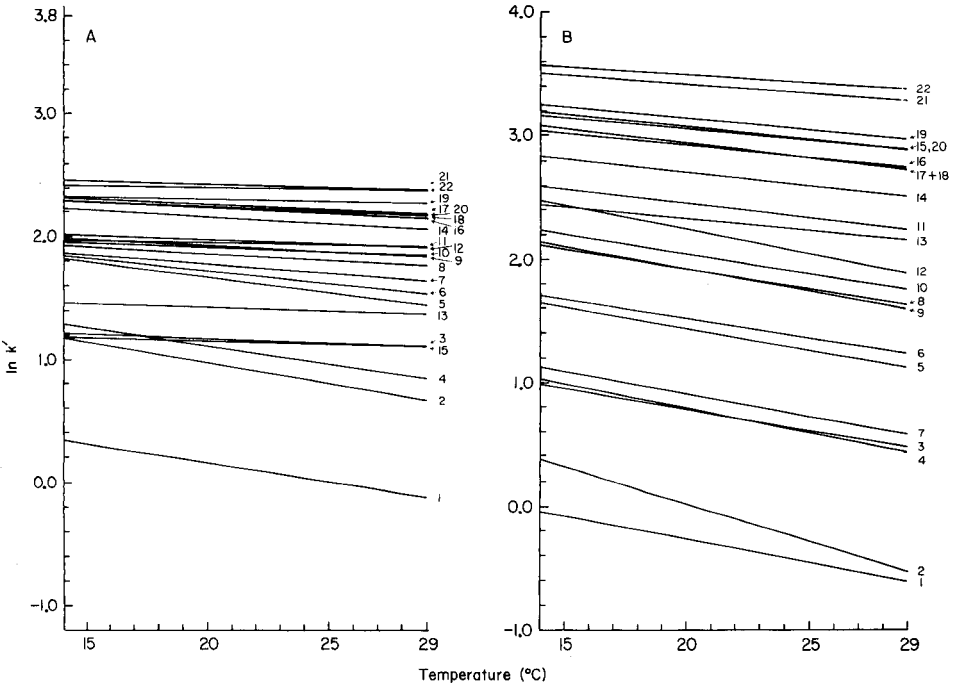

Fig. 1. Plots of ln k' vs. T for phenolic acids: (A) μBondapak column; (B) Novapak column. (See Table 2 for key to compounds.)

the effect on absolute and relative peak retention is considerable. Thus, several species change their retention times by more than 5 min over the temperature interval considered. This can be seen in Table 3, where retention time data for each species in the temperature range considered, as well as the absolute variation and the percentage variation of k' in this range (referred to the maximum value of k' obtained in each case) are collected for the two types of column. Given that the influence of temperature is much greater when 5-μm columns are used, a much more careful control of temperature will be needed in such cases.

The linearity of the relationship might have important consequences from the point of view of the optimization of gradient separations, given that once the most appropriate gradient program has been chosen for the resolution of a mixture, three or four experiments at different temperatures may help to establish the optimum working temperature with that particular gradient and the temperature margin in which the gradient will give satisfactory results. This will help to decide the temperature variation allowed in each case. Temperature could also be included in sequential optimization schemes based on simulation methods, taking advantage of this linear relationship.

The above linear variation of retention with reciprocal temperature in

TABLE 3

Values of retention time and increases in k' as a function of temperature and column[a]

Acid	μ-Bondapak				Novapak			
	t_R (min)		$\Delta k'$	$\Delta k'$ (%)	t_R (min)		$\Delta k'$	$\Delta k'$ (%)
	15°C	29°C			14°C	29°C		
1	7.51	5.91	0.50	36.2	2.40	1.88	0.42	44.2
2	13.25	9.39	1.23	38.3	2.94	1.88	0.86	61.8
3	13.51	10.04	1.10	33.4	4.41	3.05	1.14	43.5
4	14.47	10.48	1.26	35.1	4.63	3.15	1.27	44.9
5	22.15	16.11	1.92	31.8	7.61	4.96	2.20	42.1
6	22.62	17.25	1.70	27.5	8.09	5.43	2.25	39.7
7	23.43	19.14	1.36	21.1	5.06	3.43	1.34	42.8
8	24.88	21.53	1.07	15.5	11.35	7.26	3.43	41.2
9	25.68	22.58	0.98	13.7	11.82	7.49	3.63	41.6
10	25.37	22.96	0.76	10.8	12.76	8.28	3.83	40.1
11	25.68	24.35	0.42	5.9	17.39	12.25	4.36	32.7
12	26.51	23.89	0.84	11.3	15.85	11.62	3.53	29.5
13	27.04	24.83	0.70	9.2	15.50	9.23	5.23	44.6
14	32.41	27.80	1.46	15.7	22.77	16.52	5.14	29.2
15	34.71	32.11	0.83	8.3	29.75	22.67	5.80	24.9
16	33.81	29.79	1.27	13.0	26.96	19.89	5.84	27.8
17	34.24	30.33	1.24	12.6	28.47	19.89	7.04	31.7
18	33.47	29.85	1.15	11.9	28.47	19.89	7.04	31.7
19	35.66	33.43	0.71	6.9	22.29	24.34	6.5	25.7
20	34.10	30.69	1.09	11.1	30.52	22.67	6.42	26.9
21	40.07	37.05	0.96	8.2	43.37	33.96	7.67	22.4
22	38.73	36.57	0.69	6.1	44.33	36.60	6.31	18.0

[a]See Table 2 for identity of acids. t_R is retention time.

gradient elutions suggests that the equations developed for isocratic elution would be equally valid in this case. Amongst these equations, that of Dufek [7] is probably one of the simplest and most efficient for the calculation of capacity factors as a function of temperature:

$$\log k'_3 = \log k'_1 + \log (k'_2/k'_1)\,(1/T_3 - 1/T_1)/(1/T_2 - 1/T_1) =$$

$$\log k'_1 + \log (k'_2/k'_1)\,(T_2\ (T_1 - T_3)/T_3\ (T_1 - T_2))$$

where k'_1 and k'_2 are the capacity factors for a given compound measured at two different temperatures (T_1 and T_2), respectively, and k'_3 is the capacity factor of this compound at the temperature of interest (T_3) in the interval of temperatures defined by T_1 and T_2. This equation permits the prediction of capacity factors by carrying out only two measurements, with an error no greater than 3%, and therefore within the experimental errors characteristic of liquid chromatography. Given that this equation does not require the calculation of specific coefficients dependent on the nature of the compound or the column, and given that Dufek affirms its general applicability (i.e., it

is not restricted to homologous series) it was of interest to verify to what extent this equation holds true for the 22 considered species in the two columns used and with the gradients described in Table 1.

For this purpose, a computer program was developed to check the extent of agreement of the available data with Dufek's equation for all the possible combinations of temperature values in the considered range (14—29°C). For each peak, the program selects two values of temperature, and with the k' data for these temperatures, the Dufek equation was applied to obtain the k' values for the rest of the temperature data. The results of these calculations in each case were compared with the experimental values of k' for the corresponding temperature, thus establishing the absolute differences between the calculated and experimental data and also the relative error at each temperature of the value given by Dufek's equation, according to the expression $100\ (k'\ (\text{exp.}) - k'\ (\text{calc.}))/k'\ (\text{exp.})$. A new pair of temperatures is chosen and the process is continued in the same manner until all possible combinations of pairs of temperature values have been used.

The results of these calculations were expressed in a histogram, representing the percentage of trials which led to a specific relative error (between 0.1 and 12%) compared with the experimental data. These histograms are reproduced in Fig. 2 for the two columns considered. With the μBondapak column, a very high degree of agreement with the equation is observed. Approximately 90% of the combinations tried gave errors less than or equal to 3%, and in no case were errors above 12% found. The maximum in the error distribution is at 3%, precisely the value given by Dufek [7]. Analogous results, although exhibiting somewhat lesser agreement, were obtained with the Novapak column, so that it can be affirmed that Dufek's equation can be used to predict the effect of temperature on gradient elutions, or can be introduced in simulation models for the optimization of HPLC gradient separations, no matter what the complexity of the separations or the particle size of the chromatographic column.

The present work was made possible by the financial support of the Spanish Ministry of Education and Science (CAYCIT) through project (1189/84) and the collaboration of Bodegas Osborne and Cia (Puerto de Santa Maria, Spain).

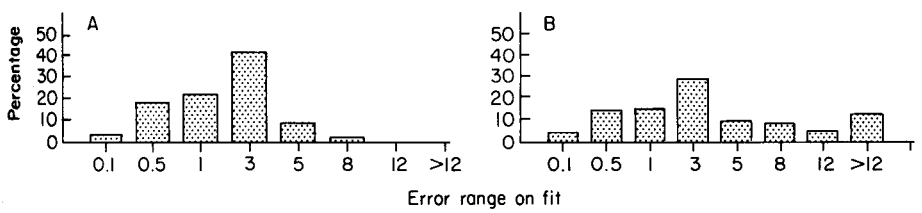

Fig. 2. Histograms of the relative error between the experimental data and those obtained through Dufek's equation: (A) μBondapak column; (B) Novapak column.

REFERENCES

1 W. R. Melander, B.-K. Chen and Cs. Horvath, J. Chromatogr., 185 (1979) 99.
2 W. R. Melander, C. A. Mannan and Cs. Horvath, Chromatographia, 15 (1982) 611.
3 W. R. Melander and Cs. Horvath, Chromatographia, 18 (1984) 353.
4 G. Vigh and Z. Varga-Puchony, J. Chromatogr., 196 (1980) 1.
5 H. Poppe and J. C. Kraak, J. Chromatogr., 282 (1983) 399.
6 E. Grushka, H. Colin and G. Guiochon, J. Chromatogr., 248 (1982) 325.
7 P. Dufek, J. Chromatogr., 299 (1984) 109.
8 L. de Galan, Trends Anal. Chem., 4 (1985) 62.
9 C. G. Barroso, R. Cela and J. A. Perez-Bustamante, Chromatographia, 17 (1983) 249.

Analytica Chimica Acta, 196 (1987) 123—134
Elsevier Science Publishers B.V., Amsterdam — Printed in The Netherlands

HIGH-RESOLUTION/HIGHER-ORDER DERIVATIVE SPECTROPHOTOMETRY FOR IDENTIFICATION AND ESTIMATION OF SYNTHETIC ORGANIC PIGMENTS IN ARTISTS' PAINTS

G. TALSKY* and MAJA RISTIĆ-ŠOLAJIĆ[a]

Institut für Technische Chemie, Lehrstuhl I, Technische Universität München, D-8046 Garching (Federal Republic of Germany)

(Received 4th August 1986)

SUMMARY

Twenty-two pigments commonly used in artists' paints were investigated by recording the fourth-derivative (d^4) ultraviolet-visible spectra. Dimethyl sulphoxide was used as a universal solvent. It was possible to distinguish pigments which were chemically very similar and of the same colour, and to quantify the components of binary mixtures without separation by using side-peak-side ratio computations. Acrylic or oil media had no influence on the derivative spectra. For mixtures of more than two components, the pigments were separated by thin-layer chromatography and the d^4-spectra were recorded directly from the developed spots; 10 ng of each pigment in 5 μl of solvent was enough for the analysis.

Since ancient times, insoluble coloured substances have been used for paintings. Mostly they were of mineral origin and dispersed in oil or water. Such pigments, e.g., oxides of iron, chrome and lead, allowed only a limited range of hues; they had good light resistance but were prone to the influence of environmental agents. In 1856, Perkin developed mauveine, the first synthetic organic dye. Since then, about 500 pigments, 400 of which are organic substances, have been synthesized. In the last 50 years, some 250 pigments have been produced commercially and over 60 of these have been identified in modern artists' paints.

Structural knowledge of the paints used is of great significance in solving the growing number of problems involved in the conservation and restoration of paintings as well as their authenticity, dating and originality. Often there is available only a minute sample from the edge or damaged area of a work of art, so that microanalytical methods are necessary for investigations. Many different ways have been reported for solving such problems. The most important of these are microscopic crystal identification, melting point determinations, chemical reactions (spot tests), infrared spectroscopy, x-ray

[a]On leave from National Museum, Belgrade (Yugoslavia).

0003-2670/87/$03.50

powder diffraction, thin-layer chromatography (t.l.c.), ultraviolet/visible spectroscopy and reflectance spectroscopy.

Ultraviolet-visible spectrophotometry is a relatively simple method and is often used for determining the concentration of known substances. But it is seldom used to identify unknown samples because many dissolved chemicals, liquids and especially solids give less characteristic electron excitation spectra with more or less well developed maxima and shoulders. To resolve such signals, higher-order derivative spectroscopy ($n > 2$) [1] is very suitable. One does not evaluate the primary absorption spectrum but the slope of the curves in dependence on the wavelength. All existing maxima and minima are sharpened, the shoulders and inflection points are resolved to maxima and minima, and unwanted background is eliminated [1—3].

In this paper, the fine resolution of spectra from different pigments in solution as well as adsorbed on thin layers of silica by using derivative spectrophotometry will be discussed.

EXPERIMENTAL

Materials and apparatus

Pigment powders and materials in tubes were supplied by the firms Talens (The Netherlands) and Hoechst (F.R.G.). Dimethyl sulphoxide (Uvasol, Merck) was used.

All absorption spectra and derivatives, up to the fourth order, were recorded with a PU-8800 spectrophotometer (Philips/Pye Unicam, Cambridge). For investigations of turbid solutions or opaque t.l.c. layers, this instrument was fitted with a second sample holder in front of the end-on multiplier. The noise of the output signals affecting the differentiation was eliminated by means of home-made higher-order low-pass analog filters or by a digital multifunction signal processor (Oriel, Stamford, CT). Digital differentiations up to the sixth order, manipulation, and storage of spectra on floppy disks were done by an intelligent plotter (BS 8110; Bascom-Turner Institute, Newton, MA).

Procedures

Derivative spectra in solution. All organic pigments were dissolved in dimethyl sulphoxide (DMSO) with the help of an ultrasonic bath (40°C; 5 min). Generally, the pigment concentration was about 25 μg ml^{-1} but for PR-4 and PO-5 (see Table 1) only 12.5 μg ml^{-1} was used, and for PG-7 and PY-100 about 300 μg ml^{-1} was better. A solution volume of 2 ml was needed for normal 1-cm Suprasil cells (Hellma); for microcells, 10—100 μl was enough. DMSO was used in the reference cell. The samples from tubes were prepared at a concentration of 300 μg ml^{-1}; sometimes it was necessary to filter them through Whatman glass microfibre filters (GF/A).

The conditions for spectrophotometry were: 850—200 nm, light pass thickness 10 mm, scan rate 10 nm s^{-1}, slit 1 nm, span 2, scale 20 nm s^{-1}, and response 5 s.

Thin-layer chromatography. Portions (5 μl) of the solution of the organic pigments in DMSO were spotted on a Polygram Sil-G plate (Macherey-Nagel; silica gel, 0.25 mm thick on a polyester sheet) and the spots were developed with benzene/chloroform/cyclohexane (25:50:25; solvent system 4) for 45 min [4]. Generally, the concentration of pigments was 25 μg ml^{-1}; for PY-1 and PY-3 (see Table 1) 150 μg ml^{-1} was better, and for samples from tubes, the optimal concentration was ca. 2 mg ml^{-1}.

Derivative spectra of t.l.c. spots. The developed spots were cut out and placed between two silica plates in a special 1-cm cell holder (Hellma) in front of the end-on multiplier of the PU-8800. A pure t.l.c. sheet was used as the reference. Then the derivatives of the absorption were recorded. The conditions for spectrophotometry were 850—300 nm, scan rate 10 nm s^{-1}, slit 1 mm or high energy, span 2, scale 20 nm s^{-1} and response 5 s.

RESULTS

Altogether 22 different pigments of different chemical types were investigated; the pigments were present in powders and also dispersed in oil or acrylic media. The substances are listed in Table 1.

Ultraviolet-visible spectrophotometry in solution

In 1889, Bamberger and Bordt [7] were the first to recognize that the solution spectrum of a dye was characteristic of its chemical structure. Formanek [8] and later Abbott and Stearns [9] proposed a systematic scheme for the identification of dyes. Saltzman and co-workers [10—12] used the different solubilities of the many classes of organic pigments for separation before identification. Nevertheless, spectrophotometry was not much applied to artists' materials, probably because of a lack of collections of reference spectra and because of the absence of truly characteristic features in the spectra.

Some years ago, higher-order derivative spectrophotometry was used here for simultaneous quantitative estimation of dye mixtures [1] and for their identification [13]. Therefore, this technique offered good prospects for successful investigations of artists' paints.

In 1889 the use of concentrated sulphuric acid as a very powerful solvent for pigments was noted by Vogel [14]; it dissolves virtually all known organic pigments [12] but its application is not very convenient. Billmeyer et al. [12] described a few solvents suitable for all pigment groups. Milovanović et al. [4] used DMSO as a universal solvent for their investigations of synthetic organic pigments in artists' paints by t.l.c. This solvent was also preferred in the present studies because it was capable of dissolving or dispersing all the pigments cited in Table 1. Depending on the absorptivity and on the cell volume, 20—300 μg of the sample was enough for measuring the spectra.

Order of differentiation. First there is the question of which order of differentiation is most suitable. Previous investigations up to the ninth order

TABLE 1

List of investigated pigments most used in artists' paints[a]

Generic name	Abbreviation	Constitution number	Pigment type	Date of introduct
Pigment Yellow 1	PY-1	11680	Monoazo-acetoacetarylide	1909
Pigment Yellow 3	PY-3	11710	Monoazo-acetoacetarylide	1911
Pigment Yellow 17	PY-17	21105	Bisazo-acetoacetarylide	
Pigment Yellow 97	PY-97	11767	Monoazo-acetoacetarylide	after 195'
Pigment Yellow 100	PY-100	19140:1	Metal monoazo salt	1884
Pigment Yellow 110	PY-110		Azamethine pigment (isoindolinone)	1964
Pigment Orange 1	PO-1	11725	Monoazo-acetoacetarylide	1926
Pigment Orange 5	PO-5	12075	Monoazo-2-naphthol	1907
Pigment Orange 43	PO-43	71105	"Vat pigment" (perinone)	1924
Pigment Red 4	PR-4	12085	Monoazo-2-naphthol	1907
Pigment Red 7	PR-7	12420	Monoazo-2-hydroxy-3-naphtharylide	1907
Pigment Red 12	PR-12	12385	Monoazo-2-hydroxy-3-naphtharylide	1921
Pigment Red 83	PR-83	58000	"Vat pigment" (anthraquinone)	1869
Pigment Red 112	PR-112	12370	Monoazo-2-hydroxy-3-naphtharylide	
Pigment Red 122	PR-122	73915	Quinacridone	1955
Pigment Brown 25	PBr-25	12510	Benzimidazolone	1960
Pigment Violet 19	PV-19	46500	Quinacridone	1955
Pigment Violet 23	PV-23	51319	Dioxazine	1935
Pigment Blue 15	PB-15	74160	Phthalocyanine	1928—19
Pigment Green 7	PG-7	74260	Phthalocyanine	1935
Pigment Green 8	PG-8	10006	Miscellaneous metal complex pigments	1921
Pigment Green 36	PG-36	74265	Phthalocyanine	

[a]The data given are from the Colour Index [5] and the Pigment Handbook [6].

indicated that for each problem there is an optimal order depending on the shape of the spectrum. Mostly, the third to sixth orders give the best results [1, 2]. Generally, the optimal conditions are reached if all shoulders and points of inflections are resolved into maxima or minima. The derivative spectra of Pigment Yellow (PY-1) up to the sixth order are given in Fig. 1. It can be seen that increasing fine resolution of the signals was achieved.

The normal u.v.-visible spectra of pigments from different classes (Fig. 2) showed only more or less flat curves, whereas the fourth-derivative (d^4) spectra showed maxima and minima and were quite similar to infrared (i.r.) fingerprint spectra.

Classification of pigments. In further studies, pigments which were chemically different but of the same colour were classified. The group of four red pigments may serve as an example. Figure 3 shows that the d^4-spectra are very suitable for the identification of unknown samples; PR-4 is a monoazo-2-naphthol, PR-12 is a 2-hydroxy-3-naphtharylide, PR-83 is an anthraquinone and PR-122 is a quinacridone.

Pigments with the same colour which were chemically similar were then tested. The chemical formulae of PY-1 and PY-3 are very similar. These two yellow pigments can provide an illustration of the use of small spectral differences (Fig.4). Qualitatively, there is a difference between the two d^4-spectra, especially in the heights of the peaks at 385 nm and 353 nm, and in the shift

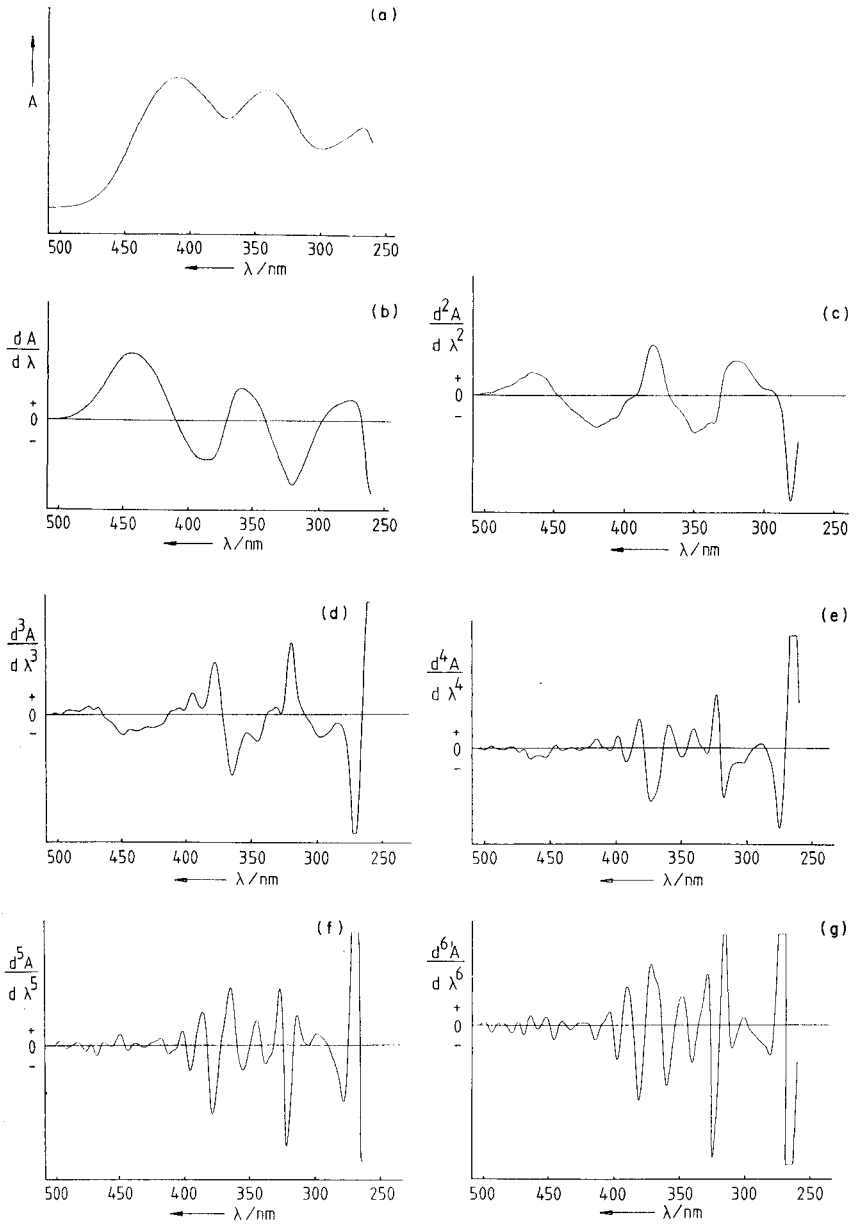

Fig. 1. Absorption spectrum (ground spectrum) of Pigment Yellow 1 (PY-1) and 1st to 6th derivatives.

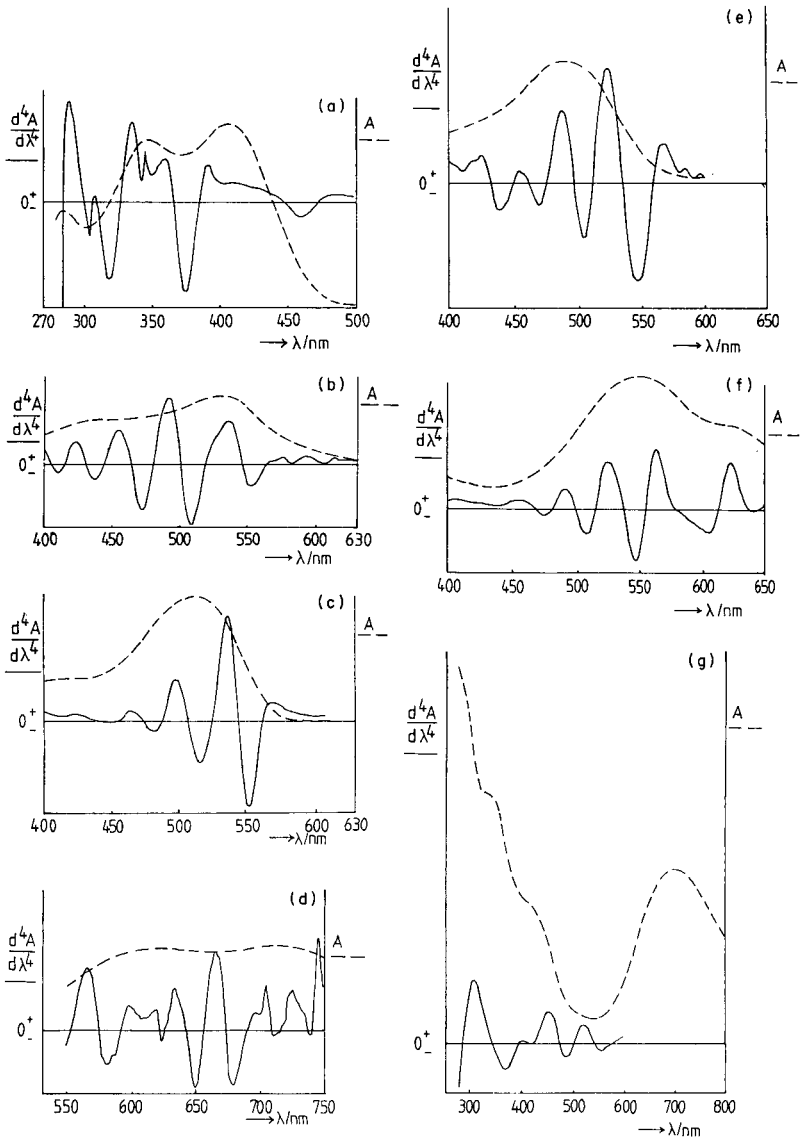

Fig. 2. Absorption spectra and 4th derivatives for different pigments: (a) PY-1; (b) PO-43; (c) PR-7; (d) PB-15; (e) PBr-25; (f) PV-23; (g) PG-8.

of the peak from 460 to 450 nm (PY-1 → PY-3). For quantitative purposes, the side-peak-side evaluation (SPS method; Table 2 and Fig. 5) and its line diagrams (Fig. 6) were very suitable.

It was important to check whether or not there was any influence of the acrylic or oil media on the derivative spectra (Fig. 7). After normalizing by

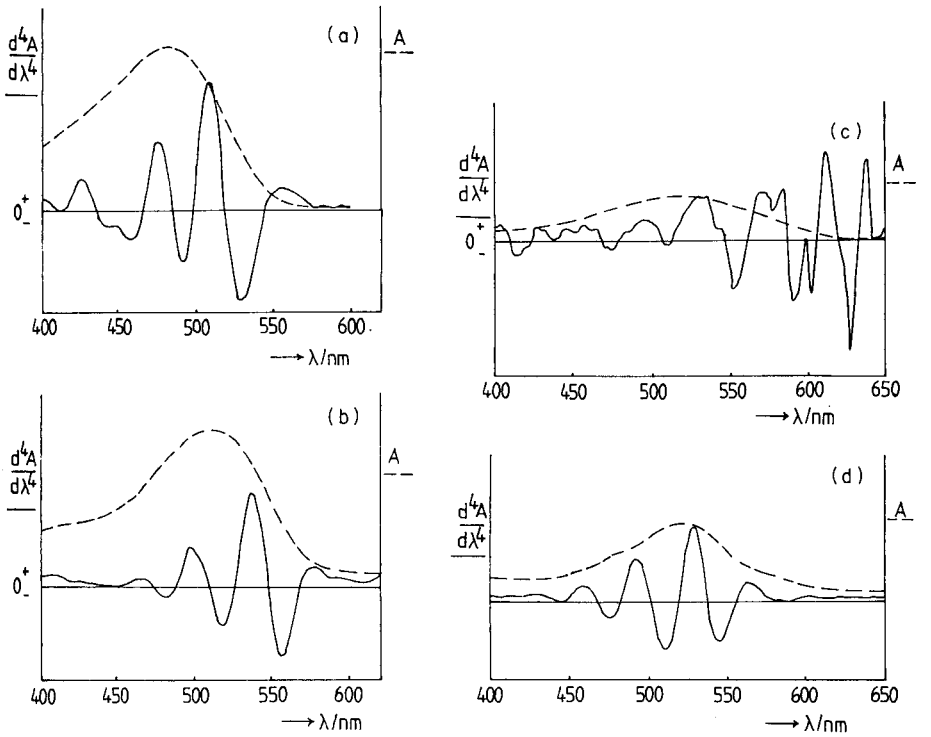

Fig. 3. Absorption spectra and 4th derivatives for four red dyes: (a) PR-4; (b) PR-12; (c) PR-83; (d) PR-122.

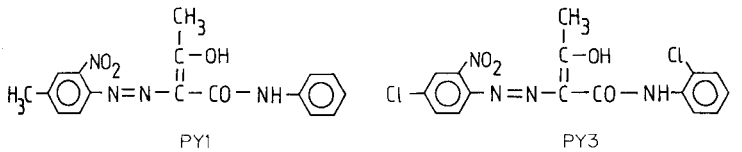

SPS evaluation, the d^4-spectra were practically the same (Fig. 8) down to 300 nm; below this wavelength, higher deviations were caused by the additives or media.

Quantitative estimation of two-component mixtures. Given a mixture of two chemically similar pigments with the same colour in oil or acrylic medium, it is possible to estimate the concentrations of both components simultaneously by higher-order derivative spectrophotometry without separation. First, the spectra of pure pigments and artificial mixtures of them are recorded, then the SPS ratios are calculated and a calibration line is drawn. The values for the peaks at 354 nm and 346 nm are shown in Fig. 9 for PY-1 and PY-3. The SPS ratio of the sample from the paint tube at 354 nm (5.29) indicates a composition of 45.8% PY-1 and 54.2% PY-3.

TABLE 2

SPS ratio calculation for PY-1 and PY-3. Maxima are indicated by plus signs and minima by minus signs

λ (nm)	460	387	369	355	344	334	320	306	298	287
SPS ratio PY-1	0.9/0.8	0.8/5.2	5.15/5.4	5.4/0.75	0.75/2.95	2.95/6.4	6.4/3.4	3.4/3.2	3.2/4.6	4.7/15.2
	−1.1	+0.15	−0.95	+7.2	−0.25	+0.46	−1.88	+1.06	−0.69	+0.31
λ (nm)	450	384	367	353	342	330	314	302	295	287
SPS ratio PY-3	1.0/1.4	0.7/6.5	6.5/8.1	8.1/2.1	2.1/2.5	2.5/5.7	5.7/3	3.0/2.3	2.3/2.5	2.5/12.5
	−0.71	+0.11	−0.80	+3.86	−0.84	+0.44	−1.9	+1.3	−0.92	+0.18

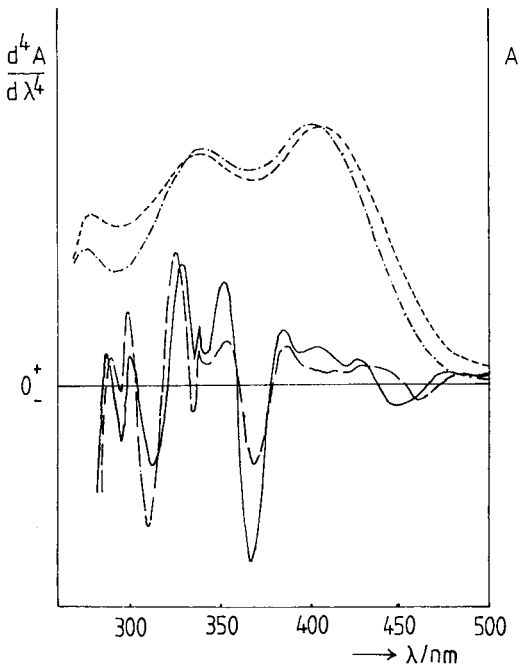

Fig. 4. Absorption spectra: (—·—·—) PY-1; (— — — —) PY-3. Fourth derivatives: (——) PY-1; (—) PY-3.

Derivative absorption spectra of thin-layer spots

When samples are very small, which is usually the case from paintings, and consist of more than two similar pigments, t.l.c. is very suitable for separation and identification. Recently, this method was used to study the palettes of Petrović [15], Konjović [16] and others [17]. In these investigations, t.l.c.

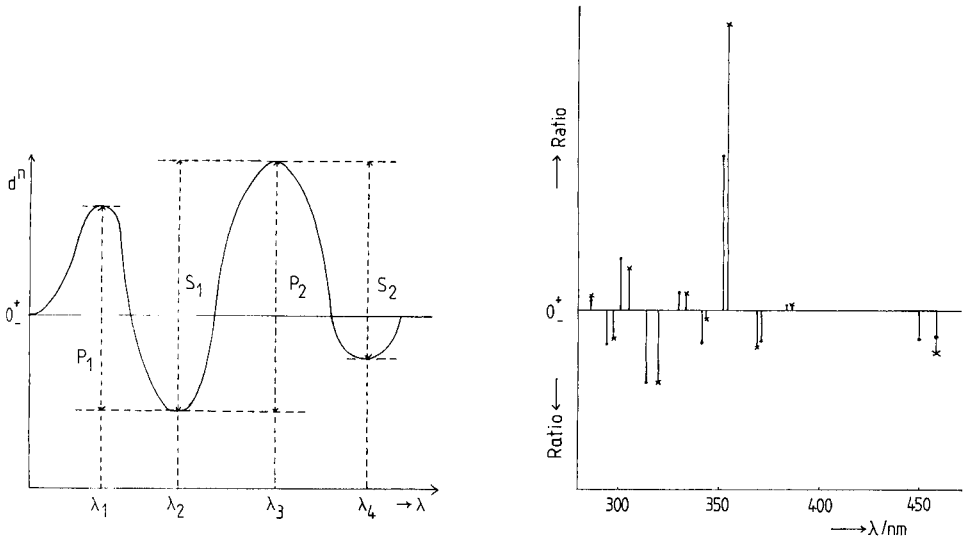

Fig. 5. PP ratio and SPS ratio shown schematically. The PP ratio (λ_1, λ_3) is $P_1(\lambda_1)/P_2(\lambda_3)$ whereas the SPS ratio (λ_3) is $S_1(\lambda_2)/S_2(\lambda_4)$.

Fig. 6. Line diagram of SPS ratios for PY-1 (×) and PY-3 (•).

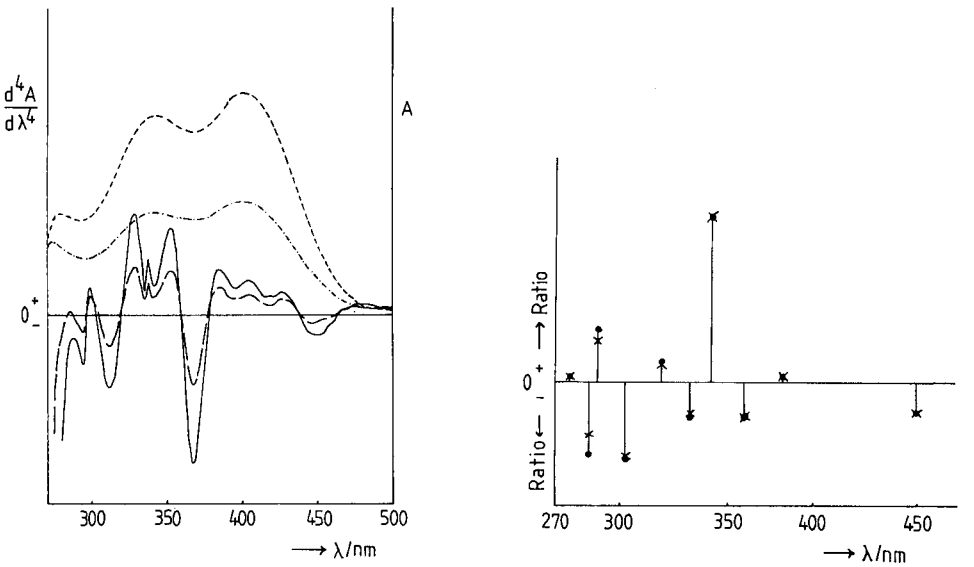

Fig. 7. Absorption spectra: (———) PY-3; (—·—·—) Talens Yellow Lemon Oil Tube (PY-3 in oil). Fourth derivatives: (——) PY-3; (— —) PY-3 in oil tube.

Fig. 8. Line diagram of SPS ratios of PY-3 (×) and PY-3 in oil tube (○).

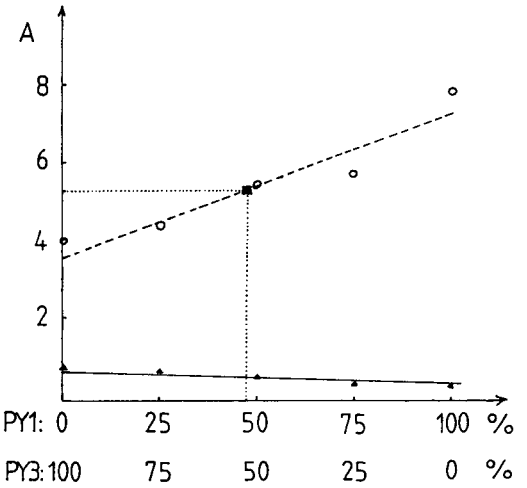

Fig. 9. Calibration lines of SPS ratios for PY-1 and PY-3, computed for 354 nm (○) and 346 nm (▲). (■) SPS value of Talens Yellow light (a mixture of PY-1 and PY-3 in oil medium).

was used in combination with u.v.-visible derivative spectrophotometry. The samples were dissolved in DMSO and the mixture was separated. The derivative spectra directly taken from the opaque spots were very similar to the d^4-spectra of the same samples in solution (Fig. 10). Differences in the fine structure were seen after the different concentrations had been normalized by SPS ratio computation (Fig. 11). The differences are caused by the adsorption effect on the thin layer. A sample of 10 ng in 5 μl of solvent was enough to identify these unknown organic pigments used for modern paintings.

DISCUSSION

In the preliminary studies, the sixth-order derivative (d^6) of the PY-1 spectrum was found to provide the highest resolution (Fig. 1) but the d^4-spectrum was quite sufficient for good resolution. Moreover, very few commercial spectrophotometers are capable of generating sixth-order derivative with small noise. Although the spectra of chemically different pigments have flat shapes, the d^4 representations show many characteristic peaks (Fig. 2). This is evident even when chemically different pigments of the same colour are compared (Fig. 3). The "finger prints" are suitable for characterization of the chemical types. Higher-order derivative spectrophotometry makes it possible to discover very small deviations from a standard spectrum and to prove whether the pigment has impurities or consists of more than one component.

For quantitative specifications, the peak-peak ratio method is very useful [1]. For example, it is possible to make evident only small differences in the

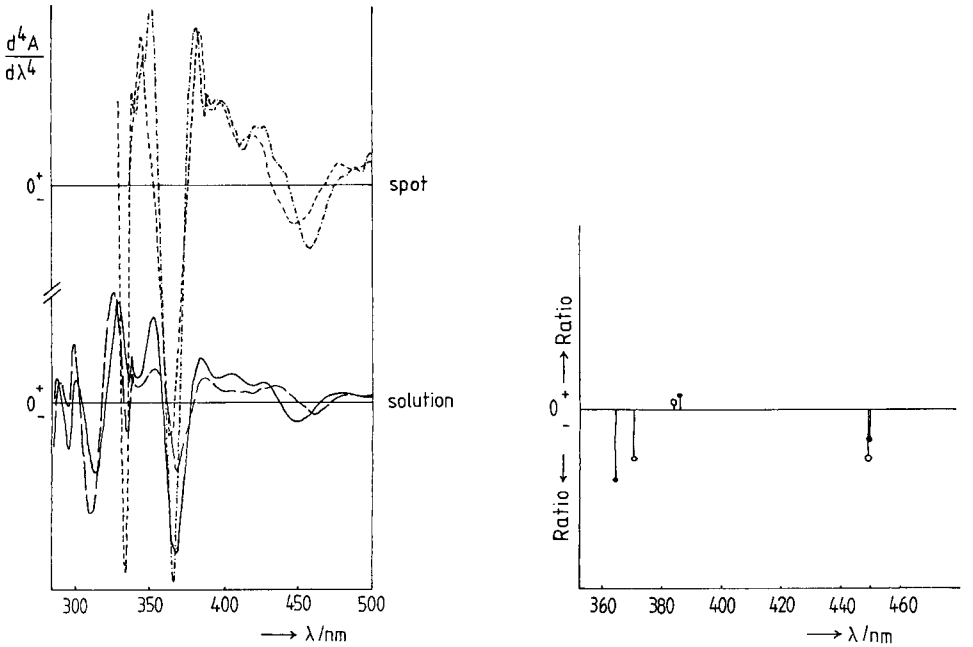

Fig. 10. Comparison of 4th derivatives of PY-1 (——) and PY-3 (——) in DMSO solution with 4th derivatives of the developed t.l.c. spots of PY-1 (— · —) and PY-3 (— — —).

Fig. 11. Line diagram of SPS ratios of PY-3 in solution (○) and of developed t.l.c. spot (●).

spectra of myoglobins [18, 19] or haemoglobins from different organisms [20] or to characterize different sorts of beers [1]. This evaluation also eliminates concentration differences in the spectra; if two spectra pertain to the same substance, the peaks will certainly be different in their heights but the peak ratios will be the same. Clearer results are given by the side-peak-side (SPS) method (Fig. 3) because only one wavelength is used. The data for the d^4-spectrum of PY-1 and PY-3 are given in Table 2 and the graphical representation is shown in Fig. 6.

Two other possibilities of eliminating the effect of concentration should be mentioned. One is the division of two derivative spectra; the other is the differentiation not of absorbance (A) but of log A [21]. Both methods are very effective, but the latter gives flatter curves and is more expensive. Billmeyer et al. [12] recommended log A to normalize pigment spectra.

For comparison of spectra, very good results were obtained by evaluation of line diagrams which are easy to understand and are also normalized. In this way, it was shown that the medium in which the pigments are suspended does not affect the results (Figs. 7 and 8).

The higher-order method also made it possible to quantify two or three pigments in mixtures without separation. The combination of t.l.c. and

examination of the developed spots by the higher-order derivative method allowed identification of complicated mixtures even when only some nanograms of sample were available.

In a later paper, the results obtained by higher-order derivative reflection spectroscopy will be reported. The pigments were directly investigated on the surfaces without destroying the paintings. Silica fiber optics and homemade adapters were used to connect the device to commercial spectrophotometers.

We thank the Deutsche Forschungsgemeinschaft and the Freunde der Technischen Universität München e.V. for supporting this investigation. This work was also made possible by the award of a grant to M. R.-Š. by the Deutscher Akademischer Auslanddienst, Bonn. All pigments and artists' paints were kindly made available by Talens BV (The Netherlands).

REFERENCES

1 G. Talsky, L. Mayring and H. Kreuzer, Angew. Chem. Int. Ed. Engl., 17 (1978) 785.
2 G. Talsky, Tech. Messen, 48 (1981) 211.
3 G. Talsky, GIT Fachz. Lab., 26 (1982) 913.
4 G. A. Milovanović, M. Ristić-Solajić and T. J. Janjić, J. Chromatogr., 249 (1982) 149.
5 British Colour Index, 3rd edn., Society of Dyers and Colorists and American Association of Textile Chemists and Colorists, Bradford, Yorkshire, Vol. 4 (1971), Vol. 6 (1975).
6 T. C. Patton (Ed.), Pigment Handbook, Wiley, New York, 1973.
7 E. Bamberger and F. Bordt, Ber. Dtsch. Chem. Ges., 22 (1889) 625.
8 J. Formanek, Untersuchung und Nachweis organischer Farbstoffe auf spektroskopischem Wege, Springer, Berlin, 1908.
9 R. Abbott and E. I. Stearns, Identification of Organic Pigments by Spectrophotometric Curve Shape, Calco Technical Bulletin 754, American Cyanamid, Bound Brook, NJ, 1944.
10 M. Saltzman, Dyestuff, 43 (1959) 57.
11 M. Saltzman and A. M. Keay, J. Paint Technol., 39 (1967) 360.
12 W. Billmeyer Jr., R. Kumar and M. Saltzman, J. Chem. Ed., 58 (1981) 307.
13 G. Talsky, S. Götz-Maler and H. Betz, Mikrochim. Acta, Part I, (1981) 1.
14 H. W. Vogel, Praktische Spektralanalyse irdischer Stoffe, 2nd edn., Nördlingen, 1889, p. 377.
15 M. Ristić-Šolajić, Die Palette von Nadežda Petrović in: Katarina Ambrozić, Nadeža Petrović (1898—1917), Neue Pinakothek München, 1985.
16 M. Ristić-Šolajić, Palette de Milan Konjović, in: Katarina Ambrozić, Milan Konjović (1898), Galeria Milan Konjović, Jugoslavia, Sombor 1985.
17 I. Strauß, Maltechnik-Restauro, 4 (1984) 29.
18 G. Talsky, M. Glasbrenner and S. Götz-Maler, Internat. Symp. on Macromolecules, IUPAC Macro Florence 1980, Preprints Vol. 2, 1980, 441.
19 G. Talsky, J. Dostal, M. Glasbrenner and S. Götz-Maler, Angew. Macromol. Chem., 105 (1982) 49.
20 G. Talsky, GIT Labor-Medizin, 6 (1983) 182.
21 G. Talsky and O. Haubensak, Proceedings 2. Kolloquium Analytische Chemie-Forschung und Anwendung, Duisburg, 1982; H.-M. Kuss, Univ. Duisburg, 1983, p. 265.

Analytica Chimica Acta, 196 (1987) 135—140
Elsevier Science Publishers B.V., Amsterdam — Printed in The Netherlands

CHEMILUMINESCENCE DETERMINATION OF IRON(II) AND TITANIUM(III) BY FLOW INJECTION ANALYSIS BASED ON REACTIONS WITH AND WITHOUT LUMINOL

ABDULRAHMAN A. ALWARTHAN and ALAN TOWNSHEND*
Chemistry Department, University of Hull, Hull HU6 7RX (Great Britain)
(Received 4th September 1986)

SUMMARY

Titanium(III) and iron(II) are shown to stimulate luminol chemiluminescence in the absence of added oxidant. Down to 10^{-9} M titanium can be determined. Both metal ions also produce chemiluminescence when injected into 0.1 M carbonate buffer (pH 10.4), allowing $\geqslant 10^{-6}$ M of each to be determined. The intensities are greater when the solutions have been deoxygenated by a stream of nitrogen, and when rhodamine B is used as a sensitizer.

The sensitivity of chemiluminescence methods for the determination of trace metals is well-known [1, 2]. Most such methods are based on the catalysis or inhibition of reactions involving the oxidation of reagents such as luminol, lucigenin, lophine and gallic acid. Methods for cobalt, copper and iron have particularly low detection limits, of the order of 1 pg ml^{-1}. The commonest oxidant has been alkaline hydrogen peroxide, but added oxidant has not always been found to be necessary [3, 4].

Seitz and Hercules [3] determined iron(II) by its catalysis of luminol chemiluminescence in the absence of added oxidant, the oxidant being assumed to be dissolved oxygen; the detection limit was 5 ng l^{-1}. Later, Klopf and Nieman [4] found that iron(II), cobalt(II), manganese(II) and copper(II) stimulated chemiluminescent emission from luminol in a flow system in the absence of hydrogen peroxide or other added oxidant. Dissolved oxygen was again considered to be the oxidant, although after removal of the oxygen there was some residual chemiluminescence. This was thought to be due to diffusion of oxygen through the plastic tubing of the flow system. Sarantonis and Townshend [5] confirmed that iron(II), but not iron(III), could be determined under these circumstances, and based a flow method for the determination of iron(II) and iron(III) in admixture on this observation. Displacement of dissolved oxygen by nitrogen decreased the emissions, but only by 28%. Incorporation of the apparatus into a nitrogen-filled box, to prevent return of oxygen by diffusion through the plastic tubing had no effect on the residual emission. These results indicate that molecular oxygen is unlikely to be the oxidant responsible for the chemiluminescent reaction under these circumstances.

0003-2670/87/$03.50

It was decided, therefore, to investigate this phenomenon in more detail. During the investigation, it was found that chemiluminescent emission could be obtained merely by mixing iron(II) with a carbonate buffer. A similar effect was found for titanium(III). This effect was also investigated, as described below.

EXPERIMENTAL

Reagents

Distilled deionized water was used throughout. AnalaR iron(II) sulphate heptahydrate, titanium trichloride solution (ca. 15% w/v $TiCl_3$ general-purpose reagent) and AnalaR anhydrous sodium carbonate were supplied by BDH, luminol (general-purpose reagent) by Sigma Chemical Co. and rhodamine B by Hopkin and Williams. Stock solutions (1×10^{-3} M) of titanium(III) and iron(II) were prepared daily by diluting 10 ml of the titanium solution to 100 ml with water, and by weighing 0.0280 g of iron(II) sulphate heptahydrate and dissolving it in 100 ml of water. Stock solutions of luminol and rhodamine B were prepared by weighing 0.0177 g and 0.0479 g, respectively, and dissolving them in 0.1 M carbonate buffer to give 100 ml of 1×10^{-3} M stock solutions. The carbonate buffer (0.1 M) was prepared by dissolving 10.6 g of sodium carbonate in water, and diluting to 1 l. Hydrochloric acid (AnalaR, 2 M) was used to adjust the buffer to pH 10.4. When required, reagent solutions were deaerated by bubbling with nitrogen for ca. 10 min.

Apparatus

All chemiluminescent measurements were made with the apparatus described previously [6]. The manifold is described in Fig. 1. Buffer solution was supplied through R_1 and R_2. The metal ion sample solution was injected into one buffer stream through a 52-μl teflon rotary injector (Rheodyne RH-5020). The emission intensity from this solution was monitored directly by an EMI 9844B photomultiplier tube, with no wavelength discrimination. The current obtained was amplified and displayed on a chart recorder. Peak-height measurements were used.

RESULTS

Initially, experiments were run in the presence of luminol (dissolved in carbonate buffer) through R_1; buffer solution only was supplied through R_2. Titanium(III) and iron(II) were both found to stimulate chemiluminescence under these conditions, and were studied in more detail. Emission intensities obtained with titanium(III) before and after deaeration are shown in Fig. 2. As with iron(II), significant emissions are produced when almost all the oxygen has been removed; in some instances, the emissions are more intense than when oxygen has not been removed. This may result from the oxidation of

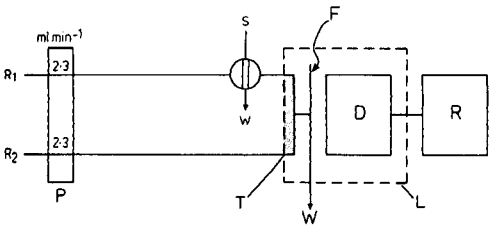

Fig. 1. Flow-injection manifold for titanium(III) or iron(II) determination: (R_1, R_2) flow streams; (P) peristaltic pump; (S) injection valve; (W) waste; (T) perspex T-piece; (F) coiled flow cell; (D) detector; (R) chart recorder; (L) light-tight box.

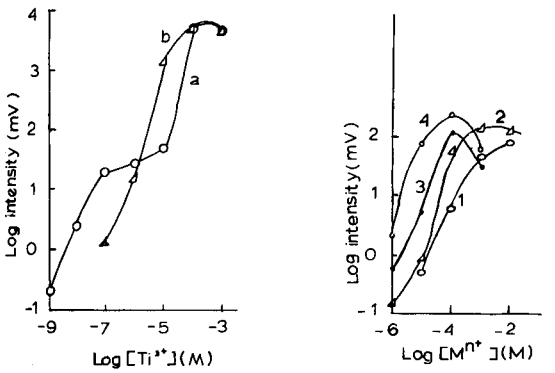

Fig. 2. Effect of titanium(III) concentration on the peak-height emission intensity from 1×10^{-5} M luminol in 0.1 M carbonate buffer: (a) in presence of molecular oxygen; (b) in its absence.

Fig. 3. Effect of metal ion concentration on the intensity obtained by mixing with 0.1 M sodium carbonate buffer: (1, 2) iron(II); (3, 4) titanium(III); (1, 3) with oxygen; (2, 4) without oxygen.

titanium(III) by oxygen, thus preventing its effect on luminol oxidation, although the results at lower titanium concentrations, where intensity is greater in the presence of oxygen, do not support this. Quenching of the luminescence by oxygen is also a possibility. Down to 10^{-9} M titanium could be detected by this reaction in solutions which had not been deaerated.

Luminescence in the absence of luminol

At this stage, the effect of adding titanium(III) and iron(II) to the alkaline buffer in the absence of luminol was investigated. Surprisingly, addition of either to the pH 10.4 carbonate buffer gave appreciable chemiluminescence, even when the buffer had been deaerated with nitrogen. The effects of various concentrations of titanium(III) and iron(II) are shown in Fig. 3. They show an increase in intensity with increasing titanium concentration up to

10^{-4} M (as in the presence of luminol) and with increasing iron concentration up to ca. 10^{-2} M. The maximum intensity in both instances is greater in the deaerated solutions; for titanium, the intensity is 1.4 orders of magnitude less than that in the presence of luminol under the same conditions.

Effect of hydrogen peroxide and of different buffers

As the presence of oxygen or added oxidant did not seem to be necessary for chemiluminescence in the systems with or without luminol, it was likely that another oxidant was involved. Such an oxidant might be peroxide ions, present in the sodium carbonate used to prepare the buffer. The effect of adding various concentrations of hydrogen peroxide to the buffer, therefore, was investigated. The results for a simple titanium(III)/carbonate system are shown in Fig. 4. They show that small concentrations of hydrogen peroxide (ca. 10^{-7} M) do slightly increase the intensity, and that there is a considerable increase above 10^{-4} M hydrogen peroxide. It seems possible, therefore, that traces of hydrogen peroxide in the buffer, or even in the water, could be responsible for the effect.

When 0.1 M sodium borate (pH 10.4) or 0.1 M ammonia/ammonium chloride buffers were used in place of the carbonate buffer, neither iron(II) nor titanium(III) gave any emission in the absence of luminol.

Effect of rhodamine B

In weakly chemiluminescent systems, it is often possible to increase the intensity by adding a fluorophore as a sensitizer. Energy from the excited-state product of the initial reaction is transferred to the more efficient

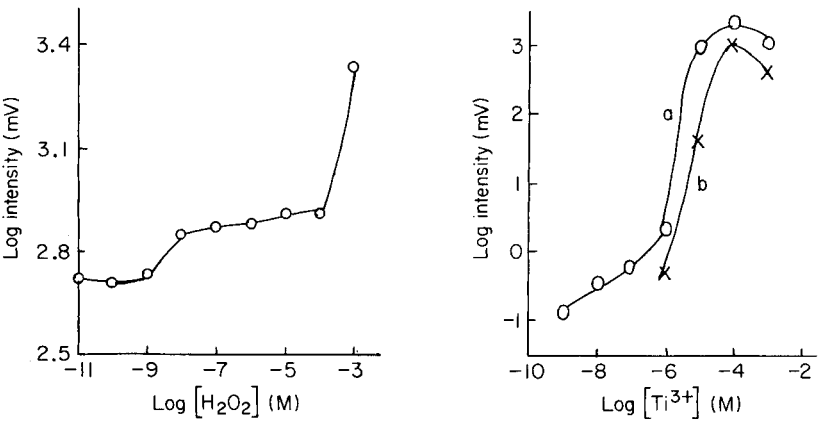

Fig. 4. Effect of hydrogen peroxide concentration on emission from 1.0×10^{-4} M titanium(III) in 0.1 M sodium carbonate buffer.

Fig. 5. Effect of titanium(III) concentration on emission in 0.1 M sodium carbonate buffer/ 1×10^{-5} M rhodamine B: (a) in presence of oxygen (b) in its absence.

emitter, thus increasing the intensity. Rhodamine B is often used for this purpose, and its effect on the titanium/carbonate emission was measured. Calibration graphs for titanium in the presence of rhodamine B are shown in Fig. 5. Maximum intensity is achieved at 10^{-5} M rhodamine B for 1×10^{-4} M titanium (although 10^{-4}—10^{-6} M rhodamine B gives almost the same sensitivity), similar to that for luminol, but with half the apparent maximum intensity obtained in the luminol system. This confirms that sensitization occurs in the titanium/carbonate system, with increase in sensitivity for $\geqslant 10^{-5}$ M titanium(III) of an order of magnitude. It also hints that the function of luminol in systems of this type, to which no oxidant is added, might itself be as a sensitizer. Interestingly, in the rhodamine B system the intensity is always less in the absence of oxygen (Fig. 5).

Effect of other metal ions

Seitz and Hercules [3], in their luminol system without added oxidant, found that cobalt(II), nickel(II), manganese(II), chromium(III) and copper(II) decreased the chemiluminescence signal obtained on addition of iron(II) to luminol in a borate buffer. Klopf and Nieman [4], however, found that cobalt(II) and copper(II) also gave rise to chemiluminescence in alkaline solutions containing luminol with no added oxidant. Emissions from carbonate buffer had the greatest intensity, as is found in the present study.

Various metal ions were tested for their effect on the titanium-induced chemiluminescence in carbonate buffer alone. At 1×10^{-4} M, chromium(III) increased the peak intensity from 1×10^{-5} M titanium(III) 24 times, and iron(III) increased it 3 times; cobalt(II) decreased it 3 times, silver 7 times, copper(II) 99 times and manganese(II) 448 times. This order of depression matches closely that observed previously [3] for iron(II) in the luminol system in the absence of added oxidant. Coprecipitation with hydrated oxides has been proposed as an explanation of the depressive effect [3], but it is notable that other metals which form hydrated oxide precipitates [iron(III), aluminium, cadmium, etc.] do not depress the emission.

Determination of iron(II) and titanium(III)

The chemiluminescent reactions described above can be used as the basis for simple procedures for determinations of iron(II) and titanium(III). The procedure for iron(II) based on luminol has already been described [4, 5], and a similar method for titanium(III) is readily achieved. Calibration graphs for titanium are shown in Fig. 2. In the absence of luminol, both ions can also be determined, albeit with less sensitivity, merely by injection into a carbonate buffer. Calibration graphs under these conditions are shown in Fig. 3.

Nature of the emissions

At present, there is no direct evidence for the nature of the emissions in the absence of luminol. However, as both iron(II) and titanium(III) are

reducing agents, it is possible that the emission arises from reduction of molecular oxygen or of traces of peroxide ions in the carbonate buffer. As removal of oxygen increased the intensity, hydrogen peroxide seems the more likely candidate but the effect of residual oxygen cannot be ruled out. The reaction of iron(II) with peroxide ions (Fenton's reagent) is well known [7] to produce $OH^{\cdot}$ and $O_2H^{\cdot}$ radicals, and the excited double oxygen molecule $(O_2O_2)^*$, produced by collision of two $O_2H^{\cdot}$ radicals [8], is therefore the possible emitter. The involvement of peroxocarbonate species is also a possibility.

The $O_2H^{\cdot}$ radical is also assumed to participate in other chemiluminescent reactions, including that of luminol. Therefore the formation of this species could also account for the luminol chemiluminescence observed in the absence of oxygen. Clearly, a much more extensive investigation of these reactions is needed. This is being undertaken, and will be reported later.

REFERENCES

1 L. J. Kricka and G. H. G. Thorpe, Analyst, 108 (1983) 1274.
2 A. Townshend, Anal. Proc., 22 (1985) 370.
3 W. R. Seitz and D. M. Hercules, Anal. Chem., 44 (1972) 2143.
4 L. L. Klopf and T. A. Nieman, Anal. Chem., 55 (1983) 1080.
5 E. G. Sarantonis and A. Townshend, Anal. Chim. Acta, 184 (1986) 311.
6 A. A. Alwarthan and A. Townshend, Anal. Chim. Acta, 185 (1986) 329.
7 J. H. Baxendale, Adv. Catal., 4 (1952) 31.
8 J. Stauff, Z. Phys. Chem. (Frankfurt am Main), 40 (1964) 64; 49 (1966) 58; 55 (1967) 39.

Analytica Chimica Acta, 196 (1987) 141—152
Elsevier Science Publishers B.V., Amsterdam — Printed in The Netherlands

ELECTROCHEMICAL STRIPPING WITH CARBON FIBER ELECTRODES IN A MICROLITER-CAPACITY CELL

WOLFGANG FRENZEL[a]

Hahn-Meitner-Institut, Spurenelemente in Gesundheit und Ernährung, Glienicker Str. 100, D-1000 Berlin 39 (Federal Republic of Germany)

(Received 30th September 1986)

SUMMARY

The construction of a microcell with an in-situ mercury-plated carbon fiber electrode for the application of electrochemical stripping techniques is described. The performance of the cell is compared to a conventional mercury-film glassy carbon electrode in large-volume cells with special emphasis on the effects of mass transport and oxygen interference. Effective mass transport is provided without forced convection and oxygen does not appear to influence the response of the carbon fiber electrode. The dependence of the a.s.v. and p.s.a. signals on the deposition time with the microcell deviated from linearity at deposition times above 3 min because of depletion effects and decreased concentration of oxidizing agent, respectively. Good reproducibility of lead determinations in the $\mu g\ l^{-1}$ range by a.s.v. and p.s.a. was achieved in successive scans at the same fiber and in consecutive tests of identical samples. Calibration plots were linear in the 0.01—10 $mg\ l^{-1}$ range. Sample volumes down to 5 μl were used in determining cadmium and lead. The detection limits for both elements obtained with a.s.v. and p.s.a. after 5-min preconcentration were 1 and 3 $\mu g\ l^{-1}$, respectively, or in absolute mass 5 pg and 15 pg, respectively.

During recent years, considerable interest has been shown in micro-scale determinations of trace elements in environmental and biological materials. Among the instrumental methods available for solution analysis, few are strictly micro-scale techniques (e.g., flameless atomic absorption spectrometry); most other methods have to be modified to meet this requirement. The analysis of small sample volumes by means of electrochemical stripping analysis is mainly limited by the size of the sensing electrode. Conventional hanging mercury drop electrodes (HMDE) and mercury film electrodes on glassy carbon substrates (MFGCE) require a minimum sample volume of about 5 ml. To allow the analysis of microliter or even smaller samples, special cell geometries can be constructed (e.g., inverted electrodes), the flow-injection technique has been applied [1, 2], or the size of the sensing electrode must be reduced. Such sensing electrodes have become known as microvoltammetric electrodes [3] and have found widespread use in the area of in-vivo neurochemistry [4—7], for studying fast electron-transfer reactions and kinetics [8—10], for fast voltammetric measurements in highly

[a]Present address: Institut für Technischer Umweltschutz, Fachgebiet Luftreinhaltung, Technische Universität Berlin, Strasse des 17 Juni 135, D-1000 Berlin 12 (Federal Republic of Germany)

0003-2670/87/$03.50

resistive solutions [11, 12], and as flow-through detectors for liquid chromatography [13—15].

Recently, several authors [16—22] have reported the application of mercury-coated carbon fiber, gold or platinum micro-electrodes for anodic stripping voltammetry (a.s.v.) and potentiometric stripping analysis (p.s.a.). The low background currents [23], improved resolution of voltammetric peaks and increased overpotential in acidic media are some of the interesting features of mercury microvoltammetric electrodes [16, 17]. In addition, the enhanced mass transport resulting from nonlinear diffusion [3, 9—12, 24—27] avoids the need for forced convection during the preconcentration step. The advantage of using very small volumes of samples has been emphasized by several authors, but the actual volumes that have been used were generally above 10 ml. The fact that the real microanalytical utility of fiber electrodes has not been demonstrated is probably due to problems associated with the design and construction of a suitable cell. Given the need for a three-electrode arrangement, a special design is required not only for the working electrode but also for the auxiliary and reference electrodes.

In the present paper, a compact and easy-to-prepare microvoltammetric cell is described. Both a.s.v. and p.s.a. responses are used to characterize the performance, with special emphasis on the conditions of mercury film formation, effects of deoxygenation and mass transport considerations. The analytical utility of the arrangement is demonstrated by determining lead and cadmium at the $\mu g\ l^{-1}$ level in sample volumes down to 5 μl.

EXPERIMENTAL

Instrumentation and reagents

Voltammetric measurements were made with a PAR model 174A three-electrode potentiostat in combination with a PAR model 315A automated electroanalysis controller (EG & G, Princeton, NY). The Striptec system (Tecator, Höganäs, Sweden) was used for p.s.a. [28].

The preparation of the carbon fiber microelectrodes which were used as working electrodes was described previously [17]. Only the cut single-fiber type (Type B [17]) was applied in the present studies. Some electrodes were modified to allow the fiber electrodes to be connected to the rotating electrode holder. This was accomplished by casting the upper end of the pipette tip into a cylindrical rod of epoxy resin. Electrical contact was made via silver epoxy. For purposes of comparison, measurements were made with a rotating disc electrode (Metrohm, EA-628, Herisau, Switzerland) equipped with a homemade glassy-carbon tip (3-mm diameter, Tokai glassy-carbon material). The electrolytic cell used was either a 10-ml teflon beaker or the microcell described in detail below.

Working standards were prepared from analytical-grade stock solutions containing 1 $g\ l^{-1}$ of the respective elements (Merck, Titrisol). The supporting electrolyte was 0.1 $mol\ l^{-1}$ potassium nitrate acidified to pH 3 with concentrated nitric acid (Merck, Suprapur reagents).

Construction of the microcell

The cell is shown schematically in Fig. 1. It consists of a glassy-carbon tube (5 mm o.d., 2 mm i.d., 8 mm long; Deutsche Carbone, Frankfurt, F.R.G.) which acts as the auxiliary electrode. This tube is stuck on a nipple in the centre of a perspex cylinder (25 mm diameter, 30 mm high). Thus a small beaker-like vessel is formed with a volume of approximately 20 μl but sample volumes as small as 5 μl can be used. A home-made Ag/AgCl (saturated) reference electrode is inserted upwards into the perspex block and connected to the cell via a 0.1-mm bore in the centre of the nipple. A diaphragm is made by plugging a small portion of quartz wool into this bore. The fiber working electrode is held by an ordinary laboratory stand and is carefully lowered into the beaker until the tip dips into the sample solution.

Procedure

When the rotating electrode compartment was used, 5 ml of base electrolyte was transferred to the cell followed by the addition of appropriate aliquots of analyte. Mercury(II) nitrate stock solution was added to give a final concentration in the 10—50 mg l^{-1} range. If necessary, samples were deaerated by purging with high-purity argon for at least 10 min, and were blanketed with argon during the entire experiment.

Mercury film deposition was done in situ by application of a constant potential of −1.0 V vs. Ag/AgCl for about 3 min. This potential was set throughout all further investigations as it is appropriate for determinations of cadmium, lead and copper. Then an anodic test scan was initiated in the quiescent solution at a rate of 50 mV s^{-1}. The background slope, overpotential and peak width at half height were used as the indicators of proper quality of any particular electrode [17]. For samples, various time intervals for preconcentration were used, depending on the metal ion concentration to be

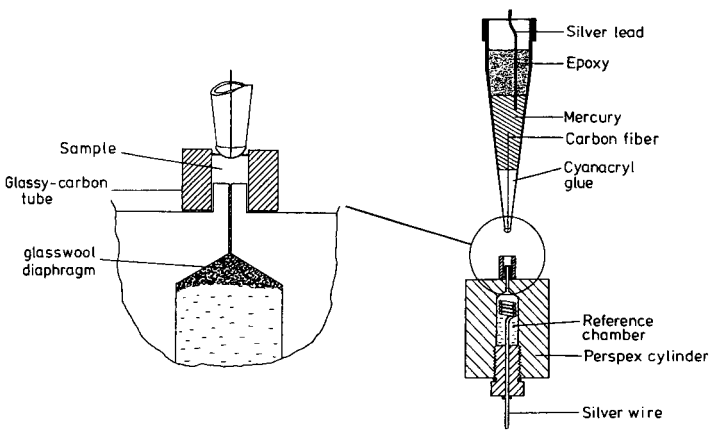

Fig. 1. Schematic representation of the microcell. For clarity, the actual cell compartment is shown in enlarged view.

determined. At least five repetitive scans were run on each sample to check reproducibility. Subsequently, p.s.a. was done under exactly the same sample and electrolysis conditions (i.e., plating potential and deposition time). Rotating of the electrode was usually not interrupted before the stripping step was initiated.

Measurements with the microcell were done as follows: 5—20-μl sample volumes were pipetted into the cell. The microvoltammetric electrode was dipped into the solution and the deposition potential was applied for 3 min. An anodic test scan was then initiated at a rate of 50 mV s^{-1}. As in the case of the large-volume cell, only well-behaved electrodes were used for further measurements. Repetitive scans were applied after variable deposition times in the 1—10 min range. P.s.a. was applied under equivalent conditions. Before a new sample was examined, the previous one was removed with a micropipette and the microcell was rinsed by repeated washings with twice-distilled water. Carry-over was checked from time to time and found to be negligible when this procedure was applied. However, the reference solution may be slowly contaminated by diffusional transport if samples with high analyte concentrations are examined and/or the residence time of the sample in the microcell is in the order of hours. This may cause contamination of subsequent samples by back-diffusion and can only be prevented by changing the reference solution. However, in the normal measuring procedure, the processing time of one sample is less than 10 min, which avoids any carry-over troubles.

RESULTS AND DISCUSSION

Mercury-film formation

The ingenious idea of in-situ plating of mercury films on glassy carbon [29] has been commonly applied in a.s.v. and p.s.a. because of the high reproducibility, extreme sensitivity and ease of preparation [30—32]. Moreover, the risk of film damage or chemical surface reactions on exposure to air during transference is avoided. In-situ plating procedures have also been used for the production of mercury micro-electrodes [16—18, 20]. Such electrodes can be used for repeated runs in the same solution or consecutive measurements in different samples with reproducible response over several hours. After working breaks of several days or removal of the mercury layer by anodic polarization, the same fiber electrode can again be used after in-situ mercury plating. It is obvious that deterioration of the mercury film by chemical or mechanical attack will immediately be remedied through coverage with a new mercury layer. However, the peak currents (a.s.v.) and stripping times (p.s.a.) obtained at such renewed electrodes deviate significantly from that at the same carbon fiber in preceding measurements or before film stripping, respectively. The irreproducible results and electrode failure observed in work involving preplated carbon-fiber electrodes [19, 21] may not arise if in-situ plating is adopted.

Mass-transport considerations

In order to achieve effective mass transport during the deposition step, forced convection either by stirring or by rotating the electrodes is needed in conventional stripping analysis. In a.s.v. the stripping step is usually done in quiescent solutions. The stripping step in p.s.a. can be done either under forced convection or into a quiescent solution, the latter yielding improved sensitivity [33, 34]. The non-linear diffusion observed at microvoltammetric electrodes [9—12, 24—27] allows effective preconcentration to be done without forced convection [3, 18]. This is of particular interest when the microcell is applied because stirring of very small volumes or rotating the electrode is difficult to achieve.

For verification, the a.s.v. and p.s.a. responses were compared for situations without rotating the electrode during both deposition and stripping, and rotating the electrode during deposition and stripping into a quiescent solution (Fig. 2). For reasons of comparison, the response of the MFGCE

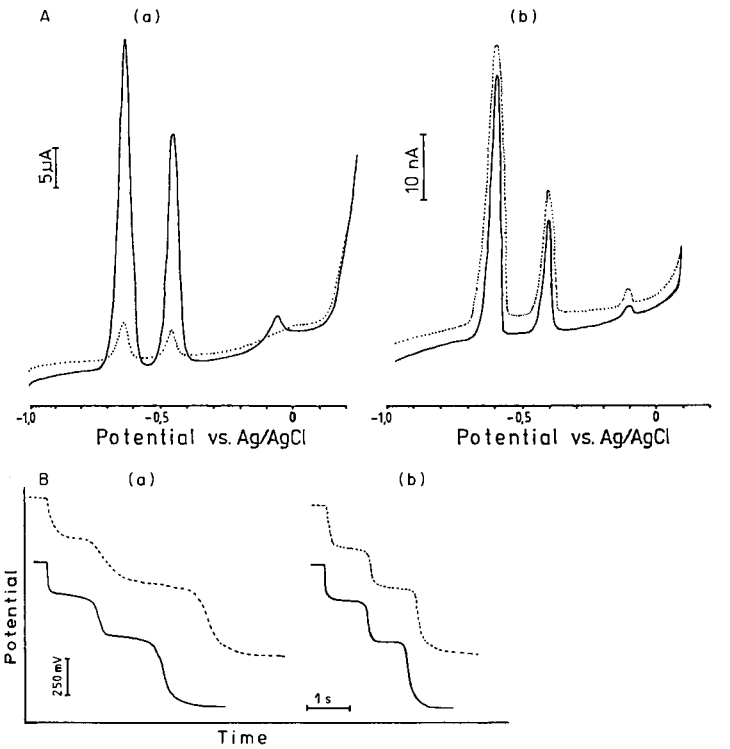

Fig. 2. Effect of convective mass transport on the a.s.v. (A) and p.s.a. (B) responses with the MFGCE (a) and the mercury microelectrode (b). (—) Stripping curves obtained with rotation of the electrode during the deposition step; (. . .) without rotation. Sample contains 500 $\mu g\ l^{-1}$ each of Cd^{2+} and Pb^{2+} and 20 mg l^{-1} Hg^{2+} in 0.1 mol l^{-1} KNO_3; deposition time 120 s; a.s.v. scan rate 50 mV s^{-1}.

under the same conditions is also shown. As expected, the a.s.v. peak currents under forced convection are substantially higher when the MFGCE is applied. The peak currents observed at the microvoltammetric electrodes, however, are hardly influenced by rotating the electrode. This agrees with theoretical predictions about time-independent faradaic currents at small electrodes in the absence of convection [24, 25] and experimental work reported by several authors [3, 5, 19, 35]. The stripping times in the p.s.a. experiments at the MFGCE are also affected by the mode of mass transport (Fig. 2).

However, as the same law of mass transport is valid for both the plating and stripping steps, the decreased preconcentration under non-convective conditions is partly compensated by the likewise slower oxidation rate [34]. The stripping times obtained at the fiber electrode with and without rotating are obviously identical which agrees with recent findings [18].

Oxygen interference

Oxygen is reduced in the cathodic potential range and therefore has usually to be removed from sample solutions prior to a.s.v. Wang [36] reported

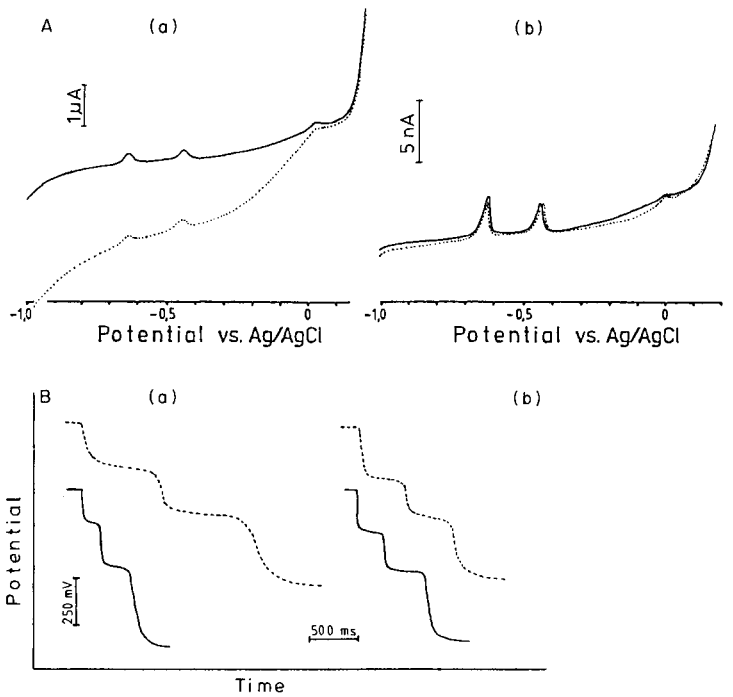

Fig. 3. Influence of oxygen on the electrode response at the MFGCE (a) and the fiber electrode (b). (A) A.s.v. in the presence (. . .) and absence (—) of oxygen. Sample contains 10 μg l^{-1} each of Cd^{2+} and Pb^{2+}, and 10 mg l^{-1} Hg^{2+} in 0.1 mol l^{-1} KNO_3; deposition time 60 s; scan rate 50 mV s^{-1}. (B) P.s.a. in the presence (. . .) and absence (—) of oxygen. Sample contains 250 μg l^{-1} each of Cd^{2+} and Pb^{2+} and 10 mg l^{-1} Hg^{2+} in 0.1 mol l^{-1} KNO_3; deposition time 120 s.

oxygen interferences even for miniature disc electrodes of 140-μm diameter. The deaeration of minute samples, however, causes significant evaporation losses and is in fact difficult to perform. Therefore, the response of the mercury microvoltammetric electrodes was investigated in deaerated and non-deaerated solutions. Figure 3 shows the anodic stripping voltammograms obtained in a typical experiment. For comparison purpose, the response of the MFGCE under similar conditions is also shown. Obviously the interference of oxygen is less pronounced in the case of the microelectrode. This can be explained by a thin layer of oxygen-free solution in the vicinity of the fiber electrode caused by electrochemical reduction during the deposition step. A similar explanation was proposed by Wojciechowski et al. [37] who reported the application of square-wave a.s.v. in the presence of oxygen. The influence of oxygen on the p.s.a. response has been extensively studied [34, 38, 39]. According to that work, deaeration of the samples is not required but a decrease in stripping time occurs because of a faster oxidation rate. However, the magnitude of the loss of sensitivity depends on the mercury ion concentration added for in-situ electrode plating [39]. The p.s.a. curves shown in Fig. 3 for the MFGCE and mercury microvoltammetric electrode essentially reflect the previous considerations although the effect of oxygen is less pronounced in the case of the fiber electrode.

Stripping analysis

In an earlier paper [17], the performance of the mercury-coated carbon fiber electrode in a.s.v. and p.s.a. was systematically investigated and the fiber electrode response was compared with that of a conventional MFGCE. Some of these measurements were repeated in the present work in order to obtain comparative data for the fiber electrode response in the large electrolytic cell and the microcell, respectively. Non-deaerated samples containing various concentrations of lead were examined without rotating the electrode, as these are the conditions applicable when the microcell is used.

The peak currents (a.s.v.) and stripping times (p.s.a.) obtained at various deposition times compare very well for the application of the large cell and microcell (Table 1). The reproducibility of the stripping signals when the microcell was used, was checked by ten successive scans at the same electrode in one sample and by analysis of five aliquots of the same solution. The electrolysis time was set to 60 s. The results obtained for two different concentrations are given in Table 2. As normally happens, the precision of repeated scans in the same solution is better than that for consecutive tests of different aliquots of a sample. This can be attributed to changes of the electrode response rather than to differences in the concentration of the particular aliquots. As usual, improved precision is obtained at higher concentrations. When long deposition times (2—5 min) were applied, a trend towards increased stripping times was observed in successive p.s.a. runs. This is probably due to a decrease of the oxygen and mercury ion concentration with time (depletion effect) and hence a decrease in the oxidation rate. The

TABLE 1

Comparison of the response of the carbon fiber electrode in the large-volume electrolytic cell and in the microcell. A.s.v. peak currents (I_p) and p.s.a. stripping times (t_s) are given for various Pb^{2+} concentrations and deposition times (t_d), respectively

$C_{Pb^{2+}}$ (mg l^{-1})	t_d (s)	Large-volume cell		Microcell	
		I_p (nA)	t_s (s)	I_p (nA)	t_s (s)
0.05	30	2.7	—[a]	2.5	—[a]
	60	5.5	0.05	5.3	0.06
	300	21.2	0.32	16.9	0.34
0.1	30	5.8	0.06	5.4	0.07
	60	11.3	0.22	10.9	0.13
	300	49.2	0.64	39.8	0.69
0.5	30	26.3	0.31	27.5	0.30
	60	52.1	0.59	51.4	0.65
	300	236.4	3.68	204.8	3.84
1.0	30	53.6	0.60	49.8	0.59
	60	100.8	1.26	106.8	1.30
	300	488.6	7.93	414.3	8.65

[a]The stripping times were below the time resolution of the strip-chart recorder.

TABLE 2

Reproducibility data obtained for the microcell. Deposition time 120 s; $C_{Hg^{2+}} = 10$ mg l^{-1}

$C_{Pb^{2+}}$ (mg l^{-1})	Repeated scans (10)[a]				Consecutive solutions[b]			
	A.s.v.		P.s.a.		A.s.v.		P.s.a.	
	I_p (nA)	*RSD* (%)	t_s (s)	*RSD* (%)	I_p (nA)	*RSD* (%)	t_s (s)	*RSD* (%)
0.05	10.9	1.6	0.12	4.1	10.4	7.3	0.10	10.3
1.0	205.2	0.9	2.39	2.3	207.3	3.1	2.64	4.8

[a]In the same solution. [b]Five separate aliquots of the same solution.

addition of higher mercury concentrations reduces this effect but at the cost of lower sensitivity.

Effect of deposition time

In conventional a.s.v. at the HMDE or MFGCE, the peak current is linearly dependent on the deposition time as long as no depletion occurs and constant mass transport during deposition is maintained. To obtain a linear dependence between deposition and stripping time in p.s.a., it is required additionally that the mass transport during the stripping step is kept constant [28, 34] by stirring of the solution, by rotating the electrode or by the

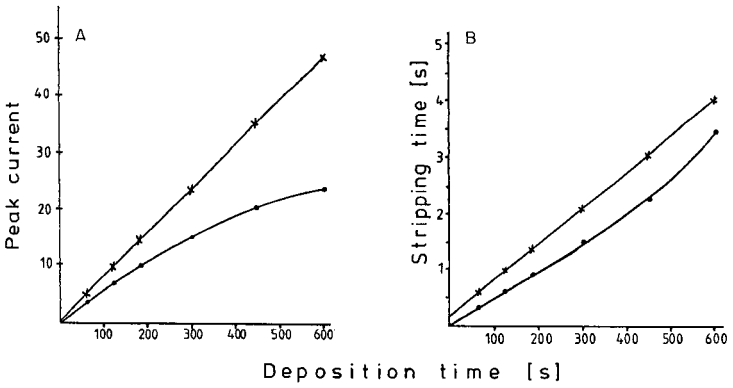

Fig. 4. Signal dependence on the deposition time in a.s.v. (A) and p.s.a. (B). (×) MFGCE in the large-volume cell; (•) fiber electrode in the microcell. Measurements were made with a sample containing 100 μg l^{-1} Pb^{2+} (a.s.v.) or 500 μg l^{-1} Pb^{2+} (p.s.a.) in 0.1 mol l^{-1} KNO_3 ($C_{Hg^{2+}}$ = 10 mg l^{-1}). The peak current unit is μA for the MFGCE and nA for the fiber electrode.

application of flow-through measurements. The experimental results shown in Fig. 4, which were obtained for the rotating MFGCE in the large-volume cell and the fiber electrode in the microcell, respectively, are substantially different. The predicted linearity between deposition time and analytical signal is found for a.s.v. and p.s.a. at the MFGCE whereas deviations from linearity occur when the fiber electrode is applied. The negative deviation in a.s.v. can be explained by depletion of metal ions in the microcell. This of course must also be valid for p.s.a. but at the same time the concentration of oxidizing agents (O_2, Hg^{2+}) also decreases with time, leading to stripping times longer than expected. Evidence for this explanation is given by the fact that with increased mercury concentrations, the deviation is shifted to longer deposition times or even turn to negative deviation.

Calibration

The calibration data for the fiber electrode in the large-volume cell have been reported previously [17]. With the microcell, linear calibration curves for lead and cadmium were found in the concentration range 0.05—10 mg l^{-1} for p.s.a. and a.s.v., respectively. Typical calibration recordings are shown in Fig. 5. As can be seen in Table 3, the longer the deposition times, the higher are the slopes of the calibration plots. However, as stated before, only a slight improvement in sensitivity can be obtained in a.s.v. when deposition times above 5 min are applied. The p.s.a. signals obtained at longer deposition times (3 min) suffer from poor reproducibility. Therefore, the plating time should be kept as short as possible to obtain just enough signal from the particular sample.

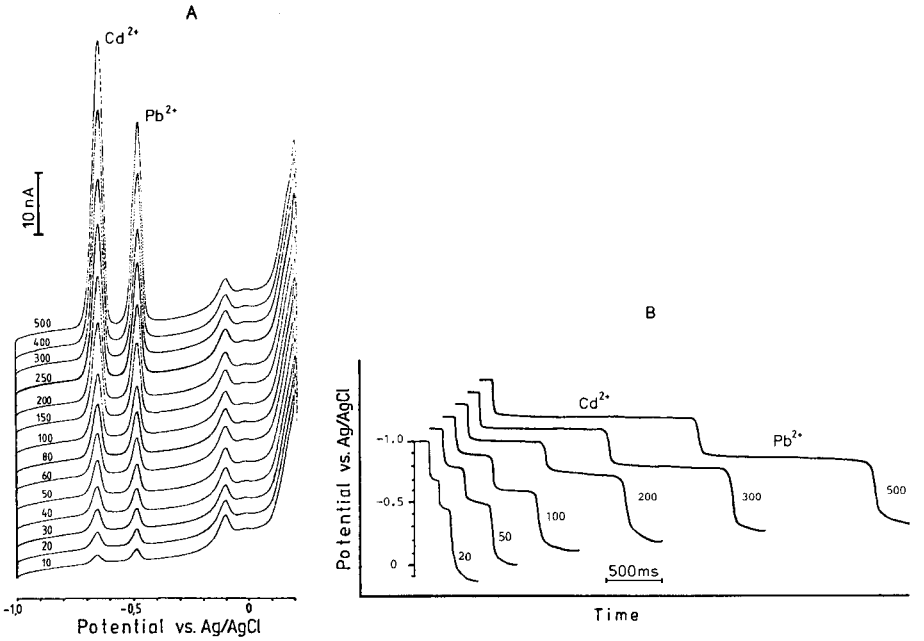

Fig. 5. Typical calibration recordings for the fiber electrode applied in the microcell. Successive scans are shown at increasing lead and cadmium concentrates for a.s.v. (A) and p.s.a. (B). The numbers on the curves refer to $\mu g\ l^{-1}$. Sample volume 20 μl; $C_{Hg^{2+}}$ = 10 mg l^{-1}; deposition time 120 s. The copper signal in the a.s.v. scans is due to contamination.

The influence of the sample volume on the response was investigated in the 5—20 μl range. No significant differences were found in the a.s.v. responses, whereas in p.s.a. the stripping times tend to be slightly shorter with smaller volumes. The detection limits in stripping analysis depend on the deposition time and therefore can only be given in relative terms. In a.s.v. at fiber electrodes, the lower limit of detection is determined by the blank value and the maximum sensitivity of the current measurement. With the equipment used, this is limited to about 0.3 nA (noise level). The detection limit found for 5-min deposition is approximately 1 $\mu g\ l^{-1}$. The detection limits in p.s.a. also depend on deposition time but additionally on the concentration of oxidizing agent [39], the oxidation rate and to some extent on the speed of data acquisition [40]. The equipment used and the experimental conditions chosen in the present work allow for detection limits of about 3 $\mu g\ l^{-1}$ cadmium or lead after 5-min preconcentration. Considering a 5-μl sample, the corresponding absolute detection limits are 5 pg and 15 pg for a.s.v. and p.s.a., respectively.

Conclusions

There are attractive attributes of mercury microelectrodes which are interesting for their application in a.s.v. and p.s.a. Effective mass transport and

TABLE 3

Calibration data for a.s.v. and p.s.a. in the determination of lead and cadmium[a]. (20-μl sample volumes containing 20 mg l^{-1} Hg^{2+} were used. Each measurement was made twice after conditioning the fiber electrode by in-situ plating for 3 min)

Concentration range (mg l^{-1})	Deposition time (s)	Lead			Cadmium		
		Slope	Intercept	Regression coefficient	Slope	Intercept	Regression coefficient
Anodic stripping voltammetry							
0.01—0.5	60	102	0.14	0.9993	108	0.22	0.9987
	120	201	0.68	0.9985	198	0.83	0.9991
	300	362	1.75	0.9991	354	−0.10	0.9998
	600	416	2.57	0.9983	419	1.55	0.9953
0.1—2	60	107	−0.07	0.9993	98	1.01	0.9997
	300	387	1.04	0.9969	343	0.79	0.9985
1—10	30	46	0.76	0.9998	56	1.23	0.9999
	60	96	1.12	0.9989	113	0.98	0.9991
Potentiometric stripping							
0.01—0.5	60	1.03[b]	0.03	0.9991	1.21[b]	0.08	0.9987
	120	2.10	0.10	0.9994	2.35	0.06	0.9992
	300	4.83	0.07	0.9984	4.76	0.10	0.9989
	600	7.95	−0.05	0.9974	8.91	0.02	0.9997
0.1—2	60	0.98	0.12	0.9991	1.14	0.04	0.9999
	300	4.76	0.08	0.9997	4.97	0.07	1.0000
1—10	30	0.51	0.04	0.9999	0.70	0.01	0.9992
	60	1.24	0.08	0.9989	1.32	0.05	0.9994

[a]In a.s.v., the slope is given in nA l mg^{-1} and the intercept in nA. In p.s.a., the slope is given in s l mg^{-1} and the intercept in seconds. [b]The regression was made in the range 0.05—0.5 mg l^{-1} because at lower concentrations no measurable results were obtained.

the negligible effect of oxygen on the electrode response renders unnecessary forced convection and deaeration of the samples, respectively. The small size of the electrodes makes them particularly useful for microanalysis. The application of carbon fiber electrodes in connection with the microcell described above offers the possibility of electrochemical stripping analysis with microliter samples. High precision and linear relations between concentration and electrode response are found over a wide range for both lead and cadmium. Furthermore, the construction principle of the microcell should find general application in electroanalytical methods such as potentiometry, voltammetry and coulometry. With a little modification and some technical skill, even smaller cell volumes should be accessible.

The skilful assistance of H. Rybczynski in the construction of the microcell is highly appreciated.

REFERENCES

1 W. Frenzel and P. Brätter, in P. Brätter and P. Schramel (Eds.), Trace Elements Analytical Chemistry in Medicine and Biology, Vol. 4, Walter de Gruyter, Berlin, 1986, p. 337.
2 W. Frenzel and P. Brätter, Anal. Chim Acta, 179 (1986) 389.
3 R. M. Wightman, Anal. Chem., 53 (1981) 1125A.
4 J.-L. Pouchon, R. Cespuglio, F. Gonon, M. Jouvet and J.-F. Pujol, Anal. Chem., 51 (1979) 1483.
5 A. Ewing, M. A. Dayton and R. M. Wightman, Anal. Chem., 53 (1981) 1842.
6 F. Gonon, R. Cespuglio, J.-L. Pouchon, M. Buda, M. Jouvet, R. N. Adams and J. F. Pujol, C. R. Acad. Sci. Ser. D., 286 (1978) 1203.
7 H. Y. Cheng, J. Schenk, R. Huff and R. N. Adams, J. Electroanal. Chem., 100 (1979) 23.
8 B. Scharifker and G. Hills, J. Electroanal. Chem., 130 (1981) 81.
9 M. Fleischmann, F. Lasserre, J. Robinson and D. Swan, J. Electroanal. Chem., 177 (1984) 97.
10 A. Fitch and D. H. Dennis, J. Electroanal. Chem., 202 (1986) 83.
11 J. O. Howell and R. M. Wightman, Anal. Chem., 56 (1984) 524.
12 A. M. Bond, M. Fleischmann and J. Robinson, J. Electroanal. Chem., 180 (1984) 257.
13 W. L. Caudill, J. O. Howell and R. M. Wightman, Anal. Chem., 54 (1982) 2532.
14 L. A. Knecht, E. J. Guthrie and J. W. Jorgensen, Anal. Chem., 56 (1984) 479.
15 K. Stulik, V. Pacakova and M. Podolak, J. Chromatogr., 298 (1984) 225.
16 M. R. Cushman, B. G. Bennett and C. W. Anderson, Anal. Chim. Acta, 130 (1981) 323.
17 G. Schulze and W. Frenzel, Anal. Chim. Acta, 159 (1984) 95.
18 V. J. Jennings and J. E. Morgan, Analyst, 110 (1985) 121.
19 K. R. Wehmeyer and R. M. Wightman, Anal. Chem., 57 (1985) 1989.
20 A. S. Baranski and H. Quon, Anal. Chem., 58 (1986) 407.
21 J. Golas and J. Osteryoung, Anal. Chim. Acta, 181 (1986) 211.
22 M. Ciszkowska and Z. Stojek, J. Electroanal. Chem., 191 (1985) 101.
23 A. N. Doronin and G. G. Muntyan, Zh. Anal. Khim., 39 (1984) 483.
24 Z. Galus, J. O. Schenk and R. N. Adams, J. Electroanal. Chem., 135 (1982) 1.
25 M. Penczek and Z. Stojek, J. Electroanal. Chem., 191 (1985) 91.
26 K. Aoki and J. Osteryoung, J. Electroanal. Chem., 160 (1984) 335.
27 M. A. Dayton, J. C. Brown, K. J. Stutts and R. M. Wightman, Anal. Chem., 52 (1980) 946.
28 G. Schulze and W. Frenzel, Fresenius' Z. Anal. Chem., 314 (1983) 459.
29 T. M. Florence, J. Electroanal. Chem., 27 (1970) 273.
30 T. M. Florence, Anal. Chim. Acta, 119 (1980) 217.
31 G. Subramanian and G. P. Rao, Rev. Anal. Chem., 4 (1979) 95.
32 D. Jagner and K. Årén, Anal. Chim. Acta, 100 (1978) 375.
33 C. Labar and L. Lamberts, Anal. Chim. Acta, 132 (1981) 23.
34 W. Frenzel, Ph.D. Thesis, Technical University, Berlin, 1984.
35 K. Aoki, K. Akimoto, K. Tokuda, M. Matsuda and J. Osteryoung, J. Electroanal. Chem., 171 (1984) 219.
36 J. Wang, Anal. Chem., 54 (1982) 221.
37 M. Wojciechowski, W. Go and J. Osteryoung, Anal. Chem., 57 (1985) 155.
38 D. Jagner, Anal. Chem., 52 (1980) 220.
39 G. Schulze and W. Frenzel, Fresenius' Z. Anal. Chem., 316 (1983) 26.
40 A. Granéli, D. Jagner and M. Josefson, Anal. Chem., 52 (1980) 220.

Analytica Chimica Acta, 196 (1987) 153—161
Elsevier Science Publishers B.V., Amsterdam — Printed in The Netherlands

A FLOW CELL WITH FLEXIBLE DEPOSITION EFFICIENCY FOR A DUAL-DETECTION SYSTEM BASED ON POTENTIOMETRIC STRIPPING ANALYSIS AND ATOMIC ABSORPTION SPECTROMETRY

G. SCHULZE*, M. KOSCHANY and O. ELSHOLZ

Institut für Anorganische und Analytische Chemie, Technische Universität Berlin, Straße des 17. Juni 135, 1000 Berlin 12 (Federal Republic of Germany)

(Received 8th August 1986)

SUMMARY

An electrochemical flow cell suitable for use with dual detection by potentiometric stripping analysis and atomic absorption spectrometry in a flow-injection system is characterized by flow pattern and dispersion measurements. The deposition efficiency can be altered from 1—2% to 24% by using a glassy carbon and a carbon felt electrode, respectively. Application to the determination of lead in water showed that after enrichment on carbon felt the sensitivity for flame atomic absorption spectrometry is increased by an order in magnitude (enrichment factor ca. 5 and 30 at sample frequencies of 60 and 12 h^{-1}, respectively). Dual-detection allows certain errors appearing in one of the methods caused by, e.g., malfunction of the apparatus or wrong sample pretreatment, to be recognized, thus providing accuracy checks.

The determination of trace elements often requires the elimination of matrix effects [1] and the enhancement of the sensitivity of the analytical method [2]. For these purposes, separation and enrichment techniques are used. On-line separation and preconcentration offers advantages such as easy handling and little risk of contamination. This can be achieved by electrochemical deposition in flow systems [3]. When porous carbon electrodes are used, a high deposition efficiency for heavy metals can be achieved [4]. In addition, two signals for the same sample at almost the same time by two different methods are obtained when a flow-injection potentiometric stripping system is connected to the nebulizer of a flame atomic absorption spectrometer [5].

With this dual-detection system, errors occurring in the malfunction of one of the methods will be indicated immediately by the other method. The new flow cell described in this paper enables two different types of dual detection. The type chosen depends on the sample concentration: if the concentration is lower than the detection limit of flame atomic absorption spectrometry (a.a.s.), a porous carbon felt electrode is inserted into the cell and potentiometric stripping analysis (p.s.a.) provides preconcentration. Although the two signals (from p.s.a. and a.a.s.) are dependent on each other to some

0003-2670/87/$03.50

extent, for both depend on the deposition process, errors in detection (e.g., by detector drift) can easily be recognized. If the concentration of the sample is in the range suitable for flame a.a.s., a glassy carbon electrode is used in the cell and two independent signals are obtained. This guarantees an efficient control of the accuracy.

EXPERIMENTAL

Apparatus

For flame a.a.s. measurements, a Pye Unicam model SP-2900 spectrometer was used. For p.s.a., a potentiostat equipped with a high speed recorder (Tecator, Model Striptec 1069) was used. Both instruments were attached to a FIAstar unit (Tecator) [6]. A schematic diagram of the system is depicted in Fig. 1.

The flow-through cell (Fig. 2) was built by inserting the electrodes into channels drilled in a plexiglas cylinder. The working electrode was a 3-mm diameter glassy carbon rod (Sigri Elektrographit) pressed into a teflon screw which allows the dead volume in the cell to be varied. The electrode surface was polished to a mirror-like finish by means of diamond pastes of decreasing particle size (30, 7, 3, 1, 0.7, 0.25 μm). A short glassy carbon tube fixed in with a cyanacryl glue (Acculite, Cotronics Corp.) served as auxiliary electrode. The silver wire of the silver/silver chloride reference electrode was stored in a silver chloride/potassium chloride solution for at least 24 h before use, and the same solution filled the reference chamber. If the cell was used with carbon felt (Deutsche Carbon, Type RVC 2000), a thin plate of Dekontakoll (Colla-Rheincollodium, Köln) was placed on the auxillary electrode

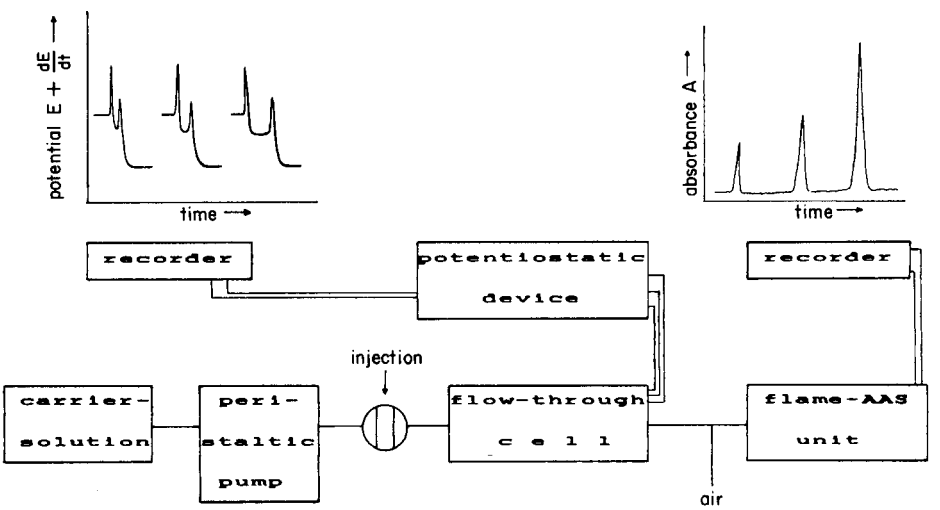

Fig. 1. Schematic diagram of the flow-injection system for p.s.a./a.a.s. dual detection.

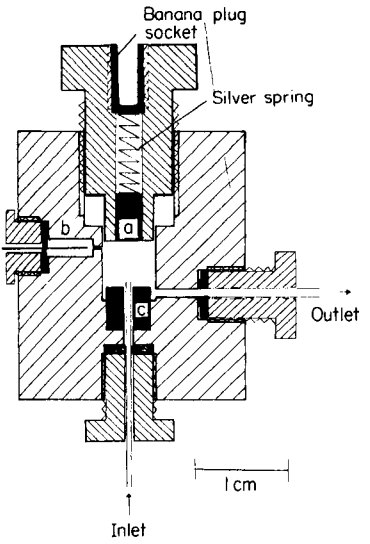

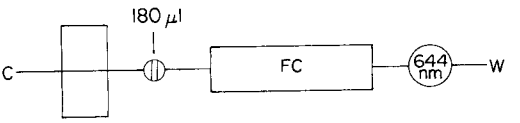

Fig. 2. Flow-through cell for potentiometric stripping analysis: (a) working electrode; (b) reference electrode; (c) auxiliary electrode.

Fig. 3. Flow-injection manifold for the determination of dispersion and the observation of the flow pattern. C, Borax carrier solution; FC, flow-through cell; W, waste.

to avoid short circuits. Electrical contact to the carbon felt chip (4 mm diameter, 3 mm thick) was made with the glassy carbon working electrode.

Dispersion was investigated with a flow-through cuvette in a photometer (Eppendorf, Model 1101 M) (Fig. 3). Injection volumes were varied by using loops of different length and inner diameter (0.7—1.6 mm i.d.). All connecting tubing was 0.7 mm i.d. teflon. The flow rate was adjusted by the speed of rotation of a peristaltic pump (Watson Marlow, Model 501-U/100).

Reagents

The filling solution for the reference electrode was prepared by adding 200 µl of silver nitrate stock solution (see below) to 5 ml of 1.0 M potassium chloride solution. For the dye stock solution, 0.4 g of bromothymol blue was dissolved in 25 ml of 96% ethanol and the solution was diluted to 100 ml with 0.01 M sodium borate solution; 1 ml of this stock solution was diluted to 200 ml with 0.01 M sodium borate solution for the dispersion measurements. The metal ion solutions were prepared by diluting stock solutions containing 1 g l^{-1} lead(II), mercury(II) and silver(I) (Titrisol, Merck) with twice-distilled water, with nitric acid added to adjust the pH to 2. The mineral acids were of high purity (Suprapur, Merck) and all the other reagents were of analytical grade.

RESULTS AND DISCUSSION

Examination of flow pattern

To study the form of the jet on its way through the cell a visible flow pattern is needed. The dye stock solution injected by means of the flow-injection system enters the flow-through cell very quickly, so that it is difficult to observe the flow pattern. To follow the process, photographic film was shot at 200 frames per second.

The photographs of three phases, which illustrate the process of sample entry into the cell, are presented in Fig. 4; the first phase is when the dye zone has just entered the cell (t_1), the next is after 50 ms (t_2), and the last is after 200 ms (t_3). At a flow rate of 5 ml min^{-1} a compact dye jet enters the cell (t_1), becomes thicker (t_2) and fills the left part of the cell (t_3). It is remarkable that the right side (opposite the outlet) remains clear. The dye obviously leaves the cell so quickly that it does not penetrate the whole compartment. If the flow rate is decreased to 3 ml min^{-1}, the dye zone splits and forms whirls which eventually almost fill the cell (t_3).

When the carbon felt has been inserted (Fig. 4, right side), the jet bounces against the felt and returns divided into two parts (t_1). Then the dye fills

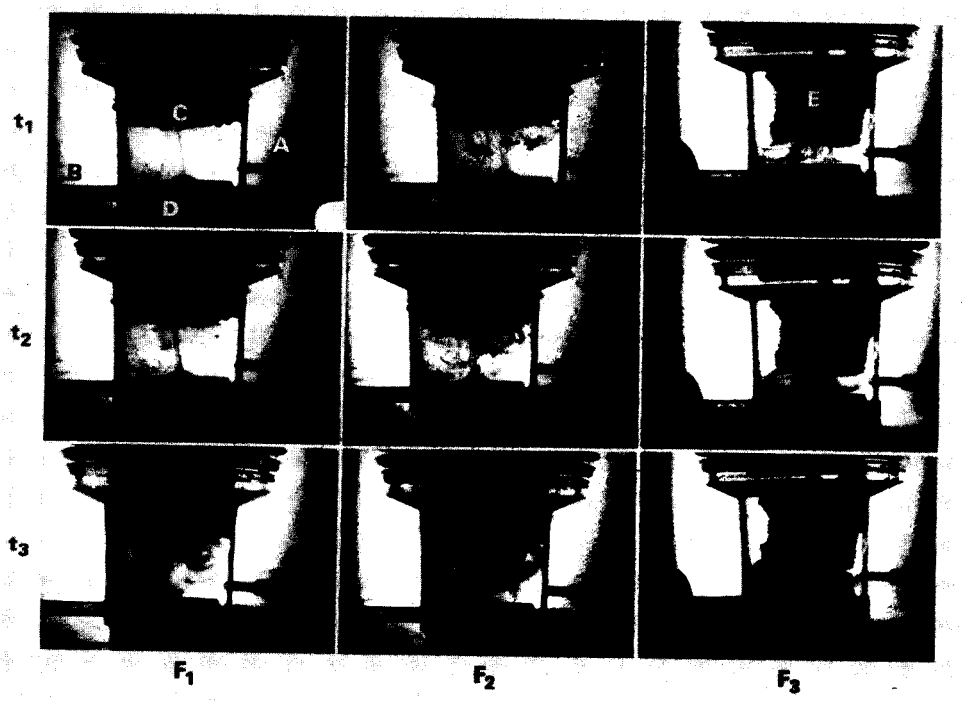

Fig. 4. Photographs of the flow pattern. (A) Reference electrode; (B) outlet; (C) glassy carbon electrode; (D) auxiliary electrode; (E) carbon felt. Flow rates: F_1, 5 ml min^{-1}; F_2, 3 ml min^{-1}; F_3, 3 ml min^{-1} with carbon felt. Times t_1—t_3 are defined in the text.

more and more of the volume between the felt and the auxiliary electrode (t_2, t_3). However, the space between the carbon felt and the wall is clear. It is most likely that the dye enters the felt, but obviously not to a great depth.

As is shown by the flow pattern, the cell with the glassy carbon working electrode may be considered to be a wall-jet type. The type of cell with carbon felt is not well defined; it seems to be intermediate between a wall-jet and a porous flow-through type. Because the jet penetrates the carbon felt, the cell cannot be classified as a wall-jet type, but the depth of penetration is very low. This prevents it being designated as a flow-through type. It is proposed to define the new cell as a "porous wall-jet" type.

Measurement of dispersion

In a dual-detection system the signal resulting from the second method (in this case, a.a.s.) mainly depends on the dispersion of the sample. To minimize loss of sensitivity, the dispersion caused by passing through the first detector (the p.s.a. cell) must be kept as small as possible. The dispersion was measured as described by Růžička et al. [6]. The injection volume was 180 μl, the flow rate 3.3 ml min^{-1} and the wavelength 644 nm. The absorbance at steady state was 0.770 and the dispersion of the flow system without the flow-through cell (D_0) was 1.098. After installation of the flow-through cell, the dispersion was measured at various distances (d) between the working and the auxiliary electrode. This distance is proportional to the dead volume of the cell. As shown in Table 1 the dispersion is very low; it decreases with decreasing dead volume, and approaches the smallest possible value, 1.00. Thus, the new cell is optimal for use in dual-detection systems. In comparison, a commercial flow-through cell, the Metrohm Model EA1096, produces a minimum dispersion of 1.36.

Deposition efficiency

Preconcentration requires a high deposition efficiency, but if dual-detection is used to monitor accuracy, the amount of deposition should be as small as possible, consistent with a reasonable p.s.a. measurement, to ensure a high atomic absorption signal. The deposition efficiency was evaluated by injection of a lead solution into the system shown in Fig. 1. The flow-rate was 5.0 ml min^{-1}, the injection volume 180 μl, the electrolysis time 400 s and the wavelength 283.3 nm. The lead solution contained 32 mg Pb l^{-1} and the carrier solution 20 mg Hg^{2+} l^{-1} in 0.01 M nitric acid. The deposition potential was altered. First, it was set to —0.2 V, a potential which is not sufficient to deposit lead, then the potential was changed to —0.9 V (and beyond) resulting in a decrease of the atomic absorption signal. The difference between the absorption signals was used to define the deposition efficiency $Eff.(d) = 1 - A_2A_1^{-1}$, where A_1 and A_2 are the absorbances without and with electrolysis, respectively. The value of $Eff.(d)$ is between 0 and 1 (0 and 100% deposition, respectively).

In recent papers, it was shown that deposition on carbon felt depends on flow rate and electrolysis potential [4, 5]. Therefore, the atomic absorbance

TABLE 1

Dependence of dispersion (D) on the distance between electrodes (d)[a]

d (mm)	4.0	3.2	2.6	1.6	0.7	min.[b]
D	1.27	1.22	1.19	1.14	1.13	1.40
$D\,D_0^{-1}$[c]	1.16	1.11	1.09	1.04	1.03	1.27

[a]All data are the average of 3 measurements. The relative standard deviation is $<0.5\%$. [b]Could not be measured exactly (≈ 0.1 mm). [c]For D_0, see text.

TABLE 2

Dependence of deposition efficiency, *Eff.* (d), on deposition potential[a]

Deposition potential (V)	GC electrode			Carbon felt		
	Absorbance	*Eff.* (d)	t_s (s)	Absorbance	*Eff.* (d)	t_s (s)
−0.2	0.125	—	—	0.099	—	—
−0.9	0.123	0.02	2.8	0.085	0.14	—
−1.2	0.125	0.00	3.0	0.076	0.24	1.6
−1.5	0.124	0.01	1.9	0.084	0.16	2.0
−2.0	0.122	0.02	0.9	0.082	0.17	1.9

[a]All data are the average of 7 measurements.

A, the stripping time t_s, and the deposition efficiency at various deposition potentials were measured. They are listed in Table 2 together with the analogous data for the glassy carbon electrode without carbon felt.

The important property of the cell is its flexible application which provides monitoring of accuracy and of the extent of enrichment. It is possible to alter the deposition efficiency from 1 or 2% (glassy carbon electrode) to 24% (carbon felt electrode). Considering the enrichment effect alone, the cell is inferior to the porous carbon flow-through cell described earlier [4, 5] probably because of the lower degree of penetration into the felt.

Owing to the re-dissolution of lead during the stripping phase in p.s.a., an additional atomic absorption signal appears as is shown in Fig. 5. Its peak height depends on the deposition efficiency. Therefore no signal is observed after stripping when the glassy carbon electrode is used. With carbon felt, however, the effect may be used for enrichment. If carbon felt is inserted in the cell described in Fig. 2, the flow rate has no effect on the atomic absorption signal (Table 3). This effect is unexpected. It may be caused by the compensation of two effects: the decrease of residence time at higher flow rates on the one hand and the increase of the electrode area by deeper penetration on the other.

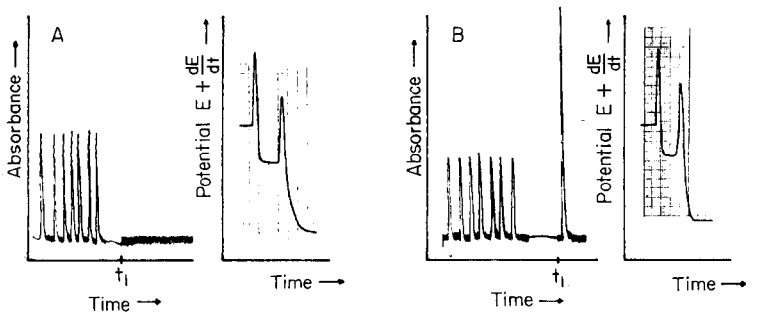

Fig. 5. Typical signals for dual-detection. (A) Glassy carbon electrode; (B) carbon felt electrode. Deposition potential, −1.2 V; flow rate, 5.0 ml min^{-1}; injection volume, 180 μl; electrolysis time, 400 s: (t_1) End of electrolysis and beginning of stripping.

TABLE 3

Dependence of atomic absorbance and stripping time on flow rate[a]

Flow rate (ml min^{-1})	1.0	2.4	5.0
Atomic absorbance	0.268	0.264	0.264
Stripping time(s)	4.8	4.8	3.6

[a]All data are the average of four measurements.

Application to water analysis

In samples of drinking water which had been analyzed routinely by anodic stripping voltammetry, the lead content was determined by using the dual-detection system. To check the accuracy, four samples with unusually high lead concentrations were selected and measured with the glassy carbon electrode. Figure 6 shows the calibration plots for p.s.a. and a.a.s. Table 4 contains the absorbance, the stripping time and the lead concentration data. The difference between the results obtained by a.a.s. and p.s.a. for sample 1 was caused by a malfunction of the apparatus, probably owing to an air-bubble in the cell. Checking the pH showed that sample 4 was not acidic enough, therefore lead did not exist totally in ionic form, leading to lower results by p.s.a.

Water samples containing lead in the μg l^{-1} range were analyzed with the carbon felt working electrode. Calibration plots obtained by different modes of evaluation are shown in Fig. 7. The atomic absorption signal obtained during electrolysis (produced by the undeposited lead) leads to lower sensitivity (curve b) than that signal obtained after stripping the lead which has been deposited by electrolysis (curve c). Compared with conventional a.a.s. (curve a), the deviation from linearity appears at higher concentrations in curve (b) but at lower concentrations in curve (c). A further advantage of the new cell is also evident, in that two atomic absorption signals are achieved from one

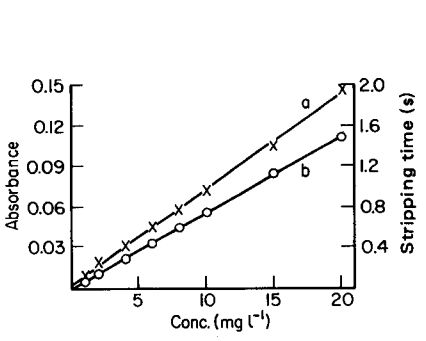

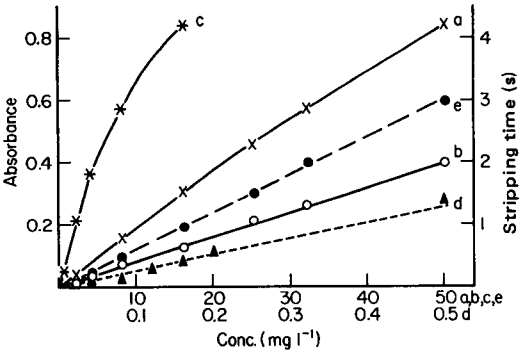

Fig. 6. Calibration plots for lead: (a) p.s.a. with the glassy carbon electrode; (b) a.a.s.

Fig. 7. Calibration plots for lead with the carbon felt electrode: (a) normal a.a.s. aspiration technique; (b, c, d) dual-detection system. Atomic absorption signal: (b) during electrolysis; (c) after stripping, injection volume 1.5 ml; (d) after stripping, injection volume 5 × 1.5 ml. (e) Potentiometric stripping signal.

TABLE 4

Results for lead in water with the dual-detection system

Sample no.	Absorbance	Conc. by a.a.s. (mg l^{-1})	t_s (s)	Conc. by p.s.a. (mg l^{-1})
1	0.078	14.0	0.56	11.6
2	0.028	4.9	0.25	5.0
3	0.049	8.9	0.42	8.9
4	0.109	19.6	0.78	16.3

injection, which gives the possibility of using two calibration plots. This enlarges the linear working range for a.a.s. by an order of magnitude.

The signals obtained after stripping depend on the number of injections (total injection volume). With one injection of 1.5 ml (curve c) the linear calibration slope (sensitivity) is 4.8 times higher than for normal a.a.s., and with five injections of 1.5 ml (curve d) it is 30.4 times higher. This enhancement permits the determination of lead in the μg l^{-1} range by flame a.a.s. A 1.5-ml injection requires an electrolysis time of 60 s.

It has already been shown that only the ionic species are detected by p.s.a. whereas the total amount of the element can be determined by a.a.s. This shows the possibility of speciation.

The valuable assistance of Mr. H. Rybczynski in constructing the flow-through cell is highly appreciated.

REFERENCES

1 Y. Thomassen, B. V. Larsen, F. J. Langmyhr and W. Lund, Anal. Chim. Acta, 83 (1976) 103.
2 T. Kempf and M. Sonneborn, Mikrochim. Acta, Part II, (1983) 445.
3 S. E. Long and R. D. Snook, Analyst, 108 (1983) 1331.
4 G. Schulze, M. Husch and W. Frenzel, Mikrochim. Acta, Part I, (1984) 191.
5 G. Schulze, O. Elsholz and W. Frenzel, Fresenius' Z. Anal. Chem., 320 (1985) 650.
6 J. Růžička, E. H. Hansen and A. U. Ramsing, Anal. Chim. Acta, 134 (1982) 55.

Analytica Chimica Acta, 196 (1987) 163—169
Elsevier Science Publishers B.V., Amsterdam — Printed in The Netherlands

ENTWICKLUNG EINER FLIEßINJEKTIONSMETHODE ZUR BESTIMMUNG VON CHLORID IM SPURENBEREICH DURCH LEITFÄHIGKEITSDIFFERENZEN

G. LACH und K. BÄCHMANN*

Fachbereich Anorganische Chemie und Kernchemie, Technische Hochschule Darmstadt, D-6100 Darmstadt (Federal Republic of Germany)

(Eingegangen den 4 August 1986)

SUMMARY

(*A flow-injection method for the determination of trace amounts of chloride.*)
The indirect determination of chloride in water is based on measurement of the difference in conductivity after the sample has passed through ion-exchange columns in the hydrogen form and silver form. The linear response range is about 0.5—10 $\mu g\ g^{-1}$ chloride (with 3 $\mu g\ g^{-1}$ nitrate and 5 $\mu g\ g^{-1}$ sulfate); the detection limit is about 50 $ng\ g^{-1}$ chloride but depends strongly on the concentrations of other anions.

ZUSAMMENFASSUNG

Prinzip der Fließinjektionsmethode ist die indirekte Bestimmung von Chlorid in wässrigen Phasen durch Messung von Leitfähigkeitsdifferenzen nach Ionenaustausch. Der Konzentrationsbereich für Chlorid liegt bei 0,5—10 $\mu g\ g^{-1}$ (mit 3 $\mu g\ g^{-1}$ NO_3^- und 5 $\mu g\ g^{-1}$ SO_4^{2-}), die Nachweisgrenze beträgt 50 $ng\ g^{-1}$ Cl^- (mit 1 $\mu g\ g^{-1}$ NO_3^- und 1 $\mu g\ g^{-1}$ SO_4^{2-}), wobei die Nachweisgrenze stark von den Konzentrationen der anderen Anionen abhängig ist.

Gasförmiger Chlorwasserstoff besitzt im Chlorkreislauf in der Luft eine zentrale Bedeutung. Als eine saure, im Wasser dissoziierte Komponente trägt er zum "Sauren Regen" bei und belastet so die Umwelt. Die Konzentrationen des gasförmigen HCl in einer Wolke oder im Nebel — die beide Teil des komplizierten Aerosol-Systems in der Atmosphäre darstellen — hängt wahrscheinlich vom pH-Wert, der Cl^--Konzentration und der Größe der Wassertropfen ab.

Die bisher üblichen Verfahren zur Cl^--Bestimmung, wie z.B. die Ionenchromatographie, besitzen für die Analyse von Wolken- bzw. Nebelwasser einige Nachteile. So ist mit ihnen weder eine zeitlich hochauflösende Analyse möglich, noch sind sie im on-line Verfahren einsetzbar, was vor allem im Hinblick auf mögliche Kontaminationsprobleme bei der Bestimmung von Cl^- im zu erwartenden Konzentrationsbereich von Nachteil ist. Deshalb sollte ein alternatives Verfahren zur Bestimmung von Chlorid in der flüssigen Phase folgende Gesichtspunkte verwirklichen: (1) zeitlich hochaufgelöste Analyse von Wolkenwasser (z.B., Bestimmung der Cl^--Konzentration als Querschnitt

0003-2670/87/$03.50

beim Durchfliegen einer Wolke), Nebelwasser und Niederschlagswasser (Unterscheidung "rain-out — wash-out"); (2) Analyse von geringen Probevolumina, bedingt durch die hohe zeitliche Auflösung; (3) On-line Verfahren, um Kontaminationsprobleme zu vermeiden; (4) Einfache und unempfindliche Technik, die einen Einsatz unter erschwerten Bedingungen, wie in Flugzeugen, gewährleistet. Um den o.g. Anforderungen zu entsprechen wurde ein System entwickelt, das auf den Prinzipien der Fließinjektionsanalyse (FIA) aufbaut. Dieses System sollte vor allem der Forderung einer hohen zeitlichen Auflösung gerecht werden können.

Die grundlegenden Arbeiten zur Theorie der Fließinjektionsanalyse wurden von Růžička und Hansen [1, 2] durchgeführt. Die indirekte photometrische Bestimmung von Chlorid in wässrigen Lösungen über die Messung eines $Fe(SCN)_2^+$-Komplexes bei 480 nm wurde von Růžička et al. [3] sowie Basson und van Staden [4] auf eine Fließinjektionsmethode übertragen. Die Intensität des gebildeten roten Komplex-Ions ist direkt proportional der Chloridkonzentration. Der Nachteil dieses Systems liegt darin, daß sich leicht höher koordinierte Komplex-Ionen bilden und somit die Linearität des Systems nur einen geringen Cl^--Konzentrationsbereich umfaßt [5]. Weitere Methoden zur Chloridbestimmung mittels FIA sind die potentiometrische Analyse mit einer Ag/AgCl-Elektrode von Trojanowicz und Matuszewski [6], sowie eine Methode von Rössner und Schwedt [7], die ein Fe(II)/Hg-Tripyridyl-*s*-triazin (TPTZ)-System für die photometrische Analyse einsetzen.

Von Ilcheva und Cammann [8] wurde eine Fließinjektionsanalyse von Chlorid in Leitungs- und Abwasser mit Detektion durch eine ionen-selektive AgCl-Einkristallmembranelektrode entwickelt. Die Methode weist allerdings Standardabweichungen von 5—10% in einem Konzentrationsbereich von 10—100 $\mu g\ g^{-1}$ Cl^- auf.

Methodische Entwicklung

Grundlage des Systems ist die indirekte Bestimmung von Chlorid durch Messung von Differenzleitfähigkeiten. Durch eine in das System integrierte, mit Ag^+-Ionen belegte Austauschersäule werden in der Probe vorhandene Chlorid-Ionen als unlösliches AgCl ausgefällt:

$$-SO_3^-Ag^+ + H^+Cl^- \rightarrow -SO_3^-H^+ + AgCl$$

$$-SO_3^-Ag^+ + Na^+Cl^- \rightarrow -SO_3^-Na^+ + AgCl$$

Das Löslichkeitsprodukt von AgCl beträgt $1{,}7 \times 10^{-10}$ $mol^2\ l^{-2}$ (25°C), d.h. in der mit Ag^+-Ionen belegten Säule (im folgenden als Ag-Säule bezeichnet) sollte eine quantitative Fällung der Chlorid-Ionen erfolgen. Die Ag-Salze von weiteren, in den Proben vorhandenen Anionen, besitzen zu hohe Löslichkeitsprodukte, um bei den vorherrschenden Bedingungen ausgefällt zu werden. Das resultierende Detektionssignal sollte dann nur von diesen Anionen, wie Sulfat und Nitrat, herrühren. In einem zweiten Schritt, der je nach Ausbaustufe des Systems zeitlich versetzt oder parallel erfolgt, wird die

Probe über eine mit Protonen belegte Säule (im folgenden als H-Säule bezeichnet) geführt, und man erhält ein Signal, welches aus der Summe aller Anionen, einschließlich der Chlorid-Ionen, resultiert. Die Differenz der Signale aus beiden Messungen sollte dann dem Gehalt an Chlorid in der untersuchten Probe proportional sein.

EXPERIMENTELLES

Abbildung 1 zeigt das Fließschema des konzipierten Systems, das auf der Messung von Differenzleitfähigkeiten nach Ionenaustausch in einem geschlossenen Kreislauf beruht. Als Trägerstrom dient entionisiertes Wasser (Milli-Q, Millipore). Der Transport des Trägerstroms erfolgt mit Hilfe einer pulsationsarmen Mehrkanal-Kassettenschlauchpumpe (IPS-4, Ismatec). Zur Probenaufgabe wird ein pneumatisch getriebenes Injektionsventil benutzt (Dionex), ebenso für die Verzweigung des Analysenstroms vor den Austauschersäulen.

Der Ionenaustauscher besteht aus einem Harz des Typs 50 WX 8 der Korngröße 200—400 mesh (Dowex). Da er in der Na-Form geliefert wird, muß er mit Hilfe von Salzsäure bzw. Silbernitratlösung in die H- bzw. Ag-Form gebracht werden. Nach Durchgang durch diese Austauschersäulen wird der Probenstrom nochmals über eine Kationenaustauschersäule in der H-Form geführt. Dies hat mehrere Gründe. In den zu untersuchenden Proben können viele verschiedene Kationen in unterschiedlichen Konzentrationen vorhanden sein. Da jedes Kation eine andere Equivalentleitfähigkeit besitzt, wäre bei jeder Probe eine neue Eichung des Systems notwendig, die jedoch voraussetzt, daß die Kationenarten und -konzentrationen bekannt sind. Dies würde jedoch einen unverhältnismäßig hohen Aufwand bedeuten und außerdem den Einsatz des Systems im on-line Betrieb verhindern. Durch den Austausch der Kationen gegen Protonen wird zudem die Empfindlichkeit des Systems in bezug auf die Anionen wesentlich erhöht, da die Equivalentleitfähigkeit der Protonen 349,82 $cm^2\ l^{-1}\ mol^{-1}$ beträgt und somit wesentlich höher als die aller anderen Kationen ist. Das Volumen bzw. die Länge der Austauschersäulen sowie der Verbindungsschläuche wird möglichst gering gehalten um die Dispersion des Probensegments zu minimieren. Man erreicht dadurch eine höhere Empfindlichkeit des Systems, was besonders bei der Analyse

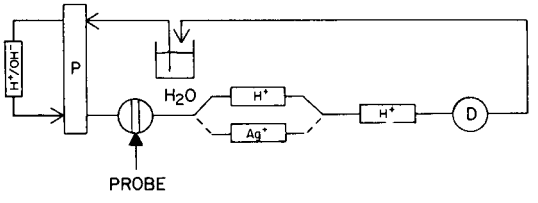

Abb. 1. Fließschema mit Kreislaufführung.

von Konzentrationen im ng ml^{-1}-Bereich von Bedeutung ist. Die Säulen wurden im Eigenbau hergestellt.

Als Detektor wird eine Leitfähigkeitsmeßzelle (Dionex) verwendet. Die Signale werden mit einem x/t-Schreiber aufgezeichnet (Linseis, Selb) und mit Hilfe eines Integrators (Minigrator, Spectra-Physics) über die Peakfläche ausgewertet.

ERGEBNISSE

Kalibrierung

Die Funktionsfähigkeit der neuen Analysenmethode für verschiedene Substanzen wurde mit Hilfe von Kalibrierungen überprüft, wodurch auch Schlußfolgerungen auf die Linearität und Reproduzierbarkeit des Systems ermöglicht wurden. Um später Niederschlagswasser untersuchen zu können, wurden die Konzentrationen für Cl^-, NO_3^- und SO_4^{2-}, die den Hauptanteil der Anionen im Niederschlagswasser ausmachen, in dem Bereich gehalten, der nach der Literatur [9] für Niederschlagswasser in Frage kommt (Tab. 1).

Um mögliche Störungen durch schwankende Grundleitfähigkeiten zu beseitigen, wurde ein System konzipiert, in dem das Trägermedium im Kreislauf geführt wird. Eine zusätzliche Mischbettaustauschersäule soll dabei eine konstante Grundleitfähigkeit garantieren, da ansonsten ein kontinuierlicher Anstieg der Leitfähigkeit durch diejenigen Stoffe erfolgen würde, die mit den zu analysierenden Proben in den Kreislauf gelangen (Abb. 1). Für den Mischbettaustauscher wurde ein Austauscherharz vom Typ 50 WX 8 in der H- bzw. OH-Form verwendet (Korngröße 200—400 mesh, Dowex).

Um die Linearität zu überprüfen, wurden für NO_3^- und SO_4^{2-} die Bezugskurven für beide Säulen, für Cl^- die Bezugskurve für die H-Säule, erstellt. Für eine typische Cl^--Kalibrierung [c(0—55 $\mu g\ g^{-1}$) vs. F(0—1800 arb.)] werden die Steigung $364{,}2 \times 10^6$, der y-Achsenabschnitt 13,427 und der Korrelationskoeffizient 0,9996 berechnet. Aus den Korrelationskoeffizienten, die Werte zwischen 0,9993 und 0,9997 aufweisen, ist erkennbar, daß die Linearität für alle fünf Bezugskurven im vorgegebenen Konzentrationsbereich gewährleistet ist.

Die Cl^--Abscheidung in der Ag-Säule liegt im Bereich von 98,3% (bei 500 ng g^{-1} Cl^-) bis 99,9% (bei 3 $\mu g\ g^{-1}$ Cl^-). Der mittlere Prozentsatz beträgt 99,1%, d.h. im Durchschnitt werden über 99% des vorhandenen Chlorids als

TABELLE 1

Werte für Niederschlagswasser [9]

	Konzentration ($\mu g\ g^{-1}$)			Konzentration (nmol ml^{-1})		
	Cl^-	NO_3^-	SO_4^{2-}	Cl^-	NO_3^-	SO_4^{2-}
Städtisch	1,14	3,36	5,70	32,11	54,29	59,38
Ländlich	0,77	2,26	3,72	21,69	36,43	38,75

AgCl ausgefällt. Nachdem die Linearität und Reproduzierbarkeit der Meßergebnisse von Einzelsubstanzen überprüft war, wurden Meßreihen mit Mischungen der einzelnen Komponenten durchgeführt. Die Konzentrationen von NO_3^- bzw. SO_4^{2-} wurden dabei konstant gehalten, während die Cl^--Konzentration im vorgegebenen Bereich variiert wurde. Die Ergebnisse wurden im Hinblick auf die Cl^--Konzentration ausgewertet, mit der Cl^--Bezugskurve verglichen und die Wiederfindungsrate des Chlorids bestimmt (Tab. 2).

Vergleich der Ionenchromatographie mit der Fließinjektionsmethode bei Analyse von Niederschlags- und Trinkwasser

Zur Überprüfung der entwickelten Methode wurde Niederschlags- und Trink wasser analysiert und mit den Ergebnissen einer ionenchromatographischen Analyse verglichen. Die jeweiligen Meßbedingungen und die Meßergebnisse sind in Tab. 3 wiedergegeben.

Nachweisgrenzen

Für Chlorid wurde eine Kalibriergerade im unteren ng g^{-1}-Bereich erstellt. Der niedrigste Konzentrationsbereich lag bei 10 ng g^{-1} Cl^-. Bei der Analyse von Gemischen mit konstanten NO_3^- und SO_4^{2-} Konzentrationen wurden akzeptable Wiederfindungsraten für Cl^- nur bis 50 ng g^{-1} Cl^- erreicht (Tab. 4). Wesentliche Störungen in diesem Konzentrationsbereich treten durch in den Proben gelöstes CO_2 auf, welches als HCO_3^- oder CO_3^{2-} ein Leitfähigkeitssignal bewirkt. Abbildung 2A zeigt das FIA-Signal eines Standards mit einer Konzentration von 10 ng g^{-1} Cl^-. Der Cl^--Peak ist gerade noch als Schulter zu erkennen, eine sinnvolle Auswertung ist nicht mehr möglich. Die Retentionszeit des CO_2-Peaks ist etwas verlängert im Vergleich zu den anderen Anionen. Dies ist wahrscheinlich darauf zurückzuführen, daß sich in den Austauschersäulen Adsorptionsgleichgewichte zwischen dem Ionenaustauschermaterial und dem CO_2 einstellen, und so zu einer verzögerten Elution führen. Als Lösungsmöglichkeit bot sich deshalb eine Reduzierung des Volumenstroms des Trägermediums an. Abbildung 2B zeigt, daß eine Verringerung des Volumenstroms von 1 ml min^{-1} auf 0,5 ml min^{-1} ausreicht, den Anionen- und den CO_2-Peak gut zu trennen.

TABELLE 2

System $Cl^-/NO_3^-/SO_4^{2-}$ mit $c_{NO_3^-}$ = 3 µg g^{-1} und $c_{SO_4^{2-}}$ = 5 µg g^{-1} [a]

c_{Cl^-} (µg g^{-1})	0,50	0,75	1	3	5
$\bar{x}_H$	21,55	22,90	23,92	32,24	40,08
$\bar{x}_{Ag}$	19,73	20,18	19,89	19,29	19,85
$\bar{x}_H - \bar{x}_{Ag}$	1,82	2,72	4,03	12,95	20,23
WFR (%)	96	99	106	113	111

[a] $\bar{x}$, Mittelwerte in Flächeneinheiten × 10^5; *WFR*, Wiederfindungsrate für Cl^-.

TABELLE 3

Meßbedingungen für der Fließinjektions methode und Ionenchromatographie und Meßwerte in Niederschlags- und Trinkwasser

	FIA	IC
System	Eigenbau	2000-i (Dionex)
Säulen	50 WX 8; 200—400 mesh H- bzw. Ag-Form	AS4 + AG4
Eluens	Deionisiertes H_2O	0,00144 M Na_2CO_3/0,0018 M NaH(
Probenschleife (µl)	50	100
Volumenstrom des Eluenten (ml min^{-1})	1	2
Meßbereich (µS cm^{-1} TS)	3 (10)	3 (10)
Cl^--Konz. (µg g^{-1})		
Niederschlagswasser	0,94 ± 0,06	0,96 ± 0,02
Trinkwasser	28,2 ± 1,5	26,5 ± 0,6

TABELLE 4

System $Cl^-/NO_3^-/SO_4^{2-}$ mit $c_{NO_3^-} = c_{SO_4^{2-}} = 1$ µg g^{-1} [a]

c_{Cl^-} (ng g^{-1})	10	50	100
$\bar{x}_H$	10,25	10,59	11,14
$\bar{x}_{Ag}$	9,81	10,03	9,99
$\bar{x}_H - \bar{x}_{Ag}$	0,43	0,56	1,15
WFR (%)	456	102	103

[a] $\bar{x}$, Mittelwerte in Flächeneinheiten × 10^5; *WFR*, Wiederfindungsrate für Cl^-.

DISKUSSION

Es wurde ein Fließinjektionssystem zur Cl^--Bestimmung entwickelt, welches auf der Grundlage des Ionenaustausches aufbaut. Die Analysen von Niederschlags- und Trink-wasser und der Vergleich mit der ionenchromatographischen Analyse erbrachten den Beweis, daß dieses System anwendungsfähig ist. Die Kalibrierungen in den untersuchten Konzentrationsbereichen dokumentieren die Linearität des Systems. Probleme treten erst im unteren ng g^{-1}-Bereich auf, wo der störende Einfluß von in den Proben gelöstem CO_2 zur Geltung kommt.

Entscheidend für die Eigenschaften des Systems sind die beiden Ionenaustauschersäulen. Man erhält optimale Ergebnisse, wenn beide Säulen absolut identisch bezüglich ihrer Abmessungen und den Packungseigenschaften (z.B. Korngröße, Packungsdichte) sind. Die mit Ag-belegte Austauschersäule arbeitet auch nach drei Monaten noch ohne irgendwelche Störungen. Die Cl^--Ionen werden weiterhin zu mehr als 99% zurückgehalten.

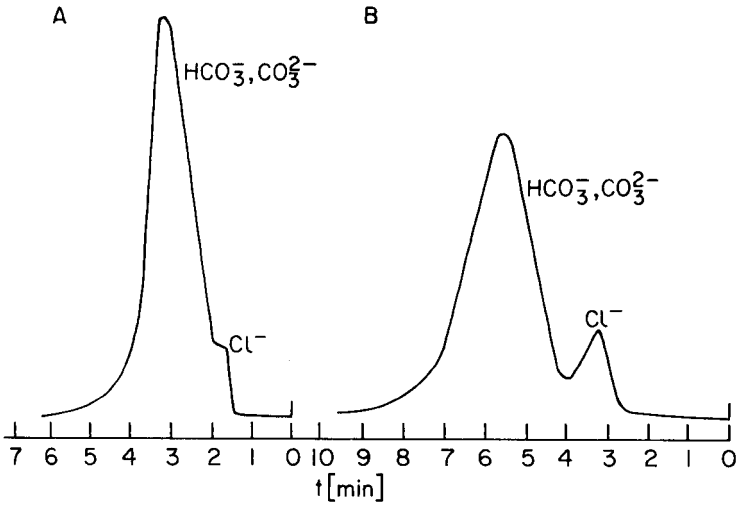

Abb. 2. FIA-Signal eines 10 ng g^{-1} Cl^--Standards (H-Säule). Volumenstrom: (A) 1.0 ml min^{-1}; (B) 0.5 ml min^{-1}.

Die in der Einleitung geforderten Eigenschaften des Systems sind wie folgt erfüllt. Eine zeitlich auflösende Analyse von Wolken-, Nebel- und Niederschlagswasser wurde noch nicht durchgeführt, erscheint aber bei weiterer Optimierung des Systems möglich. Die Analyse von geringen Probevolumina ist gewährleistet; das momentan nötige Volumen von 50 μl kann auf die Hälfte verringert werden. Alle Teile des Systems sind unempfindlich und robust; der Platzbedarf ist gering, so daß einem Einsatz unter erschwerten Bedingungen, wie z.B. in Flugzeugen, nichts im Wege Steht.

LITERATUR

1 J. Růžička und E. H. Hansen, Anal. Chim. Acta, 78 (1978) 145.
2 J. Růžička und E. H. Hansen, Flow Injection Analysis, Wiley-Interscience, New York, 1981.
3 J. Růžička, J. W. Stewart und E. A. Zagatto, Anal. Chim. Acta, 81 (1976) 387.
4 W. D. Basson und J. F. van Staden, Water Res., 15 (1981) 333.
5 J. F. van Staden, Fresenius' Z. Anal. Chem., 322 (1985) 36.
6 M. Trojanowicz und W. Matuszewski, Anal. Chim. Acta, 151 (1983) 77.
7 B. Rössner und G. Schwedt, Fresenius' Z. Anal. Chem., 315 (1983) 197.
8 L. Ilcheva und K. Cammann, Fresenius' Z. Anal. Chem., 322 (1985) 323.
9 J. Müller, Vortrag 4. Arbeitskreis Ionenchromatographie, Wiesbaden, 1985.

Analytica Chimica Acta, 196 (1987) 171—181
Elsevier Science Publishers B.V., Amsterdam — Printed in The Netherlands

DETERMINATION OF MICROGRAM AMOUNTS OF CARBON IN THE FORM OF CARBAMATE BY NON-AQUEOUS ELECTROLYTIC CONDUCTIVITY DETECTION

I. GÁCS*, K. PAYER and L. ÖTVÖS

Central Research Institute for Chemistry of the Hungarian Academy of Sciences, 1025 Budapest, Pusztaszeri ut 59-67 (Hungary)

(Received 16th June 1986)

SUMMARY

An absorption/detection system is described for the determination of carbon at and below microgram detection level. The carbon dioxide formed by combustion of an organic substance (solid or in solution) is led into a simple absorption/detection system containing 2.00 cm^3 of an ethanolic 2 M solution of 3-methoxypropylamine. The conductivity of the carbamate solution formed is measured by means of platinum electrodes built into the absorption tube, and the integrated d.c. voltage signal obtained is fed to a precision digital voltmeter. Detector response is linear up to 6.6 μg of carbon, and the detection limit is 2×10^{-2} μg. A single determination takes 5 min. Precision was found to be better than ±1.0% (P = 95%) for 1—6 μg of carbon.

The determination of carbon at and below microgram levels is important in several areas. Numerous methods utilizing different techniques for the final measurement of the carbon dioxide obtained by appropriate preparation of samples have been developed [1—3]. Small amounts of carbon dioxide can be measured by means of the change of electrolytic conductivity resulting from the absorption of the gas in aqueous alkalis or water, and this sort of detection has been applied in micro, ultramicro and trace procedures [4—18]. However, rapid and quantitative absorption in dilute aqueous solutions is difficult to achieve. Complicated equipment may be needed in some cases. A simple, sensitive and small absorption/detection system providing good precision and accuracy at low microgram levels with a detection limit of about 10^{-2} μg carbon should be of practical importance.

As shown previously [3, 19—30], various non-aqueous media are more suitable for the collection of carbon dioxide than aqueous solutions. In such absorbents, carbamate is formed [3, 29—31] by the reaction between carbon dioxide and an amine used alone or as a component. Infrared spectra of carbamate solutions show that carbamates dissociate in non-aqueous medium, while an increase in electrolytic conductivity compared to the solvent (acetonitrile) or the solution of the pure amine (diethylamine) is obtained [31]. In spite of their potential application for analytical purposes, no experimental data referring to the conductivity properties of non-aqueous

0003-2670/87/$03.50

carbamate/amine solutions are available. Therefore, the present investigations were aimed first at measurement of these data, on the basis of which the most suitable absorption/detection system for analytical purposes could be selected.

This paper presents the results of these investigations and describes a method for the determination of carbon in the form of carbamate by non-aqueous electrolytic conductivity detection. The principle of the method [32] is as follows. The carbon dioxide formed (e.g., by combustion of an organic substance) is led into a simple absorption/detection tube containing a small amount of an ethanolic solution of 3-methoxypropylamine. The integrated d.c. voltage signal obtained via a conductivity meter is linearly related to the amount of carbon trapped from the detection limit (2×10^{-2} μg) to 6.6 μg.

EXPERIMENTAL

Apparatus

The equipment is shown schematically in Fig. 1. The different parts of the apparatus are linked directly or via carefully-cleaned stainless-steel and copper capillary tubing. The oxygen used for sample combustion (flow rate 250 cm^3 min^{-1}) is led through a purification system consisting of a reactor heated to 1000°C with an electric furnace and an absorption tube for the retention of carbon dioxide. The sample feeding device made of PTFE is continuously rinsed with the purified gas to avoid contamination during sample introduction.

The sample weighed into a tin capsule (No. 76-1304, Lüdi, Switzerland) or a quartz liquid sample holder (washed with aqua regia and high-purity water then heated in an oxygen stream at 1000°C) is allowed to drop into the quartz combustion tube heated to 950°C, by turning the rotating part of the entry tap (Fig. 2). Prior to use, the combustion tube (Fig. 3) was also cleaned with aqua regia [33]. The chromium(III) oxide catalyst (Carlo Erba, Milan) pre-ignited in a stream of purified oxygen at 1000°C for at least 30 h, ensures complete oxidation of the combustion products. A perforated quartz lining tube is placed into the tube to protect its inner wall from possible damage caused by tin foil capsules during ignition. Water vapor, sulphur-, halogen- and nitrogen-containing combustion products are removed from the carrier gas stream by magnesium perchlorate (anhydrone; A_2 in Fig. 1), silver wool (A_3) heated to 550°C, and manganese dioxide (A_4), respectively. These reagents (all from Merck) are filled into microanalytical absorption tubes of the usual size. An empty bubbler (B_1) with a volume of 20 cm^3 functions as a safety vessel. The other thermostated bubbler is partly filled with ethanol (ca. 10 cm^3) to avoid loss of solvent by evaporation in the carbon dioxide absorber and detector. Details of the absorber/detector are shown in Fig. 4.

The carbon dioxide absorbent, an ethanolic 2 M solution of 3-methoxypropylamine, is fed into the absorption/detection system via stainless-steel

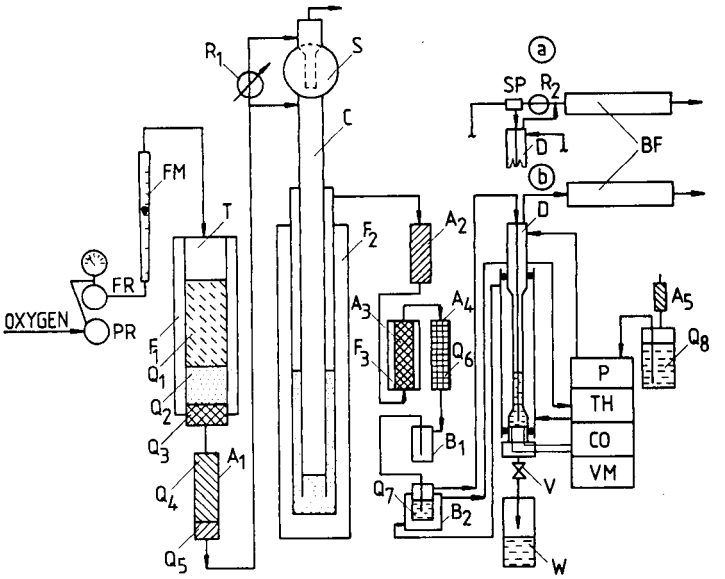

Fig. 1. Schematic diagram of the analytical instrument: (A_1, A_2, A_3, A_4, A_5) glass absorption tubes; (B_1, B_2) bubblers made of glass; (C) quartz combustion tube; (D) carbon dioxide absorber and detector; (F_1, F_2, F_3) furnaces; (P) pump; (Q_1) cerium dioxide; (Q_2) chromium(III) oxide; (Q_3) silver wool; (Q_4) ascarite; (Q_5) anhydrone; (Q_6) manganese dioxide; (Q_7) ethanol; (Q_8) absorbent solution; (R_1, R_2) pneumatic resistances; (S) sample feeder; (T) quartz reactor for oxygen purification; (V) solenoid valve; (W) waste; (CO) conductivity meter; (FM) flow meter; (FR) flow rate regulator; (PR) pressure regulator; (SP) splitter; (TH) thermostat; (VM) precision digital voltmeter; (BF) buffer vessel made of glass; (a) the absorber/detector system for ultramicro work; (b) the set-up for trace analysis.

capillary tubing by a micropump (type D-10; Labor MIM, Hungary) actuated by a time programmer (type OH-835, Chinoin, Hungary). The electrolytic conductivity of the solution thermostated at 20 ± 0.002°C is measured by circular electrodes made from platinum wire (0.5-mm diameter) and fixed into channels cut into the surface of the PTFE electrode holder (the cell constant was 0.515 cm^{-1}). The electrodes are connected to a conductivity meter (type OK-102/1, Radelkis, Hungary; measuring potential 0.2 V; measuring frequency 80 Hz) and the integrated d.c. voltage signal obtained at the appropriate output terminal (Δ 1 μS = Δ 1 mV) is fed to a precision digital voltmeter (type 1665, HIKI, Hungary) via a low-pass filter (R = 12 kohm; C = 47 μF).

Because the upper limit of the linear response of the detector was found to be 6.6 μg carbon, when the amount of the carbon in the samples exceeded this limit the inlet of the absorber was split (e.g., in a ratio of 1:174) and only a known part of the carbon dioxide obtained from the sample was used for detection (see Fig. 1a). In all other cases (e.g., trace analysis), the whole volume of the gas carrying the carbon dioxide was led into the absorption solution (see Fig. 1b).

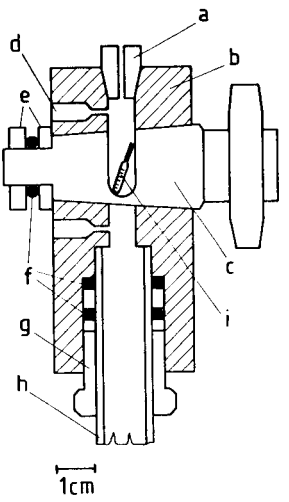

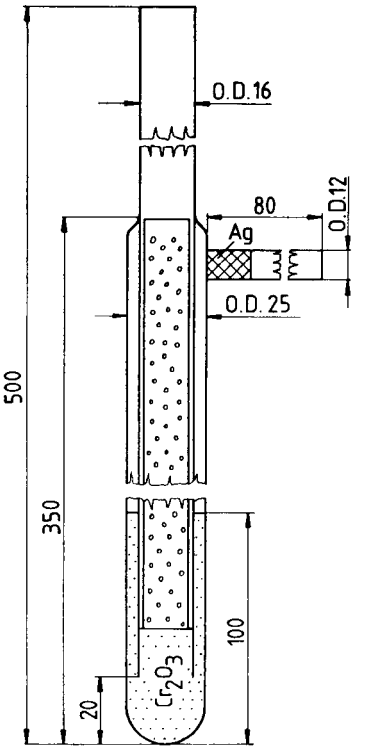

Fig. 2. Sample feeding device: (a) PTFE plug with capillary outlet; (b) PTFE body; (c) rotating part made from PTFE; (d) carrier gas inlet; (e) plastic nut and support; (f) O-rings; (g) holding nut; (h) combustion tube; (i) sample.

Fig. 3. Sample combustion tube. All dimensions in mm. For packings, see text.

The oxygen used for sample combustion can be used as the carrier gas, which is an advantage of the electrolytic conductivity detectors. Purified nitrogen can also be applied for this purpose. In the latter case, discrete amounts of pure oxygen are fed into the nitrogen stream for combustion by means of an injection valve, the arrangement of which is shown in Fig. 5.

For measurement of the absorption efficiency and splitting ratio, respectively, samples labeled with carbon-14 were combusted and the carbon dioxide passing through the absorber or the splitter was trapped by pure 3-methoxypropylamine for liquid scintillation counting [34]. For the selection of optimum conditions, in addition to the final design of absorber and detector, a larger absorber containing 28 cm^3 of solution and a commercially available electrode (type OK-9023, Radelkis) were used. The platinum black coating of this electrode was removed by aqua regia to avoid unnecessary absorption phenomena on the electrode surface.

Prior to use, the amines were freshly distilled, and the solvents were sparged with helium.

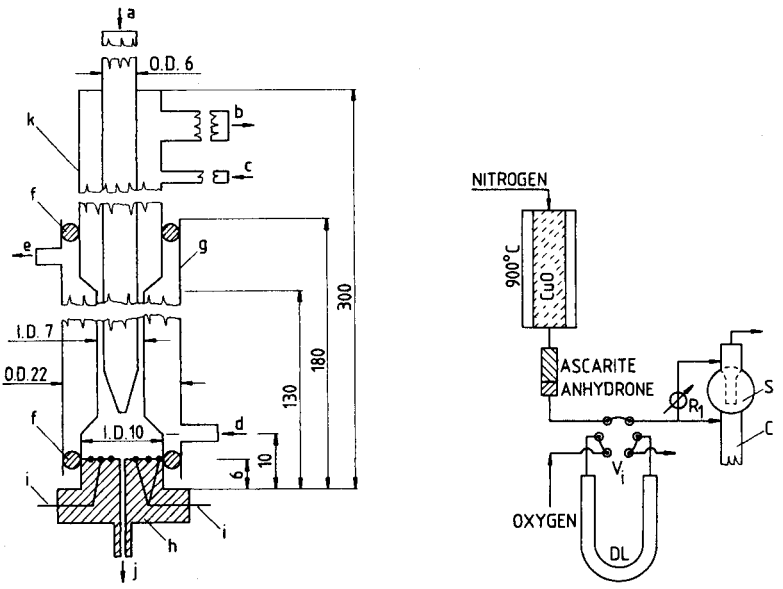

Fig. 4. Carbon dioxide absorber and detector: (a) inlet for carrier gas; (b) outlet for carrier gas; (c) inlet for absorbent; (d) inlet for water; (e) outlet for water; (f) O-rings; (g) glass jacket for water circulation; (h) PTFE electrode holder; (i) platinum electrodes; (j) outlet for the carbamate solution; (k) absorber body made of glass.

Fig. 5. Arrangement of oxygen injection valve: (C) combustion tube; (DL) dosing loop with a volume of 50 cm^3; (R_1) pneumatic resistance; (S) sample feeder; (V_i) injection valve.

Procedure

The oxygen purifying reactor, the sample combustion tube and the silver wool absorber are first heated in a stream of oxygen which escapes from the apparatus through the empty bubbler disconnected from the system. When the necessary temperatures have been reached, the connection is restored, the thermostat is turned on and the absorption/detection system is rinsed with 10 cm^3 of absorption solution by actuating the micropump and the solenoid valve for 60 s. Then, 2.00 cm^3 of absorbent is fed into the absorber (the micropump is actuated for 12 s), both the conductivity meter and the voltmeter are turned on and the buffer vessel connected to the oxygen outlet is flushed with the oxygen flowing through the absorbent. When the oxygen blank has decreased to its previously measured normal value, the analytical operational cycles can be started.

The absorber is emptied, rinsed, then filled with 2.00 cm^3 of absorption solution and the sample to be analyzed is placed into the sample feeding device. The voltage signal corresponding to the basic conductivity value is recorded and the sample is dropped into the combustion tube. A 5-min time interval was found to be sufficient for transporting the carbon dioxide to the

absorption/detection system. Thus, five minutes after the flash-type combustion, the steady signal of the voltmeter is recorded and the next analytical cycle is started. No replacement of the absorbent with fresh solution is needed until the upper limit of the linear range is reached.

RESULTS AND DISCUSSION

Selection and performance of the absorption/detection system

The type and concentration of the solute and solvent, influencing the absorption efficiency and change in specific conductance produced by absorption of carbon dioxide, are the main factors to be considered in selecting and establishing optimum performance of the absorption/detection system. As far as the role of the solute (i.e., the amine) is concerned, Fig. 6 shows that under identical experimental conditions 3-methoxypropylamine consistently ensures higher absorption efficiency, and its use provides quantitative absorption at 2 M concentration. Furthermore, 3-methoxypropylamine solutions give the relatively highest increase in specific conductance, as shown in Table 1. In this latter comparison, the slight distortion in the data caused by the difference in absorption efficiencies can be neglected. All these data show that 3-methoxypropylamine is the best trapping agent. Table 2 shows the effect of the solvent on the specific conductance of 2 M 3-methoxypropylamine solutions. In the case of apolar solvents no change in the specific conductance could be detected. Of the various protic and dipolar aprotic media applied in these experiments, ethanol can be considered as the most suitable solvent; the use of 96% alcohol instead of absolute ethanol had no effect on the analytical results.

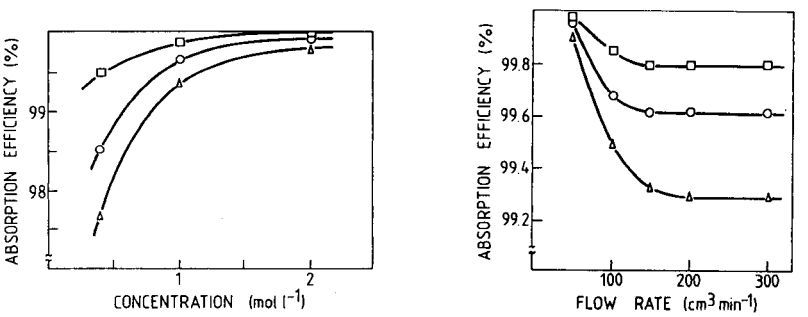

Fig. 6. Absorption efficiency as a function of the concentration of ethanolic amine solutions: (□) 3-methoxypropylamine; (○) ethanolamine; (△) 2-phenylethylamine. Conditions: temperature, 20°C; reaction volume, 28 cm^3; carrier gas flow rate, 250 cm^3 min^{-1}; amount of carbon (as CO_2) introduced, 50—500 μg.

Fig. 7. Effect of the carrier gas flow rate on the absorption efficiency. Conditions: temperature, 20°C; absorbent, ethanolic 2 M solution of 3-methoxypropylamine; amount of carbon led into the system as carbon dioxide, 1—500 μg. Absorbent volume: (□) 3.00 cm^3; (○) 2.00 cm^3; (△) 1.00 cm^3.

TABLE 1

Increase in specific conductance of ethanolic solutions of different amines caused by absorption of carbon dioxide[a]

Amine	$\Delta\kappa$ (μS cm^{-1} μg^{-1} cm^3)[b]		
	2 M soln.	1 M soln.	0.4 M soln.
2-Phenylethylamine	0.56	1.16	1.50
Ethanolamine	1.23	1.50	1.80
3-Methoxypropylamine	1.59	1.80	1.99

[a]Conditions: volume of absorbent, 28.00 cm^3; temperature, 20°C; flow rate of carrier gas, 250 cm^3 min^{-1}; electrode, type OK-9023, (Radelkis) with platinum black coating removed with aqua regia; cell constant, 1.3 cm^{-1}; conductivity meter, type OK-102/1 (Radelkis); measuring potential, 0.2 V; measuring frequency, 80 Hz. [b]Change in conductance is related to 1 μg of carbon trapped in 1 cm^3 of solution.

TABLE 2

Increase in the specific conductance of 2 M 3-methoxypropylamine solutions caused by absorption of carbon dioxide[a]

Solvent	κ (μS cm^{-1})	$\Delta\kappa$[b] (μS cm^{-1} μg^{-1} cm^3)	Absorption efficiency (%)
Methanol	100.10	1.93	100.0
Ethanol	4.30	1.59	100.0
1-Propanol	3.90	0.35	99.9
1-Butanol	0.75	0.16	99.8
Benzyl alcohol	1.00	0.03	99.8
1,4-Dioxane	0.02	0.00	99.6
N,N-Dimethylformamide	2.60	0.44	99.9
Acetonitrile	6.50	1.06	99.6
3-Methoxypropylamine	0.05	0.0008	100.0

[a]Conditions as in Table 1. [b]Change in conductance is related to 1 μg of carbon trapped in 1 cm^3 of solution.

The effect of the carrier gas flow rate on the absorption efficiency, in the case of the small-volume analytical absorber, is presented in Fig. 7. At around 250 cm^3 min^{-1}, no detectable change could be observed in the absorption efficiency, thus the effect of occasional fluctuations in the flow rate can be neglected. As a compromise between detection sensitivity and absorption efficiency, a 2.00-cm^3 absorption volume is recommended for analytical purposes.

With the use of 2.00 cm^3 of the ethanolic 2 M solution of 3-methoxypropylamine, the detector response was linear up to 6.6 μg of carbon trapped. This line follows an equation for which m = 154.93, a = 0.5, s_m = 0.271, s_a = 1.17, s_{xy} = 0.510, n = 21 and r^2 = 0.999, where m is the slope, a

is the intercept, s_m is the standard deviation of the slope, s_a is the standard deviation of the intercept, s_{xy} is the standard error of estimate, r is the regression coefficient and n is the number of determinations.

Determination of carbon

Some of the results obtained for microanalytical standards are collected in Table 3. Because the carbon content of the samples exceeded the limit of the linear range of the detector response, the inlet of the absorption/detection system was split. This also provided the advantage that the usual low but measurable blank became undetectable. These results show that (if the necessary accuracy in sample weighing is provided and the value of the

TABLE 3

Results for some microanalytical standards

Sample	Weight taken (μg)	Carbon content (μg)	Carbon led to detector[a] (μg)	Signal (10^{-2} mV)	Carbon content (%)	
					Calc.	Found[b]
Acetanilide	1128	802	4.58	710	71.10	71.05
	767	545	3.12	484		71.18
	1060	754	4.31	666		70.99
p-*Nitroaniline*	1085	566	3.23	501	52.17	52.10
	960	501	2.86	443		52.14
	1075	561	3.20	495		51.93
Mannitol	1055	418	2.39	369	39.57	39.48
	1015	402	2.30	357		39.66
	960	380	2.17	338		39.74
Benzoic acid	216	149	1.49	231	68.80	68.98
	309	213	2.13	332		69.25
	380	261	2.61	407		68.94
Sulfanilic acid	985	410	2.34	364	41.60	41.75
	1095	453	2.59	401		41.39
	1060	441	2.52	390		41.60
Triphenylphosphine	1100	906	5.18	804	82.40	82.57
	1080	890	5.09	784		81.99
	950	783	4.47	691		82.16
Dibenzyl disulphide	890	607	3.47	536	68.25	68.03
	970	662	3.78	585		68.02
	1142	779	4.45	694		68.65
S-*Benzyl-thiouronium chloride*	1028	487	2.79	430	47.40	47.15
	1002	475	2.71	419		47.16
	1043	494	2.83	436		47.15

[a]Split ratio 1:174 in all cases except 1:99 for benzoic acid. [b]Carbon (%) = (C F_i/weight) × 100, where C = signal/155 and F_1 = 175, F_2 = 100.

TABLE 4

Results for the simultaneous determination of total carbon and carbon-14

Sample		Split ratio	Carbon led to detector (μg)	Signal (10^{-2} mV)	Carbon content (%)		Activity[a] (dpm μg^{-1})
Weight (μg)	Carbon content (μg)				Calc.	Found	
Ethyluracil-^{14}C							
1418	729	1:174	4.17	646	51.42	51.46[b]	5362
730	375		2.14	333		51.54	5352
667	343		1.96	302		51.16	5377
1011	520	1:99	5.20	806		51.43	5385
999	514		5.14	797		51.47	5355
1011	520		5.20	805		51.34	5360
Aspartic acid-^{14}C[c]							
1055	1.09	—	1.09	168[d]	36.10	35.67[e]	30 329
1134	1.17		1.17	183		36.26	30 487
2376	2.46		2.46	381		36.07	30 582
2044	2.12		2.12	329		36.14	30 390
3216	3.33		3.33	516		36.08	30 859
3105	3.22		3.22	502		36.36	30 740
4091	4.24		4.24	658		36.20	30 213
4112	4.26		4.26	660		36.10	30 497
5005	5.19		5.19	799		35.85	30 342
5016	5.20		5.20	811		36.33	30 677

[a]Measured by liquid scintillation counting. [b]See footnote to Table 3. [c]Aqueous solution of ^{14}C-aspartic acid (71.751 mg in 25 g of solution). [d]Signal − blank, where μ_{blank} = (12 ± 0.4) × 10^{-2} mV; (P = 99%, n = 20), $\mu = \bar{x} \pm t\, s/n^{1/2}$. [e]Carbon (%) = (25 000 × C/71.751 × weight) 100.

blank is sufficiently low and reproducible), the method can be successfully used for micro or ultramicro determination of carbon in organic substances.

Table 4 shows the results of simultaneous determination of total carbon and carbon-14, for which the method can also be applied. The results obtained for the aqueous solution of ^{14}C-aspartic acid support the above statement; even if only a few micrograms of organic material is in the accurately weighed sample (the quartz liquid sample holder gives no blank), the precision conventional to the determination of elements in organic compounds can be achieved. The results obtained by liquid scintillation counting do not necessarily correspond with the carbon results, because these values can be affected by the counting error as well.

The results obtained for aqueous mannitol solutions (Table 5) illustrate the potential of the method when trace amounts of carbon in water have to be measured. At a 95% confidence level the limit of detection [35] is 2 × 10^{-2} μg. Detailed results of investigations regarding determination of total organic carbon in water and air, determination and detection of carbon from gas-chromatographic effluents, etc., will be dealt with in subsequent papers.

TABLE 5

Results for some aqueous solutions of mannitol

Solution	Sample weight (mg)	Signal[a] (10^{-2} mV)	Organic carbon in solution			
			Added as mannitol (ppm)	Solvent contribution (ppm)	Found	
					Total[b] (ppm)	Added (ppm)
I	27.385	24	4.95	0.97	5.65	4.68
	20.747	19			5.91	4.94
	23.217	21			5.83	4.86
	26.196	25			6.16	5.19
	20.654	19			5.93	4.96
	22.044	20			5.85	4.88
	25.592	24			6.05	5.08
	30.350	27			5.74	4.77
	23.601	22			6.01	5.04
	27.505	26			6.10	5.13
II	27.646	57	12.37	0.97	13.30	12.33
	18.093	38			13.55	12.58
III	26.477	106	24.74	0.97	25.83	24.86
	24.083	95			25.45	24.48
IV	22.605	176	48.48	0.97	50.23	49.26
	19.890	156			50.60	49.63
V	23.505	364	98.96	0.97	99.91	98.94
	20.271	313			99.62	98.65

[a]Signal — blank, where $\mu_{blank} = (12 \pm 0.4) \times 10^{-2}$ mV. [b]Calculation formula: mg l^{-1} = 1000 × signal/weight × 155.

REFERENCES

1 T. S. Ma and R. C. Rittner, Modern Organic Elemental Analysis, M. Dekker, New York, 1979.
2 E. Kozłowski and J. Namieśnik, Mikrochim. Acta, Part I (1979) 317.
3 D. H. Davies, Talanta, 16 (1969) 1055.
4 H. Malissa, Mikrochim. Acta, (1957) 553; Fresenius'Z. Anal. Chem., 181 (1961) 39.
5 W. Schmidts and W. Bartscher, Fresenius'Z. Anal. Chem., 181 (1961) 54.
6 H. Malissa, H. Puxbaum und E. Pell, Fresenius' Z. Anal. Chem., 282 (1976) 109 (and references therein.)
7 H. Puxbaum and J. Rendl, Mikrochim. Acta, Part I (1983) 263.
8 W. Stuck, Mikrochim. Acta, (1960) 421.
9 S. Greenfield, Analyst, 85 (1960) 486.
10 M. Vecera, J. Lakomy and L. Lehar, Mikrochim. Acta, (1965) 674.
11 F. Salzer, Microchem. J., 10 (1966) 27.
12 G. Kainz, K. Zidek and G. Chromy, Mikrochim. Acta, (1968) 235.
13 I. Holm-Jensen, Scand. J. Clin. Lab. Invest., 36 (1976) 493.
14 J. Bortlisz, Vom Wasser, 46 (1976) 35.
15 O. Piringer, E. Tataru and M. Pascalau, J. Gas Chromatogr., 2 (1964) 104.

16 A. Dijkstra, C. C. M. Fabrie, G. Kateman, C. J. Lamboo and J. A. L. Thissen, J. Gas Chromatogr., 2 (1964) 180.
17 R. C. Hall, J. Chromatogr. Sci., 12 (1974) 152.
18 R. J. Anderson and R. C. Hall, Am. Lab., 12 (1980) 108.
19 L. Blom and L. Edelhausen, Anal. Chim. Acta, 13 (1955) 120.
20 A. Grant, J. A. Hunter and W. H. S. Massie, Analyst, 88 (1963) 134.
21 R. F. Jones, P. Gale, P. Hopkins and L. N. Powell, Analyst, 90 (1965) 623; 91 (1966) 399.
22 P. Braid, J. A. Hunter, W. H. S. Massie, J. D. Nicholson and B. E. Pearce, Analyst, 91 (1966) 439.
23 D. C. White, Talanta, 13 (1966) 1303.
24 J. D. van der Laarse and H. C. E. van Leuven, Anal. Chim. Acta, 34 (1966) 370.
25 A. Campiglio, Mikrochim. Acta, (1968) 106.
26 W. Merz, Anal. Chim. Acta, 50 (1970) 305.
27 H. J. Boniface and R. H. Jenkins, Analyst, 96 (1971) 37.
28 A. O. Lindberg and A. Cedergren, Anal. Chim. Acta, 96 (1978) 327.
29 D. W. Whymark and J. M. Ottaway, Talanta, 19 (1972) 209.
30 A. Patchornik and Y. Shalitin, Anal. Chem., 33 (1961) 1887.
31 U. B. Mioc and S. V. Ribnikar, Bull. Soc. Chim. Beograd, 43 (1978) 603, 725; 44 (1979) 189.
32 I. Gács, K. Payer, L. Ötvös and S. Dombi, Hungarian Patent Application No. 1489/85, 1985.
33 A. E. Ezheleva and L. S. Malygina, Zavod. Lab., 49 (1983) 11.
34 I. Gács, Z. Vargay, E. Dobis, S. Dombi, K. Payer and L. Ötvös, J. Radioanal. Chem., 68 (1982) 93.
35 G. L. Long and J. D. Winefordner, Anal. Chem., 55 (1983) 713A.

Analytica Chimica Acta, 196 (1987) 183—191
Elsevier Science Publishers B.V., Amsterdam — Printed in The Netherlands

A NOVEL APPROACH TO DECOMPOSITION OF FOODSTUFFS FOR STRIPPING VOLTAMMETRIC DETERMINATION OF LEAD, CADMIUM AND COPPER

B. OGOREVC*, A. KRAŠNA and V. HUDNIK
Boris Kidrič Institute of Chemistry, P.O. Box 30, 61115 Ljubljana (Yugoslavia)
(Received 24th July 1986)

SUMMARY

Samples (ca. 0.3 g) are digested in 10-ml quartz vessels and the same vessel is used for anodic stripping voltammetry. Thus possible contamination during handling and dilution of the decomposed sample solution are avoided. A special design of column placed over the vessel provides digestion under reflux conditions without leakage and a glass cap fitted to another condenser enables the residual mineral acids (especially sulfuric acid) to be boiled out under low pressure conditions. The usual PTFE holder for electrodes and gas tubes is modified to facilitate insertion of the 10-ml vessel underneath. The system was checked on NBS standard reference materials (wheat flour and rice flour) and tested for the determination of Cd, Pb and Cu in baby foods. The limits of detection obtained for 3-min deposition times were 0.3 ng g^{-1}, 4 ng g^{-1} and 8 ng g^{-1} for cadmium, lead and copper, respectively. The levels of these elements in various commercial baby foods are given.

There is an established need for determinations of heavy metals in different biological and environmental materials and in foodstuffs, as well as for monitoring purposes in occupational hygiene, etc. [1—3]. Long-term exposure to low levels of toxic metals can be important, especially in relation to children [4, 5]. Frequently used methods are atomic absorption spectrometry, neutron activation, inductively-coupled plasma atomic emission spectroscopy, and stripping voltammetry. Voltammetry has proved to be particularly valuable for determinations of traces of heavy metals in many materials because of its reliability, sensitivity and comparative cheapness [3, 6—13]. With all these trace methods, other than neutron activation, vital aspects are the complete decomposition of the sample material and the avoidance of contamination, especially during the decomposition step.

The present paper is focused on these two aspects. The aim of the work was to improve accuracy and precision even under ordinary laboratory conditions by developing novel semi-closed equipment for stripping voltammetry. A special decomposition set-up as well as electrochemical cell was designed, in order to minimize the number of procedural steps and so the contamination risks, and to simplify the whole procedure for ultimate automation. The method developed is demonstrated for trace determinations of cadmium, lead and copper in commerical baby foods.

0003-2670/87/$03.50

EXPERIMENTAL

Equipment

A Solea-Tacussel Model PRG-5 polarograph connected to a Hewlett-Packard Model 7045-A *X-Y* recorder was used to record all stripping voltammograms. A hanging mercury drop electrode (Metrohm EA-290) was used as the working electrode with a platinum wire auxiliary electrode and a saturated Ag/AgCl (Metrohm EA 441/5) reference electrode. To control the stirring of the solution during the deposition time, a digital quartz voltammetric timer (QT-2) was used to stop the stirring automatically at a preset time and to control the stirring at precisely the desired rate. In all experiments, the stirring rate was 1100 r.p.m. The solution was purged with purified argon for 7 min at the start of each experiment and a flow of argon was maintained over the solution during the experiment.

A separate PTFE head was designed (Fig. 1) to facilitate insertion of a small 10-ml quartz vessel underneath so as to simplify using the described electrode system and purging tubes. The equipment for the decomposition of all baby food and standard reference samples is outlined in Fig. 2. The aluminum heating block has two cavities for inserting vessels, as well as a water cooling facility and a thermocouple which, together with a thermoregulator, served to control the preset temperature (to $\pm 10^{\circ}$C in the range 200—250°C). An infrared lamp, placed close over the caps during the evaporation stage, served to heat the caps so as to prevent condensation of vapors on the glass walls above the heating block. The quartz glassware consisted of 10-ml vessels with flat polished top edges, columns with flat polished bottom edges and fused in reflux aid thorns, and glass caps with shiny polished edges having an outlet tube with a joint to enter the condenser.

Reagents, standard solutions, reference materials and baby foods

All acids used were of Suprapur grade (Merck) or were prepared in the laboratory by sub-boiling distillation. Nitric acid for precleaning glassware was of analytical grade (p.a.). Double-distilled deionized water was used throughout. Stock solutions (1 g l^{-1}) of cadmium, lead and copper were prepared by dissolving the relevant metal in dilute nitric or hydrochloric acid. Working standards were made once a week by appropriate dilution of the stock with 0.01 M hydrochloric acid.

The wheat flour and rice flour standard reference materials were supplied by the U.S. National Bureau of Standards. The commercial baby foods (in powder form) were obtained from shops; they were considered as being homogeneous as a result of the manufacturing process. Both the standard reference materials and baby food samples were checked for their moisture contents as prescribed for NBS standard materials and the values were considered when calculating the results.

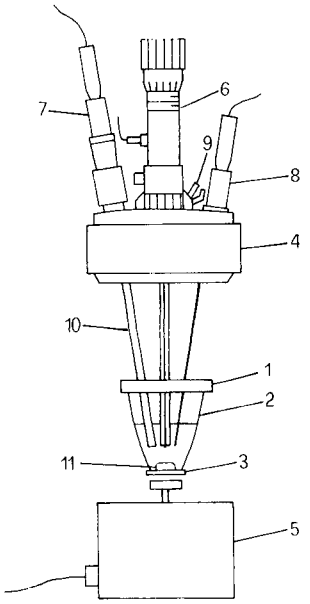

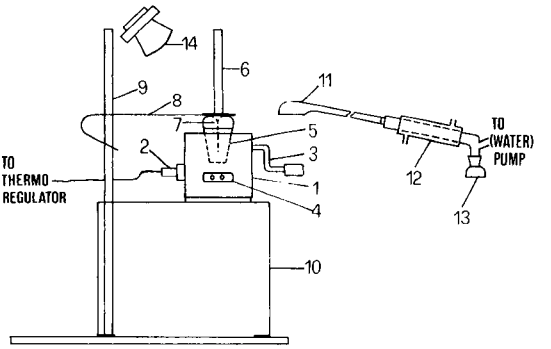

Fig. 1. Electrochemical cell: (1) small PTFE lid with holes for electrode tips, purging tubes and standard solution additions; (2) 10-ml silica vessel; (3) stainless-steel support; (4) normal PTFE voltammetric head; (5) d.c. synchronous motor mounted in an aluminium box; (6) working electrode; (7) reference electrode; (8) auxiliary electrode; (9) purging tubing leading down to the small vessel; (10) electrolyte bridge; (11) stirring bar.

Fig. 2. Decomposition set-up: (1) aluminum heating block; (2) thermocouple installation; (3) water cooling tubing; (4) mains socket; (5) 10-ml silica vessel as in Fig. 1; (6) reflux column; (7) reflux thorn aid; (8) flexible stainless-steel holder with PTFE-coated tip; (9) stainless-steel support rod; (10) stainless-steel support. For the evaporation option: (11) glass cap; (12) condenser; (13) collecting flask; (14) infrared lamp.

Procedures

Cleaning of the glassware. Before first usage the glassware was immersed for 10 days in 5—6 M (p.a.) nitric acid, during which time it was heated 4 times to boiling point for about 2 h. After being washed with water, it was soaked in fresh 2 M nitric acid, heated again and left overnight. After dipping in water, it was placed in the special distillation apparatus as described by Tschöpel et al. [14] and left over Suprapur nitric acid vapors for about 1 h. After that it was well washed with water and left to dry in a clean dustproof box.

Between analytical runs, the vessels, columns and caps were first soaked in hot 2 M nitric acid (p.a.) for 30—60 min (depending on the samples), washed thoroughly with water, and soaked in 1 M nitric acid (Suprapur) for 15—30 min. They were then immersed in water for about 10 min, washed well with water and left to dry in a clean dustproof box.

Sample decomposition. Weigh 0.3 g (0.1—0.5 g) of sample into a cleaned 10-ml silica vessel and add 2.0 ml (or pro rata) of concentrated nitric acid. Carefully insert the vessel in the cavity of the heating block preset to 60°C, place the reflux column over and fix it with the flexible holder. After foaming (if any) decreases, add 1.0 ml of 70% perchloric acid and set the temperature to 210°C. Leave at this temperature for 30—60 min and then cool to 60°C. Remove the column and put the cap on the vessel precisely edge to edge to achieve a good vacuum. Connect the tubing and turn on the water pump. Place the infrared lamp close over the cap and switch it on. Set the thermoregulator to 140°C and leave at this temperature until evaporation is complete. After cooling to 60°C or less and disconnecting the tubing, displace the infrared lamp and remove the cap. Add 20 μl of concentrated hydrochloric acid and 1.0 ml of water and leave at 60°C for a few minutes. Occasionally shake the vessel to rinse the wall. Finally, cool to room temperature, add 4 ml of water and insert the vessel into the voltammetric measurement system.

When sulfuric acid is used to assist decomposition, add 0.5 ml of concentrated sulfuric acid after adding nitric and perchloric acid as described above and after the foaming has ceased. In this case, set the regulator to 240°C for about 30 min. After cooling to 60°C, all further steps are as described above except that the temperature for evaporation is first 170°C for about 15 min and then 240°C until dry.

Voltammetric measurements. Place a clean stirring bar into the vessel, insert it underneath the small PTFE cell top and deoxygenate the solution for 7 min. Extrude a fresh drop of mercury (area of 2.20 ± 0.05 mm^2) and start stirring. Quantify cadmium, lead and copper under the following conditions: differential pulse mode, deposition potential —0.85 V vs. Ag/AgCl (saturated KCl), scan rate 10 mV s^{-1}, pulse repetition time 0.5 s, modulation amplitude 50 mV, deposition time 180 s (or appropriate), equilibration period 30 s. Change the sensitivity between the peaks (if necessary) always at the same potentials and with the same timing. Repeat the anodic stripping voltammograms at least twice before proceeding with the addition of the standard solutions. Dexoygenate the solution for about 20 s after each standard addition. Calculate the concentration of the three elements in the sample from the peaks after two standard addition experiments.

Blank values must be measured before, during and after each set of samples.

RESULTS AND DISCUSSION

The open wet-digestion technique was chosen because it is relatively simple, very flexible in terms of changing sample weight and decomposition conditions, and inexpensive. It is well known that voltammetric detection requires complete decomposition of organic samples and that different sample materials demand different approaches to decomposition. Many treatments have been described [6—11, 15—17].

The main idea behind the present work was to use only one vessel, instead of the usual two, for the decomposition and the voltammetric steps. The quantitative transference of the decomposed sample solution and its dilution can thus be avoided. Risk of contamination was also diminished by reducing the sample-handling steps and the first step towards automation of the whole procedure was possible.

Introducing the reflux column was intended to decrease the required amount of acid mixture through its refluxing back to the sample solution. The column also served as a cover to prevent contact of the solution with laboratory air. The reflux thorn aid was designed to facilitate refluxed drops slipping down into the solution and to simplify introduction of any further digestion reagent into the vessel.

The evaporation step was needed not only to facilitate the use of a definite supporting electrolyte (e.g., hydrochloric acid) but also to expel any remaining reducible components such as nitrogen oxides and peroxide. Shortening of the time required for boiling out any remaining acid mixture was usefully achieved by conducting the drying step under low pressure conditions. This meant that lower temperatures were needed and that the digest remained protected from laboratory air. This was especially useful when sulfuric acid was added for digestion. A special glass cap was designed (Fig. 2) having an outlet tube with joint connected to a condenser followed by a small collecting flask; the water pump was connected via a gas trap filled with 10% (w/v) potassium hydroxide solution.

All contacting glass surfaces were well polished first with the usual polishing material and finally with alumina powder to a mirror-like finish. For the columns, a reflux thorn aid was fused in once the polishing of the bottom edge was complete.

Various digestion treatments were tested for the baby foods as outlined in Tables 1 and 2. The use of hydrogen peroxide may be needed when the sample material is difficult to decompose but should be avoided if possible to avoid risk of contamination. A temperature/time diagram for the conduct of a typical decomposition procedure with and without use of sulfuric acid, is shown in Fig. 3. The quality of the decompositions during the digestion study was checked by applying anodic linear-sweep voltammetric tests as shown in Fig. 4.

Contamination is considered as a serious problem in any trace or ultratrace procedure. Tschöpel et al. [14] and Adeloju and Bond [18] have demonstrated how important correct pretreatment of glassware as well as laboratory conditions are in relation to the precision and accuracy of trace determinations. The results of the present study showed that laboratory conditions were not the main problem, probably because of the semi-closed procedure introduced. Similarly to Ostapczuk et al. [10], long-term experience here indicated that glassware (quartz), even after careful cleaning before first usage, must often undergo 8—10 whole digestion procedures before the blank values of all elements, but especially lead and copper, descend to low

TABLE 1

The main ingredients of different samples of baby food

No. of sample	Description of baby food	Hydro-carbons (%)	Albumin (%)	Fats (%)
1	Baby rice	85	7.1	0.9
2	Baby grits	82	9.1	1.0
3	Baby grits with apple	84	6.5	1.1
4	Babymix with vegetable	73	12	5
5	Baby grits with chocolate and nuts	78	10.0	6.5
6	Babymix with vegetable and chicken	60.2	19.7	8.0
7	Milk powder for infants up to 3 kg	57	15	22

TABLE 2

Decomposition of baby food samples. (Samples as in Table 1; 0.3-g samples taken)

No. of sample	HNO_3 (ml)	$HClO_4$ (ml)	H_2SO_4 (ml)	H_2O_2 (ml)	Temp. (°C)	Time (min)
1	2	1	—	—	210	30
2	2	1	—	—	210	30
3	2	1	—	—	210	30
4	2	1	—	—	210	40
5	2	1	—	—	210	40
6	2	1	—	—	210	60
7	2	1	—/0.5[a]	0.5[a]/—	210/240	60/30

[a]Optional.

and stable values. The acids used did not cause difficulties regarding blank values. Table 3 shows the blank values for cadmium, lead and copper per digestion as well as the calculated limits of detection for a 3-min deposition time for lead and copper and a 7-min deposition time for cadmium.

To check the accuracy and precision of the procedure, two NBS standard reference materials (wheat flour and rice flour) were analyzed; these have similar composition and approximately the same levels of cadmium, lead and copper as the baby foods tested. Table 4 shows that the results agree well with certified values and that precision is also very good. To check the results for cadmium, the analyses were repeated with addition of sulfuric acid; the results obtained were exactly the same, indicating that cadmium was not lost during the procedure.

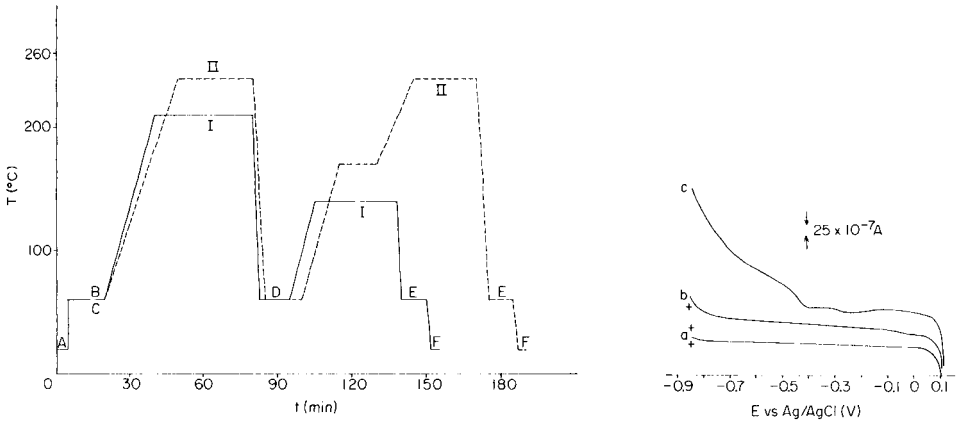

Fig. 3. Temperature/time diagram for the decomposition of a baby food sample with addition and other manipulation points: (I) without H_2SO_4; (II) with H_2SO_4. (A) Addition of HNO_3; (B) addition of $HClO_4$; (C) addition of H_2SO_4; (D) change of column to cap, pump on, infrared lamp in place; (E) disconnection of tubing, displacement of lamp, removal of cap, addition of HCl and H_2O; (F) addition of H_2O.

Fig. 4. Anodic linear-sweep voltammetric test (scan rate 40 mV s^{-1}) of completeness of decomposition: (a) supporting electrolyte after blank decomposition procedure; (b) test of complete decomposition of a sample; (c) incomplete decomposition.

TABLE 3

Blank values and limits of detection for cadmium, lead and copper for the conditions given under Experimental with or without sulfuric acid

Element	n	$\bar{x}$ (ng)	s (%)	Detection limit (ng g^{-1})
Cd	6	0.1	23	0.3
Pb	6	2.8	15	4
Cu	7	2.5	31	8

The commercial baby foods (Table 1) examined were all dry, in powder form and ready to be mixed with water or milk. The results obtained for cadmium, lead and copper in these samples are presented in Table 5. Only the milk powder required the use of sulfuric acid as is evident from Table 2. The iron contents were checked because of possible interference with the copper determination [19]. Tests of decomposed sample solutions by atomic absorption spectrometry showed that all values of total iron were under the level of 10^{-5} M, which proved that no such interferences were possible.

TABLE 4

Analyses of NBS Standard Reference Materials

Material	Metal contents (ng g^{-1})					
	Found			Certified		
	Cd	Pb	Cu	Cd	Pb	Cu
Wheat flour NBS 1567	32 ± 3	20 ± 4	2300 ± 200	32 ± 7	—	2000 ± 300
Rice flour NBS 1568	26 ± 1	41 ± 3	2300 ± 200	29 ± 4	45 ± 10	2200 ± 300

TABLE 5

Cadmium, lead and copper concentrations in baby food samples (samples as in Table 1)

No. of sample	Metal contents (ng g^{-1})[a]		
	Cd	Pb	Cu
1	22	122	1700
2	19	41	1400
3	18	60	1900
5	22	39	3400
6	26	19	2300
7	<0.3	<4	200

[a] Average of 2—5 analyses.

This work was supported by the Research Community of Slovenia, which is gratefully acknowledged.

REFERENCES

1 P. Brätter and P. Schramel (Eds.), Trace Element Analytical Chemistry in Medicine and Biology, Vol. 2, Walter de Gruyter, Berlin, 1983.
2 C. F. Jelinek, J. Assoc. Off. Anal. Chem., 65 (1982) 942.
3 H. W. Nürnberg, Anal. Chim. Acta, 164 (1984) 1.
4 T. D. Luckey and B. Venugopal, Metal Toxicity in Mammals, Vol. 1, Plenum, New York, 1979.
5 G. N. Biddle, J. Assoc. Off. Anal. Chem., 65 (1982) 947.
6 M. Puntar-Brzin, V. Hudnik and S. Gomišček, Vestn. Slov. Kem. Drus., 28 (1981) 165.
7 B. Pihlar, P. Valenta and H. W. Nürnberg, Fresenius' Z. Anal. Chem., 307 (1981) 337.
8 R. J. Gajan, S. G. Capar, C. A. Subjoc and M. Sanders, J. Assoc. Off. Anal. Chem., 65 (1982) 970.
9 S. B. Adeloju, A. M. Bond and H. C. Hughes, Anal. Chim. Acta, 148 (1983) 59.
10 P. Ostapczuk, M. Goedde, M. Stoeppler and H. W. Nürnberg, Fresenius' Z. Anal. Chem., 317 (1984) 252.
11 S. B. Adeloju, A. M. Bond and M. H. Briggs, Anal. Chem., 57 (1985) 1386.

12 A. Aliakbar and M. Popl, Collect. Czech. Chem. Commun., 49 (1984) 45.
13 A. Aliakbar and M. Popl, Collect. Czech. Chem. Commun., 49 (1984) 1140.
14 P. Tschöpel, L. Kotz, W. Schulz, M. Veber and G. Tölg, Fresenius' Z. Anal. Chem., 302 (1980) 1.
15 S. Gomišček, V. Hudnik and M. Veber, in S. S. Brown (Ed.), Clinical Chemistry and Chemical Toxicology of Metals, North Holland, Amsterdam, 1977, p. 319.
16 M. Oehme and W. Lund, Fresenius' Z. Anal. Chem., 298 (1979) 260.
17 S. B. Adeloju, A. M. Bond and M. I. Noble, Anal. Chim. Acta, 161 (1984) 303.
18 S. B. Adeloju and A. M. Bond, Anal. Chem., 57 (1985) 1727.
19 I. Šinko, Doctoral Thesis, Ljubljana, 1973.

Analytica Chimica Acta, 196 (1987) 193—204
Elsevier Science Publishers B.V., Amsterdam — Printed in The Netherlands

APPLICATIONS OF POLAROGRAPHY AND VOLTAMMETRY IN ANALYSIS FOR DRUGS

G. J. PATRIARCHE* and J.-C. VIRE

Free University of Brussels (U.L.B.), Institute of Pharmacy, Campus Plaine C.P. 205/6, Bd du Triomphe, B-1050 Brussels (Belgium)

(Received 28th August 1986)

SUMMARY

Recent developments and applications of polarographic and voltammetric techniques in drug analysis are reviewed. Typical applications to pharmacologically active compounds are described.

Polarography was applied to problems in pharmaceutical analysis quite early in the development of the method. Several reviews have been published on the topic in recent years [1—7]. The many different kinds of drugs and the numerous types of sample in which they must be determined make modern polarographic methods an interesting field of study in pharmaceutical laboratories. Such methods have become very competitive from the analytical point of view owing to sophisticated developments in electronics. The characteristics of these techniques are very suitable for the analysis of commercially available forms of drugs. It is possible to achieve direct determinations of pharmacologically active compounds in complex media without previous separation, and the appearance of an additional wave or a modification of the shape of the initial wave may indicate decomposition products or impurities. Further, determinations of bio-availability and the pharmacokinetic profile of a drug in studies of its in-vivo evolution can often be achieved by polarographic or voltammetric methods, as can detection and determination of its metabolites in blood, urine and other biological fluids.

In addition to the quantitative and qualitative aspects of polarography, studies of the electrode processes may help to elucidate some mechanisms of the action of drugs in vivo. The reproducibility of measurements allows kinetic data to be obtained with a precision similar to those obtained by other methods used in reaction kinetics.

The contribution of modern electronics has been vital to the development of electrochemical methods over the past twenty years. Among these modern techniques, differential pulse polarography can be used to solve many problems because its selectivity enables complex media to be examined, and its sensitivity makes it valuable for trace determinations. Many organic substances

0003-2670/87/$03.50

considered as poorly soluble can be studied, because it is now possible to work with aprotic media and to obtain reliable data even with very dilute solutions (10^{-6}—10^{-8} M).

During the last decade, there has been an extraordinary acceleration of progress in the discovery, synthesis and means of delivery of chemicals used in the diagnosis, prevention and treatment of human diseases. Such developments have placed increased demands on the analytical methods used. Because the newly developed drugs are often more physiologically active, they can be administered in smaller amounts, hence more sensitive analytical methods are required. Analysis of very small samples of blood is often requested and examination of single tablets containing microgram quantities of drugs is often required so that the techniques applied must have low detection limits and must be applicable to small samples. They should also be useful as indicators of the stability of drugs. Moreover, specifications concerning the purity of drugs have become more demanding with respect to both accurate knowledge of the amount of the physiologically active ingredient and the levels of unwanted trace impurities and degradation products. Polarography and related voltammetric techniques are able to solve all these problems.

Chemically modified electrodes are being extensively developed at the present time, thus the application of such sensors in pharmaceutical analysis must be mentioned. A great deal of information has been accumulated on adsorbed layers of molecules and ions and electrodes can be designed and built to exhibit properties of many kinds [8—12]. The field of electrocatalysis has also been developed and usefully explored [13]. The most studied immobilized chemicals, enzymes or drugs, are those which offer good electrochemical reactivity. The principal routes to immobilization of substances can be classified as film deposition, chemisorption and covalent bondings. The synthesis and application of chemical micro-structures onto electrode surfaces enhance the efficiency of various processes including microelectronics and semiconductors. There is intense activity in the production of new types of electrodes which may eventually lead to the production of specific materials for each kind of pharmaceutical compound.

SOME APPLICATIONS

Drugs for cardiovascular diseases

Among the drugs used for arrhythmias and cardiac failure, *N*-diethylamino-3-propyl-*N*-phenylindanamine-2 hydrochloride (aprindine) exhibits a catalytic wave at —1.4 V vs. SCE between pH 6 and 7. The oxidized form is strongly adsorbed. This surface catalytic wave is attributed to reduction of the proton and can be used to quantify aprindine [14]. Differential pulse polarography of amiodarone exhibits three irreversible two-electron peaks attributed to the reduction of the carbonyl group and both carbon-iodine bonds, respectively [15]. The linear increase of each peak with concentration is of

particular interest because the molecule can be quantified at different applied potentials if other electroactive compounds may interfere. A pH 6 phosphate/acetate/borate buffer containing 35% of methanol offers the best conditions for quantitative measurements.

Various cardiotonic drugs have been determined. For example, the adsorptive preconcentration of cardiac glycosides (digoxin, digitoxigenin and digitoxin) can be done at —0.9 V in a 0.005 M sodium hydroxide supporting electrolyte under stirring. A negative-going differential-pulse (d.p.) scan is then initiated. This procedure offers nanomolar limits of detection based on a 15-min preconcentration time. Interferences of albumin, gelatin, camphor, cholesterol and chloride have been examined and determinations are possible in urine [16].

The electrochemical oxidation of khelline, a vasodilator, at carbon-based electrodes gives rise to a quinonic structure following an irreversible two-electron process. This oxidation product exhibits reversible redox properties at less positive potentials as has been shown by using cyclic voltammetry. The oxidation peak obtained in acidic medium at a carbon polymer electrode increases linearly with concentration, the detection limit being 8×10^{-7} M [17].

Among the hemostatic drugs, naftazone, which is the semicarbazone of 1,2-naphthoquinone, gives rise to a reversible two-electron reduction wave between pH 2 and 12, the half-wave potentials appearing between 0.0 and —0.6 V vs. SCE [18]. This behaviour is quite different from that of most semicarbazone compounds which are generally reduced at more negative potentials by a four-electron transfer in acidic media only. The difference can be explained by the fact that the carbon-nitrogen double bond includes a carbon atom of the naphthalene ring, being similar in nature to the quinone structure. The reduction wave allows naftazone to be quantified down to 1×10^{-5} M by d.c. polarography. The 1×10^{-7} M level is reached by using the d.p. method.

Anti-inflammatory drugs

Piroxicam [*N*-(2-pyridyl)-4-hydroxy-2-methyl-2*H*-1,2-benzothiazine-3-carboxamide-1,1-dioxyde] is polarographically reduced; the mechanism is highly dependent on pH. At pH < 2, a four-electron transfer corresponds to the opening of the thiazine ring, immediately followed by the reduction of the enol double bond. The same mechanism is observed at pH > 9.5. Only the reduction of the enol group appears between pH 4 and 7.5 [19, 20]. The molecule can be quantified in 0.05 M sulfuric acid, in which the wave height is favorable, but also at pH 6 where the polarographic response is better defined [19, 21]. The d.p. technique is well suited for quantifying the drug in tablets and urine [21].

Oxidation of piroxicam also takes place on the enol group following a two-electron process which allows quantitative evaluation. This molecule is easily differentiated from many other non-steroidal anti-inflammatory drugs by using polarography [21].

Cytostatic drugs

2-Formylpyridine thiosemicarbazone is reduced at the dropping mercury electrode (DME) by a two-electron irreversible step at the nitrogen double bond of the side chain in the pH range 0.2—12 [22]. In alkaline media, this wave decreases progressively with increasing pH owing to the formation of an electro-inactive species. Additionally, a double anodic wave very close to the oxidation of mercury, corresponding to the formation of an organo-mercury compound, develops in neutral and alkaline media. The compound can be quantified at pH 7. A 2×10^{-8} M detection limit can be reached.

Related to the anthracycline family, the cytostatic agents aclacinomycin [23], carminomycin [24] and marcellomycin [25] exhibit a well defined reversible two-electron wave in acidic or alkaline media, which can be attributed to the reduction of their quinonic structure to the corresponding hydroquinone. Because important adsorption phenomena interfere in the reduction process, mainly in alkaline solutions, acid or neutral media should be used for quantitative purposes.

Metronidazole, known for its antimicrobial properties, exhibits a four-electron wave followed by a two-electron wave at pH 4.38. The first wave is suitable for quantifying the drug by the d.c. technique. A method for quality control of tablets has been proposed [26].

Antihistamines

Quisultidine [2-(*N*,*N*-dimethylsulfamoyl)-1-(3-quinuclidinyl)phenothiazine] has none of the antihistaminic and anticholinergic activity usually associated with the phenothiazines but possesses a unique antisecretory action. Cyclic voltammetry of this drug exhibits and unusually positive oxidation wave for this class of compounds, because of the steric hindrance caused by the 3-quinuclidinyl side chain. The oxidation product undergoes cleavage of the side chain to liberate the parent 2-(*N*,*N*-dimethylsulfamoyl)phenothiazine. The electrochemical behaviour of quisultidine is probably related to the unusual pharmacological properties of this drug [27].

Diphenhydramine hydrochloride, dimenhydrinate and chlorphenoxamine, which are themselves polarographically inactive, are able to complex cadmium ions in a pH 8.0 borate buffer. The differential-pulse peak developed by the two-electron reduction of the complexed ion occurring between —1.3 and —1.4 V vs. SCE has been used to determine these antihistaminic drugs in tablets, capsules, elixirs and injection preparations [28].

Neuroleptic, psychotropic and antidepressant drugs

A thin-layer electrochemical cell (23-μl capacity) coupled with differential pulse voltammetry has been used to determine chlorpromazine in plasma and urine, without extraction, by using a wax-impregnated graphite electrode [29]. The first one-electron oxidation peak corresponding to the formation of the cation radical is selected for quantifying the drug in a pH 7 phosphate buffer. Linear calibration plots are obtained in the range 4.8×10^{-8}—$2.4 \times$

10^{-4} M for urine and 2.4×10^{-5}—4.8×10^{-4} M for plasma without interferences from glutethimide, dextropropoxyphene, meprobamate, diazepam or methaqualone.

Electrochemical investigations of several butyrophenones (benperidol, droperidol, spiperone, azaperone) related to haloperidol have been conducted with a 20% propylene carbonate/30% methanol/50% (v/v) water mixture in acidic media and a 40% dimethylformamide/60% water solvent in alkaline media in order to favour solubility and to minimize strong adsorption phenomena. In such solutions, these ketones are reduced following a two-electron irreversible transfer in acidic medium, differing from most of the arylketones which are reduced in two one-electron steps [30]. A modification of the side chain affects neither the reduction process nor the half-wave potentials (—1.0 to —1.6 V vs. SCE in the 0—12 pH range) but may modify the intensity of the adsorption phenomenon [31]. These compounds cannot be differentiated by using polarography. Quantitative measurements have been made at pH 5 for haloperidol. These determinations must be done at pH 9 or 11 for the other compounds because adsorption phenomena are less prominent in alkaline media and because spiperone and azaperone exhibit a catalytic wave in acidic and neutral media.

Alternatively, these fluoroarylalkylketones can be oxidized at carbon electrodes, the heterocyclic moiety of the side chain being the electroactive site [32]. Spiperone gives rise to one well-defined peak but droperidol and benperidol are oxidized into two steps. Haloperidol appears to be electro-inactive. The drugs have been quantified in 0.1 M sulfuric acid, but at higher concentrations than when the differential-pulse polarographic technique is used.

The dibenzoazepine group, including clozapine, clotiapine and loxapine, can be polarographically related to benzodiazepines, owing to the electrochemical behaviour of the azomethine moiety. The two-electron transfer occurs at more negative potentials than for benzodiazepines and may be influenced by the protonation of the proximal nitrogen atom of the piperazine ring [33, 34]. Quantitation, only reported for loxapine, is possible in 0.5 M sulfuric acid containing 20% (v/v) ethanol [34]. Pharmaceutical tablets can be analyzed without interferences of excipients after extraction with ethanol.

Dibenzoazepines can also be oxidized but the mechanisms are highly dependent on pH [35]. The unprotonated form of each compound behaves similarly in aqueous or non-aqueous medium, giving rise to an unstable iminium cation, the piperazine moiety being the electroactive site. When this site is protonated, the tricyclic moiety becomes the electroactive site, mainly in aqueous solutions [36, 37]. These electro-oxidative properties are summarized in Table 1. In view of these results, various similarities have been pointed out between the in vitro oxidation processes and the pharmacological behaviour reported in the literature [38]. Linear calibration graphs have been established in a 0.1 M H_2SO_4/0.1 M $LiClO_4$ supporting electrolyte for rotating glassy-carbon or platinum electrodes but a better sensitivity can be

TABLE 1

Oxidation mechanisms of dibenzoazepines

Drug	When piperazine site is protonated		When piperazine site is not protonated	
	Aqueous	Non-aqueous	Aqueous	Non-aqueous
Clozapine	Dimerization	Dimerization	Similar behaviour for the three compounds	
Clotiapine	Sulfoxidation and sulfonation	Not oxidizable	Formation of an unstable iminium cation	
Loxapine	Not identified	Not oxidizable		

achieved by using a stationary carbon paste electrode [35]. Determinations were also possible in a pH 4.7 acetate buffer with a graphite spray electrode, which allowed a low background current and better reproducibility to be attained [39].

The two-electron reduction process of the azomethine group of imidazo-(midazolam) and triazolo-benzodiazepines (triazolam, alprazolam) is not strongly affected by the substituents, except in the case of a 3-hydroxy substitution giving rise to a four-electron transfer [40, 41]. Hydrolysis kinetic parameters, however, are highly dependent on the presence of the imidazole or the triazole ring, on the 5-*o*-phenyl substituent and on the 3-hydroxy group. At pH 6, midazolam as well as triazolam can be determined accurately by differential pulse polarography.

An extraction preconcentration can be achieved by adsorption at a glassy carbon electrode and this allows the determination of tricyclic antidepressant compounds (desipramine, imipramine, trimipramine) in pure solutions [42]. The differential-pulse voltammetric response is dependent on the electrolyte, the electrode material and the preconcentration time at 0.0 V. Replacement of the supporting electrolyte after the preconcentration step avoids interferences. Determinations in urine are also possible.

Other drugs

Sedatives and hypnotic drugs. Several barbiturate derivatives (barbital, amobarbital, pentobarbital, allobarbital, sandoptal, secobarbital and phenobarbital) exhibit a polarographic peak arising from the oxidation of mercury and formation of an organomercury derivative in a pH 9.3 borate buffer. This behaviour allows these compounds to be quantified in tablets in the 4×10^{-6}—1×10^{-4} M concentration range [43].

Neurotransmitters. The catalyzed dopamine oxidation peak appearing in the presence of ascorbic acid is suitable for its determination in a pH 7 phosphate buffer at a carbon paste electrode [44]. Calibration graphs have been established at very low concentrations by using carbon-fiber electrodes associated with a microcomputer system [45].

Hypoglycemic drugs. Several mercaptopyridine carboxylic acids, mainly the 3-mercapto-2-pyridine carboxylic acid derivatives, exhibit hypoglycemic activity [46]. A polarographic study has shown that these compounds are reduced in two two-electron steps giving rise to thiomethane or hydrogen-sulfide and other unstable products [47]. Linear calibration plots are obtained for 2 M sulfuric acid medium by using the differential pulse technique. An extended study of several homologs (i.e., 2-mercapto-5-pyridine carboxylic acids [48] and 6-mercapto-2-pyridine carboxylic acids [49] has shown that a change in the position of the substituents can strongly modify the electrochemical behaviour of the compounds.

Gout inhibitors. Allopurinol has been determined in a pH 4.85 citrate buffer containing 5% dimethylformamide; a two-electron transfer is involved. When a 0.5 M sulfuric acid medium is used, four electrons are transferred [50, 51]. The method has been applied in quality control of pharmaceutical tablets [50].

Vitamins. Differential pulse voltammetry at a carbon paste electrode has been used for trace determinations of ascorbic acid, which is often added as an antioxidant. A pH 4.7 acetate buffer was selected for the oxidation of vitamin C which occurs at +0.3 V vs. SCE. The peak height is considered after the second scan in order to avoid interferences from adsorption phenomena. Applications are proposed in analysis of pharmaceutical tablets and fresh or dehydrated fruit juices [52].

Amino acids. Tryptophane has been oxidized at glassy carbon and carbon paste electrodes to form oxyindolalanine and other oxidation products [53]. The two-electron peak appearing at +1.0 V vs. SCE in a 0.1 M phosphoric acid (pH 2) supporting electrolyte allows quantitative measurements down to 5×10^{-7} M without interferences from 5-hydroxytryptophane or serotonine. Indole, tryptamine and tyrosine may interfere [54].

Artificial sweeteners. Saccharine is frequently used as sweetener in grape jellies, gelatin desserts and beverages. A differential-pulse polarographic method for its determination has been developed after chromatographic extraction on Celite of the acidified solution with chloroform [55]. The evaporation residue, dissolved in 0.1 M sodium hydroxide, is polarographed in a 0.1 M HCl/0.1 M KCl/0.1% tetrabutylammonium bromide supporting electrolyte.

To summarize the numerous recent possibilities of the application of polarography and voltammetry in analysis for drugs, information on supporting electrolytes, wave characteristics, linear ranges and detection limits is listed in Table 2.

Thanks are expressed to the "Fonds National de la Recherche Scientifique" (F.N.R.S. Belgium) for support to one of us (G.J.P.) and to Mrs J. Sépulchre for technical assistance.

TABLE 2

Electroanalytical data on pharmaceutical compounds

Compound	Nature of sample	Supporting electrolyte or buffer[a]	pH	Characteristics of the wave[b]	Mode[c]	Working electrode[d]	$E_{1/2}$ or E_p[e] (V)	Linear range (M)	Detection limit (M)	Ref.
Aprindine	Pure soln.	ph	7	cat. (red H^+)	d.c.	DME	−1.4	6×10^{-5}—1×10^{-6}	1×10^{-6}	[14]
Amiodarone	Pure soln.	ph/ac/bor/ 35% MeOH	6	red, 3 X $2e^-$, irr	d.p.	DME	−0.65	1×10^{-4}—4×10^{-6}	4×10^{-6}	
							−1.00	1×10^{-4}—4×10^{-6}	2×10^{-6}	[15]
							−1.22	1×10^{-4}—4×10^{-6}	3×10^{-6}	
Digoxin	Pure soln.	0.005 M NaOH	—	red, $2e^-$, irr	a.s.v.	HMDE	−1.51*	2×10^{-7}—2×10^{-8}	2.3×10^{-10}	[16]
Digitoxigenine	Pure soln.	0.005 M NaOH	—	red, $2e^-$, irr	a.s.v.	HMDE	−1.42*	2×10^{-7}—2×10^{-8}	1.5×10^{-10}	[16]
Digitoxin	Pure soln.	0.005 M NaOH	—	red, $2e^-$, irr	a.s.v.	HMDE	−1.51*	2×10^{-7}—2×10^{-8}	8×10^{-10}	[16]
Khelline	Pure soln.	0.1 M H_2SO_4/ 10% MeOH	—	ox, $2e^-$, irr	d.p.	CPoE	+1.1	5×10^{-5}—3×10^{-6}	8×10^{-7}	[17]
Naftazone	Pure soln.	ph/ac/ 30% MeOH	7	red, $2e^-$, irr	d.c. d.p.	DME	−0.3	8×10^{-4}—1×10^{-7}	5×10^{-8}	[18]
Piroxicam	Pure soln., tablets	0.05 M H_2SO_4/ 20% MeOH	—	red, $4e^-$, irr	d.c. d.p.	DME	−0.96	1×10^{-4}—1×10^{-7}	5×10^{-8}	[19, 21]
	Pure soln., tablets	ph/ac/bor/ 20% MeOH	6	red, $2e^-$, irr	d.c. d.p.	DME	−1.25	1×10^{-4}—1×10^{-7}	5×10^{-8}	[19, 21]
Piroxicam	Urine	ph/ac/bor	4	red, $2e^-$, irr	d.p.	DME	−1.16	6×10^{-6}—1×10^{-6}	5×10^{-7}	[21]
Piroxicam	Pure soln.	0.05 M H_2SO_4/ 20% MeOH	—	ox, $2e^-$, irr	d.p.	GCE, CPE	+0.72	5×10^{-5}—2×10^{-6}	5×10^{-7} (CPE)	[19]
2-Formylpyridine thiosemicarbazone	Pure soln.	ph/ac/bor/ 10% MeOH	7	red, $2e^-$, irr	d.c. d.p.	DME	−0.9	1×10^{-3}—1×10^{-7}	2×10^{-8}	[22]
Aclacinomycin	Pure soln.	ph/ac/ 30% MeOH	6	red, $2e^-$, rev	d.c. d.p.	DME	−0.55	1×10^{-3}—1×10^{-5}	1×10^{-5}	[23]
	Pure soln.	ph/ac/ 30% MeOH	1	red, $2e^-$, rev	d.c. d.p.	DME	−0.22	6×10^{-4}—1×10^{-5}	1×10^{-5}	[23]
Carminomycin	Pure soln.	ph/ac/ 20% MeOH	3	red, $2e^-$, rev	d.c. d.p.	DME	−0.46	1×10^{-3}—1×10^{-5}	8×10^{-6}	[24]
Marcellomycin	Pure soln.	ph/ac/ 20% MeOH	6	red, $2e^-$, rev	d.c. d.p.	DME	−0.55	1×10^{-3}—2×10^{-5}	1×10^{-5}	[25]
	Pure soln.	ph/ac/ 20% MeOH	1	red, $2e^-$, rev	d.c. d.p.	DME	−0.28	4×10^{-4}—1×10^{-5}	1×10^{-5}	[25]
Metronidazole	Pure soln., tablets	ph/ac/bor/ 1.6×10^{-3} M Triton X-100	4.4	red, $4e^-$, irr	d.c.	DME	−0.31	7×10^{-4}—5×10^{-5}		[26]
Diphenhydramine	Tablets, elixir, injections	bor	8.0	red, $2e^-$,	d.p.	DME	−1.38	3.5×10^{-4}—1.6×10^{-4}	1.6×10^{-4}	[28]

Dimenhydrinate	Tablets, elixir, injections	bor	8.0	red, $2e^-$,	d.p.	DME	−1.33	3.0×10^{-4}—1.5×10^{-4}	1.5×10^{-4}	[28]
Chlorphenoxamine	Tablets, elixir, injections	bor	8.0	red, $2e^-$,	d.p.	DME	−1.33	2.1×10^{-4}—1.5×10^{-4}	1.5×10^{-4}	[28]
Chlorpromazine	Urine	ph	7	ox, $1e^-$, irr	d.p.	GE	+0.8	2.4×10^{-4}—4.8×10^{-8}	4.8×10^{-9}	[29]
Chlorpromazine	Plasma	ph	7	ox, $1e^-$, irr	d.p.	GE	+0.7	4.8×10^{-4}—2.4×10^{-5}	4.8×10^{-6}	[29]
Haloperidol	Pure soln.	ph/ac/bor 20% propylene carbonate/ 30% MeOH	5	red, $2e^-$, irr	d.c. d.p.	DME	−1.25	1×10^{-4}—1×10^{-6}	1×10^{-6}	[30]
Benperidol and droperidol	Pure soln.	ph/ac/bor/ 40% DMF	9	red, $2e^-$, irr	d.c. d.p.	DME	−1.45	1×10^{-4}—1×10^{-6}	1×10^{-6}	[31]
Spiperone	Pure soln.	ph/ac/bor 40% DMF	9	red, $2e^-$, irr	d.c. d.p.	DME	−1.45	1×10^{-4}—2×10^{-6}	2×10^{-6}	[31]
Azaperone	Pure soln.	ph/ac/bor/ 40% DMF	11	red, $2e^-$, irr	d.c. d.p.	DME	−1.45	1×10^{-4}—2×10^{-6}	2×10^{-6}	[31]
Benperidol, droperidol and spiperone	Pure soln.	0.1 M H_2SO_4	—	ox, , irr	d.p.	CPE, GSE, CPoE	+1.07	2.5×10^{-4}—5×10^{-5}	1×10^{-6}	[32]
Loxapine	Pure soln., tablets	0.5 M H_2SO_4/ 20% EtOH	—	red, $2e^-$, irr	d.c. d.p.	DME	−0.85	1×10^{-3}—1×10^{-7}	1×10^{-7}	[34]
Clozapine	Pure soln.	0.1 M H_2SO_4/ 0.1 M $LiClO_4$	—	ox, $2e^-$, irr	l.s. d.p.	RPE, CPE, RGCE	+0.65 +1.10 +1.10	1×10^{-4}—1×10^{-5}	5×10^{-7} (CPE) 5×10^{-6}	[35]
Clotiapine loxapine										
Clozapine clotiapine loxapine	Pure soln.	ac/ 20% MeOH	4.7	ox, $2e^-$, irr	l.s. d.p.	GSE	+0.47 +0.95 +0.95	5×10^{-5}—5×10^{-6}	2×10^{-6}	[39]
Triazolam	Pure soln.	ph/ac/bor 20% MeOH	6	red, $2e^-$, irr	d.c. d.p.	DME	−0.90	1×10^{-3}—1×10^{-7}	4×10^{-8}	[40]
Midazolam	Pure soln.	ph/ac/bor/ 20% MeOH	6	red, $2e^-$, irr	d.c. d.p.	DME	−0.85	1×10^{-3}—1×10^{-7}	6×10^{-8}	[41]
Desipramine imipramine trimipramine	Pure soln.	0.05 M ph	9	ox, $2e^-$, irr	a.s.v.	GCE	+0.70* +0.72* +0.74*	2×10^{-6}—2×10^{-7}	1.7×10^{-8} 1.5×10^{-8} 1.4×10^{-8}	[42]
Barbiturates	Tablets	0.05 M bor	9.3	ox (Hg), $2e^-$,	d.p.	DME	0.0	1×10^{-4}—4×10^{-6}		[43]
Dopamine	Pure soln. + ascorbic acid	ph	7	ox, cat	d.p.	CPE	+0.15	2×10^{-4}—1×10^{-5}		[44]
Dopamine	Pure soln. + ascorbic acid	ph		ox, cat		carbon fibers		1.5×10^{-6}—1×10^{-7} 3.0×10^{-8}—2×10^{-9}	2×10^{-9}	[45]
3-Mercapto-2-pyridine carboxylic acids	Pure soln.	2 M H_2SO_4	—	red, $2 \times 2e^-$, irr	d.c. d.p.	DME	−0.62 −0.85	1×10^{-3}—1×10^{-7}	1×10^{-7}	[47] [47]
Allopurinol	Tablets	cit/5% DMF	4.8	red, $2e^-$, irr	d.p.	DME	−1.48	5×10^{-4}—1×10^{-4}		[50]
Allopurinol	Tablets	0.5 M H_2SO_4	—	red, $4e^-$, irr	d.p.	DME	−1.10	5×10^{-4}—1×10^{-4}		[50]
Ascorbic acid	Tablets	ac	4.7	ox, $2e^-$, irr	d.p.	CPE	+0.35		1.5×10^{-7}	[52]

TABLE 2 (continued)

Compound	Nature of sample	Supporting electrolyte or buffer[a]	pH	Characteristics of the wave[b]	Mode[c]	Working electrode[d]	$E_{1/2}$ or E_p[e] (V)	Linear range (M)	Detection limit (M)	Ref.
Ascorbic acid	Dehydrated fruit juices	ac	4.7	ox, $2e^-$, irr	d.p.	CPE	+0.35		8×10^{-7}	[52]
Ascorbic acid	Fresh fruit juices	ac	4.7	ox, $2e^-$, irr	d.p.	CPE	+0.35		1×10^{-5}	[53]
Tryptophane	Pure soln.	0.1 M H_3PO_4	2	ox, $2e^-$, irr	d.p.	GCE	+1.0	2×10^{-4}—3×10^{-6}	1×10^{-6}	[54]
						CPE	+1.0	3×10^{-5}—5×10^{-7}	2.5×10^{-7}	[54]
Saccharine	Grape jellies gel desserts soft drinks	0.1 M HCl/ 0.1 M KCl/ 0.1% TBABr	—	red,	d.p.	DME	−1.15	2.3×10^{-3}—1.1×10^{-6}		[55]

[a]ph, phosphate; ac, acetate; bor, borate; cit, citrate. [b]cat, catalytic wave; red, reduction wave; ox, oxidation wave; ne^-, number of electron transferred; rev, reversible process; irr, irreversible process. [c]d.c., direct current; d.p., differential pulse; l.s., linear scan voltammetry; a.s.v.; differential-pulse adsorptive stripping voltammetry. [d]DME, dropping mercury electrode; HMDE, hanging mercury drop electrode; GSE, graphite spray electrode; CPE, carbon paste electrode; GCE, glassy carbon electrode; CPoE, carbon polyethylene electrode; RPE, rotating platinum electrode; RGCE, rotating glassy carbon electrode; GE, graphite electrode. [e]Potentials are given versus the saturated calomel electrode (SCE) or (*) versus the Ag/AgCl/KCl (satd.) electrode.

REFERENCES

1 G. J. Patriarche, M. Chateau-Gosselin, J. L. Vandenbalck and P. Zuman, in A. J. Bard (Ed.), Electroanalytical Chemistry, Vol. 11, M. Dekker, New York, 1979, p. 141.
2 H. Siegerman, in A. J. Bard (Ed.), Electroanalytical Chemistry, Vol. 11, M. Dekker, New York, 1979, p. 291.
3 P. M. Bersier and J. Bersier, Crit. Rev. Anal. Chem., 16 (1985) 81.
4 W. F. Smyth (Ed.), Electroanalysis in Hygiene, Environmental, Clinical and Pharmaceutical Chemistry, Analytical Symposia Series, Vol. 2, Elsevier, Amsterdam, 1980.
5 I. E. Davidson, in W. F. Smyth (Ed.), Polarography of Molecules of Biological Significance, Academic, London, 1979.
6 G. J. Patriarche, Labo. Pharma. Probl. Tech., 27 (1979) 953; Chem. Abstr., 92 (1980) 152942w.
7 H. S. De Boer, Polarography of Corticosteroids. Reduction mechanisms and Analytical Applications. Ph.D. Thesis, University of Utrecht, The Netherlands, 1980.
8 F. C. Anson, Acc. Chem. Res., 8 (1975) 400.
9 R. W. Murray, in A. J. Bard (Ed.), Electroanalytical Chemistry, Vol. 13, M. Dekker, New York, 1984, p. 191.
10 N. Oyama and F. C. Anson, J. Am. Chem. Soc., 101 (1979) 739.
11 G. J. Patriarche, J.-C. Vire and J.-M. Kauffmann, Chim. Nouv., 2 (1984) 91.
12 L. R. Faulkner, C. E. News, 62 (1984) 28.
13 Ch. E. D. Chidsey and R. W. Murray, Science, 231 (1986) 25.
14 O. Garcia De Alvarez and G. J. Patriarche, Analusis, 8 (1980) 26.
15 J.-C. Vire, B. Gallo Hermosa, P. Chatelain and G. J. Patriarche, Analusis, 14 (1986) 40.
16 J. Wang, J. S. Mahmoud and P. A. M. Farias, Analyst, 110 (1985) 855.
17 J.-M. Kauffmann, G. J. Patriarche, M. Chateau-Gosselin and B. Gallo Hermosa, Talanta, 33 (1986) 733.
18 J.-C. Vire, G. J. Patriarche and G. D. Christian, Fresenius' Z. Anal. Chem., 299 (1979) 197.
19 J.-C. Vire, J.-M. Kauffmann, J. Braun and G. J. Patriarche, Analusis, 13 (1985) 134.
20 J.-M. Kauffmann, J.-C. Vire, M. Gelbcke and G. J. Patriarche, Anal. Lett., 17 (1984) 2319.
21 J.-C. Vire, J.-M. Kauffmann, J. Braun and G. J. Patriarche, J. Pharm. Belg., 40 (1985) 133.
22 J.-C. Vire, R. L. De Jager, D. G. Dupont, G. J. Patriarche and G. D. Christian, Fresenius' Z. Anal. Chem., 307 (1981) 277.
23 M. Chateau-Gosselin, J.-C. Vire and G. J. Patriarche, Mikrochim. Acta, Part III, (1983) 457.
24 F. Mebsout, J.-C. Vire and G. J. Patriarche, Anal. Lett., 17 (1984) 805.
25 F. Mebsout, J.-C. Vire and G. J. Patriarche, Anal. Lett., 18 (1985) 1431.
26 A. Z. Abu Zuhri, S. I. Al-Khalil and M. S. Suleiman, Anal. Lett., 19 (1986) 453.
27 J.-M. Kauffmann, G. J. Patriarche and J.-C. Vire, Analyst, 110 (1985) 349.
28 A. Temizer and N. Özaltin, J. Assoc. Off. Anal. Chem., 69 (1986) 192.
29 T. B. Jarbawi, W. R. Heineman and G. J. Patriarche, Anal. Chim. Acta, 126 (1981) 57.
30 J.-C. Vire, M. Fischer and G. J. Patriarche, Talanta, 28 (1981) 313.
31 J.-C. Vire, M. Fischer and G. J. Patriarche, Analusis, 10 (1982) 19.
32 S. Pap, J.-M. Kauffmann, J.-C. Vire, G. J. Patriarche and M. P. Prete, J. Pharm. Belg., 39 (1984) 335.
33 J.-C. Vire, G. J. Patriarche and J. Patriarche-Sepulchre, Anal. Lett., 11 (1978) 681.
34 J.-C. Vire, J.-M. Kauffmann and G. J. Patriarche, Anal. Lett., 15 (1982) 1331.
35 J.-M. Kauffmann and G. J. Patriarche, Anal. Lett., 12(B11) (1979) 1217.
36 J.-M. Kauffmann and G. J. Patriarche, Electrochim. Acta, 27 (1982) 721.
37 G. J. Patriarche, J.-C. Vire and J.-M. Kauffmann, Anal. Proc., 22 (1985) 202.
38 J.-M. Kauffmann, J.-C. Vire and G. J. Patriarche, Bioelectrochem. Bioenerg., 12 (1984) 413.

39 J.-M. Kauffmann, A. Laudet, J.-C. Vire, G. J. Patriarche and G. D. Christian, Microchem. J., 28 (1980) 26.
40 J.-C. Vire and G. J. Patriarche, J. Electroanal. Chem., 214 (1986) 275.
41 J.-C. Vire, B. Gallo Hermosa and G. J. Patriarche, Anal. Chem. Acta, 196 (1987) 205.
42 J. Wang, M. Bonakdar and C. Morgan, Anal. Chem., 58 (1986) 1024.
43 A. Temizer and A. O. Solak, Arch. Pharm. Weinheim, Ger., 319 (1986) 149.
44 M. B. Gelbert and D. J. Curran, Anal. Chem., 58 (1986) 1028.
45 A. Akiyama, T. Kato, K. Ishii and E. Yasuda, Anal. Chem., 57 (1985) 1518.
46 B. Blank, N. W. Di Tullio, C. K. Miao, F. F. Avings, J. G. Glenson, S. T. Ross, C. E. Berkoff, H. L. Saunders, J. Delarge and C. L. Lapiere, J. Med. Chem., 17 (1974) 106.
47 R. Lejeune, J. L. Vandenbalck, G. J. Patriarche and C. L. Lapiere, Bull. Soc. Chim. Belg., 91 (1982) 751, 759; J. Pharm. Belg., 38 (1983) 33.
48 R. Lejeune, J. L. Vandenbalck, G. J. Patriarche and C. L. Lapiere, Bull. Soc. Chim. Belg., 90 (1981) 663, 881.
49 R. Lejeune, J. L. Vandenbalck, G. J. Patriarche and C. L. Lapiere, J. Pharm. Belg., 38 (1983) 200, 206.
50 L. G. Chatten, M. Boyce, R. E. Moskalyk, B. Pons and D. K. Madan, Analyst, 106 (1981) 365.
51 P. K. De and G. Dryhurst, J. Electroanal. Chem., 119 (1972) 837.
52 A. Lechien, P. Valenta, H. W. Nürnberg and G. J. Patriarche, Fresenius' Z. Anal. Chem., 311 (1982) 105.
53 N. T. Nguyen, M. Z. Wrona and G. Dryhurst, J. Electroanal. Chem., 199 (1986) 101.
54 C. R. Linders, B. J. Vincke, J.-C. Vire, J.-M. Kauffmann and G. J. Patriarche, J. Pharm. Belg., 40 (1985) 27.
55 W. Holak and B. Krinitz, J. Assoc. Off. Anal. Chem., 63 (1980) 163.

Analytica Chimica Acta, 196 (1987) 205—212
Elsevier Science Publishers B.V., Amsterdam — Printed in The Netherlands

POLAROGRAPHIC BEHAVIOUR AND HYDROLYSIS OF MIDAZOLAM AND ITS METABOLITES

J.-C. VIRE and G. J. PATRIARCHE*

Free University of Brussels (U.L.B.), Institute of Pharmacy, Campus Plaine C.P. 205/6, Bd du Triomphe, B-1050 Brussels (Belgium)

B. GALLO HERMOSA

Departamento de Quimica, Facultad de Ciencias, Universidad del Pais Vasco, Apdo 644, 48080 Bilbao (Spain)

(Received 28th July 1986)

SUMMARY

The electrochemical behaviour of midazolam [7-chloro-5-(*o*-fluorophenyl)-3*H*-(2'-methylimidazo) [1,5-a] [1,4]-benzodiazepine was studied by polarography and cyclic voltammetry. The irreversible two-electron wave is not strongly affected by the imidazole ring or the 5-*o*-fluorophenyl substituent, but the latter increases the rate of the hydrolysis in acidic media. Kinetic parameters are evaluated for midazolam and three of its hydroxylated metabolites. The hydrolysis is a first-order reaction initially but becomes second order. The 3-hydroxy metabolites are more easily hydrolyzed than midazolam. Midazolam (10^{-4}—10^{-7} M) can be quantified by using differential-pulse polarography; the detection limit is 6×10^{-8} M.

Midazolam is an imidazo-1,4-benzodiazepine of clinical interest as an anticonvulsant, sedative and anaesthetic [1, 2]; it is rapidly absorbed [3] but has a short duration of action because of its rapid metabolic inactivation [1, 4, 5]. It is excreted in a conjugated form with α-hydroxymidazolam as its major metabolite but also with 3-hydroxy derivatives as its minor metabolites [5, 6].

As an extension of an earlier study of triazolam [7], this paper is concerned with an investigation of the electrochemical properites of midazolam and a comparison of the hydrolysis kinetic parameters of this compound to those of its metabolites.

EXPERIMENTAL

Instrumentation

D.C., a.c. and differential-pulse (d.p.) polarograms were recorded on a Tacussel PRG-34 polarograph, which provided rapid-scan cyclic voltammograms on a Telequipment DM-64 oscilloscope. The following conditions were used unless otherwise stated: temperature, 25° ± 0.1°C; a.c. polarography with 10-mV sinusoidal amplitude, 90-Hz frequency, 5 mV s^{-1} scan rate and

0003-2670/87/$03.50

1.1-s drop time; or d.p. polarography with 25-mV pulse amplitude, 40-ms pulse duration, 1.9-s delay before pulse application, 2 mV s^{-1} scan rate and 2-s drop time. Potentials are given versus a saturated calomel electrode. A PAR 174A polarograph coupled with a PAR 175 programmer were used for slow-scan cyclic voltammograms. The hanging mercury drop was a PAR SMDE 303 and the potentials are referred to a silver/silver chloride/saturated KCl electrode. Controlled potential coulometry was done with a PAR 173 potentiostat equipped with a PAR 179 integrator.

Reagents

Midazolam and its metabolites (Produits Roche) were used as received. Stock solutions were prepared with methanol and renewed each day. Diluted solutions for measurements contained 20% of dimethylformamide (DMF) but metabolite solutions needed the addition of 10% of this solvent, which did not modify the characteristics of the waves. Buffers made of phosphoric, acetic and boric acids and their sodium salts were adjusted with diluted sulfuric acid or sodium hydroxide. Deoxygenation was done by passing purified nitrogen through the cell.

RESULTS AND DISCUSSION

Midazolam

Midazolam differs from the earlier studied triazolam [7] in that the triazole ring is replaced by an imidazole moiety and a 5-*o*-fluorophenyl group replaces the 5-*o*-chlorophenyl substituent. These modifications do not strongly modify the polarographic behaviour of the molecule and its reduction at a dropping mercury electrode (DME) gives rise also to a two-electron wave ($n = 1.96 \pm 0.2$, as obtained by controlled potential coulometry). The wave height remains constant in the pH range 1—11. Modifications of the polarograms appearing with time at pH <3 also indicate an acid-catalyzed hydrolysis process of the molecule (see below).

A half-wave potential shift of 65 mV per unit pH was observed up to pH 6; this decreased to 57 mV above pH 6. These values, which correspond to the classical reduction scheme of the azomethine bond following a two-electron/two-proton process, are very similar to those of triazolam [7] but the inflexion at pH 6 is less marked. This pK_a value has been attributed to the N_1 atom by several authors [1, 8] who considered it more basic than the imine nitrogen ($pK_a = 1.7$). The reverse proposition was made by Maupas and Fleury after spectrometric and polarographic investigations [9]. However, the pK_a of the imine nitrogen may vary considerably with the nature of the substituents on the diazepine moiety [9]. Interferences from the N_1 substituent have also been reported [10].

Like the imidazole ring, the 5-*o*-phenyl substituent does not markedly affect the reduction potential. A comparison between the half-wave potential/pH relationships (Fig. 1) shows that the 5-*o*-fluorophenyl derivative (midazolam)

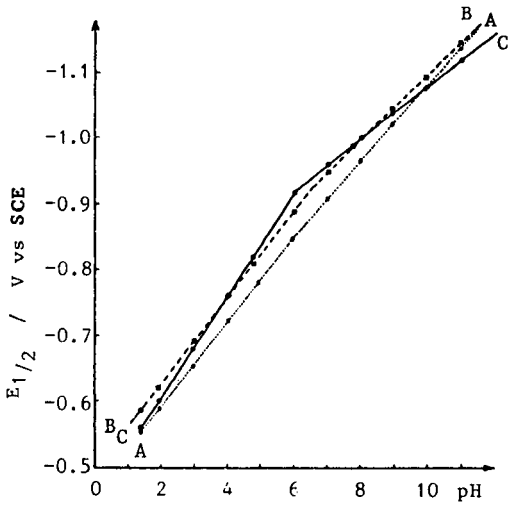

Fig. 1. Half-wave potential evolution as a function of pH for: (A) midazolam; (B) alprazolam; (C) triazolam. Concentration 2×10^{-4} M.

is more easily reduced than the chlorinated (triazolam) or hydrogenated (alprazolam) derivatives; their potentials differ at most by 50 mV. The irreversible character of the global process was demonstrated by cyclic voltammetry where no reoxidation peak appeared, despite a logarithmic analysis giving slopes about 30 mV per logarithmic unit over the whole pH range. The reduction wave is mainly diffusion-controlled as shown by the linearity of the current/temperature relationship (1.9% per degree) and the current/mercury height square root relationship. However, an adsorption phenomenon attributed to the reduced form was indicated by using a.c. polarography and cyclic voltammetry. The phenomenon is decreased in alkaline media. A second wave appears between pH 7 and 8. Its catalytic origin is evidenced by the important decrease of the current with a small increase of pH and by the current increase with a decrease of the height of the mercury column.

Hydroxylated derivatives of midazolam

The major metabolite of the drug, α-hydroxymidazolam, exhibits electrochemical characteristics similar to those of its parent compound. The situation is quite different with the 3-hydroxy and the α,3-dihydroxy metabolites. The electrochemical behaviour of these molecules has to be compared to those of oxazepam, lorazepam or temazepam [11—15] owing to the hydroxy substituent, but some differences appear.

In acidic media, a well defined wave is developed, immediately followed by a second small wave (Fig. 2). The height of both waves is constant up to pH 7. Between pH 7 and 9, the second wave increases to the detriment of the first to become of the same intensity. No further change arises in more

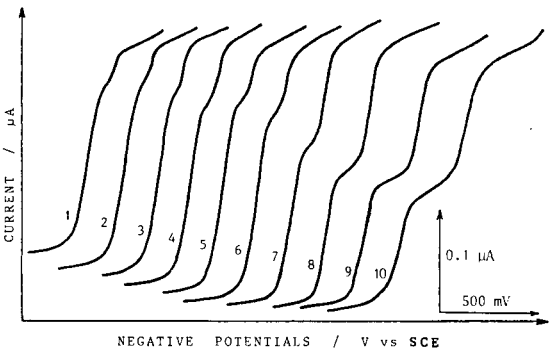

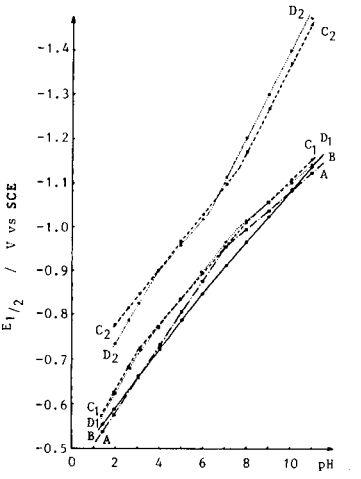

Fig. 2. D.c. polarograms of 3-hydroxymidazolam (2×10^{-4} M) as a function of pH (in parentheses is the starting potential vs. SCE): (1) 2.5 (−0.4 V); (2) 3.0 (−0.4 V); (3) 4.0 (−0.5 V); (4) 5.1 (−0.5 V); (5) 6.1 (−0.6 V); (6) 7.1 (−0.6 V); (7) 8.0 (−0.7 V); (8) 9.0 (−0.8 V); (9) 10.0 (−0.8 V); (10) 11.1 (−0.8 V).

Fig. 3. Half-wave potential evolution as a function of pH for: (A) midazolam; (B) α-hydroxymidazolam; (C) 3-hydroxymidazolam; (D) α,3-dihydroxymidazolam. For C and D: (1) first wave; (2) second wave. Concentration 2×10^{-4} M.

alkaline media. The total height remains constant and corresponds to a four-electron transfer, as shown by controlled potential coulometry. The potential/pH relationship of the first wave may be compared to that of midazolam (Fig. 3), the slopes being similar but with higher pK values than for midazolam for which the lower pK value is not polarographically detected. α,3-Dihydroxymidazolam exhibits a third pK value at pH 11 where the first wave decreases while another wave, 130 mV more negative, arises, the total height remaining constant.

Except for the fact that a four-electron transfer was observed, the reduction process must be different from that of 3-hydroxybenzodiazepinones where only one wave was detected in the whole pH range [11—14]. The appearance of a second wave more negative than the main wave cannot be explained by the reduction of the 3—4 double bond of a dehydrated species [12—14] which is easier to reduce, nor by the reduction of the initial product formed by a disproportionation reaction between the dehydrated compound and the hydroxylated reduced imine arising from the first two-electron transfer [15]. However, a slow chemical reaction must take place between the two steps, because the first wave increased to the detriment of the second when the scan rate was decreased and because coulometric measurements done on the small plateau of the first wave gave n values corresponding to more than two electrons, even in alkaline media.

Hydrolysis reaction

Like most of the benzodiazepines [16], midazolam undergoes reversible hydrolysis in acidic media [8, 17] as shown by the decrease of the azomethine reduction wave with time and the simultaneous increase of a more negative wave attributed to a benzophenone structure which appears according to a mechanism described for triazolam [7].

The reaction kinetics were studied by using cyclic voltammetry [7]. Three sulfuric acid concentrations were investigated: 1.0 M, 0.25 M and 0.10 M. Midazolam behaved similarly in the three acid concentrations; the data for 1.0 M acid are shown in Fig. 4. A first-order reaction is observed, as shown by the linear plot appearing between the natural logarithm of the current and time [18, 19]. The reaction becomes of second order after 50—60% of the compound has been hydrolyzed, the relation $X/\{[A]_0([A]_0 - X)\}$ versus time (where $[A]_0$ is the initial benzodiazepine activity and X is the activity at t time) becoming linear [18].

The calculated kinetic parameters are of same magnitude for the three acid concentrations (Table 1), showing that the hydrolysis reaction does not depend on the proton concentration in this range of acidity. This behaviour is different from that of triazolam, for which the hydrolysis increases with the proton concentration [7]. These differences are attributed to the influence of the 5-*o*-phenyl substituent. A chlorine atom (triazolam) stabilizes the molecule compared to midazolam possessing a fluorine atom or alprazolam which has no substituent, principally at the low acid concentration [7]. Similar behaviour was pointed out by Smyth and Groves [20] but it was observed here that the hydrogen derivative reacted more quickly than the fluorinated one, the reverse situation appearing with benzodiazepinones

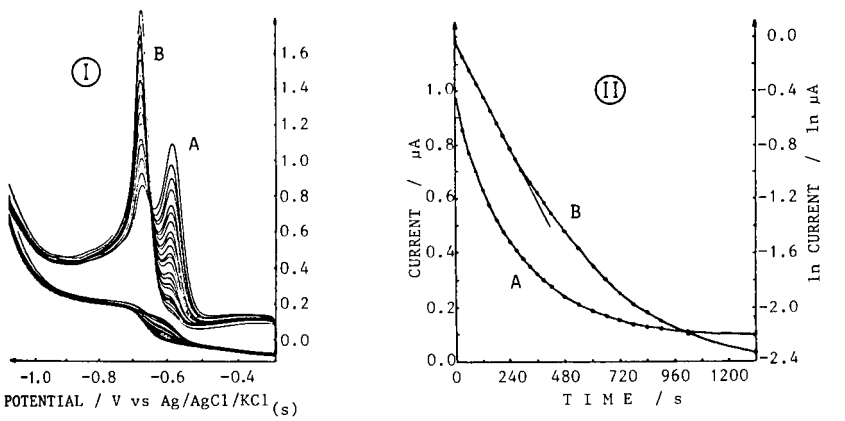

Fig. 4. (I) Cyclic voltammetric study of the hydrolysis reaction of 2×10^{-4} M midazolam (1.0 M sulfuric acid, 100 mV s^{-1} scan rate; peaks scanned over the period 0—1320 s): (A) midazolam reduction peak; (B) hydrolysis product reduction peak. (II) Kinetic plots for 2×10^{-4} M midazolam in 1.0 M sulfuric acid: (A) i_p versus time; (B) ln i_p versus time.

TABLE 1

Kinetic data of hydrolysis reactions in sulfuric acid[a]

Compound	H_2SO_4 (M)	$10^3 k$ (s^{-1})	$t_{1/2}$ (s)	Degree of completion (%)
Midazolam	1.0	3.3	210	90
	0.25	4.4	158	89
	0.10	4.1	170	84
α-Hydroxy-midazolam	1.0	2.6	267	92
	0.25	3.6	192	91
	0.10	4.1	170	86
3-Hydroxy-midazolam	1.0	9.4	74	59
	0.25	8.2	85	76
	0.10	3.6	192	73
α,3-Dihydroxy-midazolam	1.0	16.3	43	78
	0.25	5.3	130	84
	0.10	2.3	306	86

[a]Compound concentration 2×10^{-4} M; cyclic voltammetry at 100 mV s^{-1}.

[20]. It should, however, be pointed out that the reactions of the benzodiazepinones [21] are about 100-fold slower than those of the triazole or imidazole derivatives of benzodiazepines. The kinetics of the reaction for the latter is influenced by the fact that the cycle is rigid in the N_1—C_2 position instead of a linear substituent in N_1 and a carbonyl group in C_2, such a substitution modifies the conformation of the central heterocycle and favours the hydrolysis procedure.

Kinetic studies on the hydroxylated metabolites of midazolam were conducted. As for the electrochemical behaviour, α-hydroxymidazolam exhibits kinetic parameters of the same magnitude as the parent compound (Table 1); the hydroxymethyl substituent on the imidazole ring has no marked influence on the hydrolysis reaction. For both compounds, the degree of completion of the reaction decreases as the acidity decreases but the reaction rate increases slowly with a decrease of the proton concentration. When a 3-hydroxy substituent is attached, the behaviours are different. The two peaks of 3-hydroxy- and α,3-dihydroxy-midazolam developed in acidic medium disappear simultaneously with time, giving rise to one peak attributed to the benzophenone derivative. In contrast to the previous compounds, the degree of completion increases but the reaction rate decreases when the proton concentration decreases (Table 1).

As for benzodiazepinones [8, 20, 21] and triazolobenzodiazepines [7], the hydrolysis reaction is reversible. When a hydrolyzed solution of the 3-hydroxyl derivative was neutralized, the polarograms exhibited the two waves of the initial compound. That also means that the hydroxyl group is not eliminated by the hydrolysis reaction but gives rise to an amino-alcohol group in the C_3 position.

TABLE 2

Characteristics of the calibration graphs of midazolam at pH 6

Concentration range (M)	Mode	Equation	Correlation coefficient	s_b (%)
1×10^{-3}—1×10^{-4}	d.c.	$y = 107.7\,x - 6.3$	0.9999	0.8
	d.p.	$y = 101.2\,x + 10.4$	0.9995	1.6
1×10^{-4}—1×10^{-5}	d.c.	$y = 11.6\,x + 1.9$	0.9996	1.5
	d.p.	$y = 15.0\,x + 0.6$	0.9994	1.7
1×10^{-5}—1×10^{-6}	d.p.	$y = 2.63\,x + 0.08$	0.9999	0.8
1×10^{-6}—1×10^{-7}	d.p.	$y = 0.81\,x + 0.40$	0.9992	2.0

Quantitative analysis and separation

Most of the benzodiazepines can be determined polarographically [16, 22], the reduction wave of the azomethine group being well defined and mainly diffusion-controlled. The current/concentration relationship was studied at pH 6, because acidic media must be avoided to prevent hydrolysis. The results summarized in Table 2 show that d.c. polarography allows midazolam to be determined down to 1×10^{-5} M. The 1×10^{-7} M level can be reached by using the differential pulse mode; the detection limit is 6×10^{-8} M, i.e., 20 $\mu g\ l^{-1}$.

As it can be seen on Fig. 1, midazolam cannot be differentiated from triazolam or alprazolam. Figure 2 shows that this is also true for α-hydroxymidazolam. The 3-hydroxy metabolites can be distinguished from the parent drug by means of the second wave which is well separated from the first in alkaline media (Fig. 3). If both differential-pulse peaks are of the same magnitude, they can be used quantitatively at pH 11. But from a clinical point of view, 3-hydroxy derivatives are minor metabolites and midazolam is not totally metabolized, so that the first peak will always be higher than the second and overlapping of the peaks will occur.

Thanks are expressed to Produits Roche (Brussels) for the generous gift of midazolam and its metabolites and to the "Fonds National de la Recherche Scientifique" for support to one of us (G. J. P.).

REFERENCES

1 L. Pieri, R. Schaffner, R. Scherschlicht, P. Polc, J. Sepinwall, A. Davidson, H. Möhler, R. Cumin, M. Da Prada, W. P. Burkard, H. H. Keller, R. K. M. Müller, M. Gerold, M. Pieri, I. Cook and W. Haefely, Arzneim. Forsch., 31 (1981) 2180.
2 A. Forster, Arzneim. Forsch., 31 (1981) 2243.
3 R. Jochemsen, P. A. Van Rijn, T. G. M. Hazelzet, C. J. Van Boxtel and D. D. Breimer, Biopharm. Drug Dispos., 7 (1986) 53.
4 R. Amrein, J. P. Cano, M. Eckert and P. Coassolo, Arzneim. Forsch., 31 (1981) 2202.
5 P. Heizmann and W. H. Ziegler, Arzneim. Forsch., 31 (1981) 2220.
6 T. B. Vree, A. M. Baars, L. H. D. Booij and J. J. Driessen, Arzneim. Forsch., 31 (1981) 2215.

7 J.-C. Vire and G. J. Patriarche, J. Electroanal. Chem., 214 (1986) 275.
8 A. Walser, L. E. Benjamin Sr., T. Flynn, C. Mason, R. Schwartz and R. I. Fryer, J. Org. Chem., 43 (1978) 936.
9 B. Maupas and M. B. Fleury, Electrochim. Acta, 26 (1981) 399.
10 J. A. Groves and W. F. Smyth, Analyst, 106 (1981) 890.
11 H. Oelschläger, J. Volke, G. T. Lim and R. Spang, Arch. Pharm. Weinheim Ger., 302 (1969) 946.
12 H. Oelschläger, J. Volke, G. T. Lim and U. Bremer, Arch. Pharm. Weinheim Ger., 303 (1970) 364.
13 H. Oelschläger and F. I. Sengün, Pharmazie, 29 (1974) 770; Chem. Ber., 108 (1975) 3303.
14 H. Oelschläger and H. P. Oehr, Pharm. Acta Helv., 49 (1974) 179.
15 B. Maupas and M. B. Fleury, Electrochim. Acta, 27 (1982) 141.
16 H. Schütz, Benzodiazepines, A Handbook, Springer, Berlin, 1982, p. 13.
17 C. V. Puglisi, J. C. Meyer, L. d'Arconte, M. A. Brooks and J. A. F. de Silva, J. Chromatogr., 145 (1978) 81.
18 N. C. Price and R. A. Dwek, Principles and Problems in Physical Chemistry for Biochemists, 2nd edn., Clarendon Press, Oxford, 1979, p. 132.
19 E. L. King, Introduction à la Cinétique Chimique, Ediscience, Paris, 1968, p. 23.
20 W. F. Smyth and J. A. Groves, Anal. Chim. Acta, 134 (1982) 227.
21 J. A. F. de Silva, C. V. Puglisi, M. A. Brooks and M. R. Hackman, J. Chromatogr., 99 (1974) 461.
22 G. J. Patriarche, M. Chateau-Gosselin, J. L. Vandenbalck and P. Zuman, in A. J. Bard (Ed.), Electroanalytical Chemistry, Vol. 11, M. Dekker, New York, 1979, p. 141.

Analytica Chimica Acta, 196 (1987) 213—219
Elsevier Science Publishers B.V., Amsterdam — Printed in The Netherlands

VOLTAMMETRIC STUDY AND DETERMINATION OF CACOTHELINE

K. VIJAYALAKSHMI and K. SARASWATHI*
Department of Chemistry, S. V. University, Tirupati-517 502 (India)
(Received 28th July 1986)

SUMMARY

The polarographic and cyclic voltammetric characteristics of cacotheline at mercury electrodes are reported. Two well-defined, diffusion-controlled cathodic peaks are observed over the pH range 2.0—12.0. The electrode process involves two electrons for the reversible reduction of the *o*-quinone group to hydroquinone followed by a four-electron irreversible reduction of the nitro group to hydroxylamine. The effects of experimental variables on the characteristics of the waves are described. The reduction mechanism is elucidated from the results of constant-potential coulometry and infrared spectroscopy.

Cacotheline, a red product of the action of nitric acid on brucine [1], is an analytical reagent used in the detection and determination of various inorganic metal ions and organic compounds [2—5]. Although the polarographic response of the reagent in the estimation of dialkyl phosphates [6] and in the determination of strychnine in a mixture of strychnine and brucine [7] have been studied, there has been no systematic investigation of the voltammetric behaviour of this reagent.

The present paper, therefore, deals with a study of the polarographic and cyclic voltammetric behaviour of the reagent in aqueous medium at a dropping mercury electrode (DME) or a hanging mercury drop electrode (HMDE) under varying conditions of pH, temperature, surfactant, etc., to determine a mechanism for the electrode reaction. The results obtained are supported by coulometry and i.r. data.

EXPERIMENTAL

The cacotheline was prepared and purified by the well established method [1]. A 0.005 M stock solution was prepared because of the low solubility of the reagent in water. Only freshly prepared solutions were used in all studies. The supporting electrolytes used were 0.1 M Britton-Robinson (BR) (pH 2.0—12.0) and 0.1 M Walpole acetate (pH 2.0—12.0) buffers. All the experiments were done at room temperature (25 ± 0.2°C). Deaeration was done by passing oxygen-free nitrogen through the solutions. Double-distilled mercury was used. The maximum suppressor was Triton X-100.

0003-2670/87/$03.50

Polarograms were obtained with a conventional pen recording polarograph (Elico, India). A saturated calomel reference electrode (SCE) was used. The DME characteristics measured in 0.1 M KCl (open circuit) were m = 2.15 mg s^{-1} and t = 4.14 s at a mercury height of 17.3 cm. The pH measurements were made with an Elico model L'-10 pH meter with combined glass electrode.

A Wenking potentiostat and scan generator were used in cyclic voltammetric studies at the HMDE. Potentials were recorded relative to the SCE, the auxiliary electrode being a platinum wire. Unless otherwise indicated, the surface area of the HMDE was 0.03316 cm^2. Controlled potential electrolysis were done with a Radelkis (Budapest) potentiostat model OH-401'/A and a current integrator (model OH-404'/C), at the mercury pool working electrode.

From the cyclic voltammetric data, the number of electrons (n and αn_a) [8] and the diffusion coefficients (D) [9] for both reversible and irreversible processes were calculated from the following equations:

$$E_{pa} - E_{pc} = 0.058/n$$

$$E_{p/2} - E_p = 0.048/\alpha n_a$$

$$i_p = 2.75 \times 10^5 n^{3/2} A D^{1/2} C v^{1/2}$$

$$i_p = 3.01 \times 10^5 n (\alpha n_a)^{1/2} A D^{1/2} C \bar{v}^{1/2}$$

where the symbols have their conventional meanings, subscripts a and c refer to anodic and cathodic peaks, respectively, and potentials are given in volts.

RESULTS AND DISCUSSION

D.c. polarography at the DME

A typical polarogram of cacotheline in BR buffer (pH ≈4.0) is shown in Fig. 1. The nature of the polarograms remained the same in both the supporting electrolytes used. Two well defined cathodic waves are observed in the entire range of pH (2.0—12.0) and reagent concentration (0.1—2.0 mM) studied. A linear relationship between diffusion current and concentration of the reagent was observed for both the waves at all pH values (2.0—12.0) studied, indicating the diffusion-controlled nature of the waves (Table 1). The linear dependence of the diffusion current of both waves on the square root of the mercury column ($i_d^1/h^{1/2}$ and $i_d^2/h^{1/2}$) at all pH values and concentrations of cacotheline studied, strongly indicates that the electrode process is purely diffusion-controlled (Table 2).

At lower pH values (2.0—5.0) the second wave showed a maximum at the start of the limiting current, which could be suppressed by using 0.008% Triton X-100. In further studies, 0.016% Triton X-100 was added. A negative shift in half-wave potentials of about 60 mV per unit pH variation was found for both waves in the Walpole buffer, indicating proton involvement in the

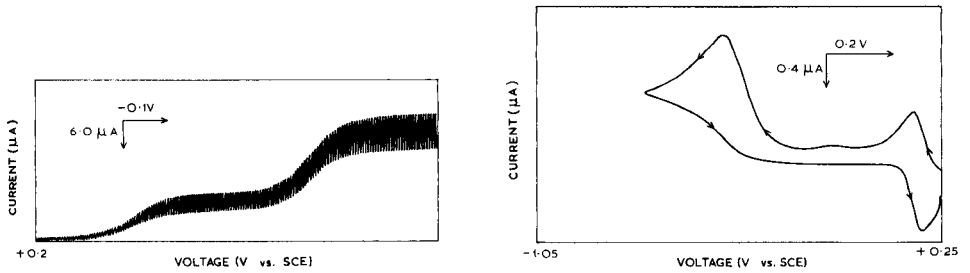

Fig. 1. D.c. polarogram of cacotheline at the DME. Conditions: 0.1 M BR buffer at pH ≈4.0, 1.0 mM cacotheline, 0.016% Triton X-100.

Fig. 2. Typical cyclic voltammogram of cacotheline at the HMDE. Conditions: BR buffer at pH ≈2.0, 0.2 mM cacotheline, scan rate 0.04 V s^{-1}.

TABLE 1

Effect of concentration of cacotheline at different pH values

pH	Cacotheline (mM)	$E^1_{1/2}$ (V vs. SCE)	i^1_d (μA)	i^1_d/C (μA mol^{-1})	$E^2_{1/2}$ (V vs. SCE)	i^2_d (μA)	i^2_d/C (μA mol^{-1})
BR buffer	0.2	+0.14	2.5	12.5	−0.28	4.85	24.3
pH ≈2.0	0.6	+0.142	7.25	12.1	−0.295	14.5	24.2
	1.0	+0.144	12.5	12.5	−0.320	24.6	24.6
	1.4	+0.146	17.0	12.1	−0.350	34.0	24.2
	2.0	+0.147	24.5	12.2	−0.380	48.75	24.3
Walpole	0.2	−0.160	2.0	10.0	−0.540	3.75	18.7
buffer	0.6	−0.165	6.38	10.6	−0.560	10.75	18.0
pH ≈6.0	1.0	−0.168	10.12	10.1	−0.575	18.38	18.3
	1.4	−0.169	14.25	10.2	−0.595	25.5	18.2
	2.0	−0.170	19.5	10.0	−0.625	37.2	18.6
BR buffer	0.8	−0.179	7.125	8.9	−0.625	15.0	18.8
pH ≈7.0	1.0	−0.179	9.0	9.0	−0.635	18.75	18.8
	1.4	−0.181	12.8	9.1	−0.665	25.5	18.2
	2.0	−0.182	18.0	9.0	−0.72	37.5	18.8
Walpole	0.3	−0.370	1.85	6.2	−0.69	6.5	21.6
buffer	0.5	−0.374	3.0	6.0	−0.71	10.75	21.0
pH ≈9.0	1.0	−0.378	6.0	6.0	−0.73	21.0	21.0
	2.0	−0.385	13.5	6.8	−0.76	41.75	20.8

electrode process (Table 3). At a fixed pH of 2.0, the half-wave potential was independent of the concentration of cacotheline and the slope of the log plot corresponded to two electrons, indicating the reversible nature of the first wave. The irreversible nature of the second wave was shown by the shift in $E_{1/2}$ with increasing concentration of cacotheline and by the $E^2_{1/4} - E^2_{3/4}$ values. The wave height ratio i^1_d/i^2_d was found to be 1:2 up to pH 8.0 indicating that the second wave may involve a four-electron process.

TABLE 2

Effect of mercury column height at different pH values with 1.0 mM cacotheline and 0.016% Triton X-100

Hg height (cm)	BR buffer pH ≈ 2.0				BR buffer pH ≈ 6.0				Walpole buffer pH ≈ 9.0			
	i_d^1 (μA)	i_d^2 (μA)	$i_d^1/h^{1/2}$	$i_d^2/h^{1/2}$	i_d^1 (μA)	i_d^2 (μA)	$i_d^1/h^{1/2}$	$i_d^1/h^{1/2}$	i_d^1 (μA)	i_d^2 (μA)	$i_d^1/h^{1/2}$	i_d^2/h
23.6	11.25	27.5	2.3	5.66	9.75	17.7	2.00	3.6	7.0	22.5	1.44	4.6
28.4	12.5	30.6	2.34	5.62	10.55	19.2	2.0	3.6	7.5	24.25	1.40	4.55
33.3	13.5	32.5	2.33	5.63	11.75	21.0	2.03	3.6	8.1	26.0	1.40	4.50
38.3	14.5	34.5	2.34	5.60	12.4	22.5	2.0	3.6	8.75	28.25	1.41	4.56
43.3	15.5	37.0	2.35	5.62	13.15	23.75	2.0	3.6	9.25	30.0	1.40	4.56

TABLE 3

Effect of pH on cacotheline waves at the DME in Walpole buffer[a]

pH	$E_{1/2}^1$ (V vs. SCE)	i_d^1 (μA)	$E_{1/2}^2$ (V vs. SCE)	i_d^2 (μA)	i_d^2/i_d^1
3.0	+0.16	7.1	−0.37	14.0	1.97
4.0	−0.050	7.5	−0.419	15.0	2.0
5.0	−0.115	7.9	−0.499	16.5	2.0
6.0	−0.17	8.0	−0.559	16.0	2.0
7.0	−0.246	9.5	−0.735	15.5	1.6
8.0	−0.285	9.4	−0.699	15.4	1.6
9.0	−0.385	6.0	−0.735	15.0	2.5
10.0	−0.55	4.86	−0.875	13.5	2.7
11.0	−0.485	4.5	−0.819	14.6	3.2
12.0	−0.56	3.4	−0.90	12.8	3.7

[a]0.8 mM cacotheline, 0.016% Triton X-100.

The nature of the waves and half-wave potentials remained the same with variation of ionic strength of the supporting electrolyte from 0.05 M to 1.0 M at pH 2.0 and 6.0 in the Walpole buffers. The concentration of Triton X-100 in the range 0.008—0.04% had no effect on the limiting currents and $E_{1/2}$ of both waves at pH 2.0 or 6.0. Temperature variations from 32°C to 60°C had little effect on the shape of the waves at pH 6.0 in BR buffer. The limiting currents of the waves increased by about 1.2%/°C, confirming the diffusion-controlled nature of both waves.

Cyclic voltammetry at the HMDE

A typical cyclic voltammogram of cacotheline at the HMDE (Fig. 2) shows two reduction peaks and one oxidation peak for a potential sweep from +0.25 V to −0.90 V at pH 2.0 (BR buffer). The first reduction peak (E_{pc}^1) was observed at +0.16 V and the second peak (E_{pc}^2) at −0.5 V. The two reduction peaks (E_{pc}^1, i_{pc}^1 and E_{pc}^2, i_{pc}^2) correspond to the first and second cathodic (E_{dc}^1, E_{dc}^2) waves of the d.c. polarograms in the same medium. By switching

off the potential at −0.25 V followed by current reversal, it was found that the reduction peak (E^1_{pc}) is coupled with its oxidation peak (E^1_{pa}), indicating the reversible nature of the first peak at low pH. But the reversibility decreased from pH 6.0 and at pH 12.0 the anodic peak (E^1_{pa}) completely disappeared. The cyclic voltammetric studies were therefore restricted to the pH range 2.0—6.0. The results obtained are summarized in Table 4.

The absence of an anodic peak corresponding to the second cathodic peak (E^2_{pc}) in the reverse scan at all pH values shows the irreversible nature of the second peak. The peak potentials for both the peaks (E^1_{pc}, E^2_{pc}) shifted to negative values with increasing pH. In the presence of 0.016% Triton X-100, the potential increment was greater for the second peak (E^2_{pc}) compared to the first cathodic peak (E^1_{pc}) at fixed pH (2.0) and concentration of the electroactive species (1.0 mM). The peak potentials of the first couple (E^1_{pc}, E^1_{pa}) remained almost constant with increasing scan rate (v) and concentration (C) of the reagent at a selected pH (2.0—6.0), confirming the reversible nature of the peak. The difference in peak potential ($E^1_{pa} - E^1_{pc}$) corresponds to a reversible two-electron process in the pH range 2.0—6.0 at all scan rates and concentrations of cacotheline in both the buffers. The invariance of the current function $i^1_{pc}/v^{1/2}$, the peak current ratio i^1_{pa}/i^1_{pc} and the peak width ($E^1_{pc/2} - E^1_{pc}$) with increasing concentration of cacotheline and scan rates in the pH range 2.0—6.0 shows the process to be purely diffusion-controlled without any involvement of adsorption or chemical reaction in the first electrode process (Table 4).

At a given pH, the peak potentials of the second peak (E^2_{pc}) shifted cathodically with increasing scan rate and concentration of the reagent, showing the irreversible nature of the peak. The plot of i^2_{pc} vs. $v^{1/2}$ was linear in the pH range 2.0—6.0 passing through the origin; this indicates that the irreversible process is purely diffusion-controlled. Based on these results, it is proposed that cacotheline in the concentration range 0.05—2.0 mg ml^{-1} can be determined by d.c. polarographic or cyclic voltammetric techniques.

Analogous to the d.c. polarographic data, the peak current ratio (i^1_{pc}/i^2_{pc}) for the first and second peaks was found to be 1:2 up to pH ≈ 6.0, confirming the four-electron transfer in the irreversible cathodic electrode process. Comparison of $i_{pc}/v^{1/2}$ data for both the peaks also confirmed this. Diffusion coefficients (D) and αn_a values are given in Table 5.

Constant-potential coulometry, in the Walpole buffer at pH 2, of a freshly prepared cacotheline solution at the limiting potential of the final wave (−0.60 V vs. SCE) gave $n = 6$ for the electron transfer.

Elucidation of mechanism

The product obtained by coulometry at the mercury pool electrode was isolated by extraction into methanol, followed by recrystallization and its infrared spectrum (KBr) was taken. The peaks at 1670 and 1700 cm^{-1} of cacotheline, representing the *o*-quinone group, and the low absorption peaks of C—NO_2 aromatic stretching at 1300 and 1340 cm^{-1} disappeared in the

TABLE 4

Cyclic voltammetric data for the reduction of cacotheline at the HMDE

Buffer pH	Cacotheline (mM)	Scan rate (V s^{-1})	E^1_{pc} (V vs. SCE)	E^1_{pa} (V vs. SCE)	$E^1_{pa} - E^1_{pc}$ (mV)	$E^1_{pc/2} - E^1_{pc}$ (mV)	i^1_{pc} (μA)	i^1_{pa} (μA)	i^1_{pa}/i^1_{pc}	$\frac{i^1_{pc}}{V^{1/2}C}$ [a]	E^2_{pc} (V vs. SCE)	i^2_{pc} (μA)	$\frac{i^2_{pc}}{V^{1/2}C}$ [a]	$\frac{i^2_{pc}}{i^1_{pc}}$	$E^2_{pc/2} - E^2_{pc}$ (mV)
Walpole	1.0	0.02	+0.09	+0.06	30	30	2.2	2.5	1.1	15.7	−0.375	4.7	33.6	2.1	40
buffer		0.06	+0.09	+0.06	30	30	3.8	3.8	1.0	15.8	−0.380	8.0	33.3	2.1	40
pH ≈ 2.0		0.10	+0.09	+0.06	30	30	5.0	5.5	1.1	15.6	−0.385	11.0	34.3	2.2	45
		0.20	+0.08	+0.06	30	30	6.8	7.0	1.0	15.5	−0.400	15.5	35.2	2.2	50
		0.40	+0.09	+0.06	30	20	9.8	10.5	1.1	15.6	−0.420	21.0	33.3	2.1	50
BR buffer [b]	0.2	0.04	+0.17	+0.20	30	30	0.88	1.0	1.1	22.0	−0.470	1.72	43.0	2.0	45
pH ≈ 2.0	0.6		+0.16	+0.19	30	30	2.64	2.7	1.0	22.0	−0.480	5.0	42.0	1.9	50
	1.0		+0.16	+0.19	30	30	4.3	4.5	1.0	22.5	−0.490	8.5	43.0	2.0	50
	1.4		+0.165	+0.20	35	30	6.0	6.3	1.0	22.5	−0.510	11.5	41.0	1.9	50
BR buffer [b]	1.0	0.02	+0.16	+0.19	30	30	3.15	3.3	1.04	22.5	−0.400	6.5	46.4	2.0	45
pH ≈ 2.0		0.10	+0.16	+0.19	30	30	7.35	7.5	1.02	22.9	−0.440	15.0	46.8	2.0	50
Walpole	0.5	0.02	−0.08	−0.05	30	35	2.55	2.5	0.98	36.4	−0.460	5.55	79.5	2.1	40
buffer		0.04	−0.08	−0.06	20	35	3.55	3.4	1.0	36.0	−0.47	8.00	80.0	2.2	35
pH ≈ 4.65		0.06	−0.085	−0.06	25	40	4.38	3.8	1.1	36.4	−0.48	9.75	81.3	2.2	30
	1.0	0.08	−0.090	−0.06	30	40	7.00	6.88	0.98	25.0	−0.49	15.0	53.5	2.1	40
Walpole	0.6	0.04	−0.12	−0.09	30	40	2.5	2.4	0.96	20.8	−0.51	4.5	37.5	1.8	50
buffer [b]	1.0		−0.14	−0.110	30	45	4.0	3.75	0.90	20.0	−0.52	7.5	37.5	1.9	45
pH ≈ 6.0	1.4		−0.10	−0.17	30	40	5.85	5.5	0.90	20.8	−0.53	10.0	35.7	1.8	50
BR buffer [b]	0.2	0.04	−0.80	—	—	50	0.5	—	—	12.5	−1.2	0.75	18.8	1.5	60
pH ≈ 12.0	0.6		−0.79	—	—	50	1.3	—	—	10.8	−1.26	2.12	17.6	1.6	60
	1.0		−0.81	—	—	50	2.65	—	—	13.25	−1.23	4.24	21.2	1.6	60

[a] Units, $\mu A\ s^{1/2}\ V^{-1/2}\ mol^{-1}\ l$. [b] Electrode area was 0.02704 cm^2; 0.016% Triton X-100.

TABLE 5

Diffusion and transfer coefficients for the reduction of cacotheline in aqueous medium

Buffer	αn_a	$D\ 10^5$ cm^2 s^{-1}			
		D.c.		Cyclic voltammetry	
	Nitro	*o*-quinone	Nitro	*o*-quinone	Nitro
BR buffer pH ≈2.0	1.2	0.232	0.488	0.111	0.212
Walpole buffer pH ≈4.65	1.2	0.142	0.228	0.189	0.335

spectrum of the product. The spectrum of the product exhibited peaks at 3460 cm^{-1} (br; —OH and NH) and 815 cm^{-1} (br; —N—O), indicating hydroxylamine formation.

The result of coulometry, cyclic voltammetry and d.c. polarography confirm that six electrons are involved in the total electrode process (in the pH range 2.0—6.0). From the data available [6, 10—12], the reduction of the *o*-quinone group of cacotheline to hydroquinone corresponds to the two-electron reversible reduction (E^1_{pc}) and the second irreversible process corresponds to the reduction of the nitro group of cacotheline to hydroxylamine at more negative potentials. Based on the above results, the following mechanism may be suggested for the reduction of cacotheline (pH 2.0—6.0):

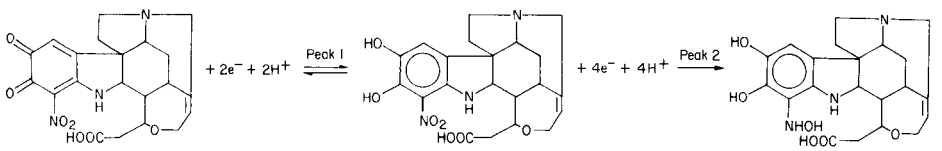

The authors thank Dr. K. I. Vasu, Director of the Central Electrochemical Research Institute Karaikudi, for providing facilities for the cyclic voltammetric and coulometric experiments.

REFERENCES

1 G. Gopala Rao, N. Krishna Murthy and V. Narayana Rao, Talanta, 12 (1965) 243.
2 See, e.g., K. Kodama, Methods of Quantitative Inorganic Analysis, Interscience-Wiley, New York, 1963.
3 G. Gopala Rao, V. Narayana Rao, G. Somidevamma and K. Lalitha, Anal. Chim. Acta, 12 (1955) 271.
4 N. Krishna Murthy, Y. Pulla Rao and V. Satyanarayana, Fresenius' Z. Anal. Chem., 272 (1974) 367.
5 N. Gallo, Ann. Chim. (Rome), 57 (1967) 54.
6 T. D. Smith, Anal. Chim. Acta, 22 (1960) 249.
7 G. Dusinsky, Cesk Farm., 10 (1961) 181.
8 H. Matsuda and Y. Ayabe, Z. Electrochem., 59 (1955) 494.
9 P. Delahay, New Instrumental Methods in Electrochemistry, Interscience, New York, 1954, p. 132.
10 N. Gallo, Gazz. Chem. Ital., 85 (1955) 1441.
11 G. Dusinsky, Acta Chem. Acad. Sci. Hung., 16 (1958) 351.
12 N. Gallo, Ann. Chim. (Rome), 55 (1965) 106.

Analytica Chimica Acta, 196 (1987) 221—227
Elsevier Science Publishers B.V., Amsterdam — Printed in The Netherlands

DETERMINATION OF LOW LEVELS OF CYANIDE WITH A SILVER/SILVER SULPHIDE WIRE ELECTRODE

VLADISLAVA M. JOVANOVIĆ*

ICTM Institute for Electrochemistry, University of Belgrade, P.O. Box 815, YU-11000 Belgrade (Yugoslavia)

MILAN SAK-BOSNAR

Pedagogical Faculty, University of Osijek, YU-54000 Osijek (Yugoslavia)

MOMIR S. JOVANOVIĆ

Department of Analytical Chemistry, Faculty of Technology and Metallurgy, University of Belgrade, P.O. Box 494, YU-11000 Belgrade (Yugoslavia)

(Received 27th August 1986)

SUMMARY

A silver/silver sulphide electrode is prepared quickly by holding a cleaned silver wire in vapours from molten sulphur. In 1000—10 mg l^{-1} cyanide solutions, the electrode exhibits a linear E/log C_{CN} function which becomes slightly sinusoidal for 10—0.1 mg l^{-1} cyanide. The average slope is slightly super-Nernstian (120 mV/decade concentration). The applicability of the electrode is demonstrated for the determinations of microgram quantities of water-soluble cyanide from the Prussian blue pigments which are constituents of externally applied cosmetics. The home-made electrode provides results agreeing with those obtained with commerically available electrodes.

The cyanide response of ion-selective electrodes is based on cyanide corrosion of the sensing phase of the electrode. As explained by Pungor and coworkers [1—3] and Veselý et al. [4], the electroactive phase creating the cyanide response can be either a silver iodide or silver iodide/silver sulphide mixture, or pure silver sulphide. In any of these cases, dicyanoargentate(I) is formed, releasing either iodide or sulphide ions from the solid phase and creating a theoretical slope of either 59 or 118 mV. Thus, the ion-selective electrode responds to the relevant primary ion, the activity of which is governed by the activity of the measured cyanide.

It is clear that the corrosion of the sensing phase shortens the lifetime of the electrode and its durability depends on the kind of silver salt applied as sensor. Thus, the silver iodide-based electrode should not be used in cyanide solutions with concentrations exceeding 10^{-2} mol l^{-1}. In fact, such electrodes, and not the silver sulphide-based ones, are usually termed "cyanide-sensitive" by manufacturers of ion-selective electrodes. Hence, it is not surprising that for the potentiometry of cyanide, some authors have investigated the applicability of membranes made of silver sulphide, which has a much lower

0003-2670/87/$03.50

solubility product than silver iodide. The most frequent requirement for the maximum cyanide concentration lies at the 0.1 mg l^{-1} or even lower level. But direct potentiometry of sub-mg l^{-1} cyanide solutions based on calibration graphs is not precise enough, because of the difficulty of preparing stable standard solutions. These aspects led Frant et al. [5] and Clusters et al. [6] to evaluate the multiple standard addition method with dicyanoargentate solutions for the determination of mg l^{-1} to μg l^{-1} cyanide levels, using the Orion 94-16A silver sulphide membrane. This procedure has been recommended as a standard method [7]. However, Penland and Fischer [8] described a single standard addition method for the determination of these cyanide levels; they added different standard potassium cyanide solutions to the unknown test solution, applying the Orion 94-06A silver iodide/silver sulphide pellet membrane. This procedure, which is much simpler than the dicyanoargentate additions, has also been accepted as a standard method [9].

The choice of method for determining trace amounts of cyanide by means of ion-selective electrodes is thus confused with regard to both procedure and electrode. Silver sulphide should have priority because it is much more resistant to cyanide corrosion and because it can easily be prepared and reconditioned. The procedure used here for the preparation of a second-kind electrode made of a silver strip coated with silver sulphide, is based on early work by Hönigschmid and Sachtleben [10]. In order to assay the atomic mass of sulphur, these authors synthesized very pure silver sulphide by keeping silver pellets in vapour from molten sulphur, all in an atmosphere of nitrogen. Other methods of preparing metal/metal sulphide wire electrodes are possible with gaseous hydrogen sulphide [11], or buffered sodium sulphide solutions [12], but the first method seemed to be the most promising.

The silver/silver sulphide wire electrodes were produced here by holding silver strips in the vapour from molten sulphur under ambient conditions. The electrodes were tested in three steps: (1) evaluation of the lowest cyanide concentration which could be titrated with silver ion; (2) determination of mg l^{-1} and μg l^{-1} concentrations of cyanide in pure solutions, by using Penland and Fischer's standard potassium cyanide addition method [8]; and (3) application of the electrode for the determination of low levels of water-soluble cyanide in iron(III) ammonium hexacyanoferrate(II), a type of Prussian blue which is used as the chief component of some cosmetic preparations. For this application, the standard extraction procedure described by Thieman et al. [13] was used; in determining the extracted cyanide, Penland and Fischer's standard addition technique [8] was preferred.

EXPERIMENTAL

Instrumentation and solutions

A MA5705 Iska (YU) model pH/mV meter and an Orion 801A "Ionalyzer" were used for potentiometric readings. Titrations were done with a Metrohm E-415 digital piston burette.

Three ion-selective electrodes were used: an Orion 94-16A and a Radiometer F1212S electrode, both of which have crystalline silver sulphide pellet membranes, and a home-made silver/silver sulphide wire electrode. The reference was a commerical saturated calomel electrode, with a salt bridge (PTFE tube) filled with potassium nitrate in agar-agar gel.

In order to avoid adsorption of cyanide on the walls of glass vessels, PTFE beakers were used throughout.

Solutions

Potassium cyanide solutions were prepared in the range from 1000 mg l^{-1} CN^- (3.8×10^{-2} mol l^{-1}) down to 10 μg l^{-1} CN^- (3.8×10^{-7} mol l^{-1}). To ensure that all the cyanide was present as free CN^-, and to maintain uniform ionic strength, solid potassium cyanide for the 1000 mg l^{-1} solution was dissolved in 0.05 mol l^{-1} sodium hydroxide, the pH being ca. 11.3. All the other cyanide solutions were made by successive ten-fold dilutions with the same hydroxide solution. Solutions with concentrations $\leqslant$100 mg l^{-1} were prepared daily. The stock solution was standardized against 0.00192 mol l^{-1} silver nitrate. To reduce adsorption of the cyanide on the glass walls, the volumetric flasks were usually pre-rinsed with the cyanide solution to be diluted.

Preparation of the silver/silver sulphide wire ion-selective electrode

Silver strips ($\geqslant$99.9% pure; ca. 0.3 mm thick, 2—3 mm wide and ca. 12 cm long) were first placed in a very low Bunsen flame until they became just red-hot; the silver must not melt. This pre-treatment provides a tiny-grain structure of the metal surface. The metal was then polished with a filter paper. Simultaneously, a few grams of pure, sublimed sulphur were melted (without the appearance of a flame) in a porcelain crucible. Immediately after all the sulphur had melted, the prepared silver strip was held in the yellow vapour (125—130°C) until there was no further change in the colour of the sulphide layer (1—2 min). The fine porosity of the silver and its slow conversion to sulphide are essential in obtaining a durable film of silver sulphide. Finally, the sulphide layer, which is black in appearance, was rubbed with filter paper in order to produce a shiny surface.

A silver sulphide film obtained in this way can resist continuous corrosion from 1000 mg l^{-1} cyanide solution for at least 24 h.

In order to achieve reproducible results, the silver/silver sulphide electrode must always be immersed to the same depth in the test solution (1 or 2 cm from the tip).

After prolonged usage, especially in concentrated cyanide solutions, the sulphide layer will be partially removed; damage can be seen as bright spots of metallic silver. In order to revive the same electrode, it can be heated part by part in a very low Bunsen flame until the black layer becomes red-hot and disappears completely. After the strip has been rubbed with filter paper, it can be recoated as described above.

Calibration graphs

Because cyanide solutions below 100 mg l^{-1} are unstable, so that daily preparation of diluted solutions was necessary, daily recalibration of the electrode was also necessary. The most negative potential values were recorded when they remained unchanged for at least 30 s.

It appeared that both the silver sulphide pellet membranes and the homemade silver/silver sulphide wire electrodes underwent a parallel potential drift each time readings were made. This phenomenon was more pronounced with the wire electrode; with the pellet membranes, only the Orion electrode exhibited linearity of the $E/\log C_{CN}$ function in the region from 1000 down to 0.1 mg l^{-1} throughout (cf. Fig. 1).

Preliminary investigations on cyanide recovery from pure solutions

As Thieman et al. [13] reported, soluble cyanide in an aqueous extract from iron(III) ammonium hexacyanoferrate(II) pigments is expected to be at the mg l^{-1} level. With the given extraction procedure, the filtrate contained a few micrograms of cyanide, and could be ca. 4 μmol l^{-1} (i.e., 0.1 mg l^{-1}) in cyanide or even less. Such low levels, almost at the detection limit of a cyanide-sensitive electrode, make the usual calibration method for the determination difficult to apply, despite the fact that it has been recommended.

Titrimetry. It is almost impossible to titrate <1 mg l^{-1} cyanide with 0.00192 mol l^{-1} silver ion; 1 ml of this titrant corresponds to 0.1 mg of cyanide, and 0.1 mg of cyanide in >100 ml of solution provided a very poor potential jump at the end-point. When 0.1 mmol l^{-1} cyanide was titrated with 0.00192 mol l^{-1} silver ion, any of the applied silver sulphide electrodes produced potential jumps of about 100 mV. For example, whether the Orion 94-16A or the Ag/Ag_2S wire was used in the titration of 100 μg of cyanide, the mean result of 5 titrations was 95 μg with a standard deviation of 0.25 μg.

Standard cyanide addition method. The titrimetric procedure was unsuitable for estimating soluble cyanide in the hexacyanoferrate(II) pigments. The standard addition method was therefore tested on pure solutions at the expected level. For this purpose, different volumes of 10 mg l^{-1} cyanide solution were diluted with 0.05 mol l^{-1} sodium hydroxide to 50 ml. Flasks and pipettes were pre-rinsed with 5 ml of the same cyanide solution. Each solution was transferred to a PTFE beaker, and the flask was rinsed with 5.00 ml of the same sodium hydroxide solution. The indicating couple was immersed into the test solution and the potential was recorded when it was constant for 1 min. Then 0.2—0.5 ml of the standard 100 mg l^{-1} potassium cyanide solution was pipetted into the beaker and the new potential was recorded. This allowed the cyanide concentration to be estimated so that the matching slope of this part of the daily calibration graph could be used in the computation procedure [8, 9]. Results obtained by this procedure are given in Table 1.

TABLE 1

Cyanide recovery test by the standard addition method

Cyanide taken (μg)	300	200	100	50.0	30.0	10.0	5.0
No. of tests	3	3	5	10	10	10	10
Recovery (%)[a]							
Orion 94-16A/SCE	99.7	97.5	107.0	101.2	101.0	110.3	108.0
	(0.2)	(0.2)	(0.4)	(0.9)	(4.5)	(9.9)	(10.2)
$Ag/Ag_2S/SCE$	101.0	103.0	108.0	106.8	103.0	120.0	108.0
	(0.3)	(0.4)	(0.4)	(1.0)	(5.5)	(10.3)	(10.7)

[a]The standard deviation from the mean is given in parentheses.

Procedure for soluble cyanide in the hexacyanoferrate(II) cosmetic preparation

The extraction step [13] was slightly modified. The soluble cyanide was extracted with ca. 20 ml of distilled water by stirring magnetically in a PTFE beaker for at least 30 min. The filtrate was collected in a 50-ml volumetric flask (pre-rinsed with 0.1 mg l^{-1} cyanide solution). Before final dilution, ca. 100 mg of sodium hydroxide was added to adjust the pH and ionic strength. This solution was transferred to a PTFE beaker, and the subsequent procedure was as described above for the standard addition method. The results obtained are shown in Table 2.

In order to check the procedure, extra cyanide was added after the filtration of the extract. This produced an acceptable cyanide recovery after subtraction of the amount added (Table 2).

RESULTS AND DISCUSSION

Figure 1 clearly shows that the differences in behaviour of cyanide-sensitive electrodes depend strongly on the manner of their production even if they are of similar morphology. Thus, the commercial electrodes, both of silver sulphide pellet membrane construction, exhibited a sub-Nernstian cyanide response and differed in the (non)linearity of their $E/\log C_{CN}$ functions. In contrast, the home-made silver/silver sulphide wire electrode, exhibited a super-Nernstian response at low concentrations before fading at 0.01 mg l^{-1} levels (Fig. 1). A probable explanation of these deviations from theoretical linearity was indicated by Veselý et al. [4] who proved that there is a sinusoidal dependence of potential on cyanide concentration and ascribed this to the different cyanoargentate complexes formed during the corrosion processes of the sensing phase.

From the analytical point of view, it is clear that the dilution technique for standards in the micromolar region is not absolutely reliable. The instability of such solutions and the tendency of cyanide to adsorb on glass create obvious problems. Calibration of the electrode to establish the $E/\log C_{CN}$

TABLE 2

Results for cyanide in the hexacyanoferrate(II) cosmetic preparation

Cell	Cyanide level found (mg kg^{-1})			s^a
	Lowest	Highest	Mean	
$Ag/Ag_2S/SCE$	1.9	3.1	2.41	0.1142(10)
$Ag/Ag_2S/SCE^b$	2.0	2.1	2.07	0.0334(3)
Orion 94-16A/SCE	2.1	2.5	2.34	0.1212(3)

[a]Standard deviation from the mean with number of tests in parentheses. [b]Results obtained after addition of 3μg of cyanide to the filtrate.

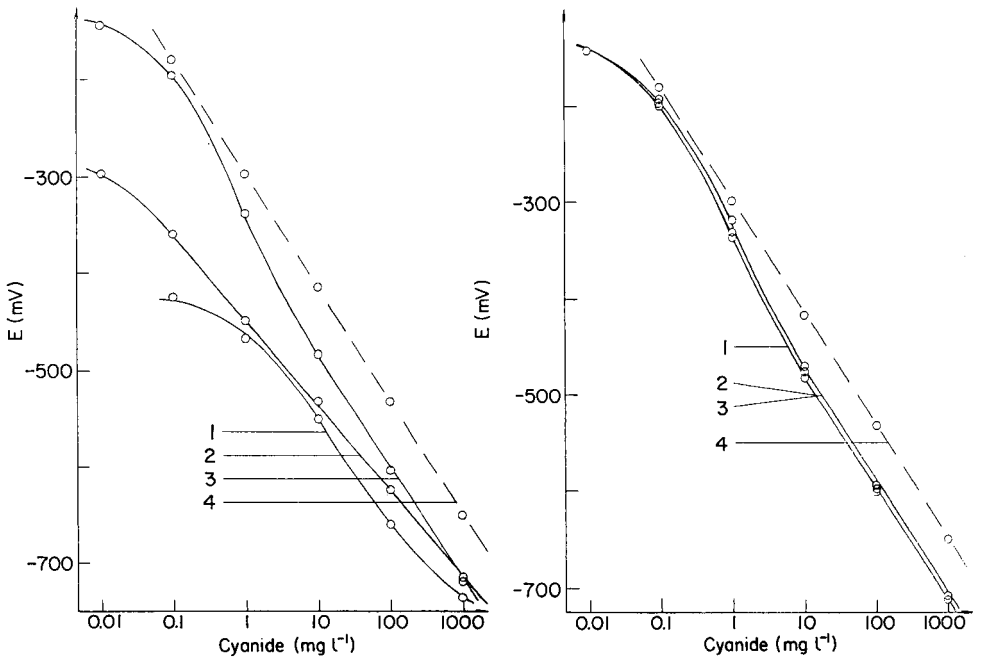

Fig. 1. Calibration graphs of different ion-selective electrodes in cyanide solutions: (1) Radiometer F1212S; (2) Orion 94-16A; (3) home-made Ag/Ag_2S; (4) theoretical 118 mV slope.

Fig. 2. Calibration graphs of the home-made Ag/Ag_2S electrode after exposure to cyanide corrosion: (1) freshly prepared electrode; (2) after 24 h exposure to 1000 mg l^{-1} cyanide; (3) next day, after conditioning in air; (4) theoretical 118 mV slope.

slope is essential for computation of the results by the standard addition method [8, 9]. Though the silver/silver sulphide wire electrode showed a very high resistance to cyanide corrosion, as shown by the calibration graphs in Fig. 2, daily recalibration was necessary because of the preparation of fresh solutions. But in all the tests conducted the simple silver/silver sulphide wire electrode proved to be as suitable as the commercial pellet membranes.

Recovery tests from pure cyanide solutions were made either by adding silver nitrate (titrimetric procedure), or by adding potassium cyanide (standard addition method). Obviously, there was a silver response of the silver sulphide sensing phase in the former case, and at the 10^{-5} mol l^{-1} cyanide level the end-point potential jump was barely recognizable. With the standard addition methods [5, 6, 8], only the cyanide response need be considered; though the reliability of the standard addition method may be less satisfactory for 100 μg of cyanide, this technique provides the only possibility of estimating $\leqslant$0.1 mg l^{-1} cyanide.

For the determination of cyanide in the cosmetic preparation (Table 2), the home-made and commercial silver sulphide electrodes provided similar results. Addition of 3.00 ml of 1 mg l^{-1} cyanide solution to the filtrate from the original cyanide extract confirmed the reliability of the results; the differences correspond to only 0.3 μg of cyanide.

It can be concluded that the proposed silver/silver sulphide wire electrode, which is simple to prepare and renew and which is resistant to cyanide corrosion, is useful for the direct potentiometry of very low concentrations of cyanide.

REFERENCES

1 B. György, L. Andrés, L. Stehli and E. Pungor, Anal. Chim. Acta, 46 (1969) 318.
2 K. Toth and E. Pungor, Anal. Chim. Acta, 51 (1970) 221.
3 E. Pungor, M. Gratzl, L. Pősos, K. Toth, M. F. Ebel, H. Ebel, G. Zuba and J. Wernisch, Anal. Chim. Acta, 156 (1984) 9.
4 J. Veselý, O. J. Jensen and B. Nicolaisen, Anal. Chim. Acta, 62 (1972) 1.
5 M. S. Frant, J. W. Ross Jr. and H. Riseman, Anal. Chem., 44 (1972) 2227.
6 H. Clusters, F. Adams and F. Verbeek, Anal. Chim. Acta, 83 (1976) 27.
7 D. Midgley and K. Torrance, Potentiometric Water Analyses, Wiley, New York, 1979, p. 306.
8 J. L. Penland and G. Fischer, Metalloberfläche, 26 (1972) 391.
9 Standard Methods for the Examination of Water and Wastewater, 14th edn., American Public Health Association, Washington, 1976, p. 372.
10 O. Hönigschmid and R. Sachtleben, Z. Anorg. Allg. Chem., 195 (1931) 207.
11 A. V. Vishnyakov, A. F. Zhukov, T. A. Lyubchak, Yu. I. Ursov and A. V. Gordievskii, Zh. Anal. Khim., 32 (1977) 840.
12 Nj. Radić, K. J. Mulligan and H. B. Mark Jr., Anal. Chem., 56 (1984) 298.
13 H. W. Thieman, H. W. Ziegler and W. H. Oakes, Drug Cosmet. Ind., 125 (1979) 78.

Analytica Chimica Acta, 196 (1987) 229—235
Elsevier Science Publishers B.V., Amsterdam — Printed in The Netherlands

ELECTROGENERATED IODINE AS A REAGENT FOR COULOMETRIC TITRATIONS IN ALCOHOLIC MEDIA

T. J. PASTOR* and V. V. ANTONIJEVIĆ

Department of Chemistry, Faculty of Sciences, University of Belgrade, 11001 Belgrade (Yugoslavia)

(Received 5th August 1986)

SUMMARY

Conditions are established for the generation of iodine with high current efficiency (>99%) in solutions of potassium acetate in methanol or ethanol, in the presence of potassium iodide or tetraethylammonium iodide at platinum or glassy carbon working electrodes, respectively. Iodine solutions in methanol are stable, but solutions in ethanol are less so. Procedures are given for coulometric titration of various thiols with anodically generated iodine in these solvents; biamperometric or potentiometric end-point detection can be used. The error of the titrations did not exceed ±2.0% for ca. 1-mg samples.

Halogens and their compounds have found wide application in volumetric and coulometric analysis in aqueous media [1—4]. They are, however, less often used in non-aqueous solvents which are important for the determination of water-insoluble organic compounds based on oxidation/reduction reactions and halogenation [2, 4—6]. In non-aqueous media, the iodine/iodide system has so far been most extensively investigated [7—10], whereas for analytical purposes iodine is most often preferred for three reasons: (a) it dissolves readily in numerous organic and mixed solvents, (b) the iodine/iodide redox couple is reversible in almost all solvents, which is very important for the choice of end-point detection, and (c) iodine [5, 6, 10—12], iodine(I) [12—15] and iodine halides [14] can be generated by anodic oxidation of iodide with high current efficiency. Electrogeneration of iodine has been done in solutions which, in addition to supporting electrolyte, contain alkali iodides [2—11], tetraethylammonium iodide [12, 13], or methyl iodide [15]. Coulometric iodimetric determinations are most often done in methanol, especially in determining water by the Karl Fischer method [5, 6], whereas absolute ethanol and ethanol containing various amounts of water are rarely applied [6].

In the present paper, the effect of the analyte composition and the material of the working electrode on the current efficiency in anodic generation of iodine in methanol and ethanol is investigated. The possibilities of biamperometric and potentiometric methods of end-point detection in coulometric iodimetric titrations are also studied.

0003-2670/87/$03.50

EXPERIMENTAL

Apparatus and chemicals

The apparatus for the generation of iodine and for the coulometric titration with biamperometric end-point detection has been described [16]. The anode of the generating circuit was a platinum spiral with a surface area of 2.0 cm^2, or a cylindrical glassy carbon electrode (GC20; Tokay Electrode). A glassy carbon rod was sealed into a glass tube, insulated by bitumen. Its active surface was 2.1 cm^2 (diameter 0.5 cm, length 1.2 cm). The indicator electrodes in the biamperometric and bipotentiometric (controlled-current potentiometric titration with two indicator electrodes) methods were platinum wires of 0.2 cm^2 surface area. They were polarized with a potential difference from 150 to 500 mV and current from 0.5 to 19 μA, respectively. The end-point in zero-current potentiometry was detected with platinum gauze and saturated calomel electrodes connected to a Radiometer PHM 26 mV-meter.

Absorption curves of solutions were recorded on a Varian Superscan-3 spectrophotometer.

All chemicals used were of analytical-reagent grade. Water was removed from them as described previously [10].

As catholyte, 0.5—1.5 M solutions of potassium acetate in methanol or ethanol were used. The anolyte was prepared by dissolving measured amounts (0.01—0.2 mol) of potassium iodide or tetraethylammonium iodide in 1 l of the chosen supporting electrolyte.

Standard 0.01—0.001 M solutions of test compounds were prepared as previously described [10].

Procedures

The following coulometric procedures [16, 17] were applied.

Method I. A suitable volume of the test solution was measured into the anode compartment prior to the titration, and iodine was generated continuously. The end-point was detected biamperometrically.

Method II. The sample solution was added to the anolyte prior to the titration and the reagent was generated discontinuously, in small amounts near the end-point. The end-point was detected biamperometrically or potentiometrically.

Method III. A known amount of the investigated solution was added to the anolyte after 90—95% of the theoretically required amount of iodine had been generated, and the titration was completed with continuous or discontinuous generation of the reagent.

RESULTS AND DISCUSSION

Conditions for the electrochemical generation of iodine with high current efficiency at platinum electrode in methanolic solutions of potassium acetate

containing potassium iodide, have been reported [10]. In the present work, titrations of the anolyte with standard solutions of 2-mercaptoethanol or 1-heptanethiol after the passage of a definite quantity of electricity, and coulometric titrations conducted as in Method III, showed that potassium iodide in the anolyte can be successfully replaced with tetraethylammonium iodide. High current efficiency in the generation of iodine was also achieved at glassy carbon working electrode (>99%) with currents of 2.00—3.00 mA.

The stability of iodine solutions in the supporting electrolytes used was followed by the biamperometric method. Iodine solutions in the anolyte prepared in methanol were stable for a longer time than those prepared in ethanol (Fig. 1); therefore, ethanol solutions were studied by methods I and II.

The absorption spectra of supporting electrolytes and anolytes, recorded before and after passage of the current, showed that the replacement of potassium iodide by tetraethylammonium iodide does not affect the form in which iodine occurs in the solution (Fig. 2). By comparing the recorded absorption spectra with each other and with spectra of iodine and iodide solutions in the aforementioned solvents [18—22], it was confirmed that iodine in the anolyte used occurs in the form of triiodide ions.

Coulometric titrations

Current efficiency in the electrogeneration of reagents can be evaluated from the results of coulometric determinations of suitable substances. Here, thiols were titrated; in methanolic solutions of potassium acetate, thiols are

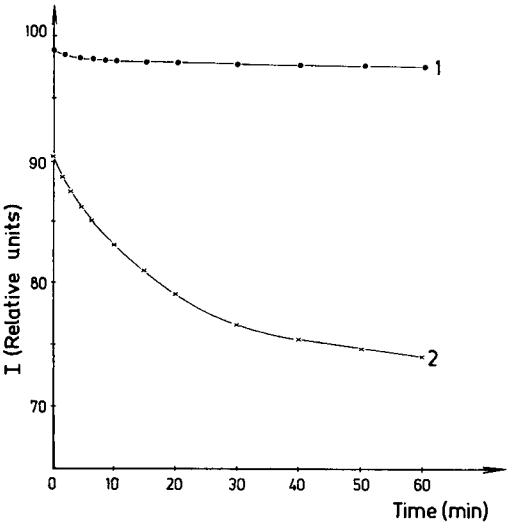

Fig. 1. Changes of iodine concentration with time in different solutions: (1) 1 M potassium acetate/0.1 M potassium iodide in methanol; (2) 1 M potassium acetate/0.05 M potassium iodide in ethanol.

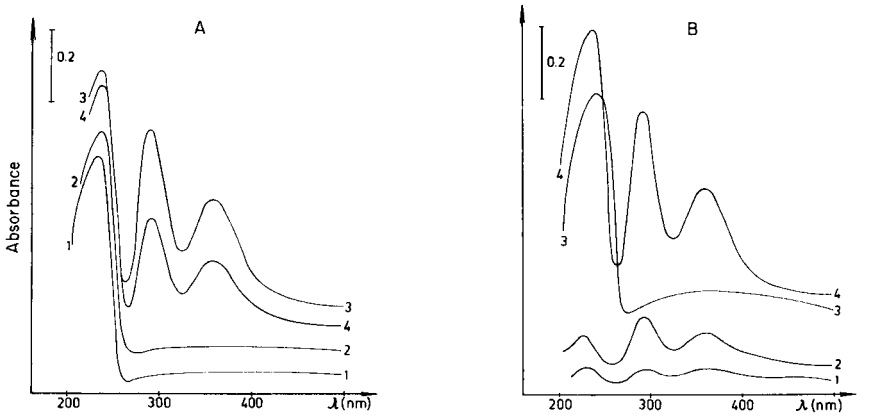

Fig. 2. Absorption spectra of various iodide solutions. In A: (1) 0.1 M potassium iodide in methanol; (2) 1 M potassium acetate/0.1 M potassium iodide in methanol; (3) 1 M potassium acetate/0.1 M potassium iodide/0.0001 M iodine in methanol; (4) 1 M potassium acetate/0.1 M potassium iodide in methanol after a definite amount of electricity had been passed. In B: (1) 0.0001 M potassium iodide in methanol, freshly prepared; (2) 0.0001 M potassium iodide in methanol, prepared 24 h prior to recording; (3) 1 M potassium acetate/0.1 M tetraethylammonium iodide in methanol; (4) 1 M potassium acetate/0.1 M tetraethylammonium iodide in methanol after a definite amount of electricity had been passed.

rapidly and quantitatively oxidized to the corresponding disulfides [10]. First, the earlier investigations were repeated by generating iodine at the platinum electrode from potassium iodide with 1.00—5.00 mA in the generating circuit and with biamperometric end-point detection. Then, under these working conditions, good results were also obtained by using the glassy carbon working electrode and generating iodine from tetraethylammonium iodide (Table 1). Methods I and II were successfully used to quantify 2-mercaptoethanol, 1-heptanethiol, 2-mercaptobenzoic acid and thioglycollic acid in solutions of potassium acetate in ethanol (Table 1). In the titration of 4-methylbenzenethiol in ethanol by method I, the results were lower than the theoretical ones, whereas in the titration of the same compound by method III, the results were about 10% higher. These findings can be explained by a slightly slower reaction of iodine with this thiol and by reaction of the reagent with the solvent.

The bipotentiometric method is usually suitable for end-point detection in non-aqueous media, thus the above coulometric titrations were examined again with this mode of end-point detection. To establish the best conditions, titration curves were recorded at various currents for the polarization of the indicator electrodes (0.5—19.0 μA). The results showed that decreasing the polarization current increased the magnitude of the potential jump at the end-point. However, with very small polarization currents, stable values of the potential differences near the end-point were achieved only slowly, after more iodine had been generated. The optimum polarization currents depend

TABLE 1

Coulometric titration of reducing substances in 1 M potassium acetate with electrogenerated iodine

Substance	Taken (mg)	No. of titns.	WE[a]	I (mA)	Method	End-point	Electrode polarization	Anolyte[b]	Recovery[c] (%)
2-Mercapto-ethanol	0.961	6	Pt	3.00	I	Biamp.	250 mV	0.1 M KI (M)	98.9 ± 0.4
	0.994	9	Pt	3.00	II	Bipot.	2.5 μA	0.1 M KI (M)	99.4 ± 0.9
	0.468	6	Pt	2.00	II	Bipot.	1.5 μA	0.1 M KI (M)	98.7 ± 0.5
	0.187	6	Pt	1.00	II	Bipot.	0.6 μA	0.1 M KI (M)	99.1 ± 0.7
	0.996	6	Pt	3.00	I	Biamp.	250 mV	0.05 M KI (E)	98.2 ± 0.3
	0.854	6	Pt	3.00	II	Bipot.	2.5 μA	0.05 M KI (E)	99.7 ± 0.4
	0.970	4	Pt	3.00	II	Pot.		0.05 M KI (M)	98.0 ± 0.1
	0.764	6	GC	3.00	I	Biamp.	250 mV	0.05 M KI (M)	99.9 ± 0.5
	0.764	6	GC	3.00	III	Biamp.	250 mV	0.05 M KI (M)	100.2 ± 0.4
	0.936	6	Pt	3.00	I	Biamp.	250 mV	0.1 M $(C_2H_5)_4NI$ (M)	100.5 ± 0.7
1-Heptane-thiol	1.345	6	Pt	3.00	I	Biamp.	250 mV	0.1 M KI (M)	99.4 ± 0.2
	1.316	6	Pt	3.00	II	Bipot.	1.9 μA	0.1 M KI (M)	98.8 ± 0.4
	0.727	6	Pt	3.00	II	Bipot.	1.9 μA	0.1 M KI (M)	99.6 ± 0.6
	0.482	6	Pt	2.00	II	Bipot.	1.5 μA	0.1 M KI (M)	100.2 ± 0.6
	1.337	6	Pt	3.00	I	Biamp.	250 mV	0.05 M KI (E)	100.6 ± 0.2
	1.221	7	Pt	3.00	II	Bipot.	1.0 μA	0.05 M KI (E)	101.4 ± 0.3
	1.187	5	GC	3.00	I	Biamp.	250 mV	0.1 M KI (M)	101.3 ± 0.5
	1.144	4	Pt	3.00	II	Pot.		0.1 M KI (M)	100.4 ± 0.3
4-Methyl-benzenethiol	1.118	6	Pt	3.00	II	Biamp.	250 mV	0.1 M KI (M)	98.7 ± 0.6
	1.008	6	Pt	3.00	II	Bipot.	1.5 μA	0.1 M KI (M)	98.7 ± 0.6
Thioglycollic acid	0.948	6	Pt	3.00	II	Bipot.	1.5 μA	0.1 M KI (M)	100.0 ± 0.5
2-Mercaptobenzoic acid	1.542	6	Pt	3.00	I	Biamp.	250 mV	0.1 M KI (M)	98.9 ± 0.8
	1.542	6	Pt	3.00	I	Biamp.	250 mV	0.05 M KI (E)	101.3 ± 0.5

[a]Working electrode. [b](M) Methanol; (E) Ethanol. [c]Mean and standard deviation.

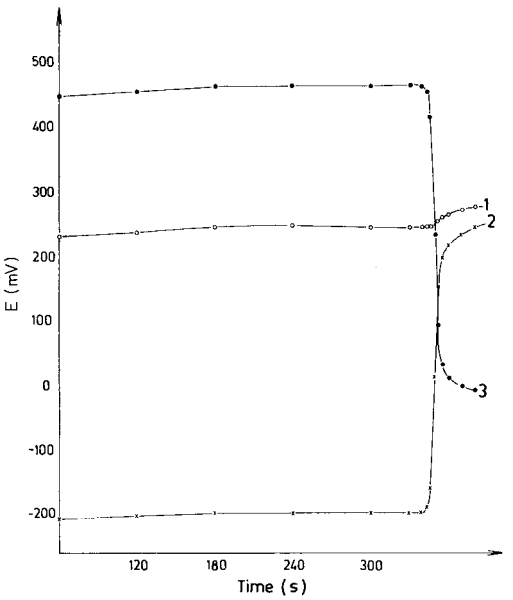

Fig. 3. Potential changes during the coulometric titration of 2-mercaptoethanol with electrogenerated iodine in 1 M potassium acetate/0.1 M potassium iodide solution in methanol: (1) positive polarized indicator electrode; (2) negative polarized indicator electrode; (3) the difference. Electrodes were polarized with 1.8 μA.

on the nature and concentration of the substance being titrated. The bipotentiometric method gave titration curves of bi-logarithmic form, as when working with one polarized electrode, i.e., with zero-current potentiometry. In order to explain these findings, the potential changes of anodically and cathodically polarized platinum electrodes were monitored during the titration versus a saturated calomel electrode. The curves thus obtained (Fig. 3) show that the potential of the anodically polarized electrode changes only negligibly during the titration, whereas the potential change of the cathodically polarized indicator electrode near the end-point is pronounced. Investigations with various concentrations of iodide in the solution (0.01—0.2 M) indicated that the potential change of the anodically polarized electrode near the end-point is inversely proportional to the concentration of iodide in the solution. Under suitable working conditions, the sensitivity of the bipotentiometric end-point detection is higher than that of zero-current potentiometry.

The authors acknowledge the financial support of the Research Fund of SR of Serbia.

REFERENCES

1 I. M. Kolthoff, R. Belcher, W. A. Stenger and G. Matsuyama, Volumetric Analysis, Vol. 3, Interscience, New York, 1957.
2 A. Berka, J. Vulterin and J. Zýka, Newer Redox Titrants, Pergamon, Oxford, 1965.
3 A. P. Zozulya, Kulonometricheskii analiz, Khimiya, Leningrad, 1968.
4 E. Bishop, in C. L. Wilson and D. W. Wilson (Eds.), Wilson and Wilson's Comprehensive Analytical Chemistry, Vol. 2D, Elsevier, Amsterdam, 1975.
5 T. J. Pastor, Glas. Hem. Drus. Beograd, 47 (1982) 153.
6 J. Barek and A. Berka, Crit. Rev. Anal. Chem., 15 (1984) 163.
7 R. T. Iwamoto, Anal. Chem., 31 (1959) 955.
8 I. W. Nelson and R. T. Iwamoto, J. Electroanal. Chem., 7 (1964) 218.
9 V. A. Macagno, M. C. Giordano and A. J. Aravia, Electrochim. Acta, 14 (1969) 335.
10 T. J. Pastor, V. J. Vajgand and V. V. Antonijević, Mikrochim. Acta, Part III, (1983) 203.
11 R. A. Aziz, P. K. Agasyan and S. I. Petrov. Zavod. Lab., 41 (1975) 641.
12 A. I. Kostromin, G. Z. Badretdinova and I. F. Abdullin, Zh. Anal. Khim., 38 (1983) 872.
13 A. I. Kostromin, G. Z. Badretdinova, I. F. Abdullin and A. R. Garifzyanov, Zh. Anal. Khim., 39 (1984) 1263.
14 A. I. Kostromin, G. Z. Badretdinova, I. F. Abdullin, K. G. Rzaev and Ya. D. Samuilov, Zh. Anal. Khim., 40 (1985) 346.
15 A. I. Kostromin, A. S. Vagizova, I. F. Abdullin and G. Z. Badretdinova, Zh. Anal. Khim., 40 (1985) 1499.
16 T. J. Pastor, V. J. Vajgand and Z. Kićović, Mikrochim. Acta, Part II, (1976) 525.
17 T. J. Pastor, V. J. Vajgand and V. V. Antonijević, Mikrochim. Acta, Part II, (1978) 131.
18 W. R. Brode, J. Am. Chem. Soc., 48 (1926) 1877.
19 J. J. Custer and S. Natelson, Anal. Chem., 21 (1949) 1005.
20 A. D. Awtrey and R. E. Connik, J. Am. Chem. Soc., 73 (1951) 1842.
21 Supplement to Mellor's Comprehensive Treatise on Inorganic and Theoretical Chemistry, Supplement II, Part I, Longmans, London, 1956, p. 923.
22 A. K. Babko and A. T. Pilipenko, Fotometricheskii analiz, Metody opredeleniya nemetallov, Khimiya, Moskva, 1974, p. 335.

Analytica Chimica Acta, 196 (1987) 237—245
Elsevier Science Publishers B.V., Amsterdam — Printed in The Netherlands

EVALUATION OF THE FUNDAMENTAL SAMPLING ERROR IN THE SAMPLING OF PARTICULATE SOLIDS

PENTTI MINKKINEN

Lappeenranta University of Technology, P.O. Box 20, SF-53851 Lappeenranta (Finland)

(Received 28th July 1986)

SUMMARY

Chemical analysis is a multi-stage process, which starts with primary sampling and ends with evaluation of the results. Especially in trace analysis and microanalysis of solid materials, sampling can far outweigh all other sources of error. For estimating the reliability of complete analytical procedures, a method is needed which can be used to estimate the errors made in the primary and the secondary sampling and sample preparation steps. Based on Gy's theory of sampling, a computer program (SAMPEX) was written for the solution of practical sampling problems. The method involves the estimation of the sampling constant, C. For well-characterized materials, C can be estimated from the material properties. If the necessary material properties are difficult to estimate, C can be evaluated experimentally. The program can be used to solve the following problems: minimum sample size for a tolerated relative standard deviation of the fundamental sampling error; relative standard deviation for a given sample size; maximum particle size of the material for a specified standard deviation and sample size; balanced design of a multi-stage sampling and sample-reduction process; and sampling for particle size determination.

Sampling is a necessary preliminary step practically in all analytical procedures. The complete analytical procedure (see Fig. 1) may have several error-generating sampling steps, and because variances, not standard deviations, are additive, the least reliable step will in practice determine the overall reliability of the whole process. Especially in trace analysis and microanalysis, the sampling operations can far outweigh all other sources of error. An error in sampling cannot be compensated later, even if the most sophisticated methods and instruments are used for the actual analysis.

The following example will clarify this: the relative standard deviation of the sampling for a determination is assumed to be 15%, and two different methods can be selected, a quick easy method with a relative standard deviation of 5% and a more tedious but precise method with a relative standard deviation of 1%. If the quick method is used, the relative standard deviation of the complete procedure is 15.8%, whereas it is 15.03% if the more precise method is used. The marginal improvement of the overall precision has then to be weighted against the increased costs when the choice between these two methods is made. It is also clear that the overall reliability of the determination can be improved only by improving the sampling procedure. A

0003-2670/87/$03.50

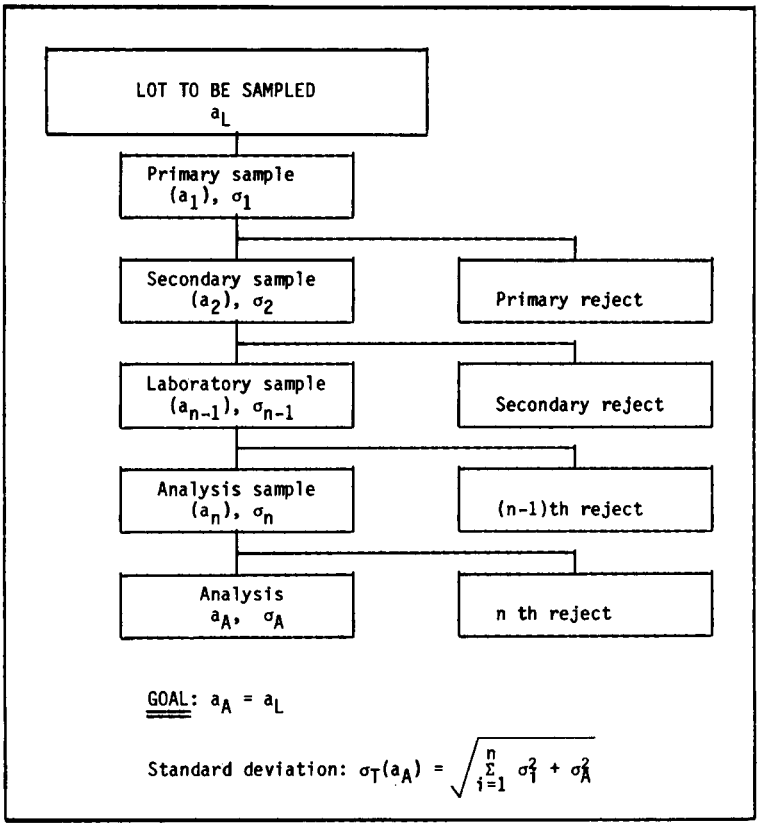

Fig. 1. The overall standard deviation, $\sigma_T(a_A)$, of the concentration estimate, a_A, is the sum of the variances of all independent operations needed to produce the final result.

practical tool, which could be used to estimate the errors of sampling procedures, would be of great value to analysts and designers of sampling procedures. The computer program SAMPEX, which is described below, can be used to help select and design optimal procedures for a given analytical determination, and to identify the weak points of existing procedures.

THEORY OF THE SAMPLING ERROR

The most complete theory of sampling, both from the theoretical and the practical point of view, was developed by Gy [1]. There are few other relevant references concerning sampling [2–7]. Although the examples considered by Gy are mainly related to the sampling of geological materials, the methods that he developed are universally applicable. Gy's method was adopted, therefore, to develop a computer program, which could help to solve sampling problems. The theory of the method is briefly outlined below.

Sources of sampling error

When a lot composed of discrete particles is sampled, three main sources of error can be identified: (1) constitutional heterogeneity, which is an intrinsic property of the material arising from its particulate nature; (2) distributional heterogeneity, caused by uneven spatial distribution of the different particle types in the lot; and (3) errors caused by incorrect sampling techniques. The errors associated with these sources are called, respectively, the fundamental error, the grouping and segregation error of the material, and the increment delimitation and extraction error. The two latter types of errors can, at least theoretically, be avoided by using correct sampling equipment and adequate sampling technique. The fundamental sampling error is avoided only if the material to be sampled is perfectly homogeneous, or the whole lot is taken as the sample, which are conditions never met in practice. The fundamental sampling error is thus the theoretical minimum error achievable in a particular sampling situation. Its estimation is of basic importance, therefore, when the adequacy of any sampling scheme is evaluated.

Estimation of the fundamental sampling error

The standard deviation of the fundamental sampling error for particulate materials can be estimated theoretically from some basic properties of the material to be sampled. Gy [1] derived the following equation to estimate it:

$$\sigma_r^2 = Z/(1/M_S - 1/M_L) \tag{1a}$$

$$= C\,d^3/(1/M_S - 1/M_L) \tag{1b}$$

where σ_r is the relative standard deviation of the fundamental sampling error, M_S the mass of the sample, M_L the mass of the lot to be sampled, and d the dimension of the largest pieces in the lot to be sampled. From experience, it was established [1] that the simplest equations could be derived when d was defined as the opening of a square mesh retaining about 5% of the total weight of the material to be sampled. C and Z are sampling constants defined later. If a is the average concentration of the substance considered in the lot and σ is the absolute standard deviation of its concentration measured in samples, then $\sigma_r = \sigma/a$. In analytical practice, σ_r is usually given in percent and then often referred to as the relative standard deviation.

Because the size of the lot to be sampled is usually very much larger than the size of the sample taken from it, Eqn. 1 simplifies further to

$$\sigma_r^2 = Z/M_S \tag{2a}$$

$$= C\,d^3/M_S \tag{2b}$$

Equations 1(a) and 2(a) express the dependence of the sampling variance on sample size, regardless of the material type, provided that the measured quantity can be regarded as randomly distributed at the used sample size.

Sampling constants C *and* Z

The sampling constant C for the particular material to be sampled is composed of four parameters, which are characteristics of the material, f, g, l and c: $C = f\ g\ l\ c$. All are dimensionless, except c, which has the dimension of density; hence C also has a dimension of density. The parameters of C can usually be estimated with an accuracy sufficient for all practical purposes.

Particle shape factor f. The shape factor f can be defined as the coefficient of cubicity (see Fig. 2). It is the ratio of the volume of a particle passing a certain sieve to the volume of a cube passing the same sieve. For a particular material, it can be regarded as constant irrespective of the size class: for a cube $f = 1$, and for a sphere $f = 0.524$. Practical experiments have shown that for most materials the average value $f = 0.5$ is a good approximation. Notable exceptions are flaky particles such as alluvial gold ores wherein $f = 0.2$, or mica with $f = 0.1$.

Size range factor g. The size range factor g can be calculated from the particle size analysis of the material. Gy [1] has shown that crushing and pulverizing operations with no size classification produces a material for which g is very near its average value of 0.25. If the size range is defined as the ratio, d/d', of the upper size limit, d, (about 5% oversize) to the lower size limit, d' (about 5% undersize), then the value of g can be estimated from Table 1.

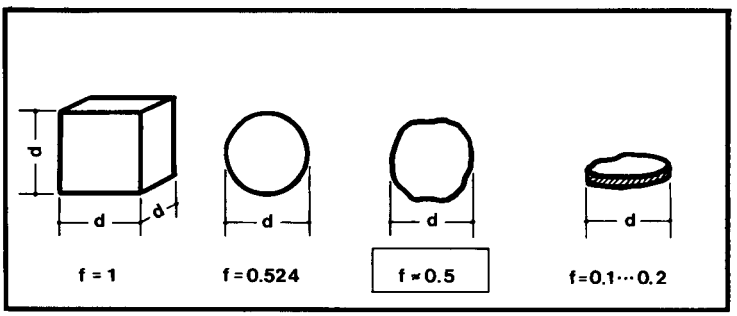

Fig. 2. To estimate the particle shape factor, f, the volume of a particle with the critical dimension, d, is compared with a cube having the same side length.

TABLE 1

Estimation of the particle size distribution factor g. d is the upper size limit and d' the lower size limit. In sieving, these correspond to the opening of sieves which retain 5% and 95% of the material tested.

Size range	d/d'	g
Large	>4	0.25
Medium	4 . . . 2	0.50
Small	2 . . . 1	0.75
Uniform	1	1.00

Liberation factor l. The maximum value is $l = 1$ for all materials in which the particles of the critical component (i.e., the mineral or compound containing the constituent to be determined) can be completely liberated. If the critical component is present as inclusions in the matrix material or gangue (Fig. 3A), then the liberation factor can be estimated from the following empirical relationship, where L is the practical liberation size of the critical particle: $l = (L/d)^{1/2}$ when $d > L$. After particle size reduction, if $d \leqslant L$, then $l = 1$ in all cases. Whenever the critical particles are completely liberated in the sampled material, $l = 1$ (Fig. 3B). In this case, d is not the upper size limit of all particles, but the upper size limit of the critical particles, and $d = L$.

Composition factor c. The composition factor c varies so much that no average value can be used. It can be calculated from

$$c = (1 - a/\alpha)^2 \rho_c/(a/\alpha) + (1 - a/\alpha)\rho_m$$

where a is the average content of the component to be determined, α is the content of this component in the pure mineral or compound containing it, ρ_c is the density of the mineral or compound containing this component, and ρ_m is the average density of the matrix (gangue). It should be noted that a and α must be given in the same units, otherwise any concentration units (%, mass fraction, mg kg^{-1}, etc.) can be used. If the component to be determined is a pure mineral, or compound, instead of an element, then $\alpha = 100\%$ (or 1 as mass fraction).

Given the particle size d and sampling constant C, the sampling constant, Z, can be defined as $Z = C\,d^3$.

Empirical estimation of sampling constants C *and* Z

If the material to be investigated is a complicated mixture (e.g., an ore having several minerals containing the required element), for which it is difficult to estimate the composition factor c and liberation factor l with sufficient precision, it is possible to estimate the sampling constants experimentally. Two different methods can be used depending on material type. For coarse materials Gy [1] suggested a method that involves analysis of individual fragments of the material to be investigated. For fine materials, C and Z can be estimated from Eqns. 1 or 2 by analyzing a sufficient number of subsamples having the same sizes. This method is identical with that suggested by

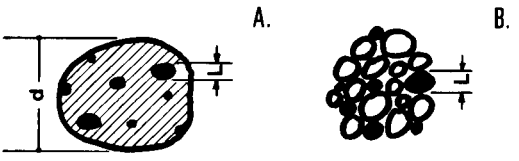

Fig. 3. Estimation of the liberation factor, l, for two different types of particulate materials. In A, the critical component is found as inclusions in the matrix material. In B, the critical components is completely liberated. In (A) $l = (L/D)^{1/2}$ and in (B) $l = 1$.

Ingamells and Switzer [5] for estimating the laboratory sampling constant K_s (and, in fact, $K_s = Z$). More than thirty individual fragments or subsamples should be analyzed, otherwise the estimate of the relative variance, which is needed to estimate the sampling constants, is not reliable.

Constant C is a function of the particle size through the liberation factor, unless the critical component is completely liberated. Therefore, if the empirical C and Eqn. 1(b) or 2(b) is used with d differing from that used for estimating C, results are likely to be somewhat optimistic, or pessimistic, depending on the case. This should be taken into account when decisions based on these values are made.

Confidence interval for the sampling error

If the error related to a sampling operation can be regarded as normally distributed, then the sampling precision, $P_{0.95}$, which gives the 95% confidence interval for the random error about the mean, is $P_{0.95} = 2\,\sigma_r$. Generally, the normal approximation and this equation are justified for values of σ_r not exceeding, say, 20%. At higher values of σ_r, the distribution becomes increasingly skewed and, consequently, a symmetrical confidence interval cannot be used for the sampling error. A value of 25% for σ_r indicates, for example, that on average there are only 16 particles of the critical component in the sample (assuming that the critical particles are randomly distributed and have uniform sizes). The 95% confidence interval for the relative sampling error about the mean concentration obtained from the Poisson distribution then covers the range from −44% to +56%. Because only the fundamental error is estimated by using Gy's method, errors arising either from segregation in the material, or from incorrect sampling technique, are not included in the confidence interval. The actual total sampling error may, therefore, be larger than predicted by the theory.

DESCRIPTION OF THE SAMPEX PROGRAM

To allow easy and practical use of Gy's method, a computer program (SAMPEX) was written in BASIC for microcomputers. It is a menu-driven program having different subroutines for different tasks. The following subroutines are included.

(1) Estimation of sampling constants can be done either by using the necessary material properties or empirical data.

(2) Relative standard deviation is calculated for a given sample size.

(3) The minimum size of a sample that is necessary to obtain a given sampling precision is calculated.

(4) The required particle size for a given sample size and relative standard deviation is calculated. This subroutine is useful when the analyst wants to know the particle size, d, to which the material should be crushed or pulverized to obtain the required sampling precision with a given sample size.

(5) A subroutine for the evaluation of multi-stage sampling processes can

be used, when the reliability of a complete analytical process, $\sigma_T(a_A)$, (see Fig. 1) is to be estimated. The options available are: (a) overall relative standard deviation, $\sigma_T(a_A)$, of a sampling scheme with given particle and sample sizes; (b) estimates for the minimum sample sizes at each sampling step for specified particle sizes and specified tolerable overall relative standard deviation, $\sigma_T(a_A)$; (c) estimates for the maximum particle sizes at each sampling step, for specified sample sizes and specified tolerable overall relative standard deviation, $\sigma_T(a_A)$. In options (b) and (c), the estimated values are calculated so that the variances of each sampling step are equal.

(6) Sampling for the determination of the particle size distribution is evaluated. The particle size distribution is given in the specifications of many commercial commodities. This subroutine can be used to evaluate the reliability of a sampling procedure for the measurement of the size distribution. The basic theory has been given by Gy (p. 254 [1]). Each size fraction is treated as the critical component and either the sampling error of a given sample size, or the minimum sample size giving a specified sampling precision, can be calculated.

Flow charts are available from the author on request.

SOME EXAMPLES

Tin as cassiterite

The problem is to estimate the particle size to which a soil or sediment sample should be pulverized, if it contains ca. 30 mg kg^{-1} tin as cassiterite and the analytical method applied is spark-source mass spectrometry. The electrodes are made by mixing 50% graphite into the sample material and about 5 mg of the electrodes is consumed during the exposure. The tolerated relative standard deviation is 10%. Complete liberation and the average values $f = 0.5$ and $g = 0.25$ can be assumed.

The tin content of cassiterite (α) is 780 g kg^{-1} and the average concentration in the electrodes is 15 mg kg^{-1}. The density values for cassiterite and for the diluent are 7.0 and 2.5 g cm^{-3}, respectively. This gives $C = 45\,500$ g cm^{-3}. To guarantee that the relative standard deviation of the sampling error caused by incomplete consumption of the electrodes does not exceed 10%, the particle size (d) should not be larger than 0.010 mm. If the fineness of the material is 100 mesh (0.147 mm), then a 50-g laboratory sample has a relative standard deviation of 3.8%, which is normally quite acceptable. But to prepare a reliable sample for analysis, further size reduction is clearly needed, because for a 1-g sample the relative standard deviation would be as high as 27%.

Aflatoxins in foodstuffs

Sampling of foodstuffs for aflatoxin determinations has been the subject of many investigations, reviewed by Campbell et al. [8]. It was found in one of the initial studies that suspect peanut kernels contained a wide range of

aflatoxin concentrations averaging 112 mg kg^{-1}. In another study, the relative standard deviation of sampling for 21.8-kg samples was 55% and the mean concentration was 0.02 mg kg^{-1} [8]. It is, therefore, interesting to compare this value with that predicted by Gy's theory. The following approximate material properties for peanut kernels were used: $f = 0.65$, $g = 0.9$ (narrow size range), density 1 g cm^{-3}, and $d = L = 10$ mm. With these values, an estimate of 39% for the relative standard deviation was obtained. The predicted estimate is lower than the measured estimate but, as the mold producing the aflatoxins tends to grow in "pockets", the grouping and segregation error is likely to be significant in the primary sampling. If it is assumed that the grouping and segregation error is equal to the fundamental error, as suggested by Gy for the sampling of segregated materials, the estimate for the total relative standard deviation is 55%, which is exactly the same value as found experimentally. Further, it can be calculated that a 82-kg sample would be needed to reduce the fundamental relative standard deviation to 20%.

Gy's theory is also very helpful when a subsampling and sample preparation plan is designed for an analysis. By using a correct technique, the grouping and segregation error, which may be significant in primary sampling, can be reduced to a low or insignificant level. For example, a representative sample weighing 100 g is made in three steps from the 21.8-kg primary peanut sample mentioned above. After initial crushing, a 5-kg subsample is extracted, then after further grinding a 1-kg subsample is taken, and after final grinding the 100-g subsample is taken. A 10% relative standard deviation can be tolerated for the whole sample preparation process, and a decision must be made on the kind of grinding equipment to be selected. In grinding, the size distribution and the shape of peanuts is not retained, therefore the average values $g = 0.25$ and $f = 0.5$ are used. A relative standard deviation of 5.8% for each sampling step totals 10%. Equation 1(b) can then be used to estimate the maximum particle sizes in each step. The following results are obtained: $d_1 = 3.1$ mm, $d_2 = 1.8$ mm, and $d_3 = 0.81$ mm (cf. Fig. 1). With this information, it is easy to select the equipment that will meet the requirements.

Conclusions

An analytical error usually costs money, either as lost work or because wrong decisions are based on erroneous results. Especially with heterogeneous materials, sampling can be the major source of error and should, therefore, be given the attention it deserves. A thoroughly tested theoretical tool, such as Gy's method, is of great value in analytical quality control. Especially in the form of a user-friendly computer program, it allows a quick study of alternative approaches to a given problem and helps to find feasible and economic solutions. With insight of the factors affecting the sampling error, problems that otherwise would need long and expensive experimentation, can often be solved in a matter of minutes.

REFERENCES

1 P. M. Gy, Sampling of Particulate Materials, Theory and Practice, Elsevier, Amsterdam, 1982.
2 P. M. Gy, Anal. Chim. Acta, 190 (1986) 13.
3 K. Sommer, Probenahme von Pulvern und körnigen Massengutern, Springer, Berlin, 1979.
4 A. A. Benedetti-Pichler, in W. M. Berl (Ed.), Physical Methods in Chemical Analysis, Vol. 3, Academic, New York, 1956, p. 183.
5 C. O. Ingamells and P. Switzer, Talanta, 20 (1973) 547.
6 C. O. Ingamells, Talanta, 21 (1974) 141; 25 (1978) 731.
7 J. Visman, J. Test. Eval., 7 (1979) 3.
8 A. D. Campbell, T. B. Whitaker, A. E. Pohland, J. W. Dickens and D. L. Park, Pure Appl. Chem., 58 (1986) 305.

Analytica Chimica Acta, 196 (1987) 247—250
Elsevier Science Publishers B.V., Amsterdam — Printed in The Netherlands

Short Communication

SIMPLIFIED POST-COLUMN REDUCTION AND FLUORESCENCE DETECTION FOR THE HIGH-PERFORMANCE LIQUID CHROMATOGRAPHIC DETERMINATION OF VITAMIN $K_{1(20)}$

W. E. LAMBERT and A. P. DE LEENHEER*

Laboratoria voor Medische Biochemie en voor Klinische Analyse, Faculteit Farmaceutische Wetenschappen, Rijksuniversiteit Gent, Harelbekestraat 72, B-9000 Gent (Belgium)

(Received 6th July 1986)

Summary. A simplification of the instrumental set-up is described for the post-column reduction and fluorescence detection in the high-performance liquid chromatographic determination of vitamin $K_{1(20)}$. The reductant (tetramethylammonium octahydridotriborate) is incorporated in the eluent, so that one pumping system can be eliminated. The system is 3—4 times more sensitive than the previous arrangement.

In the last decade, new procedures for the detection of vitamin $K_{1(20)}$ after chromatographic separation have been extensively investigated [1]. Earlier studies on the quantitation of $K_{1(20)}$ used ultraviolet detection [2, 3]. More recently, more selective detection techniques have been developed, e.g., electrochemical reduction [4, 5], mass spectrometry [6] and fluorimetry either after electrochemical [7] or photochemical reaction [8] or after reduction in solution [9, 10]. Recently, the optimization of a post-column reaction followed by fluorescence detection was described for the determination of vitamin $K_{1(20)}$ in serum [11]. This procedure was used to determine the reference interval of endogenous serum vitamin $K_{1(20)}$ [12] and to quantify $K_{1(20)}$ in serum of newborn babies. This communication describes a modification of this procedure which gives a 3—4 fold increase in sensitivity.

Experimental

Instrumentation and chemicals. The serum extraction and the liquid chromatographic system used for clean-up of the crude extract were as described previously [11]. For the post-column reactor and detector, a Model 2150 dual-piston pump (LKB), a Model CV-6-UHPa-N60 Valco injection valve with a 50-μl loop and a Model LS-4 fluorescence detector with double monochromator (Perkin-Elmer) were used. For separation, a reverse-phase column (RoSIL C18HL, 5 μm, 15 × 0.32 cm i.d.) was used; the eluent was methanol/ethyl acetate (96:4, v/v) containing the reductant (130 mg of tetramethylammonium octahydridotriborate per 100 ml) at 0.70 ml min^{-1}. A precolumn (15 cm × 0.32 cm i.d.) filled with the same packing material

0003-2670/87/$03.50

was installed ahead of the injector to saturate the mobile phase with stationary phase thus preventing the dissolution of packing material from the main column. Chromatograms were recorded on a Model PM-8251 single-pen chart recorder (Philips). Vitamin $K_{1(25)}$ was used as an internal standard.

Solvents used for extraction and chromatography were all HPLC grade (Fisher Scientific Co.). Tetramethylammonium octahydridotriborate, $(CH_3)_4NB_3H_8$, was from Alfa (Ventron). Vitamins K_1 were provided by Hoffmann-La Roche (Basel).

The post-column reactor was an open tubular knitted coil (PTFE, 5 m × 0.5 mm i.d., total volume 980 μl) placed in a silicone oil bath at 80°C. The special "knitted" configuration of the reactor tubing minimizes band broadening and provides excellent mixing [13].

Results and discussion

As vitamin $K_{1(20)}$ has no native fluorescence, conversion to the fluorescent hydroquinone form is necessary for fluorimetric detection. Such a conversion, however, increases the total time, and makes the procedure more complicated. In an off-line experiment, the fluorescence response was monitored during the first 15 min of reaction between a vitamin K standard and the reductant (tetramethylammonium octahydridoborate). From Fig. 1, which shows the results of this experiment, it is clear that the reaction has zero order kinetics, and that the reaction rate is undiminished after 15 min at $\leqslant$45°C. Furthermore, the rate is greatly increased as the temperature increases, there being only slight formation of the fluorescent hydroquinone form of vitamin $K_{1(20)}$ at 20°C. This latter observation was very important and led to an experiment in which the reductant was incorporated in the chromatographic eluent, and the chromatography was done at room temperature, thus preventing significant reaction of the reductant with vitamin $K_{1(20)}$ during the separation. After the separation, the effluent was passed directly through the knitted coil reactor at 80°C, thus allowing reduction to the fluorescent hydroquinone. This was a considerable simplification of the previous system. A typical chromatogram obtained by the new method is shown in Fig. 2. A 3—4-fold increase in sensitivity is observed as compared with the previous system using two pumps. This increased sensitivity is a result of different factors. First, in the post-column reactor, it is probably impossible to obtain such good homogeneity of reagent and eluent as is obtained by preparing a solution of the reductant in the eluent. Secondly, the reaction time is increased in the new procedure. With a dead volume of 980 μl and a total flow rate of 900 μl min^{-1} (700 μl min^{-1} from the eluent and 200 μl min^{-1} from the reductant) in the two-pump system, the reaction time was ca. 65 s. In the one-pump system, at a flow rate of 700 μl min^{-1}, the reaction time was 84 s.

The use of the saturation column inhibits the rapid dissolution of the separating column. On the chromatogram in Fig. 2, no loss in column efficiency can be observed, the total plate number (N) for the column together

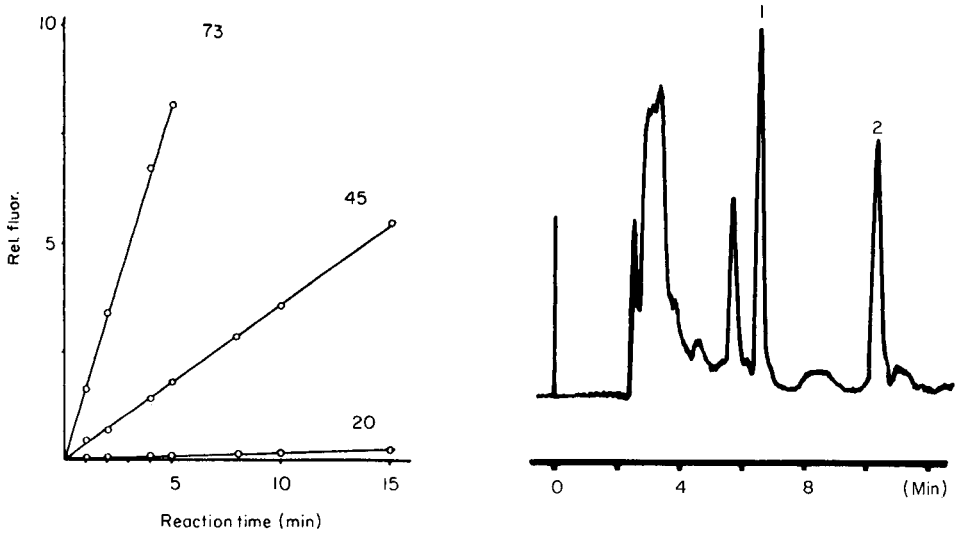

Fig. 1. Effect of temperature (°C, given on the lines) and reaction time on fluorescence intensity. Reductant concentration, 6 mg ml^{-1}; vitamin $K_{1(20)}$ concentration, 553 ng ml^{-1}; 1 ml of both solutions were mixed and allowed to react. The reductant alone (blank) did not fluoresce even after 15 min.

Fig. 2. Representative chromatogram of a serum extract. Peak identification: (1) vitamin $K_{1(20)}$; (2) $K_{1(25)}$, used as an internal standard. Detector sensitivity: x 10. Vitamin $K_{1(20)}$ concentration, 530 pg ml^{-1}.

with the reactor being ca. 5000. When this post-column reduction system was used, a relative standard deviation of 2.7% was obtained for ten replicate injections of a 542 pg ml^{-1} sample.

There was a linear relationship between the reductant concentration and the peak heights for vitamin $K_{1(20)}$ and $K_{1(25)}$. At a reductant concentration lower than 0.5 mg ml^{-1}, the fluorescence yield decreased more rapidly than at higher concentrations (Fig. 3). Without addition of the reductant, no fluorescence was observed. In the recommended procedure, the reductant concentration was 1.3 mg ml^{-1}. Although this is not a saturated solution, it remains absolutely necessary to rinse the whole chromatographic system with pure methanol after each working day. Furthermore, the reductant/eluent mixture should be prepared daily. Over several weeks, no loss in efficiency, no drift in retention times and no increase of the back-pressure were observed.

The authors thank Hoffmann-La Roche (Basel, Switzerland) for the gift of $K_{1(20)}$ and $K_{1(25)}$, and Prof. R. W. Frei (Free University Amsterdam) for providing the knitted coil reactor.

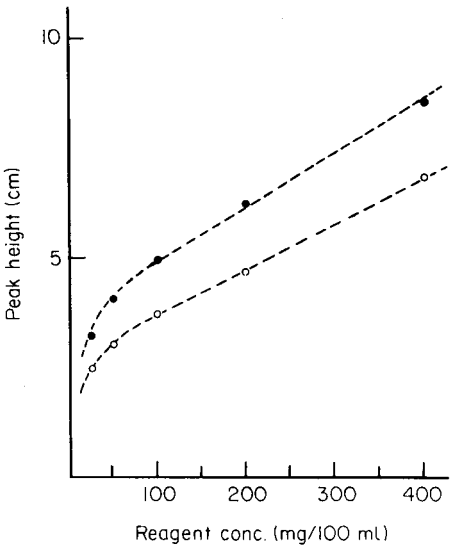

Fig. 3. Reagent concentration vs. peak height: (○) for $K_{1(20)}$; (●) for $K_{1(25)}$.

REFERENCES

1 M. F. Lefevere, A. E. Claeys and A. P. De Leenheer, in A. P. De Leenheer, W. E. Lambert and M. G. De Ruyter (Eds.), Modern Chromatographic Analysis of the Vitamins, M. Dekker, New York, 1985, p. 201.
2 M. F. Lefevere, A. P. De Leenheer, A. E. Claeys, I. V. Claeys and H. Steyaert, J. Lipid Res., 23 (1982) 1068.
3 A. L. J. M. Pietersma-de Bruyn and P. M. M. van Haard, Clin. Chim. Acta, 150 (1985) 95.
4 T. Ueno and J. W. Suttie, Anal. Biochem., 133 (1983) 62.
5 J. P. Hart, M. J. Shearer and P. T. McCarthy, Analyst, 110 (1985) 1181.
6 S. Alamercery, D. Fraisse, B. Fournier, M. Guillaumont, M. Leclercq, M. Emmelin and J. L. Rocca, Abstract of 15th International Symposium on Chromatography, Nurnberg, Oct. 1—5 1984, p. 111.
7 J. P. Langenberg and U. R. Tjaden, J. Chromatogr. Biomed. Appl., 305 (1984) 61.
8 M. F. Lefevere, R. W. Frei, A. H. Scholten and U. A. Th. Brinkman, Chromatographia, 17 (1983) 125.
9 K. Abe, O. Hiroshima, K. Ishibashi, M. Ohmae, K. Kawabe and G. Katsui, Yakugaku Zasshi, 99 (1979) 192.
10 A. Shirahata and T. Nakamura, Ketsueki to Myakkan, 16 (1985) 395.
11 W. E. Lambert, A. P. De Leenheer and M. F. Lefevere, J. Chromatogr. Sci., 24 (1986) 76.
12 W. E. Lambert, A. P. De Leenheer and E. J. Baert, Anal. Biochem., 158 (1986) 257.
13 H. Engelhardt and U. Neue, Chromatographia, 15 (1982) 403.

Analytica Chimica Acta, 196 (1987) 251—254
Elsevier Science Publishers B.V., Amsterdam — Printed in The Netherlands

Short Communication

DETERMINATION OF GLUTATHIONE IN BIOLOGICAL MATERIAL BY HIGH-PERFORMANCE LIQUID CHROMATOGRAPHY WITH ELECTROCHEMICAL DETECTION

WOLFGANG BUCHBERGER*
Department of Chemistry, Paracelsus Institute, A-4540 Bad Hall (Austria)
KARL WINSAUER
Institute of Chemistry, Analytical Department, University of Linz, A-4040 Linz (Austria)
(Received 5th August 1986)

Summary. Glutathione in biological samples is extracted by perchloric acid and separated by ion-pair chromatography on a RP-18 phase. In a post-column reaction, glutathione is converted to an isoindole derivative by reaction with *o*-phthalaldehyde and detected at a galssy carbon electrode at 800 mV v. Ag/AgCl/3 M KCl. The detection limit is 40 pmol of glutathione injected.

The tripeptide glutathione (γ-glutamylcysteinylglycine, GSH) is the major intracellular thiol and is known to be involved in many biological processes such as protection against damage by peroxides or radiation, detoxification of various xenobiotics, and maintenance of the redox potential of the cell. High-performance liquid chromatography (h.p.l.c.) has become one of the most important methods for the separation and determination of glutathione. There are several precolumn derivatization procedures [1—6] for spectrophotometric or fluorimetric detection, but the inherent possibility of side reactions must be taken into consideration. Post-column derivatization with 5,5′-dithiobis(2-nitrobenzoic acid) [7, 8] or *o*-phthalaldehyde and taurine [9, 10] has also been described. Electrochemical detection is investigated in this communication. Mercury electrodes have been used for this purpose [11—15], but they may be troublesome for routine operation. Therefore it seemed of interest to examine the use of glassy carbon electrodes. It is known that amino acids react with *o*-phthalaldehyde (OPA) in the presence of a thiol yielding electroactive derivatives with an isoindole structure [16, 17]. As glutathione contains both an amine and a thiol group, the addition of OPA alone should be sufficient.

Experimental

Instrumentation and reagents. The h.p.l.c. system consisted of a Waters M590 pump, a home-made pulse damper, a Rheodyne 7125 injection valve with a 20-μl loop, a Merck CGC glass cartridge (150 × 3 mm) filled with

0003-2670/87/$03.50

5-μm LiChrosorb RP 18, and a Metrohm VA-Detector E611 with a wall-jet cell equipped with glassy carbon as working electrode, Ag/AgCl/3 M KCl as reference electrode and gold as auxiliary electrode. The post-column reagent was added from a closed polypropylene 2l-bottle which could be pressurized to 0.2—2 bar by nitrogen; with an appropriate pressure, the reagent was fed through a teflon capillary to the mixing device. The reagent and the column effluent were mixed at a teflon T-connector (Omnifit) and then in a teflon reaction coil (3 m long, 0.45 mm i.d.). The chromatograms were recorded and integrated by an Apple IIe computer with Chromatochart software (Interactive Microware). For flow-injection experiments, the same instrumentation was used, but the column was replaced by a stainless steel capillary. The electrochemical behaviour of the derivative was investigated with a EG&G 174A polarograph.

The mobile phase (which is a modification of the eluent used by Seiler and Knodgen [18] for the separation of amino acids) was prepared by mixing 630 ml of 0.2 M phosphoric acid (containing 10 mM sodium dodecylsulphate), 270 ml of 0.2 M sodium acetate (containing 10 mM sodium dodecylsulphate) adjusted to pH 4.5 with acetic acid, and 100 ml of ethanol. The post-column derivatization reagent was prepared by dissolving 62 g of boric acid in 1000 ml of water, adding solid sodium hydroxide until a pH of 11.0 was reached, and adding 600 mg *o*-phthalaldehyde in 15 ml of ethanol. This reagent was prepared fresh daily.

The flow rates of the mobile phase and the post-column reagent were 0.5 ml min^{-1}. The detection potential was 800 mV.

Determination of glutathione in biological samples. Samples such as liver and eye lenses were homogenized with a five- to ten-fold amount of 1 M perchloric acid, 2 mM in EDTA. Blood samples were mixed with an equal volume of 2 M perchloric acid, 4 mM in EDTA. After centrifugation 1 ml of the extract was mixed with 400 μl of 2 M potassium hydroxide and diluted with water so that the anticipated concentration of glutathione was ca. 10 mg l^{-1}. This solution was subjected to h.p.l.c.

Results and discussion

A voltammogram of the derivatized glutathione is shown in Fig. 1. There was no dependence of the peak potential on the pH in the range 8—11. The derivatization reaction was complete within 10 s, as was shown by amperometry at a rotating glassy carbon disk electrode immersed in a pH 10 buffer containing OPA, to which at a definite time glutathione was added.

The detection sensitivity measured in the flow-injection system increased with increasing pH (Fig. 2). Therefore a pH of 11.0 was chosen for the post-column reagent which, after mixing with the mobile phase, gave a pH of 9.6. Reagents of pH above 11 were not used, to prevent highly caustic solutions entering the h.p.l.c. instrument. Before a series of injections, it was advantageous to polish the glassy carbon electrode with alumina in the usual way, and after connecting the cell to the chromatograph, to set the electrode to

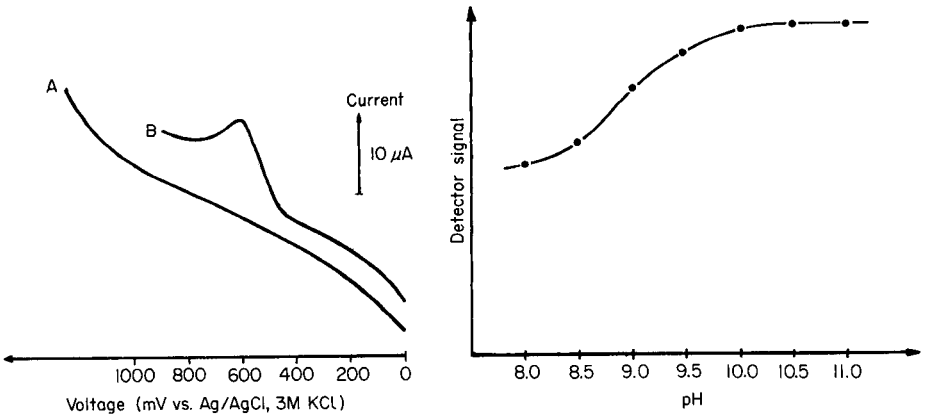

Fig. 1. Voltammograms: (A) post-column derivatization reagent/mobile phase (1+1); (B) as A but 2 mM glutathione added.

Fig. 2. Detector response as a function of pH, measured in the flow-injection system for 0.16 mM glutathione.

1500 mV for 2 mins. This pretreatment gave better stability of response.

The detection limit (signal-to-noise ratio 3:1) of the method for glutathione standards was ca. 40 pmol of glutathione injected. There was a linear relation between the amount injected and the peak area from the detection limit up to 5 nmol. The relative standard deviation of the method was 3% for the range 0.1—1 nmol injected. The method was applied to liver, blood and eye lens samples. Typical chromatograms are shown in Fig. 3.

It is often interesting to measure both glutathione (GSH) and its oxidized form (GSSG). For this purpose, the GSH content of the extract was measured, then the extract was neutralized and treated with glutathione

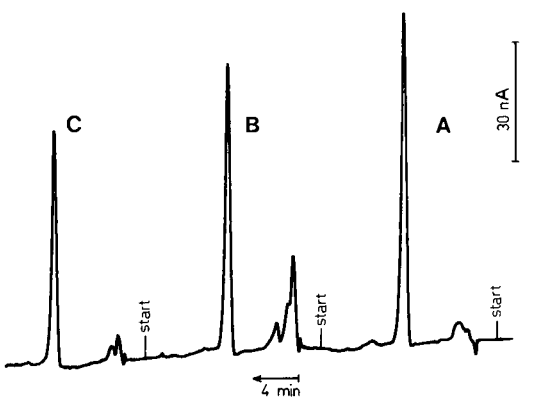

Fig. 3. Chromatograms of diluted extracts of liver and eye lens samples: (A) standard solution containing 68 μmol l^{-1} glutathione; (B) liver sample containing 3.8 μmol g^{-1} glutathione (wet weight); (C) eye lens sample containing 1.4 μmol g^{-1} glutathione (wet weight).

reductase [19], which specifically converts GSSG to GSH, and the GSH content was measured once more. Usually, however, no GSSG was detected after such treatment. Therefore, the use of a column filled with a solid-phase reagent for on-line reduction of GSSG after chromatographic separation is under investigation.

REFERENCES

1 E. P. Lankmayr, K. W. Budna, K. Müller and F. Nachtmann, Fresenius' Z. Anal. Chem., 295 (1979) 371.
2 D. J. Reed, J. R. Babson, P. W. Beatty, A. E. Brodie, W. W. Ellis and D. W. Potter, Anal. Biochem., 106 (1980) 55.
3 J. Reeve, J. Kuhlenkamp and N. Kaplowitz, J. Chromatogr., 194 (1980) 424.
4 G. L. Newton, R. Dorian and R. L. Fahey, Anal. Biochem., 114 (1981) 383.
5 A. J. Baars and D. D. Breimer, Pharm. Weekbl. Sci. Ed., 5 (1983) 145.
6 K. Mopper and D. Delmas, Anal. Chem., 56 (1984) 2557.
7 D. Beales, R. Finck, A. E. M. McLean, M. Smith and I. D. Wilson, J. Chromatogr., 226 (1981) 498.
8 A. J. Alpert and H. F. Gilbert, Anal. Biochem., 144 (1985) 553.
9 H. Nakamura and Z. Tamura, Anal. Chem., 53 (1981) 2190.
10 H. Nakamura and Z. Tamura, Anal. Chem., 54 (1982) 1951.
11 D. L. Rabenstein and R. Saetre, Anal. Chem., 49 (1977) 1036.
12 B. Zygmunt, H. B. Hanekamp, P. Bos and R. W. Frei, Fresenius' Z. Anal. Chem., 311 (1982) 197.
13 L. A. Allison and R. E. Shoup, Anal. Chem., 55 (1983) 8.
14 E. G. Demaster, F. N. Shirota, B. Redfern, D. J. W. Goon and H. T. Nagasawa, J. Chromatogr., 308 (1984) 83.
15 S. M. Lunte and P. T. Kissinger, J. Liq. Chromatogr., 8 (1985) 691.
16 M. H. Joseph and P. Davies, J. Chromatogr., 277 (1983) 125.
17 L. A. Allison, G. S. Mayer and R. E. Shoup, Anal. Chem., 56 (1984) 1089.
18 N. Seiler and B. Knodgen, J. Chromatogr., 341 (1985) 11.
19 E. Bernt and H. U. Bergmeyer, in H. U. Bergmeyer (Ed.), Methoden der enzymatischen Analyse, Vol. 2, 3rd edn., Verlag Chemie, Weinheim, 1974, p. 1688.

Analytica Chimica Acta, 196 (1987) 255—258
Elsevier Science Publishers B.V., Amsterdam — Printed in The Netherlands

Short Communication

DETERMINATION OF β-ADRENORECEPTOR ANTAGONISTS IN URINE BY HIGH-PERFORMANCE LIQUID CHROMATOGRAPHY WITH DIODE-ARRAY SPECTROPHOTOMETRIC DETECTION

LI YE and ZHANG XIANGXI*

Laboratory of Analytical Chemistry, Institute of Forensic Sciences, Ministry of Public Security, P.O. Box 2808-13, Beijing (China)

(Received 31st July 1986)

Summary. The determination of pindolol, oxprenolol and propranolol in human urine is described. The drugs are isolated with a GDX-502 resin-packed column, separated on a C_{18} (5-μm) reversed-phase column with methanol/aqueous acetic acid as mobile phase and quantified with diode-array spectrophotometric detector. The recovery was >93%, and detection limits were 2 ng for pindolol, 12 ng for oxprenolol and 2 ng for propranolol. Results are given for urine from healthy volunteers who had received the drugs orally.

β-adrenoreceptor antagonists such as pinodolol, oxprenolol and propranolol are widely used in the treatment of cardiac arrhythmias, hypertension, angina and thyrotoxicosis, but are also sometimes used as doping agents in sport. Various methods are available for determining these drugs in urine or other biological liquids involving either spectrofluorimetry [1, 2], thin-layer chromatography [3, 4], gas chromatography [5—12], gas chromatography/mass spectrometry [13—15] or high-performance liquid chromatography (h.p.l.c.) [16—26]. These methods require a time-consuming extraction precedure and are for determination of a single drug and its metabolites.

In this communication, a simple h.p.l.c. method is described for determining pindolol, oxprenolol and propranolol in human urine.

Experimental

Reagents. All reagents were of analytical grade. Methanol, ethanol and acetic acid were purchased from Beijing Chemical Works (China). The water was twice-distilled from glass. Oxprenolol and propranolol were obtained from Beijing Second Pharmaceutic Works (China). Pindolol was a gift from Shijiazhuang Pharmaceutic Works (Hebei, China).

Chromatographic system. The Hewlett-Packard HP1090 liquid chromatograph used was equipped with a DR5 solvent delivery system, variable-volume auto-injector, autosampler, HP3392A integrator, HP7470A plotter and HP1040A diode-array detector. The column (150 × 2.1 mm i.d.) was packed with 5 μm GYQG-C18 (Beijing Factory of Chemical Reagents, China). Other conditions were as follows: mobile phase, methanol/2% acetic

0003-2670/87/$03.50

acid (9:1, v/v); flow rate, 0.5 ml min^{-1}; column temperature, 30°C; detector wavelength, 260 nm (band-width 80 nm).

Standard solution and urine samples. Standard stock solutions of pindolol, oxprenolol and propranolol were prepared by dissolving the drugs in ethanol. Drug-free urine was obtained from healthy volunteers. Urine samples were also collected from healthy volunteers who had received an oral dose of 15 mg of pindolol, 20 mg of oxprenol and 20 mg of propranolol.

Procedure. A 1-ml aliquot of urine was passed through a column containing 1 g of GDX-502 resin (Tianjin Second Factory of Chemical Reagents). The loaded column was washed with 5 ml of distilled water, and then with 1 ml of methanol. The drug was eluted again with 1 ml of methanol. This solution was evaporated to dryness with a current of nitrogen at room temperature. The resulting residue was dissolved in 150 μl of methanol, and a 5-μl aliquot was injected into the h.p.l.c. column. Three calibration graphs were prepared by treating urine samples containing known amounts of pindolol, oxprenolol and propranolol in the same way.

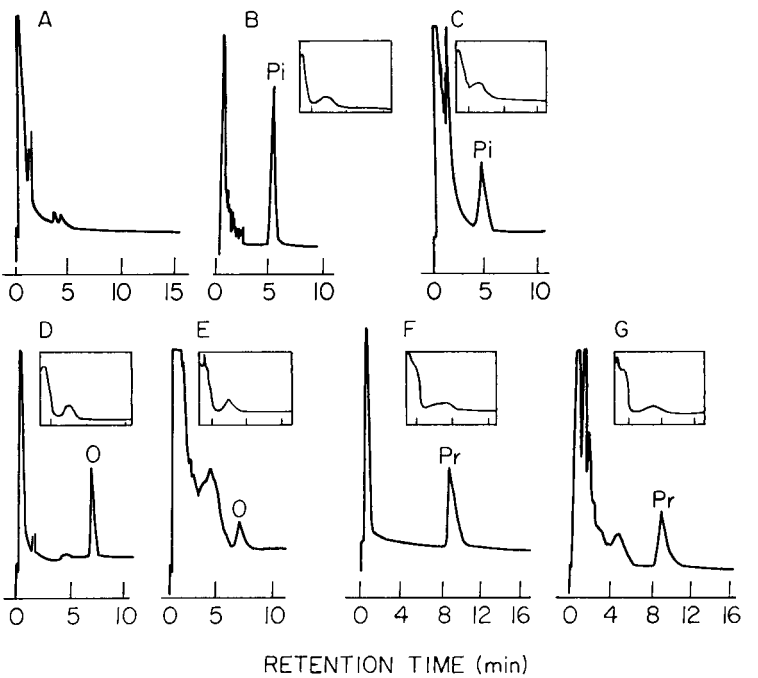

Fig. 1. Chromatograms and spectra of extracts from human urine: (A) blank urine; (B) blank urine spiked with 3.4 μg ml^{-1} pindolol; (C) urine from a volunteer, 7 h after an oral dose of 15 mg of pindolol (Pi) giving 4.2 μg ml^{-1}; (D) blank urine spiked with 5.0 μg ml^{-1} of oxprenolol; (E) urine from a volunteer, 8 h after an oral dose of 20 mg of oxprenolol (O) giving 6.1 μg ml^{-1}; (F) blank urine spiked with 3.0 μg ml^{-1} propranolol; (G) urine from a volunteer, 6 h after an oral dose of 20 mg of propranolol (Pr) giving 4.3 μg ml^{-1}. Chromatographic conditions as in the text. The inset spectra are for the wavelength range 208—400 nm at 5-nm intervals.

Results and discussion

Under the chromatographic conditions described above, the retention times of pindolol, oxprenolol and propranolol were 5.01, 7.13 and 8.71 min, respectively. Figure 1 shows chromatograms of the extracts of blank human urine (A), blank human urine spiked with pindolol (B), oxprenolol (D) and propranolol (F) and urine collected from volunteers receiving an oral dose of pindolol (C), oxprenolol (E) or propranolol (G). Figure 1 also shows the spectra recorded at the drug peaks. These spectra can be used for the identification of the drugs.

The calibration data and detection limits are shown in Table 1. The graphs showed good linearity. Table 2 shows the reproducibility of the method and the recovery of pindolol, oxprenolol and propranolol spiked in human urine. These results indicate that the method is rapid and simple, and will be suitable for use in pharmacokinetic studies and drug monitoring in patients. The

TABLE 1

Calibration data and detection limits

Compound	Linear range ($\mu g\ ml^{-1}$)	r ($n = 6$)	Detection limit[a] (ng)
Pindolol	0.2—10.0	0.997	2
Oxprenolol	1.5—15.0	0.999	12
Propranolol	0.2—10.0	0.999	2

[a]Signal/noise = 2.

TABLE 2

Reproducibility and recovery of pindolol, oxprenolol and propranolol in human urine

Compound	Concentration ($\mu g\ ml^{-1}$)	Relative standard deviation (%)[a]	Mean recovery (%)[b]
Pindolol	0.2	5.3	95.1
	1.0	3.2	
	5.0	2.8	
	10.0	3.4	
Oxprenolol	1.5	4.5	93.2
	6.0	3.6	
	10.0	2.3	
	15.0	3.1	
Propranolol	0.2	3.3	98.4
	1.0	2.5	
	5.0	1.3	
	10.0	2.7	

[a]For 6 measurements at all concentrations. [b]For all 24 experiments.

assay can be used for the detection of pindolol, oxprenolol and propranolol in doping checks.

REFERENCES

1 T. Suzuki, Y. Saitoh, S. Isozaki and R. Ishida, Chem. Pharm. Bull., 20 (1972) 2731.
2 P. S. Rao, L. C. Quesada and H. S. Mueller, Clin. Chim. Acta, 88 (1978) 355.
3 M. Schafer, H. E. Geissler and E. Mutschler, J. Chromatogr., 143 (1977) 607.
4 Y. Garceau, I. Davis and J. Hasegawa, J. Pharm. Sci., 67 (1978) 826.
5 M. Guerret, D. Lavenne and F. R. Kiechel, J. Pharm. Sci., 69 (1980) 1191.
6 M. Guerret, J. Chromatogr., 221 (1980) 387.
7 D. B. Jack and W. Riess, J. Chromatogr., 88 (1974) 173.
8 P. H. Degen and W. Riess, J. Chromatogr., 121 (1976) 72.
9 T. Walle, J. Pharm. Sci., 63 (1974) 1885.
10 D. S. Saelens, T. Walle and P. J. Privitera, J. Chromatogr., 123 (1976) 185.
11 J. F. Pritchard, D. W. Schneck, W. J. Racz and A. H. Hayes Jr., Clin. Biochem., 11 (1978) 121.
12 D. E. Easterling, T. Walle, E. C. Conradi and T. E. Gaffney, J. Chromatogr., 162 (1979) 439.
13 T. Walle, J. Morrison, K. Walle and E. Conradi, J. Chromatogr., 114 (1975) 351.
14 T. Walle, U. K. Walle, D. R. Bridges, E. C. Conradi and T. E. Gaffney, Clin. Chem., 24 (1978) 991.
15 V. T. Vu and F. P. Abramson, Biomed. Mass Spectrom., 5 (1978) 686.
16 M. Bangah, G. Jackman and A. Bobik, J. Chromatogr., 183 (1980) 255.
17 B. Diquet, J. J. Nguyen-Huu and H. Boutron, J. Chromatogr., 311 (1984) 430.
18 S. E. Tsuei and J. Thomas, J. Chromatogr., 181 (1980) 135.
19 J. F. Pritchard, D. W. Schneck and A. H. Hayes Jr., J. Chromatogr., 162 (1979) 47.
20 W. D. Mason, E. N. Amick and O. H. Weddle, Anal. Lett., 10 (1977) 515.
21 R. L. Nation, G. W. Peng and W. L. Chiou, J. Chromatogr., 145 (1978) 429.
22 A. M. Taburet, A. A. Taylor, J. R. Mitchell, D. E. Rollins and J. L. Pool. Life Sci., 24 (1979) 209.
23 F. Pritchard, D. Schneck and A. Hayes Jr., Res. Commun. Chem. Pathol. Pharmacol., 23 (1979) 279.
24 D. W. Schneck, J. F. Pritchard and A. H. Hayes Jr., Res. Commun. Chem. Pathol. Pharmacol., 24 (1979) 3.
25 M. Lo and S. Riegelman, J. Chromatogr., 183 (1980) 213.
26 H. Takei, H. Ocata and A. Ejima, Chem. Pharm. Bull., 31 (1983) 1392.

Analytica Chimica Acta, 196 (1987) 259—265
Elsevier Science Publishers B.V., Amsterdam — Printed in The Netherlands

Short Communication

EVALUATION OF ENZYMATIC KINETIC PARAMETERS BY THIN-LAYER CHROMATOGRAPHY WITH RADIOMETRIC DETECTION

ENRICO GATTAVECCHIA, DOMENICA TONELLI* and PAOLA BOSCO

Istituto di Scienze Chimiche, Facoltà di Farmacia, Università di Bologna, Via San Donato 15, 40127 Bologna (Italy)

(Received 4th August 1986)

Summary. A radiochromatographic method is described for evaluating K_m and v_{max} based on a simple modification of the integrated Michaelis-Menten equation. Experimental points are fitted directly to this equation by an iterative technique, the validity of which is tested on simulated experimental data. Results for lysine, ornithine, and glutamic acid decarboxylases are reported.

The rate, v, of most enzyme-catalyzed reactions follows the Michaelis-Menten equation $v = v_{max}S/(S + K_m)$, where S is the substrate concentration. Many methods have been published for estimating the kinetic constants K_m and v_{max} [1—9], but there is no agreement about which is the best. Most workers prefer graphical or computational methods based on the determination of initial velocities at different initial substrate concentrations. The magnitude of the error in K_m and v_{max} depends essentially on the error in the measurement of the initial velocity v_0. An accurate evaluation of v_0 presupposes the possibility of following continuously the progress of the reaction, e.g., spectrophotometrically.

Among the techniques available for studying enzyme kinetics, those based on radioactive isotopes show great sensitivity and simple applicability. Thin-layer chromatography (TLC) with radiometric detection is normally used here for determining amino acid decarboxylase activity. Its major drawback lies in the discontinuity of measurements and thus the difficulty of measuring the initial rate. In such a case it is preferable to evaluate K_m and v_{max} by fitting the integrated form of the Michaelis equation to the progress curve of the reaction.

In a previous communication [10] a radio-TLC method was described which utilized uniformly-labelled substrates for measuring amino acid decarboxylase activity. The method is based on evaluation of the ratio (R) of the peak area for the substrate to the total peak area for substrate and product(s) versus time rather than on measurement of the absolute quantity of substrate or product. For an enzymatic decarboxylation represented by

0003-2670/87/$03.50

$E + S \rightleftharpoons ES \rightarrow E + P + P_1$, where E is the free enzyme, ES is the enzyme-substrate complex, and P and P_1 are the amine and carbon dioxide products, respectively, R is defined as

$$R = S/S_0 = S/(S + P)$$

If N_S and N_P are the counts relative to the areas of substrate and product peaks, respectively, and a_S and a_P are the specific activities of the substrate and amine, respectively, ϵ is the counting efficiency, v the volume added to the gel and t the counting time, then $N_S = vSa_S\epsilon t$ and $N_P = vPa_P\epsilon t$, so that

$$R = (N_S/a_S)/[(N_S/a_S) + (N_P/a_P)]$$

For a decarboxylation reaction, if n is the number of carbon atoms in the substrate molecule (uniformly labelled), then $a_P = (n - 1)a_S/n$, and

$$R = N_S/(N_S + nN_P/(n - 1))$$

Consequently, the estimation of R is unaffected by variables such as the volume added, counting efficiency, specific activity and counting time. The main advantage in this approach therefore is that errors arising from these variables are eliminated.

Previously [10], experimental data were processed by a simple modification of the integrated Michaelis-Menten equation obtained by introducing the variable R which was valid only when the initial substrate concentration $S_0 \gg K_m$. This communication describes an elaboration of the method in order to estimate K_m and v_{max} for any initial conditions, starting only from knowledge of S_0 and the change of R with time. The theoretical aspects and the limits of applicability of the method are discussed and its validity is tested on simulated experimental data, and on experimental results for lysine, ornithine and glutamic acid decarboxylases.

Experimental

For simulated experiments, an Olivetti M-24 personal computer was used with BASIC programs. Enzymatic reactions were done in 1-ml conical Eppendorf tubes in a 100-μl final volume which contained the appropriate buffer solution supplemented with 1—100 mM L-amino acid and ca. 1 μCi (^{14}C) of the radioactive substrate. Reaction mixtures were prepared at room temperature, and each tube was incubated in a water bath at 37°C for 15 min. The reaction was initiated by addition of the enzyme solution previously thermostatted at 37°C. The tubes were capped with cotton-wool soaked with a sodium hydroxide solution in order to capture the $^{14}CO_2$ released. About 1 μl of solution was withdrawn at 4-min intervals and spotted on a pre-coated silica gel layer (0.25 mm thick) kept at ca. 80°C to stop the reaction. The layer was developed at room temperature in saturated tanks with acetone/33% (v/v) aqueous dimethylamine solution/isopropanol (1.8:2.5:5.6). After development, the radioactivity of the spots was measured by a TLC linear analyzer (Berthold LB-282) connected to an Apple IIE computer which output the integrated peak areas (counting time 5 min).

Results and discussion

The integrated form of the Michaelis-Menten equation can be formulated in terms of R as follows:

$$R = 1 - (K_m/S_0) \ln R - (v_{max}/S_0)t \quad (1)$$

where S_0 is the initial concentration of substrate. The slope of the curve at any time t is

$$\alpha = -dR/dt = v_{max}R/(S_0R + K_m)$$

and the slope at $t = 0$ is

$$\alpha_0 = -(dR/dt)_{t=0} = v_{max}/(K_m + S_0) \quad (2)$$

Equation 2 is exact, but in practice the initial slope α_0 can be estimated only approximately. To obviate this difficulty, an iterative computational method is used to fit the experimental data to Eqn. 1. For the progress curves obtained at two different initial concentrations of substrate, R_i is defined as the measured values of the dependent variable for each of n observations at several times. The average slope of any experimental progress curve from the n observations can be defined as

$$\bar{\alpha} = (1/n) \sum_{i=1}^{n} v_{max}R_i/(S_0R_i + K_m) \quad (3)$$

Combination of Eqns. 2 and 3 gives

$$\alpha_0 = \bar{\alpha}/\{[(S_0 + K_m)/n] \sum_{i=1}^{n} [R_i/(R_iS_0 + K_m)]\} \quad (4)$$

First, the slopes of the two progress curves are calculated by linear regression. The values are assumed to be the initial slopes (α'_0, β'_0) and are used to evaluate a first approximate estimate of K_m from Eqn. 2. The initial estimate is put into Eqn. 4 in order to compute new values of α'_0 and β'_0, and a more refined value of K_m. The whole process is repeated until ΔK_m becomes $<0.01\%$. The final value of K_m and the relative value of v_{max}, obtained from Eqn. 2 are put into Eqn. 1 for generating theoretical estimates of R_i corresponding to given S_0 and t values which are considered to be independent variables with errors insignificant relative to those in R_i. Computed R_i values are used to find a better value of $\bar{\alpha}$ from Eqn. 3, thus beginning a new iterative cycle. The flow chart of the program is given in Fig. 1. The program requires about 20—30 kbytes of RAM and can be run on a personal computer such as an APPLE II or IBM PC.

The method was tested on simulated experimental data obtained by considering the error in R normally distributed and caused only by counting statistics, i.e., $\sigma = N^{1/2}$ where N is the total number of counts. For each error-free curve, $K_m = v = 1$, $P_0 = 0$ and S_0 was either 0.5, 1.0 or 1.5. Experimental errors were simulated by the use of a library routine which generated normally

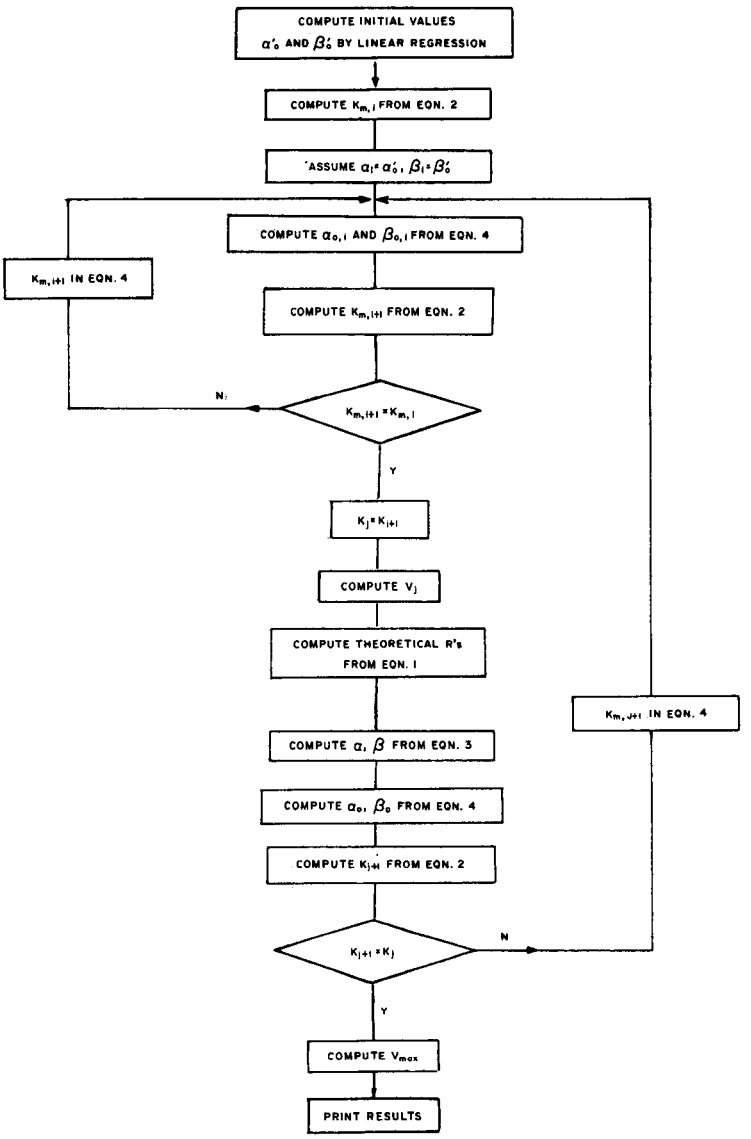

Fig. 1. Flow chart of the program.

distributed pseudo-random numbers (q), with mean = 0 and variance = 1. The error was introduced in R_i by $\sigma'_S = qN_S^{1/2}$, $\sigma'_P = qN_P^{1/2}$ and

$$R'_i = (S + \sigma'_S)/(S + \sigma'_S + P + \sigma'_P)$$

Three error levels were considered: $\sigma'_1 = qN^{1/2}$, $\sigma'_2 = 2qN^{1/2}$ and $\sigma'_3 = 3qN^{1/2}$. Ten different experimental curves were simulated at each substrate concentration and error level. Table 1 summarizes the values of the parameters

TABLE 1

Mean estimates of K_m (M) and v_{max} (M min^{-1}) for progress curves simulated at the σ_2' error level. (Values are means ± SD (n = 45))

S_0^A	S_0^B	Iterative method		Double-reciprocal plot		Direct plot	
		K_m	v_{max}	K_m	v_{max}	K_m	v_{max}
1.5	1.0	0.974 ± 0.056	0.989 ± 0.034	1.95 ± 0.28	1.19 ± 0.06	2.42 ± 0.76	1.24 ± 0.26
1.0	0.5	0.996 ± 0.019	1.002 ± 0.011	0.38 ± 0.17	0.50 ± 0.07	0.38 ± 0.16	0.50 ± 0.07
1.5	0.5	0.984 ± 0.045	0.992 ± 0.025	0.72 ± 0.17	0.70 ± 0.06	0.72 ± 0.17	0.70 ± 0.06

found by the proposed method from the progress curves generated at the error level σ_2' and setting the total counts $N_S + N_P = 10\,000$. The answers are both accurate and precise. Similar results were obtained from the progress curves obtained at the other error levels. In particular, the estimates of v_{max} seemed always to be more accurate and precise than those of K_m. The same set of data was also processed by the double-reciprocal linear plot method. As can be seen, there is no comparison between the two methods when the measurements are made only at two different concentrations of substrate.

The major limitation of the proposed method is that sometimes the procedure does not converge to a stable value of K_m. The same drawback has been pointed out previously [8]. For the initial conditions and error levels chosen in the present simulated experiments, the method always converged irrespective of the range of R values considered. But it remains to be seen how precise the initial parameter estimates must be in order to achieve convergence.

The final values of K_m and v_{max} depend on the error in the measurement of R. This error has been estimated for different total counts. The trends in the relative standard error for N = 1000 and 10 000 are reported in Fig. 2. The relative standard error in R ranges from 0.42% (R = 0.9) to 4% (R = 0.1) for total counts of 10 000 (corresponding to about 3.7×10^2 Bq of carbon-14 for a counting time of 5 min) under the present experimental conditions. Because the errors in R are very small over a wide range, enzymatic reactions can be followed from 5 to 80% completion.

To illustrate the method, K_m and v_{max} were evaluated from experimental data obtained for lysine, ornithine, and glutamic acid decarboxylase (LD, ODC and GAD). Table 2 summarizes the values of the parameters, generally evaluated from ten measurements of R in the above range, processed by the iterative method. The results obtained for K_m and v_{max} are reasonably precise.

The intrinsic precision of the radiochromatographic measurement was estimated by placing the same layer of silica gel several times under the detector of the TLC linear analyzer. The measurements always differed from one another by <1%. However, when several progress curves were obtained under identical experimental conditions, the reproducibility in the values of R was 2—4%. In practice, the error in the evaluation of K_m and v_{max} inherent in the techniques of measurement and data processing is very small and probably negligible in comparison with other sources of error.

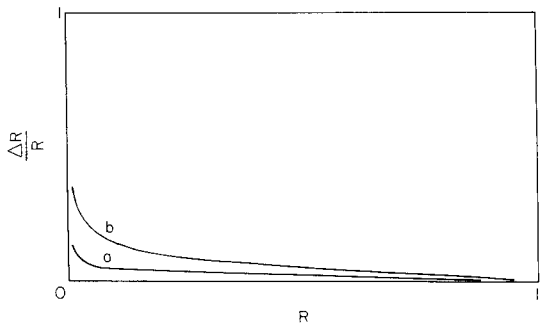

Fig. 2. Relationship between R and its relative error: (a) for N = 10 000; (b) for N = 1000.

TABLE 2

Values of K_m (mM) and v_{max} (mM min^{-1}) measured for decarboxylating enzymes

Enzyme	K_m[a]	v_{max}[a]	K_m from literature
ODC	3.56 ± 0.31 (pH 5)	0.95 ± 0.08 (pH 5)	2 [11] (pH 8.5)
GAD	20.6 ± 2.3 (pH 5)	0.92 ± 0.07 (pH 6)	27 [12] (pH 5)
LD	2.82 ± 0.27 (pH 6)	1.04 ± 0.09 (pH 6)	1.2—1.8 [13] (pH 6)

[a]Each value is the mean ±SD of five determinations; the nominal enzyme activity was 1 U ml^{-1}.

The method can therefore be used to determine enzyme kinetic parameters and for bio-analytical applications, such as the determination of enzyme activities in tissues or fluids. The TLC linear analyzer utilized here counts the whole trace simultaneously, using a position-sensitive detector thus allowing a sensitivity ca. 100 times greater than that of a TLC scanner which counts sequentially the individual areas below the slit. This marked increase in sensitivity allows a significant decrease in the counting time and/or in the quantity of radioactive material used.

This study was supported in part by The Italian National Research Council (C.N.R.), finalized Project "Oncologia", contract n. 86.00327.44 and is published with CNR permission.

REFERENCES

1 H. J. Lee and I. B. Wilson, Biochim. Biophys. Acta, 242 (1971) 519.
2 F. De Miguel Merino, Biochem. J., 143 (1974) 93.
3 R. R. Jennings and C. Niemann, J. Am. Chem. Soc., 77 (1955) 5432.
4 R. Eisenthal and A. Cornish-Bowden, Biochem. J., 139 (1974) 715.

5 A. Cornish-Bowden, Biochem. J., 149 (1975) 305.
6 N. Glick, A. D. Landman and B. D. Roufogalis, Trends Biochem. Sci., April (1979) N 82.
7 K. A. Booman and C. Niemann, J. Am. Chem. Soc., 78 (1956) 3642.
8 H. N. Fernley, Eur. J. Biochem., 43 (1974) 377.
9 J. A. Nimmo and G. L. Atkins, Biochem. J., 141 (1974) 913.
10 E. Gattavecchia, D. Tonelli and R. Budini, Radiochem. Radioanal. Lett., 59 (1983) 121.
11 E. Hölttä, J. Jänne and J. Pispa, Biochem. Biophys. Res. Commun., 47 (1972) 1165.
12 E. F. Gale, in F. F. Nord (Ed.), Advances in Enzymology, Vol. 6, Interscience, New York, 1946, p. 1.
13 E. F. Gale and H. M. R. Epps, Biochem. J., 38 (1944) 232.

Analytica Chimica Acta, 196 (1987) 267—270
Elsevier Science Publishers B.V., Amsterdam — Printed in The Netherlands

Short Communication

DETERMINATION OF MICROGRAM AMOUNTS OF AZIDE BY GAS CHROMATOGRAPHY

EUGENIUSZ KUBASZEWSKI*, ZBIGNIEW KURZAWA and MAREK ŁOŻYNSKI

Department of Chemistry, Technical University of Poznań, ul. Piotrowo 3, 60-965 Poznań (Poland)

(Received 4th August 1986)

Summary. Azide ions (5—120 μg) are oxidized by cerium(IV) in an acidic medium. The nitrogen evolved is displaced by helium carrier gas and quantified by gas chromatography with a thermal conductivity detector. The relative standard deviation is ≤5%. Many sulphur anions, cyanide and some metal ions which form azide complexes do not interfere.

Considerable importance is attached to the determination of azides because of their toxic and carcinogenic properties and to the possible application of sodium azide as a nematocide in agriculture. In a previous study, a spectrophotometric method for azide ions was described in aqueous solutions [1]. Although this method was highly sensitive, it was not very selective. Similarly, earlier spectrophotometric methods, based on coloured complexes of azide ions with iron(III) [2—4] or copper(II) [5] are limited. A better method for azide determination in aqueous solutions, therefore, was sought. The method proposed in this communication is based on oxidation of azide ions to nitrogen which is determined by gas/solid chromatography.

The oxidation product of azide depends on the oxidant and conditions. Strong oxidants such as cerium(IV) and permanganate oxidize azide to nitrogen in acidic media, but neither chromate nor iodine acts effectively under these conditions (the reaction is very slow). The oxidation in acidic media is very fast, however, when nitrite is used as the oxidant [6]. Nitrogen, nitrous oxide and nitric oxide are formed by oxidation with nitric acid at elevated temperature [7]. Azide can be oxidized to nitrous oxide only by using *N*-bromosuccinimide in the presence of mercury(II) [8]. For the proposed method, the most effective oxidant would seem to be one which yields a single gaseous product, because this will improve the sensitivity of determination. Accordingly, cerium(IV) was chosen.

Experimental

Reagents and solutions. Reagents of analytical purity were used. The sodium azide was purified as follows: a saturated aqueous solution was prepared, filtered and mixed with an equal volume of 95% ethanol; the salt

0003-2670/87/$03.50

was precipitated with an excess of diethyl ether and the crystals were washed with an ethanol/ether mixture, and air-dried. A stock solution of azide (1 mg ml^{-1}) was prepared by dissolving 1.5476 g of sodium azide in water in a 1-l volumetric flask and diluting to volume. Working solutions (50 and 100 μg ml^{-1}) were obtained by dilution of the stock solution. The stock cerium-(IV) solution (4 mg ml^{-1}) was prepared by dissolving 1.8059 g of ammonium cerium(IV) sulphate in 1 M sulphuric acid in a 100-ml volumetric flask, and diluting to volume with that acid. Solutions of $S_2O_3^{2-}$, SO_3^{2-}, SCN^-, S^{2-} and CN^- (10 mg ml^{-1}) were obtained by dissolving the sodium salts in oxygen-free water. The working solutions were prepared by dilution of stock solutions with oxygen-free water. For sulphide and cyanide, the working solutions were made alkaline with a few drops of 1 M potassium hydroxide. The solution used for absorption of hydrogen sulphide and sulphur dioxide was obtained by mixing 2 ml of 5% (w/v) barium chloride solution with 2 ml of 30% hydrogen peroxide and 1 ml of 1 M hydrochloric acid.

Apparatus. The gas chromatograph used was a model 18.3.6 (Gide, G.D.R.) with thermal conductivity detector; it was equipped with a model GP-1 six-way teflon valve with loop for gas analysis. The glass column (1 m × 4 mm) was packed with molecular sieve 5A (60—80 mesh; Serva) activated for 2 h at 350°C. Helium carrier gas was purified by a column packed with a molecular sieve 4A and activated carbon. Its flow rate was 40 ml min^{-1}. The temperatures of the injection port, column and detector were 50, 35 and 50°C, respectively. Liquid samples were injected with a Hamilton gas-tight syringe (500 or 1000 μl). The reaction vessel (10 mm diameter, 50 cm high) used for separation of the nitrogen from the solution was the same as that used by Swinnerton et al. [9]. This vessel was connected in place of the gas pipette at the six-way teflon valve (Fig. 1). The evolved nitrogen was dried with a

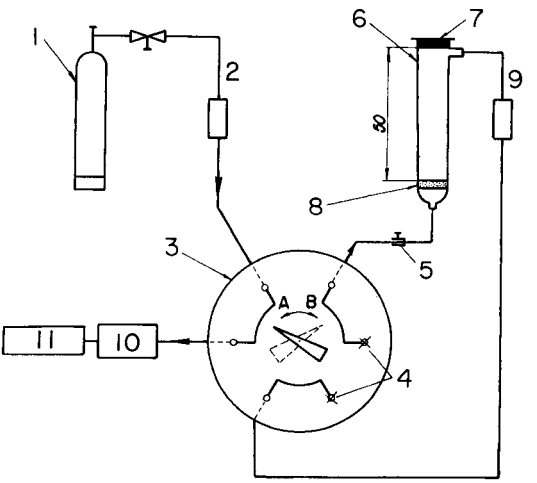

Fig. 1. Schematic diagram of the apparatus (not to scale). (1) Helium cylinder; (2) drying tube; (3) six-way valve; (4) outputs; (5) screw seal; (6) reaction vessel; (7) rubber septum; (8) coarse glass frit; (9) drying tube; (10) gas chromatograph; (11) recorder.

85 × 4-mm column packed with layers of molecular sieve 4A, magnesium perchlorate and molecular sieve 4A.

To examine the effect of foreign substances on the azide determination, an all-glass gas bubbler, the total volume of which was 4 ml, containing 2 ml of solution (to absorb unoxidized hydrogen sulphide or sulphur dioxide) was connected behind the reaction vessel, to protect the thermistor.

Procedure. Turn the valve (3; Fig. 1) to position A so that the helium flows directly to the column. Introduce 1 ml of the cerium solution into the reaction vessel and attach the vessel to the valve port. Set the valve to position B and displace air from the cerium solution until a stable baseline is obtained on the recorder. Through the rubber septum (7) inject a sample of azide solution, the volume of which must not exceed 2 ml. When the trace has returned to baseline, return the valve to position A, remove the reaction vessel, wash it, again fill it with cerium solution, and reconnect it as described above. The equipment is then ready for the next run.

Results and discussion

Azide ions are oxidized to nitrogen by cerium ions(IV) in acidic media. The nitrogen obtained is removed from the reaction mixture by helium. This method [9] proved to be the best way of determining microgram quantities of gases in liquids by gas chromatography. The reaction vessel has a coarse glass frit to break up the gas flow and thus release the nitrogen quickly and quantitatively, and prevent peak tailing. Before introduction to the chromatographic column, the gas is dried in order to avoid destruction of the filling of the chromatographic column.

If the set-up is air-tight and the analyzed sample is free of dissolved air, then the height (or area) of the chromatographic peak is proportional to the quantity of azide in the sample. If, however, the sample has not been deaerated before oxidation, an oxygen peak appears before the nitrogen peak, which indicates that the nitrogen peak is increased by the nitrogen in the air in the sample. Azide can be determined without deaerating the sample, but the blank nitrogen signal must be subtracted.

The optimization of the redox reaction between cerium(IV) and azide was described previously [1]. In the present study, it was found that, provided an excess of cerium(IV) is present, the reproducibility does not depend on the cerium(IV) concentration. Also, in order to achieve good reproducibility the sample should be deaerated thoroughly, and it should not exceed 2 ml. The presence of an excess of cerium(IV) can easily be detected by its yellow colour. Under the above conditions, 5—120 μg of azide can be determined. The sensitivity depends on the sensitivity of the instrument used. The most commonly applied detector is the katharometer, although more sensitive detectors such as ionization detectors can be used with obvious advantages. When a katharometer is used, the sensitivity of the method is similar to that of the spectrophotometric procedures with iron(III) [2, 3] or copper(II) [5], but it is poorer than the indirect spectrophotometric method [1]. To

estimate the accuracy and precision of the method, samples containing 25 and 50 μg of azide were processed six times each. The mean recoveries were 100 and 101%, respectively, and the relative standard deviations were 5.3% and 3.2%, respectively.

Effect of foreign ions. The effects of ions which interfered in other procedures, was investigated. The most important were cyanide, thiocyanate, sulphide, thiosulphate, and sulphite [2, 5]. It was found that the determination of 25 μg of azide by the present method, was not affected by 1500 μg of cyanide, 80 μg of sulphite, 50 μg of sulphide, 40 μg of thiosulphate or 20 μg of thiocyanate. Moreover, 1000 μg of iron(III), copper(II) or lead(II) did not interfere, though these cations form complexes with azide. The extremely slow oxidation of cyanide by cerium(IV) may explain why cyanide does not interfere. When the amounts of sulphur-containing ions exceeded the above values, azide recovery was decreased, even in the presence of sufficient cerium(IV) to oxidize all interfering ions as well as the azide ions. Because the reaction proceeds in acidic medium, some hydrogen sulphide or sulphur dioxide may be liberated, beside the oxidation of the sulphur compounds to elementary sulphur (H_2S) or sulphate (SO_3^{2-} and $S_2O_3^{2-}$).

This work was done within the problem MR. I-32 coordinated by the Faculty of Chemistry, Warsaw University.

REFERENCES

1 E. Kubaszewski and Z. Kurzawa, Chem. Anal. Warsaw, 30 (1985) 609.
2 C. Robertson and C. Austin, Anal. Chem., 29 (1957) 854.
3 A. Anton, J. Dodd and A. Harren, Anal. Chem., 32 (1960) 1209.
4 R. Wallace and E. Dukes, J. Phys. Chem., 65 (1961) 2994.
5 E. Neves, E. De Oliveira and L. Sant'Agostino, Anal. Chim. Acta, 87 (1976) 243.
6 R. G. Clem and E. H. Huffman, Anal. Chem., 37 (1965) 366.
7 B. M. Maya and C. J. Stedman, J. Chem. Soc. Dalton Trans., 2 (1983) 257.
8 T. S. Vivekandam and M. S. Ramachandran, Indian J. Chem., Sect. A, 22 (1983) 629.
9 J. W. Swinnerton, V. J. Linnenbom and C. H. Check, Anal. Chem., 34 (1962) 483.

Analytica Chimica Acta, 196 (1987) 271—275
Elsevier Science Publishers B.V., Amsterdam — Printed in The Netherlands

Short Communication

FACTORS INFLUENCING SENSITIVITY AND ACCURACY FOR THE DETERMINATION OF ALKYLSELENIDES AND TETRAALKYLLEAD COMPOUNDS BY GAS CHROMATOGRAPHY/ATOMIC ABSORPTION SPECTROMETRY

S. G. JIANG
Department of Chemistry, Hebei University, Baoding (China)
D. CHAKRABORTI and F. ADAMS*
Department of Chemistry, University of Antwerp (U.I.A.), B2610 Wilrijk (Belgium)
(Received 11th August 1986)

Summary. Factors affecting the quantitative collection of dimethylselenide, diethylselenide and dimethyldiselenide, as well as of tetraalkyllead compounds from the air by the cryogenic trap technique and their determination, by gas chromatography/atomic absorption spectrometry are described. Flash injection (and the addition of ca. 10% of hydrogen to the carrier gas) provide a highly sensitive detection.

The biomethylation of inorganic selenium to alkylselenide species in the environment has been discussed by several authors [1—5], but data on the determination of these volatile alkylselenides in the air are scarce because it is not easy to collect and determine these compounds quantitatively. In earlier publications [6, 7], methodology was described for the preconcentration of volatile selenium species from the air and the subsequent determination of dimethylselenide, diethylselenide and dimethyldiselenide by gas chromatography with detection by graphite-furnace atomic absorption spectrometry (GC/AAS). The present communication describes a systematic study of a number of factors affecting the recovery of the compounds from the atmosphere and the sensitivity of determinations by GC/AAS. The parameters studied are also significant for the determination of other volatile organometallic species, e.g., tetraalkyllead compounds.

Experimental

The GC/AAS assembly used was identical to that reported previously [6—9], as were the instrumental parameters for the cryogenic trap separation, gas chromatography and atomic absorption spectrometry. For the introduction of the heat-sensitive compounds into the gas chromatography, flash evaporation was applied instead of direct injection at the end of the column [10].

Alkylselenide compounds were purchased from Strem Chemicals (Newburyport, MA). Stock solutions were prepared by dissolution in analytical

0003-2670/87/$03.50

reagent-grade pentane. Working solutions at the ng l^{-1} level were prepared daily from the stock solutions. The materials used for cryogenic trapping included glass beads of 4-mm diameter, pyrex glass wool and 4-mm diameter beads of poly(vinyl chloride) and polypropylene. A 2% solution of dimethylchlorosilane (DMCS) was used for silanizing. Tetraalkyllead compounds were obtained from the Associated Octell Co., South Wirral, Gt. Britain, and were likewise dissolved in pentane.

Results and discussion

Collection efficiency on cryogenic trap. For the measurement of the collection efficiency and recovery from the cryogenic trap, a sampling system was built in which the cryogenic trap was followed by a small U-shaped tube filled with glass wool, held at liquid nitrogen temperature. The contents of this tube were also analyzed for organoselenium compounds. As is apparent from Table 1, the cryogenic trap temperature must be maintained at −140°C for quantitative collection of the three compounds investigated at a flow rate of 6 l min^{-1} with pyrex glass wool as adsorbent. By comparison, −120°C is sufficient for quantitative recovery of tetraalkyllead compounds [9]. Several adsorbents were investigated at −140°C. The results are summarized in Table 2. It appears that the surface condition has an important effect on the recovery. The best recoveries are obtained for acid-

TABLE 1

Effect on cryogenic trap temperature on collection efficiency

Temperature (°C)	Collection efficiency (%)		
	Me_2Se	Et_2Se	Me_2Se_2
−140	96	100	95
−120	90	99	98
−100	56	90	98
−78	15	20	93

TABLE 2

Collection efficiency of adsorbents for alkylselenides

Species	Glass beads	Collection efficiency (%)					
		Poly(vinyl chloride)		Polypropylene		Pyrex glass wool	
		Untreated	Washed[a]	Untreated	Washed[a]	Untreated	Silanized
Me_2Se	98	73	100	73	84	93	96
Et_2Se	89	79	97	81	80	96	100
Me_2Se_2	84	60	96	41	80	99	95

[a]Washed with 1 M hydrochloric acid before use.

washed poly(vinyl chloride) and for pyrex glass wool but for the latter material collection from a large volume of air was impossible, because of clogging by ice.

Flash injection. It appeared during the analyses that dimethyldiselenide is the most thermally labile of the compounds investigated. Figure 1 shows the thermal stability of dimethyldiselenide as a function of the injector block temperature; decomposition becomes important above 140°C. A quick flash evaporation, in which the carrier gas is preheated by passing through a short length of GC tubing before it picks up the sample, was therefore selected in order to decrease as much as possible any thermal decomposition on the chromatographic column; the inlet end of the column was kept empty for a length of ca. 10 cm, thus shortening the time of contact of the compounds with the heated injector. Table 3 gives a comparison between the sensitivity obtained by flash injection and direct injection of the compounds onto the

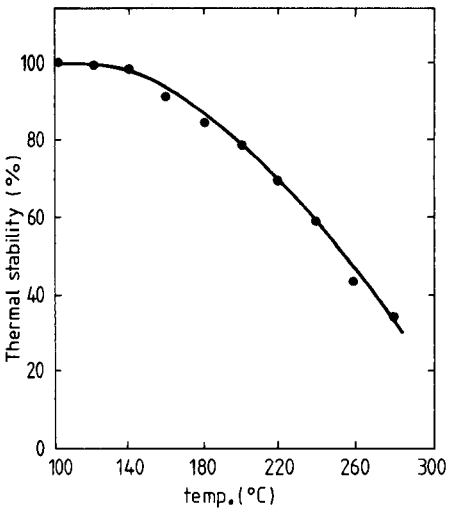

Fig. 1. Thermal stability of dimethyldiselenide in a flow system at various temperatures.

TABLE 3

Influence of injection mode and temperature on relative sensitivity for alkylselenides

Injection temp. (°C)	Relative sensitivity					
	Me_2Se		Et_2Se		Me_2Se_2	
	On-column	Flash	On-column	Flash	On-column	Flash
100	1.00[a]	0.83	1.00	1.03	2.30	3.08
200	1.24	0.93	1.07	1.11	2.00	2.97
260	1.30	1.07	1.09	1.04	1.00	2.27

[a]Arbitrary values relative to this result.

column from a dilute solution. Results obtained for tetraalkyllead compounds are summarized in Table 4.

No general conclusions can be formulated about the effect on sensitivity of flash injection of the organometallic compounds. The results confirm earlier reports that with flash injection sensitivity is significantly decreased for compounds of high thermal stability; for example, in the case of tetramethyllead, decomposition only becomes serious at ca. 265°C [11]. The overall gain in sensitivity for dimethyldiselenide must be due to the extreme heat-lability of this species whereas the more or less constant sensitivity for ethyl selenide in both injection modes probably results from a sensitivity increase caused by less thermal breakdown being compensated by a decrease caused by flash injection.

Atomic absorption detection. As was reported earlier, deuterium background correction does not correct for non-specific molecular absorption by various organic impurities at 196.1 nm [6]. The addition of ca. 10% hydrogen to the argon carrier gas circumvents this problem and, moreover, increases the sensitivity for the organoselenium species by a factor of about 2. Surprisingly, the application of this gas mixture does not enhance the sensitivity for tetraalkyllead species and even results in a slight reduction of the sensivitity for some of the compounds, as shown in Table 5.

TABLE 4

Influence of injection mode and temperature on relative sensitivity for tetraalkyllead compounds

Injection temp. (°C)	Relative sensitivity[a]									
	Me_4Pb		Me_3EtPb		Me_2Et_2Pb		$MeEt_3Pb$		Et_4Pb	
	OC	F	OC	F	OC	F	OC	F	OC	F
160	—	0.64	—	0.50	—	1.00	—	0.77	—	0.87
200	1.00[b]	0.52	1.00	0.38	1.04	0.63	1.04	0.42	1.16	0.35
220	1.05	0.56	1.13	0.37	1.26	0.58	1.33	0.42	1.71	0.35
260	1.09	0.55	1.08	0.33	1.00	0.51	1.00	0.36	1.00	0.32

[a]OC, on-column; F, flash. [b]As for Table 3.

TABLE 5

Effect on sensitivity of addition of 10% H_2 to Ar carrier gas

Species	Sensitivity gain	Species	Sensitivity gain
Dimethylselenide	1.9X	Tetramethyllead	0.6X
Diethylselenide	1.7X	Trimethylethyllead	0.5X
Dimethyldiselenide	1.9X	Dimethyldiethyllead	0.4X
		Methyltriethyllead	1.0X
		Tetraethyllead	1.0X

Under the previously reported instrumental conditions (injector temperature 100°C, detector temperature 160°C, column temperature programming from 40 to 130°C at 40°C min^{-1}, argon carrier gas with 10% H_2 at 125 ml min^{-1} and standard AAS measurement conditions at 196.1 nm), reproducible measurements for the alkylselenides were obtained with a detection limit of 0.07 ng m^{-3} for dimethylselenide, 0.03 ng m^{-3} for diethylselenide and 0.15 ng m^{-3} for dimethyldiselenide.

This work was supported financially by the National Fund for Scientific Research, Belgium.

REFERENCES

1 F. Challenger, Adv. Enzymol., 12 (1951) 429.
2 K. P. McConnell and O. W. Portman, J. Biol. Chem., 195 (1952) 277.
3 T. Hirooka and J. T. Galambos, Biochim. Biophys. Acta, 130 (1966) 313.
4 D. C. Reamer and W. H. Zoller, Science, 208 (1980) 500.
5 Y. K. Chau, P. T. S. Wong, B. A. Silverberg, P. L. Luxon and G. A. Bengert, Science, 192 (1976) 1130.
6 S. Jiang, W. De Jonghe and F. Adams, Anal. Chim. Acta, 136 (1982) 183.
7 S. Jiang, H. Robberecht and F. Adams, Atmos. Environ., 17 (1983) 111.
8 W. De Jonghe, D. Chakraborti and F. Adams, Anal. Chim. Acta, 115 (1980) 89.
9 W. De Jonghe, D. Chakraborti and F. Adams, Anal. Chem., 52 (1980) 1974.
10 L. Robbert, Modern Practice of Gas Chromatography, Wiley-Interscience, New York, 1977.
11 H. Shapiro and T. W. Frey (Eds.), Organic Compounds of Lead, Interscience, New York, 1968.

Analytica Chimica Acta, 196 (1987) 277—282
Elsevier Science Publishers B.V., Amsterdam — Printed in The Netherlands

Short Communication

DETERMINATION OF BISMUTH, CADMIUM AND LEAD IN SOIL EXTRACTS BY ATOMIC ABSORPTION SPECTROMETRY WITH LOOP SAMPLE INTRODUCTION

S. GÜCER* and M. DEMIR

Department of Chemistry, Faculty of Arts and Sciences, Inönü University, Malatya (Turkey)

(Received 11th August 1986)

Summary. Bismuth, cadmium and lead in soil extracts with aqua regia, 2 M nitric acid, 2.5% acetic acid or ammonium acetate solution from top-soils at different locations in Turkey, were determined by atomic absorption spectrometry with loop sample introduction. Detection limits were 0.8, 0.025 and 0.5 $\mu g\ ml^{-1}$ for bismuth, cadmium and lead, respectively, after concentration with ammonium pyrrolidinedithiocarbamate. Use of a silica tube for atom trapping improved the detection limits.

The determination of trace elements at $\leqslant \mu g\ g^{-1}$ levels in soil samples has become of increasing importance in agriculture. Excessive increases in the levels of some elements in soils caused by disposal of various wastes and atmospheric deposits on land can be harmful to plants and, with their introduction into the food chain, to human health. For that reason, the trace element content of soils from Erzurum has been investigated [1].

A wide range of extractants has been used in soil laboratories; for many purposes, the total trace-metal content of soil has become of less agricultural interest than the extractable content. Pickering [2] has outlined the selective chemical extraction of soil components with various extractants. Application of atomic absorption spectrometry (AAS) in the analysis of soils, fertilizers and other agricultural materials has been summarized by David [3] and lately by Bain et al. [4]. In soil testing, it is important to select a solvent that can extract many elements simultaneously, though this may result in a lower concentration of some trace species in the extracts. Thus many elements cannot be determined directly by flame AAS. For these cases, Delves cup [5] and electrothermal AAS have been used for cadmium [6—14], lead [8, 10—13] and bismuth [15] in digested and/or extracted soil samples. Hydride-generation and atom-trapping AAS techniques have been also used for bismuth [16—18] and cadmium and lead [19—21] in soil extracts, respectively.

Since its introduction to flame AAS, the applications of loop AAS have increased [22]. In previous work, chemical and spectral interferences have been investigated [23, 24] and the application of loop AAS to urine samples

0003-2670/87/$03.50

for lead has been reported [25]. This communication deals with a loop AAS procedure for the determination of bismuth, cadmium and lead in various soil extracts after an ammonium pyrrolidinedithiocarbamate-activated carbon preconcentration step.

Experimental

Reagents. All chemicals were analytical-reagent grade unless otherwise stated. Deionized water was used thoughout. The ammonium acetate solution (pH 7) was prepared by mixing 57.5 ml of concentrated acetic acid and 60 ml of ammonia (d = 0.91 g ml^{-1}) and diluting to exactly 1 l. Bismuth, cadmium and lead stock solutions (1000 mg l^{-1}) were used to prepare standard solutions by diluting with 2 M acid. Ammonium pyrrolidinedithiocarbamate (APDC; Hopkin and Williams) solution was prepared by dissolving 0.2 g of APDC in 100 ml of 50% ethanol. Activated carbon (Merck) was purified by boiling with concentrated hydrochloric acid for 3 h, washing with water, drying at 110°C and treating with aqua regia for 24 h; the solution was filtered through filter paper (Schleicher & Schüll, blue band), washed with water and dried at 110°C; 2.5 g of the activated carbon was stirred in 100 ml of water. Buffer (pH 8) was prepared by mixing 8 ml of ammonia liquor with 107 g of ammonium chloride and diluting to exactly 1 l.

Apparatus. A Perkin-Elmer model 400 atomic absorption spectrometer (without background corrector) equipped with a 5-cm air/acetylene head and a loop device [22] was used for the atomic absorption measurements. Single-element hollow-cathode lamps were used as radiation sources. Slits and wavelengths were selected from the instrument manual. Acetylene and air flow rates of 2.3 and 8.6 l min^{-1}, respectively, were used for flame/loop measurements. A silica tube (7 mm o.d.) was used as a collector and positioned ca. 0.5 cm above the primary reaction zone of the flame. Samples were injected with a Witeg pipette (10 μl) onto the loop. After a drying step (110°C, ca. 20 s) the samples were released into the flame (or under the collection tube in the flame) with a 0.2-s electrical heating pulse. Peak-height measurements were used to calculate absorbance values.

Procedure. Top-soils (0—20 cm) collected from different locations of Malatya in Turkey were used as sample material. Before extraction, the material was air-dried at room temperature and homogenized by hand grinding in an agate mortar. A 10-g sample was shaken for 2 h in a Hetofrig shaker (160 rpm) with 60 ml of extractant (ammonium acetate solution, 2.5% acetic acid, 2 M nitric acid or aqua regia). Aqua regia extracts were evaporated to dryness and the residue was dissolved in 50 ml of 2 M nitric acid. The whole extracts were filtered through Whatman 42 paper and diluted to 100 ml. After addition of 15 ml of buffer solution (pH 8), 10 ml of 20 mg ml^{-1} APDC solution (sometimes more, depending on the sample) was added, and 100 mg of activated carbon in suspension was transferred from a pipette. The suspension was shaken mechanically for 1 h and filtered, and the residue was dried at 110°C. After addition of 2 ml of concentrated nitric acid to the

residue and evaporation to dryness, the residue was shaken with 5 ml of 2 M nitric acid. The solution was separated by centrifugation and used for AAS, with either direct injection (100 μl) or loop introduction (10 μl).

Results and discussion

As in measurements by electrothermal AAS, the signal shape in loop AAS depends on factors such as the chemical species of the element introduced, the loop heating rates and the flow rates of the flame gases. The effects of acid matrices were investigated. An enhancement of cadmium absorbance was found in the presence of 2 M hydrochloric and acetic acids compared to 2 M nitric acid (Fig. 1A). This is related to the atomization mechanisms and decomposition rates which are inversely proportional to the dissociation energies, 67 and 50 kcal mol^{-1} for CdO and CdCl, respectively [26]. The increase in sensitivity in acetic acid may therefore arise from the reduction of CdO by decomposition products of acetic acid such as carbon [27]. A similar explanation can be used for lead, with dissociation energies of 51 and 90 kcal mol^{-1} for PbCl and PbO, respectively (Fig. 1B). The atomization mechanism for bismuth species seems to be more complex (Fig. 1C). When 1000 μg ml^{-1} Na, K, Ca, Mg, Fe or Al was added to acidic solutions, >90% recoveries were found for bismuth, cadmium and lead. Any interferences from iron could be eliminated by addition of sufficient APDC during the enrichment step.

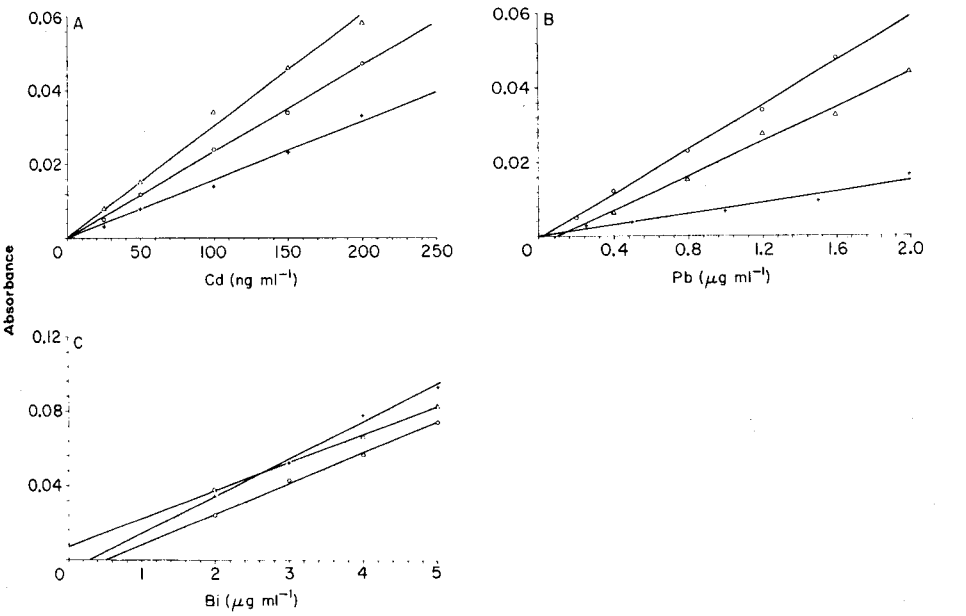

Fig. 1. Calibration graphs in various acids by loop AAS: (A) cadmium; (B) lead; (C) bismuth. Acid: (△) 2 M HCl; (○) 2 M acetic acid; (+) 2 M nitric acid.

It is interesting that, for cadmium determination, the loop could merely be heated in air, in the absence of a flame. The various peak-height calibration graphs for cadmium are shown in Fig. 2.

Detection limits derived from 3 times the signal/noise ratio for bismuth, cadmium and lead were 0.8, 0.025 and 0.5 mg l^{-1}, respectively by flame/loop AAS (0.10 mg Cd l^{-1} without the flame). When the silica collection tube was used detection limits were up to 3 times better. The relative standard deviations (RSD) for six replicate analyses of standard solutions are summarized in Tables 1 and 2. The concentration ranges for cadmium and lead extractable into acetic acid and ammonium acetate from the Turkish soils were found to be 0.12—0.48 and 0.06—5.52 $\mu g\ g^{-1}$, respectively (Table 3). The range for cadmium was shifted to higher values (0.38—0.98 $\mu g\ g^{-1}$) when

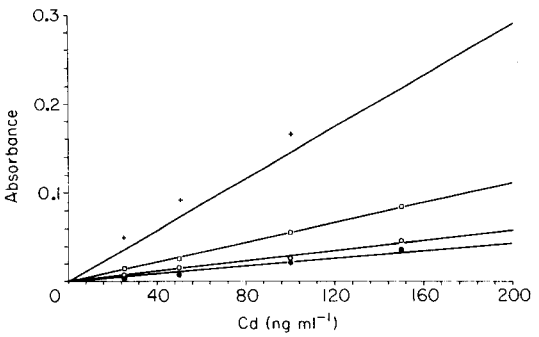

Fig. 2. Calibration graphs for cadmium: (+) in air/acetylene flame with collection tube; (□) in air with collection tube; (○) in air; (●) in air/acetylene flame.

TABLE 1

The relative standard deviation (RSD) for cadmium and lead measurements with use of the loop and silica tube

Concentration (mg l^{-1})	RSD (%) (n = 6)			
	Loop method		Silica tube method	
	Cadmium	Lead	Cadmium	Lead
0.025	29.6	—	4.9	—
0.050	17.3	20.0	1.8	27
0.100	9.2	16.2	3.0	4.3
0.150	4.9	11.6	1.5	4.4
0.200	3.5	4.2	1.8	3.1
0.400	1.0	6.7	1.5	3.3
0.800	1.3	3.0	0.7	1.0
1.200	1.0	0.9	0.8	0.8
1.600	1.6	1.7	1.3	0.5
2.000	1.5	1.3	0.8	0.7

TABLE 2

The relative standard deviation for bismuth measurements with use of the loop and silica tube

Conc. (mg l^{-1})	1.0	2.0	3.0	4.0	5.0	10.0
RSD (%): loop	—	—	11.6	14.3	5.4	2.5
Silica tube	2.9	2.0	3.3	2.9	2.8	1.2

TABLE 3

Cadmium, lead and bismuth contents in acetic acid, ammonium acetate and nitric acid extracts of twelve Turkish top-soils from Malatya[a]

Soil number	2.5% Acetic acid		Ammonium acetate (pH 7)		2 M Nitric acid	
	Cd	Pb	Cd	Pb	Cd	Bi[b]
MA02001	0.36	2.28	0.48	1.38	0.98	4.58
MA02004	0.16	2.36	0.14	1.52	0.44	3.20
MA02007	0.18	2.50	0.12	1.28	0.38	3.12
MA02010	0.14	5.52	0.14	1.44	0.44	2.18
MA02013	0.12	0.06	0.12	0.30	0.32	2.65
MA02016	0.22	1.32	0.12	0.90	0.56	2.90
MA02022	0.26	0.84	0.12	0.30	0.56	1.02
MA02023	0.18	0.84	0.18	0.44	0.38	4.30
MA02024	0.12	0.74	0.16	1.54	0.66	1.80
MA02025	0.56	1.24	0.32	1.32	0.84	2.46
MA02026	0.42	2.48	0.48	1.26	0.88	1.87
MA02027	0.36	1.64	0.34	1.46	0.62	1.60

[a] All data are given as $\mu g\ g^{-1}$ in the air-dried soil. [b] With silica collection tube.

2 M nitric acid was used as extractant. Bismuth was found only in aqua regia extracts of soils, with a range of 1.0—4.6 $\mu g\ g^{-1}$ (Table 3).

The authors are grateful to the Institut für Spektrochemie, Dortmund, for technical support.

REFERENCES

1 S. Kirimhan, T. Saglam and S. Karakaplan, Atatürk University, Journal of Agriculture, 14 (1983) 13.
2 W. F. Pickering, Crit. Rev. Anal. Chem., 10 (1981) 233.
3 D. J. David, Prog. Anal. Atom. Spectrosc., 1 (1978) 255.
4 D. C. Bain, M. L. Berrow, W. J. McHardy, E. Paterson, J. D. Russell, B. L. Sharp, A. M. Ure and T. S. West, Anal. Chim. Acta, 180 (1986) 163.
5 H. L. Kahn, F. J. Fernandez and S. Slavin, At. Absorpt. Newsl., 11 (1972) 42.
6 M. J. Dudas, At. Absorpt. Newsl., 13 (1974) 109.
7 A. M. Ure and M. C. Mitchell, Anal. Chim. Acta, 87 (1976) 283.
8 A. M. Ure, M. P. Hernandez-Artiga and M. C. Mitchell, Anal. Chim. Acta, 96 (1978) 37.
9 W. Schmidt and F. Dietl, Fresenius' Z. Anal. Chem., 295 (1979) 110.
10 K. L. Iu, I. D. Pulford and H. J. Duncan, Anal. Chim. Acta, 106 (1979) 318.

11 I. I. Petrov, D. L. Tsalev and A. E. Barsev, At. Spectrosc., 1 (1980) 47.
12 B. Pedersen, M. Willems and S. S. Jørgensen, Analyst, 105 (1980) 119.
13 G. P. Sighinolfi and A. M. Santos, Mikrochim. Acta, 1 (1976) 477.
14 R. T. T. Rantala and D. H. Loring, At. Spectrosc., 1 (1980) 163.
15 J. S. Kane, Anal. Chim. Acta, 106 (1979) 325.
16 A. M. Kersabiec, Analusis, 8 (1980) 97.
17 B. Pahlavanpour, M. Thompson and L. Thorne, Analyst, 105 (1980) 756.
18 D. S. Lee, Anal. Chem., 54 (1982) 1682.
19 C. M. Lau, A. M. Ure and T. S. West, Anal. Chim. Acta, 146 (1983) 171.
20 C. M. Lau, A. M. Ure and T. S. West, Anal. Proc., 20 (1983) 114.
21 S. M. Fraser, A. M. Ure, M. C. Mitchell and T. S. West, J. Anal. At. Spectrosc., 1 (1986) 19.
22 H. Berndt and J. Messerschmidt, Spectrochim. Acta, Part B, 34 (1979) 241.
23 S. Gücer and H. Berndt, Talanta, 28 (1981) 334.
24 S. Gücer and A. E. Karagözler, CSI XXIV, Book of Abstracts, Vol. 3, 1985, p. 490.
25 H. Berndt, S. Gücer and J. Messerschmidt, J. Clin. Chem. Clin. Biochem., 20 (1982) 85.
26 R. E. Sturgeon, C. L. Chakrabarti and C. H. Langford, Anal. Chem., 48 (1976) 1792.
27 B. V. L'vov and L. F. Yatsenko, Zh. Anal. Khim., 39 (1984) 1773.

Analytica Chimica Acta, 196 (1987) 283—286
Elsevier Science Publishers B.V., Amsterdam — Printed in The Netherlands

Short Communication

DETERMINATION OF LITHIUM IN WINES BY ATOMIC ABSORPTION SPECTROMETRY

C. BALUJA-SANTOS*, A. GONZÁLEZ-PORTAL and J. M. BOUZAS-BOUZAS

Department of Analytical Chemistry, Faculty of Chemistry, The University, Santiago de Compostella-15706 (Spain)

(Received 28th July 1986)

Summary. Lithium (10—150 ng ml^{-1}) in wine is determined by atomic absorption spectrometry by direct nebulization and after digestion with mixed acids. The results of both methods are similar. Thirty-four wines from various Spanish provinces are analysed.

Lithium was first found in ash from wine in 1878 [1], and its presence was later confirmed spectroscopically [2] but its determination in wine is ill-documented compared with the extensive research reported on other metals [3]. The concentration of lithium in wine is normally 20—300 ng ml^{-1} (though these values may be increased by the use of lithium chloride to catalyze fermentation, by adulteration or by contamination by containers). These low concentrations, together with the difficulty of determining lithium by classical techniques, have discouraged the proliferation of analytical methods. Mass spectrometry (MS) [4] and atomic emission spectrometry (AES) [5] have been used, but the application of atomic absorption spectrometry (AAS) has not received the attention it deserves, in spite of the development of long-life hollow-cathode lamps. This communication reports the determination of lithium in wine by AAS with either an air/acetylene flame, as is normal for the determination of lithium [6] or an air/propane flame that has been used for the determination of other alkali metals in wine by AES and AAS [7—10].

Experimental

Apparatus and reagents. A Perkin-Elmer model 303 atomic absorption spectrometer was used with a lithium hollow-cathode lamp run at 10 mA and a 670-nm red filter; the provided chart recorder was a model 165 (Perkin-Elmer Hitachi). When an air/propane flame was used, the standard low-temperature burner was shielded to prevent variations caused by air currents [11]. Propane and acetylene were both 99.5% pure. The instrument parameters used were: observation height above burner, 10 mm (air/C_2H_2), 15 mm (air/propane); fuel pressure, 0.35, 0.28 kg cm^{-2}; air pressure, 0.35, 0.56 kg cm^{-2}; nebulization uptake rate, 1.0 ml min^{-1} in both cases.

0003-2670/87/$03.50

Merck Titrisol standard 100 μg ml^{-1} lithium solution was diluted to yield 50.0, 75.0, 100.0 and 150.0 ng ml^{-1} solutions. All other reagents were of analytical grade and were used as received. None of the latter interfered with the atomic absorption signal under the conditions used.

Preparation of the sample. Direct injection and wet digestion methods were used. For direct injection, filter the wine sample through a 0.5-μm pore membrane, dilute if necessary and nebulize directly. For wet digestion [12], transfer 10 ml of filtered wine and 0.5 ml of concentrated sulphuric acid to a three-necked round-bottomed 100-ml flask with a thermometer in one neck, a 20-ml graduated funnel containing concentrated nitric acid in another and in the third a 100-mm condenser leading to an Erlenmeyer flask via a 14/23 mm connector joined to a vacuum line. Distil off the first alcohol fractions and add 2.5 ml of concentrated nitric acid dropwise from the funnel. Re-heat the acidified sample for a few minutes (collecting the distillate), allow to cool, add 5 ml of double-distilled water and re-heat for ca. 10 min until white fumes are given off. Allow to cool, transfer to a 10-ml volumetric flask and dilute to volume with double-distilled water. Nebulize this solution.

Results and discussion

The methods described above were used to determine the lithium contents of 34 white, red or rosé wines from various regions of Spain. Table 1 lists the maximum, minimum and mean values measured for each wine.

Direct injection method of wine samples for AAS minimizes manipulation and has been recommended [13], but it may give rise to errors in that wine contains various components capable of interfering with the measurement. In the work described here, direct nebulization and wet digestion methods were compared.

TABLE 1

Determination of lithium in spanish wines

Type of wine	Lithium conc. (ng ml^{-1})[a]					
	Maximum		Mean		Minimum	
	A	B	A	B	A	B
Air/Acetylene flame						
White	142	100	74	60	18	13
Red	119	100	53	46	25	20
Rosé	57	50	41	37	18	20
Air/Propane flame						
White	149	114	80	65	19	19
Red	124	108	62	52	30	26
Rosé	63	62	47	43	24	21

[a]Mean for 12 white, 14 red or 8 rosé wines. A, direct procedure. B, after wet digestion.

TABLE 2

Recovery of lithium added to wines

Air/Acetylene flame			Air/Propane flame		
Li total[a] (ng ml^{-1})	Li found[b] (ng ml^{-1})	Recovery (%)	Li total[a] (ng ml^{-1})	Li found[b] (ng ml^{-1})	Recovery (%)
Direct nebulization			White wines		
69.5	70.3 ± 0.5	101	80	82.3 ± 2.0	103
81.5	84.8 ± 0.6	104	92	93.6 ± 0.9	101
94.5	96.9 ± 0.6	102	115	119.6 ± 1.0	104
119.5	125.6 ± 0.7	105	130	140.4 ± 1.2	108
Wet digestion					
57	57.9 ± 0.3	102	64.5	67.2 ± 0.6	104
69	69.8 ± 0.5	101	76.5	78.8 ± 0.2	103
82	81.7 ± 0.3	100	89.5	90.7 ± 0.1	101
107	107.8 ± 0.6	101	114.5	118.3 ± 0.5	103
Direct nebulization			Red wines		
53	54.5 ± 0.1	103	54	56.0 ± 0.0	104
65	66.4 ± 0.9	102	76	77.6 ± 0.6	102
78	83.2 ± 0.4	107	89	96.6 ± 0.8	108
103	107.7 ± 1.3	105	114	121.0 ± 1.0	106
Wet digestion					
44	45.4 ± 0.3	103	51	52.2 ± 0.5	102
56	57.4 ± 0.4	102	63	64.8 ± 1.0	103
69	69.9 ± 0.6	101	76	77.9 ± 1.0	102
94	94.3 ± 0.4	100	101	101.3 ± 0.6	100

[a]Concentration added plus that originally present. [b]Mean ± standard deviation (n = 3).

The accuracy of the procedures was evaluated by measuring the recovery of lithium added to white and red wines immediately prior to their injection into the spectrometer. In all instances, quantitative recoveries were obtained (Table 2).

Precision was estimated by determining the lithium content of 7 replicates of each of two series of samples (one white wine and one red wine) to some of which known quantities of lithium were added. The relative standard deviations for the direct and wet digestion procedures were very similar, being 2—3% for wines to which no lithium had been added, and 1—2% for wines containing added lithium. There was generally no differences in precision between the two flames or types of wine used.

The methods described above for the determination of lithium in wines by AAS were satisfactory. Direct nebulization is simpler than wet digestion and is therefore recommended. The method should be applicable to other beverages of low alcohol content (<6%). The manipulation of the sample is minimal, thus reducing the risk of contamination during preparative procedures. Precision and accuracy are good. The working range is 10—150 ng ml^{-1} and the limit of detection is about 1 ng ml^{-1}.

TABLE 3

Lithium content in wines of various countries

No of samples	Method	Region	Lithium conc. (mg l^{-1})		
			Mean	Range	Ref.
25	AES	France	0.22	0.13—0.25	5
(Various)	AAS	Italy[a]	—	0.00—0.09	8
13	AAS	France	0.02	0.01—0.4	10
27	AAS	Spain	1.35	0.40—2.7	9
4	MS	—[b]	0.03	0.01—0.06	4

[a]Legal limit in Italy is 16.4 mg l^{-1}. [b]Wines of various countries.

The wines examined here had neither been treated with lithium chloride nor suffered contamination from other sources of lithium. The lithium contents measured are similar to those of wines from other countries (Table 3) and together with the lithium contents of mineral waters from the same areas suggest that the soils of these regions contain little lithium.

The authors thank Bodegas Bouzas Hnos. (Padron), La Coruña (Spain) for the gift of wine samples and F. Bermejo for assisting with the work described.

REFERENCES

1 H. W. Dahlen, 3rd Congr. of Viticulture, Würzburg, 1878.
2 J. A. Muller, Ann. Chim. Phys., 11 (1897) 394.
3 C. Baluja, A. Gonzalez-Portal and F. Bermejo, Analyst, 109 (1984) 797.
4 H. R. Schulten, U. Bahr and W. D. Lehmann, Mikrochim. Acta., (I) (1979) 191.
5 M. Ney, Ann. Falsif. Expert. Chim., 58 (1965) 263.
6 D. J. Halls, Spectrochim. Acta, Part B, 32 (1977) 397.
7 M. D. Guelbenzu, Ann. Bromatol. (Madrid), 3 (1951) 319.
8 A. Amati and R. Rastelli, Ind. Agrarie (Florence), 5 (1967) 233.
9 F. Bermejo and C. Baluja, Acta Cient. Compostelana, 9 (1972) 123; Paper presented at XVII Coll. Spectrosc. Intern (CSI) Florence, September (1973).
10 J. C. Cabanis, S. Brun and P. Bussel, Trav. Soc. Pharm. (Montpellier), 27 (1967) 111.
11 W. J. Price, Analytical Atomic Absorption Spectrometry, Heyden, London, 1972, p. 31.
12 J. Ribereau-Gayon, E. Peynaud, P. Sudraud and P. Ribereau-Gayon "Sciences et Techniques du vin. Analyse et control des vins". Vol. I, Dunod Paris (1972) p. 253.
13 J. Bonastre, Ann. Falsif. Fraudes, 48 (1955) 347.

Analytica Chimica Acta, 196 (1987) 287—292
Elsevier Science Publishers B.V., Amsterdam — Printed in The Netherlands

Short Communication

PRECONCENTRATION AND DETERMINATION OF TRACE METALS IN SYNTHETIC SEA WATER BY FLOTATION WITH INERT ORGANIC COLLECTORS

M. CABALLERO, R. LOPEZ, R. CELA* and J. A. PEREZ-BUSTAMANTE
Analytical Chemistry Department, Faculty of Sciences, University of Cadiz, Cadiz (Spain)
(Received 4th August 1986)

Summary. The preconcentration and separation of copper, cadmium, cobalt and nickel 8-quinolinolates in solutions of high salinity including synthetic sea water is studied with phenolphthalein or 2-naphthol as collector and octadecylamine as surfactant. A simplex optimization is applied. Yields >90% are achieved for Ni, Co and Cd with both collectors, but the copper yield is low. Flame atomic absorption spectrometry is used for the final measurements.

Heavy metals have received a great deal of attention in the study of marine pollution. Their low concentrations in sea water mean that preconcentration is needed during their determination. The usual preconcentration techniques, such as liquid/liquid extraction, ion-exchange, coprecipitation and evaporation, need time and large amounts of sample. These inconveniences may partly be avoided by the use of flotation techniques [1] which have proved to be of great utility [2—4] in the preconcentration of trace elements in natural [5—9], waste [6, 9—12] and marine waters [8, 13—16].

Of the flotation techniques described, co-flotation is probably most applied; numerous co-precipitants or collectors, both inorganic and organic, have been studied. In practice, however, the hydrated oxides of iron [5, 9, 10, 13—15, 17—19], indium [8, 20], aluminum [9, 10, 17], tin [21] and zirconium [22] are the compounds most used as collectors. Kuznetsov [23] and later Myasoedova [24] described the analytical use of "inert" organic collectors in separation processes. In spite of the advantages that these offer compared to classical collectors (e.g., their greater sensitivity, selectivity and ease of destruction if required before the final measurement of the collected species), they have hardly been used recently [25] and their applications as collectors in flotation processes have not been studied.

The present study describes the flotation of copper, cobalt, cadmium and nickel 8-quinolinolates in solutions of high salinity and synthetic sea water [26] with inert organic reagents (phenolphthalein or 2-naphthol) as the collector, and octadecylamine (ODA) and sodium dodecylsulfate (SDS) as the surfactants. The process was optimized by means of the COFLOT program [27].

0003-2670/87/$03.50

Experimental

Apparatus and reagents. The flotation cell has been described [28, 29]. The final measurements were made with a Pye Unicam SP9-800 atomic absorption spectrometer with an air/acetylene flame.

The reagents used were of analytical grade, except for the surfactants. Octadecylamine was from Eastman and SDS from Scharlau (pure).

Procedure for optimization. For the study of the optimum flotation conditions of the metal 8-quinolinolates with phenolphthalein or 2-naphthol, exactly 1 l of 3.5% (w/v) sodium chloride solution was placed in a beaker, and exactly 1 ml of a multistandard solution containing 1.000 $\mu g\ ml^{-1}$ each of the metals to be studied was added. The amounts of 8-quinolinol (as a 4% w/v solution in 8% v/v acetic acid) and inert collector (10% w/v solution of phenolphthalein or 2-naphthol in ethanol) established in the optimization process were also added. The pH was adjusted by addition of ammonia or sodium hydroxide solution, and the required volume of ODA (6.0 $g\ l^{-1}$ in ethanol) was added. The mixture was stirred during the induction time. The solution was placed in the flotation cell, in which the air flow had been previously adjusted to the optimum value; then 2 ml of SDS (0.01 M) was added as flotation began, and again after 2 and 5 min. Samples of ca. 5 ml were taken at 30 s, 1, 2, 4, and 10 min, in centrifuge tubes with screw tops containing 0.15 ml of concentrated hydrochloric acid. Residual concentrations in the solution of the four metals were measured by atomic absorption spectrometry (a.a.s.). The sum of the flotation percentages of all the elements was taken as the response function.

Recommended procedure. Under the optimum conditions established for the two collectors (air flow-rate 100 $ml\ min^{-1}$, 5 or 10 ml of 8-quinolinol solution, 7.5 ml of phenolphthalein solution or 5 ml of 2-naphthol solution, pH 7.0, 7.5 or 5 ml of surfactant and 10-min induction time), experiments were done with 1.5-l samples of 3.5% sodium chloride solution and synthetic sea water, to which a concentration of 16.6 $\mu g\ l^{-1}$ of each of the metals had been added. After 10 min flotation, the air stream was stopped and the mother liquor was sucked out, first through the side-drain of the column and finally under vacuum through the sintered-glass plate at the bottom of the column. The precipitate was dissolved in 20 ml of methyl isobutyl ketone/ethanol/6 M hydrochloric acid (40:40:20 by volume). The resulting solution, together with the rinsing liquid, was placed in a 50-ml volumetric flask, and made up to volume with the above solvent. The trace metal concentrations in this solution were determined by a.a.s., with use of a standard additions method.

Results and discussion

Optimization of flotation of metal 8-quinolinolates with phenolphthalein or 2-naphthol. During the optimization process, it was necessary to add a surfactant to make the foam more consistent and to inhibit its coalescence, thus avoiding re-entry of the floated material into the solution. The use of

TABLE 1

Data and results of simplex optimization for the complex formation with 8-quinolinol (8-HQ) and collection with phenolphthalein (PP)[a]

Test	Vertices retained	Air	ODA	PP	pH	Time	8-HQ	Recovery (%)				
								Ni	Co	Cu	Cd	Total
Experiment 1												
1		80	5.0	1.5	6.0	8.0	4.0	97	95	64	80	336
2		40	5.0	1.5	6.0	8.0	4.0	97	90	57	73	317
3		80	8.0	1.5	6.0	8.0	4.0	98	96	88	90	372
4		80	5.0	0.6	6.0	8.0	4.0	96	98	82	77	353
5		80	5.0	1.5	8.0	8.0	4.0	96	93	60	85	332
6		80	5.0	1.5	6.0	0.0	4.0	98	91	58	76	323
7		80	5.0	1.5	6.0	8.0	8.0	100	97	71	85	353
8	1, 3, 4, 5, 6, 7	160	6.5	1.1	7.0	4.0	6.0	94	97	61	90	342
9	1, 3, 4, 5, 7, 8	120	7.2	0.8	7.2	22.0	7.0	93	87	75	88	343
10	3, 4, 5, 7, 8, 9	140	8.4	0.5	8.2	13.0	8.5	94	85	73	90	342[b]
11	3, 4, 7, 8, 9, 10	140	8.4	0.5	5.6	13.0	8.5	93	78	82	70	323
12	3, 4, 7, 8, 9, 10	125	7.5	0.8	6.2	11.8	7.4	95	95	72	95	357
13	3, 4, 7, 8, 9, 12	42.5	2.9	2.1	2.9	4.9	1.2	—	—	—	—	—
14	3, 4, 7, 8, 9, 12	75	4.7	1.6	4.7	7.6	3.6	92	50	81	—	238
15	3, 4, 7, 8, 9, 12	91	5.6	1.3	5.5	8.9	4.8	91	89	61	46	287
16	3, 4, 7, 8, 9, 12	99.3	6.1	1.2	6.0	9.6	5.4	90	92	65	90	337
17	3, 4, 7, 5, 9, 12	103	6.3	1.1	6.2	9.9	5.7	95	92	62	89	338
Experiment 2												
1		80	5.0	1.5	6.0	8.0	4.0	97	93	62	80	332
2		150	5.0	1.5	6.0	8.0	4.0	97	94	58	67	316
3		80	1.0	1.5	6.0	8.0	4.0	97	96	84	37	314
4		80	5.0	5.0	6.0	8.0	4.0	99	95	75	77	346
5		80	5.0	1.5	4.0	8.0	4.0	98	57	53	19	227
6		80	5.0	1.5	6.0	15.0	4.0	96	91	65	76	328
7		80	5.0	1.5	6.0	8.0	1.0	94	80	76	46	296
8	1, 2, 3, 4, 6, 7	115	3.0	3.2	10.0	11.5	2.5	31	50	81	70	232
9	1, 2, 3, 4, 6, 7	68	5.7	0.9	2.0	6.8	4.5	—	—	—	—	—
10	1, 2, 3, 4, 6, 7	80	5.0	1.5	4.0	8.0	4.0	94	56	52	4	206
11	1, 2, 3, 4, 6, 7	86	4.7	1.8	5.0	8.6	3.8	100	86	62	6	254

TABLE 1 (continued)

Test	Vertices retained	Air	ODA	PP	pH	Time	8-HQ	Recovery (%)				
								Ni	Co	Cu	Cd	Total
12	1, 2, 3, 4, 6, 7	103	3.7	2.7	8.0	10.3	3.0	91	95	80	91	357
13	1, 2, 3, 4, 6, 12	127	2.3	3.8	7.0	12.7	9.5	91	83	70	89	333[c]
14	1, 3, 4, 6, 12, 13	33	2.3	3.8	7.0	12.7	5.5	91	92	75	89	347
15	1, 4, 6, 12, 13, 14	92	9.7	6.2	8.0	17.3	7.0	69	64	51	75	259
16	1, 4, 6, 12, 13, 14	88	6.8	4.6	7.3	14.2	6.0	60	72	51	83	265
17	1, 4, 6, 12, 13, 14	86	5.3	3.8	7.0	12.7	5.5	86	84	63	84	317

[a]The air flow rate is given in ml min^{-1}; time (i.e., induction time) is given in minutes. For ODA, PP and 8-HQ, the optimized parameter is the volume (ml) of the solution at the concentration given in the text. [b]Vertex 5 rejected because of the worse kinetic features. [c]Vertex 2 rejected because of the worse kinetic features.

non-ionic [30] or ionic [31] surfactants such as SDS has been recommended. The proportions of the surfactant are never critical, so it was not necessary to include this parameter in the optimization algorithm.

From the data on coprecipitation with phenolphthalein [32], two simplexes were initiated in zones close to those for optimum collection of the selected 8-quinolinolates. Their evolution, as well as the percentages flotation obtained for each ion, appears in Table 1. In both simplexes the search for optimum conditions was considered to be complete after 17 experiments because, with the exception of copper, the elements showed flotation at or above 90%. The values of the variables at the optima obtained in each case are similar, indicating that the global optimum has probably been achieved. The mean value of both vertices was chosen as the global optimum.

Flotation with 2-naphthol [32] was optimized in a similar way. The optimum conditions were very similar to those for phenolphthalein, and mean optimum recoveries were 94% (Ni, Co, Cd). Results for copper were unreliable.

Recovery of floated material. To study the analytical applicability of co-flotation with inert collectors, a series of experiments was carried out with 1.5 l of 3.5% sodium chloride solution and synthetic sea water, spiked with 16.6 $\mu g\ l^{-1}$ of each of the elements to be studied. The results obtained are shown in Table 2. From these results, several conclusions can be drawn. First, there are clear differences between the effectiveness of the collectors at such low concentrations of metal ions. Phenolphthalein gives greater recoveries than 2-naphthol, comparable with those for hydrated metal oxides as collectors [31]. Secondly, if these results are compared with those in Table 1, the difficulty of achieving complete multi-elemental separations with such

TABLE 2

Recoveries in highly saline and synthetic sea-water samples

Element	Recovery (%)[a]			
	Phenolphthalein		2-Naphthol	
	NaCl (3.5%)	Sea water	NaCl (3.5%)	Sea water
Cu	66 ± 11	70 ± 12	—	—
Co	81 ± 13	82 ± 6	40 ± 22	39 ± 29
Cd	91 ± 11	83 ± 6	74 ± 8	61 ± 20
Ni	89 ± 4	79 ± 12	78 ± 9	58 ± 19

[a]Mean ± standard deviation (n = 6) for 16 $\mu g\ l^{-1}$.

collectors becomes evident, especially for copper, although conditions do exist under which recoveries approaching 100% are achieved for some of the ions investigated. This behaviour is to be expected, taking into account the higher selectivity of the inert organic collectors as compared with the inorganic collectors.

The authors thank the Comisión Asesora de Investigación Cientifica y Técnica of the Spanish Ministry of Science and Education for financial support.

REFERENCES

1 R. Lemlich (Ed.), Adsorptive Bubble Separation Techniques, Academic, New York, 1972.
2 A. A. Clarke and D. J. Wilson, Sep. Purif. Methods, 7 (1978) 55.
3 M. Hiraide and A. Mizuike, Rev. Anal. Chem., Freund Publishing, VI (1982) 151.
4 A. Mizuike and M. Hiraide, Pure Appl. Chem., 54 (1982) 1956.
5 S. Nakashima and M. Yagi, Bunseki Kagaku, 33 (1984) 1.
6 S. D. Huang, C. H. F. Fann and H. S. Hsieh, J. Colloid Interface Sci., 89 (1982) 504.
7 S. Nakashima, Bull. Chem. Soc. Jpn., 54 (1981) 291.
8 M. Hiraide, T. Ito, M. Baba, H. Kagaguchi and A. Mizuike, Anal. Chem., 52 (1980) 804.
9 J. Y. Gau and S. D. Huang, Chie Mien K'o Hsueh, 24 (1985) 2.
10 S. D. Huang and D. J. Wilson, Sep. Sci. Technol., 19 (1984) 603.
11 M. A. Slapik, E. L. Tackston and D. J. Wilson, Procd. Ind. Waste Conf., CA., 35 (1980) 694.
12 E. L. Tackston, D. J. Wilson, J. S. Hanson and D. L. Miller; Water Pollut. Control Fed., 52 (1980) 317.
13 S. Nakashima and M. Yagi, Fresenius' Z. Anal. Chem., 314 (1983) 155.
14 R. S. Schreedhara and D. E. Ryan, Anal. Chem., 55 (1983) 682.
15 X. Feng and D. E. Ryan, Anal. Chim. Acta, 162 (1984) 47.
16 X. Feng and D. E. Ryan, Int. J. Environ. Anal. Chem., 19 (1985) 273.
17 S. M. Nemets, A. K. Charikov and Y. I. Turkin, Vestn. Leningr. Univ. Fiz. Khim., 4 (1983) 65.
18 S. Nakashima and M. Yagi, Anal. Chim. Acta, 157 (1983) 187.
19 E. H. de Carlo and D. M. Thomas, Environ. Sci. Technol., 19 (1985) 538.
20 M. Hiraide, K. Sakurai and A. Mizuike, Anal. Chem., 52 (1980) 2861.

21 U. Dietze, J. Braun and H. J. Peter, Fresenius' Z. Anal. Chem., 322 (1985) 17.
22 S. Nakashima and M. Yagi, Anal. Chim. Acta, 147 (1983) 213; Anal. Lett., 117 (1984) 1693; Bunseki Kaguku, 31 (1982) E431.
23 V. I. Kuznetsov, J. Anal. Chem. USSR-Tr. Engl., 9 (1954) 221.
24 G. V. Myasoedova, J. Anal. Chem. USSR-Tr. Engl., 21 (1966) 533.
25 S. Ostrowsky and K. Szefer, Stud. Mater. Oceanol., 25 (1979) 189, 221, 235.
26 D. R. Kester, J. W. Duedall, D. N. Connors and R. M. Pytkowicz, Limnol. Oceanogr., 12 (1967) 176.
27 M. Caballero, R. Cela and J. A. Perez-Bustamante, Sep. Sci. Technol., 21 (1986) 39.
28 R. Cela and J. A. Perez-Bustamante, Afinidad, 39 (1982) 107.
29 J. Cervera, R. Cela and J. A. Perez-Bustamente, Analyst, 107 (1982) 1425.
30 E. H. de Carlo, H. Zeitlin and Q. Fernando, Anal. Chem., 52 (1982) 898.
31 L. M. Cabezon, M. Caballero, R. Cela and J. A. Perez-Bustamante, Talanta, 31 (1984) 37.
32 W. P. Tapmeyer and E. E. Pickett, Anal. Chem., 34 (1962) 1709.

Analytica Chimica Acta, 196 (1987) 293—297
Elsevier Science Publishers B.V., Amsterdam — Printed in The Netherlands

Short Communication

THE APPLICATION OF THE RŮŽIČKA-TYPE IODIDE-SELECTIVE ELECTRODE FOR THE DETERMINATION OF CYANIDE IN ALCOHOLIC DRINKS

MILANA V. BUDIMIR*

Faculty of Agriculture, University of Osijek, YU-54000 Osijek (Yugoslavia)

MILAN SAK-BOSNAR

Pedagogical Faculty, University of Osijek, YU-54000 Osijek (Yugoslavia)

MOMIR S. JOVANOVIĆ

Faculty of Technology and Metallurgy, Department of Analytical Chemistry, University of Belgrade, P.O. Box 494, YU-11000 Belgrade (Yugoslavia)

(Received 17th July 1986)

Summary. The Selectrode with iodide Selectrode powder is used successfully to determine cyanide in pure solutions and in alcoholic drinks at 0.2—2 mg l^{-1} levels. The calibration slope was ca. 63.5 mV/decade concentration in pure solutions but changed in alcoholic solution. A double standard addition method was needed for free cyanide determinations in alcoholic drinks.

The determination of small amounts of cyanide is important in agricultural chemistry, in plant biochemistry, in the pharmaceutical industry and in various other fields, because of its extreme toxicity. Cyanide has been found in more than 2000 plant species. Glucosides containing cyanide are also common in many cultivated plants (e.g., in almonds, plums, cherries and peaches, and in distilled products of certain fruits). Although the glucoside itself is not toxic to human or animal organisms, its hydrolysis produces free hydrocyanic acid. Accurate, sensitive and simple methods for cyanide determinations are essential. Chemical methods for the determination of cyanide in plants have been reviewed by Seifert [1]. Spectrophotometric and titrimetric methods are mainly used [2], the former giving the best results for <1 mg l^{-1} cyanide. For higher concentrations, ion-selective electrodes [3] are now used increasingly. Gillingham et al. [4] used a cyanide electrode to screen forage samples for their cyanide content. György et al. [5] applied a silver iodide-based silicone-rubber electrode for the potentiometric determination of cyanide in distillates from plant hydrolysates. The Orion cyanide electrode was developed especially for cyanide [6—8]. Silver sulfide electrodes can also be used [8].

In this communication, the Růžička-type graphite/PTFE electrode is used for the determination of cyanide in some commercially available alcoholic

0003-2670/87/$03.50

drinks. This electrode is activated by powdered AgI/Ag_2S sensing material. The Růžička-type graphite/PTFE electrode and Orion 94-06 electrode are compared for their usefulness in accurate and fast determinations of cyanide at low concentrations.

Theory

The cyanide-sensitive electrode is based on a membrane of silver sulfide and silver iodide. The free cyanide ions react with the very slightly soluble silver iodide in the membrane phase according to the reaction:

$$AgI + 2CN^- \rightarrow Ag(CN)_2^- + I^- \quad (1)$$

The potential of the electrode is governed by the iodide ion activity and can be expressed by the Nernst equation:

$$E = E_0 - S \log a_{I^-}$$

Substitution of the equilibrium constant of reaction 1 in this equation and rearrangement gives the expression

$$E = E^{0'} - S \log (a^2_{CN^-}/a_{Ag(CN)_2^-})$$

Given that $a_{Ag(CN)_2^-} = 1/2a_{CN^-}$, the electrode potential is related to the cyanide ion activity by

$$E = \text{constant} - S \log a_{CN^-}$$

The major problem with the cyanide electrode is obviously the corrosion of the sensing phase. The rate of corrosion depends on the cyanide concentration, and is severe in $>10^{-3}$ mol l^{-1} cyanide solutions. Because the electrode responds only to free cyanide, sample solutions must be adjusted to pH 11.5—13 to avoid the formation of undissociated hydrocyanic acid.

Experimental

Apparatus. An Orion 801 A digital Ionalyzer was used with an Orion Model 94-06 cyanide electrode or a Radiometer Selectrode F-3012 (with S42515 Iodide powder), and an Orion Model 90-02 double-junction reference electrode with 10% (w/v) potassium nitrate in 10^{-3} mol l^{-1} potassium hydroxide in the outer compartment.

Solutions. Stock cyanide solutions (1000 mg l^{-1}) and diluted standard cyanide solutions (100, 10, 1 and 0.1 mg l^{-1}) were prepared in the usual way [2]. Solutions containing <100 mg l^{-1} cyanide were prepared daily. The stock cyanide solution was standardized against standard silver nitrate solution.

Procedure. The Selectrode was prepared in the usual way by rubbing a few milligrams of Iodide Selectrode Powder on the graphite surface and polishing the surface. Between measurements, the electrode was kept in the 0.1 mg l^{-1} cyanide solution. The Orion cyanide electrode was used and stored as suggested in the instruction manual. All measurements were done at constant

temperature and constant stirring rate. The potentials were read when they remained unchanged for at least 60 s. Both the electrodes were calibrated in the usual way.

The solutions of alcoholic drinks for measurements were prepared as follows: 5 ml of alcoholic beverage was diluted with deionized water and the pH was adjusted to 11.5 with 1 mol l^{-1} sodium hydroxide. The solutions were then diluted to exactly 50 ml.

For the standard addition method, 50 ml of sample was used. The potentials were read initially and after additions of 0.1 ml and 0.5 ml of standard 1000 mg l^{-1} potassium cyanide solution. Potential readings were stable within 60 s.

Results and discussion

Calibration of electrodes. The calibration curves obtained for 0.01—100 mg l^{-1} cyanide are shown in Fig. 1. For all calculations and statistical treatment [9], the linear region 0.1—100 mg l^{-1} was used. For six series of calibration measurements with the S electrode, the mean slope, S, was found to be 63.5 with a 95% confidence interval of ±1.1 (correlation coefficient 0.99998). There was no significant difference between the means of the six series or between the standard deviations of the means. The slopes, S, of the E/log C

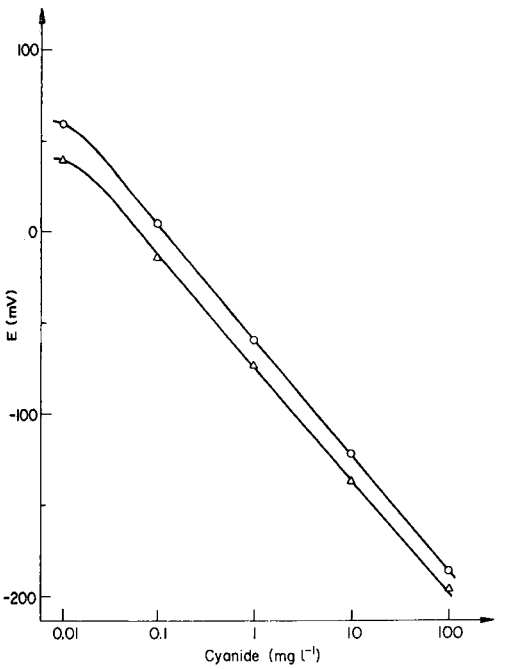

Fig. 1. Calibration graphs for cyanide: (△) Orion 94-06 electrode; (○) Selectrode F-3012 with S-42515 silver iodide powder.

plots for the Selectrode and for the Orion 94-06 electrode were in good agreement but differed from theoretical 59 mV/decade concentration by a few mV. Both electrodes could be applied for cyanide determination. For example, when the Selectrode was tested in 0.200 and 2.00 mg l^{-1} cyanide solutions, the concentrations found by the standard addition method were 0.201 and 2.06 with standard deviations of 0.017 and 0.08 (n = 5), respectively.

Determination of free cyanide levels in alcoholic drinks. Free cyanide in alcoholic drinks was determined by the double standard addition method. The results obtained showed that the cyanide concentrations calculated after the second addition were ca. 60% greater than those after the first addition. Because the standard addition method requires a reliable value of the slope, the observed differences indicated that the experimentally found slope cannot always be used in real situations. Hence, the cyanide concentration was estimated by the double standard addition method with an unknown electrode slope.

The e.m.f. of anion-selective electrode and a reference electrode dipped in a solution of unknown measured anion concentration C_x is

$$E_x = E_0 - S \log f(C_x)$$

The symbols have their usual meanings. After the additions of precisely known volumes of a standard solution to give added concentrations C_1 and C_2, the new value E_1 and E_2 are given by

$$E_1 = E_0 - S \log f(C_x + C_1)$$

$$E_2 = E_0 - S \log f(C_x + C_1 + C_2)$$

If constant ionic strength and constant liquid-junction potential are assumed and volume changes are neglected, the above equations can be solved to give

$$(E_2 - E_1) \log (C_x) - (E_2 - E_x) \log (C_x + C_1) + (E_1 - E_x) \log (C_x + C_1 + C_2) = 0$$

TABLE 1

Results obtained for the free cyanide levels in some commercial alcoholic drinks

Sample	Cyanide found[a] (mg l^{-1})	
	Orion electrode	Selectrode
Apricot	0.22 (0.03)	0.18 (0.05)
Cherry I	0.77 (0.12)	0.67 (0.13)
Cherry II	1.88 (0.21)	1.75 (0.11)
Plum brandy	1.75 (0.24)	1.55 (0.19)

[a]Mean of 5 determinations with standard deviation in parentheses.

This equation cannot be solved explicitly for C_x, but it is readily solved by computer or trial-and-error methods.

The free cyanide levels obtained by the double standard addition method with the Selectrode were computed as described above with the results shown in Table 1. The results agree well with those obtained with the Orion cyanide electrode. Application of Student's *t*-test and the *F*-test showed that there was no significant difference between the two sets of results at the 95% confidence level. The determination described takes only a few minutes.

REFERENCES

1 Pl. Seifert, Moderne Methoden der Pflanzenanalyse, Bd. IV, Springer, Berlin, 1955, p. 676.
2 Standard Methods for the Examination of Water and Wastewater, APHA Washington, 14th edn., 1976, p. 372.
3 J. H. Riseman, Am. Lab., 4 (1972) 63.
4 J. T. Gillingham, M. M. Shirer and N. R. Page, Agron. J., 61 (1969) 717.
5 B. György, L. Andre, L. Stehli and E. Pungor, Anal. Chim. Acta, 46 (1969) 318.
6 H. Clusters, F. Adams and F. Verbeek, Anal. Chim. Acta, 83 (1976) 27.
7 G. A. Rechnitz and R. A. Llenado, Anal. Chem., 43 (1971) 283.
8 M. S. Frant, J. W. Ross Jr. and H. Riseman, Anal. Chem., 83 (1976) 27.
9 K. Doerffel, Statistik in der analytischen Chemie, VEB Deutscher Verlag, Leipzig, 1984.

Analytica Chimica Acta, 196 (1987) 299—303
Elsevier Science Publishers B.V., Amsterdam — Printed in The Netherlands

Short Communication

MICRODETERMINATION OF ALKALOIDS IN ORGANIC SOLVENTS BY POTENTIOMETRIC TITRATION

WANG CHANG-YI*, ZHANG DONG-HUA, GUO YONG-LI, ZHONG HUI-MING and WEN MENG-LIANG

Department of Chemistry, Yunnan University, Kunming, Yunnan (China)

(Received 11th June 1986)

Summary. A small-interfacial voltaic cell (antimony scratch) is shown to be satisfactory for end-point detection in titrations of various alkaloids and other basic drugs and their salts in ethanol, chloroform or dibutyl ether media with picric acid in the same medium. Small (0.4—4 mg) amounts can be determined. This method has the advantages of being simple and rapid with sharp end-points. The recoveries were 96.5—100.8% for determinations of 19 drugs and their salts. The relative error was ±5% for five pharmaceutical tablets and injections.

Numerous methods have been published for the determination of alkaloids [1]. Recently, the determination has been conducted with the use of ion-selective electrodes [2]. An interfacial voltaic cell was described by Waligóra and Paluch [3] for the determination of n-tridecylamine, strychnine and some other alkaloids.

In this communication, a similar small interfacial voltaic cell is recommended for determinations of milligram levels of alkaloids and some other drugs in 10 ml of organic solvent and of microgram levels in 1 ml of organic solvent. The cell is of suitable dimensions for immersion in any type of titration vessel with a volume of 10 ml or 5 ml, and serves as an end-point indicator for acid/base potentiometric titrations in non-aqueous solvents. The cell has the advantages of being simple and of providing sharp end-points. Standard methods for alkaloids in the Pharmacopoeia [4, 5] are time-consuming, whereas the proposed method takes only about 10 min. The method is convenient for the determination of alkaloids, especially uncommon alkaloids, and is practical for use in pharmacological and phytochemical research.

Experimental

Equipment. The cell used is shown in Fig. 1. Its height is 50 mm and its width 10 mm. The electrochemical cell is Pt/antimony scratch—corundum disc/0.1 M KCl/Ag/AgCl. The cell was used with a pH/millivolt meter and a magnetic stirrer with plastic-coated stirring bar (1-mm diameter, 0.5 cm long). Microlitre syringes (100 μl and 10 μl) were also required.

0003-2670/87/$03.50

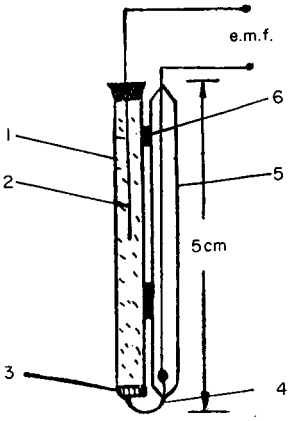

Fig. 1. The electrochemical cell. (1) Glass tube (4-mm diameter) filled with 0.1 M KCl; (2) Ag/AgCl wire; (3) corundum disc with antimony scratch; (4) Pt wire (0.5-mm diameter); (5) glass tube (3-mm diameter) with shielded connecting wire; (6) holding clips.

Reagents. Standard solutions (0.008 M) of picric acid or picrolonic acid in the required organic solvent were prepared in 50-ml volumetric flasks. The titres were determined by titration against atropine (microanalytical reagent). Analytical-reagent-grade solvents used were chloroform, ethanol and dibutyl ether.

The compounds tested were brucine, aconitine, atropine, berbamine, cinchonine, heroin, narcotine, physostigmine, reserpine, scopolamine, α-solanine, strychnine, anisodine hydrobromide, procaine hydrochloride, quinine dihydrochloride, scopolamine hydrobromide, strychnine nitrate, erythromycin and diphenhydramine hydrochloride. The tablets tested contained atropine sulphate, diphenhydramine hydrochloride, erythromycin and quinine sulphate. Procaine hydrochloride was determined in injections.

Procedure for alkaloids Weigh accurately 1—4 mg or 0.5—1 mg of the sample into a vessel with a volume of 10 ml or 5 ml, respectively. Place 10 ml or 1 ml of organic solvent into the vessel, insert the cell and stir the solution. While stirring magnetically, titrate with 0.008 M picric acid (or picrolonic acid) in the same solvent, in equal increments (100 μl or 10 μl) from the microlitre syringe. Calculate the end-point from the second derivative in the usual way. Normally, 0.050—1.500 ml of the titrant is consumed.

Procedure for alkaloids as their salts. Dissolve the salt in a little deionized water. Add 5% (w/v) sodium hydroxide solution dropwise to make the solution alkaline and liberate the alkaloid from its salt. Extract the alkaloid with the organic solvent several times. Place the organic solution in the vessel, insert the cell in the solution and titrate as described above.

Procedure for pharmaceutical preparations. For tablets containing atropine sulphate or quinine sulphate, soak 10 tablets of atropine sulphate or 1 tablet of quinine sulphate overnight in deionized water. Add the 5% sodium

hydroxide solution dropwise until the solution becomes just alkaline. Extract the solution five times with chloroform and dilute the extract to 25.00 ml with chloroform. Pipette 10.00 ml of the atropine/chloroform solution or 3.50 ml of the quinine/chloroform solution into the titration vessel. Immerse the cell in the solution and titrate with picric acid in chloroform.

For diphenhydramine hydrochloride tablets, soak one tablet in deionized water overnight. Make the solution alkaline, as described above. Extract the solution five times with dibutyl ether and dilute the extracts to 25.00 ml with dibutyl ether. Pipette 5.00 ml of this solution into the vessel and titrate with picric acid in dibutyl ether.

For erythromycin tablets, grind one tablet to a fine powder and soak overnight in ethanol. Filter the solution and dilute to 25.00 ml with ethanol. Pipette 1.25 ml of the solution into the vessel and titrate with picric acid in ethanol.

For procaine hydrochloride injections, pipette 0.50 ml of the solution and make it just alkaline as described above. Extract the solution five times with chloroform and dilute the extracts to 25.00 ml with chloroform. Pipette 7.00 ml of this solution into the vessel and titrate with picric acid in chloroform.

Results and discussion

The titration curves had the usual sigmoidal shape with well-defined end-points. For example, in the titration of 10 ml of 5.49×10^{-4} M brucine in chloroform with 8.466×10^{-3} M picric acid in chloroform, the total change in potential was ca. 220 mV during the addition of 1 ml of titrant, with a sharp 100-mV jump at the end-point.

The analytical results for alkaloids and their salts, and pharmaceutical preparations are shown in Tables 1 and 2, respectively.

These acid/base titrations are based on the Lewis concept of acids and bases in which their combination is interpreted in terms of the formation of a coordinate covalent bond. A Lewis acid can accept and share a lone pair of electrons donated by a Lewis base. This is the principle on which the above titrations are based, and it also explains why compounds like theophylline, caffeine and theobromine cannot be determined by the method. These three alkaloids have the structure

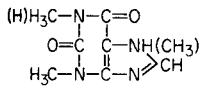

Because the lone electron pair of the nitrogen atom is affected by conjugation, its ability to donate the lone electron pair is weak, i.e., the basicity of these alkaloids is so weak that they cannot be titrated by this method.

TABLE 1

Results for alkaloids and their salts by titration with picric acid

Compound	Formula	Weight (mg)	Solvent	Recovery (%)
Brucine[a]	$C_{23}H_{26}O_4N_2$	2.021—2.575	Chloroform	99.99 ± 0.25[b]
Aconitine	$C_{34}H_{47}O_{11}N$	1.942	Chloroform	99.2
		2.490		96.3
Atropine[a]	$C_{17}H_{23}O_3N$	2.194	Chloroform	100.2
		2.946		100.4
Berbamine	$C_{37}H_{40}O_6N_2$	1.561	Chloroform	99.1
		1.102		98.8
Cinchonine	$C_{19}H_{22}ON_2$	2.520	Chloroform	98.4
		1.798		100.2
Erythromycin	$C_{37}H_{67}O_{13}N$	0.4110	Ethanol	98.4
		0.5021		99.2
Heroin	$C_{21}H_{23}O_5N$	1.925	Chloroform	99.0
		2.051		99.5
Narcotine	$C_{22}H_{23}O_7N$	2.407	Chloroform	100.1
		2.664		99.9
Physostigmine	$C_{15}H_{21}O_2N_3$	2.058	Chloroform	99.5
		2.298		100.5
Reserpine	$C_{33}H_{40}O_9N_2$	4.748	Chloroform	100.4
		1.820		100.8
Scopolamine	$C_{17}H_{21}O_4N$	2.350	Chloroform	97.1
α-Solanine	$C_{45}H_{73}O_{15}N$	0.4033	Ethanol	98.9
		0.5280		96.7
Strychnine	$C_{21}H_{22}O_2N_2$	2.837	Chloroform	99.4
		2.623		97.3
Anisodine hydrobromide	$C_{17}H_{21}O_5N \cdot HBr$	2.153	Chloroform	97.9
		3.012		96.65
Diphenhydramine hydrochloride	$C_{17}H_{21}ON \cdot HCl$	2.753	Dibutyl ether	100.1
Procaine hydrochloride	$C_{13}H_{20}O_2N_2 \cdot HCl$	3.954	Chloroform	100.7
		3.741		99.95
Quinine dihydrochloride	$C_{20}H_{24}O_2N_2 \cdot 2HCl$	4.052	Chloroform	98.25
		4.117		97.2
Scopolamine hydrobromide	$C_{17}H_{21}O_4N \cdot HBr \cdot 3H_2O$	4.112	Chloroform	99.25
		4.003		98.5
Strychnine nitrate	$C_{21}H_{22}O_2N_2 \cdot HNO_3$	2.241	Chloroform	96.9
		2.023		96.5

[a]Picrolonic acid could also be used as titrant. [b]Average recovery and average error for 8 titrations.

TABLE 2

Results for pharmaceutical preparations, tablets or injections

Sample	Amount per tablet (or injection) (mg)	Found (mg)	Relative error (%)
Atropine	0.3	0.295	−1.7
sulphate[a]		0.293	−2.3
Diphenhydramine	25	25.02	+0.1
hydrochloride[a]		25.96	+3.8
Erythromycin[a]	125	123.0	−1.6
		124.0	−0.8
Quinine	120	113.0	−5.8
sulphate[a]		126.6	+5.0
Procaine	40	39.98	−0.5
hydrochloride[b]		40.35	+0.9

[a]Tablet. [b]Injection.

This work was supported by the Science Fund of the Chinese Natural Sciences.

REFERENCES

1 N. D. Cheronis and T. S. Ma, Organic Functional Group Analysis, Wiley, New York, 1964, p. 279.
2 T. S. Ma and S. S. M. Hassan, Organic Analysis Using Ion-Selective Electrodes, Academic Press, London, 1982, p. 150.
3 B. Waligóra and M. Paluch, Anal. Chim. Acta, 119 (1980) 375; 132 (1981) 229.
4 Chinese Pharmacopoeia, 1977.
5 British Pharmacopoeia, 1980.

Analytica Chimica Acta, 196 (1987) 305—310
Elsevier Science Publishers B.V., Amsterdam — Printed in The Netherlands

Short Communication

NATIVE PEROXYOXALATE CHEMILUMINESCENCE FROM THE REACTION OF BIS(2,4-DINITROPHENYL) OXALATE AND HYDROGEN PEROXIDE PERTURBED BY NONFLUOROPHORES

A. C. CAPOMACCHIA*, R. N. JENNINGS, S. M. HEMINGWAY, P. D'SOUZA, W. PRAPAITRAKUL AND A. GINGLE

The University of Georgia, College of Pharmacy, Athens, GA 30602 (U.S.A.)

(Received 1st September 1986)

Summary. The reaction of bis(2,4-dinitrophenyl) oxalate and hydrogen peroxide yields an excited-state product that luminesces with greatest intensity at ca. 400 nm. The weak intensity is enhanced by some agents that normally do not fluoresce. In pure solutions, the detection limits for the nonfluorophores ouabain and urea, based on this effect, are 2.0 and 20 pmol, respectively.

The use of peroxyoxalate chemiluminescence for determinations of efficient fluorophores is well known [1—6]. The use of bis(2,4-dinitrophenyl) oxalate (DNPO) in the experimental system is not common because it is less stable than other aryl oxalate esters, in particular bis(2,4,6-trichlorophenyl) oxalate (TCPO) [7], but DNPO has recently been recommended for the pH range 2—4 [1]. In later tests, it was found here that in some cases as much as a thousand-fold increase in sensitivity can be achieved with DNPO compared to TCPO; but the background intensity was invariably large, which initially was considered a nuisance. This background was present regardless of the solvent used or which synthetic batch the DNPO was obtained from. By accident it was discovered that the injection of a nonfluorophore enhanced the background signal from solutions of DNPO and hydrogen peroxide, but not as strongly as a fluorophore. These effects are investigated below.

Experimental

Procedures. Chemiluminescence reactions were studied with an in-house designed and constructed flow-injection or static-injection system (Fig. 1). For flow-injection work, the two 50-ml syringes S_1 and S_2 were driven by an infusion pump (Harvard Apparatus Company). Syringe S_1 was filled with hydrogen peroxide solution and syringe S_2 with oxalate ester solution. Analyte sample solutions, which may be either a fluorophore or nonfluorophore, were injected into the peroxide stream by means of a Rheodyne valve (Model 7010) with a 20-μl sample loop, or a Hamilton syringe. The peroxide and ester solutions mixed at a teflon Y-shaped joint and were delayed for ca. 30 s in a stainless-steel coil before passing through the flow

0003-2670/87/$03.50

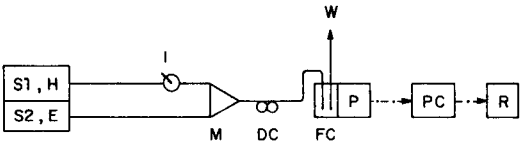

Fig. 1. Flow-injection system: S_1 S_2, syringes 1 and 2; H, hydrogen peroxide, E, ester; I, injection port; M, mixing point; DC, delay coil; FC, flow cell; W, waste; P, photomultiplier tube; PC, photon counter; R, recorder.

cell (3 μl). Emission was monitored and amplified by a photomultiplier tube (Hamamatsu R464) and a photon counter (Hamamatsu Model C-1230). Signals were recorded on either a strip-chart recorder or integrator. All connecting tubing was teflon or stainless steel.

Static-injection work was done on the same apparatus after disconnecting the delay coil. Injections of oxalate ester (100 μl) followed by hydrogen peroxide (100 μl) were made directly into a larger flow cell (300 μl) and the emission intensity was immediately recorded. Injections of solvent (10—100 μl) and nonfluorescing agents (10—100 μl) were made immediately after peroxide addition, and the emissions were recorded.

Fluorescence was measured with a Perkin-Elmer MPF-44A fluorimeter. Spectra were obtained for the luminescent reaction product(s) from the reaction of DNPO and hydrogen peroxide in chloroform, butyl or ethyl acetate, or acetonitrile. Spectra for TCPO and TBTO (bis(6-trifluoromethyl-benzotriazol-1-yl) oxalate) could not be obtained because of the native fluorescence of these agents and their breakdown products. Attempts to "blank out" the native fluorescence electronically with a microprocessor failed. DNPO and its precursor DNP (2,4-dinitrophenol) did not fluoresce in the above solvents even when the highest possible electronic amplification and maximum excitation and emission bandpass (20 nm) were used. Each solvent used and all hydrogen peroxide solutions also did not fluoresce under these instrumental conditions. Native chemiluminescence spectra were recorded after the excitation shutter was closed. The spectra were maintained at the same relative intensity by altering electronic amplification, but maintaining the emission bandpass at 20 nm in order to more easily compare peak position and vibrational structure. Therefore, the spectral intensity shown in Fig. 2 for the reaction in acetonitrile is actually 20% of that in the other three solvents. Intensity enhancement by ouabain (1×10^{-7} M) and urea (1×10^{-6} M) as shown later in Fig. 2 is roughly eightfold.

Flow-injection experiments showing native chemiluminescence enhancement by the nonfluorophores ouabain and urea were done with the assembly shown in Fig. 1.

All measurements were made at least in quadruplicate.

Chemicals. Chloroform and ethyl acetate were "resi-analyzed"-grade (for pesticide analysis with low trace hydrocarbon) solvents, and acetonitrile was HPLC-grade (J. T. Baker). Butyl acetate was "spectro"-grade (Aldrich

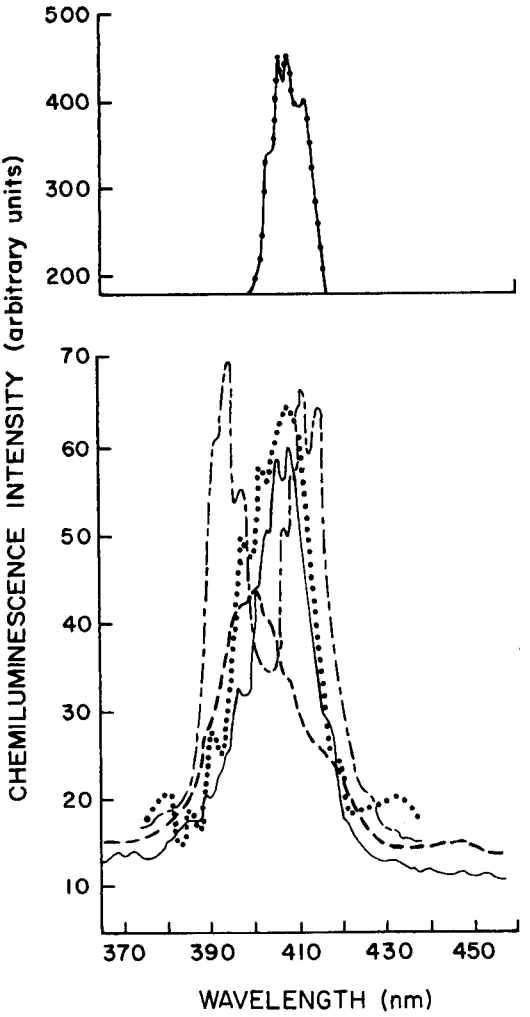

Fig. 2. Chemiluminescence spectra recorded after adding 100 μl of H_2O_2 in chloroform (—), ethyl acetate (---), butyl acetate (...) or acetonitrile (-·-) to 2.0 ml of 1.0×10^{-2} M DNPO in the same solvent in a quartz cuvette. The H_2O_2 concentration was 0.088 M for acetonitrile and 0.88 M for the other solvents. An example of native peroxyoxalate chemiluminescence intensity enhancement by ouabain (1×10^{-7} M) in chloroform is shown in the upper part.

Chemical). All solvents were used as received and displayed no inherent fluorescence. Hydrogen peroxide (30%) and urea (Fisher Scientific Company) were used as received. Ouabain was obtained from Sigma Chemical Company and DPA (diphenylanthracene) and pyrene from Aldrich. Solutions of ouabain, urea and hydrogen peroxide in the above solvents demonstrated no fluorescence. DNPO was synthesized from the above and other fluorescence-free chemicals as described by Rauhut et al. [8] (39.8% C calc., 39.7% found;

1.4% H calc., 1.5% found). TCPO and TBTO were purchased from the Chemical Dynamics Company.

Results and discussion

The native peroxyoxalate chemiluminescence spectra from the reaction product(s) of DNPO and hydrogen peroxide in chloroform and butyl acetate solutions demonstrate vibrational structure and a maximum at around 406 nm (Fig. 2). In ethyl acetate the spectrum shows less structure with a maximum at 400 nm. In acetonitrile, it shows distinct vibrational character and two sharp bands with maxima at 390 nm and 419 nm, respectively.

The spectra are strong evidence that an excited-state species is formed during the reaction of DNPO and hydrogen peroxide (Fig. 3). The postulated reactive intermediate is 1,2-dioxetanedione (D in Fig. 3 [8, 9]). The most likely breakdown product is carbon dioxide. However, according to Lechtken and Turro [10], the generation of excited singlet carbon dioxide ($^1CO_2$) is unlikely because of its high-lying electronic states (singlet excitation energy = 103.5 kcal mol^{-1}) and because the upper limit of energy production from an oxalate ester/hydrogen peroxide reaction seems to be ca. 105 kcal mol^{-1}. If for these reasons $^1CO_2$ is ruled out as the intermediate, then ^1D or ^3D or some other carbonyl species may be responsible for the luminescence. The state of the intermediate is important in understanding how the fluorophore is chemically excited during indirect peroxyoxalate chemiluminescence. It has been thought that degradation of the constrained ring system in D supplied the chemical excitation energy [8, 11]. However, if an excited product is the intermediate, then energy transfer may occur via the interaction between excited-state product and ground-state fluorophore, either by classical charge or electron transfer, similar to that reported for tetramethyldioxetane [12].

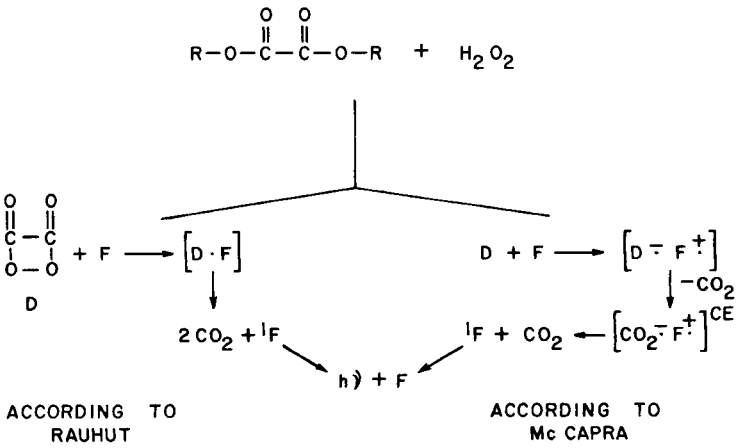

Fig. 3. Postulated mechanisms for peroxyoxalate chemiluminescence as developed by Rauhut et al. [8] and McCapra [9].

The use of DNPO may have been fortuitous because neither it nor DNP fluoresces in solution, most likely because of the heavy atom effect of the nitro groups. Similar native peroxyoxalate chemiluminescence spectra could not be generated with TCPO and TBTO because of the fluorescence of both the esters and their degradation products TCP and trifluoromethyl-1H-benzotriazole, respectively. It is suspected that the background emission spectrum published for TCPO [3] may be due in part to TCPO and TCP fluorescence. Chemiluminescence from degradation products has been reported during the thermolysis of secondary peroxyesters [13]. Background emission from bis(2,4,5-trichloro-6-carbopentoxyphenyl)oxalate has also been reported and attributed to the solvents used [6].

Luminescence from the DNPO/H_2O_2 reaction may be perturbed by fluorophores and nonfluorophores (Figs. 2, 4, 5). The addition of a fluorophore to the reaction medium yields luminescence identical to fluorophore photoluminescence. A large intensity enhancement (Fig. 4, points b and c) proportional to fluorophore concentration is also observed. Such effects are not discussed further because they are well documented [1, 7, 8]. Some nonfluorophores like ouabain and urea also produce an intensity enhancement, but 1000-times less intense than for fluorophores in both static (Fig. 4, points d and f) and dynamic (Fig. 5, points b and c) systems. The limits of detection are 20 μl of 1×10^{-7} M oubain and 1×10^{-6} M urea. The addition of a pure solvent blank in either the static (Fig. 4, points a and e) or dynamic (Fig. 5, point a) system yields an intensity decrease, probably because of dilution. The enhancement is actually greater than apparent because it incorporates the dilution effect.

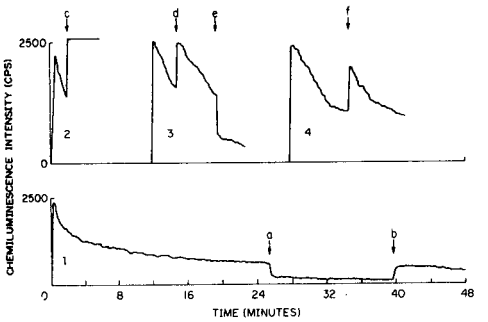

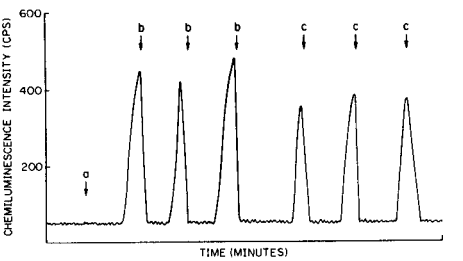

Fig. 4. Native chemiluminescence intensity decay versus time for DNPO and H_2O_2 in acetonitrile. Each curve was obtained by adding 100 μl of H_2O_2 (8.8×10^{-2} M) to 100 μl of DNPO (1×10^{-3} M) in the static mixing assembly. On curves 1 and 3, arrows a and e indicate 20-μl injections of pure acetonitrile. On curves 1 and 2, arrows b and c are 20-μl injections of DPA (1×10^{-8} M). Arrows d and f on curves 3 and 4 are 20-μl injections of ouabain (1×10^{-7} M) and urea (1×10^{-6} M), respectively, in acetonitrile.

Fig. 5. Native chemiluminescence enhancement by 20-μl injections of ouabain (1×10^{-7} M) and urea (1×10^{-6} M) at points b and c. Point a is an acetonitrile solvent blank. DNPO (1×10^{-3} M) and H_2O_2 (8.8×10^{-2} M) were mixed in the flow system shown in Fig. 1.

In order to ensure that it was not a trace fluorescent impurity, that was being monitored, the DNPO solutions were doped with DPA and pyrene (each DNPO solution contained 1×10^{-12} M of either DPA or pyrene) and the above experiments were repeated. In each case, the addition of ouabain or urea to DNPO solutions containing DPA or pyrene caused ca. 30% quenching of the indirect luminescence from DPA or pyrene rather than the enhancement of native chemiluminescence previously observed. These results agree with those recently published by van Zoozen et al. [14], who reported quenching of indirect chemiluminescence from TCPO and aminofluoroanthracene immobilized on a solid substrate by a wide variety of agents including two urea derivatives (thiourea and ethenyl thiourea). The results presented here together with those of the above workers strongly indicate that it is not a trace fluorescent impurity that is being monitored. Therefore, the luminescence from the reaction between DNPO and hydrogen peroxide must indicate the presence of an excited-state species.

DNPO is not as widely used as TCPO because of its relative instability in solution. Degradation appears to occur more rapidly in acetonitrile than in either chloroform or ethyl or butyl acetate. DNPO solutions in the latter solvents are stable for 8—12 h but acetonitrile solutions must be replaced after 4—6 h. Mixing must also be controlled very closely because the solution mixing rate has a marked effect on the final intensity measured. Because of these problems, exploitation of DNPO peroxyoxalate chemiluminescence for the detection of nonfluorophores as well as fluorophores is a challenging task. However, DNPO provides nearly 1000-fold more sensitivity than any other oxalate ester, and the work is justified. Standard techniques are being developed for the sensitive determination of nonfluorophores and fluorophores based on DNPO peroxyoxalate chemiluminescence, which will be reported in a later publication.

REFERENCES

1 See, e.g., K. Honda, K. Miyaguchi and K. Imai, Anal. Chim. Acta, 177 (1985) 103, 111 (and references therein).
2 M. Yamada, Anal. Chim. Acta, 155 (1983) 259.
3 K. W. Sigvardson and J. W. Birks, Anal. Chem., 55 (1983) 432.
4 G. Gelboin, J. Liq. Chromatogr., 6 (1983) 1603.
5 R. Weinberger, J. Chromatogr., 314 (1984) 155.
6 M. L. Grayeski and W. R. Seitz, Anal. Biochem., 136 (1984) 277.
7 A. G. Mohan and N. J. Turro, J. Chem. Ed., 51 (1974) 528.
8 M. M. Rauhut, L. J. Bollyky, B. G. Roberts, M. Loy, R. H. Whitman, A. V. Iannotta, A. M. Semsel and R. A. Clarke, J. Am. Chem. Soc., 89 (1967) 6515.
9 F. McCapra, Prog. Org. Chem., 8 (1973) 231.
10 P. Lechtken and N. J. Turro, Mol. Photochem., 6 (1974) 95.
11 M. M. Rauhut, Acc. Chem. Res., 2 (1969) 80.
12 N. J. Turro, P. Lechtken, N. E. Schore, G. Schuster, H. C. Steinmetzer and A. Yekta, Acc. Chem. Res., 7 (1974) 97.
13 B. G. Dixon and G. B. Schuster, J. Am. Chem. Soc., 103 (1981) 3068.
14 P. van Zoozen, D. A. Kamminga, C. Gooijer, N. H. Velthorst and R. W. Frei, Anal. Chem., 58 (1986) 1245.

Analytica Chimica Acta, 196 (1987) 311—316
Elsevier Science Publishers B.V., Amsterdam — Printed in The Netherlands

Short Communication

SPECTROPHOTOMETRIC DETERMINATION OF ZINC IN COOKING SALTS, TAP AND MINERAL WATERS WITH PHENYLGLYOXAL MONO(2-PYRIDYL)HYDRAZONE

A. G. ASUERO*, M. L. MARQUES and M. A. HERRADOR

Department of Bromatology, Toxicology and Applied Chemical Analysis, Faculty of Pharmacy, The University of Seville, 41012 Seville (Spain)

(Received 4th August 1986)

Summary. The behaviour of phenylglyoxal mono(2-pyridyl)hydrazone (PGMPH) with various metal ions was studied by spectrophotometry. The reaction of zinc with PGMPH provides a sensitive and precise method for the determination of zinc in tap and mineral waters and in cooking salts. Zinc ion reacts with PGMPH at pH 7.2—8.5 in solutions containing 40% (v/v) ethanol to form a yellow-orange complex with maximum absorbance at 464—470 nm. The molar absorptivity of the 1:2 Zn—PGMPH complex is 71 300 1 mol^{-1} cm^{-1}. Interferences are considered in detail.

Numerous pyridylhydrazones and related compounds have been synthesized and investigated for the determination of traces of metals [1, 2]. Spectral data have been given for various metal complexes of *N*-heterocyclic derivatives of pyridylhydrazone [3]; e.g., phenanthridine-2-aldehyde 2-pyridylhydrazone permits the extraction-spectrophotometric determination of <0.5 mg l^{-1} zinc, but cadmium interferes. It has been shown [4] that 2-(3′-sulfobenzoyl)pyridine 2-pyridylhydrazone forms an anionic complex with zinc (and other metal ions). 2-Benzoylpyridine 2-pyridylhydrazone forms a complex with zinc in alkaline medium (pH >10.5) with maximum absorbance at 455 nm and a molar absorptivity of 51 000 1 mol^{-1} cm^{-1} [5]; 0.01% zinc in aluminum can be determined directly. The lack of selectivity of these reagents can be overcome by using appropriate masking agents or by a differential demasking technique [6]; 2,2′-dipyridyl 2-pyridylhydrazone [7] and 2,2′-dipyridyl 2-quinolylhydrazone [8] have been proposed for the direct determination of zinc ions. The mono- and bis-pyridylhydrazones derived from dipyridylglyoxal [9] as well as 3-hydroxypyridine-2-aldehyde 2-pyridylhydrazone [10] also form highly coloured zinc chelates. The results obtained in the reaction of zinc ion with the monopyridylhydrazone derivative of phenylglyoxal (PGMPH) are reported in this communication, together with several practical applications concerning the determination of zinc in potable and mineral waters and in cooking salts. This communication forms part of a systematic investigation into the uses of Schiff bases derived from biacetyl and related compounds as analytical reagents [11].

0003-2670/87/$03.50

Experimental

Apparatus. Absorption spectra and absorbances were measured with a Bausch and Lomb Spectronic 2000 spectrophotometer. A Crison Model 502 pH meter was used with a combined glass–Ag/AgCl electrode pair. All measurements were made at room temperature. All glassware was cleaned with dilute hydrochloric acid and then thoroughly washed with distilled water.

Reagents. Phenylglyoxal mono(2-pyridyl)hydrazone was prepared by refluxing the appropriate amounts of 2-hydrazinopyridine (Aldrich) and phenylglyoxal (Ega Chemie) dissolved in a minimum amount of ethanol with several drops of anhydrous acetic acid [12]. The reagent was used as a 0.1% (w/v) solution in ethanol.

The standard zinc(II) solution was prepared by dissolving 11.386 g of zinc sulphate heptahydrate (Merck) in distilled water and diluting to 1 l. This solution was standardized against EDTA by using eriochrome black T as indicator [13]. Working standards were prepared by appropriate dilution.

Tris buffer, pH 8.47, was made by mixing 50 ml of 0.5 M tris(hydroxymethyl)aminomethane (Scharlau) with 6.2 ml of 1 M hydrochloric acid and diluting to 100 ml with distilled water.

All other reagents were of the highest available purity and glass-distilled water was used throughout.

Recommended procedure for the spectrophotometric determination of zinc. The solution containing 1.25–15 μg of zinc(II) was pipetted into a 25-ml volumetric flask followed by 7.5 ml of ethanol, 1 ml of pH 8.47 Tris buffer and 2.5 ml of the 0.1% (w/v) PGMPH solution. After dilution to 25 ml with water, the solution was left for 15 min and then the absorbance was measured in 10-mm glass cells against distilled water. The absorbance of the blank was measured similarly and subtracted from the absorbance for the sample. Concentrations were calculated from a calibration graph or empirical equation.

Results and discussion

Reactivity of phenylglyoxal mono(2-pyridyl)hydrazone with metal ions. The reactions of PGMPH with 40 cations, up to concentrations of 20 mg l^{-1}, at pH 4.7 (acetate buffer) and at pH 8.6 (boric acid/sodium hydroxide) were investigated. The order of addition of reagents was as given in the above procedure, unless otherwise specified. The characteristics of the most important PGMPH complexes in solution are shown in Table 1. The most sensitive reactions were those of Ni(II), Cu(II), Zn(II), Cd(II) and Mn(II), the molar absorptivity for the zinc complex being particularly attractive. The determination of zinc was therefore examined.

Spectrophotometric determination of zinc with phenylglyoxal mono(2-pyridyl)hydrazone. Zinc ions react with PGMPH in basic medium (pH > 7) to form a yellow-orange complex. The absorption spectra (Fig. 1) indicated the formation of a single complex with maximum absorbance at 464–470 nm,

TABLE 1

Reactivity of PGMPH with metal ions

Metal ion	pH 4.7[a]		pH 8.6		Metal ion	pH 8.6	
	λ_{max} (nm)	ϵ^b	λ_{max} (nm)	ϵ^b		λ_{max} (nm)	ϵ^b
Co(II)	518.5	28 400	469	36 800	Zn(II)	464	71 300
Cu(II)	475	26 600	466	57 300	Cd(II)	466	68 000
Ni(II)	471.5	52 800	471	60 100	Mn(II)[c]	471	55 700
Fe(II)	462	38 300	465	13 700	Pb(II)[c]	483	32 300
Hg(II)[c]	465	5800	468	36 200			

[a]At this pH, the Pd(II) complex had ϵ = 9600 l mol^{-1} cm^{-1} at 470 nm. The Fe(III) complex had ϵ = 32 500 at 462 nm. [b]Molar absorptivity in l mol^{-1} cm^{-1}.

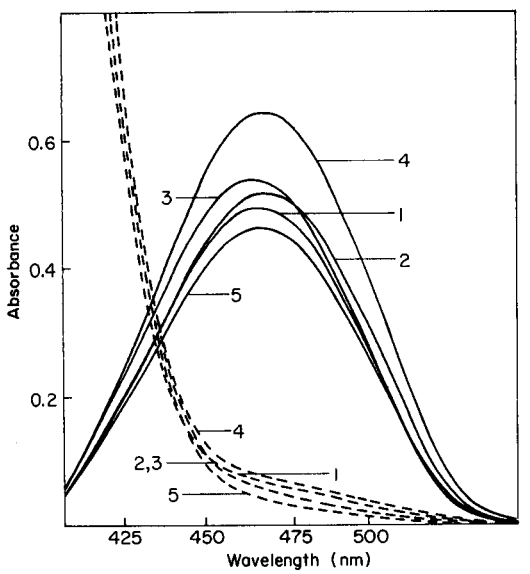

Fig. 1. Spectra of the zinc-PGMPH complex in different solvents: (1) dimethylsulphoxide; (2) dimethylformamide; (3) ethanol; (4) acetone; (5) dioxane. Broken lines indicate reagent blanks.

at which wavelength (470 nm) the absorbance of the reagent blank is low. The absorbance of the PGMPH complex with zinc was independent of pH over the range 7.2—8.5. The formation of zinc hydroxide complexes prevented the use of higher pH. A Tris pH 8.47 buffer was selected; 1 ml of this buffer gave a final pH of 8.2.

The spectrum of the Zn—PGMPH complex was recorded in various solvents miscible with water (Fig. 1). Although maximum absorbance (ϵ = 83 700 l mol^{-1} cm^{-1}) was attained with acetone, ethanol was preferred because of its

greater ability to dissolve PGMPH and its lower volatility. The ratio of ethanol to water in the final solution did not affect the wavelength of maximum absorbance, but maximum absorbance was attained in a medium containing 30—60% (v/v) ethanol. A medium containing 40% ethanol was chosen for the recommended procedure to maintain overall solubility on standing.

The colour intensity depended on the amount of reagent added unless the excess was at least 40-fold. The recommended amount of reagent provided a 97:1 mole ratio of reagent to zinc (0.3 mg l^{-1}). The coloured complex was then formed within 15 min and remained stable for at least 24 h. The order in which the reagents were added was not important. More than 2 ml of buffer reduced the absorptivity of the zinc—PGMPH complex; 1 ml of the Tris buffer is recommended. When necessary, preliminary adjustment of pH was done with hydrochloric acid or sodium hydroxide.

Beer's law was obeyed over the concentration range 0.05—0.6 mg l^{-1} zinc. A least-squares treatment of a typical set of results gave the following calibration equation: $y = 0.0029 + 1.0939\ x$ (correlation coefficient 0.9987; $n = 7$), where y is the absorbance of a solution containing x mg l^{-1} zinc. The molar absorptivity coefficient was 71 300 l mol^{-1} cm^{-1}. This value is larger than those for other zinc pyridylhydrazone complexes [1, 2] and compares well with those found for other zinc complexes used for spectrophotometry [14]. The Sandell sensitivity is 0.0009 $\mu g\ cm^{-2}$. The optimum range concentration as evaluated by a Ringbom plot is 0.05—0.3 mg l^{-1} zinc. The relative standard deviation (s_r) was 1.2% for 0.30 mg l^{-1} zinc ($n = 7$). The between-day variability was larger ($s_r = 2\%$; $n = 28$) than the within-day range. The detection limit was 0.02 mg l^{-1}, evaluated from three times the standard deviation of the blank ($s_b = 0.0075$; $n = 6$).

For the sake of comparison, the most sensitive of similar reagents reported earlier were phenanthridine-2-aldehyde 2-pyridylhydrazone, which provided a molar absorptivity of 64 000 l mol^{-1} cm^{-1} in benzene/hexane after extraction from solution at pH 9 [3], and 2,2′-dipyridyl 2-quinolylhydrazone, which gave a molar absorptivity of 63 000 l mol^{-1} cm^{-1} in 5% ethanolic medium at pH 11.5—12.7 [8].

Composition of the complex. The PGMPH molecule when complexed exhibits a single negative charge by loss of the imine proton. Charge neutrality requires the formula ZnL_2 for the complex, HL being the neutral form of the ligand. The method of Rosales et al. [15] was applied to the data obtained in a study of the optimum amount of reagent; the conditional formation constants were found to be $\log \beta_1 = 3{,}32$ and $\log \beta_2 = 8.91$.

Interferences. Results of various tests for interferences are given in Table 2. The criterion for interference was an absorbance varying more than 5% from the expected value for zinc alone. For some interfering ions, increased tolerance was achieved by addition of masking agents as indicated in Table 2. Tartrate was effective in suppressing interference from iron(III). Thiosemicarbazide (freshly prepared 4% solution in dimethylformamide) masked the interference from small amounts of copper, cobalt and manganese. Iodide

TABLE 2

Effect of diverse ions on the determination of 0.3 mg l^{-1} zinc

Ion	Tolerance limit (mg l^{-1})	Ion	Tolerance limit (mg l^{-1})	Ion	Tolerance limit (mg l^{-1})
I^-	>380 000	Citrate	<30	Fe(III)	1 (12[b])
CH_3COO^-	>30 000	$C_2O_4^{2-}$	12	V(V)	1
$S_2O_3^{2-}$	>6000	CrO_4^{2-}	1	Mn(II)	0.6 (1.5[b], 0.9[c])
Thiourea, tartrate	>3000	NH_4^+	>1200	Al	<0.6 (30[d])
Thiosemicarbazide	3000	Ca, Mg	>600	Pb	<0.3 (0.6[a], 2[b])
F^-	1800	W(VI)	120	Hg(II)	0.1 (30[a])
Cl^-, Br^-, SO_4^{2-}	>300	As(III)	30	Cd	0.03 (6[e])
NO_3^-	120	Mo(VI)	5	Cu(II)	0.03 (0.3[a], 0.9[c])
CO_3^{2-}, PO_4^{3-}	60	Bi, Au, Ag	1 (12[a])	Co(II)	0.03 (1.2[c])
IO_4^-	30			Ni(II)	<0.03 (0.03[a])

[a]In presence of 600 mg l^{-1} thiosulphate. [b]In presence of 3000 mg l^{-1} tartrate. [c]In presence of 3000 mg l^{-1} thiosemicarbazide. [d]In presence of 1800 mg l^{-1} fluoride. [e]With 10 ml of 50% (w/v) KI added.

effectively masked cadmium. Mixtures of tartrate and thiourea (each at 3000 mg l^{-1}) were effective in masking iron(III), Mn(II) and copper(II) when all were present at similar concentrations to zinc (ca. 0.3 mg l^{-1}). Tartrate alone was less effective in such cases, though it was satisfactory when copper was absent. When masking agents were added, absorbances were measured within 10—20 min.

Applications. The recommended procedure for the determination of zinc was applied to cooking salts and water samples in order to evaluate its effectiveness. Data for triplicate analysis of different tap and mineral water samples from the Andalusia country are presented in Table 3. Statistical comparison with determinations by atomic absorption spectrometry and by the zincon method showed excellent agreement. Trace amounts of zinc in cooking salts were also determined (Table 4). Comparison of the variances and mean values obtained by the proposed method and by the zincon method

TABLE 3

Determination of trace amounts of zinc in tap and mineral waters

Water	Water pH	Ca (mg l^{-1})	Mg (mg l^{-1})	Zn(II) (mg l^{-1})	
				PGMPH	AAS[a]
1	7.22	16.4	3.2	0.45 ± 0.005	0.46
2	7.90	27	10	0.45 ± 0.011	—
3[b]	7.55	119.6	26.3	0.04 ± 0.004	0.04
4[b]	7.15	24	11	1.565 ± 0.010	1.60
5	7.83	17.6	4.4	0.45 ± 0.012	0.45

[a]Atomic absorption spectrometry. [b]Mineral water.

TABLE 4

Determination of trace amounts of zinc in salts[a]

Trade name	PGMPH	Zincon	Trade name	PGMPH	Zincon
	$\bar{X} \pm S_d$	$\bar{X} \pm S_d$		$\bar{X} \pm S_d$	$\bar{X} \pm S_d$
Marine salt PROA	1.44 ± 0.11	1.42 ± 0.07	Iodide salt	1.42 ± 0.08	1.54 ± 0.07
Raw marine salt	1.64 ± 0.08	1.67 ± 0.08	TORREMAR	1.53 ± 0.07	1.59 ± 0.10
Marine salt POLA	1.89 ± 0.09	2.05 ± 0.09	BAR	1.39 ± 0.08	1.35 ± 0.08
IBARRA	0.88 ± 0.12	0.93 ± 0.06			

[a]Dissolved in distilled water at 10% (w/v).

[16] using the variance ratio test and the Student *t*-test [17] showed no significant differences between the two methods; the methods are equally accurate and precise.

Conclusions

Few spectrophotometric procedures for trace amounts of zinc are selective enough for direct application [11, 16, 18]. Virtually all the pyridylhydrazone reagents proposed for zinc, including the present method, are subject to interferences notably from cadmium, iron, cobalt, nickel and copper. Isolation of the zinc or masking of foreign ions is therefore required. The method proposed here is safe, rapid, precise and sensitive, and affords an efficient means of determining traces of zinc, especially in cases where lack of selectivity is not a serious disadvantage, e.g., potable waters and cooking salts.

REFERENCES

1 M. Katyal and Y. Dutt, Talanta, 22 (1975) 151.
2 R. B. Singh, P. Jain and R. P. Singh, Talanta, 29 (1982) 77.
3 V. Zatka, J. Abraham, J. Holzbecher and D. E. Ryan, Anal. Chim. Acta, 54 (1971) 65.
4 J. E. Going, G. Wesenberg and G. Andrejat, Anal. Chim. Acta, 81 (1976) 349.
5 J. E. Going and R. T. Pflaum, Anal. Chem., 42 (1970) 1098.
6 J. A. Platte and V. M. Marcy, Anal. Chem., 31 (1959) 1226.
7 H. Alexaki-Tzivanidou, Microchem. J., 22 (1977) 388.
8 R. B. Singh, P. Jain, B. S. Garg and R. P. Singh, Analyst, 104 (1979) 1188.
9 A. A. Schilt, J. F. Wu and F. H. Case, Talanta, 22 (1975) 915.
10 J. M. Cano Pavon, M. L. Trujillo and A. G. de Torres, Anal. Chim. Acta, 117 (1980) 319.
11 See, e.g., A. G. Asuero, A. M. Jimenez and M. A. Herrador, Analyst, 111 (1986) 747 and references therein.
12 M. L. Marqués, Ph.D. Thesis, University of Seville, 1986.
13 F. Bermejo and A. Prieto, Aplicaciones Analíticas del AEDT y Análogos, Departamento de Química Analítica, Santiago de Compostela, 1975.
14 G. Ackerman and J. Köthe, Talanta, 26 (1979) 693.
15 D. Rosales, A. G. González and J. L. Gómez Ariza, Talanta, 32 (1985) 467.
16 J. Fries and H. Getrost, Organic Reagents for Trace Analysis E. Merck, Darmstadt, 1977.
17 S. Akhnazarova and V. Kafarov, Experiment Optimization in Chemistry and Chemical Engineering, MIR Publishers, Moscow, 1982.
18 F. D. Snell, Photometric and Fluorometric Methods of Analysis, Part II, Wiley, New York, 1976.

Analytica Chimica Acta, 196 (1987) 317—322
Elsevier Science Publishers B.V., Amsterdam — Printed in The Netherlands

Short Communication

SPECTROPHOTOMETRIC DETERMINATION OF TRACES OF PLATINUM IN PALLADIUM WITH DITHIZONE AFTER MATRIX PRECIPITATION AS A COMPOUND WITH AMMONIA AND IODIDE

Z. MARCZENKO* and S. KUŚ
Department of Analytical Chemistry, Technical University, 00-664 Warsaw (Poland)
(Received 23rd April 1986)

Summary. Palladium is precipitated with ammonia and iodide; platinum remains in solution and is completely extracted with dithizone in carbon tetrachloride. The precipitated palladium compound is shown to be $Pd(NH_3)_2I_2$ by thermogravimetry and by determinations of ammonia and iodide. To separate small amounts of palladium from platinum in the dithizone extract, the resistance of platinum dithizonate to oxidizing agents is utilized; platinum dithizonate is converted to an oxidized form which is easily reduced to the initial form. The separation and spectrophotometric procedure enable about 1×10^{-3}% platinum to be quantified in palladium(II) chloride with good precision and accuracy.

Palladium(II) and platinum(II) are among the platinum metals which can be determined spectrophotometrically with dithizone, at room temperature, after shaking acidic solutions with dithizone in carbon tetrachloride or chloroform [1—4]. Previous work [5, 6] on the separation and determination of platinum and palladium with dithizone (in the presence of iodide or tin(II) chloride) has led to useful spectrophotometric determinations of the two metals in similar amounts, and of trace amounts of palladium in platinum.

In this communication, the spectrophotometric determination of trace amounts of platinum in palladium, with dithizone after preliminary separation of the palladium matrix from acidic medium as a sparingly soluble compound with ammonia and iodide, is reported.

Experimental

Reagents. A platinum standard solution (1 mg Pt ml^{-1}) was prepared by dissolving 0.5000 g of suitably pure platinum metal in 20 ml of aqua regia. Nitrogen oxides were removed by triple evaporation with added portions of hydrochloric acid almost to dryness. The residue was dissolved in 10 ml of concentrated hydrochloric acid and the solution was diluted to the mark with water in a 500-ml volumetric flask. Working solutions were obtained by suitable dilution with water.

A palladium standard solution (10 mg Pd ml^{-1}) was prepared by dissolving 8.40 g of palladium(II) chloride in 20 ml of concentrated hydrochloric acid and evaporating to about 5 ml. The residue was dissolved in water and diluted

0003-2670/87/$03.50

to the mark with water in a 500-ml volumetric flask. Working solutions were obtained by suitable dilution with water.

Dithizone (H_2Dz) solution, 4×10^{-4} M in carbon tetrachloride, was standardized by extractive titration of silver standard solution [7]. Iodine solution was freshly prepared by adding 0.2 ml of 0.1 M potassium iodate, 0.5 ml of 0.1 M potassium iodide, and 0.5 ml of 2 M sulphuric acid to 10 ml of water. Reducing solution was freshly prepared by adding 1 ml of 2 M potassium iodide, 2 drops of 1% (w/v) sodium pyrosulphite ($Na_2S_2O_5$) solution and 1 ml of (1 + 1) sulphuric acid to 8 ml of water.

Apparatus. A Specord M40 u.v.-visible spectrophotometer with 1-cm and 5-cm cells, a Specord 75 infrared spectrophotometer, and a derivatograph (Q-1500D, MOM, Hungary) were used.

Procedure. Dilute the slightly acidic (HCl) palladium solution ($\leqslant$0.25 g in 40 ml) containing $\leqslant$40 μg of platinum with water so that the palladium concentration is $\leqslant$5 mg ml^{-1}. Add concentrated ammonia solution (1 ml for 50 mg of palladium), mix and allow the solution to stand for 2 min. Add successively solid potassium iodide and (1 + 1) sulphuric acid to provide 0.5 M iodide and 2 M sulphuric acid in the solution. Filter the precipitate and wash it with 10 ml of water. Transfer the filtrate to a separatory funnel and shake for 5 min with exactly 10 ml of dithizone solution. Before the end of shaking (ca. 30 s) add 2 drops of 1% sodium pyrosulphite solution. Shake the organic extract with 10 ml of diluted ammonia (1 + 100) for 15 s, and then again with 10 ml of iodine solution for 15 s. Shake the organic phase (15 s) with 10 ml of ammonia (1 + 100), and then with 10 ml of the reducing solution (15 s). Measure the absorbance of the clear $Pt(HDz)_2$ solution at 720 nm against carbon tetrachloride.

Results and discussion

Separation of palladium as $Pd(NH_3)_2I_2$. Palladium(II) and platinum(II) in acidic medium (HCl or H_2SO_4) in the presence of iodide, form brown-red and red iodide complexes, respectively. Absorption spectra are given in Fig. 1.

When ammonia in excess is added to a weakly acidic solution of palladium(II), a colourless ammine complex is formed. Addition of potassium iodide and sulphuric acid then produces a compound composed of palladium(II), ammonia and iodide, soluble (turning the solution yellow, Fig. 1, curve 2) provided that the amount of palladium is less than about 1 mg in 20 ml of the solution. With an increase of palladium concentration, a heavy yellow precipitate precipitates.

The precipitate, washed with water and a little ethanol, was studied thermogravimetrically. Figure 2 shows that the compound is stable up to 160°C. In the range of 160—250°C, the mass loss corresponds to exactly two ammonia molecules, the change in mass being 8.6%. Between 410 and 645°C a further loss of mass follows corresponding to two iodine atoms for each palladium atom (64.4% change in mass). This allows the formula $Pd(NH_3)_2I_2$ to be ascribed to the sparingly soluble palladium compound. This result was

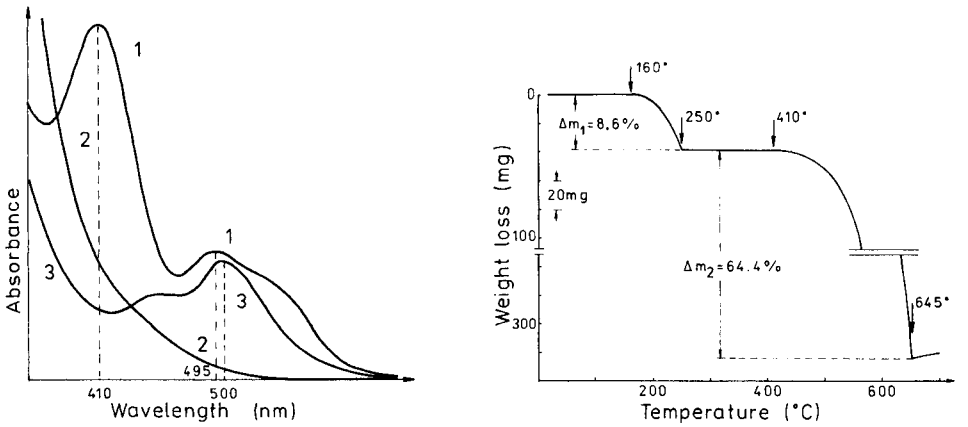

Fig. 1. Absorption spectra in 1 M sulphuric acid medium: (1) palladium iodide complex, (2) palladium/ammonia/iodide complex, (3) platinum iodide complex. Concentrations of metals 10 $\mu g\ ml^{-1}$, 0.5 M KI.

Fig. 2. Thermogravimetric curve of the palladium(II) compound with ammonia and iodide. The initial mass was 441 mg and the heating rate was 10°C min^{-1} in air.

confirmed by titration of the ammonia evolved from the compound by sodium hydroxide solution [8]. Earlier data [9, 10] do not agree as to the number of NH_3 molecules in the discussed palladium compound. The iodide content of the compound was determined by titration with standard silver nitrate solution and dithizone as an indicator [1].

Consecutive addition to ammonia in excess, potassium iodide and sulphuric acid to acidic solutions of platinum (in microgram amounts) allows the platinum(II) to remain in solution as the red iodide complex. The slow formation of the platinum ammine complex (in contrast to that of palladium) [11, 12] makes the formation of the ternary compound (with ammonia and iodide) impossible (Fig. 1, curve 3).

When a solution contains microgram amounts of platinum besides small amounts of palladium (1—5 mg), the ternary palladium compound remains in solution or partly precipitates forming a suspension. In such a case, it is possible to extract platinum quantitatively with dithizone in carbon tetrachloride, at appropriate concentrations of iodide and sulphuric acid (Fig. 3). But increasing amounts of palladium make complete extraction of platinum difficult (Fig. 3, curve 3). Under the given conditions, the extraction of palladium is small.

The quantitative extraction of platinum from the filtrate after the separation of palladium in large quantities as $Pd(NH_3)_2I_2$ precipitate was studied. Under the optimal conditions for the precipitation of palladium (0.05—0.2 M KI, 0.1—0.2 M H_2SO_4, solution volume ca. 50 ml), about 1 mg of palladium remained in solution, but the platinum losses reached 30%. When the iodide

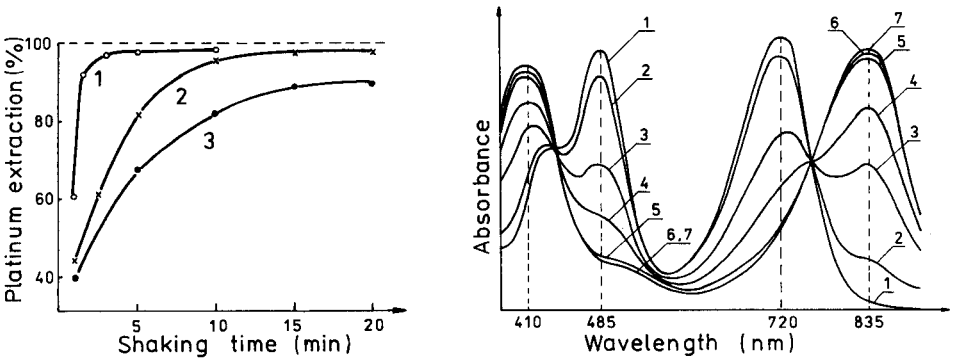

Fig. 3. Dependence of the platinum extraction on shaking time with dithizone in carbon tetrachloride for different amounts of palladium present: (1) 1 mg, (2) 5 mg, (3) 25 mg. Conditions: 10 ml of 5 × 10^{-5} M H_2Dz, 3 M H_2SO_4, 0.1 M KI.

Fig. 4. Oxidation of the platinum dithizonate with increasing permanganate concentration (in ammonia medium). Molar ratio $Pt(HDz)_2/MnO_4^-$: (1) 1/0, (2) 1/0.25, (3) 1/1, (4) 1/1.5, (5) 1/2, (6) 1/3, (7) 1/5.

concentration was increased to 0.5 M and the sulphuric acid to 2 M, the amount of the unprecipitated palladium was a little larger, but almost all the platinum was found in the filtrate.

Extraction of platinum with dithizone after separation of the palladium matrix. Under the conditions chosen for the removal of palladium, the quantitative extraction of platinum demands dithizone in considerable excess. After a 5-min shaking time, the organic phase contains all the platinum, part of the palladium (as dithizonates), and free dithizone. Other metals are not then extracted by dithizone in carbon tetrachloride (see Table 2 [6]).

During shaking of the phases, oxygen oxidizes some iodide and some dithizone. In order to reduce the iodine and the oxidized products of dithizone, a reductant must be added at the end of shaking. Sodium pyrosulphite is a suitable reductant. The next shaking of the extract with dilute ammonia (1 + 100) removes all the free dithizone.

Before the absorbance of the platinum dithizonate is measured, it is essential to remove palladium from the extract because $Pd(HDz)_2$ absorbs a little at 720 nm, the λ_{max} of $Pt(HDz)_2$. When iodine is added to the extract, which is then shaken with dilute ammonia solution, palladium passes to the aqueous phase; hypoiodite decomposes palladium dithizonate. The platinum dithizonate remaining in the organic phase after those operations shows an essential change in the shape of the absorption spectrum. Absorption maxima appear at 410 and 835 nm instead of at 485 and 720 nm (Fig. 4). Shaking the carbon tetrachloride solution of the changed platinum dithizonate with pyrosulphite restores its normal absorption spectrum (with λ_{max} at 720 nm).

TABLE 1

Results obtained for platinum in palladium(II) chloride (p.a.)

Sample (mg)	Platinum (μg)		Platinum in sample (%)
	Added	Found[a]	
17.7	—	<0.5 (2)	—
	2.0	2.25 (2)	
	5.0	5.15 (2)	
88.6	—	0.97 (3)	
	2.0	2.85 (2)	1.2×10^{-3}
177	—	1.9 (5)	
	2.0	3.63 (3)	1.2×10^{-3}
355	—	3.67 (5)	
	2.0	5.5 (2)	1.1×10^{-3}

[a]Mean of n determinations with n in parentheses.

Other oxidizing agents act similarly to iodine (in alkaline medium), namely, bromine, permanganate, cerium(IV), and sufficiently concentrated (ca. 3 M) nitric acid. Each of these oxidants gives the same oxidation product which is converted to the original form of platinum dithizonate on reduction. Figure 4 illustrates the conversion of platinum dithizonate to the oxidized form when increased amounts of permanganate in the aqueous phase (about 0.1 M ammonia) are shaken with the extract. An exchange of two electrons is associated with the reaction of $Pt(HDz)_2$ and permanganate.

The infrared spectra of the two forms of platinum dithizonate were recorded. The infrared bands at 3240 and 1525 cm^{-1} disappeared after the oxidation was complete; this may mean the absence of NH groups [2].

Determination of traces of platinum in palladium. The proposed method was applied to the determination of platinum traces in palladium(II) chloride (p.a.; POCh, Gliwice). The palladium(II) chloride (8.86 g corresponds to 5 g of palladium) was dissolved in a mixture of 25 ml of concentrated hydrochloric acid and 3 ml of concentrated nitric acid and nitrogen oxides were removed by three evaporations with 5-ml portions of hydrochloric acid. The residue (ca. 5 ml) was dissolved in water and transferred to a 500-ml flask. Portions corresponding to different masses of the sample were taken and the procedure given above was applied. The absorbances were measured in 5-cm cells.

Table 1 shows that the proposed method is precise; the recovery for 2 μg of platinum was about 90%. The platinum content in the palladium chloride tested was 1.2×10^{-3}%.

This work was supported by Research Program MR-I-32.

REFERENCES

1 G. Iwantscheff, Das Dithizon und seine Anwendung in der Mikro-und Spurenanlyse, 2nd edn., Verlag Chemie, Weinheim, 1972.
2 H. M. Irving, Dithizone, The Chemical Society, London, 1977.
3 J. Minczewski, M. Krasiejko and Z. Marczenko, Chem. Anal. Warsaw, 15 (1970) 43.
4 E. E. Rakovskii and A. N. Shkil, Zh. Anal. Khim., 34 (1979) 1795.
5 Z. Marczenko, S. Kuś and M. Mojski, Talanta, 31 (1984) 959.
6 Z. Marczenko and S. Kuś, Analyst, 110 (1985) 1005.
7 Z. Marczenko, Separation and Spectrophotometric Determination of Elements, 2nd. edn., Horwood, Chichester, 1986.
8 A. I. Vogel, Quantitative Inorganic Analysis, 3rd edn., Longmans, London, 1961.
9 S. I. Ginzburg, N. A. Ezerskaya, I. V. Prokof'eva, N. V. Fedorenko, V. I. Shlenskaya and N. K. Belskii, Analytical Chemistry of Platinum Metals (in Russian), Nauka, Moscow, 1972.
10 S. E. Livingstone, The Chemistry of Ruthenium, Rhodium, Palladium, Osmium, Iridium and Platinum, Pergamon, Oxford, 1973.
11 M. A. Khattak and R. I. Magee, Talanta, 12 (1965) 733.
12 S. I. Al-Bazi and A. Chow, Talanta, 31 (1984) 815.

Analytica Chimica Acta, 196 (1987) 323—327
Elsevier Science Publishers B.V., Amsterdam — Printed in The Netherlands

Short Communication

COMPARISON OF TWO CHELATING AGENTS IMMOBILIZED ON CONTROLLED-PORE GLASS FOR THE PRECONCENTRATION OF ALUMINIUM FROM AQUEOUS SOLUTIONS

E. A. ALLEN, M. C. BOARDMAN and B. A. PLUNKETT*

Department of Chemistry, Portsmouth Polytechnic, St Michael's Building, White Swan Road, Portsmouth, PO1 2DT (Great Britain)

(Received 30th July 1986)

Summary. Aluminium at low $\mu g\ cm^{-3}$ levels can be preconcentrated on columns of 8-quinolinol or EDTA immobilized on controlled-pore glass. Distribution coefficients are ca. 45 and 370 $cm^2\ g^{-1}$, respectively, and recoveries of aluminium are >80% at pH >4.6 and pH >4.0, respectively. The eluted aluminium is determined by atomic absorption spectrometry in a nitrous oxide/acetylene flame.

Aluminium is present at high concentrations in the earth's crust (8 wt.% [1]) but it is a trace metal in the biosphere owing to the very low solubility of its ores in natural waters. Little is known about its metabolism, although it may activate succinic dehydrogenase and δ-aminolaevulinate hydrolase [2]. If levels in blood are high, aluminium acts as a neurotoxin and causes presenile dementia [3, 4]. Aluminium may also be involved in osteodystrophy and in liver problems in people who have very high industrial exposures to aluminium dust. Haemodialysis patients have suffered from dementia with aluminium levels as low as 8 $\mu g\ l^{-1}$ in the water used [5].

Pollution of natural waters by aluminium is caused in two major ways. First, soluble aluminium sulphate is often added in water treatment processes as a flocculating agent. Precipitation of aluminium should be complete under these circumstances but this has been found not to be the case [6]. Secondly, acid rain increases the dissolution of aluminium from soils [7]. Typical freshwater contains 30 ng Al cm^{-3}, but acidic water may contain 400 ng Al cm^{-3} [7]. An additional means of liberating aluminium is by cooking acidic foods in aluminium containers [8].

Direct determinations of aluminium at the levels in natural waters is difficult with the range of techniques routinely available and pre-concentration is normally required. Column chromatrography is often effective for preconcentration and can also provide sample clean-up. Chelating agents immobilized on controlled-pore glass (CPG) have proved effective for this purpose. Studies of such materials have largely centred on immobilized 8-quinolinol (CPG/8-Q) and immobilized EDTA (CPG/ED_3A). CPG/8-Q has received the

0003-2670/87/$03.50

most attention; the efficiency of extraction has been evaluated over a range of pH values for copper(II) [9—12], lead [10, 11] and aluminium [9]. Studies of CPG-ED_3A have been restricted to copper and lead extraction from solutions of pH 5.6 [13, 14]. Allen et al. [10] compared the extraction of copper from dilute solution with CPG/8-Q and an ammonium tetramethylenedithiocarbamate-based liquid/liquid extraction; Guedos da Mota et al. [14] compared CPG/8-Q with an ion-exchange resin.

In the present study, the efficiencies of CPG/8-Q and CPG-ED_3A are compared for the preconcentration of aluminium from dilute aqueous solution prior to determination by flame atomic absorption spectroscopy (AAS). The distribution coefficients of aluminium between the solid phase and aqueous solutions are reported.

Experimental

Reagents. All water used was demineralized and distilled. All reagents were of AnalaR grade (BDH). Solutions were prepared in water and stored in polyethylene bottles. The stock 0.01 M aluminium solutions for distribution coefficient measurements and stock aluminium solutions (1000 $\mu g\ cm^{-3}$) for column extraction studies and AAS calibration were prepared from aluminium nitrate nonahydrate and stabilized with 5 $cm^3\ dm^{-3}$ of concentrated hydrochloric acid. The immobilized chelating agents (Pierce Chemicals) were CPG/8-Q (23750) and CPG/ED_3A (23520), both with pore diameter 50 nm and particle size 125—177 μm.

Apparatus. All glassware was soaked overnight in 25% nitric acid, rinsed thoroughly with water and ethanol, and dried in a stream of nitrogen. For the column extractions, the apparatus used was similar to that used previously [10], modified to allow only one passage of any given aluminium solution through the CPG bed. The sample solution was sucked through a percolating filter inserted via a 3-way tap into a glass column (1-cm diameter, 10 cm high); the effluent passed to a container via a peristaltic pump (Schuco Analytical) set to the required flow rate. All PTFE tubing and polythene sample containers were degreased with hexane before use, washed with and finally rinsed with large quantities of water.

Atomic absorption measurements were made with a Baird Alpha 4 spectrometer and a nitrous oxide/acetylene flame at the 309.3-nm aluminium line. A Pye Unicam model 291 pH meter was used with an Ingold combined glass electrode.

Procedures. For distribution coefficient measurements, appropriate volumes of standard aluminium solution (1000 $\mu g\ cm^{-3}$) and 200 ml of potassium nitrate solution (5000 $\mu g\ cm^{-3}$) were transferred to 500-cm^3 volumetric flasks and diluted to volume with water to give standard solutions containing 0.2, 3, 7, 10, 12, 17 and 20 μg Al cm^{-3}. The standards were prepared freshly for each run.

For equilibrium studies, dry, immobilized chelating agent (0.1 g) was weighed accurately into a dry 50-cm^3 conical flask. A 15-cm^3 portion of standard (0.01 M) aluminium solution was adjusted to pH 4.6 with sodium

hydroxide, hydrochloric acid and sodium acetate/acetic acid buffer and diluted to 250 cm^3 to give 6×10^{-4} M aluminium. To the weighed quantity of immobilized reagent was added 20 cm^3 of this aluminium solution, and the mixture was degassed under vacuum for 1 min. This helped to clear the pores of air and ensured complete wetting of the immobilized reagent. The flask was stoppered and shaken mechanically for 30 min. A 10-cm^3 portion of the solution was pipetted from the flask and sufficient potassium nitrate solution added to make the solution 2000 $\mu g\ cm^{-3}$ in potassium. The aluminium was determined by AAS as described above. The CPG reagent was washed with water ($2 \times 20\ cm^3$) and the washings discarded. The chelated metal was removed from the CPG by washing with 1 M hydrochloric acid ($2 \times 5.0\ cm^3$). The acid washings were combined and the aluminium determined as above.

Column extractions were examined for each immobilized reagent with solutions of pH 2.0, 3.8, 4.6, 6.1, 7.0 and 8.0. The CPG reagent was covered with buffer solution, degassed under vacuum for 3 min, and packed into the column as a slurry to give a bed depth of ca. 3 cm, held in place by a sintered glass plate. Standard aluminium solution (1000 $\mu g\ cm^{-3}$) was diluted to 10 $\mu g\ cm^{-3}$ with water, and 10 cm^3 of this solution was diluted to 150 cm^3. The pH was adjusted with sodium hydroxide, hydrochloric acid or the acetate buffer, and the mixture was diluted to 200 cm^3. This solution (500 ng cm^{-3} aluminium) was pumped through the column at $5 \pm 0.5\ cm^3\ min^{-1}$. The column was washed with 25 cm^3 of water and the chelated metal was eluted with 25 cm^3 of 1 M hydrochloric acid which was 2000 $\mu g\ cm^{-3}$ in potassium nitrate.

Aluminium in the eluent was determined by the method of multiple standard additions. To each of four 5-cm^3 portions of the eluent was added an aliquot of the aluminium standard (0.0, 1.0, 2.0 or 5 cm^3 of 20 $\mu g\ cm^{-3}$ aluminium in 1 M HCl/2000 $\mu g\ cm^{-3}$ KNO_3). Aluminium was measured in each solution by AAS. The column was regenerated by washing with 1 M hydrochloric acid (25 cm^3) followed by water until the effluent attained pH 7.

Results and discussion

Distribution coefficients. The distribution coefficients, D_g, were calculated from the expression D_g = (amount of metal chelated on CPG (mol) $\times$ volume of solution (cm^3))/(amount of metal remaining in solution (mol) $\times$ mass of CPG (g)). The values obtained are shown in Table 1 together with the sum of the metal chelated and that remaining in solution. The values of D_g show that aluminium is very strongly bound to CPG/ED_3A, much more strongly than to CPG/8-Q. The former would thus seem to be the preferred reagent for the preconcentration of aluminium. The slightly low total aluminium recoveries are difficult to account for, but suggest that the 1 M hydrochloric acid used to strip the CPG was too dilute. If this is so, the values of D_g given will be slightly low.

Column extraction. The concentration of aluminium in the 25 cm^3 of solution collected from the column in each experiment should be 4 $\mu g\ cm^{-3}$

TABLE 1

Results of distribution coefficient measurements

Reagent	D_g (cm^2 g^{-1})	Total Al (%)[a]
CPG/8-Q	44	82
	46	84
CPG/ED_3A	365	89
	382	90

[a]Sum of aluminium chelated and remaining in solution as a % of the initial amount of aluminium.

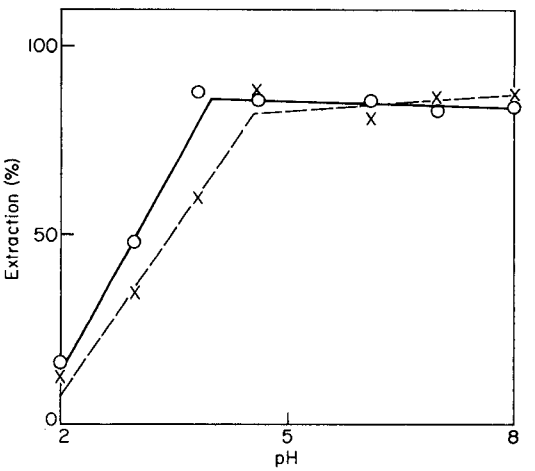

Fig. 1. Effect of pH on % extraction of aluminium by: (○) CPG/ED_3A; (X) CPG/8-Q (for conditions, see text).

if complete extraction followed by complete leaching is achieved. Figure 1 shows the percentage extraction of aluminium achieved in the pH range 2–8. It is clear that at low sample pH competition between the hydrogen and aluminium ions leads to low % extraction. As the pH increases, the percentage extraction of aluminium increases until a limiting value is achieved. For CPG/8-Q this limit is reached at ca. pH 4.6 and for CPG/ED_3A at pH 4.0. In each case the limiting percentage extraction is similar, 81–89%. The lower onset of the limit for CPG/ED_3A is due to its more stable aluminium complex. The results for CPG/8-Q agree well with those obtained by Sugawara et al. [9]. Although the extent of extraction is lower than would be desirable, the bed depth used was only 3 cm, the flow rate was 5 cm^3 min^{-1} and the solution passed through the column only once. The contact time between the CPG and the solution is thus small. Greater bed depths and lower flow rates should achieve complete extraction; a stronger hydrochloric acid eluent could also improve recoveries.

The columns were found to have an appreciable lifetime. The CPG/8-Q has been in use for some four years and the CPG/ED_3A for three years without detectable loss of activity.

The above results show that column preconcentration of aluminium from sub-μg cm^{-3} levels to those within the optimum analytical concentration range for determination by flame atomic absorption spectrometry is easily achieved from sample solutions of pH greater than 4.6 by using controlled-pore glass with immobilized 8-quinolinol or EDTA. Work on the collection of extremely low levels of aluminium is underway.

The authors thank Mr N. Armstrong and Mr R. Tite for their technical assistance.

REFERENCES

1 E. Ochiai, Bioinorganic Chemistry, an Introduction, Allyn and Bacon, Boston 1977.
2 J. E. Huheey, Inorganic Chemistry, Harper and Row, New York, 1983.
3 A. C. Alfrey, Aluminium and Tin, in Disorders of Mineral Metabolism, Vol. 1, Academic Press, New York, 1981.
4 M. R. Wills and J. Savoury, Lancet, 8340 (1983) 29.
5 A. M. Davison and H. Oli, Lancet, 8302 (1983) 785.
6 H. L. Elliot and F. Dryburgh, Br. Med. J., 6120 (1978) 1101.
7 U. Forstner and G. T. W. Wittmann, Metal Pollution in the Aquatic Environment, Springer, Berlin, 1981.
8 Zhang Jinshen, Wu Baotai, Wang Zhuyin and Wei Qiaoai, Chem. Abstr., 99 (1983) 211285d.
9 K. F. Sugawara, H. N. Weetall and G. D. Schucker, Anal. Chem., 46 (1974) 489.
10 E. A. Allen, P. K. N. Bartlett and G. Ingram, Analyst, 109 (1984) 1075.
11 F. Malamas, M. Bengtsson and G. Johansson, Anal. Chim. Acta, 160 (1984) 1.
12 M. A. Marshall and H. A. Mottola, Anal. Chem., 57 (1985) 729.
13 M. M. Guedos da Mota and B. Griepink, Fresenius' Z. Anal. Chem., 290 (1978) 317.
14 M. M. Guedos da Mota, M. A. Jonker and B. Griepink, Fresenius' Z. Anal. Chem. 296 (1979) 345.

Analytica Chimica Acta, 196 (1987) 329—332
Elsevier Science Publishers B.V., Amsterdam — Printed in The Netherlands

Short Communication

COMPLEXATION OF IRON(III) BY PIMELYLDIHYDROXAMIC ACID

R. McMAHON, N. Ni CHOILEAIN and J. D. GLENNON*
Department of Chemistry, University College, Cork (Ireland)
(Received 29th July 1986)

Summary. Pimelyldihydroxamic acid forms strong complexes with iron(III) in aqueous solution at pH 2—9. Plots of $\bar{n}$ and proton liberation against pH show plateaux regions at values of 1.5 and 3.0, respectively, over the pH range 4.0—8.0 supporting a formulation of Fe_2L_3 ($\log \beta = 41.06$). The orange-red complex exhibits maximum absorbance at 420 nm, and a well-defined peak at 0.6 V vs. SCE in differential pulse polarography.

Hydroxamic acids are an important class of chelating agent with analytical applications in the areas of gravimetric and extraction-spectrophotometric determinations [1—3]. Research in this laboratory has led to the development of a convenient synthesis of strongly chelating dihydroxamic acids, HOHN—CO—$(CH_2)_n$—CO—NHOH (n=3—14) which were previously not readily available [4]. The reagents have a particularly strong affinity for iron(III) and have been investigated with respect to their biological activity, coordination chemistry [5] and analytical applications [6]. Recently, decane-1, 10-dihydroxamic acid has been used for the extraction-photometric determination of vanadium(V) [7].

The optimization of procedures for determinations of metal ions is facilitated by knowledge of the complex species in aqueous solution [8]. To aid investigations into the applications of the dihydroxamate reagents, the nature and stability of the complex species formed with iron(III) were studied potentiometrically. In the present work, the proton liberation on Fe(III) complexation to pimelyldihydroxamic acid is measured and computer-assisted data refinement is applied. The complex in aqueous solution is also examined by polarography and spectrophotometry.

Experimental

Apparatus. The Radiometer automatic titrimeter used consisted of a digital PHM84 pH meter, autoburette ABU80, titrator TTA80 and a Servograph REC61 recorder. The 50-ml titration vessel was thermostatted at 25 ± 0.05°C. The electrodes were a Radiometer G2040-C glass electrode and a K4040 calomel reference electrode. A computer interface to a BBC microcomputer was constructed, allowing automatic data collection at every 0.1 pH. A PAR Model 174A polarographic analyzer and a Shimadzu UV-260 spectrophotometer were also used.

0003-2670/87/$03.50

Materials and solutions. Pimelyldihydroxamic acid was synthesized as described previously [4] and was ⩾98% pure. Stock solutions were prepared with distilled/deionized water and were stored under nitrogen. Carbonate-free 1.010 M sodium hydroxide was standardized against weighed amounts of dried potassium hydrogenphthalate. A stock solution of iron(III) nitrate nonahydrate (AnalaR), 0.515 M in 0.02 M nitric acid, was prepared. The stock acid/salt solution was 0.024 M nitric acid in 0.15 M sodium nitrate.

Procedure. Titration curves were recorded with metal and ligand concentrations varied at constant mineral acid concentration [9]. An excess of ligand over metal was used to ensure full coordination and to prevent metal precipitation. Titration curves were obtained for C_L = 3.452 × 10^{-3} M, 5.460 × 10^{-3} M and 7.720 × 10^{-3} M with C_{Fe} = 1.029 × 10^{-3} M and for C_{Fe} = 5.148 × 10^{-4} M, 1.029 × 10^{-3} M and 1.389 × 10^{-3} M with C_L = 5.460 × 10^{-3} M.

Species distribution. The equilibrium reactions between the metal ion M, hydrogen ion and hydroxamate L can be represented by

$$pM + qH + rL \rightleftharpoons M_pH_qL_r$$

where p, q and r are the stoichiometric quantities of M, H and L, respectively. The stoichiometric equilibrium constant is $\beta_{pqr} = [M_pH_qL_r]/m^ph^ql^r$, where m, h and l are the concentrations of free metal ion, hydrogen ion and the hydroxamic acid, respectively. Three BASIC programs PLOT-3, GUESS-3 and LEASK-4 were used to process the titration data [9].

Results and discussion

The ultraviolet-visible absorption characteristics of the Fe(III)/pimelyldihydroxamic acid system indicate typical hydroxamate coordination. The wavelength of maximum absorption shifts from 460 nm at pH 2 to 420 nm at neutral pH with a corresponding increase in absorption (Fig. 1), which is consistent with increasing total Fe(III) complexation and with increasing coordination number.

The nature and response of the Fe(III) complex was examined by differential pulse polarography in 1 M KNO_3 at pH 7.5. The complex gave one well-defined peak at 0.6 V vs. SCE. A linear response with increasing concentration was obtained over the range 10^{-6}—10^{-4} M iron(III).

A fuller understanding of the complex species was obtained from the molar proton liberation values $\delta H^+/\delta C_M$ evaluated from potentiometric data (Fig. 2). It is evident from the proton liberation that complexation is well advanced by pH 2. The levelling off of the proton liberation at a value of three in the pH range 4—8 is characteristic of a definite predominant complex. A levelling off of $\bar{n}$, the average ligand number, towards a value of 1.5 coincides with the plateau region of the proton liberation plot. The evidence is strongly in favour of a complex with Fe_2L_3 stoichiometry. The predominant dimeric complex is clearly shown in the final species distribution diagram for the Fe(III)/pimelyldihydroxamic acid system (Fig. 3). The initial strong visible absorption at 460 nm can be explained by the presence of a FeL (log β_{pqr} =

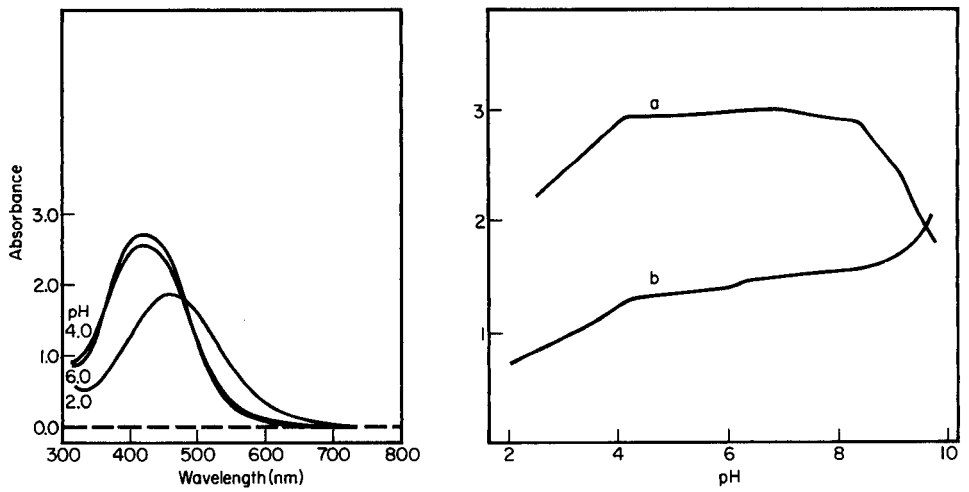

Fig. 1. Ultraviolet-visible absorption spectra of the Fe(III)/pimelyldihydroxamic acid system as a function of pH (indicated on the curves). C_{Fe} = 1.03 × 10^{-3} M, C_L = 5.47 × 10^{-3} M.

Fig. 2. Molar proton liberation $\delta H^+/\delta C_M$ (a) and $\bar{n}$ (b) as a function of pH for the Fe(III)/pimelyldihydroxamic acid system.

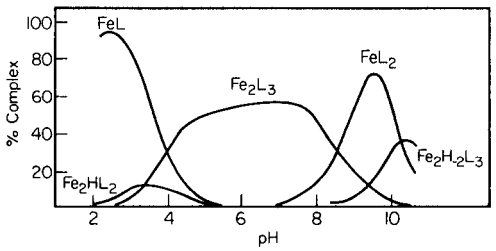

Fig. 3. Species distribution diagram for the Fe(III)/pimelyldihydroxamic acid system as a function of pH. C_{Fe} = 1.03 × 10^{-3} M, C_L = 5.46 × 10^{-3} M.

17.30) complex species which at its maximum at pH 2.7 represents >90% of the total Fe(III). By pH 4, this complex is replaced by the Fe_2L_3 species (log β_{pqr} = 41.06) which is the major complex up to pH 8.5. Other complexes formed are Fe_2HL_2 (log β_{pqr} = 23.50), FeL_2 (log β_{pqr} = 25.78) and $Fe_2H_2L_3$ (log β_{pqr} = 32.22).

The pattern of coordination of Fe(III) displayed by pimelyldihydroxamic acid is expected to be representative of the aliphatic dihydroxamic acid reagents in general. While sharing many attributes with those monohydroxamic acids already used as analytical reagents, the dihydroxamic acids appear to combine a strong affinity for Fe(III) with interesting dimeric chelation.

REFERENCES

1 Y. K. Agrawal and R. D. Roshania, Bull. Soc. Chim. Belg., 89 (1980) 3.
2 Y. K. Agrawal and S. A. Patel, Rev. Anal. Chem., 4 (1980) 237.
3 J. Aznarex, J. Galban, F. Palacios and J. C. Vidal, Analyst, 110 (1985) 193.
4 J. D. Glennon, N. Ni Choileain, D. A. Brown and R. A. Geraty, Synth. Commun., 15 (1985) 1159.
5 D. A. Brown, R. Geraty, J. D. Glennon and N. Ni Choileain, Inorg. Chem., 25 (1986) 3792.
6 A. T. Senior and J. D. Glennon, Anal. Chim. Acta, 196 (1987) 333.
7 H. Wu, D. Lu and Q. Liu, Fenxi-Haxue, 13 (1985) 523.
8 J. Inczedy, Analytical Applications of Complex Equilibrium, Horwood, Chichester, 1976.
9 B. Sarkar and T. P. Kruck, Can. J. Chem., 51 (1973) 3541.

Analytica Chimica Acta, 196 (1987) 333—336
Elsevier Science Publishers B.V., Amsterdam — Printed in The Netherlands

Short Communication

USE OF ACETOHYDROXAMIC ACID IN THE DIRECT SPECTROPHOTOMETRIC DETERMINATION OF IRON(III) AND IRON(II) BY FLOW INJECTION ANALYSIS

A. T. SENIOR and J. D. GLENNON*
Department of Chemistry, University College, Cork (Ireland)
(Received 29th July 1986)

Summary. The direct spectrophotometric determination of iron(III) and iron(II) by flow injection analysis with acetohydroxamic acid and 1,10-phenanthroline as reagents is reported. The working ranges are 0.5—10 and 10—60 mg l^{-1}, respectively. Results obtained for synthetic mixtures of Fe(III) and Fe(II) and for acid extracts of haematite samples were accurate. Interference studies indicate that the method is highly selective.

Flow injection analysis is increasingly recognised as an important tool for metal speciation [1]. The determination of iron(III) in the presence of iron(II) has received particular attention. Methods have for the most part involved the calculation of the Fe(III) concentration by a difference method after reduction of Fe(III) to Fe(II) [2, 3]. A spectrophotometric method based on parallel flow-injection manifolds with simultaneous sample injection has also been described [4]. More recently, ion chromatography with post-column derivatization [5] and a flow-injection system with diode-array detection have been used [6].

In the present work, the direct spectrophotometric determination of Fe(III) and Fe(II) by FIA by means of 1,10-phenanthroline in conjunction with a hydroxamic acid chelating agent is reported. Hydroxamic acids from both naturally-occurring and synthetic sources have a strong affinity for Fe(III) [7, 8] and a large variety of synthetic hydroxamic acids have been used for extractive-spectrophotometric determinations [9]. The simplest member of this class of reagent is acetohydroxamic acid, which undergoes a series of rapid stepwise reactions with Fe(III) to yield a strong 1:3 complex at neutral pH. An investigation of the utility of acetohydroxamic acid for Fe(III) determinations in the working range 0.5—100 mg l^{-1} and in the presence of Fe(II) are reported here.

Experimental

Apparatus. A Tecator 5001 FIAstar system was used with a Shimadzu UV-260 spectrophotometer. The injection and flow-through cell volumes were 20 μl and 70 μl, respectively. The total flow rate was 2 ml min^{-1} at

0003-2670/87/$03.50

0.2 bar pressure (nitrogen) with equal flow rates in each stream. Atomic absorption was measured with a Pye-Unicam SP191 spectrometer.

Direct determination of Fe(III) and Fe(II). Separate reagent solutions of acetohydroxamic acid and 1,10-phenanthroline were prepared at concentrations of 2×10^{-2} M and 2×10^{-3} M, respectively, in acetate buffer. The acetate buffer solution was prepared by mixing 20 ml of 2.0 M ammonium acetate with 180 ml of 2.0 M acetic acid to yield a reagent pH of 3.7. The carrier stream consisted simply of triply-distilled water. The flow injection manifold is shown in Fig. 1. At a given time, only one reagent stream is allowed to merge with the carrier stream, while the other reagent stream is stopped. This necessitates two injections of each sample for the speciation of Fe(III) and Fe(II). The wavelengths of maximum absorption were 512 nm and 440 nm for the Fe(II) and Fe(III) determinations, respectively.

Stock solutions of iron (200 μg ml^{-1}) were prepared from iron(III) nitrate and iron(II) ammonium sulphate in acid (2.0% v/v nitric acid and sulphuric acid, respectively). Synthetic Fe(III) and Fe(II) mixtures were prepared by appropriate dilutions of the two stock solutions. Analytical-grade salts were used for the interference studies, which involved alternating injections of a 20 μg ml^{-1} Fe(III) standard with injections of the standard-plus-diverse ion solutions.

Iron(III) was also determined in a diluted acid extract of a haematite geological sample by the flow-injection method and also by flame atomic absorption spectrometry (a.a.s.).

Results and discussion

The flow-injection method outlined here takes advantage of the high affinity of the hydroxamic acid reagent for Fe(III) and of the relatively strong but broad absorption band in the 420—440 nm region for Fe(III) complexation. This direct determination of Fe(III) in the presence of Fe(II) has distinct advantages, particularly as the level of interference from other metals on the Fe(III) determination is also reduced.

Calibration graphs for Fe(III) with acetohydroxamic acid and for Fe(II) with 1,10-phenanthroline were constructed for the ranges 1—10 mg l^{-1} and 10—60 mg l^{-1} with correlation coefficients greater than 0.999. The limit of detection for the Fe(III) determination was calculated to be 0.2 mg l^{-1} for

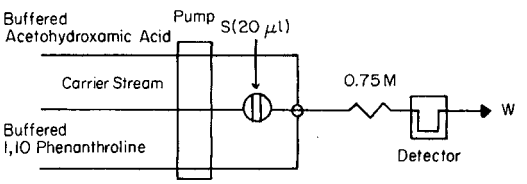

Fig. 1. Flow-injection manifold for the determination of Fe(III) and Fe(II). The reaction coil is 0.75 m long. All tubing was polyethylene (0.75 mm i.d.).

the 20-μl injection volume. For each standard injected six times, the relative standard deviation did not exceed 2%.

To verify the selectivity of the hydroxamic acid reagent for Fe(III) and the accuracy of the method, synthetic mixtures of Fe(III) and Fe(II) were prepared and examined while fresh by the flow-injection method and by flame atomic absorption spectrometry. The results obtained at pH 3.7 for various mixtures are shown in Table 1. The Fe(III) and Fe(II) levels found by the flow-injection method are in good agreement with the expected values and the total iron concentrations are in good agreement with the results obtained by a.a.s.

The interference study was done with 20 mg l^{-1} Fe(III); interference was considered to have occurred if the detector response differed by more than 2% relative from the interference-free standard [4]. As shown in Table 2, Cr(III), Sn(II) and Cu(II) exhibit the lowest tolerance levels. However, the level for the interference of Cu(II) is a considerable improvement over that attainable with the iron(III) thiocyanate system.

To test the accuracy of the Fe(III) determination, aliquots of a diluted acid extract of a haematite geological sample were examined by the flow-injection method and by flame a.a.s. The results were in good agreement (13.0, 23.8 and 73.8 mg l^{-1} by the proposed method and 13.2, 22.9 and 75.0 mg l^{-1} by a.a.s.). Investigations into other applications of this approach to the speciation of Fe(III) and Fe(II) are continuing, and other water-soluble hydroxamic acids are under study with a view to improving the sensitivity and selectivity of the method.

TABLE 1

Levels of Fe(III) and Fe(II) found for synthetic mixtures by flow injection analysis and flame atomic absorption spectrometry

Sample	Iron concentration (mg l^{-1})[a]			
	Flow-injection			A.a.s.
	Fe(II)	Fe(III)	Fe(Total)	Fe(Total)
1	35.5(36.0)	5.5(5.0)	41.0(41.0)	41.0
2	31.0(30.0)	10.2(10.0)	41.5(40.0)	41.5
3	30.0(30.0)	30.0(30.0)	60.0(60.0)	61.5
4	20.6(20.0)	20.7(20.0)	41.3(40.0)	42.0
5	10.0(10.0)	30.0(30.0)	40.0(40.0)	41.0
6	1.8(2.0)	40.0(40.0)	42.0(42.0)	42.5

[a]Added levels are given in parentheses.

TABLE 2

Interference studies for the spectrophotometric Fe(III) flow-injection method

Element	Diverse ion	Tolerance level (mg l^{-1})	Element	Diverse ion	Tolerance level (mg l^{-1})
Al(III)	$Al(NO_3)_3 \cdot 9H_2O$	500	Mn(II)	$MnSO_4 \cdot 4H_2O$	>1200
Cd(II)	$Cd(NO_3)_2 \cdot 4H_2O$	>1200	Ni(II)	$NiCl_2 \cdot 6H_2O$	>1600
Co(II)	$CoCl_2 \cdot 6H_2O$	>800	Pb(II)	$Pb(NO_3)_2$	1500
Cr(III)	$CrCl_3 \cdot 6H_2O$	200	Sn(II)	$SnCl_2 \cdot 2H_2O$	100
Cu(II)	$Cu(NO_3)_2 \cdot 3H_2O$	200	Zn(II)	$ZnSO_4 \cdot 7H_2O$	>900

REFERENCES

1 G. E. Pacey and B. P. Bubnis, Am. Lab., 16 (1984) 17.
2 T. P. Lynch, N. J. Kernoghan and J. N. Wilson, Analyst, 109 (1984) 839.
3 J. Mortatti, F. J. Krug, L. C. R. Passenda, E. A. G. Zagatto and S. S. Jorgensen, Analyst, 107 (1982) 659.
4 T. P. Lynch, N. J. Kernoghan and J. N. Wilson, Analyst, 109 (1984) 843.
5 H. Saitoh and K. Oikawa, J. Chromatogr., 329 (1985) 247.
6 F. Lazaro, A. Rios, M. D. Luque de Castro and M. Valcárcel, Anal. Chim. Acta, 179 (1986) 279.
7 D. A. Brown and M. V. Chidambaram, Bioinorg. Chem., 9 (1978) 255.
8 D. A. Brown, M. V. Chidambaram and J. D. Glennon, Inorg. Chem., 19 (1980) 3260.
9 Y. K. Agrawal and S. A. Patel, Rev. Anal. Chem., 4 (1980) 237.

Analytica Chimica Acta, 196 (1987) 337—343
Elsevier Science Publishers B.V., Amsterdam — Printed in The Netherlands

Short Communication

RADIO-ISOTOPE NEUTRON ACTIVATION ANALYSIS FOR VANADIUM, MANGANESE AND TUNGSTEN IN ALLOY STEELS

SERGIO MARIO LINS GALDINO and CARLOS COSTA DANTAS*

Department of Nuclear Energy, Federal University of Pernambuco, Recife, PE 50 000 (Brazil)

RENE VAN GRIEKEN

Department of Chemistry, University of Antwerp (UIA), Universiteitsplein 1, B-2610 Wilrijk (Belgium)

(Received 28th September 1986)

Summary. An instrumental neutron activation method for V, Mn and W in alloy steels with a ^{241}Am/Be isotopic neutron source is described. The samples were irradiated to induce the nuclear reactions ^{51}V(n, γ) ^{52}V, ^{55}Mn(n, γ) ^{56}Mn, and ^{186}W(n, γ) ^{187}W. The activities were measured with a NaI(Tl) detector. Interferences on the measured photopeaks were shown to be negligible by measuring the half-lives of ^{62}V, ^{56}Mn and ^{187}W. These three elements were determined in the range 1.5—12.9% in special steels; manganese in the range 0.5—1.6% was measured in cast irons. Calibration was done by comparison with results from wet chemistry and x-ray fluorescence spectrometry. The processing times for the vanadium, manganese and tungsten determinations were 11 min, 3 h and 26.3 h, respectively, but these were reduced greatly by introducing a scheme wherein six samples were simultaneously irradiated and the ^{56}Mn and ^{187}W nuclides were measured sequentially for a series of 66 samples. The average processing time was reduced to 45 min for tungsten with a precision of 4.0% and accuracy of 3.4% and 22.8 min for manganese with a precision of 3.8% and accuracy of 3.1%.

Small-scale manufacturing industries, particularly in developing countries, often find sophisticated multi-element instrumental methods, e.g., emission spectrometry or wavelength-dispersive x-ray fluorescence methods, too costly for laboratory control, whereas wet chemistry is too slow. In particular, the tool industry needs fast results for only a few elements in special steel alloys and cast irons; fast and precise determinations of vanadium, manganese and tungsten are often required.

Radio-isotope neutron activation analysis (NAA) can be sufficiently sensitive and precise for such applications. A low-activity neutron source for irradiation, a NaI(Tl) gamma counter and a single-channel analyzer are the only equipment required. A general review of problems in activation with various neutron sources has been given by Gijbels [1]. In several papers, the analysis of large iron and steel samples by radio-isotope NAA for V, Mn and W has been regarded as an unsolved problem; indeed, small samples are usually irradiated in a high reactor neutron flux and this is usually followed by

0003-2670/87/$03.50

chemical separation [2, 3]. A similar solution has been proposed for aluminium alloys for a few elements including vanadium and manganese [4]. Large samples of ferromanganese have been manipulated in radio-isotope NAA for manganese [5]. No reference in the literature was found regarding the problems of instrumental radio-isotope NAA based on isotopes with such different half-lives as ^{52}V ($t_{1/2}$ = 3.75 min), ^{56}Mn ($t_{1/2}$ = 2.58 h) and ^{187}W ($t_{1/2}$ = 23.8 h).

Experimental

Samples. Special steel, used in a small factory to make tools and with a typical composition of 84% Fe, 6% W, 3.6% Mo, 1.35% V, 0.33% Ni, 0.35% Co, 0.23% Mn and 0.02% Zn, was machined prior to irradiation into 35-g rods (6.0 cm long, 1.0 cm diameter). Cast iron samples, typically containing >90% Fe, 2—5% C, >0.5% Si and 0.2% S, were machined into 75-g discs (0.8 cm thick, 0.4 cm diameter).

Seven of the steel samples were split after the activation, one half for wet chemical analysis and the other part for x-ray fluorescence spectrometry (XRF).

Irradiation arrangements and counting equipment. The $^{241}Am/Be$ neutron source with an activity of 5 Ci had a neutron flux of 5×10^6 s^{-1}. The irradiation arrangement contained the neutron source inserted in the center of a 40-cm diameter cylindrical paraffin block, which served as a neutron moderator-reflector. The neutron flux was mapped for the radial and vertical axes by irradiating and measuring the radioactivity induced through the ^{51}V (n, γ) ^{52}V reaction in small discs of vanadium metal. Previously [6], by irradiating aluminium and measuring the induced activities from ^{27}Al (n, γ) ^{28}Al and ^{27}Al (n, p) ^{27}Mg, the neutron flux was calculated to be 6×10^4 cm^{-2} s^{-1} and the ratio of the thermal-to-fast flux around 35. The irradiation arrangement, with one irradiation position shown in Fig. 1, allows the steel rod sample to be placed in a defined irradiation position at the maximum thermal neutron flux. The irradiation arrangement shown in Fig. 2, allows six disc samples to be placed concentrically in the same neutron flux.

After irradiation, the samples were measured by γ-counting, the rods in a well-type detector, and the discs positioned directly on a 2 × 2-in. detector; both NaI(Tl) detectors were coupled to a single-channel analyzer.

Procedures. The selected γ-ray counting channels were: 1220—1550 keV for ^{52}V (main peak at 1434 keV), 760—940 keV for ^{56}Mn (main peak at 847 keV) and 610—745 keV for ^{167}W (prominent peak at 686 keV). In preliminary experiments, the irradiation and counting times were 5 min each for the determination of vanadium; for the determination of manganese, the samples were irradiated for 20 min and counted for 20 min after a 40-min decay; for tungsten, the samples were irradiated for 2 h, allowed to decay for 24 h and counted for 20 min. Under the given conditions, the ^{52}V, ^{56}Mn and ^{187}W were measured practically free of any interference. For all the measured radionuclides, the number of counts was above 2×10^4 in each sample. For

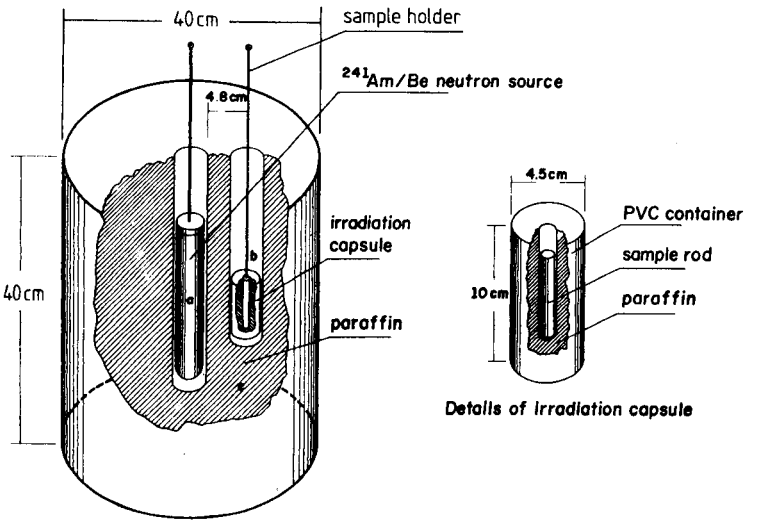

Fig. 1. Irradiation arrangement with 1 irradiation position (a) ^{241}Am/Be source (5 Ci); (b) irradiation capsule at the maximum flux position; (c) paraffin as neutron moderator/reflector.

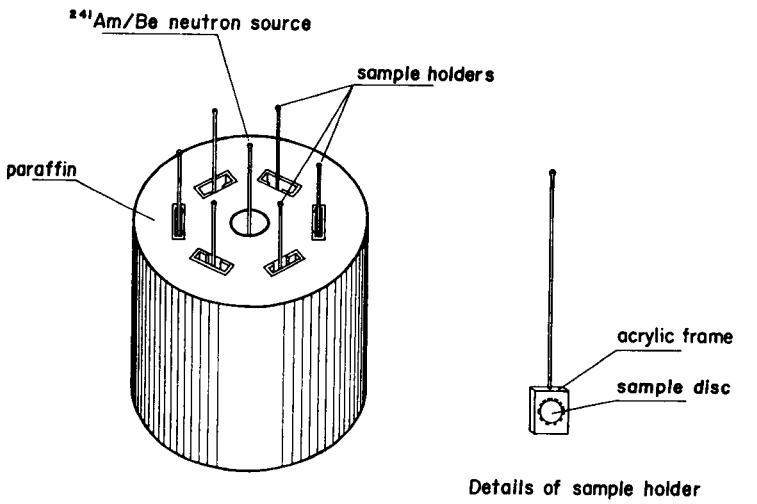

Fig. 2. Irradiation arrangement with 6 irradiation positions.

calibration, the measured activities of a series of typical samples were related to the results from wet chemistry and from XRF [7].

This procedure allowed the purely instrumental determination of vanadium, manganese and tungsten in the special steel samples with precision and accuracy equivalent to those of XRF. However, the total time needed for the manganese and especially the tungsten determinations was not compatible with the industrial requirements.

The solution was a sequential irradiation/counting scheme for a number of

samples so that the average time would decrease significantly. For this scheme, the basic requirement was simultaneous irradiation of several samples. The counting system would remain the same with one detector coupled to a single-channel analyzer. To maintain the same neutron flux, the number of samples to be irradiated simultaneously was limited to a maximum of six. In this scheme of analysis, the irradiation time should be six times the counting time for both ^{56}Mn and ^{187}W. An irradiation arrangement was thus constructed with six irradiation positions (Fig. 2); the induced activity was exactly the same for the six positions, within the counting statistics. The sequential irradiation/counting scheme involved a suite of 66 samples to be irradiated in the six positions. In the sequence of analysis, one sample goes into the irradiation arrangement every 20 min and after 2 h of irradiation, the sample is removed to decay. After a decay of 40 min, the sample is ready for measurement of ^{56}Mn and after 24 h for measurement of ^{187}W. The scheme for sequential irradiation and counting is shown in Fig. 3. For the 66 samples, the mean processing time is 23 min for manganese and 45 min for tungsten. This sequential scheme was checked with a block of 18 samples by simultaneous irradiation, decay and counting for the ^{56}Mn radionuclides. Three samples were taken from each of six different cast iron batches in order to check the stability of the counting equipment during long measurements and also the time needed for changing the samples within the total processing time.

Sources of errors. Although tungsten has the highest concentration and the highest neutron absorption among all the alloy elements in special steel, variations in its neutron self-shielding effect were found to be negligible by the calculation given earlier [8], taking into account the typical variation in the tungsten concentration among the special steel samples. The manganese

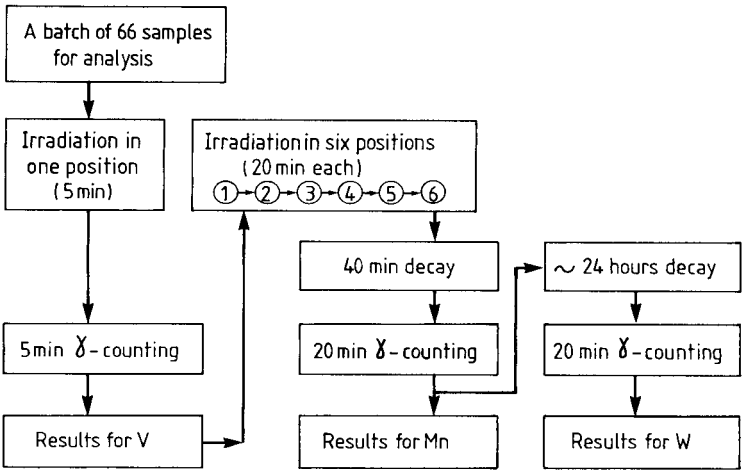

Fig. 3. Scheme for sequential irradiation and counting.

concentration is lower in the special steels than in the ferromanganese samples for which Alaerts et al. [5] reported a significant neutron self-shielding error; the manganese concentration varied only over 0.1% Mn at maximum while it varied over 5% Mn in ferromanganese [5]. However, for the cast iron samples, the variation in manganese concentration can induce differences in the self-shielding effect of around 3%. No correction was introduced, because this error was acceptable for the 0.5—1.5% manganese contents typical of cast iron. The γ-attenuation caused by the density variation among the sample profile produced a negligible effect. The samples were machined to identical dimensions and the variation in weight caused by density variation was 0.5% at most.

Because of the chosen irradiation, decay and counting times, practically only one radionuclide was present in each measurement. The production of ^{56}Mn by the ^{56}Fe (n, p) ^{56}Mn reaction proved to be negligible in a pure iron sample. To confirm the absence of any interference in the measured energy region, the apparent half-lives of ^{52}V, ^{56}Mn and ^{187}W were measured for typical steel samples; the values found were 3.88 ± 0.15 min, 2.62 ± 0.08 h and 23.72 ± 0.08 h, respectively, compared to values of 3.75 min, 2.58 h and 23.8 h obtained from nuclide charts, i.e., the agreement was within 4%.

Results and discussion

The concentrations of vanadium, manganese and tungsten in the special steel samples were calculated in relation to the results given by the wet chemical and XRF procedures. Results from wet methods were available for samples 1—7 and XRF results for samples 1—5. In both cases sample 5 was chosen as the standard to calculate the elemental concentration of the other samples. Sample 5 was selected because of its intermediate values for V, Mn and W among the results from the wet methods and because it provided the minimum standard deviation among the XRF results. In Table 1, the results found by the radio-isotope activation method using the data from wet methods as the reference value are listed as NAA-I and those based on XRF results as reference value as NAA-II. Except for vanadium, there appears to be a systematic difference between wet chemistry and XRF. Table 2 shows the mean relative deviations between the three techniques. Obviously, the radioisotope NAA method is better with the XRF results than with wet chemistry results. When the XRF results were taken as the true values, the accuracies for vanadium, manganese and tungsten in a special steel were within 1.9, 3.1 and 3.1%, with coefficients of variation of 1.5, 5.1 and 3.8%, respectively. The result for manganese in a cast iron, based on the same calibration, was within 6% of the XRF result, with a 4% coefficient of variation. The ^{56}Mn activity for 18 disc samples of six cast iron batches containing 0.5—1.6% manganese was shown to have a good linear relation to the results obtained by atomic absorption spectrometry.

While the total processing times for a single run for V, Mn and W were 11 min, 3.1 h and 26.3 h, respectively, they were reduced to 5 min, 23 min

TABLE 1

Comparison of the results for vanadium, manganese and tungsten in steel samples

Sample	Metal found (%)			
	Wet Chemistry	NAA-I[a]	XRFA	NAA-II[a]
Vanadium				
1	2.15	2.19 ± 0.03	2.02 ± 0.02	2.07 ± 0.03
2	2.05	2.19 ± 0.05	1.98 ± 0.002	2.07 ± 0.05
3	2.15	2.14 ± 0.07	2.00 ± 0.02	2.02 ± 0.06
4	2.15	2.08 ± 0.05	1.96 ± 0.02	1.96 ± 0.05
5	2.15	—	2.03 ± 0.01	—
6	2.30	2.29 ± 0.09	—	2.17 ± 0.08
7	2.15	1.93 ± 0.07	—	1.82 ± 0.06
Manganese				
1	0.20	0.21 ± 0.03	0.27 ± 0.01	0.29 ± 0.04
2	0.20	0.21 ± 0.02	0.27 ± 0.03	0.28 ± 0.03
3	0.20	0.21 ± 0.03	0.28 ± 0.01	0.28 ± 0.04
4	0.29	0.25 ± 0.03	0.35 ± 0.01	0.34 ± 0.04
5	0.25	—	0.34 ± 0.01	—
6	0.29	0.25 ± 0.02	—	0.34 ± 0.03
7	0.29	0.21 ± 0.03	—	0.29 ± 0.04
Tungsten				
1	4.23	4.52 ± 0.21	6.17 ± 0.12	6.46 ± 0.31
2	4.12	4.43 ± 0.17	6.10 ± 0.01	6.34 ± 0.24
3	4.12	4.45 ± 0.28	6.14 ± 0.02	6.36 ± 0.39
4	4.12	4.18 ± 0.22	5.96 ± 0.06	5.97 ± 0.32
5	4.17	—	5.96 ± 0.01	—
6	3.70	4.36 ± 0.21	—	6.24 ± 0.30
7	4.20	4.03 ± 0.37	—	5.76 ± 0.53

[a]Results were normalized with respect to sample 5; wet chemistry was used for NAA-I and XRF for NAA-II.

TABLE 2

Comparison of mean relative deviation in the results for V, Mn and W

Element	Mean relative deviation[a]		
	Wet method/NAA-I	XRF/NAA-II	Wet method/XRF
V	3.8	1.9	6.2
Mn	10.8	3.1	33.3
W	7.6	3.1	46.1

[a]Defined as $100\left[\sum_{i=1}^{n}(x1_i - x2_i)/x1_i\right]/n$; $n = 5$.

and 45 min, respectively, with the irradiation-counting scheme for many samples.

S. M. L. G. is a research fellow of Pronuclear, Commissao Nacional de Energia Nuclear, Brazil. C. C. D. is a scientist of the CNPq, Brazil. Part of this work was financed by FINEP, Brazil. L. Van't dack carried out the XRF measurements.

REFERENCES

1 R. Gijbels, Miner. Sci. Eng., 5 (1973) 304.
2 H. Jaskolska, L. Rowinska and M. Radwan, J. Radioanal. Chem., 20 (1974) 419.
3 H. Jaskolska, L. Rowinska, L. Walis and M. Radwan, J. Radioanal. Chem., 13 (1973) 41.
4 T. Z. Bishay, J. Radioanal. Chem., 13 (1973) 87.
5 L. Alaerts, J. P. Op de Beeck and J. Hoste, J. Radioanal. Chem., 15 (1973) 601.
6 G. Carvalho, M.Sc. Thesis, DEN, Federal University of Pernambuco, Brazil, 1980.
7 P. Van Dyck and R. Van Grieken, in J. Albaiges (Ed.), Analytical Techniques in Environmental Chemistry, Vol. 2, Pergamon, Oxford, 1982, p. 315.
8 C. C. Dantas, PhD. Thesis, University of Ghent, Belgium, 1973.

Analytica Chimica Acta, 196 (1987) 345—350
Elsevier Science Publishers B.V., Amsterdam — Printed in The Netherlands

Short Communication

n-OCTYLPHENYL HYDROGEN PHOSPHATE AS AN EXTRACTANT FOR SOME LANTHANIDES

S. S. V. RAMA KUMAR, O. V. SINGH and S. N. TANDON*
Department of Chemistry, University of Roorkee, Roorkee-247 667, U.P. (India)
(Received 28th August 1986)

Summary. n-Octylphenyl hydrogen phosphate (OPHP) is examined for the extraction of neodymium, gadolinium and terbium. The effects of pH and metal ion and extractant concentrations are reported. The extraction constants are 39.5, 40.7 and 43.4 for Nd, Gd and Tb, respectively. The extraction efficiency of OPHP for these lanthanides is better than that of commoner alkylphosphorus acids.

Numerous alkyl, aryl and mixed alkyl—aryl phosphorus acids have been reported as potential extractants for lanthanides as well as other metals. Of these, di-2-ethylhexyl phosphoric acid (DEHPA) has received by far the most attention. Peppard et al. [1] indicated the superiority of n-octylphenyl phosphonate over DEHPA for the extraction of transition metals. It was thought that n-octylphenyl hydrogen phosphate (OPHP) would also prove to be an effective extractant. Nothing significant appears to have been reported on this extractant. Here, the potential of OPHP for the extraction of some lanthanides (neodymium, gadolinium and terbium) from nitric acid solutions is examined. The efficiency of extraction with OPHP is compared with that of some other alkyl phosphorus acids.

Experimental

Materials. All the alkylphosphorus acids tested were obtained from Mobil Chemical Company (U.S.A.) and were used as received. The acid solutions were standardized by conventional non-aqueous titrimetry [2]. All other chemicals used were of analytical purity.

The γ-activity of ^{147}Nd, ^{153}Gd and ^{160}Tb was counted with a well-type NaI(Tl) scintillation counter.

Procedure. Equal volumes (10 ml) of the aqueous phase (usually 1.0×10^{-4} M metal ion in nitric acid) and organic phase (usually 0.10 M OPHP in toluene) were shaken at 23 ± 2°C for 2 min to complete equilibration. The two phases were separated and suitable aliquots of each phase were counted for γ-activity.

0003-2670/87/$03.50

Results and discussion

The extraction equilibrium of the alkylphosphorus acids can be represented [3] as follows

$$[M^{m}]_{aq} + (m/2)[R_2H_2]_0 \rightleftharpoons [MR_n(m-n)RH]_0 + n[H^+]_{aq} \quad (1)$$

where M^{n+} is the metal ion, R_2H_2 is the dimeric acidic extractant and m is the total number of extractant molecules (exchanging and solvating) involved in the complex formation. The distribution ratio, D, is

$$\log D = \log K + \mathrm{pH} + (m/2)\log [R_2H_2]_0 \quad (2)$$

Differentiating this equation with respect to pH gives $[\delta \log D/\delta \mathrm{pH}] = m$. Equation 2 in terms of $pH_{0.5}$ becomes

$$pH_{0.5} = -(1/n) \log K - (m/2n) \log [R_2H_2]_0 \quad (3)$$

When the extracted species polymerizes in the organic phase, Eqn. 2 becomes [4]

$$\log D = \log K + n\mathrm{pH} + (m/2) \log [R_2H_2]_0 + (1/X) \log X + [(X-1)/X] \times \log [M]_0$$

where X is the degree of polymerization or the average number of MR_n units. Then

$$[\delta\ pH_{0.5}/\delta \log [M_{total}]]\ [R_2H_2]_0\, X = -(X-1)/nX$$

Extraction of neodymium, gadolinium and terbium. When the extraction of these metal ions into various solvents was studied, no regular trend was observed with changing dielectric constant (Table 1). Toluene was selected as the diluent for further studies.

If the acid extractant is present as a dimer in the organic phase, the slope of the linear relationship between $\log [HR]_{aq}$ and $\log [HR]_0$ should be two. Distribution studies showed that OPHP exists in dimeric form in toluene. This was confirmed by infrared spectroscopy; a downward shift in the phosphoryl (P—O) bond stretching frequency indicated intermolecular hydrogen bonding in the dimer [5].

As indicated above, the slope of the pH vs. $\log D$ plot at constant extractant concentration in the organic phase gives the number of extractant molecules involved. The variation of $\log D$ with pH at various OPHP concentrations for Nd(III), Gd(III) and Tb(III) is shown in Fig. 1. For each of these metal ions, the expected slope of 3 was obtained, indicating that three OPHP molecules are involved in the extraction.

The relationship between $pH_{0.5}$ and $\log [R_2H_2]_0$ should be linear with a slope of $-m/2n$ (Eqn. 3), from which the value of m (total number of exchanging and solvating OPHP molecules) can be obtained. Plots of $pH_{0.5}$ vs. $\log [H_2R_2]_0$ for all the three metal ions are given in Fig. 2. From the slopes of these plots, the m values are about 3 in all cases; this indicates that OPHP is not involved in solvating the extracted species.

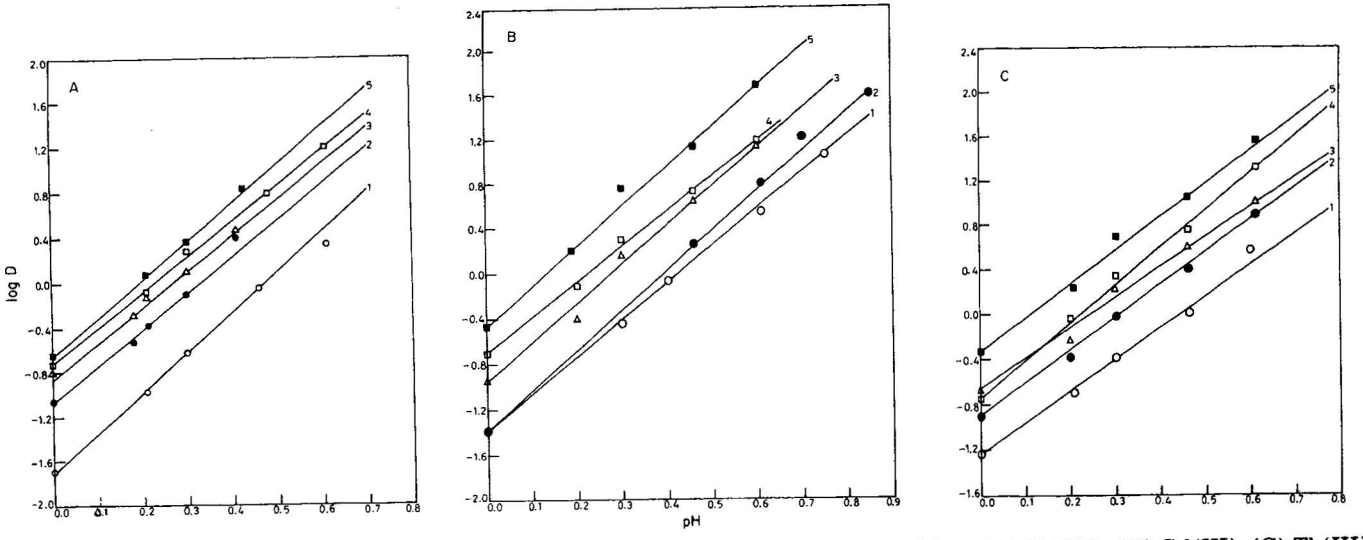

Fig. 1. Effect of pH on the metal extractions at various OPHP concentrations. Metal ion: (A) Nd(III); (B) Gd(III); (C) Tb(III). OPHP concentration: (○) 0.02 M; (●) 0.04 M; (△) 0.06 M; (□) 0.08 M; (■) 0.10 M. The respective m values for these extractant concentrations were as follows: (A) 3.4, 3.3, 3.0, 3.0, 3.4; (B) 3.0, 3.2, 3.1, 3.0, 3.3; (C) 2.8, 3.0, 2.9, 3.3, 2.9. In all cases, the correlation coefficients for the plots were >0.98.

TABLE 1

Extraction of Nd(III), Gd(III) and Tb(III)[a] with OPHP (0.10 M) in different solvents of varying dielectric constants

Solvent	Dielectric constant	Percentage extraction		
		Nd(III)	Gd(III)	Tb(III)
n-Hexane	1.89	79.6	94.7	96.2
Cyclohexane	2.02	86.4	46.3	93.1
Xylene	2.20	64.7	84.9	81.0
Benzene	2.28	62.0	—	70.8
Toluene	2.44	62.8	87.3	88.5
Chloroform	4.50	56.8	—	—
Carbon tetrachloride	4.80	67.1	77.8	83.5
Cyclohexanone	18.30	5.2	1.1	50.1

[a]In 1.0 M nitric acid.

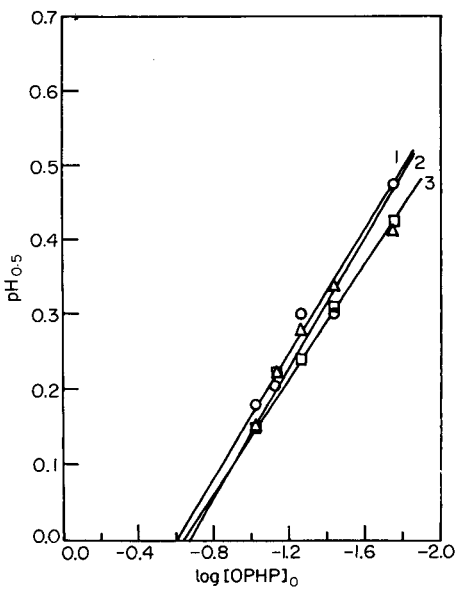

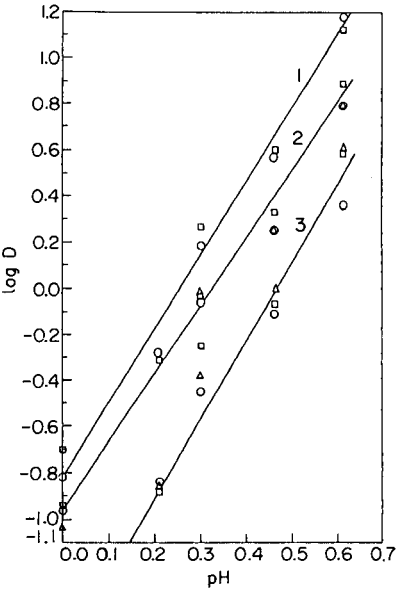

Fig. 2. Effect of OPHP concentration on the extractions: (○) Nd(III); (△) Gd(III); (□) Tb-(III).

Fig. 3. Effect of metal concentration on the extraction of the metals: (1) Nd(III); (2) Gd-(III); (3) Tb(III). Metal concentration: (○) 5×10^{-4} M; (△) 1.0×10^{-4} M; (□) 5.0×10^{-5} M.

To check the possibility of further polymeric species being formed, $pH_{0.5}$ was plotted against log $M_{(total)}$; $pH_{0.5}$ was obtained from the plots of pH vs. log D for solutions of different metal ion concentrations. The results are shown in Fig. 3. For each metal ion, the $pH_{0.5}$ values fall on the same straight line suggesting that no polymeric species are formed.

TABLE 2

Calculation of extraction constants (K)

Log $[OPHP]_0$	Neodymium $pH_{0.5}$	K	Gadolinium $pH_{0.5}$	K	Terbium $pH_{0.5}$	K
−1.32	0.11	39.5	0.11	40.7	0.10	43.4
−1.42	0.20		0.22		0.22	
−1.55	0.30		0.27		0.24	
−1.73	0.30		0.39		0.31	
−2.05	0.48		0.41		0.45	

TABLE 3

Comparison of the efficiency of extraction with OPHP and other alkylphosphorus acids in toluene

Extractant[a]	Extraction (%)		
	Nd	Gd	Tb
OPHP	62.8	87.3	88.5
H_2EHPA	6.2	65.0	22.8
DEHPA	1.8	0.5	0.8
DBBP	7.0	1.1	<0.1
DT-23	1.9	0.7	<0.1

[a]H_2EHPA, mono-(2-ethylhexyl)phosphoric acid; DEHPA, di-(2-ethylhexyl)phosphoric acid; DBBP, di-butylbutyl phosphonate; DT-23, a mixture (77:23) of DEHPA and trioctyl phosphine oxide (TOPO).

The above studies indicate that the extracted species of all the three metals studied is MR_3, where M is the metal ion and R is the n-octylphenyl phosphate ion. The extraction constants were calculated from Eqn. 3 and the results are given in Table 2. The constants follow the expected trend and increase with increasing atomic number, i.e., Tb > Gd > Nd.

Comparison with some other alkylphosphorus acids. The extraction efficiency of OPHP was compared with other widely used alkylphosphorus acids under identical conditions. The results shown in Table 3 indicate that OPHP is a better extractant for the lanthanides. The effectiveness of OPHP in comparison with its alkyl counterparts may be due to its increased acidity.

The authors are grateful to Mobil Chemical Company for donating the alkylphosphorus acids. The financial assistance of Council of Scientific and Industrial Research, India, is gratefully acknowledged.

REFERENCES

1 D. F. Peppard, G. W. Mason, S. McCarty and F. D. Johnson, J. Inorg. Nucl. Chem., 24 (1962) 321.
2 T. Sato, J. Inorg. Nucl. Chem., 9 (1954) 188.
3 A. W. Fletcher and D. S. Flett, J. Appl. Chem., 14 (1964) 250.
4 Y. Marcus, Chem. Rev., 63 (1963) 139.
5 J. R. Ferraro, J. Inorg. Nucl. Chem., 24 (1962) 475.

Analytica Chimica Acta, 196 (1987) 351—354
Elsevier Science Publishers B.V., Amsterdam — Printed in The Netherlands

Short Communication

OXIDIMETRIC TITRATION OF TRIPHENYL DERIVATIVES OF PHOSPHORUS, ARSENIC, ANTIMONY AND BISMUTH WITH *N*-BROMOSUCCINIMIDE

Y. A. GAWARGIOUS*, M. E. M. HASSOUNA[a] and H. N. A. HASSAN
Microanalytical Research Laboratory, National Research Centre, Dokki, Cairo (Egypt)
(Received 9th July 1986)

Summary. A simple direct titration for milligram and microgram amounts of triphenyl-phosphorus, -arsenic, -antimony, and -bismuth is described. The methanolic sample solution, with a little water, hydrochloric acid and bromide added, is titrated with *N*-bromosuccinimide to a methyl red end-point. All four compounds were titrated in the same way with recoveries of 99—100% and relative standard deviations of 1—5% were obtained.

The extensive use of the triphenyl derivatives of phosphorus, arsenic, antimony and bismuth in various industrial fields [1] requires accurate simple methods for their determination. No single procedure has been reported for this group of related compounds. Triphenylphosphine has been estimated via oxidation with iodine chloride [2] or bromine chloride [3] followed by iodimetric titration of the excess of reagent. Organo-arsenic compounds have been determined [4] iodimetrically. Triphenyl-arsenic, -antimony and -bismuth have been determined with chloramine-T [5], the excess of which was titrated iodimetrically; triphenylantimony was estimated with chloramine-B [6]. Organic arsenicals and antimonials have been decomposed by acid digestion followed by oxidation and iodimetric titration [7]. Oxidation with periodate and titration of the iodate released was recently applied to some of these derivatives [8].

N-Bromosuccinimide has been used as titrant for antimony trichloride and tartar emetic [9] and for arsenites [10]. In the work described here, the oxidative efficiency of *N*-bromosuccinimide as titrant for trivalent phosphorus, arsenic, antimony and bismuth, each bonded to the triphenyl moiety, was studied in order to develop a single procedure for the direct determination of all four compounds at both micro and submicro levels.

[a]Present address: Chemistry Department, Faculty of Science at Beni-Suef, Cairo University, Beni-Suef, Egypt.

0003-2670/87/$03.50

Experimental

Reagents and materials. All reagents used were of analytical grade and doubly-distilled water was always used. Aqueous 4×10^{-3} and 5×10^{-4} M *N*-bromosuccinimide solutions were prepared and standardized [11] daily. Methyl red indicator was used as a 0.125% (w/v) solution in 70% ethanol.

The sample solutions were prepared in methanol, 4×10^{-3} M for the micro method and 5×10^{-4} M for the submicro method.

Procedure. Transfer an aliquot of the sample solution containing 0.08–5 mg of the triphenyl compound to a 100-ml conical flask and dilute to 5 ml with methanol. Add a few drops of water, 0.1 ml of dilute (1 + 99) hydrochloric acid, 0.1 ml of 1% (w/v) potassium bromide solution and one drop of methyl red indicator. Titrate with the appropriate *N*-bromosuccinimide solution at a moderate rate until the red colour fades; continue adding the titrant dropwise with shaking until complete decolorization is obtained. Run a blank experiment and deduct the blank before calculating the result.

Results and discussion

The first point studied was the oxidation route of each of the four triphenyl derivatives of trivalent P, As, Sb and Bi with *N*-bromosuccinimide under conditions closely related to those established recently [12] for the determination of antibilharzial antimony(III) compounds. With all four compounds, the oxidation proceeded rapidly at room temperature according to the equation

$$(C_6H_5)_3M + \begin{matrix} CH_2{-}CO \\ | \quad\quad > NBr \\ CH_2{-}CO \end{matrix} + H_2O + 2HCl + 2KBr \longrightarrow$$

$$(C_6H_5)_3MO + \begin{matrix} CH_2{-}CO \\ | \quad\quad > NH \\ CH_2{-}CO \end{matrix} + 2KCl + 3HBr \qquad (1)$$

where M = P, As, Sb, or Bi. In previous work [8] with periodate as oxidant for the same compounds (other than triphenylbismuth), the respective triphenyl oxide derivatives were formed quantitatively; benzene and the element oxides were not formed as stated eariler [13]. The formation of the $(C_6H_5)_3MO$ was confirmed by extraction and crystallization of the four products individually from benzene; triphenylbismuth oxide separated only on slow addition of petroleum ether to the concentrated benzene extract. The white solids were shown to be the corresponding oxide derivatives through melting points and mixed melting points with authentic samples [14].

The best medium for general application of the oxidation reaction was found to be methanol, which gave the lowest blank value, in the presence of bromide, compared with ethanol and acetone. The blank value also depended on the strength of the *N*-bromosuccinimide solutions, increasing at concentrations less than 5×10^{-4} M. As is evident from reaction 1, the presence of

water as ionizing agent [15] is essential for completion of oxidation. The amount of water possible is limited by the solubility and concentration of the test compound in methanol. 5—6 drops of water sufficed; more produced turbidity.

With regard to acidity, Pahil and Sharma [5] dissolved arsines and stibines by heating with acetic acid, then adding water to incipient precipitation and more acetic acid to clear the solution; addition of excess of chloramine-T and back-titration followed. For bismuthines, a mixture of anhydrous acetic acid and 2 M hydrochloric acid with heating to 90—100°C was used for dissolution. A strong hydrochloric acid medium was used earlier for direct titration of trivalent antimonials with *N*-bromosuccinimide [9, 16]. In the present study, it was found that addition of 0.1 ml of dilute (1 + 99) hydrochloric acid to the methanolic sample solution was efficient for both micro and submicro levels thus avoiding the drastic conditions previously recommended [8, 13]. No signs of any bromination of the triphenyl organic moiety could be seen under the present mild acidity conditions with any of the four compounds tested.

A general procedure was then worked out for both micro and submicro sample amounts with methyl red as indicator. Application of the recommended procedure produced highly satisfactory results (Tables 1 and 2) showing total average recoveries of 99.97 and 99.78%, respectively. The

TABLE 1

Microdetermination of triphenyl derivatives of phosphorus, arsenic, antimony and bismuth

Compound	No. of detns.	Wt. taken (mg)	Average found (mg)	Average recovery (%)	Standard deviation
Triphenyl-phosphorus	3	2.098	2.095	99.8	0.144
	3	5.246	5.249	100.1	0.058
	6[a]	3.339—5.924	4.391	99.9	0.153
Triphenyl-arsenic	3	3.675	3.673	99.9	0.051
	3	4.900	4.900	100.0	0.060
	10[a]	3.200—5.454	4.313	100.0	0.178
Triphenyl-antimony	3	2.824	2.828	100.1	0.202
	3	5.649	5.630	99.7	0.144
	6[a]	3.415—5.645	4.603	99.9	0.080
Triphenyl-bismuth	3	2.642	2.648	100.2	0.190
	3	5.284	5.280	99.9	0.085
	6[a]	2.010—5.920	4.315	99.9	0.203

[a]Weighed samples.

TABLE 2

Submicrodetermination of the same triphenyl derivatives

Compound	Wt. taken (μg)	Average[a] found (μg)	Average recovery (%)	Standard deviation (*S*)
Triphenyl-phosphorus	65.6	65.3	99.6	0.35
	262.3	262.5	100.1	0.14
Triphenyl-arsenic	76.6	76.4	99.8	0.14
	459.4	459.5	100.0	0.12
Triphenyl-antimony	88.3	88.0	99.7	0.58
	353.1	351.3	99.8	0.29
Triphenyl-bismuth	111.0	109.1	99.1	0.23
	660.5	661.2	100.1	0.19

[a]Average of 3 determinations.

blank values did not exceed 0.1 and 0.15 ml for the two molarities of *N*-bromosuccinimide used.

REFERENCES

1 M. Dub, Organometallic Compounds. Methods of Synthesis, Physical Constants and Chemical Reactions, Vol. III, 2nd edn., First supplement, Springer, Berlin, 1972, p. 531.
2 P. N. K. Nambisan, R. Lalithakumari, C. N. Kumaran and C. G. R. Nair, Indian J. Chem., 11 (1973) 964.
3 C. G. Nair and R. Lalithakumari, Indian J. Chem., Section A, 14 (1976) 115.
4 S. S. Singh, S. S. Pahil and K. D. Sharma, Anal. Chim. Acta, 56 (1971) 145.
5 S. S. Pahil and K. D. Sharma, Z. Anal. Chem., 270 (1974) 127.
6 D. V. Końkova and K. Z. Zonenberg, Khim. Prom-st., Ser.: Reakt. Osobo Chist. Veschestva, 1 (1980) 1; Anal. Abstr., 41 (1981) 4C88.
7 M. Bigois and M. Marchand, Talanta, 19 (1972) 157.
8 Y. A. Gawargious, A. Besada and M. E. M. Hassouna, Microchem. J., 33 (1986) 116.
9 M. Z. Barakat and S. K. Shehab, Analyst, 90 (1965) 50.
10 M. Sarwar, A. K. Rana and S. P. Hamdani, Microchem. J., 16 (1971) 184.
11 M. Z. Barakat, M. F. Abd El-Wahab and M. M. El-Sadr, Anal. Chem., 27 (1955) 536.
12 Y. A. Gawargious, M. E. M. Hassouna, H. N. A. Hassan and I. H. Habib, Pharmazie, 41 (1986) 59.
13 Y. A. Gawargious, L. S. Boulos and A. Besada, Analyst, 101 (1976) 458.
14 T. S. Ma and R. C. Rittner, Modern Elemental Analysis, M. Dekker, New York, 1979, pp. 235—252.
15 R. D. Tiwari and U. C. Pande, J. Indian Chem. Soc., 51 (1974) 112.
16 A. Berka and J. Zýka, Collect. Czech. Chem. Commun., 23 (1958) 402.

Analytica Chimica Acta, 196 (1987) 355—357
Elsevier Science Publishers B.V., Amsterdam — Printed in The Netherlands

Short Communication

DETERMINATION OF SULPHUR IN ORGANOMETALLIC COMPOUNDS BY THE OXYGEN FLASK METHOD

PETER BORDA

Chemistry Department, 2036 Main Mall, The University of British Columbia, Vancouver, B.C. V6T 1Y6 (Canada)

(Received 31st July 1986)

Summary. A simple technique of determining sulphur in organometallic compounds by the oxygen flask method is presented. It is based upon the oxidative destruction of the sample; precipitation and cation exchange separation of interfering ions and the titrimetric determination of sulphuric acid. From the variety of substances analyzed, the method would appear to be applicable to all kinds of sulphur-containing organic and organometallic compounds.

Because of its simple mode of operation and economy, the oxygen-flask method [1] of decomposition is frequently used for the determination of halogens and sulphur in organic and organometallic compounds. However, after such oxidative destruction, the titration of sulphur (as sulphate with barium perchlorate [2]) is rather tedious if both phosphate and metal ions are present in the absorbing solution. Before sulphate can be successfully titrated, the common procedures require conversion of the interfering phosphates to insoluble entities, separation of these by filtration [3—5] and removal of cations with ion exchangers or EDTA [4, 5].

In the present study, the procedure was simplified by using a cation-exchange column to retain both metal ions and the insoluble phosphate precipitates, while the sulphate was eluted free of interferences. Before this method was considered, however, attempts were made to use cation-exchange resins to separate metal and phosphate ions from the sulphate. These experiments were based on an earlier observation [6] that cation exchangers not only absorb metal ions but temporarily retain the phosphate ion. Therefore, more washing is necessary for removal of phosphate from a column than is normally required for other acids. Thus, after decomposition, the absorbing solution and washes were passed through a cation-exchange column and the sulphate in the eluate was titrated in the usual way with barium perchlorate. This procedure for removing interferences worked well when the phosphate concentration was low. Larger concentrations could be handled if 10 mg of zinc acetate or lanthanum nitrate was added to the absorbent solution before it was transferred to the cation-exchange column, thus providing clean separation of interferences.

0003-2670/87/$03.50

Experimental

Mineralization of organic and organometallic samples was done in the usual manner by the oxygen-flask method. When absorption of the products was complete, the stopper and gauze were rinsed down with 3 ml of distilled water. Then 10 mg of zinc acetate or lanthanum nitrate was added to the solution, which was boiled for 3 min. After the solution had cooled to room temperature, the solution and the metal phosphate precipitate were transferred to a column (1 cm i.d., 25 cm long, 10-cm resin bed) containing Amberlite IR-120 cation exchanger in the hydrogen form. The eluate and washings (total volume 40—45 ml) were diluted with isopropanol and the sulphate was titrated with 0.01 M barium perchlorate in the presence of thorin/methylene blue as indicator [2].

Results and discussion

The determination of sulphur in test samples by this simple technique gave the results summarized in Table 1. Even complex organometallic compounds can be analysed. In the final titration there was no interference from phosphate, showing that the insoluble (acid-sensitive) precipitates did not break down on the cation-exchange resin. The utilization of thorium nitrate afforded no advantage as the removal of its phosphate from the column was more difficult than those of zinc or lanthanum. Because zinc and lanthanum phosphates are soluble in dilute acids, reconditioning of the column after each determination was easily accomplished with 2 M hydrochloric acid.

TABLE 1

Determination of sulphur in organometallic compounds

Compound	Weight taken (mg)	Sulphur (%)		
		Calc.	Found	Error
$C_4H_{12}P_2S_2$	2.989	34.43	34.62	+0.19
	4.059		34.60	+0.17
	3.616		34.72	+0.29
	5.004		34.92	+0.49
$C_4H_{13}NP_2S_2$	3.747	31.87	31.90	+0.03
	4.129		32.17	+0.30
$C_{38}H_{32}O_2P_2SRu$	4.575	4.48	4.40	−0.08
$C_{40}H_{36}O_2P_2SRu$	5.008	4.31	4.00	−0.31
$C_{45}H_{38}O_2P_2SRu$	7.113	3.98	3.96	−0.02
$C_{50}H_{44}OCl_2P_4SPd_2$	5.597	2.91	3.08	+0.17
			2.90	−0.01
$C_{51}H_{46}Cl_2P_4SPd_2$	7.602	2.92	2.88	−0.04

REFERENCES

1 W. Schöniger, Mikrochim. Acta, (1956) 869.
2 H. Wagner, Mikrochim. Acta, (1957) 19.
3 R. Belcher, A. D. Campbell, P. Gouverneur and A. M. G. Macdonald, J. Chem. Soc., 1962, 3033.
4 R. B. Balodis, A. Comerford and C. E. Childs, Microchem. J., 12 (1967) 606.
5 S. W. Bishara, M. E. Attia and H. N. A. Hassan, Rev. Roum. Chim., 19 (1974) 1099.
6 F. C. Saville, in C. L. Wilson and D. W. Wilson (Eds.), Comprehensive Analytical Chemistry, Vol. 2B, Elsevier, 1968, p. 289.

ANALYTICA CHIMICA ACTA, VOL. 196 (1987)

AUTHOR INDEX

INFORMATION FOR AUTHORS

Detailed "Information for Authors" was published in Vol. 190, No. 2, pp. 375–378. A free reprint is available from the Editors or from:

Elsevier Editorial Services Ltd., Mayfield House, 256 Banbury Road, Oxford OX2 7DH (Great Britain)

Types of contribution. The journal welcomes original research papers, short communications and reviews. Reviews are written by invitation of the editors, who welcome suggestions for subjects. Short communications are usually complete descriptions of limited investigations, and should generally not exceed six printed pages. Preliminary communications of important urgent work can be printed within four months of submission, if the authors are prepared to forego proofs.

Manuscripts. The preferred language of the journal is English, but French and German manuscripts are also acceptable. For authors whose first language is not English, French or German, linguistic improvement is provided as part of the normal editorial processing. Authors should submit three copies of the manuscript in double-spaced typing on one side of the paper only, with a margin of 4 cm, on pages of uniform size. If any variety of machine copying is used (e.g. xerox), authors should ensure that all copies are easily legible and that the paper used can be written on with both ink and pencil. Authors are advised to retain at least one copy of the manuscript. Manuscripts should be preceded by a sheet of paper carrying (a) the title of the paper, (b) the name and full postal address of the person to whom proofs are to be sent, (c) the number of pages, tables and figures.

Information on the *submission of papers* is given on the inside front cover.

Summary. Research papers and reviews begin with a Summary (50–250 words) which should comprise a brief factual account of the contents of the paper, with emphasis on new information. Short communications and preliminary communications require summaries, which should not exceed 50 words. Uncommon abbreviations, jargon and reference numbers must not be used. The Summary should be suitable for use by abstracting services without rewriting. Papers in French or German require a Résumé or Zusammenfassung preceded by a Title and Summary in English; authors are encouraged to provide translations where necessary.

Introduction. The first paragraphs of the paper should contain an account of the reasons for the work, any essential historical background (as briefly as possible and with key references only) and preliminary experimental work.

Figures. Figures should be prepared in black waterproof drawing ink on drawing or tracing paper of the same size as that on which the manuscript is typed. One original (or sharp glossy print) and two photostat (or other) copies are required. Attention should be given to line thickness, lettering (which should be kept to a minimum) and spacing on axes of graphs, to ensure suitability for reduction during printing. Axes of a graph should be clearly labelled, along the axes, and outside the graph itself.

All figures should be numbered with Arabic numerals, and require descriptive legends. Explanatory information should be placed not in the figure, but in the legend, which should be typed on a separate sheet of paper. Simple straight-line graphs are not acceptable, because they can readily be described in the text by means of an equation or a sentence. Claims of linearity should be supported by regression data that include slope, intercept, standard deviations of the slope and intercept, standard error, and the number of data points; correlation coefficients are optional.

Photographs should be glossy prints and be as rich in contrast as possible; colour photographs cannot be accepted. In general, line diagrams are more informative and less liable to dating than photographs of equipment, which are therefore not usually acceptable.

Computer outputs for reproduction as figures must be good quality on blank paper, and should preferably be submitted as glossy prints.

Nomenclature, abbreviations and symbols. In general, the recommendations of the International Union of Pure and Applied Chemistry (IUPAC) should be followed, and attention should be given to the recommendations of the Analytical Chemistry Division in the journal *Pure and Applied Chemistry* (see also *IUPAC Compendium of Analytical Nomenclature*, 1978).

References. The references should be collected at the end of the paper, numbered in the order of their appearance in the text (*not* arranged alphabetically), and typed on a separate sheet.

In the list of references, the following forms should be adopted.

Journals

1 W. Lund and M. Salberg, Anal. Chim. Acta, 76 (1975) 131.

2 M. McDaniel, A. D. Shendrikar, K. D. Reizneir and P. W. West, Anal. Chem., 48 (1976) 2240.

The title of the journal must be abbreviated as in the Bibliographic Guide for Editors and Authors.

Books

1 D. D. Perrin, Masking and Demasking of Chemical Reactions, Interscience–Wiley, New York, 1970, p. 188.

2 S. Hofmann, in G. Svehla (Ed.), Wilson and Wilson's Comprehensive Analytical Chemistry, Vol. 9, Elsevier, Amsterdam, 1979, p. 89.

Titles of papers are unnecessary. Citations of reports which are not widely available (e.g., reports from government research centres) should be avoided if possible. Authors' initials should not be used in the text, unless real confusion could be caused by their omission. If the reference cited contains three or more names, only the first author's name followed by et al. (e.g., McDaniel et al.) should be used in the text; but the reference list must contain the initials and names of *all* authors.

Chemometrics: a textbook

by **D.L. Massart,** *Farmaceutisch Instituut, Vrije Universiteit Brussel, Belgium,* **B.G.M. Vandeginste,** *Laboratorium voor Analytische Chemie, Katholieke Universiteit Nijmegen, The Netherlands,* **S.N. Deming,** *Department of Chemistry, University of Houston, Texas, U.S.A.,* **Y. Michotte** *and* **L. Kaufman,** *Farmaceutisch Instituut, Vrije Universiteit Brussel, Belgium*

(Data Handling in Science and Technology, 2)

Most chemists, whether biochemists, organic chemists, pharmaceutical or clinical chemists and most medical doctors, pharmacists, and biologists who apply a chemical discipline need to carry out chemical determinations, i.e. perform chemical analysis. This book is addressed to all those scientists.

Its purpose is to give an introduction to the science of chemometrics - the chemical discipline that uses mathematical and statistical methods to design or select optimal procedures and experiments, and to provide maximum chemical information by analyzing chemical data.

The first book on chemometrics by D.L. Massart, A. Dijkstra and L. Kaufman appeared some ten years ago. The subject was then very new, but it has evolved considerably since then. After three reprints of this book, the need was felt for what, at first, was thought would be a new, updated edition of the first book. However, it has finally become a completely new book. Less weight is given in this new book to information theory, systems theory, and operations research and more to time series, correlation, and transformation methods, filtering, smoothing, etc. The authors' aim which went beyond that of the original book, was to write a tutorial book. Since, in didactical texts, too many references are irritating, citations appear in the text only when strictly necessary, and additional references are given at the end of most chapters.

Contents: Introduction. 1. Chemometrics and the Analytical Process. 2. Precision and Accuracy. 3. Evaluation of Precision and Accuracy. Comparison of Two Procedures. 4. Evaluation of Sources of Variation in Data. Analysis of Variance. 5. Calibration. 6. Reliability and Drift. 7. Sensitivity and Limit of Detection. 8. Selectivity and Specificity. 9. Information. 10. Costs. 11. The Time Constant. 12. Signals and Data. 13. Regression Methods. 14. Correlation Methods. 15. Signal Processing. 16. Response Surfaces and Models. 17. Exploration of Response Surfaces. 18. Optimization of Analytical Chemical Methods. 19. Optimization of Chromatographic Methods. 20. The Multivariate Approach. 21. Principal Components and Factor Analysis. 22. Clustering Techniques. 23. Supervised Pattern Recognition. 24. Decisions in the Analytical Laboratory. 25. Operations Research. 26. Decision Making. 27. Process Control. Subject Index.

1987 ca. 464 pages
US$ 77.75 / Dfl. 175.00
ISBN 0-444-42660-4

ELSEVIER SCIENCE PUBLISHERS
P.O. Box 211 - 1000 AE Amsterdam - The Netherlands
P.O. Box 1663 - Grand Central Station - New York, NY 10163